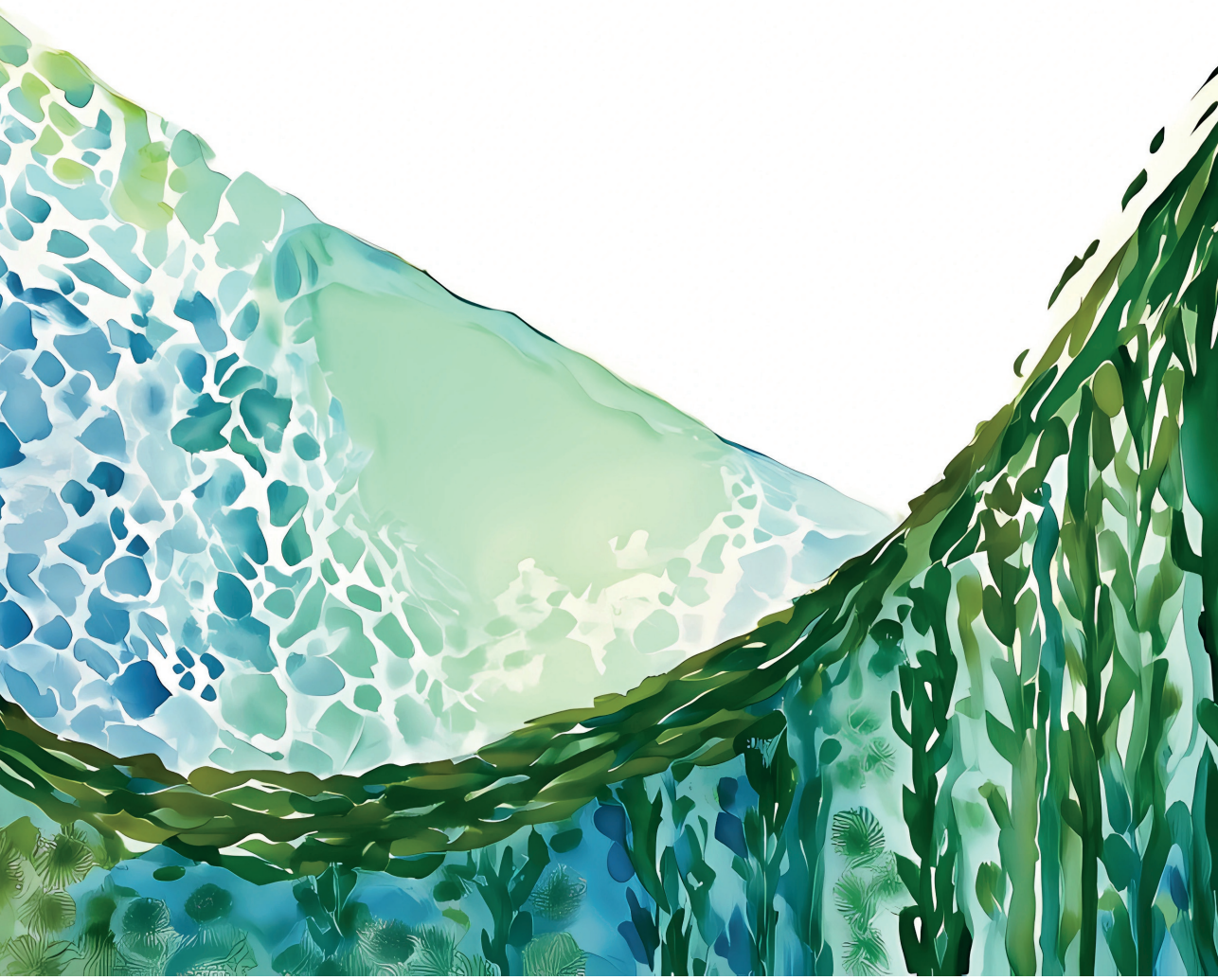
From Solvents to Solutions

Deep Eutectic Solvents for Circular Seaweed Biorefineries



Isa Sara Aimée Hiemstra

Propositions

1. Eutectic solvents are an essential part of life (this thesis)
2. Bioprocess engineering requires intuition to navigate unpredictability of biological systems (this thesis)
3. Musicians make better scientists
4. Manuscript reviewers should never be anonymous
5. A 36-ECTS master's thesis should be an elective pathway for aspiring researchers rather than a compulsory requirement for future industry professionals.
6. True autonomy lies not in controlling external circumstances, but the governance of the internal space that decides how reality is received
7. Who we become matters more than what we leave behind

Propositions belonging to the thesis, entitled

From Solvents to Solutions: Deep Eutectic Solvents for circular seaweed biorefineries

Isa Sara Aimée Hiemstra

Wageningen, 27 November 2026

From Solvents to Solutions

Deep Eutectic Solvents for Circular Seaweed Biorefineries

Isa Sara Aimée Hiemstra

Thesis committee

Promotors

Prof. Dr *ir.* Rene H. Wijffels

Professor of Bioprocess Engineering

Wageningen University & Research

Prof. Dr Michel H. M. Eppink

Professor of Bioprocess Engineering

Delft University of Technology

Co-promotors

Dr Antoinette Kazbar

Associate Professor in Bioprocess Engineering

Wageningen University & Research

Other members

Prof. Dr *ir.* Maarten Schutyser, Wageningen University & Research

Dr Elinor Scott, Wageningen University & Research

Prof. Dr Sónia Ventura, University of Aveiro, Portugal

Dr Edgar Suarez Garcia, Revyve

This research was conducted under the auspices of VLAG Graduate School (Biobased, Biomolecular, Chemical, Food and Nutrition Sciences).

From solvents to solutions

Deep Eutectic Solvents for Circular Seaweed Biorefineries

Isa Hiemstra

Thesis

submitted in fulfilment of the requirements for the degree of doctor
at Wageningen University
by the authority of the Rector Magnificus,
Prof. Dr C. Kroeze,
in the presence of the
Thesis Committee appointed by the Academic Board
to be defended in public
on Friday 27 November 2026
at 10:30 a.m. in the Omnia Auditorium.

Isa Hiemstra

From solvents to solutions – Deep eutectic solvents for circular seaweed biorefineries

388 pages

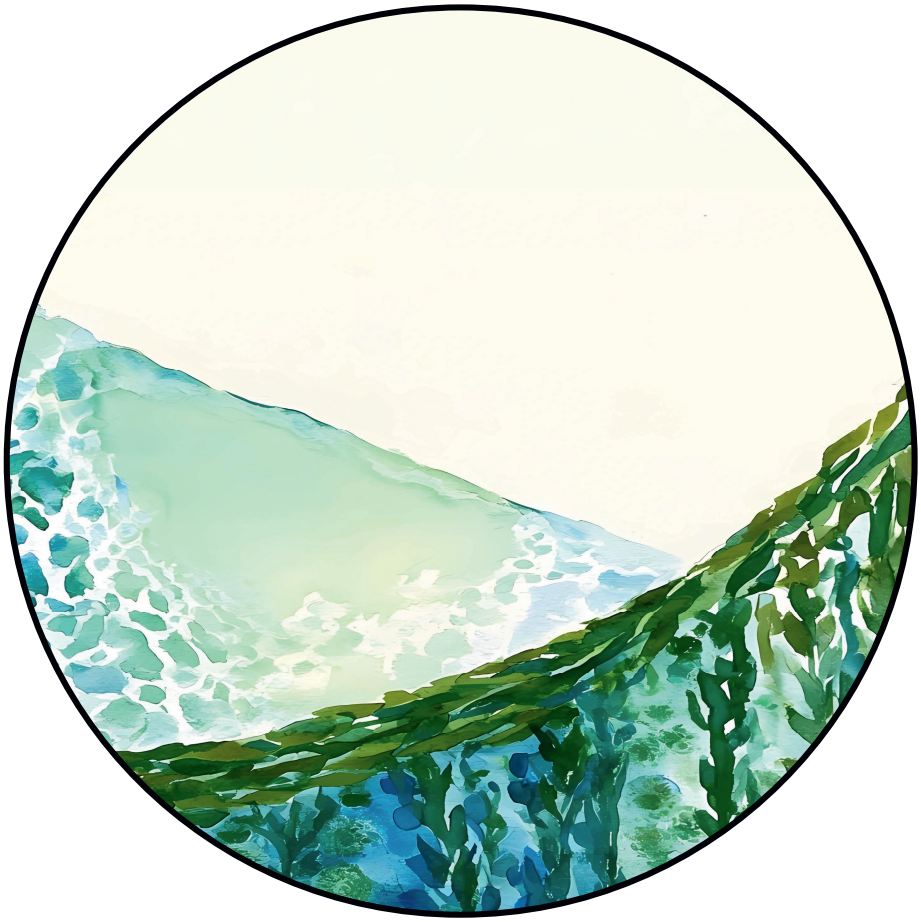
PhD thesis, Wageningen University, Wageningen, the Netherlands (2026)

With references, with a summary in English

DOI: 10.18174/682015

Table of contents

Chapter 1	*Introduction*	9
Chapter 2	*Towards selective alginate solvation: A capacity–selectivity analysis of deep eutectic solvents*	29
Chapter 3	*Choline chloride-based solvents as alternative media for alginate extraction from brown seaweed*	59
Chapter 4	*Pressure-driven membrane processes for the recovery and recycling of deep eutectic solvents: A seaweed biorefinery case study*	85
Chapter 5	*Process intensification of seaweed biorefinery using reusable natural deep eutectic solvents*	101
Chapter 6	*Separation of alginate and recycling of deep eutectic solvents using temperature-responsive aqueous two-phase systems*	133
Chapter 7	*Mechanistic insights into temperature-responsive deep eutectic solvent for alginate recovery and solvent recycling*	161
Chapter 8	*Direct alginate recovery and solvent recycling from deep eutectic solvents via interfacial precipitation in aqueous two-phase systems*	197
Chapter 9	*Disruption or partitioning? Deep eutectic solvent biphasic systems for integrated seaweed biorefineries*	225
Chapter 10	*Techno-economic and life cycle assessment of DES-based multiproduct seaweed biorefinery*	257
Chapter 11	*General discussion*	293
References		325
Summary		369
Appendices		375



Chapter 1

Introduction, aim and thesis outline

1.1. Introduction

There is an increasing need for alternative green biorefinery technologies for the sustainable extraction of bioactive compounds from biomass resources, as conventional extraction processes frequently depend on solvents and chemicals associated with environmental and health concerns [1]. In integrated biorefinery concepts, not only extraction efficiency but also solvent recyclability and multiproduct recovery are essential for process sustainability. Currently, organic solvents are widely applied for the recovery of biomass-derived products, yet several of these solvents present challenges related to toxicity, volatility, flammability, or fossil-based origin [2]. In addition, harsh extraction conditions and unsuitable processing media may compromise the structural integrity and functionality of sensitive compounds, thereby potentially reducing product quality and application potential [3, 4]. Conventional extraction routes are also often resource-intensive and inefficient, owing to limited solvent regeneration and the incomplete valorisation of biomass streams.

Therefore, integrated biorefinery approaches that combine efficient extraction with solvent recyclability and multiproduct recovery are increasingly recognised as essential for improving overall process sustainability. Consequently, the development of safer, circular, and more selective extraction platforms is essential to support sustainable biorefinery concepts.

1.2. Eutectic solvents

As alternatives to conventional extraction media, eutectic and deep eutectic solvents (DES) have emerged as promising solvents for sustainable biorefinery applications [5–7]. Deep eutectic solvents belong to the broader class of eutectic solvents, which are mixtures of two or more components that exhibit a melting point lower than that of the individual parent compounds. The term “eutectic” is derived from the Greek word εὐτηκτος (eutektos), meaning “easily melted” [8], reflecting this characteristic melting point depression. This melting point depression behaviour enables combinations of otherwise solid constituents to form liquids at or near room temperature, thereby allowing their use as solvents. Thermodynamically, such behaviour arises from favourable interactions between the mixture components, which reduce crystal lattice formation and stabilise the liquid phase [9, 10]. The extent of this melting point depression in eutectic systems can be expressed thermodynamically in **Equation 1.1**:

$$\ln(x_i\gamma_i) = \frac{\Delta_{fus}H}{R}\left(\frac{1}{T_m} - \frac{1}{T}\right) \qquad \textbf{(1.1)}$$

where x represents the mole fraction of component i and γ_i its activity coefficient, with γ_i= 1 corresponding to ideal mixture behaviour. $\Delta_{fus}H$ denotes the enthalpy of fusion of pure compound i, R is the ideal gas constant (8.314 J mol^{-1} K^{-1}), T_m is the melting temperature of the pure component, and T is the melting temperature of the resulting mixture [11]. Under the assumption of ideal mixing behaviour ($\gamma = 1$), the melting temperature of the system can be predicted as a function of composition when the melting enthalpy and melting point of the pure components are known. By applying (**1.1**) to each constituent, two solid–liquid equilibrium curves can be constructed. The intersection of these curves defines the eutectic composition and the corresponding eutectic temperature, at which the mixture exhibits its minimum melting point (**Figure 1.1**).

1.2.1 Deep eutectic solvent behaviour

A specific subclass of eutectic solvents, termed deep eutectic solvents (DES), was first described by Andrew Abbott and co-workers in 2003 [12], describing solvent behaviour of a choline chloride and urea mixture. DES are characterised by a melting point depression that is significantly greater than that expected for an ideal eutectic mixture (**Figure 1.1**). This non-ideal behaviour ($\gamma < 1$) is commonly attributed to strong intermolecular interactions, particularly hydrogen bonding, electrostatic interactions, and van der Waals forces between the constituents. Owing to these extensive and tuneable interaction capabilities, DES have attracted considerable interest as promising solvents for several applications, including selective extraction and biomass fractionation [13].

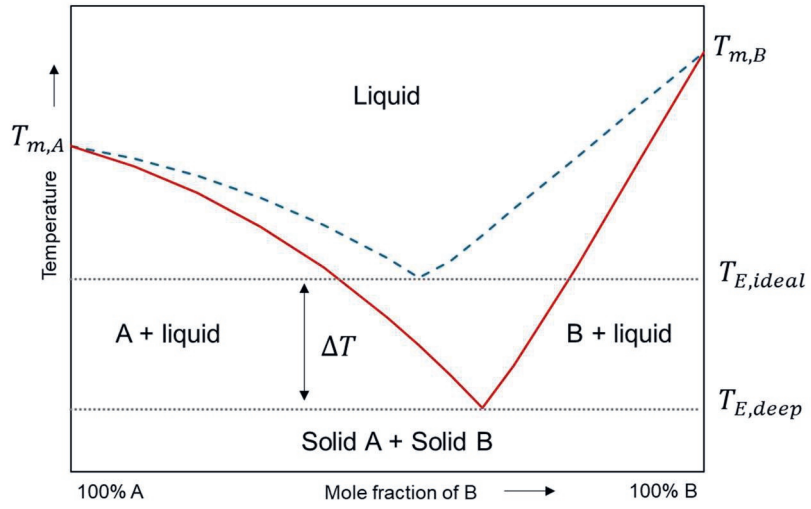


Figure 1.1 Schematic solid–liquid equilibrium phase diagram of a (deep) eutectic mixture, illustrating the eutectic point and melting point depression.

1.2.2 DES types

DES are commonly represented by the general formula (**Equation 1.2**):

$$Cat^{+}X^{-}zY \quad (\mathbf{1.2})$$

where Cat^{+} refers to a cationic species, generally ammonium, phosphonium, or sulfonium, X^{-} generally is a Lewis base, Y to a Lewis or Brønsted acid, and z to the number of Y molecules interacting with the corresponding anions [14]. In most DES systems, one component acts as a hydrogen bond acceptor (HBA), frequently a quaternary ammonium salt such as choline chloride, while the second component functions as a hydrogen bond donor (HBD), such as organic acids, polyols, amides, or sugars.

DES composed of a quaternary ammonium salt with a hydrogen bond donor (Type III) are the most widely studied due to their tunability and relatively low toxicity. Additionally, DES composed entirely of non-ionic molecular compounds, are increasingly studied, thereby expanding the design space and enabling the development of systems with tailored polarity and reduced toxicity [15, 16].

When DES are composed of naturally derived components, they are referred to as natural deep eutectic solvents (NADES), typically consisting of primary metabolites such as sugars, amino acids, and organic acids. The concept of NADES was first introduced by Choi and co-workers [17], who proposed that such solvent systems may naturally occur in living organisms and contribute to tolerance against environmental stresses such as dehydration and temperature fluctuations. As an example, the wood frog (*Rana sylvatica*) is capable of surviving prolonged exposure to subzero temperatures through a remarkable cryoprotective response. In preparation for seasonal freezing and dehydration, the frog accumulates urea, while the onset of freezing rapidly triggers the conversion of liver glycogen into high concentrations of glucose. Together, these metabolites form highly concentrated intracellular mixtures that reduce water availability, suppress ice damage, and stabilise proteins and cellular structures. This metabolite-rich environment resembles a NADES-like system, where strong solute–solute interactions and hydrogen-bonding networks effectively replace bulk water and enable biological function under extreme environmental stress. The ability of such metabolite-rich systems to stabilise and interact with biological molecules has inspired the development and application of NADES as extraction and processing media.

Within the broader class of DES, NADES are particularly attractive for extraction and biorefinery applications due to their renewable and biocompatible composition. Their formation from naturally abundant metabolites enables tuneable solvation behaviour while maintaining the inherent advantages of DES, such as strong intermolecular interactions and high structural diversity, making them promising media for biomass processing and integrated valorisation strategies.

The definition of DES is still subject to debate, as no universally accepted description exists [18]. Therefore, Martins *et al*. [8] described DES as mixtures of two or more components that exhibit a melting point significantly lower than that of an ideal mixture, due to strong non-ideal interactions between the constituents. When this melting point depression is insufficient to maintain a liquid state under operating conditions, the system is more appropriately referred to as a eutectic solvent rather than a deep eutectic solvent. In this thesis, the term DES is used to refer to solvent systems reported as such in literature, without independent thermodynamic verification of eutectic behaviour. Consequently, some of the systems studied may more accurately be classified as eutectic rather than deep eutectic solvents. However, for consistency with the literature, the term DES is retained throughout this thesis.

1.3. DES applications

Even though DES offer several advantages over conventional solvents, it should be noted that these favourable characteristics are highly dependent on the specific DES composition, as the choice of components largely determines solvent performance, stability, and environmental profile. A major advantage of DES is their high tunability as physicochemical properties can be readily adjusted through selection of different hydrogen bond acceptors, hydrogen bond donors, and molar ratios [9, 10]. This compositional flexibility enables the rational design of solvents for different targeted applications.

As a result of these attributes, DES have attracted increasing interest across a broad range of industrial and environmental applications. Reported uses include CO_2 capture [19, 20], air pollutant removal [21, 22], drug solubilisation and delivery [23, 24], cryopreservation [25, 26], metal extraction and recovery [27, 28] and biomass delignification [29, 30]. More recently, DES have emerged as promising extraction media for the recovery of valuable compounds from different biomass resources, including plants [31, 32], yeast [33], and algae [34, 35]. Their tuneable selectivity and flexible composition make DES particularly attractive as selective and potentially more sustainable alternatives to conventional solvents for the extraction of bioactives

including lipids, pigments, and polysaccharides within integrated biorefinery processes.

1.3.1 DES as extractants

Deep eutectic solvents (DES) have emerged as promising extraction media for the recovery of bioactive compounds from biomass due to their favourable properties [16, 36]. Their strong solvation capacity and tuneable selectivity enable efficient dissolution of target compounds [16], while their solvent environment can contribute to the stabilisation of sensitive bioactives during extraction [37]. In addition, DES are proposed to act as a disruptive medium, facilitating the breakdown of biomass structures and promoting the release of intracellular components [33]. The extraction performance of DES is governed by the interactions between the solvent constituents and the target molecules, primarily through hydrogen bonding, polarity-driven interactions, and the disruption of the cell wall matrix [16]. Key solvent properties influencing extraction behaviour include polarity, viscosity, density, conductivity and surface tension, all of which are strongly dependent on the chemical nature and composition of the hydrogen bond acceptor (HBA) and hydrogen bond donor (HBD). These combined properties have made DES increasingly relevant for biomass processing applications, particularly for the extraction of value-added compounds from complex natural matrices. Among renewable biomasses, marine biomass has gained increasing attention due to its diverse composition, availability and broad potential for valorisation, including pharmaceuticals, nutraceuticals and cosmetics [38]. In particular, seaweeds have emerged as highly attractive candidates for biorefinery applications due to their high content of structurally diverse compounds, such as polysaccharides, pigments, and other bioactive molecules, enabling multiproduct valorisation strategies.

1.4. Seaweed as renewable biomass

Marine macroalgae, commonly referred to as seaweeds, have attracted increasing interest as renewable biomass resources for sustainable biorefinery applications. Unlike terrestrial crops, seaweeds exhibit rapid growth rates, high areal productivity, and can be cultivated in marine environments without requiring arable land, freshwater, or substantial fertiliser input [39, 40]. Their rich and diverse biochemical composition makes seaweeds particularly attractive for integrated multiproduct valorisation, in which several valuable compounds can be selectively recovered from a single biomass stream.

Among the three major seaweed groups (green, red and brown seaweed), brown seaweeds are of particular relevance due to their high carbohydrate content and abundance of structurally diverse polysaccharides (**Figure 1.2**). Species such as *Saccharina latissima*, *Laminaria digitata*, and *Ascophyllum nodosum* contain significant quantities of the carbohydrates alginate (15-40% DW), fucoidan (3-11% DW), laminarin (2–35% DW), and mannitol (5-20% DW) [41–43], alongside pigments, proteins, and phenolic compounds.

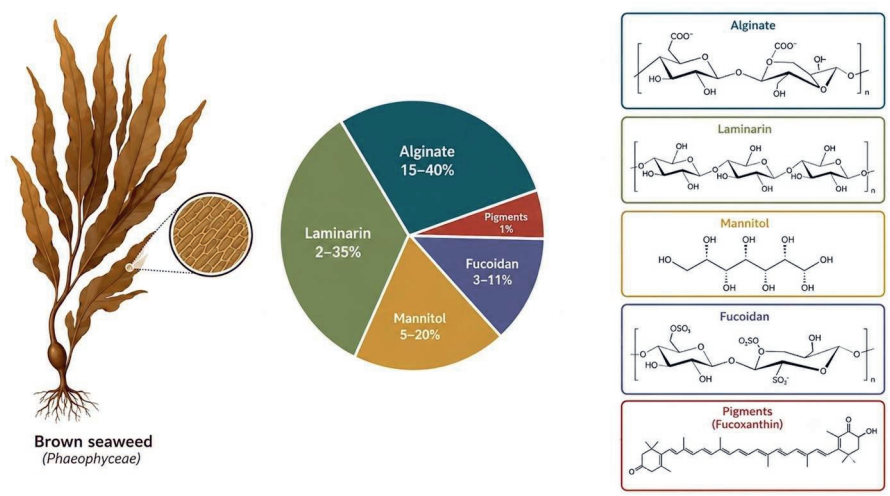


Figure 1.2 Composition and relative abundance of major carbohydrates in brown seaweed.

This coexistence of multiple valuable fractions makes brown seaweeds highly suitable feedstocks for integrated processing strategies aimed at maximising biomass utilisation and product value, further potentially increasing their commercial potential. The complex and layered architecture of the brown seaweed cell wall emphasises the need for selective extraction approaches. Alginate and fucoidan form the primary structural matrix, while proteins, phenolic compounds, and pigments are embedded within or associated with this network (**Figure 1.3**). Consequently, efficient fractionation requires solvent systems capable of selectively disrupting and solubilising specific components while preserving opportunities for sequential or simultaneous recovery of multiple products. In this context, the tuneable solvation behaviour and selectivity of DES make them promising candidates for seaweed-based multiproduct biorefinery applications.

Among these constituents, alginate is of particular interest because of its gelling ability, biocompatibility, and broad use in the food, pharmaceutical, biomedical, and materials sectors [44]. Alginate is widely used as a thickening and gelling agent in the

food industry and has found applications in the medical field for drug delivery and wound dressings [45, 46].

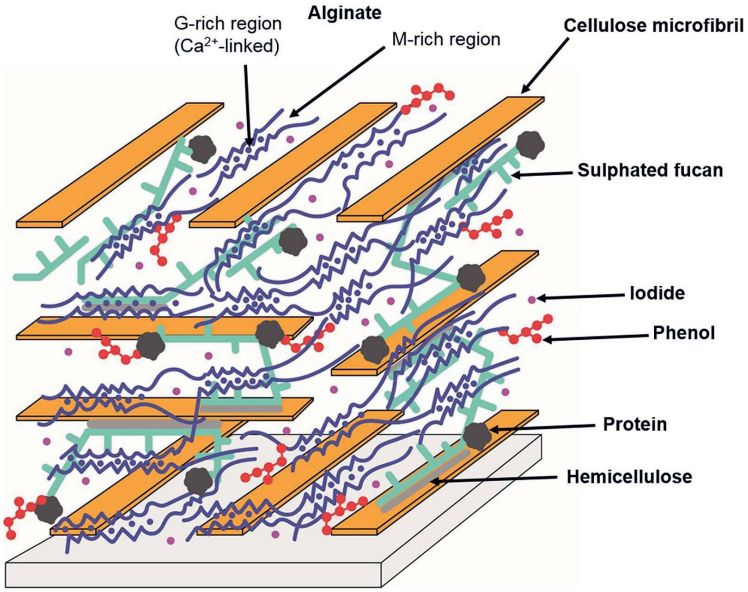


Figure 1.3 Brown seaweed cell wall model. Alginate and phenolic compounds are closely associated and may form high-molecular-weight complexes. Proteins can interact with sulphated fucoidans and are covalently bound to phenolic compounds. Certain sulphated fucoidans are strongly associated with cellulose microfibrils and are embedded within the surrounding alginate matrix. Hemicellulosic components, typically present as shorter-chain polysaccharides, interact hydrophobically with cellulose and form additional connections with the sulphated fucoidans (Figure adapted from Charoensiddhi *et al*. [47] with permission).

1.4.1 Alginate

Alginate is a linear anionic polysaccharide present in the cell wall, composed of β-D-mannuronic acid (M) and α-L-guluronic acid (G) residues arranged in homopolymeric (MM, GG) and heteropolymeric (MG) block sequences (**Figure 1.4**). The relative abundance and distribution of these blocks influence parameters including viscosity, gel strength, elasticity, and affinity for divalent cations, thereby determining end-use functionality [48]. Alginate gels with a high M/G ratio generally exhibit greater flexibility and permeability, whereas gels with a low M/G ratio tend to form stronger, more rigid networks [49]. G-rich blocks possess a more ordered and less conformationally flexible structure, which promotes tighter ionic cross-linking and enhanced mechanical strength compared with alginates containing higher proportions of mannuronic acid blocks (**Figure 1.4**). Within the cell wall, alginate serves multiple structural and protective roles, acting as a flexible but strong matrix that helps the seaweed withstand mechanical stresses in marine environments. Due to alginate's properties, it can be

applied as a thickener, stabiliser, encapsulation matrix, wound dressing material, and hydrogel-forming biopolymer [50]. Given that alginate functionality is closely linked to its molecular structure, extraction methods should aim to preserve these native characteristics while achieving efficient recovery. This is particularly relevant in the development of alternative extraction systems, where solvent–polymer interactions may influence polymer composition, viscosity, and overall material performance.

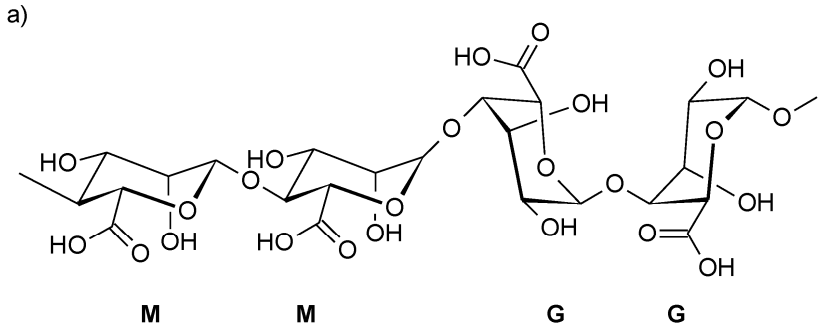


Figure 1.4 Structural organisation of alginate: (**a**) conformation of the polysaccharide chain, (**b**) arrangement of mannuronic acid (M) and guluronic acid (G) block sequences within the polymer backbone. Adapted from Rosiak *et al*. [51] under the Creative Commons CC BY license.

1.4.2 Other seaweed components

In addition to alginate, brown seaweeds contain several other valuable fractions that contribute to their attractiveness as multiproduct biorefinery feedstocks. Fucoxanthin, the principal carotenoid pigment in brown algae, has attracted attention due to its antioxidant, anti-inflammatory, and potential anti-obesity properties, as well as its high market value, making it an attractive target for valorisation [52]. Fucoidan, a sulphated polysaccharide located in the cell wall matrix, is of interest for nutraceutical and pharmaceutical applications because of its reported anticoagulant, antiviral, and immunomodulatory activities [42, 53]. Laminarin serves as a storage glucan with potential prebiotic and bioactive functionality [43, 54], while mannitol is a readily soluble sugar alcohol that can be recovered as a platform chemical or sweetener [43, 55].

The simultaneous presence of structural polysaccharides, bioactive compounds, and soluble metabolites provides opportunities for integrated fractionation and multiproduct recovery from a single biomass stream. From a process and economic

perspective, valorisation of multiple fractions alongside alginate may improve biomass utilisation, increase product value generation, and enhance the feasibility of seaweed biorefineries. Consequently, selective extraction and separation strategies capable of targeting different compound classes are required, motivating the development of integrated solvent-based processing approaches.

1.5. Current and novel seaweed processing

1.5.1 Conventional alginate extraction

Conventional alginate extraction from brown seaweed is typically a multistage process aimed at converting naturally occurring insoluble alginate salts, primarily calcium and magnesium alginates present in the cell wall, into purified sodium alginate (**Figure 1.5**). After harvesting, the seaweed is often treated with formaldehyde to enhance storage stability and to improve alginate yields in subsequent extraction steps [56]. Initially, the biomass is washed, dried, and mechanically reduced in size to increase surface area and improve mass transfer during extraction. This is followed by an acid pretreatment using dilute hydrochloric or sulfuric acid to remove polyvalent cations and convert alginate into insoluble alginic acid. Subsequently, alkaline extraction is performed using sodium carbonate under elevated pH, whereby alginic acid is transformed into water-soluble sodium alginate. The resulting viscous extract is diluted and subjected to solid–liquid separation, typically through filtration, flotation, or centrifugation, to remove residual biomass solids. The clarified solution is often further treated by bleaching and acidification to remove colour impurities and facilitate purification prior to recovery [56, 57]. Alginate is then recovered through alcohol precipitation or calcium-induced fibre formation, followed by washing, neutralisation, drying, and milling to obtain the final product [58]. Variations of this process are applied depending on the seaweed species used and the targeted alginate quality.

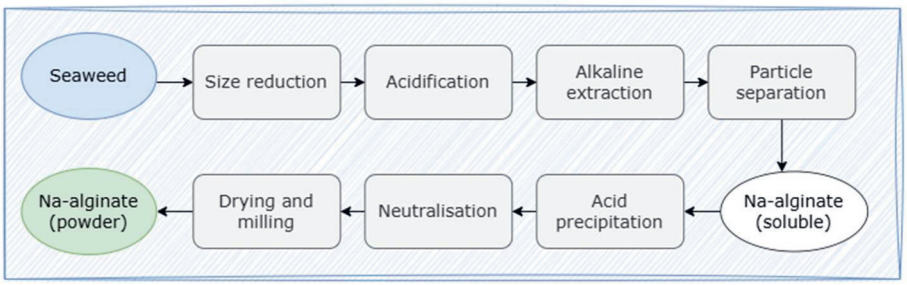


Figure 1.5 Schematic representation of the conventional alginate extraction process. Adapted from Saji *et al.* [56].

The conventional extraction approach described above relies on multiple chemical-intensive steps and may considerably alter the structural characteristics of alginate,

particularly its molecular weight and mannuronic-to-guluronic (M/G) block distribution [57, 59]. Prolonged exposure to highly alkaline conditions and elevated temperatures can induce polymer depolymerisation and modify alginate block composition, thereby affecting functional properties such as viscosity, gelation behaviour, and mechanical performance [60]. These chemically induced structural changes can also result in significant batch-to-batch variability in alginate quality, which is undesirable from a process standardisation and industrial application perspective. In addition, conventional alginate extraction is associated with substantial consumption of chemicals, water, and thermal energy, owing to extensive washing, pH adjustment, dilution, and temperature-controlled extraction stages. The use of harsh chemicals also generates alkaline and acidic effluents, thereby raising environmental and processing concerns [56, 60].

Furthermore, conventional processing largely focuses on alginate recovery, while underutilising or degrading other valuable seaweed constituents, including fucoidan, laminarin and pigments such as fucoxanthin. As a result, the broader valorisation potential of brown seaweed biomass remains insufficiently exploited [57, 61]. Consequently, there is a clear need for alternative, milder extraction strategies that enable efficient alginate recovery while preserving polymer properties and supporting integrated multiproduct valorisation of seaweed biomass.

1.5.2 Alternative extraction

As a result, DES have recently emerged as a promising alternative for the extraction polysaccharides from brown seaweed. For example, DES have been applied in combination with techniques such as microwave-assisted [62] and ultrasound-assisted [63, 64] extraction for polysaccharide recovery from brown seaweed, demonstrating their potential to enhance extraction efficiency.

However, despite these promising results, several critical aspects remain insufficiently explored. Most reported studies primarily focus on extraction performance, while limited attention has been given to downstream processing, including product isolation from the DES phase, solvent recovery, and recyclability, which are critical prerequisites for translating DES-based extraction systems into viable integrated circular biorefinery processes. In addition, the majority of studies rely on the integration of DES with energy-intensive auxiliary techniques, whereas the use of DES as a standalone extraction medium remains largely unexplored. This limits the understanding of DES as a complete processing platform rather than merely an extraction additive.

More importantly, current literature lacks integrated process designs that combine selective extraction, product recovery, product quality and solvent recycling within a unified biorefinery concept. As a result, the potential of DES for enabling circular and sustainable seaweed valorisation has not yet been fully established. Therefore, further research is required to develop integrated DES-based extraction and recovery strategies and to evaluate their applicability within complete biorefinery frameworks.

1.5.3 Solvent screening

The large number of possible DES combinations, resulting from the many available HBA, HBD and compositional ratios, make experimental solvent selection inefficient and resource intensive. Therefore, more rational approaches are needed to prioritise promising solvent systems prior to laboratory screening.

In solid–liquid extraction processes, solute transfer from biomass into the solvent is governed by thermodynamic interactions between the solute and the surrounding medium, which can be described using the activity coefficient (γ). In general, lower activity coefficients indicate stronger solute–solvent interactions and therefore higher affinity of the solute for the solvent phase [65]. With the activity coefficient, extraction performance indicators such as distribution coefficients, selectivity, and solvent capacity can be derived.

Experimentally determining these parameters for a large number of DES compositions would require extensive screening in terms of time, materials, and analytical effort. As a result, in silico computational approaches have become increasingly important for guiding solvent selection and reducing experimental workload [32, 66]. Among these, the Conductor-like Screening Model for Real Solvents (COSMO-RS) is widely used to predict thermodynamic behaviour in liquid systems based on molecular surface charge distributions, enabling estimation of solute–solvent interactions and relative affinities without requiring experimental input [67, 68]. This makes COSMO-RS a powerful tool for rapidly narrowing down large DES design spaces and guiding experimental efforts toward the most promising solvent candidates. However, its ability to reliably predict interactions with complex seaweed-derived polysaccharides and bioactive mixtures still requires further researching and validation. Following computational screening, experimental studies remain essential to confirm extraction performance and optimise process conditions.

1.6. DES recycling

Once suitable DES and extraction parameters have been identified, the main limitation of DES-based processes lies in the separation of target products from the solvent and the subsequent recovery and reuse of the DES [69, 70]. Due to their generally low vapour pressure, DES cannot be removed by evaporation, which limits straightforward product isolation and subsequent solvent recycling [71]. To compete with current extraction solvents, effective product recovery and solvent recyclability is required to ensure process sustainability and circularity. Several approaches have been applied for the recovery of DES (**Figure 1.6**).

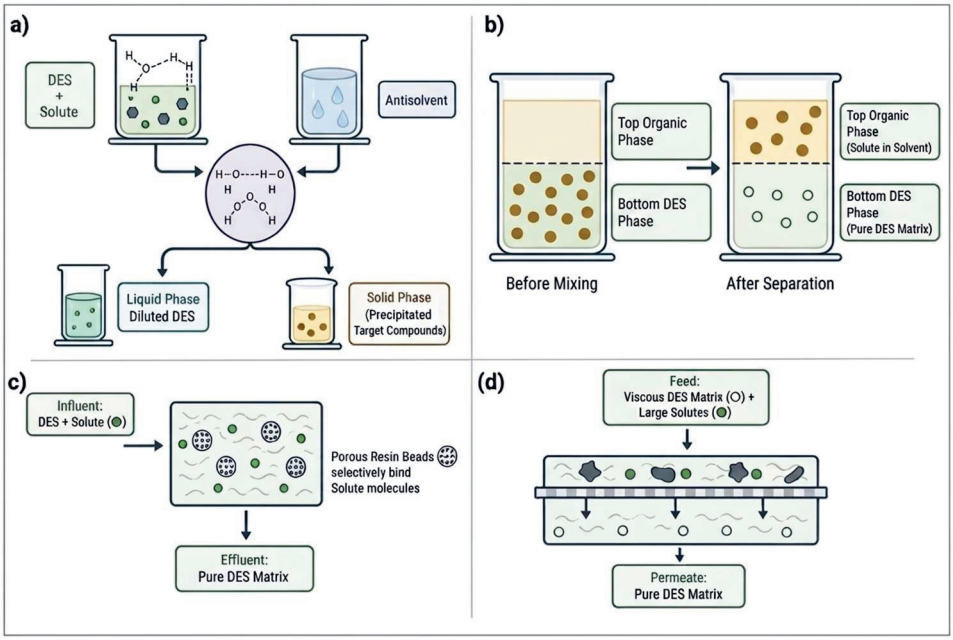


Figure 1.6 Schematic overview of possible product recovery strategies from DES via (**a**) antisolvent addition, (**b**) liquid-liquid extraction, (**c**) adsorption and (**d**) membrane filtration.

1.6.1 Antisolvent extraction

Among the reported strategies for product recovery from DES, antisolvent addition is one of the most widely applied methods [70]. In this strategy, a solvent is added to disrupt DES–solute interactions, thereby reducing solubility and inducing precipitation of the target compound. Water has frequently been used as antisolvent for the recovery of compounds, including phenolics [72], flavonoids [73] and lignin [74] from DES. Precipitation with water often takes several hours (up to 6 hours) at low temperatures (0-4 ◦C) and is generally followed by vacuum evaporation or drying to remove the added water, which is often operated for prolonged times at elevated temperatures (up to 105

◦C) [72, 75, 76]. Although effective, this approach generally requires subsequent water removal, which can be energy-intensive, time-consuming, and costly at larger scale [77].

Ethanol has also been widely explored as an alternative antisolvent, particularly for the precipitation of polysaccharides from DES extracts [69]. In these systems, multiple volumes of ethanol are commonly added, often followed by prolonged cooling or standing periods to complete precipitation (e.g. 12 h at 4 °C) [78, 79]. Subsequent centrifugation, washing, redissolution, and dialysis steps are frequently performed for further purification [78]. While ethanol may reduce the need for high-temperature evaporation compared with water-based antisolvent systems, these methods rely on substantial solvent consumption, extended processing times, and multiple downstream operations. In addition, certain DES components may themselves precipitate or become destabilised upon alcohol addition, which can further complicate solvent recycling [70].

1.6.2 Liquid-liquid extraction

Liquid–liquid extraction has also been explored for product recovery from DES by contacting the extract with an immiscible organic solvent. Commonly reported solvents include hexane [80], 1-butanol [81] and diethyl ether [82], allowing transfer of the target compound into the organic phase followed by straightforward phase separation. However, the use of volatile and potentially hazardous organic solvents reduces the sustainability of this approach. In addition, its applicability is limited to compounds that exhibit favourable partitioning between the DES and the selected organic solvent.

1.6.3 Adsorption

Membrane filtration represents a promising downstream strategy for DES-based processes, enabling selective product separation while allowing recovery and recycling of the solvent. Different membrane-driven approaches have been explored for DES recovery, including pressure-driven processes such as ultrafiltration, concentration gradient-driven techniques such as dialysis, and electrically driven separations such as electrodialysis [69]. Although research on DES–membrane systems remains limited, coupled membrane configurations combining ultrafiltration and electrodialysis have demonstrated potential for integrated product and solvent recovery [83, 84]. However, energy demand and limited ease of scale-up may restrict large-scale implementation of electrodialysis [85, 86]. Nevertheless, membrane technologies remain promising for DES recovery and recycling, particularly commercially established pressure-driven processes.

Despite their operational simplicity and scalability, membrane-based approaches still face several challenges when applied to DES-containing streams. The relatively high viscosity of DES solutions can reduce mass transfer and increase susceptibility to membrane fouling [70], thereby affecting separation efficiency and membrane lifetime. In addition, membrane processes often require substantial water use for dilution, washing, or diafiltration, which may compromise overall process sustainability. The recovery of highly concentrated products and solvents can further be limited by operational constraints [70], highlighting the need for optimised membrane designs and process integration strategies for DES-based separations.

Overall, current recovery strategies demonstrate that product isolation from DES is feasible, but often at the expense of process simplicity, solvent efficiency, and energy demand (**Table 1.1**) To compete as sustainable alternatives to conventional solvents, mild and effective solvent recycling must also be incorporated. This emphasises the need for alternative separation concepts that enable direct product recovery while preserving DES recyclability, while avoiding prolonged evaporation steps and the use of toxic organic solvents.

Table 1.1 Product recovery strategies from DES

Method	Advantages	Disadvantages
Antisolvent extraction	Simple setup; highly effective for large solids like lignin or oils; fast separation.	High water consumption; requires high energy to evaporate the antisolvent later; low yields for highly polar compounds.
Liquid-liquid extraction	High recovery yield; can keep DES intact; does not require heavy dilutions.	Uses volatile organic solvents; risks phase emulsification; cross-contamination between phases.
Adsorption	High selectivity; possibility to regenerate and reuse the resin adsorbent	Requires a volatile elution solvent; limited by adsorption capacity; expensive
Membrane filtration	Allows precise fractioning by size; Chemical-free process; potential to scale up	Membrane fouling; high viscosity of DES drops flux; limited by high osmotic pressure

1.7. Process viability

Despite the promise of DES as selective and potentially recyclable processing media, enhanced extraction performance alone does not necessarily translate into industrial feasibility or environmental sustainability**.** The overall viability of DES-based processes is determined by the full process chain, including solvent preparation, downstream separation and product recovery, solvent regeneration, and associated water and energy requirements. In particular, product recovery and solvent recycling operations

may introduce additional process complexity and material requirements that significantly affect both economic and environmental performance.

Consequently, evaluation of DES-based processes must extend beyond extraction efficiency and consider the system as a whole. A comprehensive techno-economic assessment (TEA) and life cycle assessment (LCA) are therefore required to evaluate DES-based processes for both economic and environmental performance at process scale. TEA provides quantitative insight into process economics, including capital and operating expenditures, whereas LCA assesses environmental impacts associated with resource consumption, energy use, emissions, and waste generation. Together, these methodologies are essential to determine whether DES-based extraction strategies can be translated into viable, scalable, and sustainable biorefinery concepts.

1.8. DES-based circular seaweed biorefineries

Overall, the comprehensive evaluation of DES-based processing requires an integrated assessment across the entire value chain, beginning with molecular-level solvent screening to understand solvent–solute interactions and predict selective affinities toward target compounds and biomass components, thereby supporting the rational selection of suitable DES. This should be complemented by validation and optimisation of extraction conditions at laboratory scale to maximise product yields, selectivity, and process performance. In parallel, mechanistic insight into biomass disintegration and compound partitioning remains important for the targeted design of improved DES-based extraction systems. In addition, efficient downstream separation strategies are essential for the recovery of both target products and the DES itself, enabling solvent recycling and the development of circular processing concepts. Such recovery approaches should minimise energy demand, solvent losses, and additional purification requirements to ensure practical implementation. Finally, techno-economic assessment (TEA) and life cycle assessment (LCA) are required to determine the industrial feasibility, environmental performance, and scalability of DES-based biorefinery systems.

In the present work, this integrated framework was applied using brown seaweed biomass as a case study to evaluate the potential of a complete, circular DES-based multiproduct biorefinery process.

1.9. Aim and thesis outline

The aim of this thesis is to evaluate the feasibility of a circular DES-based multiproduct biorefinery using brown seaweed biomass as a case study, by integrating molecular

solvent screening, extraction process optimisation, while focussing on product recovery and DES recycling.

In this thesis, the following research questions are addressed:

- What molecular descriptors and which DES screening criteria enable the identification of solvent systems with high affinity and selectivity toward alginate?
- To what extent does DES-based extraction improve alginate extraction and preservation of properties relative to conventional processing?
- How can DES-based processing contribute to process intensification in brown seaweed biorefineries?
- How can DES-based processes be designed to achieve effective and sustainable product recovery and solvent recycling?
- How can biphasic DES systems couple biomass pretreatment and selective multiproduct recovery within a single intensified process?
- What is the economic feasibility and environmental impact of a biphasic DES-based brown seaweed biorefinery?

To address these research questions, this thesis is structured into several chapters. In **Chapter 2**, a range of DES were computationally screened to evaluate their interactions, affinity, and selectivity toward alginate. Based on these results, a subset of promising DES was selected in **Chapter 3** for experimental alginate extraction from brown seaweed, followed by optimisation of extraction conditions using response surface methodology. As alginate recovery from DES was not addressed in **Chapter 3**, **Chapters 4–8** focus on the development and evaluation of different strategies for alginate recovery, DES regeneration, and solvent recycling.

In **Chapter 4**, the recovery of alginate and DES was investigated using pressure-driven membrane separation as a proof-of-concept for full membrane-based separation. A model mixture consisting of alginate dissolved in DES was employed to evaluate technical feasibility and solvent recovery under controlled conditions. While the approach demonstrated the potential of membrane-based DES recovery, the use of a model system does not fully capture the complexity of real seaweed extracts, where additional components may influence separation performance, and process stability. Moreover, membrane processes remain associated with limitations such as high-water demand, and operational complexity. Therefore, alternative phase-based recovery strategies including three-phase partitioning, aqueous two-phase systems and temperature-responsive DES systems, were investigated in the subsequent chapters to enable integrated product separation and solvent recycling.

As an alternative approach, **Chapter 5** explores three-phase partitioning (TPP) using a hydrophobic DES for the simultaneous extraction of alginate and pigments from seaweed. In this system, the DES functioned both as a pretreatment medium for alginate and as an extraction solvent for pigments, while its hydrophobic nature facilitated recovery and reuse. Although effective, this approach requires dialysis for alginate recovery from the salt-rich aqueous phase, and fucoxanthin was not recovered from the DES phase.

In **Chapter 6**, a thermo-separating aqueous two-phase system (ATPS) was developed for the continuous and cyclic extraction and separation of alginate, employing a temperature-responsive copolymer (EOPO) for product recovery. This system enables successful recovery and recycling of both DES and EOPO. However, its complexity, arising from the integration of multiple phase systems and recycling streams, motivated the exploration of alternative approaches.

Accordingly, **Chapter 7** evaluates temperature-responsive deep eutectic solvents (TRDES) for continuous alginate extraction and recovery. Although DES recycling was achieved, the requirement for potentially toxic components to induce temperature responsiveness, along with the need for downstream dialysis of the aqueous alginate phase, limits the overall sustainability of this approach.

Building on the strengths of previous systems developed **Chapter 5** and **Chapter 6**, **Chapter 8** presents a DES-based aqueous two-phase system that integrates the precipitation principle of three-phase partitioning. This approach enables direct alginate isolation through precipitation, while maintaining solvent recyclability, thereby simplifying downstream processing.

Subsequently, **Chapter 9** investigates a DES-based biphasic system (FABU) for one-pot multiproduct extraction, thereby enhancing product properties of alginate while extracting pigments simultaneously.

To evaluate the feasibility of this approach, **Chapter 10** presents a techno-economic assessment (TEA) and life cycle assessment (LCA) of the biphasic DES-based biorefinery system, assessing its economic feasibility and environmental performance.

Finally, **Chapter 11** reflects on the major findings of the thesis, discusses limitations, and presents an outlook and recommendations for further DES-based bioprocessing and research.

Figure 1.7 provides a schematic overview of the chapters included in this thesis.

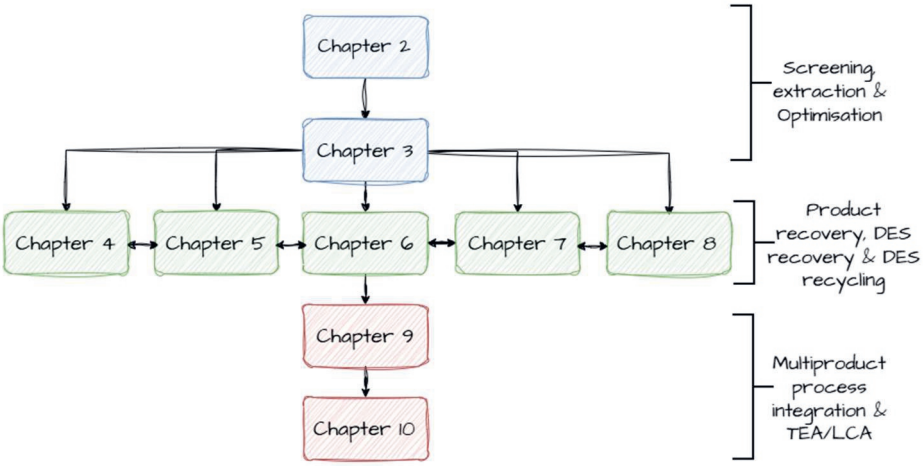
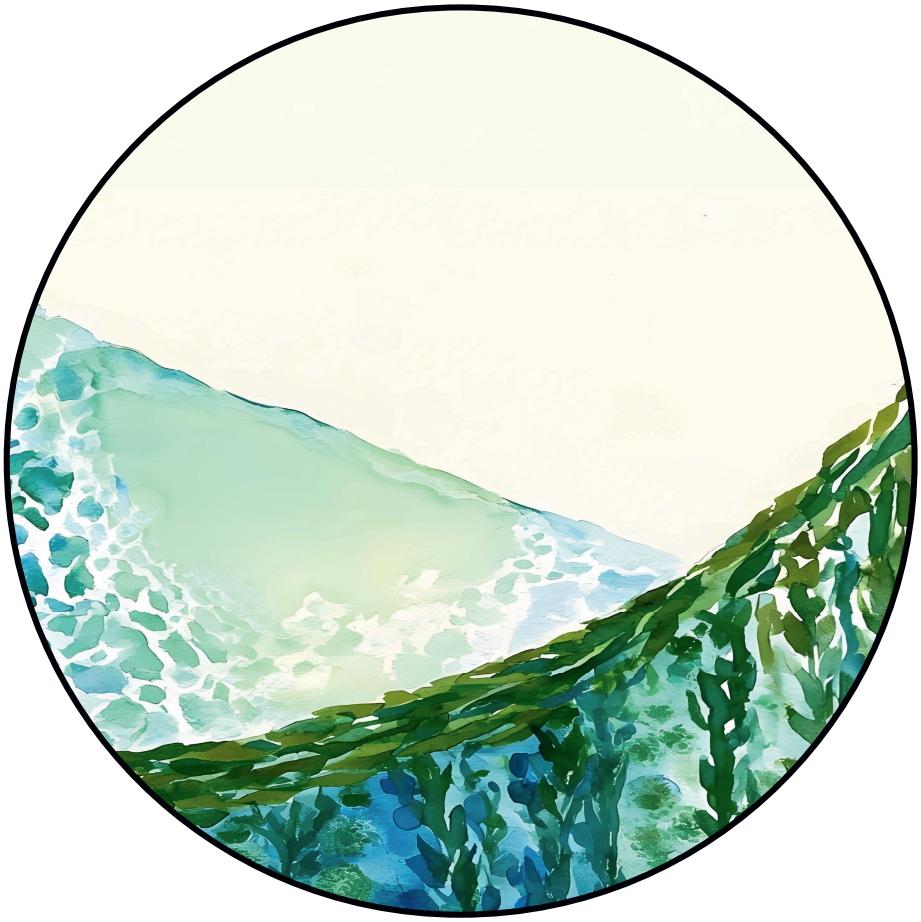


Figure 1.7 Overview of the thesis structure. Chapters 2 and 3 (blue boxes) focus on DES screening, alginate extraction, and process optimisation. Chapters 4–8 (green boxes) address product recovery, DES regeneration, and solvent recycling strategies. Chapters 9 and 10 focus on multiproduct process integration and the evaluation of techno-economic feasibility and environmental performance through TEA and LCA.



Chapter 2

Towards selective alginate solvation: A capacity–selectivity analysis of deep eutectic solvents

Isa S.A. Hiemstra, Michel H.M. Eppink, Rene H. Wijffels, Antoinette Kazbar

Manuscript is in preparation for submission

Abstract

Rational design of deep eutectic solvents (DES) for extraction of bioactives remains limited by the lack of selective screening strategies, capable of discriminating between structurally related compounds. In this work, a computational framework was developed to enable selective DES screening for alginate solvation in the presence of other polysaccharides laminarin and fucoidan. A total of 115 DES were evaluated using COSMO-RS (Conductor-like Screening Model for Real Solvents) to predict relative thermodynamic affinity, solubilisation capacity, and selectivity, allowing quantitative comparison of solvent–polysaccharide interactions. The effects of hydrogen bond acceptor (HBA) and hydrogen bond donor (HBD) identity, and HBA:HBD molar ratio were systematically assessed to elucidate how solvent composition governs electrostatic and hydrogen-bonding interactions with the target polymer. The results demonstrate that structurally similar polysaccharides exhibit sufficiently distinct interaction profiles to permit computational discrimination. The combined evaluation of capacity and selectivity enabled comparative ranking of DES systems according to predicted preferential affinity toward alginate. A performance index integrating both metrics was established to rank DES according to defined solvation objectives. The analysis further demonstrated that hydrogen-bonding characteristics, polarity, and HBA:HBD ratio collectively govern the balance between solubilisation strength and selectivity. Overall, this study presents a computational screening framework for evaluating DES–polysaccharide interactions and identifying promising solvent systems for selective alginate solvation. The proposed methodology may support future experimental studies aimed at selective and sustainable extraction processes.

2.1. Introduction

The search for alternative extraction solvents has gained significant attention due to environmental and safety concerns associated with conventional organic solvents. Deep eutectic solvents (DES) have emerged as a promising green alternative, offering advantages such as low toxicity, biodegradability, and tuneable physicochemical properties [87]. Deep eutectic solvents (DES) are formed by combining one or more hydrogen bond acceptors (HBA) with one or more hydrogen bond donors (HBD). When mixed in a specific molar ratio, these components interact through hydrogen bonding, resulting in a significant depression of the melting point, leading to the formation of a stable liquid mixture [9, 10].

DES have been successfully applied in the extraction of bioactive compounds from seaweed [88], which is a rich and renewable source of diverse polysaccharides. Brown seaweeds, in particular, contain alginate, fucoidan, and laminarin (**Figure S2.1**, **Figure S2.2**). Among these, alginate is of special interest due to its gelling ability, biocompatibility, and wide-ranging applications in the food, pharmaceutical, and biomedical industries [89]. Alginate consists of linear copolymers of β-D-mannuronic acid (M) and α-L-guluronic acid (G) residues arranged in homopolymeric and heteropolymeric block structures (**Figure S2.1**). For many of its applications, especially in food and biomedical fields, high purity is essential, as residual polysaccharides including fucoidan and laminarin (**Figure S2.2**), can affect its physicochemical properties and performance. Therefore, in addition to achieving high extraction yields, the development of effective separation and purification strategies is crucial when applying DES-based processes for alginate recovery.

However, the large chemical space of possible DES combinations makes the experimental identification of suitable solvents time-consuming and costly. In liquid–liquid extraction processes, the distribution of a solute between two phases is governed by differences in chemical potential, which determine the solute's affinity for each phase [90]. This affinity is commonly expressed through thermodynamic parameters such as the activity coefficient (γ), which reflects the strength of solute–solvent interactions. A low activity coefficient indicates favourable interactions and thus a higher tendency of the solute to dissolve in that solvent phase. From these parameters, distribution coefficients, selectivity, and solvent capacity can be derived, which are key performance indicators in extraction processes.

Experimentally determining these thermodynamic properties for many potential DES combinations would require extensive laboratory work. Therefore, computational

screening approaches are increasingly employed to efficiently narrow down promising candidates prior to experimental validation [32, 66]. The Conductor-like Screening Model for Real Solvents (COSMO-RS) is a quantum-chemical model widely used to predict thermodynamic properties of fluids and mixtures. By calculating the molecular surface charge density and deriving the chemical potential of species in solution, COSMO-RS enables the estimation of activity coefficients and, consequently, solute–solvent affinities [67, 91]. In the context of alginate extraction, COSMO-RS can thus be applied to screen DES systems based on their predicted affinity toward alginate, accelerating the identification of effective and sustainable solvent systems while reducing experimental effort. More broadly, this computational screening strategy can be extended to other bioactive compounds, providing a general framework for rational solvent selection in DES-based extraction processes.

Despite these advances, DES screening strategies have predominantly emphasised extraction capacity or affinity for a single target compound, often without explicitly considering solvent selectivity in complex biomass matrices [92, 93]. In the case of brown seaweed, screening DES solely for alginate solubilisation therefore carries a potential of co-extracting structurally related polysaccharides such as fucoidan and laminarin (**Figure S2.2**), which can compromise the purity of the alginate fraction. While COSMO-RS and related screening approaches have primarily been applied to identify solvents with strong affinity or solubilisation capacity for a single component, selective screening strategies that discriminate between structurally related polysaccharides present in the same biomass remain comparatively underexplored. As a result, identifying DES formulations that preferentially solubilise alginate while minimising interactions with laminarin and fucoidan remains a bottleneck.

Addressing this challenge requires computational screening strategies that move beyond solubility or affinity alone and incorporate comparative selectivity analysis. By evaluating relative interactions between DES systems and multiple polysaccharides, COSMO-RS may be used to identify solvent systems with predicted preferential affinities toward alginate relative to laminarin and fucoidan. Such comparative screening can provide insight into how DES composition influences thermodynamic interaction trends between structurally related polysaccharides. More broadly, this type of computational pre-screening approach may support future experimental studies aimed at selective solvent development for biomass fractionation.

Therefore, this study aimed to investigate whether COSMO-RS-based computational screening could be used to comparatively evaluate DES–polysaccharide interactions relevant to alginate solvation. A total of 115 DES systems were assessed in terms of

predicted capacity and selectivity toward alginate relative to laminarin and fucoidan, with particular attention to the influence of HBA identity, HBD identity, and HBA:HBD molar ratio. In addition, a performance index integrating both capacity and selectivity was applied to comparatively rank DES systems according to predicted interaction behaviour. The study further examines how solvent composition influences the balance between solubilisation strength and selectivity, thereby providing insight into DES structure–property relationships relevant to polysaccharide solvation.

Overall, this study investigates the use of computational screening to comparatively evaluate DES–polysaccharide interactions relevant to alginate solvation. The present work focuses on relative thermodynamic interaction trends at infinite dilution and does not aim to directly predict full extraction performance from complex biomass systems. Nevertheless, the framework provides insight into DES structure–property relationships governing predicted capacity and selectivity and may support future experimental studies aimed at solvent screening and biomass fractionation.

2.2. Methodology

Alginate, fucoidan, and laminarin were selected for this study, as they represent the major polysaccharides found in brown seaweed. For the computational screening, 12 HBAs and 53 HBDs were selected. In total, 115 DES systems were evaluated to comparatively assess predicted capacity and selectivity toward alginate relative to laminarin and fucoidan. Only DES systems previously reported in literature as liquid and stable at the specified molar ratios were included in the screening. The selected HBAs and HBDs are presented in **Table S2.1**.

2.2.1 COSMO-RS

COSMO-RS calculations were performed using COSMO-RS implementation within the Amsterdam Modelling Suite (version 2022.103, Software for Chemistry and Materials BV (SCM), Amsterdam, The Netherlands) was utilised within the Amsterdam Density Functional (ADF) package for the computational analyses. Molecular geometries of the polysaccharide fragments and DES constituents were geometry-optimised using the universal force field (UFF), followed by quantum chemical calculations using the GGA:BP86 density functional and TZP basis set. The σ-profile, which represents the surface charge density distribution of a molecule, was used to comparatively analyse intermolecular interaction tendencies in different DES systems.

2.2.2 DES capacity and selectivity calculations

The extractive efficiency of a solvent is primarily governed by two main parameters: selectivity and capacity at infinite dilution. These parameters can be calculated with the activity coefficient. The activity coefficient describes the interaction between a solute and solvent at an infinitesimal concentration of the solute and can be calculated using the chemical potential (**Equation 2.1**):

$$\gamma_i^S = \exp\left\{\frac{\mu_i^S - \mu_i^i}{RT}\right\} \qquad (\mathbf{2.1})$$

where γ_i^S is the activity coefficient of compound i in phase S, μ_i^S is the chemical potential of compound i in phase S, μ_i^i is the chemical potential of compound i in in an ideal state (reference state), R is the molar gas constant and T is the absolute temperature. Lower γ values correspond to stronger solute–solvent interactions and thus a higher thermodynamic affinity of the solute for the respective phase.

Within COSMO-RS, the activity coefficient at infinite dilution for alginate (γ_A^∞), fucoidan (γ_F^∞) and laminarin (γ_L^∞) was calculated for each selected DES. However, COSMO-RS

cannot directly calculate the activity coefficient of polymers, since these quantum chemical calculations would require large, expensive and time-consuming computer resources [94]. Therefore, the studied polymers were represented using a fragment-based trimer approach in which the σ-profile of a representative monomer unit is calculated and subsequently scaled to approximate the behaviour of the full polymer, thereby avoiding computationally demanding calculations on the entire macromolecule, as has been described previously [95].This fragment-based modelling approach has been previously applied for computational studies of polymeric systems [94, 96]. This approximation assumes that relative solvent affinity trends are primarily governed by repeating-unit chemistry rather than full polymer chain architecture. Consequently, the calculated activity coefficients should be interpreted as comparative indicators of relative thermodynamic interaction tendencies rather than quantitative predictors of absolute polymer solubility or extraction performance.

The activity coefficient was calculated according to the molar ratio composition of their constituents [93]. Different combinations of HBAs and HBDs were selected, and the molecular ratios were altered to assess the effect on the activity coefficient and subsequently the capacity and selectivity. With the activity coefficient, the capacity and selectivity for each DES could be calculated. The capacity indicates the maximum solubility in the DES [93]. Accordingly, a higher capacity corresponds to a lower activity coefficient and indicates a higher predicted maximum solubility of the solute in the respective DES. The capacity towards alginate for each solvent was calculated as the inverse of the activity coefficient at infinite dilution of alginate (**Equation 2.2**):

$$C_A^{\infty} = \frac{1}{\gamma_A^{\infty}} \qquad (\mathbf{2.2})$$

The selectivity parameter quantifies the preferential solvation of alginate by a DES and is defined as the ratio between the activity coefficient of alginate and that of either fucoidan or laminarin, with higher values indicating greater discrimination in favour of alginate. The selectivity of each DES towards alginate compared to fucoidan, was calculated with the activity coefficients (**Equation 2.3**):

$$S_{A-F}^{\infty} = \frac{\gamma_F^{\infty}}{\gamma_A^{\infty}} \qquad (\mathbf{2.3})$$

Similarly, the selectivity towards alginate compared to laminarin was calculated as (**Equation 2.4**):

$$S_{A-L}^{\infty} = \frac{\gamma_L^{\infty}}{\gamma_A^{\infty}} \quad \textbf{(2.4)}$$

where γ_i^{∞}represents the activity coefficient of compound *i* at infinite dilution. Since lower activity coefficients correspond to stronger solute–solvent interactions, selectivity values greater than unity (S > 1) indicate a preferential affinity of the DES for alginate over the competing polysaccharide. Increasing selectivity values therefore reflect stronger discrimination in favour of alginate, whereas S ≈ 1 suggests limited differentiation between the compounds.

The total combined selectivity score for a DES towards alginate compared to fucoidan and laminarin was calculated using both selectivity values (**Equation 2.5**):

$$S_{total}^{\infty} = (S_{A-F}^{\infty} + S_{A-L}^{\infty})/2 \quad \textbf{(2.5)}$$

This parameter represents the overall discrimination of a DES for alginate relative to both fucoidan and laminarin. Since selectivity values greater than unity indicate preferential interactions with alginate, higher S_{total}^{∞}values correspond to stronger overall selectivity toward alginate. DES with larger combined selectivity scores were therefore considered more promising candidates for selective alginate extraction.

2.2.3 Performance index calculations

The overall performance of each DES was evaluated using a Performance Index (P.I.), defined as a weighted combination of the total selectivity and the alginate capacity (**Equation 2.6**):

$$Performance\ Index\ (P.I.) = 0.25\, S_{total}^{\infty} + 0.75 C_A^{\infty} \quad \textbf{(2.6)}$$

where S_{total}^{∞}represents the combined selectivity toward alginate and C_A^{∞}denotes the capacity for alginate. A larger weighting factor was assigned to the capacity term, as strong alginate solvation was considered more critical for effective extraction performance than selectivity alone. In general, solvents with high selectivity tend to have a low capacity for target molecules due to strong but limited interactions, and vice versa [93]. Selecting a solvent based solely on its ability to interact effectively, rather than on its efficiency per volume, is not economically viable. Therefore, a solvent combining both high capacity and high selectivity is essential to minimise solvent usage while maximising targeted extraction [97]. Ideally, DES with both high capacity and high selectivity are needed for extraction. The weighting factors were chosen to

assign greater importance to capacity than to selectivity. Higher P.I. values indicate DES systems with a more favourable balance between alginate solubility and preferential selectivity over competing polysaccharides. DES with the highest P.I. values were therefore considered the most promising candidates for experimental validation.

2.2.4 Polarity

The overall performance of each DES was evaluated using a Performance Index (P.I.), defined as a weighted combination of the total selectivity and the alginate capacity (**Equation 2.7**):

$$Performance\ Index\ (P.I.) = 0.25\, S_{total}^{\infty} + 0.75 C_A^{\infty} \quad (\mathbf{2.7})$$

where S_{total}^{∞}represents the combined selectivity toward alginate and C_A^{∞}denotes the capacity for alginate. A larger weighting factor was assigned to the capacity term, as strong alginate solvation was considered more critical for effective extraction performance than selectivity alone. In general, solvents with high selectivity tend to have a low capacity for target molecules due to strong but limited interactions, and vice versa [93]. Selecting a solvent based solely on its ability to interact effectively, rather than on its efficiency per volume, is not economically viable. Therefore, a solvent combining both high capacity and high selectivity is essential to minimise solvent usage while maximising targeted extraction [97]. Ideally, DES with both high capacity and high selectivity are needed for extraction. The weighting factors were chosen to assign greater importance to capacity than to selectivity. Higher P.I. values indicate DES systems with a more favourable balance between alginate solubility and preferential selectivity over competing polysaccharides. DES with the highest P.I. values were therefore considered the most promising candidates for experimental validation.

2.3. Results and discussion

2.3.1 σ-profile analysis of polysaccharides

Alginate, fucoidan and laminarin were analysed using their σ-profile, which illustrates the charge density distribution across the molecular surface. Within this profile, regions with charge densities below -0.085 e/Å^2 correspond to hydrogen bond donors, whereas areas exceeding +0.085 e/Å^2 indicate hydrogen bond acceptors [98]. Surfaces with charge densities ranging from -0.085 to +0.085 e/Å^2 are considered too non-polar to participate in hydrogen bonding.

The σ-profiles and σ-potentials can be used to predict the chemical nature of the polysaccharides, including the polarity and hydrogen-bonding. This, in turn, can be used to guide solvent selection by identifying molecular polarity and interaction patterns, enabling comparative evaluation of solute-solvent compatibility [99]. The σ-profiles of the polysaccharides show that each compound has surface charge densities distributed across both polar and non-polar regions (**Figure 2.1**), indicating that hydrogen bonding, Van der Waals forces, and hydrophobic interactions likely contribute to their extraction behaviour [97].

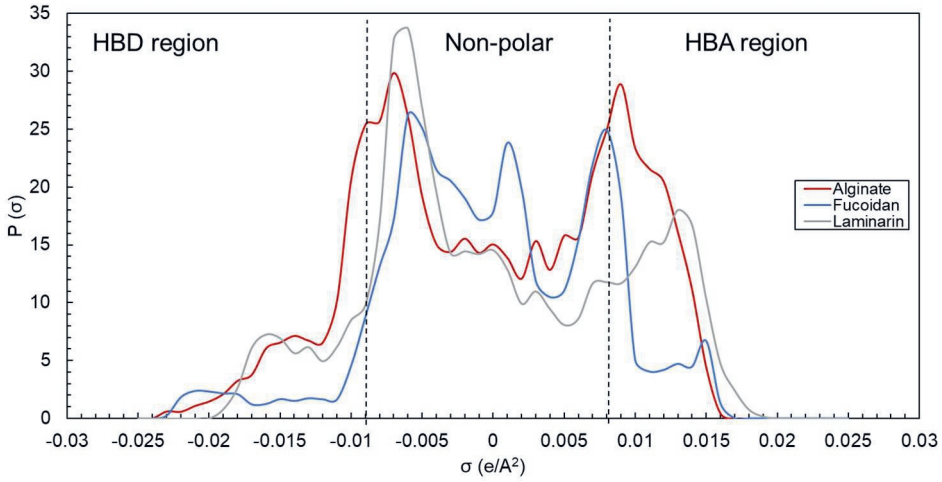


Figure 2.1 σ-profiles of alginate (red), fucoidan (blue) and laminarin (grey).

For alginate, two main polar peaks (-0.007 and 0.009 e/A^2) are observed in the hydrogen bond acceptor and donor regions (**Figure 2.1**). The polar peaks are associated with the presence of hydroxyl groups in D-mannuronic acid and L-guluronic acid, which arise due to the electronegativity difference between oxygen and hydrogen. Conversely, the non-polar regions correspond to neutrally charged areas containing C-H bonds. These findings indicate that alginate may exhibit favourable interactions with solvents

possessing both hydrogen bond donor (HBD) and hydrogen bond acceptor (HBA) functionalities [100].

The σ-profiles of fucoidan and laminarin showed differences in their interaction potentials. Fucoidan exhibited three major peaks (-0.006, 0.001 and 0.008 e/A^2) in the non-polar region coming from fucoidan's backbone and alkyl groups, together with a small, lower-intensity peak in the HBA region, possibly from sulphate or carboxyl groups and a broad, low-intensity peak in the HBD region, likely from the hydroxyl groups (**Figure 2.1**). This indicates that fucoidan is largely dominated by hydrophobic surface areas, with only limited hydrogen-bonding capacity. In contrast, laminarin displayed one high-intensity peak in the non-polar region, coming from the hydrophobic surface areas of the backbone of laminarin, a medium-sized peak in the HBA region, probably coming from oxygen atoms in hydroxyl groups and glycosidic linkages, and a small peak in the HBD region due to hydroxyl groups present (**Figure 2.1**). Compared to fucoidan, laminarin therefore shows a more pronounced hydrogen bond acceptor character, which may facilitate stronger interactions with hydrogen bond donor solvents as well as non-polar interactions.

Overall, although all three polysaccharides exhibit both polar and non-polar surface regions, clear differences are observed in their σ-profile distributions. Alginate shows more pronounced hydrogen bond donor and acceptor peaks, indicating a stronger polar interaction capacity, whereas fucoidan is predominantly non-polar and laminarin exhibits a more moderate hydrogen bond acceptor character. These differences indicate that alginate possesses a sufficiently distinct interaction profile compared to the other two polysaccharides, suggesting that computational discrimination based on relative intermolecular interaction tendencies may be feasible. Based on this molecular differentiation, further comparative analysis screening through capacity and selectivity calculations can be conducted (**Section 2.3.2**). It should be noted that σ-profile analysis reflects relative intermolecular interaction tendencies and does not fully capture the effects of polymer molecular weight, conformational flexibility, or biomass matrix interactions on experimental extraction behaviour.

2.3.2 Structure-property relationships

2.3.2.1 DES affinity towards alginate

The capacity of 115 DES combinations towards alginate was assessed via COSMO-RS (**Table S2.1**). The five DESs with the highest capacities were ChCl:Thiourea (4828), Bet:1,4-Butanediol (3287), ChCl:1,2-Butanediol (2135), ChCl:Isosorbide (1902) and ChCl:Methyldiethanolamine (1546) (**Table S2.1**).

The high predicted affinity of ChCl:Thiourea, Bet:1,4-butanediol, ChCl:1,2-butanediol, ChCl:Isosorbide, and ChCl:Methyldiethanolamine towards alginate may be attributed to their ability to establish multiple stabilising interactions with the polymer. In DES–polysaccharide systems, such interactions have been identified as the main drivers of solvation behaviour, where DES components effectively compete with intramolecular polysaccharide hydrogen bonds and promote polymer dissolution [101, 102]. These DESs contain hydrogen bond donors (HBDs) rich in hydroxyl (-OH) or amine (-NH) groups (**Table S2.2**), which facilitate extensive hydrogen-bonding networks with the hydroxyl and carboxylate functionalities of alginate (**Figure S2.1**). ChCl:Thiourea exhibited the highest affinity for alginate, likely due to the complementary roles of its components. Thiourea contributes versatile hydrogen-bonding interactions, acting as a donor through its –NH groups and as an acceptor via its C=S moiety (**Table S2.2**), while the choline cation can engage in electrostatic interactions with alginate's negatively charged carboxylate groups**.** Importantly, unlike acidic DES systems, these components are less likely to promote protonation of alginate's carboxylate groups, thereby preserving its polyanionic character and solubility. Previous studies have shown that the dissolution of polysaccharides such as cellulose increases with DES basicity, indicating that stronger hydrogen-bond-accepting components enhance disruption of intermolecular hydrogen-bond networks [101]. Although alginate differs structurally due to its polyanionic nature, a similar mechanism may contribute to the enhanced predicted affinity observed for amine-based DESs in this study.

2.3.2.2 Effect of HBD

The effect of the HBD on the capacity and selectivity of the 115 DESs towards alginate was evaluated using COSMO-RS. The choice of HBD clearly influenced the predicted solvent capacity (**Figure 2.2**). DESs containing polyol- and amine-based HBDs exhibited high affinities towards alginate, whereas acid-based HBDs resulted in consistently lower capacities for both ChCl and Bet as HBAs. As discussed previously (**Section 2.3.2.1**), polyol- and amine-containing HBDs provide multiple hydroxyl or amine functionalities that promote extensive hydrogen-bonding interactions with the hydroxyl and carboxylate groups of alginate. This trend is consistent with previous studies [62, 63], which reported increased dissolution and extraction behaviour using polyol-based DESs such as ethylene glycol and 1,2-propanediol, attributed to their high hydroxyl density and strong hydrogen-bonding capability. However, since these studies did not target specific polysaccharides, the reported improvements may reflect a combination of increased overall solubilisation and altered selectivity, underscoring

the importance of distinguishing between extraction efficiency and selective extraction behaviour.

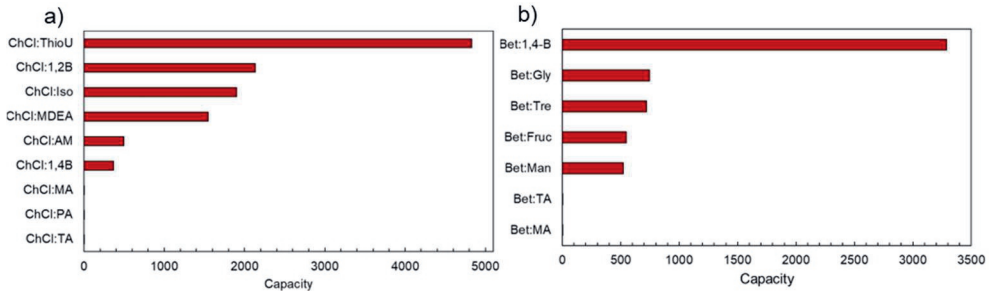


Figure 2.2 Effect of the HBD on the solubility capacity for (a) choline chloride as HBA and (b) Betaine as HBA.

The capacity results indicate that acidic DESs are not suitable for alginate extraction (**Figure 2.2, Table S2.1**). This behaviour can be attributed to protonation of alginate's carboxylate groups under acidic conditions, which neutralises its negative charge and weakens electrostatic interactions with cationic HBAs, thereby reducing solubility and interaction strength [103]. Nevertheless, literature reports that carboxylic acid-based HBDs can effectively interact with hydroxyl-containing polysaccharides and have been successfully applied in pectin extraction and biomass pretreatment processes [103–105]. This suggests that although acidic DESs are unfavourable for direct alginate solubilisation, they may be valuable as pretreatment agents capable of disrupting structural polysaccharide networks and enhancing accessibility for subsequent extraction steps.

When assessing the effect of different HBDs on the selectivity of ChCl-based DESs towards alginate, ChCl:Menthol (ChCl:Men) exhibited the highest predicted selectivity (**Figure 2.3**). In contrast to the capacity screening, where other DESs showed superior performance, this highlights that selectivity and capacity are governed by different interaction mechanisms and must be evaluated independently. The performance of ChCl:Menthol could be attributed to its relatively low polarity [106] and limited hydrogen-bonding capacity compared with more hydrophilic DESs such as ChCl:Thiourea (**Table S2.1**). The reduced polarity of ChCl:Menthol disfavours the solvation of highly charged polysaccharides such as fucoidan, whose extensive sulphate groups require a strongly polar environment for stabilisation. Similarly, laminarin, being neutral and structurally compact with fewer accessible hydroxyl groups, forms limited specific interactions with the solvent. Alginate, which possesses both carboxylate and hydroxyl functionalities and exhibits intermediate polarity among the studied polysaccharides, can still establish sufficient hydrogen bonding with

menthol's hydroxyl group and electrostatic interactions with the choline cation. As a result, although ChCl:Menthol does not maximise overall predicted capacity, it may preferentially stabilise alginate relative to the other polysaccharides.

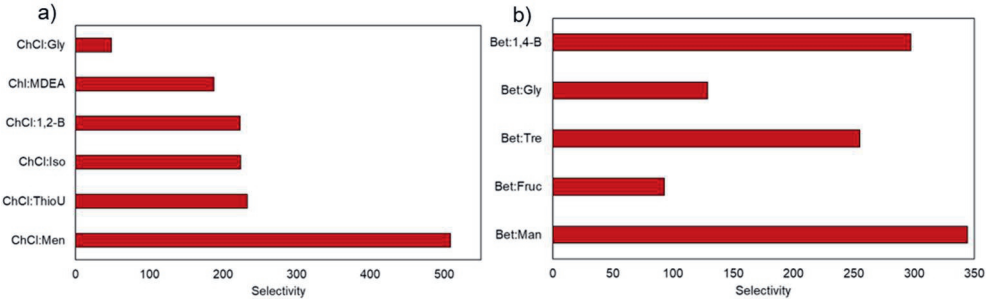


Figure 2.3 Effect of the HBD on the selectivity for (a) choline chloride as HBA and (b) Betaine as HBA.

In contrast, ChCl:Thiourea forms multiple strong hydrogen bonds with all three polysaccharides, leading to high overall solubilisation but reduced discrimination between them. Therefore, the enhanced selectivity of ChCl:Menthol arises from its lower polarity and limited hydrogen-bonding network, which accentuates differences in charge density and hydrophilicity between the polysaccharides.

For the betaine-based DESs, Betaine:mannose (Bet:Man) exhibited the highest selectivity for alginate, followed by betaine:1,4-butanediol (Bet:1,4-B). While diol- and polyol-based HBDs generally demonstrated favourable selectivity, notable differences were observed among them (**Figure 2.3, Table S2.1**). Mannose possesses a relatively rigid pyranose structure, which results in a well-defined spatial distribution of hydroxyl groups [107]. This structural rigidity may promote more cooperative and consistent hydrogen-bonding interactions with alginate's regularly distributed carboxylate and hydroxyl functionalities. In contrast, fructose can adopt multiple cyclic and conformational forms [108], leading to a more variable hydroxyl arrangement that may reduce interaction specificity and facilitate interactions with competing polysaccharides such as fucoidan and laminarin.

These observations suggest that, beyond hydroxyl group density, the rigidity and spatial organisation of HBD functional groups can influence selectivity in betaine-based DESs, likely by affecting the balance between specific and non-specific hydrogen-bonding interactions.

2.3.2.3 Effect of HBA

The type of HBA strongly influenced the predicted capacity of the DES towards alginate (**Figure 2.4**). When glycerol or lactic acid was used as HBD, the highest capacities were obtained with betaine as HBA (748 and 3.7 for Bet:Gly and Bet:LA, respectively). In contrast, lower capacities were observed for DESs containing TEA (tetraethylammonium chloride) or TBAC (tetrabutylammonium chloride) as HBA.

The reduced capacity of TEA- and TBAC-based systems may be related to their higher logP values (4.84 and 5.31, respectively) compared to the other HBAs (**Table S2.1**), indicating a more hydrophobic character that limits favourable interactions with the polyanionic alginate. These findings suggest that HBA polarity and ionic character play a critical role in promoting complementary electrostatic and hydrogen-bonding interactions.

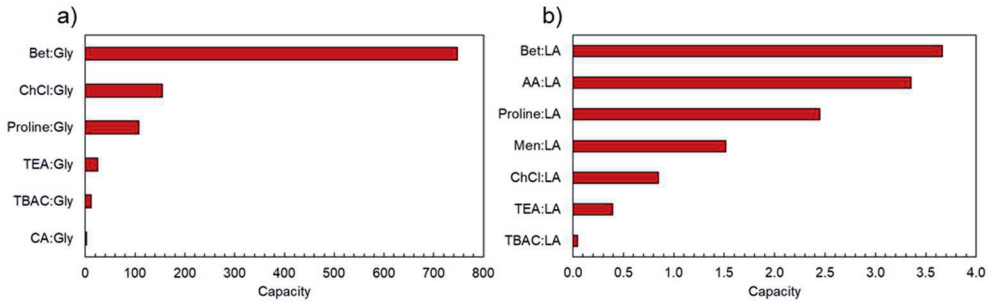


Figure 2.4 Effect of the HBA on the solubility capacity for (a) glycerol as HBD and (b) lactic acid as HBD.

As shown in **Figure 2.4**, the choice of HBA substantially influences the predicted solubility capacity of a DES, even when the HBD is fixed. This indicates that, beyond hydrogen-bond donation from the HBD, the polarity and ionic character of the HBA play a decisive role in governing interactions with the polyanionic alginate. In particular, HBAs with lower hydrophobicity and stronger charge complementarity appear to promote more favourable interactions. These findings are consistent with literature highlighting the importance of complementary solvent–polymer interactions in polysaccharide dissolution [101, 109].

Interestingly, different trends were observed for solvent selectivity (**Figure 2.5**). Among DESs containing glycerol as HBD, TEA:glycerol exhibited the highest selectivity (237), which may be attributed to strong electrostatic interactions between the cationic tetraethylammonium ion and the negatively charged carboxylate groups of alginate [110]**.** These interactions likely promote preferential stabilisation of alginate relative to competing polysaccharides with different functional group chemistry. In contrast,

betaine is a zwitterionic HBA containing both a quaternary ammonium and a carboxylate group [111]. While this dual functionality enhances overall hydrogen-bonding capacity and improves general solubilisation, it may reduce electrostatic specificity, resulting in lower selectivity compared to TEA-based DESs. For DESs containing lactic acid as HBD, consistently low selectivities were obtained (0.40–2.60), suggesting that the acidic character of the HBD may dominate the interaction behaviour and limit the influence of HBA variation on selectivity (**Figure 2.5**). Notably, these trends differ from the capacity results, where certain DES, for instance TEA-based, showed relatively low solubilisation capacity despite their high selectivity. This contrast demonstrates that capacity and selectivity are governed by distinct interaction mechanisms.

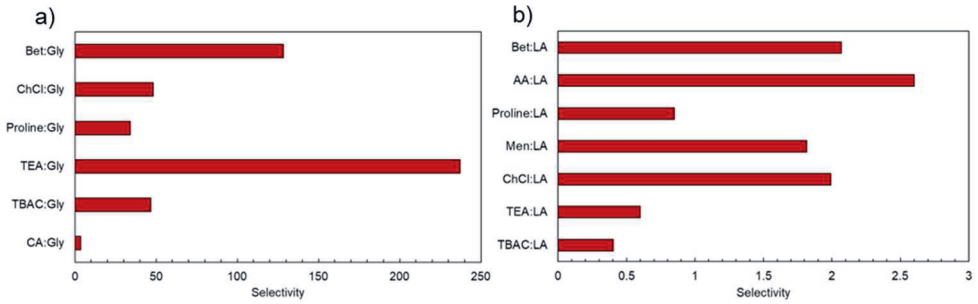


Figure 2.5 Effect of the HBA on the selectivity for (a) glycerol as HBD and (b) lactic acid as HBD.

While overall polarity and hydrogen-bonding ability enhance solubilisation, specific electrostatic complementarity between the HBA and alginate appears to drive preferential stabilisation. Therefore, tuning the HBA structure provides a means to steer solvent systems towards either higher solubility or greater specificity, depending on the targeted extraction objective.

2.3.3 Effect of HBA:HBD molar ratio

The effect of the HBA to HBD molar ratio on the capacity and selectivity of DES towards alginate was investigated. For the selected DES, the HBA:HBD ratios were varied across 4:1, 3:1, 2:1, 1:1, 1:2, 1:3, and 1:4 for both choline chloride- and betaine-based systems (**Figure 2.6**). Interestingly, varying the HBA:HBD ratio affected capacity and selectivity in opposite directions for the two HBAs (**Figure 2.6**). For ChCl-based DESs, decreasing the HBA:HBD ratio from 4:1 to 1:4 led to an increase in both capacity and selectivity (**Figure 2.6 a-b**), whereas for Bet-based DESs, the same change caused a decrease in these parameters (**Figure 2.6 c-d**).

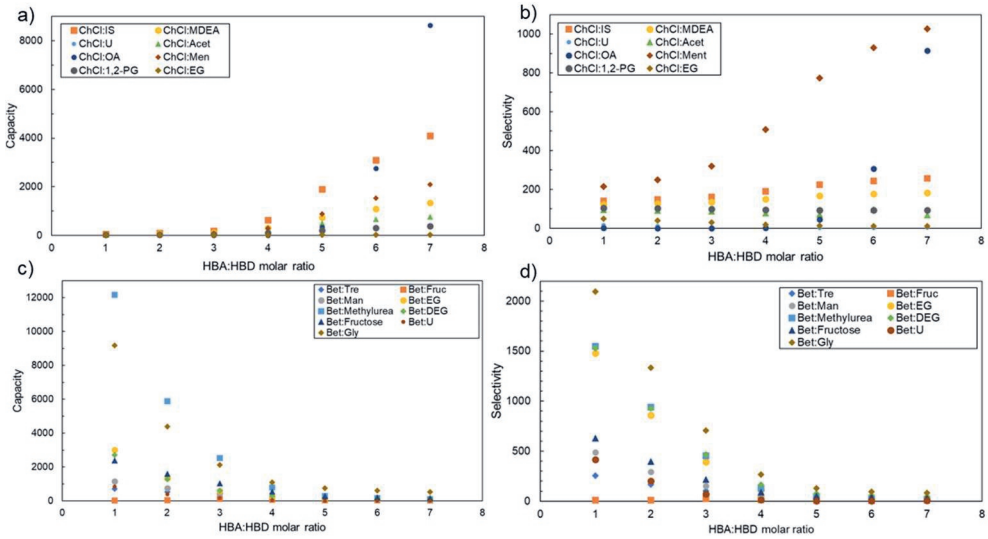


Figure 2.6 Effect of the HBA:HBD ratio for choline chloride-based DES on the (a) capacity and (b) selectivity, and the effect of the HBA:HBD ratio for betaine-based DES on the (c) capacity and (d) selectivity. HBA:HBD ratios of 4:1, 3:1, 2:1, 1:1, 1:2, 1:3 and 1:4 were assessed.

These opposing trends can be explained by the distinct hydrogen-bonding characteristics of the two HBAs. Choline chloride acts as a hydrogen-bond acceptor via the chloride ion, while the choline cation's hydroxyl group can also participate in hydrogen-bond donation [112]. Additionally, the cationic choline moiety provides electrostatic stabilisation of alginate's carboxylate groups. Increasing the HBD proportion therefore strengthens the hydrogen-bond network and enhances solvation capacity. Betaine, in contrast, is a zwitterionic species that functions primarily as a hydrogen-bond acceptor. Its carboxylate group forms strong interactions with hydrogen-bond donors, but excess HBD can oversaturate these acceptor sites, disrupting the optimal HBA–HBD balance. As demonstrated by Abranches *et al*. [113], betaine-based DESs exhibit unusually strong interactions between HBA and HBD within a narrow compositional window, and excess HBD destabilises the structured network. Consequently, decreasing the HBA:HBD ratio in betaine-based DESs weakens betaine–HBD interactions, reducing alginate solubilisation, whereas a higher betaine proportion favours ionic and hydrogen-bonding interactions with alginate's carboxylate groups.

These results demonstrate that the solubilisation and selectivity of DES are governed by the balance between hydrogen-bond donors and acceptors, and that the optimal HBA:HBD ratio depends on the HBA. This illustrates that both the choice of HBA and its ratio with the HBD must be considered in tandem to achieve selective solubilisation.

These insights establish guiding principles for DES composition, providing a foundation for systematic performance screening and the identification of optimal formulations in subsequent computational studies.

2.3.4 Performance index

The performance Index (P.I.) provides a metric to evaluate the combined performance based on the capacity and selectivity. PI values ranged from 0.05 for TBAC: Acetic acid to 3679 for DES ChCl:Thiourea (**Table S2.1**). The five DES with highest P.I. were ChCl:Thiourea, Bet:1,4-B, ChCl:1,2-B, ChCl:Iso and ChCl:MDEA**)**. These DESs were subsequently analysed in greater detail based on their predicted interaction behaviour toward alginate. Sensitivity analysis using alternative weighting factors produced comparable ranking trends (**Table S2.1**), indicating that the overall DES ranking was not strongly dependent on the selected weighting scheme.

The capacity–selectivity scatter plot (**Figure 2.7**) exhibited a diagonal arrangement of DESs, reflecting the interdependence between solubilisation capacity and selectivity towards alginate. DESs positioned in the lower-right region, including TEA:glycerol (selectivity of 238, capacity of 25), exhibits high selectivity but moderate capacity, indicating potential for high-purity alginate isolation, whereas DESs in the upper-right region, including ChCl:MDEA (selectivity of 187, capacity of 1546) achieves both high capacity and moderate selectivity, favouring maximal extraction yields. These observations suggest that solvent selection that solvent choice may be tailored according to the target outcome, depending on whether stronger predicted capacity or higher predicted selectivity is prioritised.

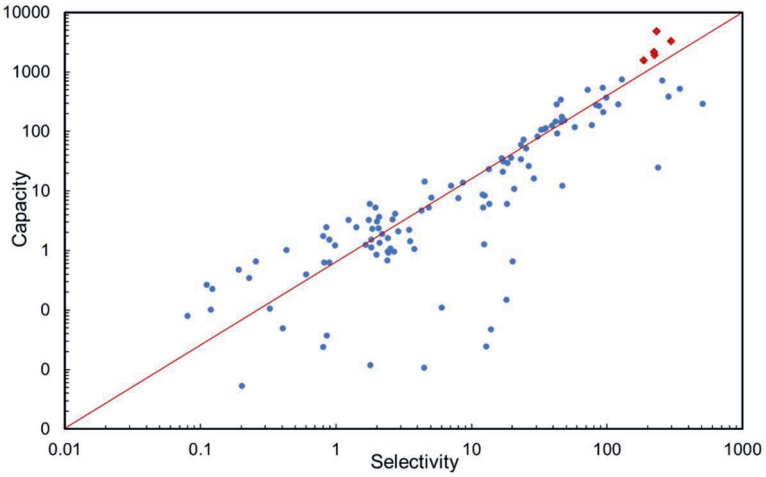


Figure 2.7 Selectivity versus the capacity for alginate of the 115 DES. Red diamonds indicate the 5 highest-ranked DES.

These results indicate that this computational screening approach provides a rapid and rational manner to identify promising DES candidates for alginate extraction. While experimental validation remains essential, the method substantially reduces the number of solvents to be tested. By calculating the activity coefficients from a variety of HBA and HBD combinations, the capacity and selectivity of each DES can be comparatively assessed, allowing solvent systems to be evaluated based on either stronger predicted solubilisation or higher predicted selectivity, as summarised in **Figure 2.8**. Importantly, this approach may also be applicable to other extraction processes and target compounds. Furthermore, it allows solvent selection to be tailored depending on whether stronger predicted solubilisation or selective intermolecular interactions are prioritised, thereby providing insight into DES structure–property relationships.

However, it should be noted that favourable thermodynamic predictions do not necessarily directly translate into high experimental extraction yields, as extraction performance is also influenced by factors such as biomass disruption efficiency, mass transfer limitations, solvent viscosity, and interactions with other biomass constituents. In addition, the fragment-based trimer approximation represents local intermolecular interactions rather than full polymer behaviour. Nevertheless, this approach provides valuable insight into solvent–solute interactions and serves as an effective pre-screening tool to narrow down suitable DES candidates prior to experimental evaluation.

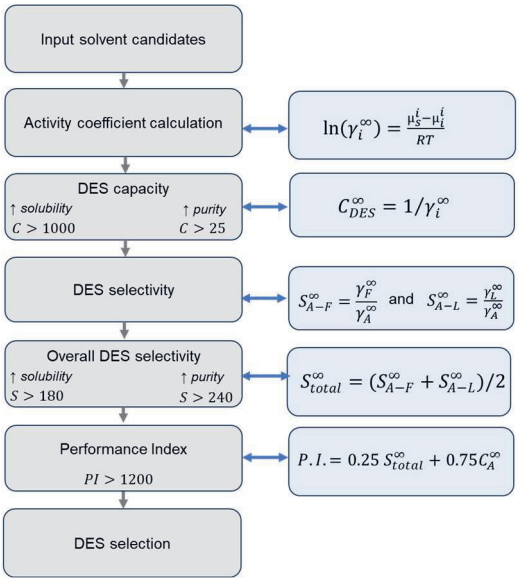


Figure 2.8 Process overview for selective DES design for alginate solubilisation.

2.4. Conclusion

This study demonstrated that computational screening can be used to comparatively evaluate DES–polysaccharide interaction trends for structurally related polysaccharides. Initial σ-profile analysis revealed distinct surface charge distributions among alginate, laminarin, and fucoidan, indicating differences in predicted intermolecular interaction behaviour between the polysaccharides. Systematic evaluation of hydrogen bond donor and acceptor identity, as well as HBA:HBD molar ratio, showed that solubilisation capacity and selectivity are governed by distinct yet interrelated interaction mechanisms. While overall polarity and hydrogen-bonding capacity primarily influence predicted solubilisation extent, electrostatic complementarity and functional group organisation may contribute to preferential stabilisation. Importantly, solvent composition and molar ratio must be considered in tandem, as their combined effects influence the balance between predicted selectivity and solvation strength. Integration of capacity and selectivity into a unified performance index enabled comparative solvent ranking based on predicted interaction behaviour.

Overall, this work presents a computational screening approach for evaluating DES–polysaccharide interactions and identifying promising solvent systems for alginate solvation. Although the present framework focuses on comparative thermodynamic interaction trends at infinite dilution, the approach may support future experimental solvent screening studies and provide insight into DES structure–property relationships relevant to biomass fractionation.

2.5. Supplementary information

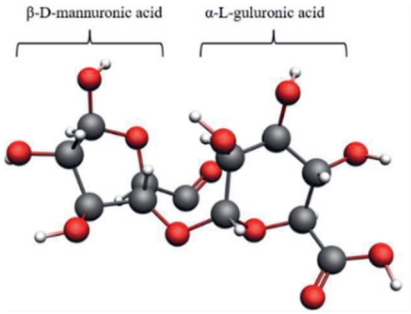


Figure S2.1 Chemical structure of part of alginate, represented by linked β-D-mannuronic acid and α-L-guluronic acid monomers.

The chemical structure of fucoidan is composed of α-L-fucopyranose residues linked by (1→3) or (1→4) or alternating (1→2) and (1→3) glycosidic bonds. It is branched featuring sulfation at C-2 or C-4 positions. Laminarin is composed of linear backbone of β(1→3)-D-glucopyranose units.

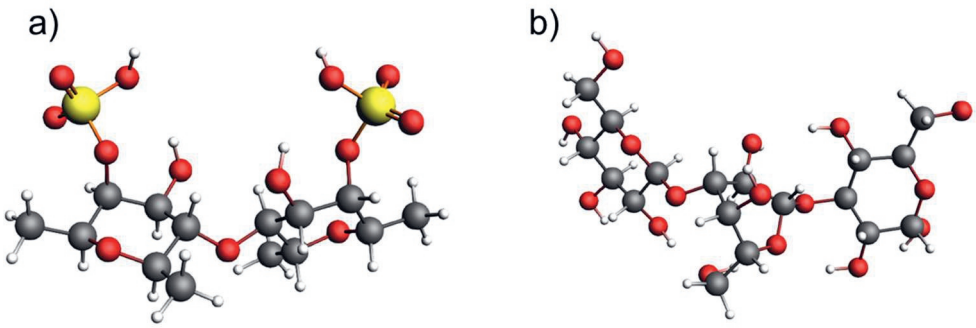


Figure S2.2 Chemical structures of (a) fucoidan and (b) laminarin.

Table S2.1 Selected DES used for activity coefficient calculations for alginate, fucoidan and laminarin.

				Activity coefficient			Capacity			LogP	P.I.
HBA	**HBD**	**Ratio**	**Ref**	**Alginate**	**Fucoidan**	**Laminarin**	**Alginate**	**Fucoidan**	**Laminarin**	**Alginate**	
ChCl	Ethylene glycol	1:2	(Gonzalez–Diaz & García–Núñez, 2023)	0.043	0.059	1.083	2.3×10^{1}	1.7×10^{1}	9.2×10^{-1}	0.352	2.1×10^{1}
ChCl	1,2-propylene glycol	1:2		0.005	0.009	0.866	2.1×10^{2}	1.1×10^{2}	1.2	0.871	1.8×10^{2}
ChCl	Lactic acid	1:1		1.177	0.191	4.505	8.5×10^{-1}	5.2	2.2×10^{-1}	1.320	1.1
ChCl	Lactic acid	1:2		0.811	0.351	1.241	1.2	2.8	8.1×10^{-1}	0.709	1.2
ChCl	Lactic acid	1:3		0.661	0.494	0.686	1.5	2.0	1.5	0.403	1.4
ChCl	Malic acid	1:3		0.405	1.145	0.002	2.5	8.7×10^{-1}	4.4×10^{2}	1.115	2.2
ChCl	Glucose	1:2		0.435	0.383	1.229	2.3	2.6	8.1×10^{-1}	0.697	2.2
ChCl	Acetic acid	1:2		1.583	0.266	2.555	6.3×10^{-1}	3.8	3.9×10^{-1}	1.038	7.0×10^{-1}
ChCl	1,2-Butanediol	1:2		0.000	0.002	0.207	2.1×10^{3}	4.1×10^{2}	4.8	0.811	1.7×10^{3}
ChCl	Citric acid	1:2		0.241	1.311	0.001	4.1	7.6×10^{-1}	1.0×10^{3}	1.356	3.8
ChCl	Malonic acid	1:2	(Cheng et al., 2018)	0.190	0.741	0.001	5.3	1.4	1.2×10^{3}	1.161	4.4
ChCl	Oxalic acid	1:2		0.003	0.267	0.000	3.4×10^{2}	3.7	5.0×10^{6}	1.279	2.7×10^{2}
ChCl	Phenylacetic acid	1:1		26.66	0.352	45.21	3.8×10^{-2}	2.8	2.2×10^{-2}	2.631	2.4×10^{-1}
ChCl	3-Phenylpropionic acid	1:1		41.40	0.409	66.34	2.4×10^{-2}	2.4	1.5×10^{-2}	2.922	2.2×10^{-1}
ChCl	Levulinic acid	1:2		0.191	0.114	4.537	5.2	8.8	2.2×10^{-1}	1.072	7.0
ChCl	Itaconic acid	1:1		4.428	0.589	0.496	2.3×10^{-1}	1.7	2.0	1.943	2.0×10^{-1}
ChCl	Xylitol	1:1		0.115	0.052	2.724	8.7	1.9×10^{1}	3.7×10^{-1}	1.319	9.6
ChCl	Sorbitol	1:1		0.038	0.033	1.999	2.6×10^{1}	3.1×10^{1}	5.0×10^{-1}	1.363	2.6×10^{1}
ChCl	Acetamide	1:2		0.002	0.009	0.280	5.0×10^{2}	1.2×10^{2}	3.6	0.252	3.9×10^{2}
ChCl	Isosorbide	1:2	(Maugeri & Domínguez De María, 2012)	0.001	0.005	0.230	1.9×10^{3}	2.0×10^{2}	4.3	0.357	1.5×10^{3}
ChCl	Triethylene glycol	1:4	(Cheng et al., 2018)	0.008	0.030	0.950	1.2×10^{2}	3.3×10^{1}	1.1	0.850	1.0×10^{2}
ChCl	Propionic acid	1:2		9.897	0.524	1.839	1.0×10^{-1}	1.9	5.4×10^{-1}	1.457	1.1×10^{-1}

ChCl	Urea	1:2	(Gonzalez–Diaz & García–Núñez, 2023)	0.163	0.296	0.284	6.1	3.4	3.5	-0.233	5.0
ChCl	1,2-propanediol	1:1	(Zainal-Abidin et al., 2017)	0.165	0.028	5.973	6.1	3.5×10^{1}	1.7×10^{-1}	1.537	9.1
ChCl	Sucrose	1:1		0.047	0.066	1.545	2.1×10^{1}	1.5×10^{1}	6.5×10^{-1}	1.066	2.0×10^{1}
ChCl	Tartaric acid	2:1		12.56	0.606	1.413	8.0×10^{-2}	1.7	7.1×10^{-1}	2.367	8.0×10^{-2}
ChCl	Maltose	1:2	(Fernández et al., 2018)	0.014	0.093	0.570	7.3×10^{1}	$1.1E\times10^{1}$	1.8	-0.669	6.0×10^{1}
ChCl	1,4-Butanediol	1:2	(Shishov et al., 2020)	0.003	0.009	0.525	3.7×10^{2}	1.1×10^{2}	1.9	0.808	8.0×10^{2}
ChCl	1,3-Butanediol	1:2	(Abbasi et al., 2021)	0.004	0.010	0.587	2.8×10^{2}	1.0×10^{2}	1.7	0.816	2.3×10^{2}
ChCl	Glycerol	1:2	(Al-Maari et al., 2024)	0.006	0.026	0.599	1.5×10^{2}	3.8×10^{1}	1.7	0.235	1.3×10^{2}
ChCl	Menthol	1:1	(Al-Maari et al., 2024)	0.003	0.002	3.512	2.9×10^{2}	5.3×10^{2}	2.8×10^{-1}	3.195	3.4×10^{2}
ChCl	Zinc chloride	1:2	(Wojeicchowski et al., 2021)	0.121	3.025	0.000	8.3	3.3×10^{-1}	2.1×10^{-3}	1.449	9.4
ChCl	1,6-Hexanediol	1:2	(Abbasi et al., 2021)	0.004	0.007	0.843	2.8×10^{2}	1.4×10^{2}	1.2	1.555	2.4×10^{2}
ChCl	Nonanoic acid	1:1	(Al-Maari et al., 2024)	84.56	0.487	300.9	1.2×10^{-2}	2.1	3.3×10^{-3}	3.618	4.5×10^{-1}
ChCl	Imidazole	3:7	(Hou et al., 2008)	0.008	0.003	1.188	1.3×10^{2}	3.7×10^{2}	8.4×10^{-1}	0.632	1.2×10^{2}
ChCl	Thiourea	1:2	(Y. Li et al., 2023)	0.000	0.096	0.000	4.8×10^{3}	1.0×10^{1}	4.5×10^{5}	1.250	3.7×10^{3}
ChCl	Methyldiethanolamine	1:6	(Adeyemi et al., 2018)	0.001	0.004	0.238	1.5×10^{3}	2.6×10^{2}	4.2	0.372	1.2×10^{3}
ChCl	Maleic acid	1:1	(Dai, Van Spronsen, et al., 2013)	3.750	0.686	0.145	2.7×10^{-1}	1.5	6.9	1.813	2.3×10^{-1}
ChCl	Aconitic acid	1:1		2.114	0.715	0.096	4.7×10^{-1}	1.4	1.0×10^{1}	1.825	4.0×10^{-1}
ChCl	Adonitol	5:2		9.428	0.365	5.750	1.1×10^{-1}	2.7	1.7×10^{-1}	2.350	1.6×10^{-1}
ChCl	Ascorbic acid	2:1		0.062	0.023	3.540	1.6×10^{1}	4.3×10^{1}	2.8×10^{-1}	2.401	1.9×10^{1}

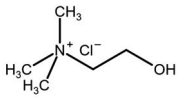
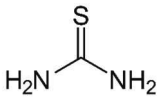
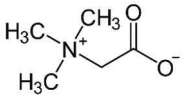
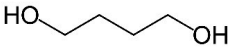
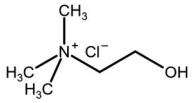
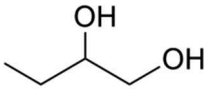
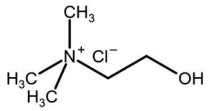
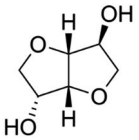
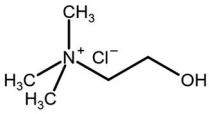
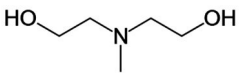
ChCl	Adipic acid	1:1		1.579	0.362	2.229	6.3×10^{-1}	2.8	4.5×10^{-1}	1.650	6.8×10^{-1}
ChCl	Succinic acid	1:1		2.913	0.465	0.864	3.4×10^{-1}	2.2	1.2	1.666	3.1×10^{-1}
Glycerol	Urea	1:1	(Lazović et al., 2022)	0.165	3.584	0.872	6.0	2.8×10^{-1}	1.1	-1.575	7.9
Glycerol	Lactic acid	1:1		0.073	0.698	0.561	1.4×10^{1}	1.4	1.8	-0.869	1.2×10^{1}
Glycerol	L-Ascorbic acid	1:1		0.531	1.877	0.455	1.9	5.3×10^{-1}	2.2	-0.388	2.0
Glycerol	Sucrose	3:1	(Jeong et al., 2017)	0.009	0.195	0.429	1.1×10^{2}	5.1	2.3	-1.173	9.4×10^{1}
Glycerol	Sorbitol	2:1		0.009	0.176	0.427	1.1×10^{2}	5.7	2.3	-0.958	8.9×10^{1}
Glycerol	Maltose	3:1		0.008	0.205	0.424	1.3×10^{2}	4.9	2.4	-1.563	1.0×10^{2}
Glycerol	Glucose	3:1		0.032	0.493	0.592	3.2×10^{1}	2.0	1.7	-1.051	2.8×10^{1}
Glycerol	Maltitol	3:1		0.012	0.259	0.483	8.2×10^{1}	3.9	2.1	-1.560	6.9×10^{1}
Glycerol	Xylitol	2:1		0.017	0.283	0.500	5.9×10^{1}	3.5	2.0	-0.988	5.0×10^{1}
Glycerol	Fructose	3:1		0.006	0.186	0.341	1.8×10^{2}	5.4	2.9	-1.453	1.4×10^{2}
Glycerol	Galactose	3:1		0.165	3.584	0.872	6.0	2.8×10^{-1}	1.1	-1.262	3.2×10^{1}
Betaine	Glycerol	1:2	(Gonzalez–Diaz & García–Núñez, 2023)	0.001	0.014	0.329	7.5×10^{2}	7.1×10^{1}	3.0	-0.169	5.9×10^{2}
Betaine	L,D-Lactic acid	1:2		0.273	0.263	0.867	3.7	3.8	1.2	0.304	3.3E+00
Betaine	Levulinic acid	1:2	(Al-Maari et al., 2024)	0.093	0.102	3.734	1.1×10^{1}	9.8	2.7×10^{-1}	0.667	1.3×10^{1}
Betaine	Citric acid	1:1		0.577	0.914	0.013	1.7	1.1	7.9×10^{-1}	1.199	1.5
Betaine	Malic acid	1:1		1.532	0.644	0.138	6.5×10^{-1}	1.6	7.3	1.188	5.5×10^{-1}
Betaine	Ethylene glycol	1:2		0.007	0.029	0.541	1.5×10^{2}	3.5×10^{1}	1.8	-0.053	1.2×10^{2}
Betaine	Urea	1:2	(Zainal-Abidin et al., 2017)	0.070	0.285	0.346	1.4×10^{1}	3.5	2.9	-0.637	1.2×10^{1}
Betaine	1,4-Butanediol	1:2	(Al-Maari et al., 2024)	0.000	0.003	0.178	3.3×10^{3}	3.2×10^{2}	5.6	0.404	2.5×10^{3}
Betaine	1,2-Propanediol	1:3	(He et al., 2024)	0.029	0.030	1.329	3.4×10^{1}	3.3×10^{1}	7.5×10^{-1}	0.425	3.1×10^{1}
Betaine	Diethylene glycol	1:4	(He et al., 2024)	0.007	0.039	0.594	1.4×10^{2}	2.6×10^{1}	1.7	0.073	1.2×10^{2}
Betaine	Tartaric acid	1:1	(Mohd Fuad & Mohd Nadzir, 2022)	0.974	0.830	0.009	1.0	1.2	1.1×10^{2}	1.368	8.8×10^{-1}

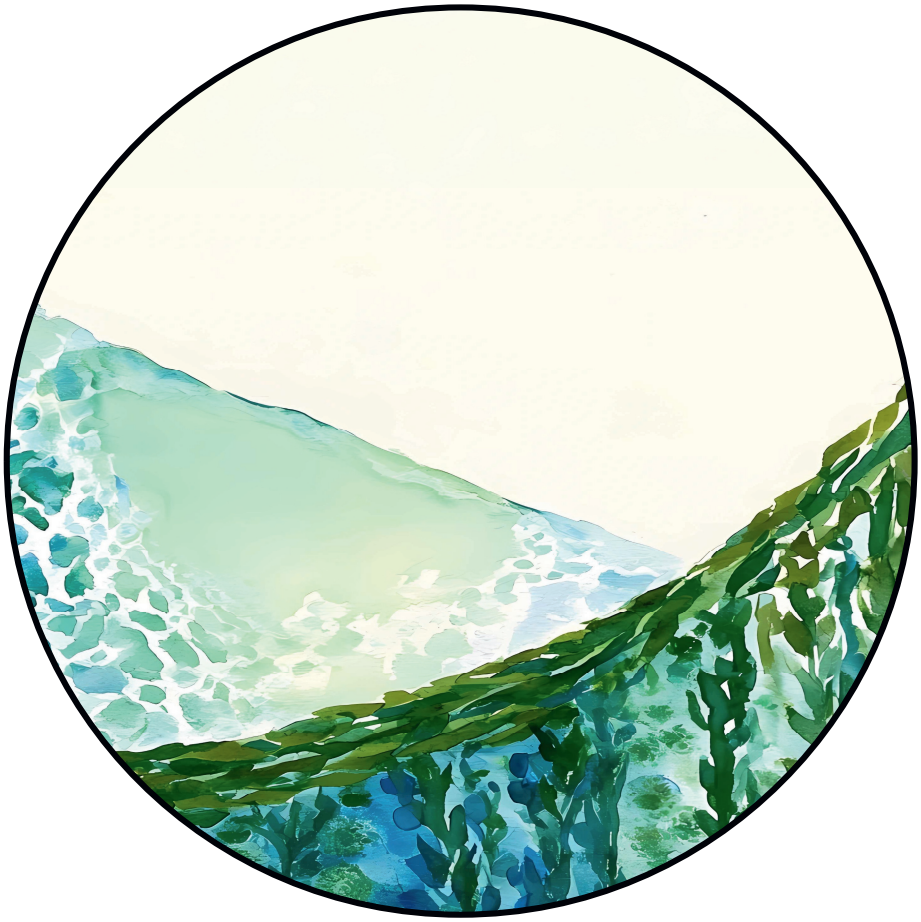
Betaine	Xylitol	1:2	(Mohd Fuad & Mohd Nadzir, 2022)	0.034	0.071	1.174	3.0×10^{1}	1.4×10^{1}	8.5×10^{-1}	0.303	2.7×10^{1}
Betaine	Sorbitol	1:2	(Mohd Fuad & Mohd Nadzir, 2022)	0.011	0.039	0.878	9.3×10^{1}	2.6×10^{1}	1.1	0.362	8.1×10^{1}
Betaine	Glucose	1:1	(Mohd Fuad & Mohd Nadzir, 2022)	0.132	0.118	1.999	7.6	8.5	5.0×10^{-1}	0.704	7.7
Betaine	Fructose	1:1	(Alcalde et al., 2024)	0.002	0.013	0.326	5.5×10^{2}	7.6×10^{1}	3.1	-0.101	4.3×10^{2}
Betaine	Methyl urea	1:2	(N. Li et al., 2016)	0.004	0.016	0.282	2.8×10^{1}	6.1×10^{1}	3.5	-0.094	2.2×10^{2}
Betaine	Sucrose	2:1	(Dai, Van Spronsen, et al., 2013)	0.004	0.013	0.636	2.7×10^{2}	7.5×10^{1}	1.6	0.953	2.2×10^{2}
Betaine	Trehalose	4:1	(Dai, Van Spronsen, et al., 2013)	0.001	0.004	0.704	7.2×10^{1}	2.6×10^{2}	1.4	1.036	6.0×10^{2}
Betaine	Mannose	5:2	(Dai, Van Spronsen, et al., 2013)	0.002	0.004	1.316	5.2×10^{2}	2.5×10^{2}	7.6×10^{-1}	0.805	4.8×10^{2}
Lactic acid	Sucrose	4:1	(Gonzalez–Diaz & García–Núñez, 2023)	0.214	1.096	0.730	4.7	9.1×10^{-1}	1.4	-0.615	4.6
Lactic acid	Urea	3:1		0.698	4.538	0.390	1.4	2.2×10^{-1}	2.6	-0.866	2.0
Lactic acid	Glycine	3:1		0.323	1.040	0.259	3.1	9.6×10^{-1}	3.9	-0.512	2.8
Lactic acid	Glucose	3:1	(Zainal-Abidin et al., 2017)	0.616	2.645	0.337	1.6	3.8×10^{-1}	3.0	-0.518	1.8
Lactic acid	Sodium acetate	3:1	(Zainal-Abidin et al., 2017)	0.019	0.186	0.797	5.2×10^{1}	5.4	1.3	-0.415	4.5×10^{2}
Lactic acid	Alanine	9:1	(Skulcova et al., n.d.)	0.419	1.501	0.220	2.4	6.7×10^{-1}	4.5	-0.460	2.3
Tartaric acid	Xylitol	1:2	(Gonzalez–Diaz &	0.808	2.411	0.270	1.2	4.1×10^{-1}	3.7	-0.078	1.3

			García–Núñez, 2023)								
Citric acid	Xylitol	1:2	(Gonzalez–Diaz & García–Núñez, 2023)	0.745	2.844	0.290	1.3	3.5×10^{-1}	3.4	-0.191	1.5
Citric acid	D-Fructose	1:1	(Dai, Van Spronsen, et al., 2013)	0.924	4.164	0.505	1.1	2.4×10^{-1}	2.0	-0.842	1.4
Citric acid	Sucrose	1:1		0.477	1.972	0.779	2.1	5.1×10^{-1}	1.3	-0.282	2.3
Citric acid	D-Sorbitol	1:1		0.881	3.053	0.149	1.1	3.3×10^{-1}	6.7	0.015	1.3
Citric acid	Trehalose	2:1		1.045	4.730	0.301	9.6×10^{-1}	2.1×10^{-1}	3.3	-0.555	1.3
Citric acid	Xylose	1:1		1.048	5.288	0.328	9.5×10^{-1}	1.9×10^{-1}	3.0	-0.749	1.4
Citric acid	Maltose	2:1	(Jeong et al., 2017)	1.045	4.730	0.301	9.6×10^{-1}	2.1×10^{-1}	3.3	-0.555	1.3
Citric acid	Glucose	1:1		0.952	7.185	0.030	1.1	1.4×10^{-1}	3.3×10^{1}	-0.037	1.7
Citric acid	Maltitol	2:1		1.091	5.014	0.288	9.2×10^{-1}	2.0×10^{-1}	3.5	-0.551	1.3
Citric acid	Glycerol	1:2		0.446	2.630	0.453	2.2	3.8×10^{-1}	2.2	-0.663	2.5
Proline	Malic acid	1:1	(Lazović et al., 2022)	0.305	0.747	0.005	3.3	1.3	1.9×10^{2}	0.633	2.8
L-Proline	Glycerol	2:5	(Zainal-Abidin et al., 2017)	0.009	0.035	0.597	1.1×10^{2}	2.8×10^{1}	1.7	-0.637	9.0×10^{1}
Proline	Xylitol	1:1	(Nam et al., 2015)	0.081	0.075	1.073	1.2×10^{1}	1.3×10^{1}	9.3×10^{-1}	0.157	1.1×10^{1}
D/L-Proline	Sucrose	2:1	(Dai, van Spronsen, et al., 2013)	0.028	0.052	0.892	3.5×10^{1}	1.9×10^{1}	1.1	0.213	3.1×10^{1}
D/L-Proline	Lactic acid	1:1	(Dai, van Spronsen, et al., 2013)	0.408	0.286	0.407	2.5	3.5	2.5	0.158	2.0
Proline	Levulinic acid	1:2	(Vieira Sanches et al., 2023)	0.130	0.142	1.178	7.7	7.0	8.5×10^{-1}	0.297	7.0
Ammonium acetate	Lactic acid	1:3	(Zainal-Abidin et al., 2017)	0.298	1.245	0.307	3.4	8.0×10^{-1}	3.3	-0.415	3.2
Menthol	Lactic acid	1:2		0.659	0.301	2.093	1.5	3.3	4.8×10^{-1}	0.737	1.6

Menthol	Acetic acid	1:2	(Xu et al., 2022)	1.464	0.249	6.783	6.8×10^{-1}	4.0	1.5×10^{-1}	1.066	1.1
Menthol	Decanoic acid	1:1	(Devi et al., 2023)	21.06	0.325	586.9	4.7×10^{-2}	3.1	1.7×10^{-3}	3.914	3.5
Menthol	1-Butanol	1:1		0.002	0.004	1.316	5.2×10^{2}	2.5	7.6×10^{-1}	2.220	4.8
Menthol	Octanoic acid	1:1	(Al-Maari et al., 2024)	6.772	0.211	245.2	1.5×10^{-1}	4.7	4.1×10^{-3}	3.275	4.6
Menthol	Thymol	1:1		92.63	0.494	826.7	1.1×10^{-2}	2.0	1.2×10^{-3}	3.491	1.1
Menthol	Butyric acid	1:1		1.521	0.117	61.11	6.6×10^{-1}	8.6	1.6×10^{-2}	2.197	5.5
Menthol	Dodecanoic acid	1:1		40.61	0.423	1042	2.5×10^{-2}	2.4	9.6×10^{-4}	4.461	3.2
TBAC	Glycerol	1:2	(Xu et al., 2022)	0.081	0.029	7.550	1.2×10^{1}	3.4×10^{1}	1.3×10^{-1}	0.798	2.1×10^{1}
TBAC	1,2-Ethanediol	1:2		0.793	0.074	19.62	1.3	1.4×10^{1}	5.1×10^{-2}	0.914	4.1
TBAC	1,2-Butanediol	1:2		0.003	0.002	1.455	3.9×10^{2}	4.3×10^{2}	6.9×10^{-1}	1.374	3.6
TBAC	Lactic acid	1:2		20.49	0.600	15.98	4.9×10^{-2}	1.7	6.3×10^{-2}	1.271	1.4×10^{-1}
TBAC	Acetic acid	1:2	(Al-Maari et al., 2024)	188.3	1.350	74.45	5.3×10^{-3}	7.4×10^{-1}	1.3×10^{-2}	1.600	5.4×10^{-2}
TBAC	Levulinic acid	1:2		9.064	0.362	108.9	1.1×10^{-1}	2.8	9.2×10^{-3}	1.634	1.6E+00
TEA	Glycerol	2:1		0.040	0.005	19.11	2.5×10^{1}	2.0×10^{2}	5.2×10^{-2}	3.132	7.8×10^{1}
TEA	Lactic acid	1:2		2.536	0.358	2.698	3.9×10^{-1}	2.8	3.7×10^{-1}	1.428	4.5×10^{-1}
B-Alanine	DL-Malic acid	1:1	(Dai, van Spronsen, et al., 2013)	0.307	1.058	0.011	3.3	9.5×10^{-1}	9.1×10^{1}	0.229	2.9
B-Alanine	Citric acid	1:1		0.190	1.832	0.002	5.3	5.5×10^{-1}	4.0×10^{2}	0.240	5.2

Table S2.2 Molecular structures of the five deep eutectic solvents with the highest predicted alginate solubilisation capacities based on computational screening.

DES	HBA	HBD
ChCl:Thiourea (1:2)		
Bet:1,4-butanediol (1:2)		
ChCl:1,2-butanediol (1:2)		
ChCl:Isosorbide (1:2)		
ChCl:Methyldiethanolamine (1:6)		



Chapter 3

Choline chloride-based solvents as alternative media for alginate extraction from brown seaweed

Isa S.A. Hiemstra, Jenne T. Meinema, Michel M.H. Eppink, René H. Wijffels, Antoinette Kazbar

This chapter has been published as:

Hiemstra, I. S.A, Meinema, J. T., Eppink, M. M., Wijffels, R. H., & Kazbar, A. (2024). Choline chloride-based solvents as alternative media for alginate extraction from brown seaweed. *LWT*, 214, 117174. https://doi.org/10.1016/j.lwt.2024.117174

Abstract

This study demonstrated an effective method for extracting alginate from the brown seaweed *Ascophyllum nodosum* using deep eutectic solvents (DES), achieving a higher yield than traditional alkaline extraction methods. Eight choline chloride-based DESs were tested, with DES ChCl:Urea (1:2) yielding the most alginate. The extraction conditions were optimised using response surface methodology (RSM), which identified the biomass to liquid ratio as the most significant factor influencing extraction efficiency. The optimised parameters resulted in a 74% extraction efficiency of alginate. Characterisation through FTIR and size exclusion chromatography showed that the extracted alginate was comparable to that obtained via the conventional alkaline extraction method. Overall, DES extraction offers a more efficient and sustainable alternative to conventional methods, which typically extract only 10% to 24.5% of total alginate.

3.1. Introduction

There is a pressing need to adopt green biorefinery technologies for the sustainable extraction of bioactive compounds from biomasses, as current methods often rely on environmentally and health hazardous solvents. These conventional extraction techniques not only involve toxic solvents but also generate significant chemical waste due to the lack of solvent regeneration. The food processing sector has expanded dramatically over the past decade, particularly regarding products rich in biologically active compounds. Consequently, the efficacy and safety of food extraction techniques have gained increased attention. This has led to a surge in research focused on developing new extraction methods that are not only rapid and cost-effective but also more efficient and environmentally friendly, thereby enhancing yields and extract quality without the use of potentially harmful organic solvents [114]. The use of green solvents is a critical area of study in pursuit of sustainable development goals.

Deep eutectic solvents (DES) offer a promising alternative as green solvents for bioactive compound extraction [115–117]. DES are recognised as excellent substitutes for organic solvents due to their simple manufacturing process, low cost, potential biodegradability and negligible toxicity [9, 10, 118]. They have emerged as versatile and effective solvents with proven applications in a variety of processes, including the extraction of a wide range of food components. Composed of a combination of hydrogen bond donors (HBD) and hydrogen bond acceptors (HBA), DES demonstrate a melting point depression when mixed in specific ratios, resulting in a liquid at a certain temperature [14, 15].

DES have been effectively utilised for extracting various biological compounds, such as polysaccharides, lipids and phenolic compounds, from diverse biomass sources including plants, microalgae and lignocellulosic biomass [32, 115, 119–121]. However, there is limited research on the use of DES for extracting phycocolloids from seaweed biomass. Brown seaweeds predominantly consist of phycocolloids, with alginate comprising approximately 30-35% of their dry weight. Alginate, found in the cell walls of brown seaweed, consists of the uronic acids β-D-mannuronic acid and α-L-guluronic acid (**Figure S3.1**). These two uronic acids are present in varying sequences and ratios [122]. This hydrocolloid is widely used as a thickening and stabilising agent in the food and pharmaceutical industry due to its ability to form stable gels [123]. Current alginate extraction methods involve harsh chemicals, including formaldehyde, under acidic and alkaline conditions across multiple processing stages, leading to excessive water use and high energy consumption [56, 124]. Moreover, these methods only yield 10% to 24.5% of the total alginate [122, 125, 126].

As a more sustainable alternative, DES could be used for alginate extraction from brown seaweed. Das *et al*. [119] reported a maximum extraction yield of 60.25% k-carrageenan from the red seaweed *Kappaphyccus alvarezii* using ChCl:glycerol (1:2) (10% water). Another study applied microwave-assisted DES extraction from *Fucus vesiculosus*, achieving 11.63% yield of polysaccharides using DES ChCl:1,4-butanediol (1:5) with 32% of water [127]. Similarly, ultrasound-assisted DES extraction of polysaccharides from *Sargassum horneri* yielded 11.31% using ChCl:1,2-propanediol (1:2) with 30% water [63]. Additionally, Saravana *et al*. [128] demonstrated that 28.12% alginate could be extracted from *Saccharina japonica* using subcritical water extraction with ChCl:Gly (1:2) containing 70% of water. Due to the high water content, this solution cannot be classified as a DES and is considered as a subcritical water extraction with solubilised HBA and HBD components.

While the aforementioned studies achieved considerable extraction yields, they employed additional techniques alongside DES. There is currently no literature on the use of DES as sole extracting agent for alginate. By omitting additional techniques such as ultrasound, microwave or subcritical water assistance, the extraction process could be simplified, reducing both equipment and operational costs.

In this research, alginate was extracted from brown seaweed *Ascophyllum nodosum* using eight different choline chloride-based deep eutectic solvents as a more sustainable extraction method. Prior to extraction, the interactions between the DES and alginate were evaluated through σ-potential using COSMO-RS (Conductor-like Screening Model for Real Solvents), a quantum chemistry-based method that predicts the behaviour of compounds in solvents. This theoretical approach assessed the compatibility of the DESs with alginate extraction. The effects of various operating parameters, including extraction temperature, time, biomass content, and water content in the DES, were experimentally analysed using response surface methodology (RSM), significantly increasing alginate yield compared to traditional alkaline extraction. Additionally, the extracted alginate was characterised using FTIR and SEC analysis. These results indicated that alginate extracted with DES was similar to alkaline extraction regarding functional groups. Overall, this study demonstrates that DES-based extraction of alginate can not only surpass current industrial yields but also improve process efficiency, positioning DES as a highly promising extraction agent for alginate in the food sector. This approach not only supports sustainable production but could also enhance alginate's functional properties, making it ideal for diverse food application. This work sets a foundation for future DES-based processes that can improve both extraction efficiency and the quality of food-grade products.

3.2. Materials and methods

3.2.1 Materials

All chemicals used were purchased from Sigma Aldrich (Merck). DESs were prepared using the following materials: choline chloride (≥ 98%), urea (≥ 99.5%), imidazole (≥ 99%), thiourea (≥ 98%), methyldiethanolamine (≥ 99%), ethylene glycol (≥ 99.8%), glycerol (> 99.5%), levulinic acid (≥ 98%) and acetic acid (≥ 99%). For the uronic acid assay, a 0.125% solution of carbazole (purity ≥ 95%) in absolute ethanol (≥ 99.9%) was prepared and a 5 mM solution of sodium tetraborate (≥ 99%) in concentrated sulfuric acid (95-98%) was prepared. The carbazole and sodium tetraborate solutions were stored in the dark at 4 ºC. Fresh *Ascophyllum nodosum* was provided by project partner Algaia (France) in March 2023 (**Figure S3.2**). The seaweed was frozen using liquid nitrogen and stored at -80 ºC until it was used for extraction. Before extraction, the seaweed was freeze dried and subsequently crushed into powder by grinding it with a mortar and pestle.

3.2.2 Instrumentation

The Tecan Infinite M200 plate reader was used for alginate quantification. The extracted alginate, the DES and DES constituents were analysed with Fourier transform Infrared Spectroscopy (FTIR). FTIR Nicolet Summit X attenuated total reflection (ATR) FTIR Spectrometer (ThermoFisher Scientific) was used, with a range of 400-4000 cm^{-1}. For alginate size determination, HPLC size exclusion chromatography (SEC) was used [129]. Standards of pullulan, ranging from 0.18 to 1250 kDa were used. An AdvanceBio SEC 300A (2.7 µm 7.8 * 300 mm) was used for determining the size. Alginate was detected by a DAD detector (203 nm), while pullulan was detected by RID [129]. A 0.1 M ammonium phosphate buffer (pH 4.4) was used with a flow rate of 0.8 mL/min.

3.2.3 Methods

3.2.3.1 DES preparation

For extraction of alginate, eight different deep eutectic solvents were used (**Table 3.1** and Supplementary Information **Table S3.1**). These DESs were selected to study the effect of choline chloride-based DES with different HBDs on the extraction yield of alginate. The selected ratios were obtained from literature (**Table 3.1**). These DESs were prepared by combining the HBA and HBD in the appropriate ratios and were heated in a water bath at 80 ºC until a transparent solution was obtained. For the DES ChCl:I and ChCl:ThioU 20 wt% of water was added and for ChCl:Gly and ChCl:LevA 10 wt% of water was added.

Table 3.1 Deep eutectic solvents and the molar ratios used for alginate extractions.

DES	HBA	HBD	Ratio	Abbreviation	Reference
DES1	ChCl	Urea	1:2	ChCl:U	[130, 131]
DES2	ChCl	Imidazole	3:7	ChCl:I	[132]
DES3	ChCl	Thiourea	1:2	ChCl:ThioU	[130, 131]
DES4	ChCl	Methyldiethanolamine	1:6	ChCl:MDEA	[133]
DES5	ChCl	Ethylene glycol	1:2	ChCl:EG	[119]
DES6	ChCl	Glycerol	1:2	ChCl:Gly	[119]
DES7	ChCl	Levulinic acid	1:2	ChCl:LevA	[134]
DES8	ChCl	Acetic acid	1:2	ChCl:AA	[135]

3.2.3.2 Extraction and quantification of alginate

Alginate was extracted from *A. nodosum* with eight different DESs. For initial extractions, 500 mg of powdered seaweed was added to 10 g of DES and this was vortexed before it was put in a water bath for the extraction [119]. Extractions were performed at 80 ºC for 1 hour and samples were vortexed every 10 minutes. For the extraction optimization, these extraction conditions were altered. As control method, the conventional alkaline extraction was performed. For alkaline extraction, acid water containing H_2SO_4 (pH 1.9) was added in a 1:1 (w/w) ratio to seaweed and this was set for one hour at room temperature. Next, Na_2CO_3 was added in a ratio 0.0325:1 (w/w) for a one hour extraction at 65ºC. Extractions with the different DESs and controls were performed in triplicates. After extraction, the samples were centrifuged and the supernatant was used for analysis of alginate content (**Figure 3.1**). For the total alginate content determination of *A. nodosum*, 10 mg of *A. nodosum* was hydrolysed using 2.5 M H_2SO_4 and incubated at 96 ºC for 3 hours, after which 2.5 M NaOH was added to neutralise the samples. Alginate quantification was performed using the 96-well plate uronic acid carbazole reaction as proposed by Cesaretti *et al*. [136]. The alginate yield was quantified using **Equation 3.1**:

$$Yield\ (\%) = \frac{\frac{C_{extract}}{100\rho_L}}{m_{biomass}x_{dry}} * 100 \qquad (\mathbf{3.1})$$

where $C_{extract}$ is the concentration of the extract, $\rho_L$is the density of the solvent, $m_{biomass}$ is the weight of the initial biomass and x_{dry} is the weight fraction of the biomass that is dry biomass. With this expression the yield is a function of the dry biomass weight.

3.2.3.3 Characterisation of alginate and DES

The alginate extracts were subsequently isolated and purified by first precipitation with calcium chloride dihydrate 1% w/v, followed by two washing steps with 80% ethanol. The precipitated alginate was dried under nitrogen and analysed with FTIR. FTIR was selected due to its widespread application and established reliability in the characterisation of seaweed polysaccharides [119, 128, 137]. Extracts with the conventional alkaline extraction method and DES extraction were compared. The optimal DES and its components were also analysed using FTIR, a commonly used and suitable method for characterising DES [138–140]. For alginate size determination, HPLC size exclusion chromatography (SEC) was used (**Section 3.2.2**) [129].



Figure 3.1 Pictorial representation of the alginate extraction process with deep eutectic solvents.

3.2.3.4 COSMO-RS evaluation

COSMO-RS (Software for Chemistry and Materials BV (SCM), Amsterdam, The Netherlands) version 2022.103 within the Amsterdam density functional (ADF) package was used for the COSMO-RS analyses [67]. The molecular geometry of all used molecules was pre-optimised using a universal force field (UFF) at density functional level GGA:BP86 basis set TZP. The σ-profile and σ-potential analyses of alginate and the DESs were conducted with COSMO-RS. The monomer D-mannuronic acid was considered using the polymer function, considering the σ-profile of an average monomer. A representation of the alginate polymer was obtained by multiplying the monomer σ-profile by a factor equal to the number of repeat units in the polymer. In this way, a σ-profile for the polymer was created while not being an exorbitantly expensive calculation. Previous research showed that this trimer representation was sufficiently accurate for calculating various thermodynamic properties while not being an expensive and time-consuming calculation [141, 142].

3.2.3.5 Optimisations study

The software Design-Expert 13 (version 13.0.14) was used for the optimisation study. Response surface methodology (RSM) combined with Box Behnken Design (BBD) was used to study the influence of four different factors on the extraction yield of alginate (**Table 3.2**). A three-level BBD was used, as this has widely been applied in literature for optimising DES extraction conditions [32, 62, 128, 143, 144]. The factors extraction temperature (40 to 95 ºC), extraction time (0.25 to 3 hours), biomass to DES amount (2.5 to 25% w/v) and water content in the DES (0 to 30 wt %) were considered in the optimisation of alginate extraction (**Table 3.2**). These values were selected to have a broad range of extraction conditions, therefore allowing to study interactions of these factors. Within BBD, first and second order coefficients can be investigated. The optimisation experiment consisted of 25 runs, with 5 replicates and 5 lack-of-fit points. As a response, the alginate extraction yield was selected, expressed as a function of the dry biomass weight.

Table 3.2 The factors and three levels per factor for the BBD experiment.

Factor	Level		
	-1	0	1
Extraction temperature (ºC)	40	60	95
Extraction time (hours)	0.25	1.5	3
Biomass (% w/v)	2.5	10	25
Water content (wt %)	0	10	30

Subsequently, the extraction conditions were optimised using a numerical solution of the software, displaying a desirability of 1. For this, the response (alginate yield) was set at a maximum. Experimental validation was performed in triplicate with these optimised conditions.

3.2.3.6 Statistical analysis

All experiments were performed in triplicates. Statistical analysis for the extraction yield of alginate with different solvents was performed by Duncan's multiple range test. P values < 0.05 were considered statistically significant. Error bars represent the standard deviations of the triplicate measurements. For the optimization study, the model was verified using an analysis of variance test (ANOVA) to validate the accuracy of the predictive model.

3.3. Results and discussion

3.3.1 DES-alginate molecular interactions

Alginate and the different DESs can be evaluated using their σ-profiles and σ-potentials (**Figure 3.2** and **Figure 3.3**), which represent the charge density distribution of the molecular surface. In this way, predictions regarding the performance of the solvents in the extraction of alginate can be made. The hydrogen bond donating region is located at less than -0.085 e/A^2, while the hydrogen bond accepting region is present at greater than +0.085 e/A^2 [93]. The molecular surface is considered too non-polar to contribute to hydrogen bonding when its value is between -0.085 and +0.085 e/A^2. The σ-profile of alginate indicates that predominantly polar regions are present alongside some non-polar regions within the molecule (**Figure 3.3**). The σ-potential of alginate and the DESs were used to assess the affinity of alginate towards the DESs. Identifying complementary interactions would enhance the compatibility between the DES and the compound [93, 145]. Higher negative values of the σ-potential y-axis (chemical potential) indicate a stronger interaction between compounds, while increased positive values suggest repulsive forces [93, 99]. The σ-potential of alginate shows negative values in both the HBD and HBA regions (**Figure 3.2**). In the non-polar region, the values are positive. Polar peaks are attributed to the OH-groups present in D-mannuronic acid, which contribute to the difference in electronegativity between the O and H, while the non-polar regions are attributed to the neutrally charged areas containing C-H atoms. This suggests that alginate is likely to dissolve in solvents containing both HBD and HBA regions. However, slightly more negative values are observed in the HBD region, indicating that a DES with marginally better HBA properties could be a more suitable extractant.

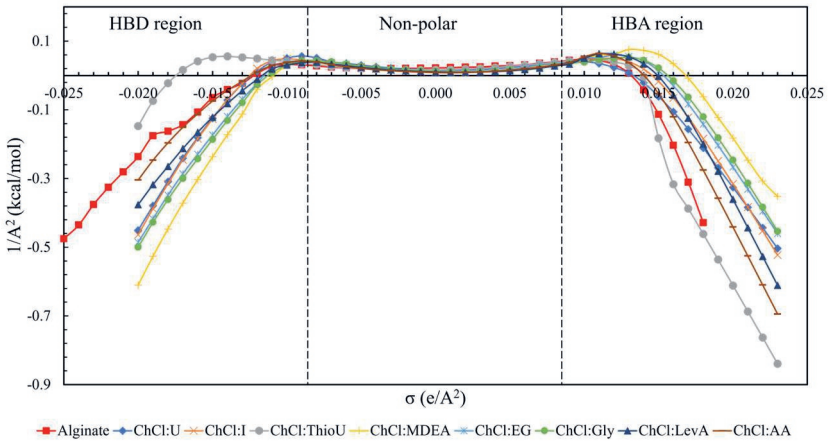


Figure 3.2 σ-potential of alginate (red), ChCl:U (blue), ChCl:I (orange), ChCl:ThioU (grey), ChCl:MDEA (yellow), ChCL:EG (light blue), ChCl:Gly (green), ChCL:LevA (dark blue), ChCL:AA (brown).

All DESs showed a similar σ-potential, with slight positive values in the non-polar regions and negative HBA and HBD regions (**Figure 3.2**). Similar σ-potentials indicate that there is an affinity between the DES and the compound [146]. Due to the presence of both HBA and HBD groups, alginate could form hydrogen bond interactions with all studied DES. In particular, ChCl:U, along with ChCl:I and ChCl:LevA, shows a symmetric curve with a slightly stronger HBA region than HBD, indicating that complementary hydrogen bonding interactions could occur between the OH groups of alginate and cholinium cations acting as HBA (**Figure 3.2**, **Figure S3.3**). Hence, these solvents could potentially extract more alginate compared to the other solvents. However, interactions in the non-polar region may also influence the extraction mechanism [145], potentially contributing to variations in experimentally observed extraction yields.

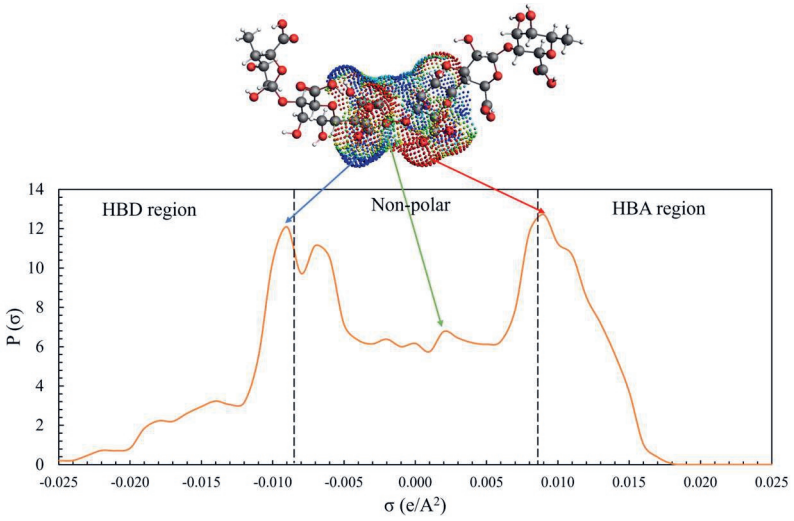


Figure 3.3. σ-surface (top) and σ -profile (graph) of alginate. The red parts of the σ -profile represent electronegative regions of the molecule, while blue indicates electropositive regions. Green areas represent neutral regions.

Additionally, it must be noted that, apart from the interactions between DES and alginate, other interactions could also occur during alginate extraction. Compounds present in the cell wall, such as laminarin and fucoidan, could interact with the DES, as well as hydrophilic proteins, thereby influencing the extraction efficiency. In *Ascophyllum nodosum*, the protein content is relatively low, comprising only 5-10% DW [147]. As a result, proteins were excluded from consideration. The majority of the carbohydrate fraction in *A. nodosum* consists of alginate (15-30% DW), with smaller contributions from laminarin (0-10% DW) and fucoidan (4-10% DW) [147]. Given their lower contents of laminarin and fucoidan, it is likely that most interactions will occur between the DES and alginate.

Based on σ-potential analysis, complementary interactions of hydrogen bonding interactions between the HBD and HBA of alginate and the DES could occur. Thus, according to these analyses, all DES should be able to interact with alginate and were subsequently used for the extraction of alginate from *A. nodosum*.

3.3.2 Alginate extraction

Alginate was successfully extracted with the DESs used in this study and with the alkaline extraction control. Among the DESs, extraction yields ranged from 5.58 ± 1.71% per DW for ChCl:U, to 2.15 ± 0.33% for ChCl:AA (**Figure 3.4**). From total alginate content determination in the biomass (**Section 3.2.3.2**), it was determined that *A. nodosum* biomass contained approximately 27% alginate in dry weight. This indicates that with ChCl:U, an extraction efficiency of 20.7% was reached (20.7% of the total alginate content was extracted) while with ChCl:AA this was 7.9%. DESs ChCl:ThioU and ChCl:I also extracted similar amounts of alginate compared to ChCl:U, with yields of 5.20% ± 0.81 g /g DW (19.3% alginate extraction efficiency) and 4.68 ± 0.37% g/g DW (17.3% of alginate extraction efficiency), respectively. Variations in extraction efficiency within the same DES were probably due to the sensitivity of the colorimetric assay. For future studies, alternative quantification methods beyond colorimetric assays could be employed, such as HPLC, to enhance accuracy and specificity in measurement. The alkaline control showed similar extraction yields compared to DES extraction, with an extraction yield of 4.9 ± 0.6% (**Figure 3.4**).

Some DES showed decreased extraction yields compared to others. However, the σ-potential plots for most DESs were similar. This could indicate that the interaction between DES and biomass is an important factor to consider for the ability to extract compounds from biomass. Previous studies have shown that certain DESs can affect the permeability and availability of intracellular components in plant cell walls, microalgae and bacteria [148–150], indicating that factors beyond the affinity of the DES for the product may be crucial for extractions.

Even though the conventional method extracted similar amounts of alginate compared to DESs (**Figure 3.4**), the DES process is intensified compared to alkaline extraction. With the applied DES extraction, only one extraction step of an hour is applied. Alkaline extraction comprises of two one-hour steps, including soaking in acid conditions, followed by alkaline extraction. Besides, the usage of DES in the alginate extraction process could decrease the high water usage currently employed in the alkaline process. Industrial alginate processing methods require approximately 1000-1500 m^3 of water per ton of sodium alginate produced [151]. Additionally, a milder extraction can be performed using DES compared to alkaline extraction, making use of extraction

solvents that are environmentally less harmful. Nevertheless, a concrete techno-economic analysis and life cycle assessment (LCA) need to be conducted to compare these processes and assess the sustainability of DES [152].

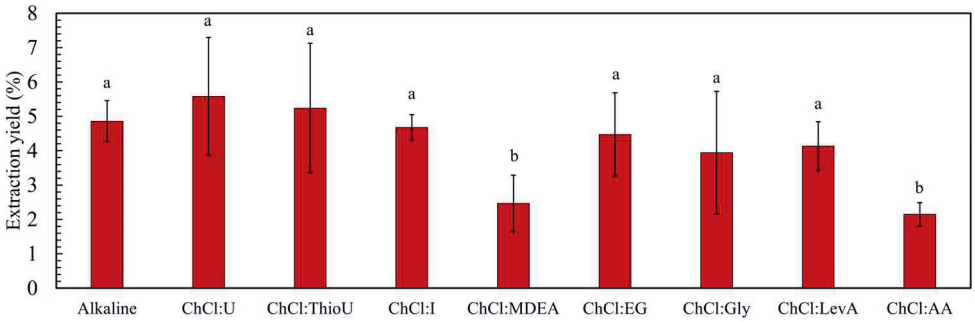


Figure 3.4 Extraction yields of alginate with different DESs and alkaline extraction (control). Extraction yields are expressed as a percentage of alginate extracted per dry weight content.

So far, the focus has only been on the DESs, while the operating extraction parameters (temperature, extraction time, the water content of the DES and the biomass to DES ratio) were fixed. The obtained alginate extraction (20.7% of the total alginate for ChCl:U) with DES could possibly still be improved further. By testing different extraction conditions, the influence of these different parameters and the main influential contributors can be assessed. By understanding these influences on the extraction process, the alginate extraction yield could be enhanced. To further improve the obtained extraction yield of alginate by using DES, an optimization was performed with one of the DESs for the extraction temperature, extraction time, the biomass to solvent ratio and the water content in the DES.

3.3.3 Optimisation of alginate extraction

To enhance the alginate extraction yield, four factors were optimised using ChCl:U. DES ChCl:U was selected due to the highest alginate extraction efficiency obtained with this DES before optimization (**Section 3.3.2**). The data was analysed with multiple regression with a reverse square root transformation. Based on this, an equation was formed (**Equation 3.2**). This equation describes the interaction between the extraction yield of alginate and the extraction factors. The quadratic polynomial equation obtained, was:

$$\text{Yield} = 0.4514 - 0.0364\,A - 0.0109\,B + 0.1828\,C - 0.0329\,D + 0.0565\,AB - 0.0215\,AC + 0.0380\,AD + 0.0154\,BC + 0.0611\,BD + 0.0022\,CD - 0.0124\,A^2 + 0.0175\,B^2 - 0.0135\,C^2 + 0.0894\,D^2. \quad \textbf{(Eq. 3.2)}$$

Within the optimisation study, 25 experimental runs were performed using a BBD (**Table S3.3**). This model was verified using an analysis of variance test (ANOVA), which validated the accuracy of the predictive model (**Table S3.2**). The R^2 value of this model was 0.9706, and the Adjusted R^2 and Predicted R^2 (0.9293 and 0.8097, respectively) had a difference of less than 0.2, indicating these are in reasonable agreement. Furthermore, the value of adequate precision was found to be 19.069. This value should be greater than 4 for the model to be useful in navigating the design space.
The overall model was found to be significant, with a p-value of < 0.0001 and a non-significant lack of fit value of 0.3345 (**Table 3.3**). The Model F-value of 23.55 indicates that the model is significant, with only a 0.01% chance that an F-value this large could occur due to noise.

The significant model terms include temperature (A), biomass concentration (C), water content (D), and temperature with time (AB), temperature with water (AD), time with water (BD) as well as the quadratic water term (D^2), all with p-values less than 0.0500. In contrast, the terms time (B), temperature with biomass (AC), time with water (BD), biomass with water (CD) were not significant, as they had a p value above 0.05. The quadratic terms for temperature (A^2), time (B^2) and biomass (C^2) were also not significant (**Table 3.3**).

Subsequently, RSM 3D surface plots were generated to analyse the interactions between various factors affecting the alginate extraction yield**.** The biomass content ($p < 0.0001$) was identified as the primary influential factor on the extraction yield (Table 3). Regardless of the temperature, time and water content of the DES, the 3D surfaces indicated that the highest extraction efficiencies were obtained with the lowest biomass concentration (2.5% w/v) compared to solvent added (**Figure S3.4**).

Table 3.3 Analysis of variance (ANOVA) test for response surface of the quadratic model for the alginate extraction efficiency.

Source	Sum of Squares	df	Mean Square	F-value	p-value	
Model	0.7586	14	0.0542	23.55	< 0.0001	significant
A-Temperature	0.0192	1	0.0192	8.33	0.0162	significant
B-Time	0.0014	1	0.0014	0.5880	0.4609	not significant
C-Biomass	0.4097	1	0.4097	178.01	< 0.0001	significant
D-Water	0.0153	1	0.0153	6.67	0.0273	significant
AB	0.0290	1	0.0290	12.62	0.0053	significant
AC	0.0050	1	0.0050	2.18	0.1703	not significant
AD	0.0149	1	0.0149	6.46	0.0293	significant
BC	0.0018	1	0.0018	0.7922	0.3944	not significant
BD	0.0257	1	0.0257	11.17	0.0075	significant
CD	0.0000	1	0.0000	0.0212	0.8871	not significant
A^2	0.0006	1	0.0006	0.2535	0.6255	not significant
B^2	0.0013	1	0.0013	0.5526	0.4744	not significant
C^2	0.0005	1	0.0005	0.2010	0.6635	not significant
D^2	0.0271	1	0.0271	11.76	0.0064	significant
Residual	0.0230	10	0.0023			
Lack of Fit	0.0138	5	0.0028	1.50	0.3345	not significant
Pure Error	0.0092	5	0.0018			
Cor Total	0.7816	24				

Extraction yields increased due to higher mass transfer at lower biomass concentrations. Furthermore, the surface plots demonstrated that high temperature (**Figure S3.4b**) and extended extraction time, combined with low biomass content (2.5% w/v), resulted in increased extraction efficiency compared to lower temperatures or shorter extraction times. Higher temperatures reduce the viscosity of the DES, thereby enhancing mass transfer during extraction.

The significant impact of the biomass to solvent ratio on the extraction efficiency could be attributed to the diffusion of alginate into the DES. An increased extraction efficiency at lower biomass to solvent ratios may arise from an increased concentration gradient between the biomass and solvent [153, 154]. In a study focussed on polyphenolic extraction with DES, an increase in solid to liquid ratio significantly enhanced the extraction yield for each studied DES [154]. It was noted that a higher amount of solvent could enhance contact between both phases and enhance penetration into the cell matrix. Therefore, increased extraction efficiency at lower biomass to solvent ratios (2.5% biomass) could lead to a better diffusion of alginate in the DES, enhancing the

extraction efficiency. Dardavila *et al*. [153] conducted extractions of phenolic and carotenoid compounds from the microalga *Chlorella vulgaris*, finding an optimal biomass to solvent ratio of 1:40 (2.5% biomass) after optimisation. Yue *et al*. [144] investigated ultrasound-assisted DES extraction of palmatine and berberine from *Phellodendron* chinense Schneid, obtaining an optimized biomass to solvent ratio of 1:30 (3% biomass). Our model suggests that further lowering the biomass-to-DES ratio could increase yield. However, a too low solid to liquid ratio makes the process impractical due to excess solvent, leading to challenges such as increased solvent use and sample concentration. Thus, a biomass to solvent ratio of 2.5% was chosen for further experiments.

Additionally, the 3D surface plots indicated that the water content of the DES influenced the extraction efficiency, particularly at low biomass concentrations (**Figure 3.5 a-b**). A short extraction time (0.25 h) yielded the highest alginate extraction with a high temperature (95 ºC) and a water content in the DES of approximately 20 wt% (Figure 5a). In contrast, a longer extraction time (2.8 h), at a low extraction temperature (40 ºC), resulted in higher alginate extraction efficiency with a water content of approximately 15 wt% (**Figure 3.5b**). This difference in optimal water content in the DES may be attributed to hydrogen bonding availability and the diffusion rates. At a short extraction times and high temperatures, an increased water content in the DES can enhance hydrogen bonding with alginate, making it more accessible. Conversely, at longer extraction times and lower temperatures, the water content can be reduced due to the extended extraction duration.

Similar trends were observed in interaction between the extraction time and water content at different temperatures (**Figure 3.5 c-d**). When a lower extraction temperature (44 ºC) was employed, a longer extraction duration resulted in higher alginate extraction yields (**Figure 3.5c**). Extraction efficiencies remained sub-optimal regardless of the water content at shorter extraction times. However, a high extraction temperature (90 ºC) increases alginate extraction efficiency when a short extraction time (0.25 h) was used (**Figure 3.5c**). Additionally, as extraction time increased from 0.25 to 3 hours, the optimal water content slightly increased from approximately 11 to 18 wt% (**Figure 3.5d**). Over time, the available alginate in the biomass decreases, making it less accessible. However, the increased water content improves the diffusion coefficient, helping to maintain sufficient alginate extraction efficiency.

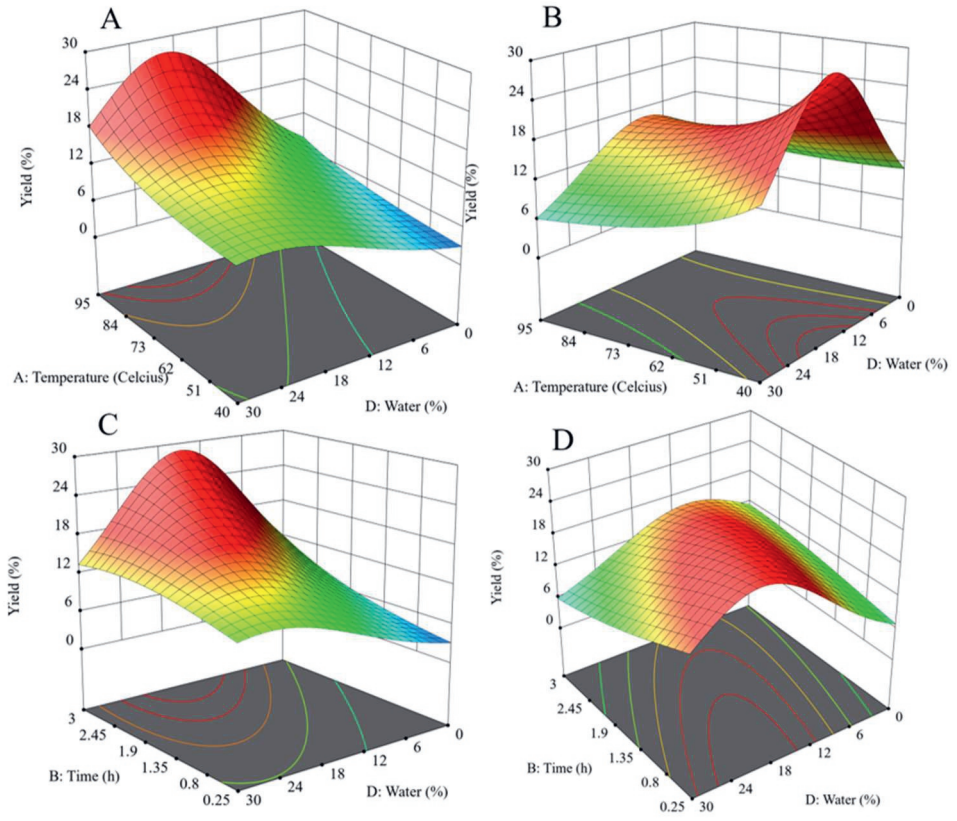


Figure 3.5 3D surface plots of alginate extraction efficiency with ChCl:U for interaction with (A) temperature and water content (biomass content = 2.5%, time = 0.25 h), (B) temperature and water (biomass content = 2.5%, time = 2.8 h), (C) extraction time and water content (biomass content = 2.5%, temperature = 43.9 ºC) and (D) extraction time and water content (biomass content = 2.5%, temperature = 90 ºC.

When comparing response surface methodologies for DES extractions from different biomasses, it is evident that optimal settings and interactions vary for each application. A study by Wojeicchowski *et al*. [32] found that increasing the extraction temperature enhanced antioxidant extraction from rosemary, using a DES composed of 15 wt% of N3333Cl, 55 wt% of 1,2-propanediol and 30 wt% of water. Additionally, a solid to liquid ratio of approximately 1:21 (4.8% of biomass) was identified as optimal. Saravana *et al*. [128] reported a sufficient solid to liquid ratio at 1:30 (3% of biomass) for extraction with the DES ChCl:Gly (1:2) (70% water) during subcritical water extraction from *Saccharina japonica*. They noted no significant impact for changing the water content of the DES between 50 and 70 wt%. In contrast, our study did observe a notable impact of the water content on alginate extraction, as here the water content remained lower (0-30 wt %), thus maintaining the DES hydrogen bonding. Shang *et al*. [62] studied

polysaccharide extraction using microwave-assisted DES extraction from *Fucus vesiculosus*. In their study, extraction with DES ChCl:1,4-butanediol (1:5) showed that only the water content (p=0.0029) was significant, while other factors, such as the solid to liquid ratio, did not significantly affect the results (p=0.3601). Given that the biomass content was the most influential parameter in this study, it suggests that extraction parameters differ among various brown seaweed species and DES.

These studies indicate that the influence of extraction parameters varies depending on the biomass, the extracted compound, and the composition of the DES used. Therefore, when investigating the extraction of a specific compound, all extraction parameters and different DESs must be considered.

Subsequently, optimised conditions were experimentally tested to increase the alginate extraction yield. A value of 20.02% ± 1.5 of alginate was extracted per g DW when operating at 93.89 ºC, for 1.69 hours, with 2.54% biomass and a water content of 16.89 wt% (**Figure S3.5**). With these optimised conditions, approximately 74% of the total alginate content was extracted from brown seaweed using solely DES as the extraction method. The yield obtained from the optimisation extraction was similar to the yield (20.6%) predicted by the model. Optimised DES extraction (74% extraction efficiency) thus greatly exceeds the conventional alginate extraction methods, which currently have alginate extraction efficiencies between 10% and 24.5% [122, 125, 126].

3.3.4 Alginate and DES characterisation

3.3.4.1 Alginate characterisation

The extracted alginate was identified using FTIR spectroscopy and SEC, to determine whether these different extraction procedures yield alginate with similar characteristics. The DES extraction with ChCl:U was compared to the current alkaline extraction (**Figure 3.6**). The spectra of isolated alginate for both extracts contained clear bands at 1400 and 1600 cm^{-1}, corresponding to carboxyl group (C=O) stretching (**Figure 3.6**). These two bands are characteristics of alginate [155]. Additionally, a broad band at 3300 cm^{-1} and a weak band at 2925 cm^{-1} were observed, correlating to hydrogen-bonded O-H and C-H stretching vibrations, respectively [155]. The bands at 813 and 900 cm^{-1} are assigned to α-L-gulopyranuronic asymmetric ring vibration and to the mannuronic acid residues, respectively, which are representative of alginate [122]. The molecular size of the extracted alginate from both the DES and alkaline methods was identified using SEC. From the standards, a polynomial equation was obtained with an R^2 of 0.9857 (**Figure S3.6**). The DES extracts contained, on average, 44% of alginate above 40 kDa, while the alkaline extract contained 55%. The molecular size of

the DES extract above 40 kDa was 582 kDa, while for the alkaline extract, it averaged 438 kDa (**Figure 3.6**).

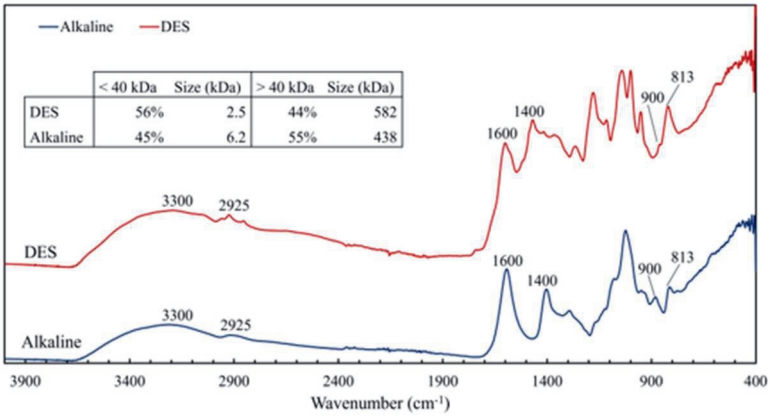


Figure 3.6 FTIR spectrum from alkaline extraction (1) and DES extraction (2) and molecular size distribution of isolated and purified alginate.

Based on the FTIR and SEC results, it can be observed that alginate extracted with DES does not differ significantly from that obtained through the current alkaline extraction process. Similar functional groups were detected in both extracts, and the extracted alginate displayed comparable molecular weights. Therefore, the DES extraction is unlikely to affect the extracted alginate differently compared to the alkaline method. Additionally, the molecular sizes of the extracted alginate were similar.

3.3.4.2 DES characterisation

FTIR spectroscopy was used to characterise DES ChCl:U, to analyse functional groups and assess hydrogen bond interactions between the hydrogen bond acceptor and donor [156]. Additionally, the integrity of the DES after addition of water, applied in the optimised extraction settings, was assessed. The FTIR spectra of pure choline chloride, pure urea and ChCl:U without water and with the optimal water content (16.89 wt%) were evaluated (**Figure 3.7**).

For pure choline chloride (**Figure 3.7a**), vibration bands at 3290 and 3020 cm^{-1} were present, corresponding to O-H and C-H stretching vibrations, respectively [157]. The band at 1490 cm^{-1} corresponded to an alkyl group [157, 158]. For pure urea (**Figure 3.7b**), the bands at 3455 and 1625 cm^{-1} are due to N-H stretching and deformation frequencies, respectively, while the band at 1677 cm^{-1} corresponds to C=O stretching. C-N stretching is indicated at 1455 cm^{-1} [159]. The DES ChCl:U showed bands at 3390-

3220 cm^{-1}, corresponding to the stretching bands of O-H and N-H groups (**Figure 3.7c**). The N-H bands appeared as deformed group due to hydrogen bond formation between urea and choline [160]. Previous research determined that hydrogen bonding with this DES occurs through the NH group of urea and the Cl of choline [161], confirming the trends observed in the FTIR spectra. Between the pure DES and the DES containing 16.89 wt% water (**Figure 3.7d**), no clear differences were observed, indicating that the DES maintained its hydrogen bonding between the HBA and HBD.

From the FTIR spectra, it was concluded that different functional groups from choline chloride and urea were present in the formed ChCl:U DES. Thus, the FTIR peaks observed in the formed DES indicate that the functional groups of the DES derive from those of choline chloride and urea. Upon the addition of water, the functional groups remain intact, thereby preserving the structure of the DES.

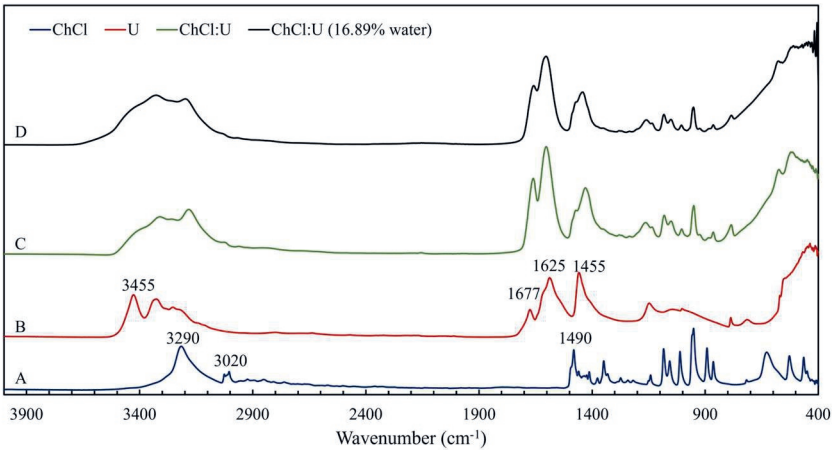


Figure 3.7 FTIR spectrum of pure choline chloride (A), pure urea (B), eutectic mixture ChCl:U (1:2) (C), and ChCl:U (16.89 %wt water) (D).

After optimising the DES extraction, an extraction efficiency of 74% of the total alginate was achieved, exceeding the conventional alkaline extraction method. Furthermore, the DES extraction using the natural deep eutectic ChCl:Urea could be a milder and more intensified process that does not employ toxic chemicals. ChCl:Urea is composed of non-hazardous substances and exhibits good biodegradability and relatively low ecotoxicity [162]**.** Deep eutectic solvents could be utilised for industrial applications to extract various bioactive components and can be applied to different biomasses due to their high extraction yields. A standardised methodology is needed to simplify the screening of DESs based on specific products, applications, and biomass types. When examining factors such as extraction temperature, duration, water content in the DES, and biomass concentration, it becomes clear that optimal

conditions are strongly dependent on the type of biomass and the desired extracted product. The primary influential factor for alginate extraction is the biomass to DES ratio. Additionally, the selection of DES, along with the specific compound to be extracted is crucial, as DES can have a disruptive effect on the biomass. Nevertheless, using DES as the sole extraction agent for alginate could serve as an intensified, suitable, and more environmentally friendly alternative to conventional extraction methods.

One of the main challenges remaining is the recovery of the extracted compounds from the DES and the recycling of the DES. Due to the low vapour pressure of these solvents, they cannot be evaporated. Suitable separation methods for recovering the DES from alginate need to be assessed before this process can be applied industrially and the solvent can be reused. The potential of using switchable DES for alginate extraction and separation should be considered, such as pH (acid base) [163, 164], temperature [165, 166] and CO_2 [167, 168] responsive DESs. These switchable DES could facilitate product recovery while allowing for solvent recycling. The effectiveness of these solvents for alginate separation needs further investigation.

3.4. Conclusion

This study investigated alginate extraction from *Ascophyllum nodosum* using eight different deep eutectic solvents (DESs) and optimised the process for maximum yield. Initial screening revealed that the DES-based process successfully extracted alginate with final product characteristics comparable to those obtained through traditional extraction. Among the solvents tested, ChCl:Urea (1:2 molar ratio) achieved the highest alginate yield at 5.58 ± 1.71% of dry weight. To further improve extraction, key parameters—extraction time, temperature, biomass-to-solvent ratio, and DES water content—were optimised. Results from ANOVA and response surface methodology (RSM) indicated that the biomass to solvent ratio was the most significant factor, with a 1:40 ratio maximising yield, likely due to enhanced alginate diffusion into the DES. For lower biomass levels, the water content of DES also influenced efficiency. Short extraction times (under one hour) resulted in higher yields with increased water addition (20 wt%) compared to longer extraction times, where only 15 wt% water was preferred. Under optimized conditions, the process achieved a yield of 20.02 ± 1.5% alginate per dry weight, which is 74% efficiency relative to total alginate content. FTIR and SEC analyses confirmed that DES-extracted alginate closely resembled traditionally extracted alginate, supporting DES as a mild, effective, and sustainable alternative for industrial extraction. This foundational work suggests that DES-based technology could be further explored in future studies to characterise the techno-functional properties of alginate for enhanced applications.

3.5. Supplementary Information

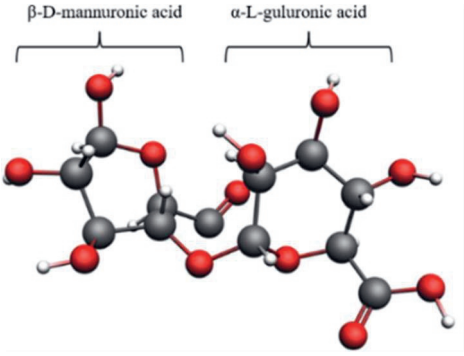


Figure S3.1 Chemical structure of part of alginic acid, represented by linked β-D-mannuronic acid and α-L-guluronic acid monomers.



Figure S3.2 Fresh *Ascophyllum nodosum* from Algaia used in the study.

Table S3.1 Molecular structures of the DES combinations used in this work.

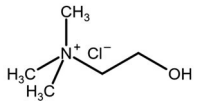
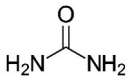
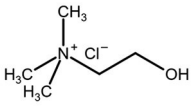
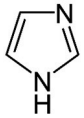
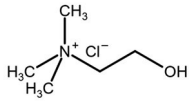
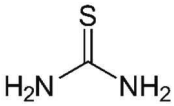
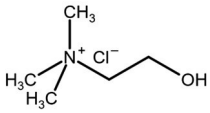
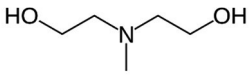
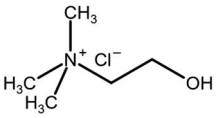
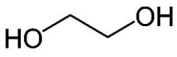
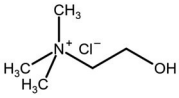
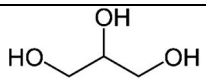
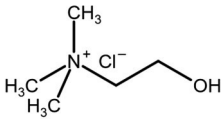
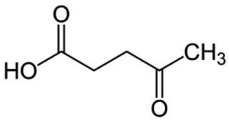
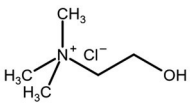
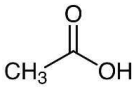
	DES	HBA	HBD
DES1	Choline chloride: Urea (1:2)		
DES2	Choline chloride: Imidazole (3:7)		
DES3	Choline chloride: Thiourea (1:2)		
DES4	Choline chloride: Methyldiethanolamine (1:6)		
DES5	Choline chloride: Ethylene glycol (1:2)		
DES6	Choline chloride: Glycerol (1:2)		
DES7	Choline chloride: Levulinic acid (1:2)		
DES8	Choline chloride: Acetic acid (1:2)		

Table S3.2 ANOVA fit values for the predictive model of alginate extraction.

Factor		Factor	
Std. Dev.	0.0480	R^2	0.9706
Mean	0.5047	Adjusted R^2	0.9293
C.V. %	9.50	Predicted R^2	0.8097
		Adeq Precision	19.0694

Solution for optimised alginate extraction conditions, with response (yield) set at a maximum.

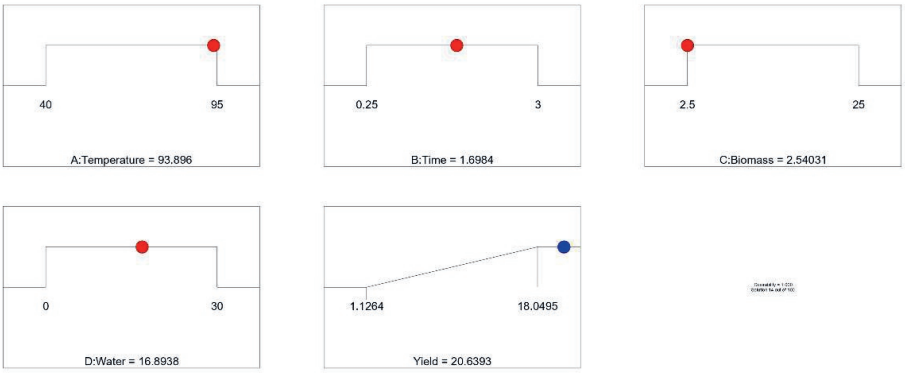


Figure S3.3 Optimised alginate extraction solution with a desirability of 1.

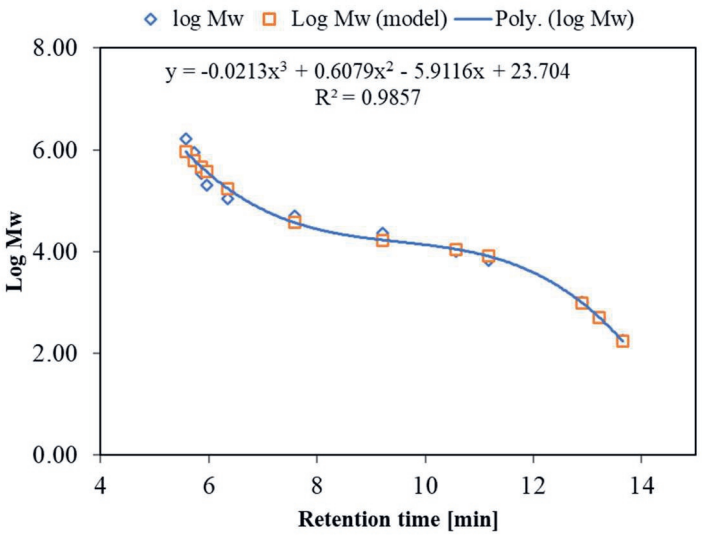
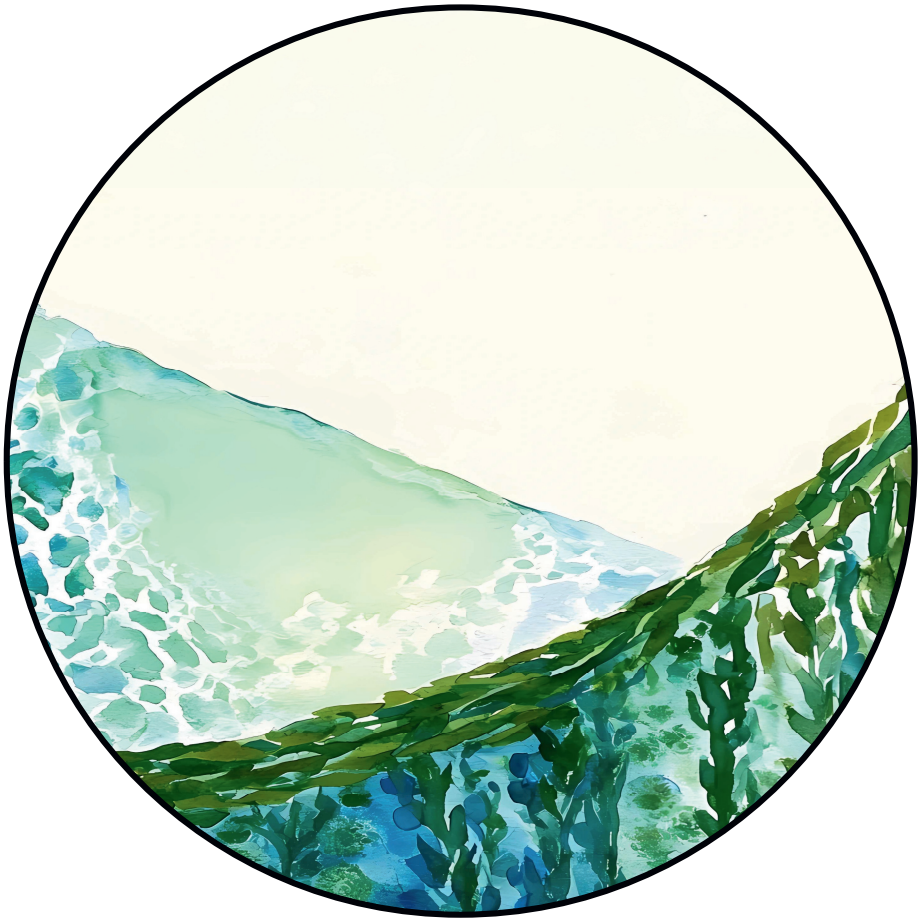


Figure S3.4 Standard curve of pullulan standards for size exclusion chromatography.



Chapter 4

Pressure-driven membrane processes for the recovery and recycling of deep eutectic solvents: A seaweed biorefinery case study

Oscar M. Elizondo Sada, Isa S.A. Hiemstra, Nattawan Chorhirankul, Michel Eppink, Rene H. Wijffels, Anja E.M. Janssen, Antoinette Kazbar

This chapter has been published as:

Elizondo Sada, O. M. E., Hiemstra, I. S. A., Chorhirankul, N., Eppink, M.H., Wijffels, R. H., Janssen, A. E., & Kazbar, A. (2024). Pressure-driven membrane processes for the recovery and recycling of deep eutectic solvents: A seaweed biorefinery case study. *Biotechnology Reports*, *43*, e00849. https://doi.org/10.1016/j.btre.2024.e00849

Abstract

Deep eutectic solvents (DES) are green alternatives for conventional solvents. They have gained attention for their potential to extract valuable compounds from biomass, such as seaweed. In this framework, a case study was developed to assess the feasibility of pressure-driven membrane processes as an efficient tool for the recovery of deep eutectic solvents and targeted biomolecules. For this purpose, a mixture composed of the DES choline chloride and ethylene glycol (ChCl:EG) 1:2, water and alginate was made to mimic a DES extraction from seaweed. An integrated separation process design was proposed where ultrafiltration-diafiltration-nanofiltration (UF-DF-NF) was coupled. UF and DF were found to be effective for the separation of alginate with an 85% yield. DES was likewise recovered by 93%, proving the membrane filtrations' technical feasibility. The NF performance to separate the DES from the water, for its recycling, laid by a 45%-50% retention and a final concentrated DES solution of 18%(v/v).

4.1. Introduction

The use of biomass to obtain bioproducts through biorefinery has become more feasible over the last years [169]. For sustainability reasons biorefineries must focus on the reduction of waste streams and hazardous chemicals employed [170]. Common extraction techniques still involve an unsustainable series of strong mineral acids and alkaline treatments [171]. To evade environmentally benign processes, new-age solvents such as deep eutectic solvents (DESs) have emerged as a promising alternative to conventional solvents, due to their sustainable nature and the possibility of intensifying processes by the prevention of mechanical cell disruption [172, 173].

DESs are composed of two (or more) compounds (a hydrogen bond donor -HBD- and a hydrogen bond acceptor -HBA-) that form a eutectic mixture when added in a specific molar ratio [174]. When compared to conventional solvents or even earlier-considered "green" solvents as ionic liquids (ILs), DESs exhibit lower to no toxicity, have lower production costs, are renewable and biodegradable [175, 176]. Furthermore, DESs have been praised for their excellent solvent capabilities, and their thermodynamic characteristics such as high thermal stability, low volatility, low vapor pressure, and tuneable polarity [9, 117]. As a result of their proven technical feasibility, DESs can be implemented for the development of sustainable and circular biorefineries [177, 178]. Nevertheless, DESs are difficult to separate from their extracted products due to the low volatility and low vapour pressure and strong intramolecular interactions with the extracted products as well [179]. The challenge on back extraction limits the use of DESs in the industrial and commercial market, as recovery and recycling are important for the reduction of costs and carbon footprint [178].

Separation processes such as liquid-liquid extraction, solid-liquid extraction, crystallization, short-path distillation, and anti-solvent addition have been studied for DES. Results, however, have not been consistent, mostly due to scarce research and yield variability in dependence on targeted compound and type of DES used [69]. Membrane processes have a lower energy consumption, higher flexibility, lower cost-to-performance ratio, and favour more recycling when compared to other separation processes [180]. Thus, membrane processes have been listed as alternatives for the recovery and recycling of DESs.

Despite this, too little research has been performed employing this type of separation process. As a matter of fact, only a coupled ultrafiltration and electrodialysis module has been used as was reported previously in the work by Liang *et al*. [83], where DES was recovered with a yield of 97%. This result shed light on the potential application of membrane technology for the recovery and recycling of DESs.

The aim of this study is to explore the use of a coupled membrane filtration system for the separation of a bioproduct from DES, while recycling the solvent. This is used as a case study and proof of concept, for the first time, under the seaweed biorefinery scope. Alginate was the target molecule, because it currently recovered from seaweed in an unsustainable process [181]. The DES selected was choline chloride – ethylene glycol 1:2 (ChCl:EG 1:2), as it has been reported to have significant extraction yield of alginate from brown seaweed [128]. Physiochemical parameters of this DES were assessed experimentally and via the software COSMO-RS. An ultrafiltration-diafiltration process was applied to separate alginate and recover the DES by washing it out. Different pressure levels, concentration factors and water content were evaluated for their impact on the membrane separations. A nanofiltration unit was further coupled to the process to concentrate the DES by permeating water through the membrane to explore the feasibility of stream recirculation.

4.2. Materials and methods

4.2.1 DES preparation

The DES ChCl:EG was prepared in a 1:2 molar ratio, by mixing choline chloride and ethylene glycol (Sigma Aldrich) at 80 °C in a water bath for 1 h until a translucid liquid was obtained. The molecular weight (MW) of this DES is 263.76 g/mol. Due to the hygroscopic nature of choline chloride, the Metrohm KF Coulometer was used to verify the absence of water (<0.65 wt.%) in the produced DES.

4.2.2 DES physicochemical characterisation

The Anton Paar ViscoQC 300 Rotational Viscometer was used to measure the viscosity of the DES over a temperature range between 25 °C – 70°C.

Viscosity can be described by the Arrhenius-type model, (**Equation 4.1**), which is the most used [182]. Here, η_0 (mPa·s) is a constant, Ea (kJ/mol) the activation energy, R = 8.314 J·mol/K the ideal gas law constant, and T (K) the temperature.

$$\eta = \eta_0 e^{\frac{-Ea}{RT}} \quad (\mathbf{4.1})$$

The software COSMO-RS (Conductor-like Screening Model for Real Solvents) was used for the confirmation of the DES's affinity towards alginate, and for generating the activity coefficient plot. The Mettler Toledo Seven Compact Conductivity Meter was employed to measure the conductivity of the DES. Due to the known relationship between conductivity and DES fraction, it has been proposed as a fast and efficient method to quantify DES in streams [183, 184]. The DES presence in the different streams was measured by correlating it with a DES ChCl:EG 1:2 conductivity standard calibration curve, shown in **Figure 4.1**.

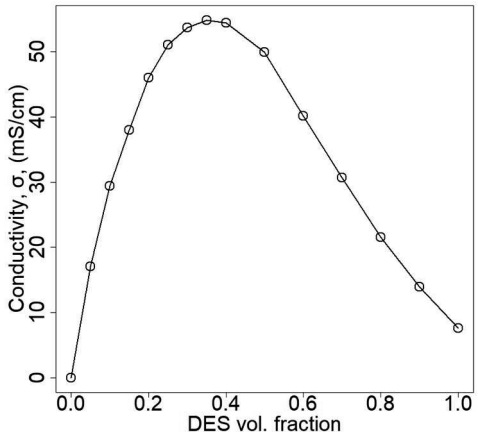


Figure 4.1 Conductivity as a function of the DES ChCl:EG 1:2 molar fraction.

4.2.3 Sample preparation and alginate determination

Samples consisting of DES/H_2O in 10%, 25%, 50% (v/v%) were prepared to evaluate the effect of water during the membrane filtrations. Alginic acid sodium salt from brown algae (Sigma Aldrich) was added to each sample in a concentration of 1 g/L to mimic a mixture from an alginate extraction. Alginate determination was carried out following the 96-well plate uronic acid carbazole reaction proposed by Cesaretti *et al*. [136]. The reagents carbazole, sulphuric acid, sodium tetraborate, absolute ethanol and D-galacturonic acid were obtained from Sigma Aldrich.

4.2.4 Membranes

For the UF- DF experiments, a polyethersulfone (PES) ultrafiltration flat sheet membrane (LY series) from Synder Filtration™ with molecular weight cutoff (MWCO) of 100 kDa was used.

For the NF experiments, a spiral wound membrane (GE series) made of polyamide-TFC from SUEZ with a MWCO of 1000 Da and an effective membrane area of 0.37 m^2 was employed.

4.2.5 Ultrafiltration and diafiltration set-up and experimental procedure

Dead-end ultrafiltration was performed in a pressurized and mechanically stirred set-up, utilizing a Millipore Stirred Cell (Amicon® Stirred Cell 400 mL) with an effective membrane area of 44.2 cm^2. The stirrer velocity was kept constant throughout all experiments at 400 rpm (1.57 m/s). The pressure levels of 1.4, 2.0, 2.8 bar were tested for each of the samples with a volume of 200 mL. The experiments ran for 120 min, which provided enough time to reach a steady-state condition. Analysis of variance (ANOVA) was performed to test the effects of the conditions. Before each experiment, the membranes were flushed with MilliQ water under pressure, and permeability tests were performed at the same pressure levels of all experiments. The UF/DFs were performed in the same set-up. The pressure was kept constant at 1.4 bar based on the preliminary UF experimental results. Three different volumetric concentration factors (VCF = 2, 3, 4) were investigated and MilliQ water was added as diafiltrate buffer to bring the total volume back to the original volume after each filtration. Diavolumes (N) were performed in each experiment until the conductivity in the permeate laid below 1 mS/cm, as that indicated that the DES concentration was insignificant and therefore washed-out. All tests were performed at room temperature. The permeate flux was calculated by first sampling over time and weighting on an Ohaus™ Explorer™ analytical balance and subsequently converted to volumes utilizing the density, as shown in **Equation 4.2**:

$$J = \frac{1}{A\rho}\frac{m}{\Delta t} \quad (\mathbf{4.2})$$

Where J is the permeate flux ((L/(m^{-2}h)), A is the effective membrane area (m^2), ρ is the density (g/L), m the weight of the permeate (g), and Δt the time the sample was collected (h).

The alginate rejection was defined by **Equation 4.3** [185]:

$$R = \left[\frac{\ln\left(\frac{C_R}{C_F}\right)}{\ln(VCF)}\right] \quad (\mathbf{4.3})$$

Where R is the rejection of alginate expressed in percentage, C_F and C_R are the concentrations of alginate in the feed and retentate, respectively. VCF is the volumetric concentration factor (given by: $\frac{V_F}{V_R}$, where V_F and V_R are the volumes of the feed and retentate, respectively).

DES recovery was calculated following **Equation 4.4.**

$$\%R_{DES} = \frac{V_{DES}^F}{\sum V_{DES}^P} * 100 \quad (\mathbf{4.4})$$

Where $\%R_{DES}$ is the recovery of the DES and V_{DES}^F the volume of the DES in the initial feed solution and V_{DES}^P the volume of DES permeated from each stage of the UF/DF.

4.2.6 Nanofiltration set-up and experimental procedure

Nanofiltration of the resulting DES/H_2O mixture post UF/DF was done in a continuous pilot and spiral wound set-up [186, 187]. The feed solution, comprised of DES/H_2O at a 6.4% (v/v%) ratio, was circulated with an operational crossflow velocity of 0.1 m/s. Pressure levels of 10, 15 and 20 bar were set. The temperature was held constant throughout the experiments at 25±0.5°C. Each condition ran for 45 min to reach steady state. After the time had elapsed, samples from the permeate and retentate were collected to analyse the DES fraction in each stream. Cleaning-in-place (CIP) was performed before and after the experiment following the cleaning procedure from Sealed Air, Diversey Care (The Netherlands).

4.3. Results and discussion

4.3.1 DES characterisation

The viscosity and activity coefficient of the DES ChCl:EG (1:2) were assessed for the membrane filtration case study. Viscosity can be one of the main roadblocks of DESs for practical purposes due to mass transfer limitations [188, 189]. The viscosity of the DES showed no shear rate dependency on the viscosity, indicating Newtonian fluid behaviour. Moreover, the relation between viscosity and temperature fitted validly within an Arrhenius model (Ea = -27.03 kJ/mol and η_0 = 8.52x10^{-4} mPa·s, **Figure 4.2**).

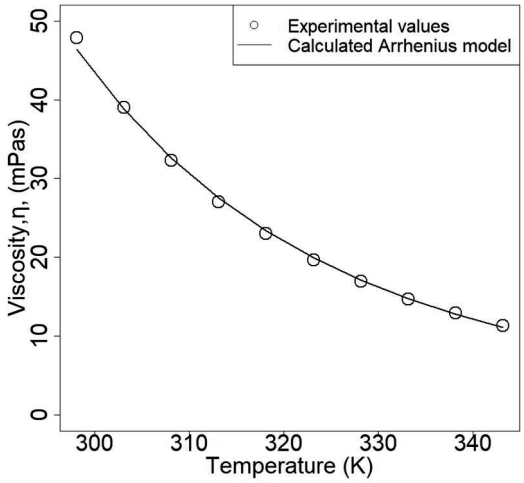


Figure 4.2 Experimental and calculated viscosity values for the DES ChCl:EG 1:2 over a range of temperatures.

The viscosity of the DES at 25°C (47.8 mPa·s) was approximately 50 times higher than that of water, thus posing possible mass transfer challenges during extraction. To improve mass transfer of alginate to the DES, either the temperature or the water content of the DES can be increased. The first option would require extra energy input for heating and the viscosity would still be approximately 10-fold higher than water (**Table 4.1**). On the contrary, the addition of 25% water decreases the viscosity fivefold, and a fifteen times decrease is obtained when 50% of water is added. This decrease in viscosity not only allows better mass transfer, but also it can avoid membrane fouling during the separation process [190].

Table 4.1 Viscosity of DES ChCl:EG 1:2 at different concentrations.

	DES concentration v/v% / (mol. fraction, *x*)			
	100% (*1*)	50% (*0.07*)	25% (*0.04*)	10% (*0.01*)
γ (-)	1.00	4.77	7.32	18.03
η (mPa·s)	47.82	3.20	1.60	1.12

Water addition does impact, however, the activity coefficient (γ) of the DES. The activity coefficient describes the thermodynamic intermolecular interactions and is used for the evaluation of the extracting capacity of solvents [191, 192]. For extraction operating conditions, γ values from 10 to 100 indicate weaker interactions, whereas values below 10 indicate strong interactions between solute and solvent [193]. The γ- value of ChCl:EG (1:2) in a mixture with water remains within practical purposes limits until the point where the mixture is composed of less than 0.01 mole fraction DES (**Figure 4.3**). Therefore, for this study the DES/H_2O ratios presented (**Table 3.1**) were selected to evaluate its effect on the membrane filtration performance.

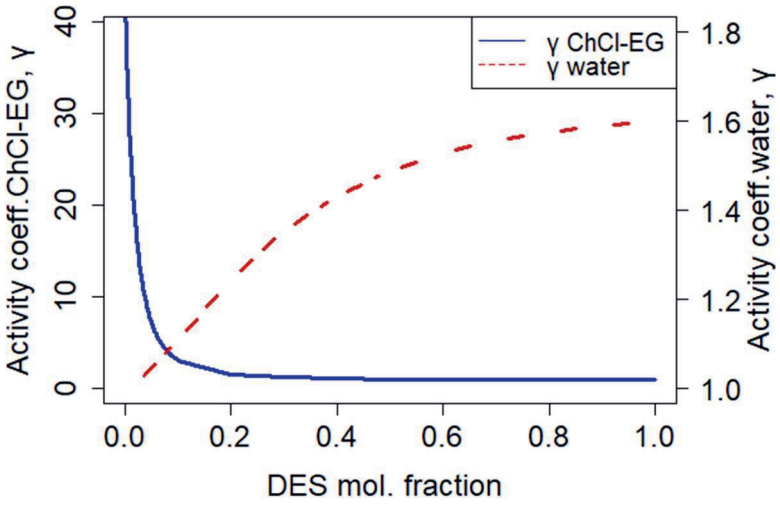


Figure 4.3 Activity coefficient of DES ChCl:EG 1:2 and water as a function of the DES mol fraction.

4.3.2 Ultrafiltration and diafiltration

Dead-end ultrafiltration was carried out to understand what the effects of the water content and the pressure are on the DES on the filtration performance when alginate is targeted to be retained. The permeability of the flat sheet membrane was found to be 64.1±1.1 L/($m^2 \cdot h \cdot bar$). The permeate flux behaviour for each DES/H_2O ratio with 1 g/L alginate is shown in **Figure 4.4**.

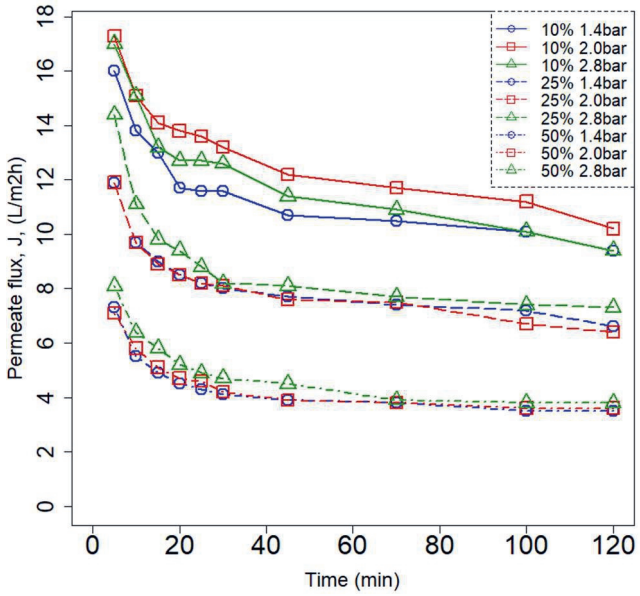


Figure 4.4 Permeate fluxes at 10%, 25% and 50% DES/water ratios under three pressure levels. The PES membrane had a cut-off of 100 kDa.

A significant decrease in flux occurs as the DES concentration is increased. Nonetheless, the pressure levels do not affect the permeate flux ($p > 0.05$), thus an increase in pressure would not directly translate into a flux increase. This behaviour may be attributed to two factors. On one hand, the viscosity of the solvent is higher as the DES concentration increases. In accordance with Fick's Law and the Einstein Stokes relation, this will result in diffusion limitation through the membrane [194]. On the other hand, formation of a layer on the membrane surface, either by alginate or species of the DES, could have developed and hindered permeation through the membrane. This in turn would prevent the pressure from having a direct effect on the permeate flux. Alginate was successfully rejected as shown in **Table 4.2**. At a DES /H_2O ratio of 50%, the alginate rejection was lower. A possible explanation could be that the diffusivity of the solutes affected the mass transfer mechanism at the polarization layer.

Table 4.2 Alginate and DES rejections at different DES/water concentrations and pressures.

Alginate rejection	**1.4 bar**	**2.0 bar**	**2.8 bar**
10% DES/H_2O	0.95	0.95	0.96
25% DES/H_2O	0.92	0.93	0.94
50% DES/H_2O	0.82	0.81	0.84

Conductivity measurements were done to quantify the DES in the permeate stream and evaluate its recovery. For the 10%, 25% and 50% samples, the DES recovery was 47.9±2.7%, 32.6±0.9% and 16.1±1.4%, respectively. Based on the results, ultrafiltration-diafiltration (UF/DF) steps were carried out to fully recover the DES while retaining the alginate. The ultrafiltration works as a pre-concentration step, whereas the diafiltrations are targeted to wash out the DES. This type of configuration, with involving DESs, has been reported previously by Gholami *et al*. [195]. For this coupled membrane process, the pressure was set at 1.4 bar, and a 25% DES/H_2O ratio was used. The latter is due to its resemblance to a pure DES extraction on fresh seaweed which contains approximately 80% water. Besides, it has been reported that a high water content in DES (≈70%) improves polysaccharide extraction yield from brown seaweed [128, 196]. Furthermore, at a 25% v/v DES/H_2O, values for both viscosity and the activity coefficient are within operating conditions (**Table 4.1**). The volumetric concentration factor (VCF), defined in **Section 4.2.6**, and the number of diavolumes (N) were variables that were studied. **Figure 4.5** shows the behaviour of the UF/DF permeate flux over time. Since the concentration of the DES decreases in every filtration step by the addition of water in each diavolume, the solution becomes less viscous, resulting in an increasing flux pattern of 1.90, 2.49, and 2.51 times for the VCF 2,3,4, respectively. The diavolume additions are graphically seen as the peaks in each of the curves.

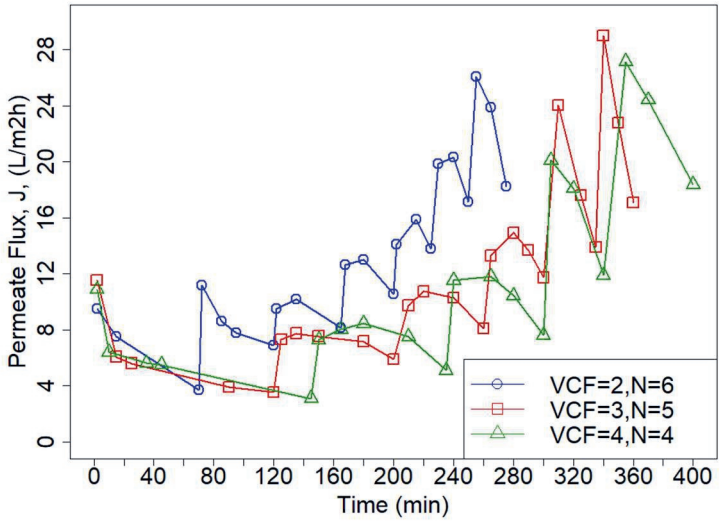


Figure 4.5 UF/DF permeate fluxes over time.

Conductivity measurements revealed that after 4 filtrations (UF - 3 DF), the maximum possible recovery of the DES was reached for the three of the conditions (82.2%, 93.3%, 93.5%), as shown in **Figure 4.6**. Additionally, the rejection coefficient of the membrane

for the DES was found to be 0.37±0.06. No difference between the experiments with a VCF of 3 and 4 was observed. However, for a VCF of 2, the recovery of the DES laid below 90%. This could be due to the bigger volume still held at the retentate side compared to the other two conditions.

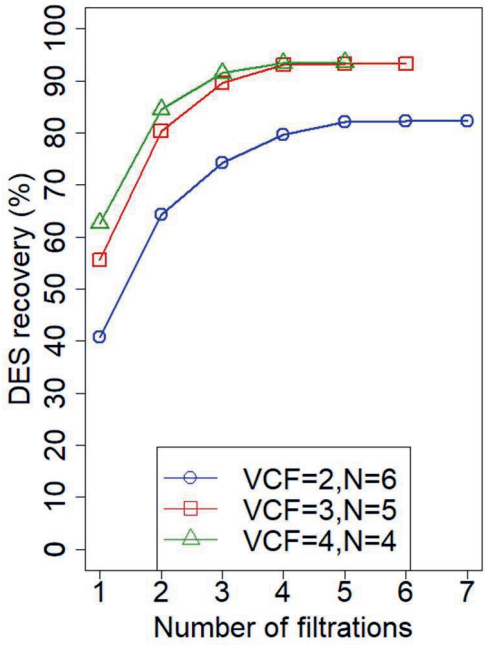


Figure 4.6 DES ChCl:EG 1:2 recovery as a function of filtration steps.

Based on the experimental results, proving the efficacy of UF/DF for DES and alginate separation, a separation process design is proposed in **Figure 4.7**. This overall process is a coupled cascade membrane filtration system with three final outlet streams. In this process, the feed solution enters a continuous ultrafiltration-diafiltration system with a working pressure of 1.4 bar. The ultrafiltration step is applied as a pre-concentration step to reduce the volume and to keep the alginate retained. The diafiltrations will dilute the previous retentate stream in order to permeate the DES and to retain alginate. The DF process with a VCF of 3 can be regarded as most suitable option out of the tested conditions. This is due to the high DES recovery yield (93.3%) obtained here and the lower processing time required than a VCF of 4. After the UF/DF, the permeated total volume had a 6.4% (v/v) DES/H_2O concentration, thus being highly diluted. Therefore, a nanofiltration was coupled to the process design to further concentrate the DES and to possibly recover both streams.

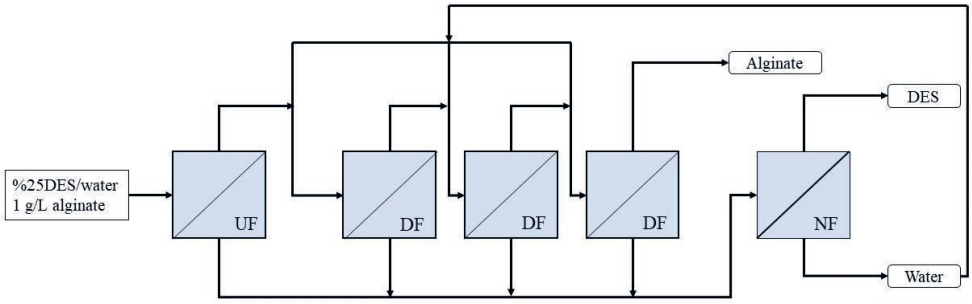


Figure 4.7 Proposed integrated separation process for alginate retention and DES recovery and recycling.

4.3.3 Nanofiltration

Nanofiltration was performed in a pilot spiral wound single-stage configuration, graphically shown by Montesdeoca *et al*. [186]. The separation of the DES ChCl:EG (1:2) from water was studied. This allows for solvent recirculation, as well as reutilisation of the water stream. The feed for the nanofiltration was a 6.4% (v/v) DES/H_2O solution permeated after the UF/DF. The permeability of the spiral wound membrane was 2.12 L/($m^2 \cdot h \cdot bar$). **Figure 4.8** shows the results from the NF experiments. The permeate flux increased linearly in each pressure level, meaning that the flux was not hindered in the studied pressure range.

After reaching steady state, the permeate conductivity was measured to quantify the DES that passed through the membrane. Retention of the DES was found to lay at 44.2%, 45.0% and 51.7% for the pressure levels of 10, 15 and 20 bar, respectively. The results are in agreement with previous studies. Abels *et al*. [183] reported that at lower feed mass fractions, the applied pressure plays a main role in the separation of the solvent from the aqueous mixture. Haerens *et al*. [184] used a nanofiltration and reverse osmosis (RO) module to separate the DES ChCl:EG (1:2), obtaining just a 20% retention with the NF and up until 88% with the RO. The higher retention obtained compared to the previously mentioned study, could be due to the dissociation of the DES into its components and possibly the chlorine ion adsorbing to the membrane due to its negative charge.

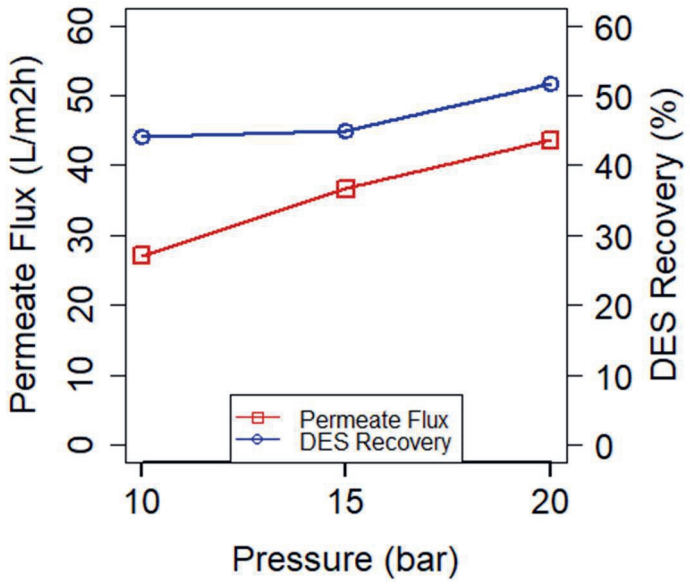
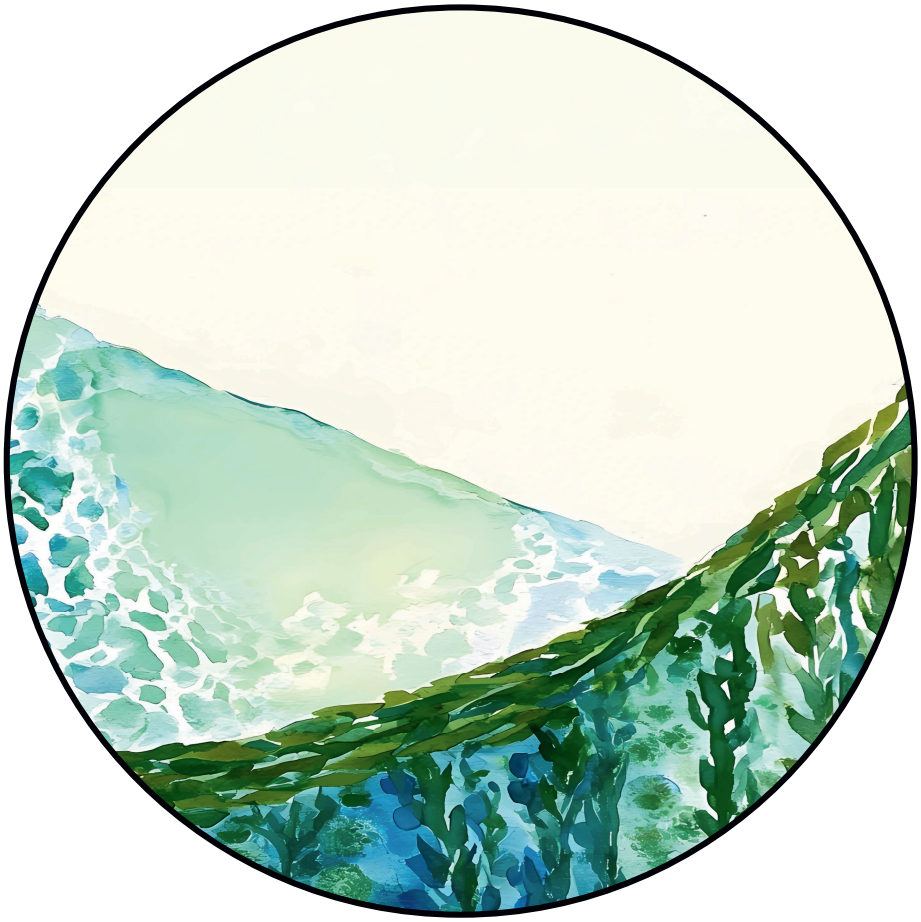


Figure 4.8 Permeate flux and DES recovery during the nanofiltration experiment. The process was configured in a pilot spiral wound set-up.

4.4. Conclusion

The use of deep eutectic solvents in a commercial scale can be hindered by difficulties in the separation of extracted compounds, and the recovery of them. In this study, the concept to use ultrafiltration/diafiltration and nanofiltration was proven to be effective as a sustainable alternative for the separation and recovery of deep eutectic solvents and alginate. And for the first time a membrane filtration separation process design involving DESs was proposed for a seaweed biorefinery case study. The process consisted of coupled membrane filtrations (UF-DF-NF), with the aim of separating alginate from a DES/H_2O mixture. Ultrafiltration and diafiltration effectively separated alginate with an 85% yield from the DES, and the DES was recovered by 93%. Nanofiltration underperformed to further purify the recovered DES, as the DES ChCl:EG 1:2 was retained to a final 18% concentration (v/v%). Further research on the separation of DES from water is recommended and different pressures and MWCO to be tested. Notwithstanding, this case study approach leads to conclude that there is technical feasibility for the use of pressure driven membrane processes for the separation of targeted biomolecules from DESs. Likewise, the use of membrane filtrations may be used for the recovery and recycling of deep eutectic solvents.



Chapter 5

Process intensification of seaweed biorefinery using reusable natural deep eutectic solvents

Isa S.A. Hiemstra, Michel H.M. Eppink, Marco Bravi, Rene H. Wijffels, Antoinette Kazbar

This chapter has been published as:

Hiemstra, I. S.A., Eppink, M. H., Bravi, M., Wijffels, R. H., & Kazbar, A. (2025). Process intensification of seaweed biorefinery using reusable natural deep eutectic solvents. *Journal Of Environmental Chemical Engineering*, *13*(5), 119184. https://doi.org/10.1016/j.jece.2025.119184

Abstract

Conventional alginate extraction methods from brown seaweed typically rely on harsh chemicals that are not reused, and valuable pigments are lost during this process. This study applied a novel approach utilising reusable natural deep eutectic solvents (DES) in three-phase partitioning (TPP) to simultaneously extract alginate and pigments from *Saccharina latissima*. The hydrophobic DES effectively released alginate from the algal cell wall in the aqueous phase and served as a solvent for pigment extraction. Computational screening confirmed that all selected DES had an affinity for pigments chlorophyll *a* and fucoxanthin, while alginate extraction confirmed their role in disrupting the algal cell wall. Extraction conditions were optimised, resulting in an alginate yield of 101.8 ± 3.1 mg/g DW compared to 55.3 ± 14.1 mg/g DW for conventional alkaline extraction. According to physicochemical characterisation through FTIR and M/G ratio (mannuronic to guluronic) analysis, the extracted alginate was comparable to that obtained via alkaline extraction, exhibiting similar functional groups and M/G ratios. The DES was reused successfully, showing that it could be reused for up to seven extraction cycles, during which pigments accumulated. After the seventh cycle, alginate yield declined, likely due to partial transfer into the DES phase, possibly driven by reverse micelle formation in the system. This study highlights a novel, mild multiproduct approach of a DES-based TPP system, enhancing economic feasibility by employing gentler and quicker extraction conditions. It facilitates the concurrent recovery of alginate and pigments while allowing for the repeated reuse of the DES.

5.1. Introduction

The need for alternative, greener extraction solvents is becoming increasingly urgent due to the environmental and health risks associated with conventional solvents [197]. Traditional solvents can be toxic, flammable, and volatile, contributing to pollution, human health issues, and hazardous waste. Therefore, the development of sustainable alternative solvents is essential. Deep eutectic solvents are an emerging class of novel solvents that could potentially replace these organic extraction solvents [198, 199]. DES are solvents composed of one or more hydrogen bond donors (HBD) and hydrogen bond acceptors (HBA), that are formed upon a large depression in melting point when mixed at a certain ratio. They are favourable solvents due to their low volatility, ease of preparation, low costs, and potential recyclability [10, 200, 201].

Over the past decades, DES have gained attention in a wide range of fields, including pharmaceuticals [202, 203], separation processes [203], and renewable energy [204]. Thanks to their tuneable properties and environmental compatibility, these solvents are being explored for applications such as drug solubilization, metal recovery, and used as electrolytes in energy systems [205, 206]. Specifically, DES have been successfully used to extract various bioactive compounds, including polysaccharides [119, 207], lipids [208], proteins [209], and polyphenols [72] from diverse biomass sources, including plants, microalgae, and seaweed. However, many studies do not report on recovery and reuse, which compromises the environmental sustainability of the process. The overall impact is also strongly influenced by the preparation step, as the choice of constituents used to form a DES largely determines it environmental footprint [152, 210]. Furthermore, Life Cycle Assessment (LCA) studies have demonstrated that DES can be more sustainable than conventional organic solvents, provided they are efficiently recovered and reused [211]. Yet, their low vapour pressure poses challenges for product isolation and solvent recovery, meaning that research on reuse strategies remains limited and warrants further investigation [70].

Seaweed emerges as an attractive, sustainable, renewable biomass for DES extraction due to its high abundance, rapid growth rate, and diverse biochemical composition. Brown seaweeds, in particular, are rich in compounds such as alginate, fucoidans, and valuable pigments [212]. Among these components, alginate stands out for its versatility and wide range of applications (**Figure S5.1**). This polysaccharide is widely used within a variety of sectors, including food processing as a thickening and gelling agent and medicine for drug delivery and tissue engineering [123]. In addition to its polysaccharide content, brown seaweed is a rich source of high-value pigments, including chlorophylls and fucoxanthin (**Figure S5.2**). Chlorophyll *a* is a bioactive compound with health-related benefits, including antimutagenic and antioxidant

activities [213]. Fucoxanthin is a xanthophyll that exhibits antioxidant, anti-inflammatory, and anti-cancer properties [214, 215]. Due to their market value and diverse biological activities, both pigments present a wide range of potential applications. Conventional alginate extraction methods typically rely on hazardous chemicals and involve multiple acidic and alkaline processing steps, resulting in excessive water consumption and high energy demand [56, 124]. Additionally, pigments are lost during the process and cannot be recovered due to the harsh chemical conditions employed.

Our previous study demonstrated that alginate can be efficiently extracted using DES [100]. However, DES reuse was not addressed, as alginate recovery relied on precipitation. Direct extraction with hydrophilic DES complicates recovery due to strong hydrogen bonding. Moreover, the study focused solely on alginate, without considering the recovery of other valuable compounds such as pigments, limiting full biomass utilisation. To overcome these challenges and maximise biomass utilisation, hydrophobic DES offer a promising alternative. They could be applied as a novel approach for indirect alginate extraction while facilitating easy DES recovery and subsequent reuse. As an extraction agent, hydrophobic DES would allow alginate to migrate to a separate, hydrophilic phase. Simultaneously, hydrophobic DES could also be employed for pigment extraction from brown seaweed. Several studies have already demonstrated the effectiveness of DES in extracting pigments from various biomasses, including brown seaweed [216], microalgae [93] and plants [217].

Building on this concept, three-phase partitioning (TPP) with DES presents an innovative approach to further enhance the extraction process. TPP is a liquid-liquid extraction technique that enables the simultaneous concentration and purification of biomolecules. It offers a mild and efficient approach for separating alginate and pigments from brown seaweed. In traditional TPP systems, an organic solvent and an aqueous salt solution are usually applied to the biomass [218], resulting in three distinct phases: an organic top phase containing pigments or lipids, a middle phase containing the residual biomass, and an aqueous bottom phase containing polysaccharides or soluble proteins. Replacing the widely used toxic solvent *t*-butanol with DES [219–221] could enhance the environmental sustainability of the system while preserving its extraction efficiency. DES have already been successfully integrated into TPP systems for the extraction and purification of polysaccharides from grape seeds [163] and tomato peroxidase [222]. However, they have not yet been applied in a multiproduct approach, utilising both the salt and DES phases. The dual application of DES as both a biomass pretreatment agent for alginate release and an extraction solvent for pigments represents a novel and innovative approach to

integrated biorefinery processes. This strategy enhances resource efficiency and has the potential to maximise the economic viability of the process through the simultaneous recovery of both high- and low-value products, while enabling DES reuse.

In line with this, this study developed a three-phase partitioning system that uses natural deep eutectic solvents for a multi-product extraction of alginate and pigments from *Saccharina latissima*. Nine DES were computationally evaluated with the software COSMO-RS (Conductor-like Screening Model for Real Solvents) to evaluate their pigment extraction capabilities. This was followed by laboratory testing to determine their alginate extraction yield. Under optimised conditions, the DES's reuse potential within a three-phase partitioning (TPP) system was assessed while enabling pigment accumulation in the DES phase. This study introduces an innovative and sustainable multi-product approach to extract various compounds from brown seaweed efficiently.

5.2. Materials and methods

5.2.1 Materials

Brown seaweed *Saccharina latissima* was harvested in May 2023 from Kamperland (Zeeland, The Netherlands). The collected biomass was stored at -80 °C until it was utilised. Prior to extraction, the biomass was ground into a fine powder using a GRINDOMIX GM 200 (Retsch) grinder. The ground seaweed was then freeze dried until it reached a dry weight content of at least 93% After freeze drying, the seaweed was sieved using 710 µm and 90 µm mesh sizes. The fraction between 90 and 710 µm was collected and used for subsequent extraction. To extract and isolate bioactive compounds from the seaweed using TPP, nine different DES were employed. Fatty acid-based and linalool-based HBAs and HBDs were selected (**Table 5.1**). Dodecanoic acid (purity 98%), octanoic acid (purity > 99%), nonanoic acid (purity > 97%), decanoic acid (purity > 98%), hexanoic acid (purity > 98%), linalool (purity > 97%), ammonium sulphate (purity > 99.5%), Jeffamine D-230, hydrochloric acid (purity 37%), menthol (purity 99%) and thymol (purity >98.5%) were purchased from Sigma Aldrich (Merck).

Table 5.1 Composition of DES used in this study.

	HBA	HBD	Mole ratio	Reference
DES1	Dodecanoic acid	Octanoic acid	1:1	[163]
DES2	Dodecanoic acid	Nonanoic acid	1:1	[163]
DES3	Dodecanoic acid	Decanoic acid	1:1	[163]
DES4	Dodecanoic acid	Hexanoic acid	1:1	
DES5	Octanoic acid	Decanoic acid	2:1	[223]
DES6	Linalool	Dodecanoic acid	1:1	
DES7	Linalool	Decanoic acid	1:1	[224]
DES8	Linalool	Nonanoic acid	1:1	[224]
DES9	Linalool	Octanoic acid	1:1	[224]

5.2.2 DES preparation

The DES were prepared according to the heating method [200]. The HBA and HBD were mixed in the appropriate molar ratio provided from literature and experimental screening (**Table 5.1**). The mixture was then heated at 50 °C for approximately 15 minutes until a translucent solution was formed. These DES solutions were subsequently used for the extraction of alginate and pigments with TPP.

5.2.3 Computational DES screening for pigment affinity

The software COnductor-like Screening MOdel for Real Solvents (COSMO-RS) was applied for the initial affinity screening of the pigments chlorophyll *a* and fucoxanthin, and for determining the octanol-water partitioning coefficient (logP) of the DES and pigments. The octanol-water partitioning coefficient (logP) was estimated using COSMO-RS to assess the hydrophobicity of both the DES and pigments. Less polar compounds have higher logP values than polar compounds. COSMO-RS is a quantum chemical software that can predict the thermodynamic properties of fluid mixtures [141]. With COSMO-RS (Software for Chemistry and Materials BV (SCM), Amsterdam, The Netherlands), the DES were screened by generating the activity coefficient of the solvents, followed by calculating the capacity of each DES. The activity coefficient (γ) is defined as the ratio of a species' activity to its mole fraction, and it reflects the deviation from ideal solution behaviour. It represents the interaction between the pigments and each DES at infinite dilution. COSMO-RS within the ADF (Amsterdam Density Functional) was used for screening. The settings used were selected according to Xu *et al*. [93]**.** The capacity of each solvent, indicating the maximum solubility in the DES, was calculated using the inverse of the activity coefficient as shown in **Equation 5.1**:

$$Capacity = 1/\gamma \quad (\mathbf{5.1})$$

where γ represents the activity coefficient of chlorophyll *a* or fucoxanthin at infinite dilution in the solution.

5.2.4 Alginate extraction, characterisation and quantification

Alginate was extracted by combining dried seaweed and an ammonium sulphate solution (30 wt%) with a DES in a solid to liquid ratio of 1:40. Ammonium sulphate was chosen as salt in the aqueous phase due to its widespread use in three-phase partitioning [221, 222, 225, 226]. The DES and ammonium sulphate were added in a 0.5:1 volume ratio. As a control, alginate was extracted with only the ammonium sulphate solution. A second control involved alkaline extraction to allow comparison with conventional alginate recovery methods. For alkaline extraction, acid water containing H_2SO_4 (pH 1.9) was added to the seaweed in a 1:1 (w/w) ratio and left to rest at room temperature for one hour. Next, Na_2CO_3 was added in a ratio of 0.0325:1 (w/w) to the stream for a one-hour extraction at 55 ºC [56]. The extractions were performed at 55 ºC for 30 minutes, and the solutions were vortexed every 5 minutes. After extraction, solutions were centrifuged, resulting in a three-phase separation. The DES phase and precipitation phase were separated from the bottom salt solution phase. The salt phase was dialysed and thereafter analysed for alginate content.

Subsequently, extraction time, extraction temperature, solid to liquid ratio, mass fraction of ammonium sulphate, type of salt, and DES to salt ratio were altered to assess the influence of these factors on the extraction yield. For alginate quantification, a colorimetric assay adapted from Cesaretti *et al*. [136] was used. The alginate extraction yield was determined following **Equation 5.2**:

$$Yield\ \left(\frac{mg}{g\ DW}\right) = \frac{C_{extract} * V_{total}}{m_{biomass} * x_{DW}} \quad (\mathbf{5.2})$$

where $C_{extract}$ is the concentration of the extract, $m_{biomass}$ is the weight of the initial biomass, x_{DW} is the weight fraction of the dry biomass and V_{total} is the total volume of the extract.

The alginate fraction obtained through TPP was dried and subsequently characterised using Fourier transform Infrared Spectroscopy (FTIR), and its spectral profile was compared to those of alginate extracted via alkaline and acid treatment. Additionally, the DES fraction before and after extraction was characterised using FTIR. Spectral analysis was performed with a Nicolet Summit X attenuated total reflection (ATR) FTIR Spectrometer (ThermoFisher Scientific), covering a range from 400-4000 cm^{-1}.

The mannuronic to guluronic (M/G) ratio of the extracted alginate was determined through methanolysis, followed by high-performance anion exchange chromatography with pulsed amperometric detection (HPAEC-PAD), as described by Bojorges *et al*. [227]. The analysis was conducted using a Dionex ICS-6000 system (Thermo Fisher) equipped with a CarboPac 1 mm column. Alginate extracted using DES was compared to that obtained through conventional alkaline extraction. The extracted alginate was precipitated using 80% ethanol with 1% NaCl, followed by two washing steps with 80% ethanol. The samples were subsequently re-solubilised in Milli-Q water, and 50 µL aliquots were used for methanolysis.

5.2.5 Pigment extraction and quantification

Pigments chlorophyll *a* and fucoxanthin were extracted in the DES phase under the previously mentioned conditions (**Section 5.2.4**). Pigment quantities were estimated using a UV-Vis microplate reader (TECAN Infinite M200) as this provides a rapid and non-destructive means for assessing pigment contents in solution [89] and has been applied for quantification [228]. The absorption spectra of the DES were measured from 300 to 800 nm. Chlorophyll and fucoxanthin contents were estimated using calibration curves established in DES1, based on absorbance at 667 nm for chlorophyll (R^2 = 0.9985) and 457 nm for fucoxanthin (R^2 = 0.9967), as shown in **Figure S5.3** [228].

5.2.6 DES reusing

To reuse the DES fraction, the optimal DES was selected, and optimal extraction conditions were applied. The multiproduct extraction of alginate and pigments was performed 12 times to assess the impact on the yield by reusing the DES fraction. Alginate content and pigment extraction yields were assessed per extraction cycle.

Figure 5.1 gives a schematic overview of the integrated multi-product extraction, phase separation and DES regeneration process. Initially, seaweed is added to the DES and aqueous salt solution to facilitate the simultaneous extraction of alginate and pigments. Following extraction, phase separation results in three distinct fractions: (1) a hydrophobic DES-rich upper phase containing lipophilic pigments, (2) an aqueous salt-rich lower phase containing solubilised alginate, and (3) an intermediate solid fraction composed of undissolved residual biomass. The DES phase containing pigments is recovered and reused for subsequent extraction cycles, while the alginate fraction is dialysed. The residual biomass fraction is discarded.

5.2.7 Alginate determination in DES

To determine the potential alginate content in the hydrophobic DES, the DES was switched to a hydrophilic solution to release the alginate content. This was achieved by adding water to the DES in a 5:1 ratio, along with Jeffamine D-230 at a 1:10 ratio relative to water, to increase the pH and induce the formation of a hydrophilic fraction (**Figure S5.4**). The aqueous fraction was precipitated and subsequently analysed with Dionex through methanolysis (**Section 5.2.4**).

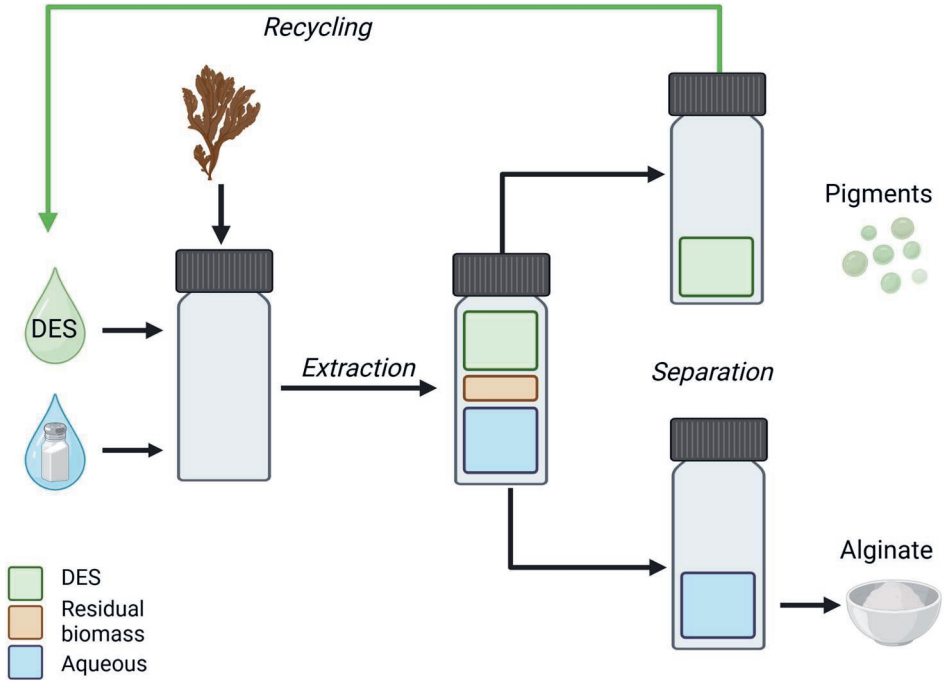


Figure 5.1 General overview of multi-product brown seaweed biorefinery using three-phase partitioning with a hydrophobic DES and an ammonium sulphate aqueous solution.

5.3. Results and discussion

5.3.1 DES screening for alginate and pigment extraction

Before assessing the ability of each DES to release alginate from the cell wall within the TPP, the affinity of these DES towards pigments was determined computationally. This assessment ensured that the DES selected for subsequent alginate extraction with TPP could also effectively extract pigments, thereby enabling a multi-product biorefinery. A multiproduct biorefinery approach maximises biomass valorisation by allowing the extraction of not only alginate but also high-value pigments, thereby enhancing both economic viability and sustainability. This integrated strategy aligns with circular bioeconomy principles by reducing waste, diversifying product streams, and meeting the growing demand for natural bioactives in food, cosmetic, and pharmaceutical sectors [229].

5.3.1.1 Pigment affinity screening

The capacity of each DES and benchmark solvent ethanol was calculated as the inverse of the activity coefficient at infinite dilution (**Section 5.2.3**). The solvent capacity indicates the maximum amount of pigment that can be dissolved in DES, making it an important parameter to consider for extraction solvents. Screening results from COSMO-RS showed that all DES have affinity with the pigments chlorophyll *a* and fucoxanthin, with capacities ranging from 2.14×10^4 to 2.99 (**Table 5.2**). When comparing the linalool-based DES (DES6-DES9) with the fatty acid-based DES, we observed that the fatty acid-based DES (DES1-DES5) had higher capacities for both pigments. This difference could be due to the lower logP of linalool compared to the C9, C10, and C12 fatty acids (**Table S5.1**). Capacities could reach a factor 10^4 for chlorophyll *a*, while for fucoxanthin, this could reach a factor of 10^3 (**Table 5.2**). For fucoxanthin, the capacity decreased with increasing chain length of the carboxylic acid HBD in dodecanoic acid-based DES. Conversely, an increased capacity was observed for chlorophyll *a* as the carbon chain length of the HBD increased when using dodecanoic acid as HBA. The difference in capacities could be due to the higher logP chlorophyll exhibits (18.4) compared to fucoxanthin (13.6) (**Table S5.1**), indicating its greater hydrophobicity. This suggests that chlorophyll has a stronger affinity toward more non-polar solvents. Fatty acid-based DES, composed of long hydrophobic chains, exhibit a lower polarity than DES based on monoterpenes like linalool (**Table S5.1**). As a result, these fatty acid-based solvents provide a more compatible environment for solubilising highly non-polar compounds such as chlorophyll, which may explain their higher extraction capacity in this case compared to fucoxanthin. Moreover, each DES displayed a higher capacity compared to the benchmark extraction solvent ethanol, highlighting their superior solubilising ability for algal

pigments. This supports the potential of DES as promising green alternatives for efficient and selective pigment extraction.

By plotting the σ-potential of the pigments and DES, we could assess the affinity of the pigments towards the DES [93]. σ-Potential plots provide insight into the interaction tendencies between the pigments and the DES. A more negative σ-potential indicates a stronger attractive interaction, whereas less negative or positive values suggest weaker affinity or repulsion between the species [93, 99]. As observed from the σ-potential, chlorophyll *a* and fucoxanthin display high negative values in their HBD regions and positive values in both the neutral and HBA regions (**Figure S5.5**). This indicates that these pigments can be solvated best in DES with strong HBD groups, meaning DES with more negative σ-potential values in the HBD region ($\sigma \leq -0.085$ e/A^2) (**Figure S5.5**). Additionally, to enhance the extraction efficiency of DESs for both pigments, the DES should exhibit negative σ-potential values in the HBA region to enable strong complementary interactions with the pigments, together with increased capacity values (**Table 5.2**). The fatty acid-based DES (DES1-5) have stronger negative values in the HBA region (>+0.085 e/A^2) compared to the linalool-based DES (DES6-9) (**Figure S5.5**). This indicates that the fatty acid-based DES have a stronger affinity with HBA molecules compared to the linalool-based DES. Additionally, the fatty acid-based DES display less negative values in the HBD region (<-0.085 e/A^2) compared to the linalool-based DES, thereby having less affinity to HBD molecules.

As a result, the fatty acid-based DES should solvate the pigments more effectively than the linalool-based DES due to complementary hydrogen bonding interactions that can occur, thereby reducing the self-association between the HBA and HBD of the DES. Due to the high capacity all DES exhibited for chlorophyll *a* and fucoxanthin (**Table 5.2**), all DES were considered in the TPP for alginate extraction.

Table 5.2 Calculated capacities of DES and ethanol for chlorophyll *a* and fucoxanthin.

	Chlorophyll *a*	Fucoxanthin
DES1	2.04×10^4	2.10×10^3
DES2	2.10×10^4	2.02×10^3
DES3	2.14×10^4	1.94×10^3
DES4	1.88×10^4	2.23×10^3
DES5	1.88×10^4	2.31×10^3
DES6	1.12×10^1	2.87
DES7	1.08×10^1	3.15
DES8	1.36×10^1	3.89
DES9	7.98	2.99
Ethanol	8.86×10^{-3}	3.01×10^{-1}

5.3.1.2 Alginate characterisation and isolation

Alginate was successfully extracted with TPP using the nine studied DES (**Figure 5.2**). During the extraction process, the hydrophobic DES interact with seaweed biomass primarily through hydrogen bonding and hydrophobic interactions. These DES may disrupt the polysaccharide-rich cell wall structure, aiding the release of alginate. Due to alginate's hydrophilic and anionic nature, it has limited solubility in the hydrophobic DES phase. Therefore, the aqueous phase permits the selective migration of alginate into the aqueous phase. In the aqueous phase, alginate can strongly interact with ammonium sulphate through electrostatic interactions between the negatively charged carboxylate groups on the alginate backbone and the positively charged ammonium ions [230], thereby influencing the solubility of alginate [231].

Among the DES types, DES1 (dodecanoic acid: octanoic acid) resulted in the highest alginate release, with an extraction yield of 55.7 ± 6.4 mg alginate per g DW. The control using the conventional alkaline extraction resulted in similar amounts of alginate with a yield of 55.3 ± 14.1 mg/g DW (**Figure 5.2**). DES1 and DES2 performed comparably to the alkaline extraction regarding alginate yield (**Figure 5.2**), while the other DES had a lower performance compared to the alkaline extraction. Although the alkaline treatment provides an extraction yield similar to those of DES1 and DES2, this method can be objectionable for safety, environmental and engineering (corrosion) reasons, as it requires strong alkaline and acidic conditions. Furthermore, solvent regeneration cannot be applied with this treatment.

When only the aqueous salt solution was applied without adding a DES, the extraction yields were considerably lower (4.8 ± 1.2 mg/g DW) compared to extracting with salt and DES (**Figure 5.2**). This indicates that, even though the hydrophobic DES is not directly involved in extracting alginate, the DES can act as a synergistic extracting agent together with the aqueous phase, facilitating enhanced alginate extraction into the aqueous salt phase. Previous studies have demonstrated that certain DES can affect the permeability and integrity of the cell walls of plants [149, 163, 232] and microalgae [148]. Therefore, in the TPP system, alginate could have been released in the aqueous phase through the disruption of the cell wall with DES. However, scanning electron microscopy would be required to confirm this. Hydrophobic DES can disrupt cell walls primarily by reconfiguring the hydrogen-bond network within structural polysaccharides of the biomass [206]. The hydrophobic DES constituents interact with non-polar cell wall regions through van der Waals forces [37], enhancing membrane permeability, thereby facilitating the release of compounds, including alginate. It must be noted that the effect of a single component (HBA or HBD separately) could also influence permeability rather than the DES. However, comparing DES and single

components is difficult because part of the used fatty acids are in a solid state at room temperature as single components, resulting in less exposure to cellular material [33].

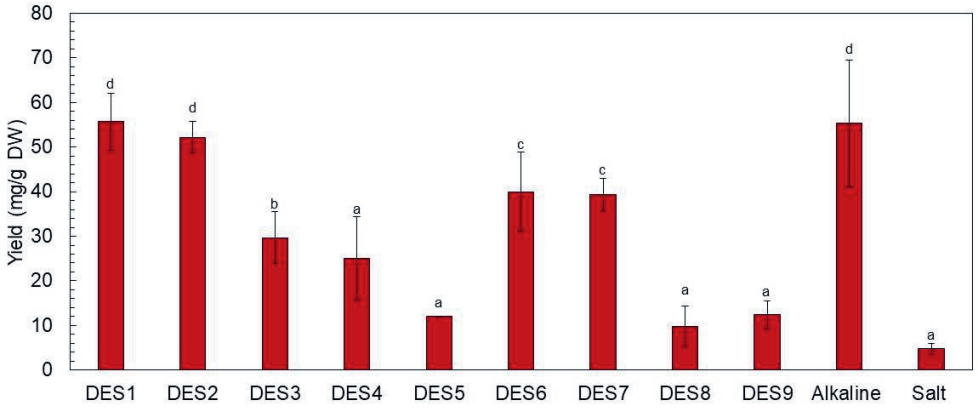


Figure 5.2. Alginate extraction yield for TPP systems with DES1-DES9. Alkaline extraction and extraction with only salt (ammonium sulphate) were used as controls.

For the dodecanoic acid-based DES (DES 1-4), it was observed that increasing the chain length of the HBD resulted in a decrease in alginate extraction yield. (**Figure 5.2**). Conversely, for the linalool-based DES (DES 6-9), using dodecanoic and decanoic acid as HBD resulted in a higher alginate extraction yield compared to using nonanoic and octanoic acid as HBDs (**Figure 5.2**). Differences in alginate yield may be due to the differences in polarity of these DES. The DES with the lowest alginate extraction yields (DES5, DES8 and DES9) displayed a logP below 4 (3.9, 3.8 and 3.6, respectively) (**Table S5.1**), while all the other DES had logP values larger than 4. However, DES3 displayed a logP of 5.1 and had a decreased yield compared to DES1 and DES2. This suggests that a certain degree of non-polarity (logP between 4 and 5) of the DES is required to act on the algal cell wall and to destabilise it. Furthermore, greater hydrophobicity of DES could cause more alginate to migrate into the aqueous phase because of repulsion between alginate molecules and the hydrophobic solvent, enabling alginate to partition into the more hydrophilic phase.

For the dodecanoic acid-based DES, an increased chain length of HBD decreased the alginate extraction yield (**Figure 5.2**). These observations are in line with Chen *et al.* [163], where grape seed polysaccharides were extracted in a TPP system using fatty acid-based DES. Here, the highest extraction yield of polysaccharides was also obtained with dodecanoic acid: octanoic acid. The viscosity of the DES may be a factor influencing the extraction yield. Out of the dodecanoic acid-based DES, DES1 displayed the lowest viscosity.

The higher extraction yields observed with dodecanoic acid-based DES compared to linalool-based DES may be due to the ability of fatty acids to interact with the seaweed's cell wall. Cao *et al*. [172] stated that hydrophobic DES containing fatty acids can interact with the outer cell membrane of recombinant *E. coli* cells, causing it to destabilise. When fatty acids are deprotonated, they can function as surfactants known for their cell-disrupting properties [33]. As the permeability of the outer membrane increases, the hydrophobic DES can penetrate the inner phospholipid layer, thereby disrupting the phospholipid bilayer. This phenomenon could have led to the release of more alginate with the dodecanoic acid-based DES compared to the linalool-based DES.

In a separate study on the pretreatment of lignocellulosic biomass with hydrophilic DES [233], it was demonstrated that choline chloride-based DES disrupts the cell wall structure by dissolving lignin from the lignocellulosic microfibrils. This disorganisation led to an increased cellulose availability. In another study performed by Huang and coworkers [234], a choline chloride-based DES (choline chloride: formic acid 1:2) was used as a pretreatment to extract lipids from the microalga *Nannochloropsis oceanica*. Density Functional Theory (DFT) calculations revealed that DES could disorganise the intermolecular interactions between microalgal molecules through the reconstruction of the hydrogen bond network, therefore increasing lipid availability for extraction. In our study, the hydrophobic DES may have disrupted the cell membrane, while also disorganising the algal cell wall. This could have facilitated the penetration of the aqueous salt phase, enhancing the release of alginate. As a result, the application of DES likely led to a significant increase in alginate extraction yield compared to using the aqueous solution alone.

Given its high alginate extraction efficiency and strong capacity for chlorophyll *a* and fucoxanthin, DES1 was chosen for further single-factor experiments.

5.3.2 Extraction conditions

TPP is a technique that involves both extraction and separation within a one-pot system. Operational parameters can affect the system's extraction yield. Therefore, the effect of extraction time, extraction temperature, the concentration of ammonium sulphate, the liquid to solid ratio, DES to ammonium sulphate ratio and the type of salt on the alginate yield were studied (**Figure 5.3 a-e**).

5.3.2.1 Extraction time

The extraction time was assessed, ranging from 5 to 60 minutes. The alginate extraction yield initially increased between 5 and 10 minutes, then gradually decreased from 20

to 60 minutes (**Figure 5.3a**). The highest alginate extraction yield of 86.6 ± 13.0 mg/g DW was achieved after just 10 minutes of extraction. In contrast to traditional alkaline extraction, which generally involves one hour for the acid treatment followed by an additional hour of alkaline extraction (**Section 5.2.4**), TPP extraction is more time-efficient. The decrease in yield from 10 to 60 minutes (**Figure 5.3a**) could be attributed to the increased dissolution of other components [163] and an increase in viscosity of the DES over time [206]. However, a notable reduction in alginate yield was observed at 60 minutes, suggesting that alginate might be partially transferred into the DES phase due to the saturation of the DES. This could occur through the formation of reverse micelles, created by the algal phospholipids or proteins, as they can act as surfactants [235], similar to methods used for encapsulating polysaccharides, proteins and enzymes [236].

5.3.2.2 Extraction temperature

The effect of the extraction temperature was investigated across a range of 20 to 70 °C. The alginate extraction yield increased with increasing temperature, reaching its highest value of 100.2 ± 2.4 mg alginate/g DW at 70 °C (**Figure 5.3b**). The increase in yield with higher temperatures (**Figure 5.3b**) may be due to the reduced viscosity of the DES at elevated temperatures, which enhances mass transfer [220, 237]. In addition, higher temperatures within the TPP can lead to increased thermal molecular movement [163], facilitating the formation of more hydrogen bonds, as more hydroxyl groups of alginate are exposed. This results in increased solubility of alginate in the aqueous phase, yielding a higher extraction [221]. Additionally, higher temperatures can help in rupturing the cell wall [238], thereby improving the alginate accessibility. Even though the alginate yield increased with increased temperatures, fucoxanthin is susceptible to thermal degradation above 36 °C [93]. For energy efficiency and pigment protection, 35 °C was chosen as the optimal extraction temperature.

5.3.2.3 $(NH_4)_2SO_4$ concentration

The mass fraction of $(NH_4)_2SO_4$ was tested from 0 to 40 wt%. The alginate extraction yield increased as the amount of $(NH_4)_2SO_4$ rose to 15 wt%, above which the alginate yield gradually decreased (**Figure 5.3c**). A clear optimum was observed at 15 wt%, with an extraction yield of 124.6 ± 18.1 mg/g DW. The increased presence of $(NH_4)_2SO_4$ in the solution enhanced the alginate extraction yield, as NH_4^+ and SO_4^- ions help stabilise macromolecular interactions [221]. Specifically, NH_4^+ ions can interact with the negatively charged carboxylate groups on alginate, reducing intermolecular aggregation and thereby enhancing alginate solubilisation [231]. However, further increases in the mass fraction of $(NH_4)_2SO_4$ led to a decrease in yield, likely due to reduced dissolution as the aqueous layer became increasingly saturated [219, 239].

This saturation reduced the amount of water available for dissolving alginate, lowering the extraction yield. Additionally, higher salt concentrations can interfere with hydrogen bonding between alginate and water, further decreasing the yield [240]. Therefore, a 15 wt% mass fraction of $(NH_4)_2SO_4$ was selected as optimal.

5.3.2.4 Liquid to solid ratio

Total liquid (DES and ammonium sulphate solution) to solid ratios ranging from 30:1 to 70:1 were evaluated. The extraction yield improved as the liquid to solid ratio increased, with a maximum extraction yield at a ratio of 60:1 (48.8 ± 15.8 mg/g DW) (**Figure 5.3d**). Further increasing the ratio to 70:1 did not result in a higher extraction yield. Higher liquid to solid ratios provide a larger extraction volume, allowing more alginate to dissolve in the aqueous phase. A 60:1 ratio was found to be optimal for alginate extraction, as increasing the ratio to 70:1 did not result in a further improvement in yield. When applying low liquid to solid ratios, the extraction yield was low (**Figure 5.3d**). This could be due to solubility-limited extraction, in which alginate reaches saturation in the aqueous phase [241]. On the other hand, mass transfer constraints could have caused no extraction improvement from 60:1 to 70:1. An insufficient amount of extractant results in incomplete extraction, while excessive amounts lead to waste and negatively impact the extraction process [163, 240]. Therefore, a 60:1 ratio was selected as the ideal for extraction.

5.3.2.5 DES to salt ratio

Various DES to salt volume ratios, ranging from 0.25:1 to 3:1, were tested. It was found that increasing the amount of DES relative to salt resulted in higher alginate extraction yields (**Figure 5.3e**). The highest extraction yield, 98.3 ± 15.8 mg/g DW of alginate, was achieved with a 2:1 DES to salt ratio. Increasing the concentration of DES could enhance van der Waals interactions with hydrophobic regions of the cell structure [37], thereby improving membrane permeability and promoting the release of alginate. However, increasing the volume ratio to 3:1 resulted in a reduced extraction yield (38.6 ± 8.6 mg/ g DW). The optimal DES to salt ratio was determined to be 2:1 (**Figure 5.3e**), aligning with findings from previous studies [237, 242]. At lower DES to salt ratios, the DES and $(NH_4)_2SO_4$ cannot effectively synergise, compromising the system's stability [163]. These findings suggest that DES enhances the buoyancy of macromolecules, including alginate, facilitating its separation into the aqueous phase while solubilising the lipid fraction into the DES [220]. Further increasing the amount of DES may raise

the system's overall viscosity, which could impede mass transfer of alginate to the salt phase [237]. Thus, a 2:1 DES to salt volume ratio was selected as the optimal condition.

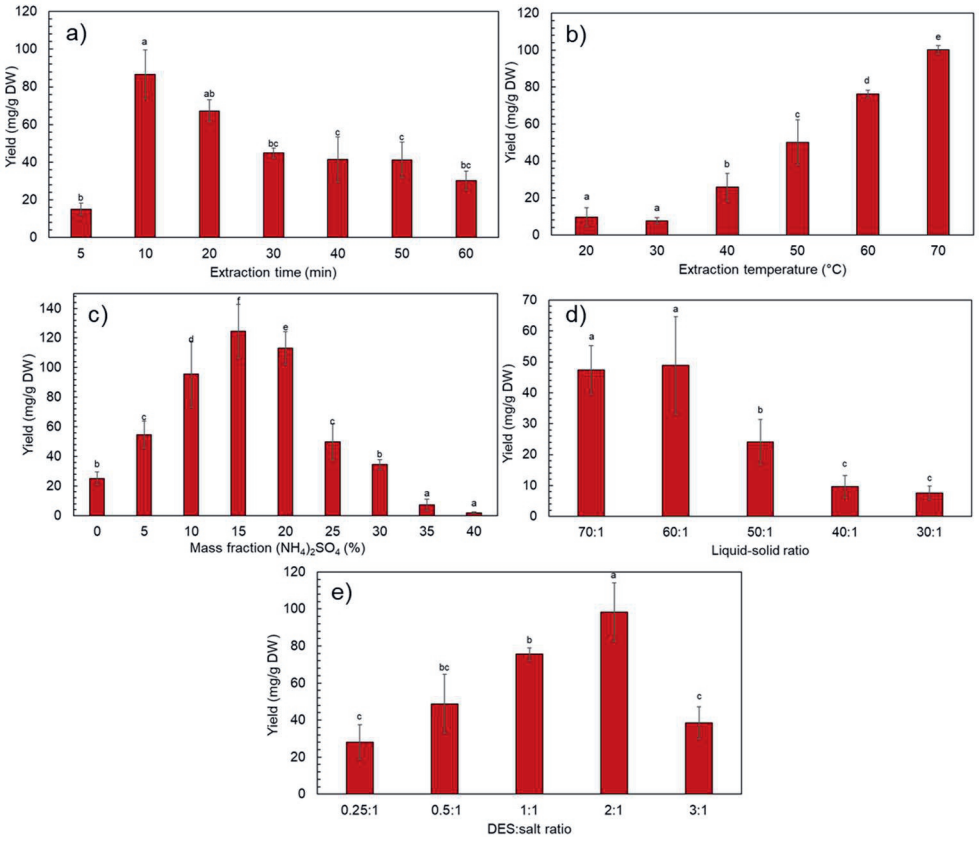


Figure 5.3 Effect of (a) the extraction time, (b) extraction temperature, (c) mass fraction of $(NH_4)_2SO_4$, (d) the liquid-solid ratio and (e) the DES to salt ratio on the extraction yield of alginate. Conditions were standardised at 30 wt% $(NH_4)_2SO_4$, 55 °C, liquid-solid ratio of 60:1, 30 minutes extraction time and a DES:salt ratio of 0.5:1 when one of the extraction parameters was altered.

5.3.3 Extraction optimisation and characterisation

Subsequently, the optimal extraction conditions were selected for DES reusing, except for the extraction temperature. For temperature, 35 °C was selected. The following conditions were applied: 10 minutes, 35 °C, 15 wt% $(NH_4)_2SO_4$, liquid to solid ratio of 60:1 and DES to salt of 2:1. For temperature, the suboptimal extraction condition at 35 °C was selected as higher temperatures lead to increased energy consumption. Under optimised conditions, 101.8 ± 3.1 mg/g DW of alginate was extracted, while 0.144 mg/g DW and 0.026 mg/g DW of chlorophyll *a* and fucoxanthin were obtained, respectively. Taking into account that *S. latissima* contains approximately 19% alginate and 90% of

the biomass is dry weight, this indicates that approximately 55% of the total alginate content was extracted.

Although a temperature of 35 °C was chosen, which was not the optimal temperature, high alginate extraction yields were still achieved under the optimised conditions. This temperature, combined with optimal extraction parameters, could have facilitated a synergistic effect, resulting in a high yield with a relatively low extraction temperature. Additionally, lower extraction temperatures are advantageous for pigment extraction [93]. Compared to the initial extraction conditions, the optimised process employed shorter extraction times, lower temperatures, and reduced salt concentrations, thereby enhancing its economic viability.

Compared to other novel extraction methods, similar yields were achieved. Direct alginate extraction using hydrophilic DES choline chloride: urea (1:2) resulted in 74% alginate after optimisation [100]. However, the reuse of DES was not examined since alginate was recovered through precipitation. Additionally, the approach focused only on alginate extraction, without considering the recovery of other valuable bioactive compounds. In a study by Bojorges *et al*. [243]**,** hydrostatic pressure-assisted extraction was used for *S. latissima*, using 0.1 M $NaHCO_3$ for 2 hours at room temperature. An alginate yield of 13.9% was obtained, which is significantly lower than the TPP extraction of alginate. Moreover, the treatment is relatively long (2 hours compared to 10 minutes), and no other compounds were extracted. Saravana *et al*. [128] employed subcritical water extraction at 125 °C and 10 bar using a choline chloride: glycerol (1:2) DES containing 70% water, achieving an alginate yield of 28%. Despite its potential, this approach yielded lower extraction efficiencies and requires high-pressure equipment, which increases capital investment and raises safety and material corrosion concerns**.**

The FTIR spectra of alginate extracted using TPP and alkaline treatment exhibited similar characteristic patterns (**Figure 5.4**). Both extracts exhibited peaks at 1020 cm^{-1} and 1080 cm^{-1}, as well as at 1600 cm^{-1} and 1400 cm^{-1}. Additionally, a minor peak at 2900 cm^{-1} was detected for both extracts (**Figure 5.4**). The sharp peaks observed at 1080 and 1020 cm^{-1} are attributed to mannuronic and guluronic acid units [244]. The peaks around 1600 and 1400 cm^{-1} correspond to the asymmetric and symmetric stretching modes of carboxylate groups, respectively [244–246]. Additionally, the low-intensity peak at 2900 cm^{-1} is associated with -CH_2 groups [245]. The presence of these characteristic bands indicates that the proposed TPP system is effective for extracting

alginate from brown seaweed, producing a profile similar to that of the conventional alginate extraction method.

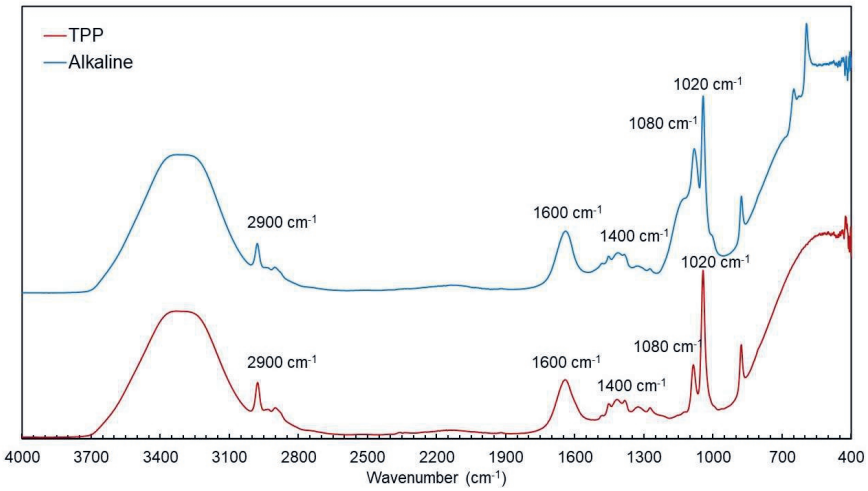


Figure 5.4 FTIR spectra of alginate extracted with DES-based three-phase partitioning and conventional alkaline extraction.

The M/G ratio is an important factor in alginate extraction, as it impacts the physical properties of the alginate [227]. Alginates with a higher M/G ratio generally form more permeable gel matrices, whereas those with a lower M/G ratio produce mechanically stronger structures. This difference is attributed to the higher affinity of guluronic acid blocks for calcium ions, which leads to enhanced cross-linking and gel strength compared to mannuronic acid blocks [247].

The M/G ratio of alginate extracted using the TPP system was 1.05 ± 0.00, whereas the conventional alkaline extraction yielded a higher ratio of 1.57 ± 0.02. These values are comparable to values reported in literature (ranging from 1.17 to 1.40) for *S. latissima* [227, 248] indicating that the M/G ratios of TPP and alkaline extraction methods are similar. However, alginate extracted with TPP could probably produce stronger and less permeable gels, whereas the conventional method could yield softer and more elastic gels. Both the FTIR analysis and M/G ratio results suggest that alginate extracted and recovered using TPP is comparable to that obtained through conventional alkaline extraction, with similar functional groups and M/G ratios. Therefore, physicochemical characterisation indicates that TPP could be a viable method for alginate extraction.

5.3.4 DES reuse

5.3.4.1 Pigment extraction

Reusing the DES was conducted to evaluate the alginate and pigment yield per extraction cycle. As the DES is reused without removal of pigments, it is anticipated that chlorophyll and fucoxanthin will progressively accumulate until the solvent reaches saturation. The extraction yield for both chlorophyll and fucoxanthin increased from cycles 1 to 10 (**Figure 5.5**). For chlorophyll *a*, the extraction yield reached a plateau at cycle 7 (1.98 ± 0.04 mg/g DW) with no further increase up to cycle 12. The yield for fucoxanthin increased up to cycle 6 (0.18 ± 0.00 mg/g DW), followed by a decrease in cycle 7. Extraction yields increased again between cycles 7 and 12, reaching 0.21 ± 0.21 mg/g DW. The fluctuating fucoxanthin yields could be due to partial degradation of this pigment in the DES.

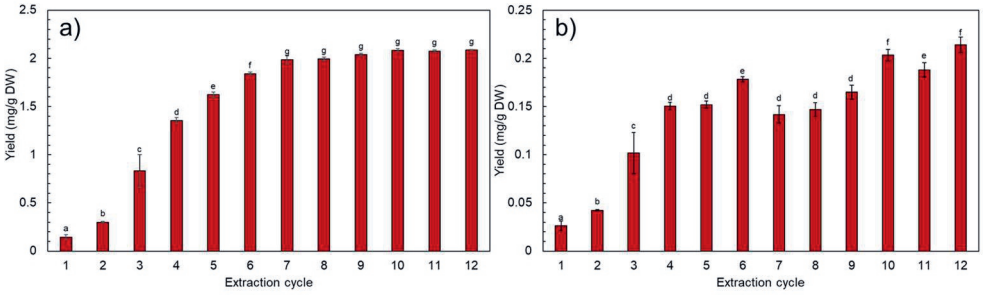


Figure 5.5 Extraction yield of (a) chlorophyll *a* and (b) fucoxanthin when reusing the DES fraction.

Previous research focused on fucoxanthin extraction from *S. latissima* [216] found an optimised extraction yield of 0.137 mg fucoxanthin/g DW and 0.08 mg/g DW chlorophyll using menthol: levulinic acid (1:1). These results are similar to the fucoxanthin yields obtained in our study after seven reuse cycles of the DES. In a study by Fernandes *et al*. [249], fucoxanthin yields ranging from 0.02 to 0.12 mg/g DW were obtained from *S. latissima* using acetone containing 0.05% butylated hydroxytoluene, depending on the season. These values are comparable to those achieved with the TPP system. In contrast, Martins *et al*. [228] reported 1.96 mg/g DW and 4.93 mg/g DW of fucoxanthin and chlorophyll, respectively, when using a phosphonium-based ionic liquid combined with sunflower oil. Although high pigment yields were obtained, the isolation step relies on back-extraction using toluene, which limits the process's suitability for sustainable industrial applications. However, it must be noted that fucoxanthin content is subject to seasonal variation as well as differences related to the geographic location of seaweed collection [250]. Therefore, direct comparison of pigments extracted per dry weight between different studies is challenging due to variability.

To evaluate the DES extract, FTIR analysis was conducted on both the pure DES and the DES extract. The pure DES exhibited characteristic peaks, including a strong stretching vibration of the carbonyl group (COOH) at 1703 cm^{-1} and a bending vibration of the hydroxyl group (-OH) in the carboxyl functional group at 917 cm^{-1} [163] (**Figure S5.6**). Upon extraction, the DES extract exhibited additional peaks that could be attributed to the presence of fucoxanthin and chlorophyll. Specifically, the low-intensity absorption at 3427 cm^{-1} corresponds to O–H stretching vibrations, present in fucoxanthin [89], while distinct carbonyl (C=O) groups were observed through a high-intensity peak at 1623 cm^{-1} [89, 251], which is consistent with functional groups found in chlorophyll and fucoxanthin. These additional peaks may suggest the solubilisation of these compounds in the DES.

For product recovery, a biphasic system can be employed, as proposed by Kholany *et al*. [216]. By introducing a hydrophilic choline chloride-based DES, fucoxanthin and chlorophyll can be effectively separated, with fucoxanthin partitioning into the hydrophilic phase. Subsequently, fucoxanthin can be recovered through water addition to the hydrophilic DES. Chlorophyll remains in the hydrophobic DES and could be directly applied, for instance, for cosmetic applications [216].

5.3.4.2 Alginate extraction

DES reusing was performed for twelve cycles using the optimised extraction conditions (**Figure 5.6**). Per extraction cycle, the alginate yield was determined in the aqueous phase. Interestingly, the alginate extraction yield decreased from cycle 1 to 3 (101.8 ± 3.1 to 54.1 ± 12.5 mg/g DW) and increased again from cycle 4 (95.4 ± 15.2 mg/g DW) up to cycle 7 (118.0 ± 22.4 mg/g DW). From cycle 8, the alginate yield decreased again. The decrease in extraction yield from cycle 1 to 3 and from cycle 7 could be due to increased dissolution of other components in the DES, therefore lowering the effectiveness of the DES [163]. However, this does not explain the increase in alginate yield from cycle 4 to 7. As discussed in **Section 5.3.2**, this trend could be due to the formation of reverse micelles by the DES, capturing alginate in the DES phase. An overview of the extracted target analytes and approximate quantities are given in **Table 5.3**.

Table 5.3 Approximate concentrations of alginate, chlorophyll a, and fucoxanthin after seven extraction cycles with DES1.

Target analyte	Alginate	Chlorophyll *a*	Fucoxanthin
mg/g DW	118.0 ± 22.4	1.98 ± 0.04	$1.4*10^{-1}$

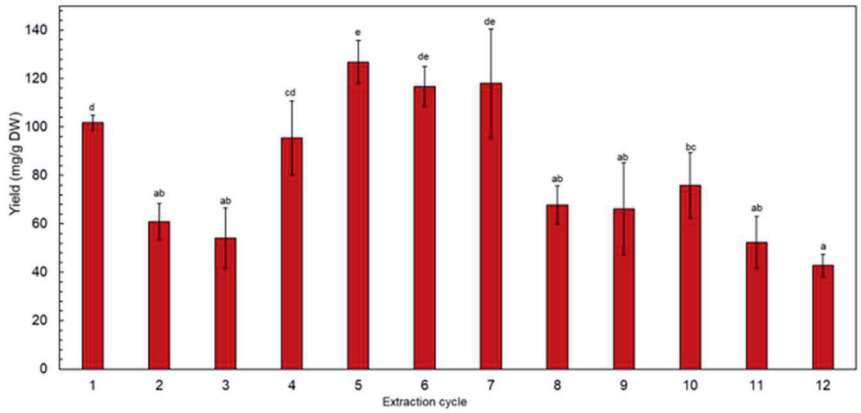


Figure 5.6 Extraction yield of alginate when reusing the DES fraction twelve times.

5.3.5 Proposed extraction mechanism

As previously mentioned (**Section 5.3.2**), the fluctuations in alginate yield could be attributed to the formation of reverse micelles, potentially caused by the release of phospholipids or proteins acting as emulsifiers when DES is applied to the biomass. However, the fatty acid-based DES could also play a role in reverse micelle formation, as studies have reported the use of fatty acids in reverse micellar systems [252, 253]. Bukman *et al*. [252] utilised dodecanoic acid, hexadecenoic acid and octadecanoic acid to extract methylene blue from an aqueous solution via reverse micelle formation. Under optimised conditions, this method achieved a dye removal efficiency of 99%.

The combination of phospholipids from the seaweed and fatty acids from DES is hypothesised to have promoted enhanced micellar formation. A study by Kittipongpittaya *et al*. [254] examined the influence of phospholipids and free fatty acids on reverse micelle formation. Their findings demonstrated that higher fatty acid concentrations significantly increased the concentration of micelles. This effect was attributed to the ability of fatty acids to alter the pH, which enhanced the positive charge on the phospholipid head groups. The resulting electrostatic repulsion between phospholipid molecules further facilitated the formation of reverse micelles. Penttila *et al*. [253] found that adding fatty acids to phospholipids improved the stability of reverse micelles against precipitation. Additionally, it was observed that the cores of the reverse micelles expanded, allowing them to accommodate more water.

To confirm the presence of alginate in the DES phase, this phase was converted into an aqueous solution by adding water and an amine solution (**Section 5.2.7**). Notably, mannuronic and guluronic acid were detected in the aqueous DES phase (**Figure S5.7**), suggesting that alginate was indeed present in the DES. Therefore, alginate may have been encapsulated within reverse micelles formed by phospholipids released during DES treatment, in combination with fatty acids present in the DES. This process could have facilitated the transfer of alginate to the upper phase (**Figure 5.7**). Initially, the fatty acid-based DES functioned as a pretreatment, disintegrating the algal cell wall and releasing the alginate. During this release, phospholipid fractions and fatty acids from the DES could have interacted, forming reverse micellar structures (**Figure 5.7**). These micelles, present in the DES fraction, could encapsulate alginate, thereby reducing the alginate yield in the aqueous phase. The formation and release of reverse micelles may account for the fluctuations in extraction yield across the extraction cycles.

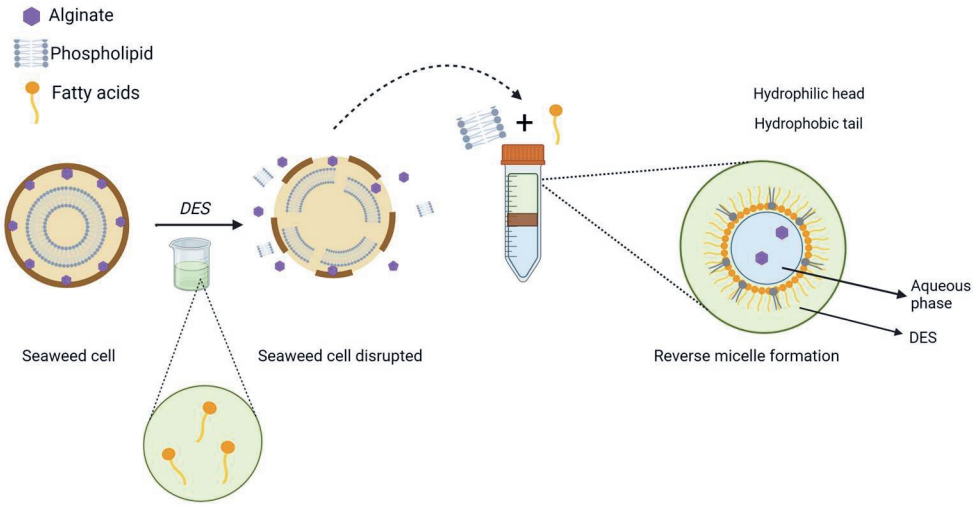


Figure 5.7. Proposed TPP extraction mechanism with fatty acid-based DES.

Given the low total lipid content (0.69-1.88 % per DW) [255] and protein content (5-13% per DW) [209] in brown seaweed, reverse micelle formation is likely primarily driven by the addition of fatty acids. To evaluate the role of fatty acids in this system, a different hydrophobic DES without fatty acids was used in TPP. When TPP extraction was performed with menthol: thymol (1:1), a different trend emerged when the DES was reused five times (**Figure S5.8**). The alginate extraction yield decreased from cycles 1 to 2 (95.9 ± 4.8 mg/g to 87.4 ± 5.5 mg/g) and did not significantly change between cycles 3 and 5 (**Figure S5.8**). No fluctuations in alginate yield were observed, likely due to the absence of fatty acids. The decrease in yield between cycles 1 and 3 is probably

attributed to the accumulation of impurities in the DES. The stable yield observed in cycles 3 to 5 suggests that alginate may have been encapsulated when using fatty acid-based DES, possibly enhanced by phospholipid release from the seaweed. To overcome this limitation, reverse micelle structures can be destructed [252]. Through basification, the fatty acids can form a homogeneous aqueous phase, thereby releasing the micelle structure [237]. This, in turn, could result in alginate release. The DES can be recovered through subsequent acidification and reused within the TPP extraction.

Biodegradable fatty acids and terpenes are relatively inexpensive compounds and display low solubility in water, making them suitable, bio-based hydrophobic extraction solvents [93, 256]. Moreover, they can be easily reused and facilitate simultaneous pigment extraction in three-phase partitioning. Overall, natural hydrophobic DES based on fatty acids are suggested to be effective both as biomass pretreatment for alginate release from the cell wall and as an extraction solvent for pigments. For the first time, a DES-based TPP was employed to enable a multi-product biorefinery, wherein the DES served a dual function as both pretreatment agent and extractant. Reuse of the DES up to seven cycles resulted in a relatively stable alginate yield and pigment saturation, demonstrating its potential for sustainable and efficient resource utilisation.

5.4. Conclusion

This study investigated the use of natural deep eutectic solvents (DES) in three-phase partitioning (TPP) as a novel and mild approach for simultaneous extraction and purification of alginate and pigments from S*accharina latissima* as an alternative to conventional alkaline processing. A multi-product DES-based TPP was employed, with DES functioning as both a pretreatment and extraction solvent. Alginate extraction showed that hydrophobic DES disrupted the algal cell wall, releasing alginate in the aqueous phase while extracting pigments with DES. DES1 (dodecanoic acid: octanoic acid) yielded the highest alginate output (55.7 ± 6.4 mg/g DW). A short extraction time (10 minutes) at a low temperature (35 °C) improved alginate yield to 101.8 ± 3.1 mg/g DW. The DES proved reusable for up to seven extraction cycles, although partial alginate transfer into the DES phase was observed due to reverse micelle formation. This work highlights the multi-product potential of the DES-based TPP system, improving economic viability through milder and shorter extraction conditions while facilitating the recovery of both alginate and pigments, along with DES reuse.

5.5. Supplementary information

The chemical structure of the alginate monomers β-D-mannuronic acid (M) and α-L-guluronic acid (G) monomers. linked by β-1,4-glycosidic bonds. Their composition and arrangement of M and G blocks can vary depending on the seaweed species and seasonal conditions.

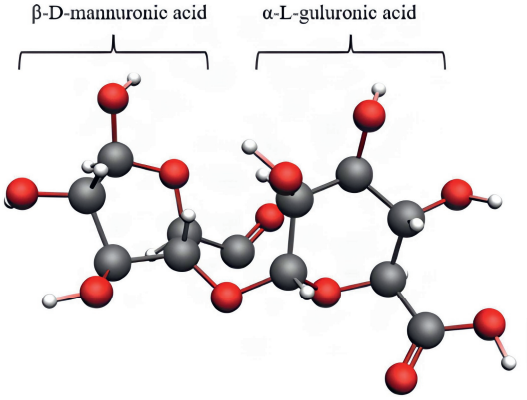


Figure S5.1 Chemical structure of part of alginic acid, represented by linked β-D-mannuronic acid and α-L-guluronic acid monomers.

The molecular geometries of chlorophyll *a* and fucoxanthin were pre-optimised using a universal force field (UFF) at density functional level GGA:BP86 basis set TZP. The surface charge densities (**Figure S5.2**) were used as an input for predicting the activity coefficients for each DES.

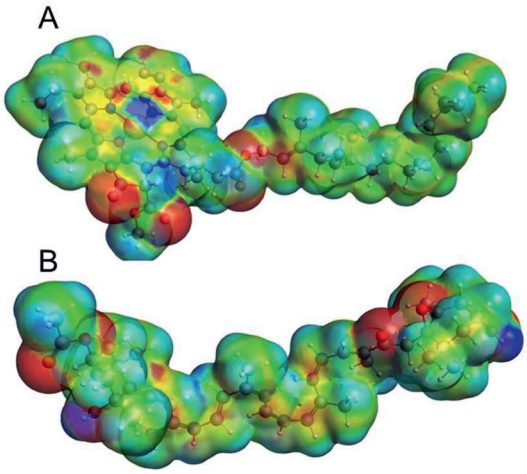


Figure S5.2 Molecular structures of pigments (A) chlorophyll *a* and (B) fucoxanthin. Blue regions represent the hydrogen bond donating areas, red regions represent the hydrogen bond accepting areas, and green regions represent the non-polar surface areas.

Pigment quantities were estimated using the calibration curves prepared in DES, with an R^2= 0.9985 at 667 nm and R^2 = 0.9967 at 457 nm for chlorophyll and fucoxanthin, respectively.

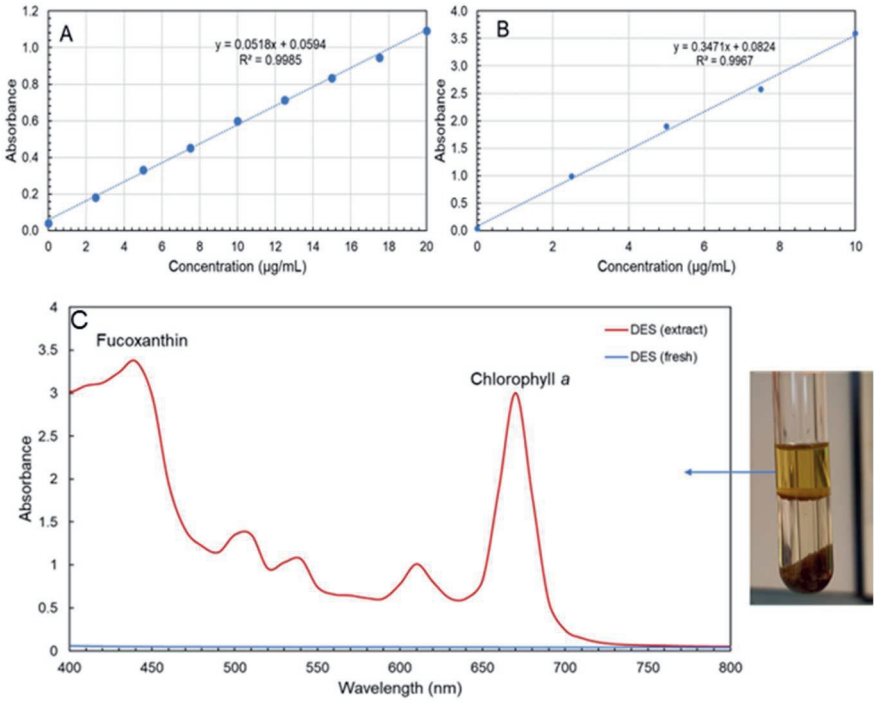


Figure S5.3 Calibration curves of (A) chlorophyll *a* and (B) fucoxanthin in DES1. (C) UV-vis spectra of fresh and used DES1.

The hydrophobic DES was switched to an aqueous solution to determine the potential alginate content in this phase. The DES was made aqueous through the addition of water in a 5:1 ratio to DES, together with Jeffamine D-230 in a 1:10 ratio to water. The obtained fraction was analysed for alginate.

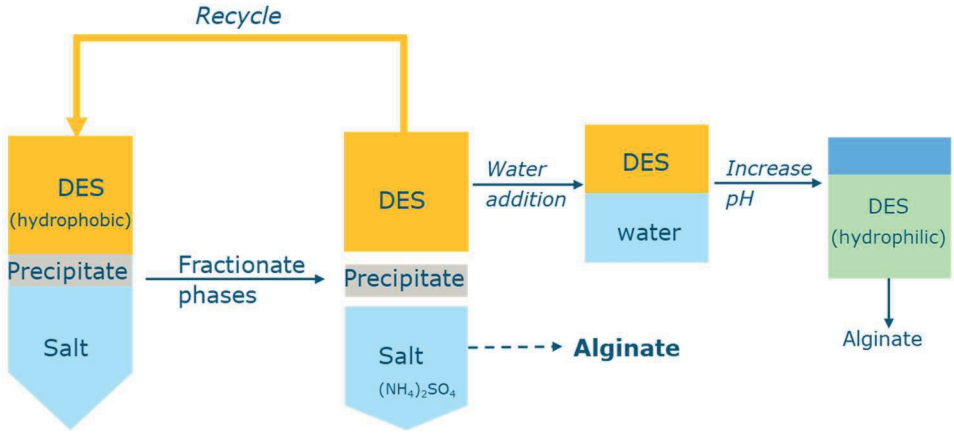


Figure S5.4 Schematic overview of alginate determination in the reused DES phase.

The octanol-water partitioning coefficient (logP) was estimated in COSMO-RS to assess the hydrophobicity of the DES and pigments. The LogP estimations were used for assessing both the pigment affinities towards each DES and were used to assess the degree of hydrophobicity needed for alginate release.

Table S5.1 LogP values of DES constituents, DES1-DES9 and pigments.

Compound	LogP
Linalool	3.5979
Dodecanoic acid	5.6841
Octanoic acid	3.3123
Nonanoic acid	4.0838
Hexanoic acid	2.3744
Decanoic acid	4.5908
DES1	4.4982
DES2	4.8839
DES3	5.1375
DES4	4.0293
DES5	3.9516
DES6	4.6410
DES7	4.0943

DES8	3.8408
DES9	3.4551
Chlorophyll *a*	18.377
Fucoxanthin	13.569

σ-potential plots can be applied to identify the affinity of a component towards another component. A more negative σ-potential value indicates stronger interactions between components, whereas a more positive value reflects increased repulsive behaviour.

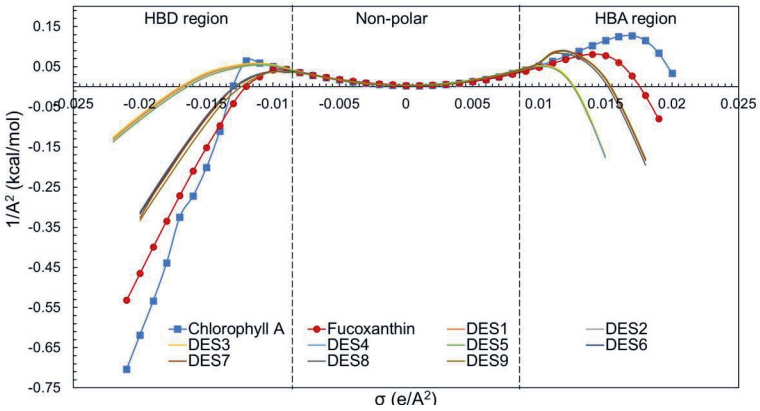


Figure S5.5 σ-potential of chlorophyll *a*, fucoxanthin and DES1 to DES9.

FTIR of the DES fraction from DES1 was performed before and after extraction with TPP, to characterise the DES and its distinctive peaks, and to evaluate the presence of pigments.

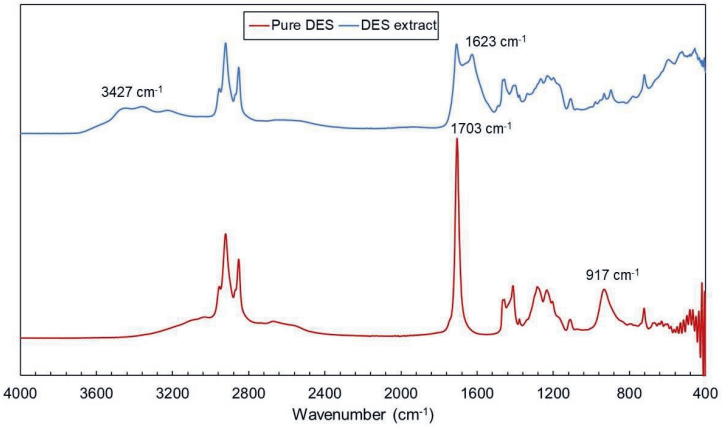


Figure S5.6 FTIR spectra of pure DES and the DES after extraction within TPP.

The Dionex ICS-6000 system was used for the identification of mannuronic and guluronic acid in the hydrophobic DES phase, as an indication for the presence of alginate in the hydrophobic DES phase.

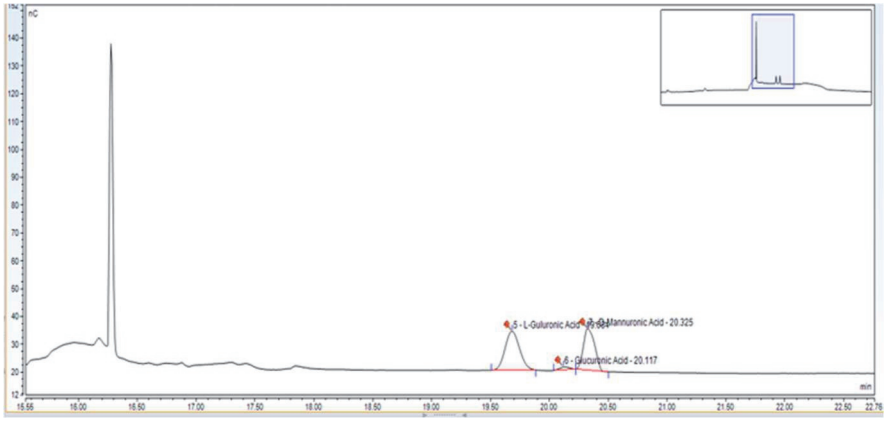


Figure S5.7 Chromatogram of recycled DES phase from 15 to 22 minutes.

Three-phase partitioning was performed with DES menthol: thymol (1:1), to evaluate the potential role of the fatty acids in reverse micelle formation, affecting the alginate yield as observed in the studied fatty acid-based DES. Conditions used were the same as the optimal extraction conditions for DES1.

Three-phase partitioning was performed with DES menthol: thymol (1:1), to evaluate the potential role of the fatty acids in reverse micelle formation, affecting the alginate yield as observed in the studied fatty acid-based DES. Conditions used were the same as the optimal extraction conditions for DES1.

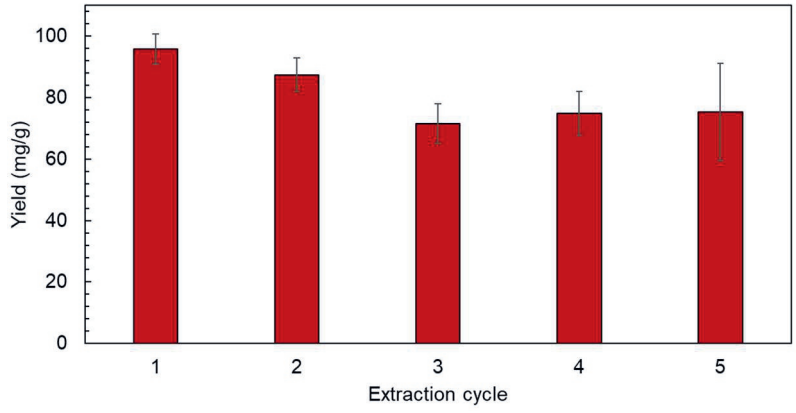
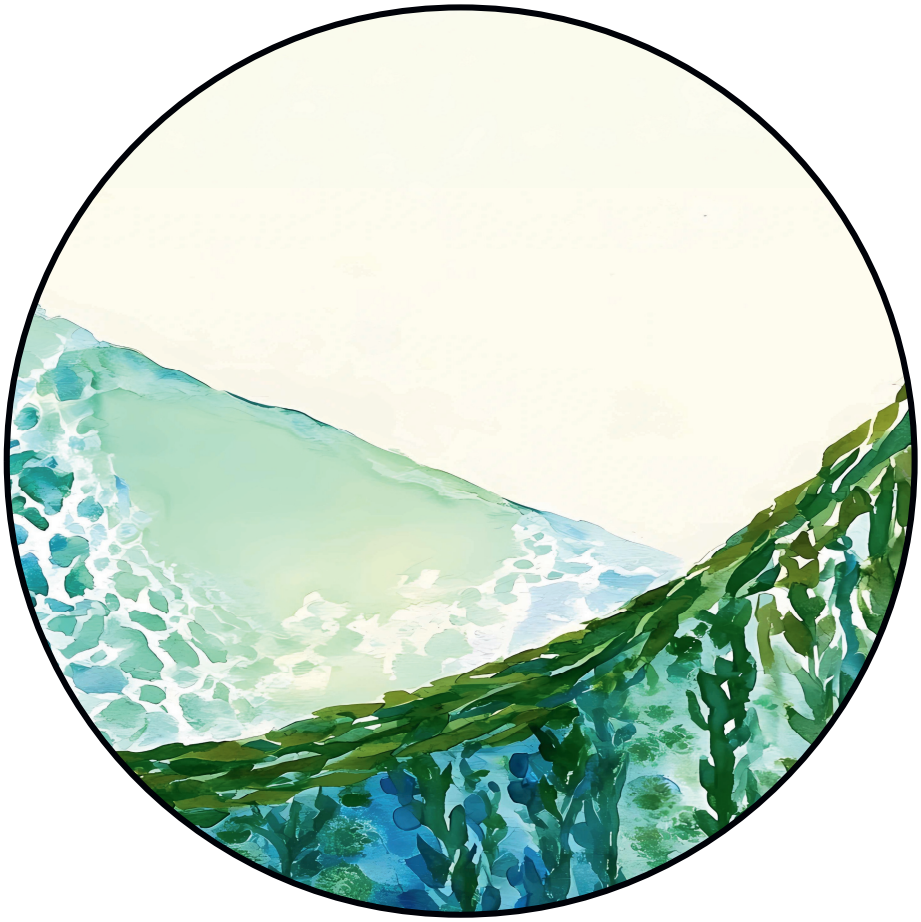


Figure S5.8. Extraction yields of alginate in the reusing test of menthol:thymol DES.



Chapter 6

Separation of alginate and recycling of deep eutectic solvents using temperature-responsive aqueous two-phase systems

Isa S.A. Hiemstra, Niels Lustig, Michel M.H. Eppink, Rene H. Wijffels, Antoinette Kazbar

This chapter has been published as:

Hiemstra, I. S. A., Lustig, N., Eppink, M. H. M., Wijffels, R. H., & Kazbar, A. (2025). Separation of alginate and recycling of deep eutectic solvents using temperature-responsive aqueous two-phase systems. *Journal Of Cleaner Production*, *536*, 147186. https://doi.org/10.1016/j.jclepro.2025.147186

Abstract

Deep eutectic solvents (DES) have emerged as green alternative extraction solvents. However, challenges in DES recovery and recycling limit their broader application. In this study, a novel thermo-separating aqueous two-phase system (ATPS) was developed for the continuous, cyclic extraction and separation of alginate from *Laminaria digitata* using DES and temperature-responsive copolymers. The system enables a novel approach by repeatedly reusing both the DES phase and the EOPO copolymer phase five times, thereby reducing waste generation and enhancing process sustainability. This research demonstrated that DES can be efficiently recycled for ten cycles using temperature-responsive ethylene oxide-propylene oxide (EOPO) copolymers, remaining stable yields. For the extraction and subsequent separation of alginate, three different DESs were evaluated, all of which demonstrated to extract and recover alginate. DESs ChCl:Ethylene glycol and ChCl:Urea exhibited a preference for EOPO1000 (66 and 75% recovery, respectively), whereas Bet:Urea achieved the highest recovery with EOPO3900 (66% recovery). Subsequent recycling of the recovered DES showed that DES could be recycled for ten cycles, maintaining stable extraction yields between 74 and 86 mg alginate/g DW and alginate recovery yields of 55 to 65%. Furthermore, combined DES and EOPO recycling could be performed for up to five cycles while maintaining an alginate recovery yield between 50 and 65 mg/g DW. This thermo-separating ATPS presents a novel, circular and sustainable approach for DES recycling compared to the non-circular conventional alkaline extraction. This proposed method can be applied in a simple and effective manner to both recover and recycle DES.

6.1. Introduction

Many industrial processing and extraction methods currently depend on conventional organic solvents, such as methanol, ethanol and sulphuric acid, which pose environmental, health and safety risks and are often not recycled, generating chemical waste [257–259]. To address these issues, alternative and more sustainable processes are being investigated [260–262], with particular focus on green solvents. One promising class of solvents are deep eutectic solvents (DESs). These solvents offer several advantages over traditional solvents, including lower toxicity, biodegradability, and the potential for recycling [117, 263]. DES are solvents composed of one or more hydrogen bond donors (HBD) and one or more hydrogen bond acceptors (HBA), formed upon a large depression in melting point when mixed at a certain ratio [9, 264].

One potential application of DES is the extraction of valuable marine constituents. For instance, alginate, a polysaccharide present in the cell wall of brown seaweed [265], is widely employed as a thickening agent in food processing and in diverse biomedical applications [123]. Brown seaweeds contain approximately 20-35% dry weight of the phycocolloid alginate [266]. Alginate is composed of two uronic acids: β-D-mannuronic acid and α-L-guluronic acid (**Figure S6.1**), with their composition and arrangement varying depending on the seaweed species, habitat, and seasonal conditions [267]. Conventional processes for alginate extraction from seaweed rely on large amounts of harsh solvents and often yield limited efficiency [56, 124]. Hence, there is a strong need to develop novel and sustainable processes, such as the use of DES for alginate extraction and recovery.

Recent studies have demonstrated that DES are effective for extracting polysaccharides from a variety of biomass sources, including seaweed [62, 100], molluscs [268], plants [79, 269] and fungi [270]. However, DES are characterised by their low vapour pressure, which complicates both solvent recovery and product isolation. As a result, DES removal is typically performed through ethanol [63] or isopropanol [119] precipitation, followed by multiple washing steps and vacuum evaporation. Wu *et al*. [79] and Wang *et al*. [78] employed ethanol precipitation combined with dialysis. Shang *et al*. [62] used a brominated macroporous resin to load the DES phase, followed by washing with water. Although polysaccharides were successfully recovered, the DES was simultaneously washed out and therefore could not be reused.

To enhance process sustainability in industrial applications, DES recycling is essential. Zhang *et al*. [270] recovered both polysaccharides and DES by repeatedly adding the DES to anhydrous ethanol for precipitation. The DES–ethanol precipitate was distilled

via rotary evaporation, allowing the DES to be reused for up to five extraction cycles. While antisolvent addition is a straightforward and selective approach, it poses challenges in process control due to potential loss of DES components. In addition, anti-solvent removal often requires long evaporation times (16–24 hours) [77], and some DESs may themselves precipitate upon alcohol addition, further limiting their recyclability [70]. Membrane-based separation processes, especially electrodialysis combined with ultrafiltration [83, 84], have been used for DES recovery and product separation [271]. Liang *et al*. [84] demonstrated the recycling of DES up to four times using ultrafiltration coupled with bipolar membrane electrodialysis. Although these techniques are easy to operate and cost-effective, they impose strict requirements on membrane performance due to the high viscosity of DES solutions, which increases the risk of membrane fouling [272]. Moreover, the recovery of concentrated extract is limited by concentration constraints inherent to the process [70].

In this context, aqueous two-phase systems (ATPS) present a promising and environmentally friendly alternative for recovering polysaccharides from DES and the potential recycling of the DES itself. ATPS is a liquid–liquid fractionation method that relies on the immiscibility of two aqueous solutions at specific concentrations [273] and is widely used for gentle, efficient, and straightforward separation of biomolecules and cells [274]. Several ATPS types have been explored, including polymer-polymer, polymer–salt, alcohol–salt, and thermo-separating polymer–salt systems [275, 276]. Among these, thermo-separating ATPSs are particularly attractive due to their ability to induce phase separation and product recovery simply by altering the temperature [277, 278]. These systems have been applied in the purification of several biomolecules, including anthraquinones [279], saccharides and proteins [280], vitamin B12 [281], lincomycin [282] and tea saponins [283]. Thermo-separation is achieved by increasing the temperature to a point at which the copolymer becomes insoluble, resulting in phase separation. Ethylene oxide-propylene oxide (EOPO) is a thermo-sensitive copolymer that can induce phase separation upon temperature changes [284]. EOPO has been used for EOPO-salt ATPS separation methods to separate products based on temperature change, including peptides [285], hyaluronic acid [284], polysaccharides [286] and polyphenols [287]. Limited studies have explored the use of thermo-separating aqueous two-phase systems (ATPS) for product recovery from DES. Gao *et al*. [288] demonstrated that polysaccharides extracted from *Camellia oleifera* using DES could be recovered using a temperature-responsive ATPS, achieving recovery yields of up to 86%. Similarly, Zhou *et al*. [289] showed that polysaccharides from American ginseng could be extracted with DES and subsequently recovered through a thermo-separating ATPS. However, in both studies, while the polysaccharides were successfully recovered, the DES was not reused in subsequent extractions. Recovering

both the bioactive compounds and the DES is essential for enhancing the sustainability of DES-based extraction processes by minimising solvent waste.

In the present study, we aimed to develop a novel and circular thermo-separating ATPS for the simultaneous recovery of functional alginate and recycling of both DES and EOPO after extraction from the brown seaweed *Laminaria digitata*. Various DESs and ethylene oxide–propylene oxide (EOPO) copolymers were evaluated to determine the most effective combination for alginate recovery. A recycling study was conducted to assess the extraction efficiency and recovery yield of the reused DES. In addition, the feasibility of the combined recycling of EOPO and DES was investigated, allowing repeated reuse of both phases, thereby minimising waste generation. Overall, this study introduces an innovative and sustainable method for alginate recovery from DES while enabling effective solvent recycling, without significantly compromising extraction yields. These findings lay the groundwork for more environmentally friendly DES-based extraction processes, where both product and solvent can be efficiently recovered and DES can be reused.

6.2. Materials and methods

6.2.1 Materials

Brown seaweed *Laminaria digitata* was used for the extraction of alginate. Sun-dried *L. digitata* was obtained from Algaia in March 2023 (**Figure S6.2**). Before use, the biomass was shredded, its dry weight was determined, and it was sieved using 710 µm and 90 µm mesh sizes. The fraction between 90 and 710 µm was collected and stored at 4 °C for extraction. For alginate extraction and isolation, three DESs were used, containing 15 wt% of water (**Table 6.1**, **Table S6.1**). As HBA, either choline chloride or betaine was used and as HBD, ethylene glycol or urea was used.

Table 6.1 Composition of DESs used in this study.

	HBA	HBD	Mole ratio	Abbreviation	Viscosity [a] (mPa*s)	Density [a] (g/cm^3)
DES 1	Choline chloride	Ethylene Glycol	1:2	ChCl:EG	17.11	1.105
DES 2	Choline chloride	Urea	1:2	ChCl:U	7.36	1.142
DES 3	Betaine	Urea	1:2	Bet:U	91.48	1.195

[a] Measured at 20 °C.

The DES constituents choline chloride (≥98%), betaine (≥98%), ethylene glycol (≥99%), and urea (≥99.5%) were purchased from Sigma-Aldrich (Merck). EOPO copolymers with Pluronic® 10 wt% PEG block-copolymers (PEG-PPG-PEG) with average molecular weights of 1000, 2500 and 3900 were purchased from Sigma-Aldrich (Merck).

6.2.2 DES preparation and characterisation

The DESs were prepared using the heating method [200]. The HBA and HBD were mixed in a molar ratio of 1:2 (**Table 6.1**) with 15 wt% of water, and this was put in a water bath at 80 °C for one hour until a transparent solution was obtained. Subsequently, the formed DES was used for the extraction of alginate. The dynamic viscosity of each DES and EOPO was measured over a temperature range from 20 °C and 60 °C with 10 °C intervals using an Anton Paar rotational viscometer (Anton Paar ViscoQC 300 Rotational Viscometer) with measuring probe B-SC4-18. The density of the DES and EOPO was measured using an Anton Paar density and sound velocity meter (DSA 5000M) at 20 °C.

6.2.3 Alginate extraction and quantification

Three DESs were used to extract alginate from *L. digitata* (**Table 6.1**). A solid:liquid ratio of 1:40 was applied [119]. The extractions were performed at 80 °C for one hour. During the extractions, the samples were regularly vortexed. As a control, alkaline extraction was performed. Acid water containing H_2SO_4 (pH 1.9) was added in a 1:1 (w/w) ratio to the seaweed, and this was set for one hour at room temperature. Subsequently, Na_2CO_3 was added in a ratio of 0.0325:1 (w/w), and the extraction was performed for one hour. DES and alkaline extractions were performed in triplicate. After extraction, the samples were centrifuged, and the supernatant was taken for alginate quantification. Quantification was performed using a method adapted from Cesaretti *et al*. [136]. Subsequently, the DES layer was separated from the supernatant and used for the first ATPS. The alginate extraction yield from *L. digitata* represents the quantity of alginate obtained using DES per gram of dry seaweed, and was determined using **Equation 6.1**:

$$Extraction\ yield\ \left(\frac{mg}{g\ DW}\right) = \frac{C_{extract} * V_{total}}{m_{biomass} * x_{DW}} \quad (\mathbf{6.1})$$

where $C_{extract}$ is the concentration of the extract, $m_{biomass}$ is the weight of the initial biomass, x_{DW} is the weight fraction of the dry biomass and V_{total} is the total volume of the extract.

6.2.4 Alginate isolation

6.2.4.1 Aqueous two-phase separation between EOPO and DES

To all DESs, EOPO was added to obtain an EOPO wt% of either 30%, 40%, 50%, 60% or 70% (**Table 6.2**). For each DES, EOPO copolymers with molecular weights of 1000, 2500, and 3900 were added to facilitate aqueous two-phase separation (**Table 6.2**). After EOPO addition, the solution was mixed thoroughly for 15 minutes and left for at least one hour until phase separation was observed. The EOPO-containing layer was subsequently transferred to the second ATPS to recover alginate from the EOPO phase (**Figure 6.1**).

Table 6.2 Different variables tested per DES in the first ATPS.

	EOPO1000	**EOPO2500**	**EOPO3900**
EOPO (wt %)	30	30	30
	40	40	40
	50	50	50
	60	60	60
	70	70	70

6.2.4.2 Temperature-dependent aqueous two-phase separation

For the removal of alginate from the EOPO layer, a temperature-dependent aqueous two-phase separation was used (**Figure 6.1**). To the isolated EOPO fraction, water was added in a 1:1 mass ratio. The solution was vortexed to mix the two layers. Once the EOPO was dissolved, the solution was heated at 60 °C for at least two hours until phase separation occurred. From the observed phase separation, the position of the aqueous layer was determined. The alginate concentration was determined from the aqueous layer. The percentage of alginate recovery (%) was determined by comparing the initial alginate extracted to the alginate recovery yield obtained in the aqueous layer after the second ATPS. The alginate recovery yield represents the quantity of alginate obtained in the aqueous phase after the ATPS separations, and was calculated using **Equation 6.2**:

$$Recovery\ yield\ \left(\frac{mg}{g\ DW}\right) = \frac{C_{aqueous} * V_{aqueous}}{m_{biomass} * x_{DW}} \qquad (\mathbf{6.2})$$

where $C_{aqueous}$ is the concentration of alginate in the aqueous phase, $m_{biomass}$ is the weight of the initial biomass, x_{DW} is the weight fraction of the dry biomass and $V_{aqueous}$ is the volume of the aqueous phase.

6.2.5 Alginate characterisation

The alginate fraction was characterised using Fourier Transform Infrared Spectroscopy (FTIR) and compared to alginate extracted through alkaline treatment. Characterisation was conducted with a Nicolet Summit X ATR-FTIR Spectrometer (ThermoFisher Scientific) over a spectral range of 400–4000 cm^{-1}. The alginate extracts were isolated through a precipitation step using 1% w/v calcium chloride dihydrate, followed by two successive washes with 80% ethanol. The resulting precipitate was dried under a nitrogen flow and characterised using FTIR spectroscopy.

The mannuronic to guluronic (M/G) ratio of the extracted alginate was determined through methanolysis followed by high-performance anion exchange chromatography with pulsed amperometric detection (HPAEC-PAD) as described by Bojorges *et al*. [227]. The Dionex ICS-6000 system (ThermoFisher) with CarboPac 1 mm column was used. Alginate extracted using DES was compared with alginate obtained via conventional alkaline treatment. The extracted alginate was precipitated with 80% ethanol containing 1% NaCl, followed by washing twice with 80% ethanol. Subsequently, the samples were resolubilised in Milli-Q water. Samples of 50 µL were used for the methanolysis.

6.2.6 DES recycling

For DES recycling, the optimal DES and EOPO conditions for alginate recovery were selected. The alginate extraction and subsequent alginate and DES separation were repeated up to ten times. In each cycle, both extraction and recovery yields were measured to evaluate the impact of DES reuse. After each extraction step, the alginate content was determined. After each cycle, the alginate recovery was assessed.

6.2.7 Combined DES and EOPO recycling

To assess the influence of recycling of both fractions, combined DES and EOPO recycling was performed. The same conditions were applied as for DES recycling (**Section 6.2.6**). Both fractions were recycled up to six times. Each cycle, the alginate extraction yield and recovery were assessed.

An overview of the extraction, two-step aqueous two-phase separation and solvent recycling is presented in **Figure 6.1**. First, alginate is extracted using DES. In the initial aqueous two-phase system (ATPS1), EOPO is introduced, enabling alginate to partition into the EOPO-rich phase. After phase separation, the EOPO and DES phases are isolated, and the DES is recycled for subsequent extractions. The EOPO phase is then subjected to the second ATPS (ATPS2), where water is added and the temperature is increased to induce phase separation between EOPO and water. This facilitates the transfer of alginate into the aqueous phase, which is collected, while EOPO was recovered for reuse in the next ATPS1 cycle.

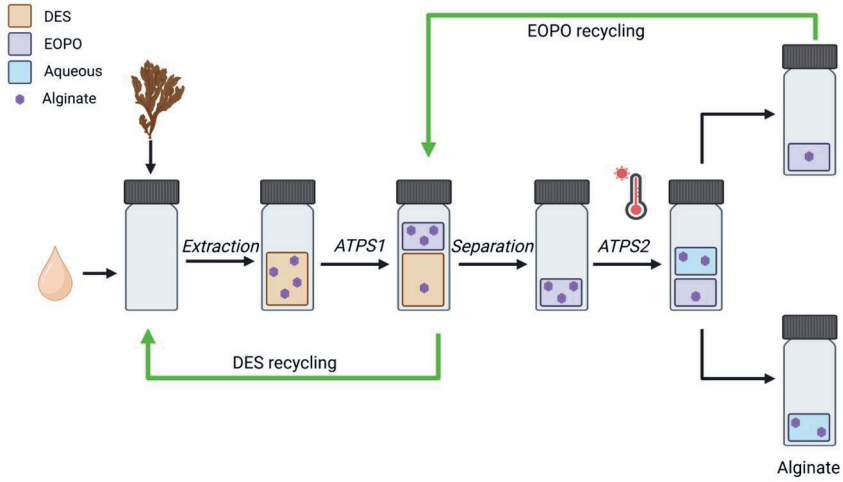


Figure 6.1 Schematic overview of the alginate extraction and separation procedure. Alginate is first extracted using DES, after which EOPO is added in ATPS1 to transfer alginate into the EOPO-rich phase while the DES phase is recovered and recycled. In ATPS2, water addition and heating induce the separation of EOPO and water, enabling alginate to move into the aqueous phase. The aqueous phase is collected, and EOPO is reused in the next ATPS1 cycle.

6.3. Results and discussion

6.3.1 Extraction and isolation of alginate

6.3.1.1 Extraction of alginate

Alginate was successfully extracted using each DESs (**Figure 6.2**). Among them, ChCl:EG yielded the highest alginate content with an extraction yield of 100.3 ± 8.0 mg/g DW. ChCl:U resulted in the lowest yield, extracting 71.4 ± 2.4 mg/g DW, while Bet:U achieved an intermediate yield of 83.3 ± 10.5 mg/g DW. The conventional alkaline control method yielded 89.0 ± 3.6 mg/g DW, which was comparable to ChCl:EG and Bet:U. Although the extraction yields obtained via the alkaline method were similar to those of ChCl:EG and Bet:U, and higher than those of ChCl:U, this approach poses environmental concerns due to the harsh alkaline conditions and the use of sulfuric acid. Conventional alginate extraction relies on acidification with concentrated acids, including sulphuric acid, to remove divalent cations, thereby converting alginate salts into alginic acid. Subsequently, alkaline hydrolysis is applied for alginate extraction. This two-step process generates effluents that require neutralisation and waste management [56]. Additionally, solvent regeneration is not feasible in the conventional method, further limiting its sustainability. The three DESs were subsequently utilised for alginate separation through the two-step ATPS separation.

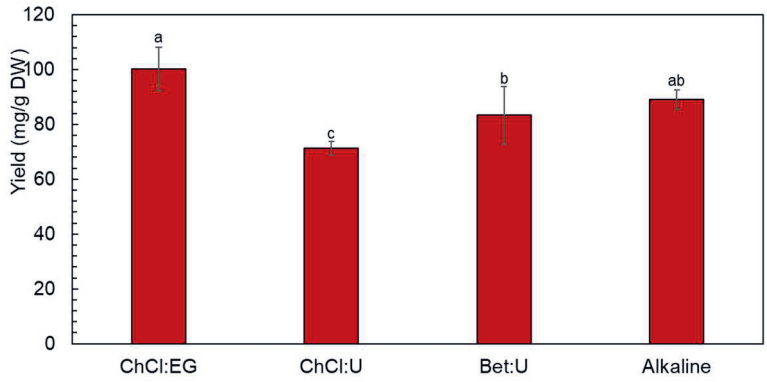


Figure 6.2 Extraction of alginate from L. digitata with three DESs and alkaline extraction as control.

6.3.1.2 Isolation of alginate

To assess the performance of the different DESs per EOPO, evaluating the recoveries of alginate per DES is essential (**Table 6.2**). A high extraction rate with a low recovery could still be less efficient. By combining alginate yield and recovery, the overall performance of the isolation method could be determined. For the first ATPS, three

EOPOs were used in different ratios for each DES (**Section 6.2.4.1**). The phase separation of all combinations of DESs with EOPOs (**Figure S6.3**) showed that the type of EOPO affects its behaviour towards the DESs. For all DESs, EOPO1000 and EOPO3900 appeared as the top layer in the system. For EOPO2500, no clear phase separation occurred for DES ChCl:EG and Bet:U (**Figure S6.3**). Gao *et al*. [288] used DES ChCl:EG, containing 30 wt% water, for the extraction and isolation of polysaccharides from *Camellia oleifera* Abel. The highest recovery was observed when using EOPO2500 with ChCl:EG (30 wt% water). The difference in water content between this DES and the DES used in our study probably affected phase separation differently, as increased water content reduces viscosity and density, thereby altering the physicochemical properties of the DES [290]. These changes can significantly impact the performance of the ATPS. In the case of EOPO2500, the intermediate molecular weight may result in an intermediate hydrophilic–hydrophobic character, providing insufficient polymer–solvent incompatibility to promote complete phase separation. Additionally, when combined with ChCl:EG and Bet:U containing 15 wt% water, EOPO2500 may lie closer to the binodal curve of the ATPS, making phase separation highly sensitive to DES composition and water content. This behaviour could explain the poor separation observed. Due to insufficient phase separation, EOPO2500 was excluded from further experiments.

In the consecutive thermo-separating ATPS step, the alginate recovery was assessed. For phase separation with EOPO1000, the EOPO was situated at the top layer because the density of this copolymer is 0.988 g/cm^3 (**Table S6.2**). In contrast, for EOPO3900, the EOPO was placed at the bottom layer since this copolymer has a density greater than water, measuring 1.056 g/cm^3 (**Figure S6.4 and S6.5** and **Table S6.2**).

DES ChCl:EG and ChCl:U displayed a preference for EOPO1000, while Bet:U recovered more alginate with EOPO3900 (**Figure 6.3**). For ChCl:EG, the highest recovery reached was 66.0 ± 6.2%, at 40 wt% of EOPO1000 (**Figure 6.3a**). When taking into account the extraction yield, 66.2 mg/g alginate was recovered (**Table 6.3**). The recovery using EOPO1000 was approximately twice that observed with EOPO3900 for ChCl:EG (**Figure 6.3a**). This difference could be due to the larger viscosity of EOPO3900 at 20 °C (**Figure S6.6**), which may hinder efficient mass transfer and phase separation compared to EOPO1000. When applying DES ChCl:U, the highest alginate recovery was reached (75.4%) at 50 wt% of EOPO1000 (Figure 3b). This resulted in an alginate recovery yield of 53.8 mg/g DW (**Table 6.3**). ChCl:U resulted in the highest percentage of alginate recovery, which was the DES with the lowest viscosity (**Figure S6.7**). The lower viscosity of ChCl:U compared to the other DES (**Figure S6.7**) may have facilitated more efficient mass transfer into the copolymer phase [291, 292]. For this DES, a clear influence of

the EOPO concentration on alginate recovery was observed. The highest recovery yields were achieved at an EOPO1000 to DES ratio of approximately 1:1. Reducing the ratio to 30 wt% or increasing it to 70 wt% caused the recovery to drop to 17 % or, in the latter case, resulted in no detectable alginate recovery. Increasing the EOPO concentration up to 50 wt% likely enhances the contact area between alginate and EOPO (**Figure 6.3b**), promoting the preferential partitioning of alginate into the EOPO-rich phase. However, further increasing the EOPO concentration to 60 or 70 wt% led to a decrease in alginate recovery. This decline may be attributed to the volume exclusion effect that becomes significant at high EOPO concentrations. The entropic effect is predominant at high EOPO concentrations, thereby hindering solute partitioning [293, 294]. At elevated polymer contents, the EOPO-rich phase becomes increasingly crowded, reducing the available free volume for alginate. This crowding increases the entropic penalty associated with alginate entering the polymer-rich phase. As a result, alginate is thermodynamically disfavoured from partitioning into the EOPO phase, leading to reduced recovery. Such behaviour is well-described in polymer–salt and polymer–polymer ATPS [275], where high polymer concentrations limit solute accessibility due to steric constraints and reduced solvent activity. Additionally, higher EOPO content increases the system's viscosity, which can reduce mass transfer efficiency and impair recovery yields [295].

For ChCl:EG and ChCl:U, the average molecular weight of the EOPO copolymer was found to significantly influence the alginate recovery yield. EOPO1000, which has a lower molecular weight than EOPO3900, possesses shorter polymer chain lengths. These shorter chains may provide more free volume within the solution [287], thereby enhancing the accommodation and solubility of alginate in the EOPO phase. As a result, up to eight times more alginate was recovered using EOPO1000 compared to EOPO3900 for ChCl:U at 50 wt%. Bet:U had the highest recovery (66%) at 30 wt% of EOPO3900 (**Figure 6.3c**), indicating that an alginate recovery yield of 54.8 mg/g DW was obtained (**Table 6.3**). In contrast to the behaviour observed for ChCl:EG and ChCl:U systems, both EOPO copolymers exhibited comparable recovery efficiencies when Bet:U was used. This could be due to the increased viscosity of this DES at 20 °C compared to ChCl:EG and ChCl:U (**Figure S6.7**). The hydrophobicity of the polymer increases when the molecular weight increases, due to the increase in hydrophobic area compared to hydrophilic groups [296]. Therefore, an EOPO with a higher molecular weight requires lower concentrations to form an ATPS, due to the increased hydrophobicity [277, 297]. This will, in turn, lead to enhanced phase separation. This trend correlates with the results obtained from Bet:U, where the highest recovery of

alginate was obtained using the lowest weight percentage of EOPO3900. For EOPO1000 with the same DES, the highest recovery was obtained at 50 wt%.

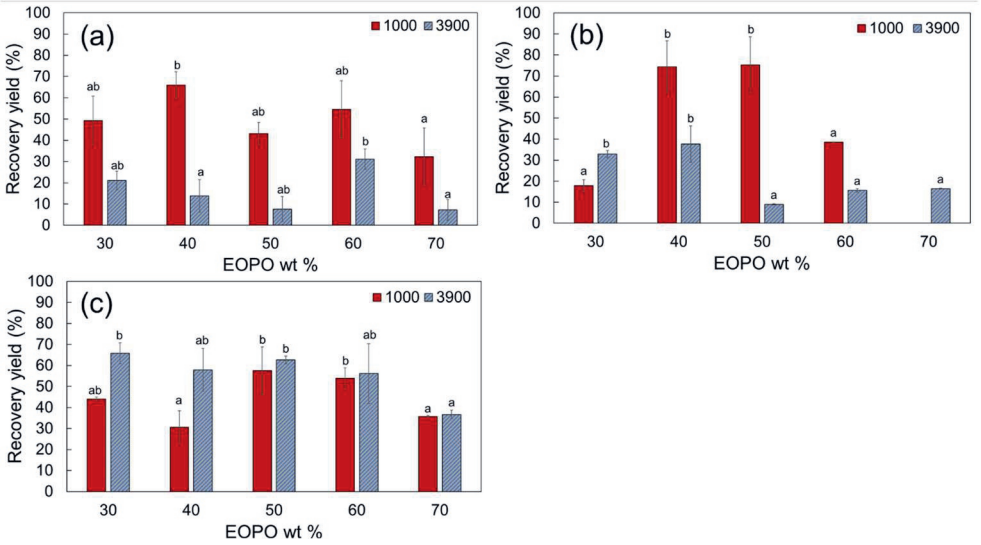


Figure 6.3 Recovery yields of alginate for (a) ChCl:EG, (b) ChCl:U and (c) Bet:U using EOPO1000 and EOPO3900.

No literature is available on the effect of the molecular weight of the EOPO on alginate separation. However, for the protein bromelain, previous studies have shown that increasing the molecular weight of EOPO leads to a higher partitioning coefficient [298]. Similarly, lower separation of the enzyme guanylyltransferase was observed when EOPO with a lower molecular weight was used [296]. For polyphenol extraction, a reversed trend was observed. A shorter chain length of EOPO resulted in a lower polyphenol yield [287]. For alginate, notable differences in recovery were observed between EOPO1000 and EOPO3900 across the three DES systems. This suggests that the hydrogen bond acceptor (HBA) in the DES may influence alginate isolation. Specifically, Bet:U yielded higher alginate recoveries with EOPO3900, whereas ChCl:EG and ChCl:U showed greater recoveries when EOPO1000 was used. This indicates that the selection of the DES constituents and thus the DES extract composition largely influences the recovery and the optimal choice of EOPO.

Interestingly, the DES with the highest extraction yield (ChCl:EG) gave lower alginate recovery, while the lowest-yielding DES (ChCl:U) achieved the highest recovery (**Table 6.3**). This indicates that recovery efficiency depends not solely on extraction yield but on alginate partitioning between the DES and copolymer phases. An optimal equilibrium between these phases appears to enhance recovery. Despite differences

in efficiency, final alginate yields were similar (55–66 mg/g DW), highlighting the importance of this phase equilibrium in governing overall recovery performance.

Table 6.3 Alginate extraction yield, optimal recovery (%) and alginate recovery yield per DES.

	ChCl:EG	ChCl:U	Bet:U
Extraction yield (mg/g DW)	100.3 ± 8.0	71.4 ± 2.5	83.3 ± 10.5
Alginate recovery (%)	66.0 ± 6.2	75.4 ± 12.3	66.0 ± 5.0
Alginate recovery yield (mg/g DW)	66.2 ± 8.2	53.8 ± 9.0	54.8 ± 8.1

Since the final alginate yields were similar (**Table 6.3**), Bet:U was selected for characterisation and subsequent DES recycling as the lowest amount of EOPO could be applied compared to ChCl:EG and ChCl:U (30 wt% for Bet:U compared to 40 and 50 wt% for ChCl:EG and ChCl:U, respectively).

6.3.2 Alginate characterisation

The alginate recovered from the DES Bet:U was characterised using FTIR and analysed for its mannuronic to guluronic acid (M/G) ratio. The M/G ratio is a critical parameter in alginate characterisation, as it influences the polysaccharide's physical and functional properties [227]. Alginates with a higher M/G ratio typically form more permeable and flexible gel matrices, whereas those with a lower M/G ratio tend to produce mechanically stronger gels. This is due to the higher affinity of guluronic acid (G) blocks for calcium ions compared to mannuronic acid (M) blocks, resulting in stronger cross-linking and firmer gel structures [247]. The M/G ratio for alginate extracted with Bet:U was 1.96 ± 0.02. Compared to alkaline extraction, this ratio was 1.49 ± 0.02 (**Table S6.3**). These values are comparable to the reported values (1.44 to 1.82) for *L. digitata* [56, 299], indicating that the alginate is flexible and can form soft and elastic gels.

The FTIR spectra of alginate extracted through DES and alkaline treatment displayed similar patterns (**Figure 6.4**). Both extracts showed characteristic peaks at 1035 cm^{-1} and 1080 cm^{-1}, as well as at 1600 cm^{-1} and 1400 cm^{-1}. The distinct peaks at approximately 1080 cm^{-1} and 1035 cm^{-1} are associated with mannuronic and guluronic acid units, respectively [246, 300]. The bands at 1600 cm^{-1} and 1400 cm^{-1} are associated with asymmetric and symmetric stretching modes of carboxylate groups [244–246]. Additionally, a broad band at 3500 cm^{-1} and a weak band at 2900 cm^{-1} were observed, correlating to hydrogen-bonded O-H and C-H stretching vibrations, respectively [245]. The appearance of these characteristic absorption bands

demonstrates that the DES-EOPO system effectively extracts alginate and produces a spectral signature consistent with that of conventionally extracted alginate.

Based on FTIR and MG data, it was observed that alginate extracted and recovered with Bet:U in a temperature-responsive ATPS is not affected differently compared to the current alkaline extraction. Similar functional groups and similar M/G ratios were defined. Therefore, DES-based alginate extraction and subsequent recovery with a temperature-responsive EOPO could be a suitable approach that maintains alginate characteristics.

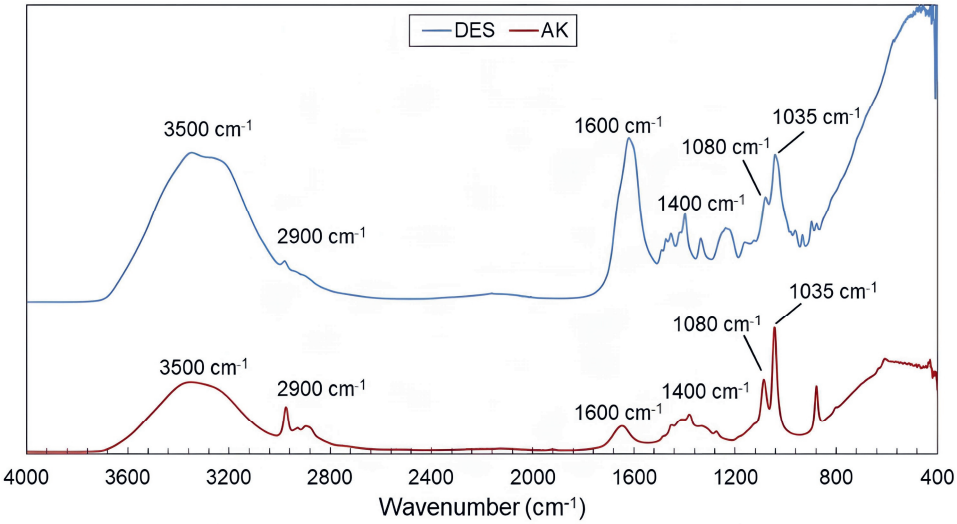


Figure 6.4 FTIR spectra of alginate extracted with DES (Bet:U) and with the conventional alkaline (AK) extraction.

6.3.3 Recyclability of recovered DES

Previous studies have reported DES recovery using temperature-responsive copolymers [288, 289]. However, whether the recovered DES can be effectively reused as an extraction solvent has not yet been investigated. Therefore, Bet:U was utilised for extraction, recovered, and subsequently recycled for additional alginate extraction cycles. The optimal recovery conditions at 30 wt% EOPO3900 (**Section 6.3.2.1**) were used. Thus, it was investigated whether the alginate extractability or recovery capability would be impacted by reusing the DES within this system. For DES recycling, the process of alginate extraction followed by its separation from DES was repeated over ten consecutive cycles. After the first ATPS, the DES was reused for the next extraction cycle (**Section 6.2.6**). After ten extraction cycles with Bet:U, the alginate extraction yields remained stable between 74 and 86 mg alginate/g DW (**Figure 6.5**). After cycle

seven, a slight decrease in extraction yield was observed. The accumulation of other constituents in the DES [301, 302], present in low amounts, such as proteins, could have influenced the alginate yield. These additional solutes may compete with alginate for dissolution, alter the hydrogen-bonding environment, or increase the viscosity of the DES, thereby reducing the solvent's effective capacity to extract alginate. The results indicate that the extraction yield is not majorly influenced when reusing the DES up to ten times. The recovery of alginate when reusing the DES was found to remain stable between 55 and 65% (56.0 ± 0.9 and 41.2 ± 5 mg/g recovery yield) (**Figure 6.5**).

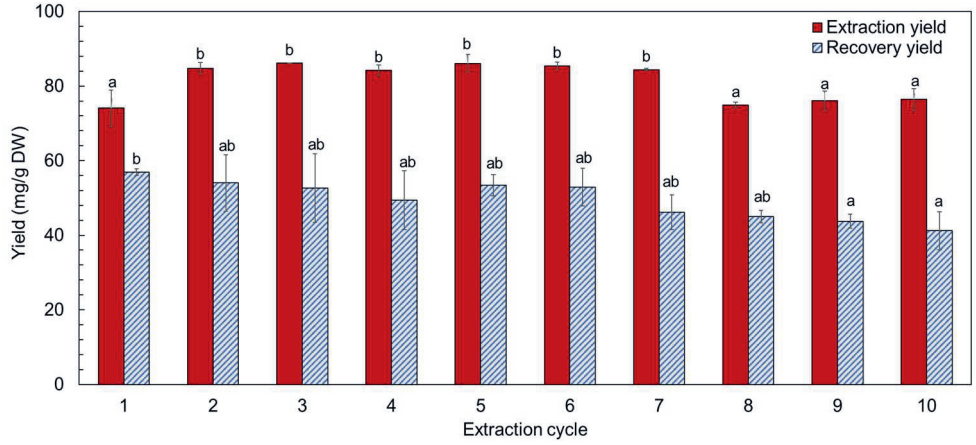


Figure 6.5 Alginate extraction and recovery yield during DES recycling.

To the best of our knowledge, no studies have been performed yet on the recycling of DES after product recovery through EOPO addition. However, several studies have reported the recycling of DES through different approaches. For recycling DES that was used for pre-treating plant biomass, a highly used approach is anti-solvent addition [303, 304]. For this approach, DES could be recycled between 2 and 4 times. Jeong *et al*. [305] recycled a DES composed of glycerol, L-proline, and sucrose (9:4:1) three times after performing extractions of ginsenoside from Korean ginseng. Recycling involved diluting the DES threefold with water, loading onto hydrophilic-lipophilic balance cartridges, followed by rinsing and vacuum drying. Xie *et al*. [306] employed DES for the pretreatment of lignocellulosic biomass and recovered it by removing the water from the DES through rotary evaporation. This approach enabled the DES to be reused for up to five pretreatment cycles. For the extraction of ferulic acid from oil palm empty fruit bunch fibre, Ng *et al*. [301] applied antisolvent addition to precipitate ferulic acid, followed by filtration. The DES was subsequently recycled successfully up to five times.

Compared to the other recycling strategies, the proposed ATPS-based approach enables a greater number of recycling cycles within the integrated extraction–separation system. Since both alginate yield and recovery remain stable, this indicates that DES can be recycled within a temperature-responsive ATPS for continuous extraction of alginate from brown seaweed.

To further improve the circularity and sustainability of the process, the potential of recycling EOPO together with DES was investigated, as this has not been assessed previously in literature. Both DES and EOPO fractions were recycled after each cycle for six cycles (**Figure 6.6, Table S6.4**). As can be observed, the alginate extraction yield decreased from cycles 1 to 3 from 80.3 ± 10.5 to 64.2 ± 9.0 mg/g, followed by an increase from cycle 4. However, when considering the amount of alginate in the final aqueous phase, the recovery remained rather stable between 54.8 ± 7.8 and 46.6 ± 6.5 mg/g from cycles 1 to 5 (**Figure 6.6**). Since the amount of recovered alginate increased while the extraction yield decreased, this could be due to the accumulation of alginate in the EOPO fraction. When the EOPO gets more saturated, the alginate in the DES phase increases (starting from cycle 3), as alginate cannot be fully transferred to the EOPO in the first ATPS. Even though more alginate is present in DES, recovered alginate decreased to 25.1 ± 7.7 mg/g in cycle 6.

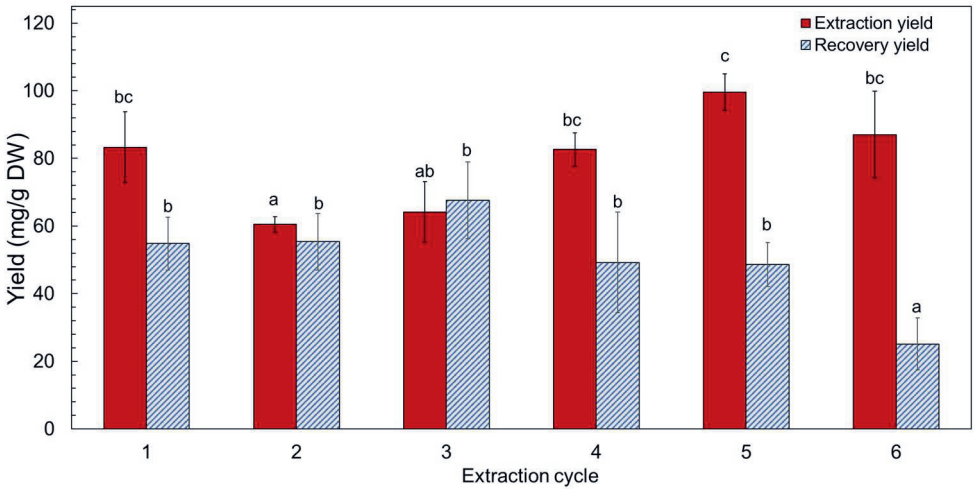


Figure 6.6 Alginate extraction and recovery yield during simultaneous DES and EOPO recycling.

6.3.4 Overall extraction and recovery process

Two approaches can be employed for the temperature-responsive ATPS recovery process: (1) recycling only DES, and (2) recycling both the DES and the EOPO fraction. In the first scenario, up to ten reuse cycles are achievable. However, this strategy

results in continuous EOPO consumption, potentially generating chemical waste. In contrast, simultaneous recycling of both DES and EOPO is feasible for up to five cycles, during which alginate extraction yields fluctuate between 60 and 100 mg/g DW, and the alginate recovery yields remain stable at approximately 50-65 mg/g DW (**Figure 6.7**). The ability to recycle both phases is supported by the stable transfer of alginate from the DES to the EOPO phase over multiple cycles, indicating that the ATPS1 partitioning step remains effective under simultaneous recycling conditions. However, when only the DES fraction is recycled, the recovery yield remains constant despite repeated cycles, suggesting that alginate progressively accumulates in the EOPO phase. This accumulation likely impairs alginate partitioning efficiency, altering the EOPO phase properties, such as viscosity, polymer–solute interactions, or available partitioning capacity, ultimately reducing the number of effective EOPO reuse cycles. Introducing a washing step to remove residual alginate from the EOPO fraction could mitigate this issue, potentially improving the transfer efficiency from DES to EOPO and enabling more recycling cycles.

Although recycling only the DES allows for greater reuse frequency, the dual-component recycling approach offers a more integrated and sustainable solution. By reducing chemical consumption and minimising waste, the combined recycling of DES and EOPO contributes to a more circular and environmentally friendly alginate extraction process (**Figure 6.7**). Therefore, despite the reduced number of cycles, the second approach may be considered more favourable for long-term, sustainable operation.

Scaling up the DES–EOPO ATPS process may present challenges, particularly related to the high viscosity of DESs and the energy requirements for heating to induce phase separation. Elevated viscosity could hinder efficient mixing, mass transfer, and phase separation at larger volumes, while heating costs could increase operational expenses. Potential solutions include optimising DES composition to reduce viscosity, such as increasing the water content, provided that the impact on ATPS formation at the required EOPO concentration is systematically evaluated. Mechanical agitation or static mixers may further enhance phase contact, and alternative heating strategies such as localised or continuous heating could improve overall energy efficiency. This may further facilitate scalability while maintaining extraction performance. In addition, incorporating spectroscopic analyses (e.g. FTIR) on the used DES and EOPO fractions into future scale-up studies could help identify potential chemical or structural changes in the DES or EOPO phases, thereby supporting more informed optimisation at larger scales.

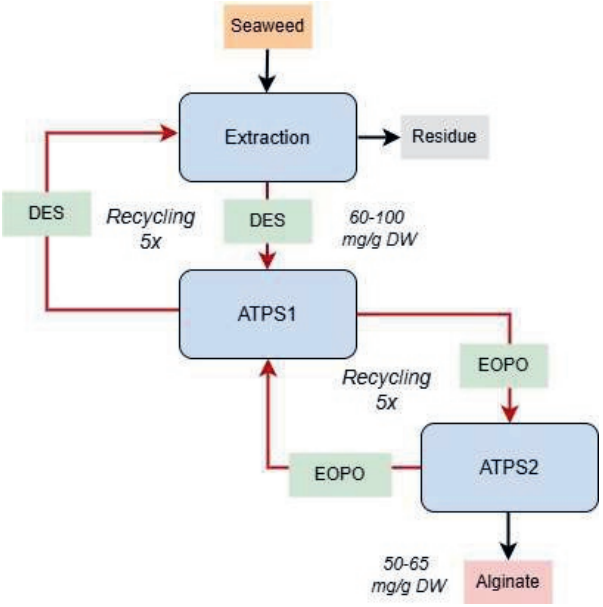


Figure 6.7 Alginate extraction and recovery yields during simultaneous recycling of both DES and EOPO phases over five consecutive cycles. Extraction yields remain within 60–100 mg/g DW across cycles, while recovery yields are consistently maintained at approximately 50–65 mg/g DW.

6.4. Conclusion

In this study, a thermo-separating aqueous two-phase system (ATPS) was developed for the continuous extraction and separation of alginate using DES as an alternative, circular extraction process compared to conventional alkaline extraction. This research demonstrated, for the first time, that DESs can be effectively recycled for at least ten cycles using a temperature-responsive ethylene oxide–propylene oxide (EOPO) copolymer. The three different DESs all successfully extracted and recovered alginate. Bet:U was selected for further recycling studies with EOPO3900 (54.8 ± 8.1 mg/g), as it required the lowest amount of copolymer for separation. The DES reusability study showed that the alginate extraction yield remained between 74 and 86 mg/g DW over ten cycles, with consistent recovery yields (55-65%). Furthermore, the combined recycling of both the DES and EOPO was successfully performed for up to five cycles while maintaining stable recovery performance (between 54.8 ± 7.8 and 46.6 ± 6.5 mg/g).

This study presents a novel, efficient, and circular approach for DES recycling. The thermo-separating ATPS offers a suitable and straightforward method for the recovery and reuse of DES. Additionally, the simultaneous recycling of DES and EOPO could enhance process sustainability and significantly reduce solvent waste. The proposed system provides a viable, eco-friendly alternative for alginate extraction and isolation, while enabling effective regeneration of DES.

6.5. Supplementary information

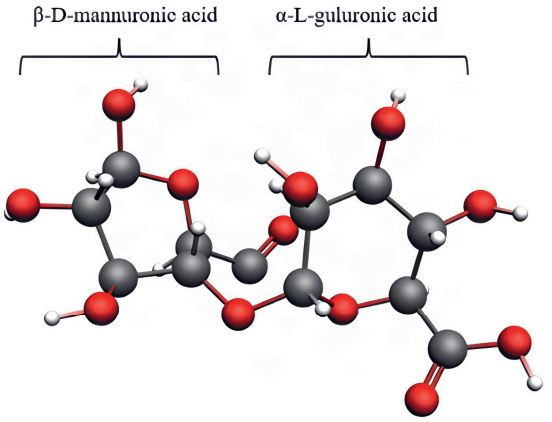
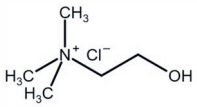
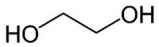
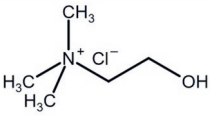
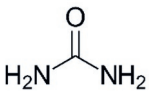
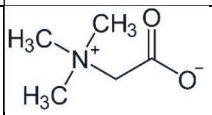
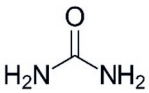


Figure S6.1 Chemical structure of alginate monomers β-D mannuronic acid and α-L guluronic acid.



Figure S6.2 Sun-dried *Laminaria digitata* used in this study.

Table S6.1 Molecular structures of the DES combinations used in this work.

DES1	Choline chloride: Ethylene glycol (1:2)		
DES2	Choline chloride: Urea (1:2)		
DES3	Betaine: Urea (1:2)		

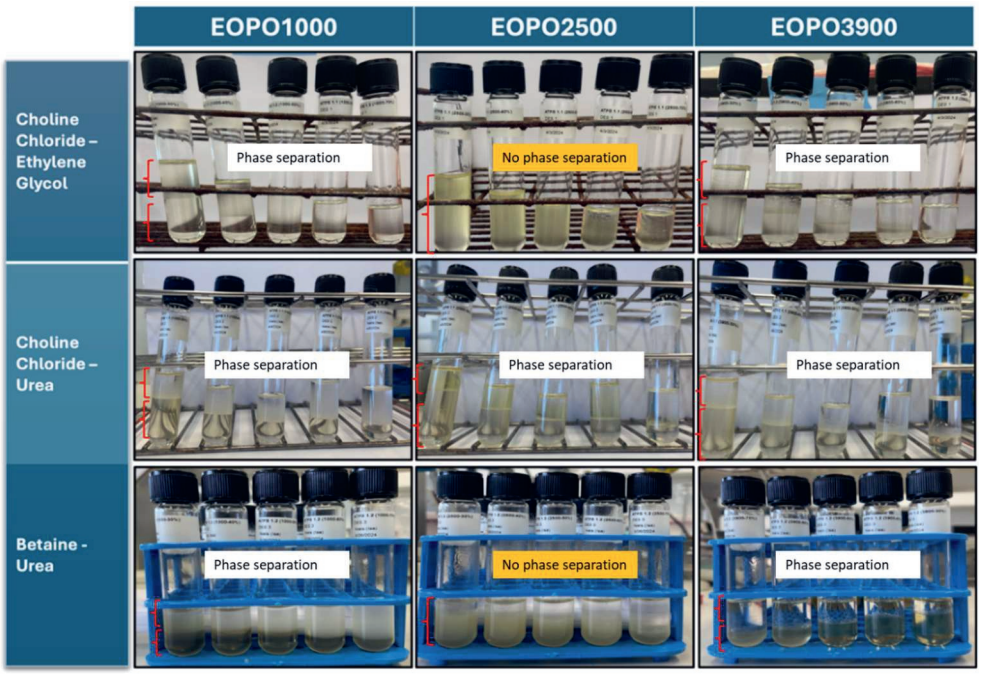


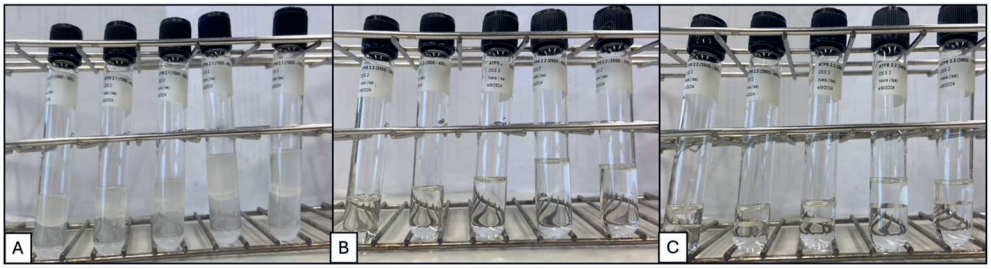
Figure S6.3 First ATPS (DES and EOPO) for ChCl:EG, ChCl:U and Bet:U using different wt% of EOPO.

Table S6.2 Density of the studied DESs and EOPOs.

	Density (g/cm^3)[a]
ChCl-EG	1.106 ± 0.00
ChCl-U	1.142 ± 0.00
Bet-U	1.195 ± 0.00
EOPO1000	0.989 ± 0.00
EOPO2500	1.095 ± 0.00
EOPO3900	1.056 ± 0.00

[a] Density was measured at 20 °C.

Figure S6.4 A) Phase separation with EOPO1000 in second ATPS B) Phase separation with EOPO2500 in second ATPS C) Phase separation with EOPO3900 in second ATPS.



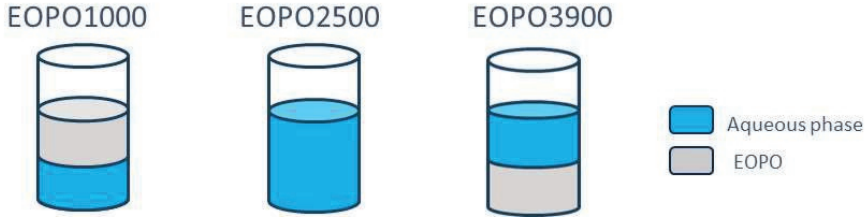


Figure S6.5. Schematical representation of phase separation for the second ATPS.

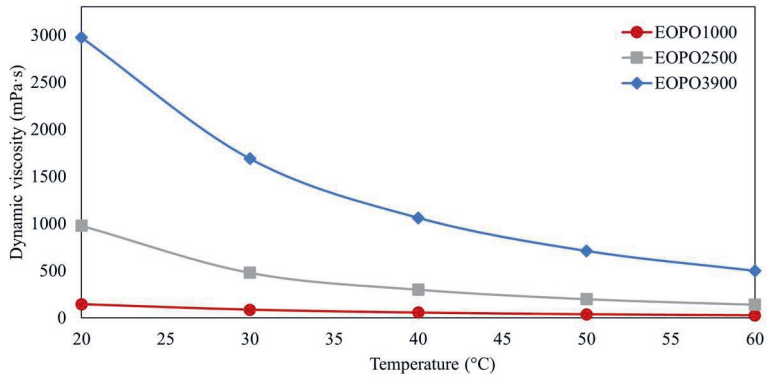


Figure S6.6 Viscosity of EOPO1000, EOPO2500 and EOPO3900 from 20 to 60 °C.

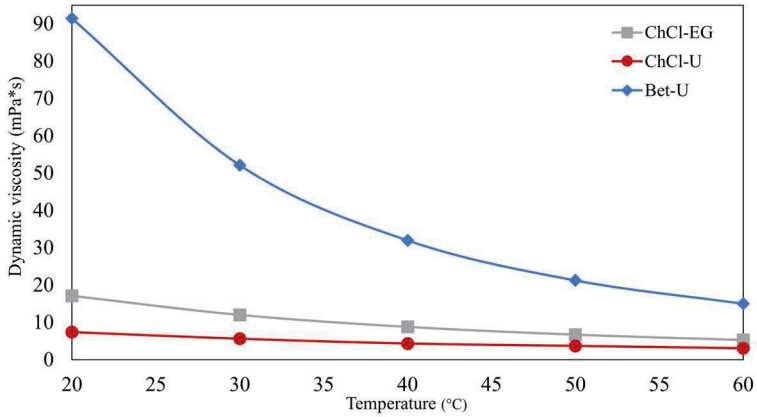


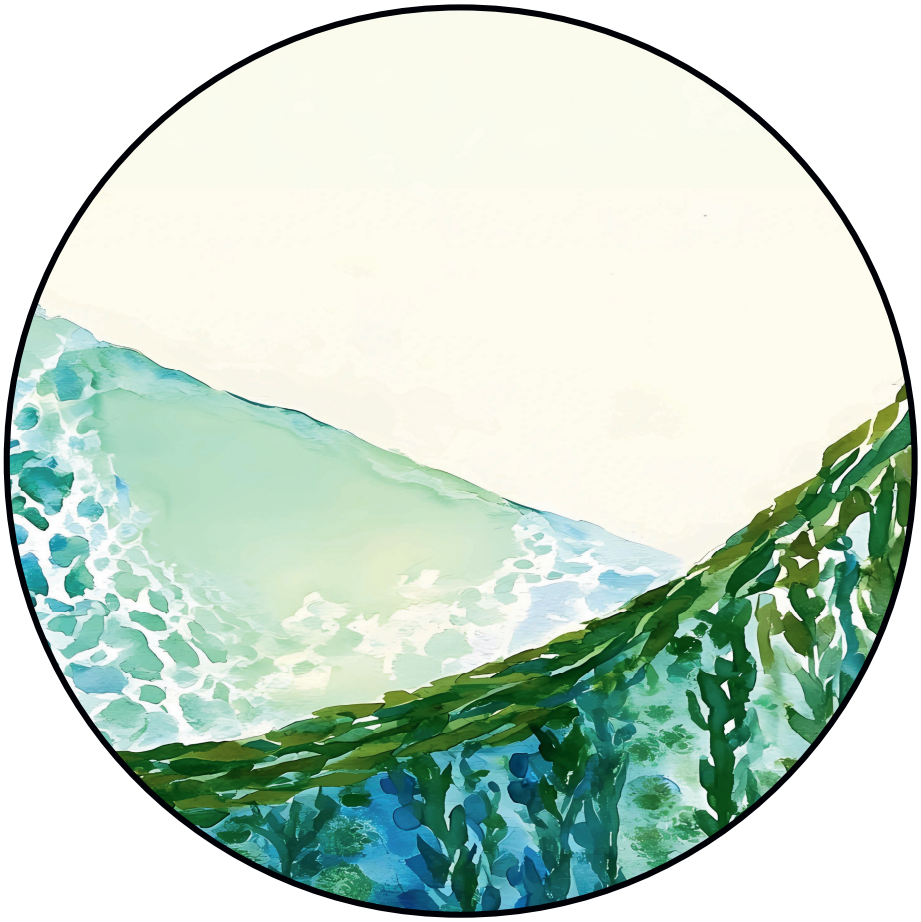
Figure S6.7 Viscosity of ChCl-EG, ChCl-U and Bet-U from 20 to 60 °C.

Table S6.3 M/G ratios of alginate for the DES extract, alkaline extract and alginate standard.

Sample	M/G ratio
DES extract	1.96 ± 0.02
Alkaline extract	1.49 ± 0.02

Table S6.4 Alginate extraction yield (mg/g), alginate recovery yield (mg/g) and recovery (%) when recycling DES and EOPO simultaneously.

Cycle	**1**	**2**	**3**	**4**	**5**	**6**
Extraction yield (mg/g)	83.3 ± 10	60.5 ± 2	64.2 ± 9	82.6 ± 5	99.6 ± 5	87.0 ± 13
Recovery yield (mg/g)	54.8 ± 8	55.4 ± 8	67.3 ± 11	49.2 ± 15	48.6 ± 7	25.1 ± 8
Alginate recovered (%)	65.8 ±8	83.9 ± 10	105.4 ± 16	59.6 ± 15	48.8 ± 9	28.9 ± 7



Chapter 7

Mechanistic insights into temperature-responsive deep eutectic solvent for alginate recovery and solvent recycling

Isa S.A. Hiemstra, Faridah Husna, Michel H.M. Eppink, Rene H. Wijffels, Antoinette Kazbar.

This chapter has been published as:

Hiemstra, I. S. A., Husna, F., Eppink, M. H., Wijffels, R. H., & Kazbar, A. (2026). Mechanistic insights into temperature-responsive deep eutectic solvent for alginate recovery and solvent recycling. *Separation And Purification Technology*, *388*, 136807. https://doi.org/10.1016/j.seppur.2026.136807

Abstract

Conventional alginate extraction from brown seaweed typically relies on harsh, non-recyclable chemicals, limiting process sustainability. This study presents temperature-responsive deep eutectic solvents (TRDES) as circular, recyclable extractants for alginate recovery. Using computational screening with COSMO-RS and experimental validation of TRDES affinity and alginate partitioning, TRDES1 (o-cresol: ethanolamine) was identified as the most promising combination, and was optimised and reused over eight cycles, yielding up to 55.6 ± 14.4 mg/g DW. COSMO-RS modelling validated the observed increase in extraction efficiency over successive cycles, showing enhanced partition coefficients and reduced Gibbs free energy of transfer with reuse. The process enabled mild extraction of functional alginate with increasing efficiency over the cycles. The main solvent parameters for TRDES design found to govern extraction and recyclability were capacity (C), partition coefficient (K), and Gibbs free energy (ΔG). Optimal performance was achieved with moderate TRDES–water capacity (1.27×10^{1} to 3.15×10^{1}), low TRDES capacity (<1.2), and $K > 1$. This work establishes a theoretical framework with design rules for future TRDES development based on computational and experimental analysis and highlights the need for novel, biocompatible TRDES systems. As demonstrated, combining computational screening with these design principles enables the use of recyclable solvents. Incorporating natural compounds into TRDES design enhances both process efficiency and sustainability, facilitating the integration of DES technologies into circular biorefineries and supporting environmentally responsible biomass valorisation.

7.1. Introduction

The valorisation of renewable biomass has become a valuable asset in the development of sustainable and circular bioeconomies. Brown seaweeds are an interesting renewable biomass that can be used for valorisation. These macroalgae contain valuable bioactive compounds, including polysaccharides, proteins, lipids and polyphenols, with antibacterial, antiviral and antifungal properties [307–309]. Among these compounds, alginate is a polysaccharide that is widely used in the food, pharmaceutical, and biomedical industries due to its gel-forming and biocompatible properties [310]. This polysaccharide has a simple molecular structure, containing two uronic acid units, D-mannuronic acid (M) and L-guluronic acid (G). These two uronic acids are present in varying sequences and ratios and are linked by β-1,4-glycosidic bonds [122] (**Figure S7.1**).

Efficient extraction of these compounds is essential for applications in pharmaceuticals, food, and materials science. However, conventional alginate extraction relies on multiple processing stages that use harsh chemicals, under both acidic and alkaline conditions, resulting in significant water consumption and a high energy input [56]. Moreover, the solvents used in alkaline extraction are typically not recyclable, leading to environmental and economic concerns.

Deep eutectic solvents (DES) have emerged as a promising class of alternative extraction solvents [87]. Formed by the complexation of one or more hydrogen bond donors (HBD) and acceptors (HBA), the depression in melting point leads to the formation of a DES. DES can be classified as green solvents due to their low volatility, high thermal stability, tuneable physicochemical properties, simple preparation without chemical reactions, and the possibility of selecting biocompatible, biodegradable components that can be recycled [9, 10], making them attractive candidates as extraction solvents. DES show significant potential in the extraction of various bioactive compounds from different biomasses. DES have been successfully applied for the extraction of bioactives from various biomasses, including plants [79, 207], microalgae [93, 311], and seaweed [62, 63].

Although alginate was successfully extracted using DES in our previous study, achieving a higher extraction yield compared to conventional processing [100], the main challenge associated with DES is the efficient isolation of the extracted compounds from the solvent and the subsequent recycling of the DES. DES recycling is complicated due to the low vapour pressure DES exhibits [70].

Several approaches have been proposed for DES recovery, including membrane separation [312], antisolvent addition [78, 79], and the use of macroporous resins [62]. Nonetheless, these methods often involve additional solvents, a high energy input, or lead to incomplete solvent recovery. Additionally, these studies do not address DES recycling but only focus on extractant recovery. Therefore, efficient recycling strategies are essential to ensure that DES-based processes are not only effective but also reusable and circular.

To address this issue, research has recently turned toward the development of a novel class of DES, known as responsive deep eutectic solvents (RDES) [262]. RDES are a novel subclass of DES designed to undergo physical or chemical changes in response to external stimuli. These systems can respond to external triggers, including carbon dioxide (CO_2), changes in pH, or temperature, allowing for controlled phase transitions through changes in polarity or solubility that facilitate selective extraction and solvent recovery [262, 313]. Among these, temperature-responsive DES (TRDESs) are particularly appealing due to the simplicity of temperature manipulation. By exploiting the reversible solubility in response to temperature shifts, TRDES offer a promising alternative for DES recovery and recycling without the need for additional reagents or complex equipment [313]. TRDES can exhibit either upper (UCST) or lower critical solution temperature (LCST) behaviour. UCST-type systems are immiscible with water at low temperatures due to strong hydrogen bonding between DES components but become miscible upon heating as thermal energy disrupts these interactions [165, 313]. In contrast, LCST behaviour involves phase separation at high temperatures, driven by entropy and the weakening of hydrogen bonds between the DES and water [314].

Despite growing interest in TRDESs, their application in marine biomass extraction remains limited, and fundamental thermodynamic governing extraction, separation, and recyclability are often overlooked. Understanding DES–water–compound affinity and partitioning behaviour is essential for rationally optimising extraction efficiency, phase switching, and solvent recovery. Integrating predictive modelling could offer valuable thermodynamic insights and support the systematic design of DES-based biorefinery processes, rather than relying solely on empirical solvent screening. Such an approach also holds broader potential, enabling the prediction of solvent behaviour across diverse compounds and feedstocks, and guiding the development of more versatile and ultimately more sustainable extraction systems.

Therefore, this study aimed to evaluate the feasibility of extracting and recovering alginate using UCST-type TRDES, with the aim of establishing a mechanistic

understanding of TRDES behaviour during extraction and recycling, thereby enabling simultaneous alginate isolation and solvent recovery. First, 22 TRDES were selected and evaluated for their phase switching behaviour. By addressing the solubility capacity and partition coefficient in COSMO-RS (Conductor-like Screening Model for Real Solvents), a model used to predict thermodynamic properties of fluids and solutions, the performance of different TRDES and the alginate partition behaviour was modelled. Subsequently, alginate extraction and recovery were conducted. The optimal TRDES was used, extraction was optimised, and the alginate was characterised. The TRDES fraction could be recycled for up to eight rounds of alginate extraction.

This study provides an effective framework and design criteria that can be translated to the future development of greener and biocompatible TRDES systems. By combining experimental extraction with COSMO-RS modelling, the main solvent parameters for TRDES design that govern extraction and recovery were established. This work contributes to the advancement of deep eutectic solvent (DES) recycling and promotes circularity in extraction processes, supporting the rational design of sustainable and resource-efficient biorefinery approaches.

7.2. Materials and methods

7.2.1 Materials

Brown seaweed *Saccharina latissima* was obtained from Algaia, France, in September 2024. The biomass was freeze-dried, ground, sieved and stored in the dark at 4°C. Monoethanolamine (>98%), diethanolamine (>98%), triethanolamine (>99%), 2-(Methylamino)ethanol (>98%), (Dimethylamino)ethanol (>99,5%), o-cresol (99%), p-cresol (99%), m-cresol (99%), guaiacol, 3- Methoxyphenol (96%), 4-Methoxyphenol (99%), L-menthol (99%), methyltrioctylammonium chloride, decanoic acid (>98%), phenyl salicylate (99%), octanoic acid (>98%) and D-galacturonic acid monohydrate (>97%), sodium tetraborate (99%), sulfuric acid (95-98%), carbazole (>95%) and ethanol (>99%) were purchased from Sigma-Aldrich.

7.2.2 TRDES preparation

In total, 22 TRDES were selected for the screening. The TRDESs were prepared by mixing the HBA and HBD at 60 °C until a clear and homogeneous liquid formed. The details of the TRDES formulation tested are listed in **Table 7.1** and **Figure S7.2**.

Table 7.1 Details of the TRDES used in this study.

	HBAs	HBDs	Molar ratios	Reference
TRDES1	Monoethanolamine	o-cresol	1:1	[165]
TRDES2	Monoethanolamine	p-cresol	1:1	
TRDES 3	Monoethanolamine	m-cresol	1:1	
TRDES 4	Diethanolamine	o-cresol	1:1	
TRDES 5	Diethanolamine	p-cresol	1:1	
TRDES 6	Diethanolamine	m-cresol	1:1	
TRDES 7	Triethanolamine	o-cresol	1:1	
TRDES 8	Triethanolamine	p-cresol	1:1	
TRDES 9	Triethanolamine	m-cresol	1:1	
TRDES 10	Monoethanolamine	Guaiacol	1:1	
TRDES 11	Monoethanolamine	3-Methoxyphenol	1:1	[315]
TRDES 12	Monothanolamine	4-Methoxyphenol	1:1	
TRDES 13	2-(Methylamino)ethanol	Guaiacol	1:1	
TRDES 14	2-(Methylamino)ethanol	3-Methoxyphenol	1:1	
TRDES 15	2-(Methylamino)ethanol	4-Methoxyphenol	1:1	
TRDES 16	(Dimethylamino)ethanol	Guaiacol	1:1	
TRDES 17	(Dimethylamino)ethanol	3-Methoxyphenol	1:1	
TRDES 18	(Dimethylamino)ethanol	4-Methoxyphenol	1:1	
TRDES 19	L-menthol	Methyltrioctylammonium chloride	1:1	[232]

TRDES 20	L-menthol	Decanoic acid	1:1
TRDES 21	L-menthol	Phenyl salicylate	1:1
TRDES 22	L-menthol	Octanoic acid	1:1

7.2.3 TRDES screening

7.2.3.1 Laboratory

The TRDES were first tested to assess whether phase separation would occur between the DES and aqueous phase. Phase separation was examined at 50% v/v TRDES concentration. The solution was heated to 60 °C in a water bath for one hour and vortexed every 10 minutes. Then, the solution was refrigerated at 4 °C to allow it to cool down and separate into two phases. If phase separation did not occur in the solution, sodium chloride was added to achieve 8% salt concentration to facilitate phase separation further [315]. The TRDES that phase separated from the aqueous fraction were then used for alginate extraction, whereas the formulations that did not phase separate were discarded for alginate extraction.

7.2.3.2 COSMO-RS

7.2.3.2.1 TRDES comparison

The COSMO-RS (Conductor-like Screening Model for Real Solvents) software is an effective computational tool for predicting the thermodynamic behaviour of fluid mixtures [67]. Analyses were performed using COSMO-RS version 2022.103 (Software for Chemistry and Materials BV, Amsterdam, The Netherlands) integrated within the Amsterdam Density Functional (ADF) package. Molecular geometries of all compounds were pre-optimised using the universal force field (UFF), followed by density functional theory (DFT) calculations at the GGA:BP86 level with a TZP basis set [93].

The direct application of COSMO-RS to polymers such as alginate is impractical, as it requires extensive quantum chemical COSMO calculations, making the process highly time-consuming [96, 316]. Therefore, a trimer of alginate was selected for the modelling, as this allows feasible quantum chemical calculations while still capturing the essential structural characteristics of the polymer [94, 317].

With COSMO-RS, the activity coefficient of alginate was determined using **Equations 7.1** and **7.2:**

$$\ln(\gamma_i^{\infty}) = \frac{\mu_s^i - \mu_i^i}{RT} \quad (\mathbf{7.1})$$

$$\gamma_i^{\infty} = limit_{xi \to 0 \gamma_i} \quad (\mathbf{7.2})$$

where $\gamma_i^{\infty}$is the activity coefficient of alginate (i) at infinite dilution, which is defined as the limiting value of the activity coefficient as the concentration of alginate approaches zero; it is determined based on the chemical potential of the solvent μ_s and the chemical potential of the pure compound μ^0 [65, 318].

The solubility capacity (C) of each TRDES was calculated to determine the maximum amount of solute that can be dissolved in the TRDES, following **Equation 7.3** [318]**:**

$$C_i^{\infty} = 1/\gamma_i^{\infty} \quad (\mathbf{7.3})$$

The partition coefficient was calculated to evaluate the distribution of the solute between the DES and aqueous phases [319, 320], providing insights into the alginate extraction and recovery efficiency. The partition coefficient was determined following **Equation 7.4**:

$$K_{water/TRDES} = \frac{\frac{1}{\gamma_i^{\infty}(water)}}{\frac{1}{\gamma_i^{\infty}(DES)}} \quad (\mathbf{7.4})$$

7.2.3.2.2 TRDES recycling simulation

The partitioning behaviour of alginate across multiple extraction cycles was assessed by calculating the partition coefficient $K_{water/TRDES}$ and through calculating the Gibbs free energy of transfer (ΔG) for the partitioning of alginate. This computational approach enables the evaluation of thermodynamic trends and insights into whether cumulative effects within the TRDES could account for the enhanced alginate release observed in later extraction cycles. The Gibbs free energy of transfer was calculated following **Equation 7.5**:

$$\Delta G_{Partitioning} = -RTln\left(K_{water/DES}\right) \quad (\mathbf{7.5})$$

where R is the molar gas constant ($8.314 \frac{J}{mol*K}$) and T is the separation temperature (K).

The recycling process was modelled using COSMO-RS to evaluate the partitioning behaviour of alginate over successive cycles. After each extraction cycle, it was assumed that 2% of the total alginate accumulated in the DES phase. This retained alginate was then included in the solvent mixture composition for the subsequent

cycle. At each stage, the updated solvent composition was used to recalculate the activity coefficient and partition coefficient of alginate.

7.2.4 Alginate extraction and recovery

A TRDES-water system was prepared to achieve a 50% v/v TRDES concentration [165], and this was used to extract alginate from S. *latissima* at a solid-to-total liquid ratio of 1:40. The extraction was performed at 60 °C for one hour in a water bath, with the solution vortexed every ten minutes to ensure thorough homogenisation.

As a control, water extraction was performed using the same conditions as applied with the TRDES extraction. Alkaline extraction was performed as a control for the conventional alginate extraction. For alkaline extraction, acidified water containing H_2SO_4 (pH 1.9) was added to the seaweed at a 1:1 (w/w) ratio and incubated for one hour at room temperature. Subsequently, Na_2CO_3 was added at a 0.0325:1 (w/w) ratio, followed by extraction for 1 hour at 60 °C. All extractions, including those using different DESs and controls, were performed in triplicate.

Subsequently, the mixtures were centrifuged to separate the biomass residue. The supernatant was stored at 4 °C to facilitate phase separation between the aqueous and TRDES phases. Once phase separation occurred, the aqueous phase was collected and dialysed using a membrane with a molecular weight cutoff of 3.5-5 kDa. The alginate recovery yield of the dialysed aqueous phase was analysed using a colorimetric assay as proposed by Cesaretti *et al*. [136]. The alginate recovery yield was calculated following **Equation 7.6**:

$$Yield\ \left(\frac{mg}{g\ DW}\right) = \frac{C_{aqueous} * V_{aqueous}}{m_{biomass} * x_{DW}} \qquad (\mathbf{7.6})$$

where $C_{aqueous}$ is the concentration of the extract in the aqueous phase, $m_{biomass}$ is the weight of the initial biomass, x_{DW} is the weight fraction of the dry biomass and $V_{aqueous}$ is the volume of the aqueous phase.

The schematic diagram of the TRDES extraction and recovery process is illustrated in **Figure 7.1**.

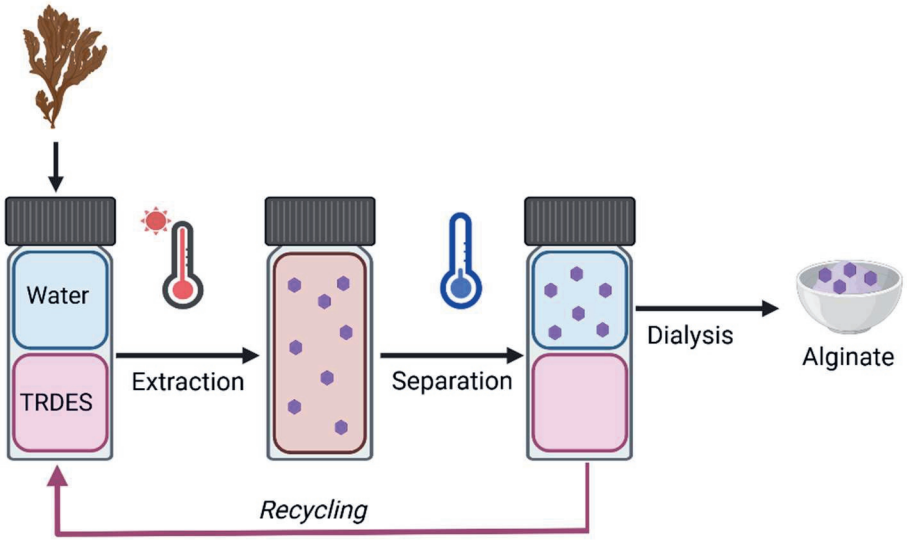


Figure 7.1 Schematic diagram of alginate extraction using temperature-responsive deep eutectic solvents.

7.2.5 Extraction optimisation

7.2.5.1 FTIR analysis

The TRDES, their individual components and alginate were analysed using Fourier-transform infrared (FTIR) spectroscopy. Spectra were recorded in the range of 400–4000 cm^{-1} using a Nicolet Summit X ATR-FTIR spectrometer (Thermo Fisher Scientific). For alginate, the extracts were isolated from the aqueous phase and purified by precipitation with 80% ethanol containing 1% NaCl, followed by two washes with 80% ethanol. The resulting precipitate was dried under nitrogen and characterised using FTIR spectroscopy, Size Exclusion Chromatography (SEC) and for the mannuronic to guluronic acid (M/G) ratio. Extracts obtained using the conventional alkaline method and water extracts were compared with those from DES-based extraction.

7.2.5.2 Molecular weight

Size exclusion chromatography (SEC) was performed to analyse the molecular weight of alginate extracted with TRDES, water and alkaline extraction, as described previously [48]. Alginate solutions (0.15% w/v) were prepared in Milli-Q water. A 20 µL sample was injected into an Agilent 1290 Infinity HPLC system equipped with two PL aquagel-OH MIXED-H columns (8 µm, 300 × 7.5 mm) in series. Elution was carried out using 0.1 M ammonium phosphate monobasic at pH 4.5 (Sigma-Aldrich) at a flow rate of 0.8 mL/min. Detection was performed with a refractive index detector (RID). A calibration curve was constructed using pullulan standards (PSS-PULKITR1, Agilent),

and molecular weights were converted to alginate equivalents via the Mark-Houwink relation [48]. The average molecular weight (M_w) was calculated following **Equation 7.7:**

$$M_w = \frac{\Sigma(M_i^2 * c_i)}{\Sigma(M_i * c_i)} \quad (7.7)$$

where M_i represents the molecular weight of fraction i corresponding to a specific retention time in the chromatogram, and c_i is the intensity (area) of fraction i, which is proportional to its concentration.

7.2.5.3 Mannuronic to guluronic acid ratio

The mannuronic to guluronic (M/G) ratio of the extracted alginate was analysed via methanolysis, followed by analysis using high-performance anion-exchange chromatography coupled with pulsed amperometric detection (HPAEC-PAD), following the methodology reported previously [227]. Measurements were performed on a Dionex ICS-6000 system (Thermo Fisher Scientific) equipped with a 1 mm CarboPac column. Alginate samples obtained via DES extraction were evaluated alongside those recovered through water extraction and conventional alkaline treatment. Prior to methanolysis, the samples were precipitated, redissolved in Milli-Q water, and 50 µL aliquots were used.

7.2.6 TRDES recycling

TRDES recycling was assessed after selecting the optimal TRDES formulation and optimal extraction conditions (**Sections 7.2.4** and **7.2.5**). The recycling capabilities of the TRDES were evaluated by repeating the same extraction procedure five times using the switched, recovered DES. The alginate recovery yield was measured in the aqueous phase after each extraction cycle.

7.2.7 Statistical analysis

Statistical analysis was performed using IBM SPSS Statistics version 30.0.0.0. The least significant difference (LSD) test and Duncan's multiple range test were applied to determine significant differences, with statistical significance set at $p < 0.05$. Error bars represent the standard deviation of three independent experiments. Different letters in the histogram indicate statistically significant differences at $p < 0.05$.

7.3. Results and discussion

7.3.1 TRDES phase behaviour

First, the 22 selected TRDES were assessed for their phase-switching ability. It was observed that alkanolamine:phenol-based TRDES (1 to 18) were immiscible with water at room temperature and became homogeneous mixtures with water when the solution was heated up to 60°C (**Table S7.1)**.

For TRDES 2–4, TRDES 10, and TRDES 12 and 16–18, phase separation occurred only upon cooling after adding 8% sodium chloride. The addition of salt can enhance phase separation in TRDES systems, following a mechanism similar to salt-induced precipitation [315]. The less soluble component tends to precipitate out, while the more soluble component remains in the aqueous phase. In this case, sodium chloride is more soluble in water than the TRDES, promoting TRDES aggregation and separation from the aqueous phase at lower temperatures. In TRDES 10, incomplete phase separation occurred. An increased aqueous volume occurred after phase separation, indicating residual DES in the water. Therefore, it was discarded from further alginate extractions.

Out of the 22 TRDES, 17 could perform reversible phase separation. TRDES 10, 11, 13, 14 and 15 did not fully reverse during phase separation and were therefore discarded from the alginate extractions and partition behaviour.

7.3.2 Partitioning behaviour and extraction performance of TRDES

7.3.2.1 Computational analysis of capacity and partition coefficient

Prior to experimental extraction, COSMO-RS modelling was conducted to evaluate the capacity and partition coefficient ($K_{water/DES}$) across the switchable TRDES systems for alginate. The capacity quantifies the solute's ability to dissolve in the solvent, reflecting the extent of solute–solvent interactions. It is determined from the solute's activity coefficient, with lower activity coefficients indicating higher solubility within the DES. These thermodynamic parameters were used to estimate the potential effectiveness of each TRDES system and to predict the affinity of alginate for both the aqueous and DES phases. This computational analysis enabled the selection of TRDES candidates with favourable partitioning behaviour for subsequent experimental validation (**Table 7.2**).

Table 7.2 Capacities (C) and partition coefficients (K) of alginate in the TRDES-water systems at 20 °C.

	Capacity DES-water[a]	Capacity DES[a]	$K_{Water/DES}$[a]
TRDES 1	3.15×10^{1}	1.21	4.54
TRDES 2	2.53×10^{1}	1.07	5.17
TRDES 3	2.93×10^{1}	1.29	4.27
TRDES 4	1.79×10^{1}	1.68	3.28
TRDES 5	1.52×10^{1}	1.53	3.59
TRDES 6	1.72×10^{1}	1.79	3.07
TRDES 7	1.45×10^{1}	2.53	2.18
TRDES 8	1.27×10^{1}	2.34	2.35
TRDES 9	1.42×10^{1}	2.69	2.05
TRDES 12	2.44×10^{1}	1.70	3.23
TRDES 16	2.15×10^{1}	1.01	5.44
TRDES 17	2.12×10^{1}	3.26×10^{1}	1.69×10^{-1}
TRDES 18	4.93	9.71	5.68×10^{-1}
TRDES 19	1.48×10^{3}	1.85×10^{-6}	2.97×10^{6}
TRDES 20	5.36×10^{-1}	3.29×10^{-3}	1.67×10^{3}
TRDES 21	1.49	8.28×10^{-3}	6.66×10^{2}
TRDES 22	7.07×10^{-1}	5.73×10^{-3}	9.62×10^{2}
Water	5.51		

[a] Calculations were performed at 20 °C.

In addition to calculating the activity coefficients (γ) of the DES and water at 20 °C, the variation of the capacity and the partition coefficient (K) was also examined across a range of temperatures for each DES (**Figure 7.2, Figure S7.3**). This analysis was performed to investigate the influence on alginate partitioning when enabling temperature-responsive product recovery.

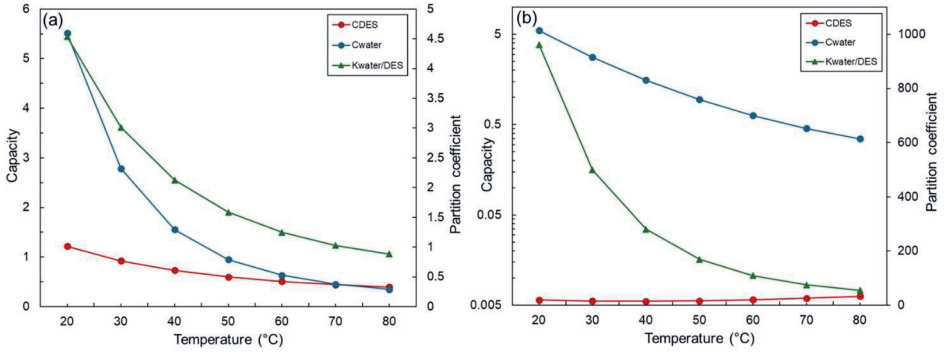


Figure 7.2 Capacity and partition coefficient (K) of (a) TRDES1 with water and (b) TRDES20 with water as a function of temperature (20–80 °C).

7.3.2.1.1 Capacity

The capacity of the TRDES-water systems for alginate decreased progressively from HBA monoethanolamine (31.5 for TRDES1) to diethanolamine (17.9 for TRDES4) and triethanolamine (12.9 for TRDES9) (**Table 7.2**). Monoethanolamine (MEA) based DES-water systems exhibited superior capacities due to their balanced hydrogen bonding capacity and favourable basicity [321]. Featuring both a primary amine ($–NH_2$) and a hydroxyl (–OH) group (**Figure S7.2**), MEA can act as both a strong hydrogen bond donor and acceptor [322], enabling effective interactions with the carboxylate ($–COO^-$) and hydroxyl (–OH) groups of alginate (**Figure S7.1**). Additionally, MEA's relatively high basicity (pKa ~9.5) compared to diethanolamine (DEA, pKa ~8.7) and triethanolamine (TEA, pKa ~7.7) [165, 323] allows for partial protonation under aqueous conditions. The resulting $–NH_3^+$ groups can engage in electrostatic interactions with negatively charged alginate, further enhancing affinity. In contrast, DEA and TEA contain secondary (–NH) and tertiary (–N) amines, respectively, which exhibit weaker hydrogen bonding capabilities and lower basicity, making MEA the most effective HBA in terms of capacity among the ethanolamines studied.

The DES–water (50:50) system exhibited significantly higher capacity than the DES without water (**Table 7.2**). This improvement is attributed to the role of water in increasing solvent polarity, enhancing hydrogen bonding, and reducing viscosity [290], which together promote more effective solvation of the alginate. In contrast, the DES without water offers limited capacity due to its lower polarity (**Table S7.2**) and higher viscosity compared to DES with water. The menthol-based DES (TRDES19-22) with water showed low capacity towards alginate (less than 1.5) (**Table 7.2**). This could be due to their predominantly hydrophobic nature (**Table S7.2)**, which reduces their solvation capacity towards alginate.

7.3.2.1.2 Partition coefficient

When considering the partition coefficient, it can be observed that the partition coefficient is above 0 for all TRDES at 20 °C (**Table 7.2**) and across 20-80 °C (**Figure 7.2** and **Figure S7.3**). This indicates that alginate prefers partitioning into the water phase over the DES phase at all temperatures for each DES. Additionally, the partition coefficient decreased at higher temperatures for each TRDES (**Figure S7.3**). For TRDES1, this decrease is from approximately 4.54 at 20 °C to 0.88 at 80 °C (**Figure 7.2**), suggesting that alginate is more likely to partition into the water phase at lower temperatures. This indicates that temperature affects the relative solubility of alginate in the two phases, with lower temperatures enhancing its distribution toward water. This is desirable, as TRDES-water phase separation occurs at 20 °C, making it convenient for efficient partitioning of alginate into the aqueous phase.

For TRDES 18-22, the partition coefficient was significantly larger than 1 at 20-80 °C (**Table 7.2, Figure 7.2** and **Figure S7.3**), indicating that alginate preferentially partitions in the water phase over the DES phase. Due to the hydrophobicity of these DESs (**Table S7.2**), they exhibit poor compatibility with alginate, as indicated by the low capacities. This, in turn, results in minimal solubilisation within the DES phase and thus good separation ability.

Since all TRDES showed a positive partition coefficient at 20 °C and demonstrated moderate to good capacities, these DESs were considered for laboratory alginate extraction.

7.3.2.2 Experimental evaluation of alginate extraction yields

All of the TRDESs that could undergo phase separation recovered alginate in the aqueous phase (**Figure 7.3**). The highest yield was obtained by TRDES 1 (ethanolamine:o-cresol 1:1) and TRDES 16, which recovered 25.0 ± 3.6 and 23.6 ± 4.2 mg/g DW, respectively, in their aqueous phase (**Figure 7.3**). Compared to water extraction, TRDES 1 and 16 resulted in a two-times higher alginate yield, which could be due to the higher capacities of these DESs compared to water due to their improved hydrogen bonding capacities (**Section 7.3.2.1**).

In general, it was observed that the alkanolamine: phenol-based DES could recover more alginate than the menthol-based DES (TRDES 19-22) (**Figure 7.3**). This may be attributed to the mildly alkaline conditions created by the alkanolamine–phenol-based DES [165]. Since the pKa of an alginate polymer is in the range of 3.5 – 4.6 [324], this causes alginate to dissolve in alkaline conditions. The increased yield compared to the menthol-based DES is consistent with the computationally obtained capacities (**Section 7.3.2.1**).

Differences among yields for alkanolamime: phenol-based DES could be due to the interaction between the DES and biomass. In addition to solute–solvent affinity, the capacity of DES to alter biomass structure by modulating cell membrane permeability and compromising structural integrity also contributes to its extraction performance [148, 149, 325]. This, in turn, can affect the accessibility of alginate and may significantly influence the extraction efficiency. Specifically, previous studies have demonstrated that certain TRDES and DES can alter the permeability and integrity of plant and microalgal cell walls, thereby enhancing the release of target compounds [148, 232].

Alkaline extraction reached a yield of 42.1 ± 3.7 mg/g DW. Despite the lower yield of TRDES 1 and 16 compared to alkaline extraction, TRDES extraction could offer advantages in process intensification and process circularity. Extraction with TRDES enables the simultaneous extraction and separation of product and DES in a single one-hour step, compared to two one-hour steps for alkaline extraction. In addition, TRDES extraction allows for direct alginate recovery from the aqueous phase. Furthermore, TRDES allow for the recycling of the extraction solvent, thereby enhancing its sustainability.

TRDES 1 was selected for further optimisation due to its high solubility capacity and favourable partition coefficient.

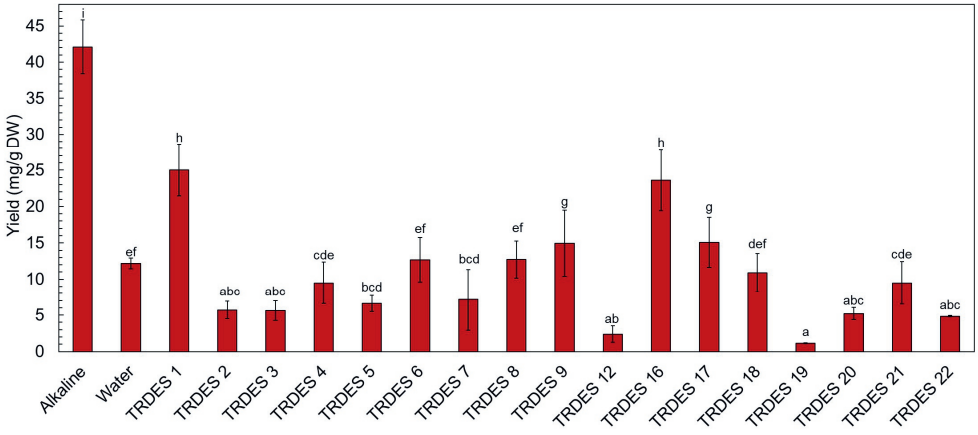


Figure 7.3 Alginate extraction yield for TRDES-water systems for TRDES1-TRDES22. Extraction with only water and alkaline extraction were used as controls.

7.3.3 Extraction parameters

From the previous section (**Section 7.3.2**), TRDES 1 was selected for extraction optimisation. Optimisation was performed to identify the impact of extraction parameters on the alginate yield. In this study, TRDES concentrations, solid to total liquid ratio, extraction temperature and extraction time were investigated to enhance alginate recovery yield (**Figure 7.4**). Single-factor experiments were employed to evaluate the effect of each parameter independently, an approach widely applied and effective in responsive solvent optimisation studies [163, 232, 326].

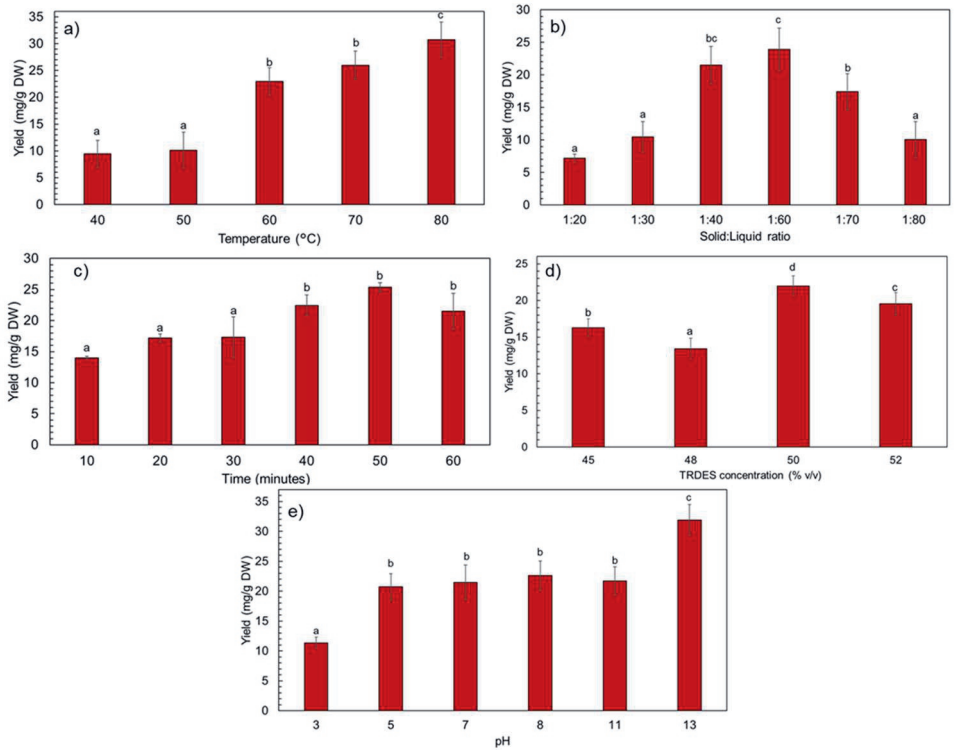


Figure 7.4 Effect of (a) the extraction temperature, (b) the solid:liquid ratio, (c) the extraction time, (d) the TRDES concentration and (e) the pH on the alginate extraction yield. Conditions were standardised at 60 °C, solid:liquid ratio of 1:40, one hour extraction time, at 50% v/v TRDES concentration and pH 7 of the water when one of the extraction parameters was altered.

7.3.3.1 Effect of extraction temperature

The influence of extraction temperature on the alginate recovery yield was examined from 40 to 80 °C. The extraction yield increased as the temperature increased (**Figure 7.4a**). The UCST of TRDES1 is 55 °C [165], indicating that a homogeneous solution forms above 55 °C, where TRDES1 becomes fully miscible with water. Consequently, a marked difference in alginate yield is observed when comparing extraction temperatures below the UCST (50 °C, 10.2 ± 3.3 mg/g DW) and above it (60 °C, 23.0 ± 2.6 mg/g DW). Below the UCST, a heterogeneous system is formed because TRDES is insoluble in water, which impairs mass transfer and molecular diffusion [262]. Above the UCST, TRDES1 becomes fully miscible with water and forms micelle-like aggregates [165]. This arises from the amphiphilic nature of its components: monothanolamine provides polar headgroups capable of hydrogen bonding, while o-cresol contributes hydrophobic aromatic moieties (**Figure S7.2**). Elevated temperatures increase molecular mobility and weaken hydrogen bonding, allowing the amphiphilic molecules to self-assemble into micelles. These structures create

localised microenvironments of differing polarity, enhancing alginate solubilisation and mass transfer [165]. Below the UCST, partial phase separation suppresses micelle formation, resulting in a heterogeneous system with limited diffusion and reduced extraction efficiency. Additionally, elevated temperatures can promote the rupture of the cell wall [238]. thereby enhancing alginate release. Therefore, 80 °C was selected as the optimal temperature.

7.3.3.2 Effect of solid-liquid ratio

Solid-liquid ratios from 1:20 to 1:80 (g/mL) were assessed. The results show that from 1:20 to 1:60, the alginate yield increases and then decreases when further increasing the solid-liquid ratio (**Figure 7.4b**). The extraction yield increased noticeably with an increase in the liquid–solid ratio. A higher concentration of extractant enhances the dissolution of target compounds into the extraction medium due to improved mass transfer [327], thereby increasing the yield from 7.2 ± 0.6 to 23.0 ± 3.3 mg/g DW when using 1:20 and 1:60 solid-liquid ratios, respectively. However, an excessive amount of extractant not only adversely affects the extraction efficiency but may also lead to resource waste [217, 315, 328]. Therefore, a solid-liquid ratio of 1:60 was selected.

7.3.3.3 Effect of extraction time

The extraction time of 10 to 60 minutes was examined. The alginate yield increased up to 40 minutes, but extracting longer than 40 minutes did not significantly affect the extraction yield. (**Figure 7.4c**). This initial increase is due to the progressive diffusion of alginate into the extraction solvent. During the early stages of extraction, the concentration gradient between the polysaccharide in the biomass and the solvent is high, which promotes mass transfer [329]. However, beyond 40 minutes, the extraction yield plateaued, which could be due to the accumulation of impurities [163] or because the extraction process has reached equilibrium [330]. Therefore, 40 minutes was chosen as the optimal extraction time.

7.3.3.4 TRDES concentration

The TRDES concentration of 45 to 52% was investigated for alginate extraction. The optimal yield was obtained when having a 50% TRDES concentration and increasing or decreasing the concentration resulted in lower yields (**Figure 7.4d**). At lower TRDES concentrations, the solvent may be too diluted, reducing its ability to break down the cell structure [165], which will in turn result in less alginate release. Additionally, lower TRDES concentrations can weaken the interactions between the solvent and alginate. At higher TRDES concentrations, the viscosity of the mixture increases, which can hinder mass transfer and diffusion of target compounds into the solvent phase [288, 328]. Therefore, a 50% TRDES concentration was selected as the optimal condition.

7.3.3.5 Effect of pH

The pH value of the water was adjusted from pH 3 to pH 13. The extraction yield increased when the pH was increased (**Figure 7.4e**). This improved yield when elevating the pH could be because the pKa of an alginate polymer is in the range of 3.5 – 4.6 [324, 331], which makes alginate dissolve in alkaline conditions. On the other hand, acidic conditions promote the protonation of carboxyl groups in alginate, leading to polymer precipitation or gel formation, thereby limiting its solubility [50], resulting in a decreased extraction yield. Therefore, pH 13 was selected as the optimal pH value. Although this pH falls within the alkaline range, this treatment fundamentally differs from conventional extraction, as no concentrated sulphuric acid is used and the process occurs in a single step. Moreover, the TRDES can be recovered and reused, reducing reagent consumption compared to traditional alkaline extraction.

7.3.4 TRDES and alginate characterisation

Based on the optimal conditions identified in **Section 7.3.2**, the subsequent extraction was performed based on these conditions and characterisation of both the extracted alginate and the DES was performed.

7.3.4.1 TRDES characterisation

To confirm the temperature-responsive behaviour of the DES system, TRDES1 was characterised across the phase transition temperature with FTIR (**Figure 7.5, Table S7.3**). This evaluation aimed to verify the reversible switching of the DES between biphasic and monophasic states.

For ethanolamine, the FTIR spectrum typically shows a broad O–H/N–H stretching band around 3000–3400 cm^{-1} and distinct C–N stretching near 1075 cm^{-1} [332]**.** For o-cresol, characteristic peaks include aromatic C=C stretching at approximately 1600 cm^{-1}, and C–O stretching near 1200 cm^{-1} [333]. Upon DES formation, a small peak is observed at 3344 cm^{-1} corresponding to hydrogen bonding interactions between ethanolamine and o-cresol, consistent with previous reports [165]. Upon the addition of water to the DES and heating, a broader band emerges at 3400 cm^{-1}, indicating the formation of additional hydrogen bonds between water molecules and the DES components [165]. In addition, the aqueous phase obtained after switching was analysed (**Figure S7.4**). The FTIR spectrum of this water phase was compared to that of

pure water. No distinct peaks attributable to DES components were observed, suggesting the absence of detectable DES traces in the aqueous phase (**Figure S7.4**).

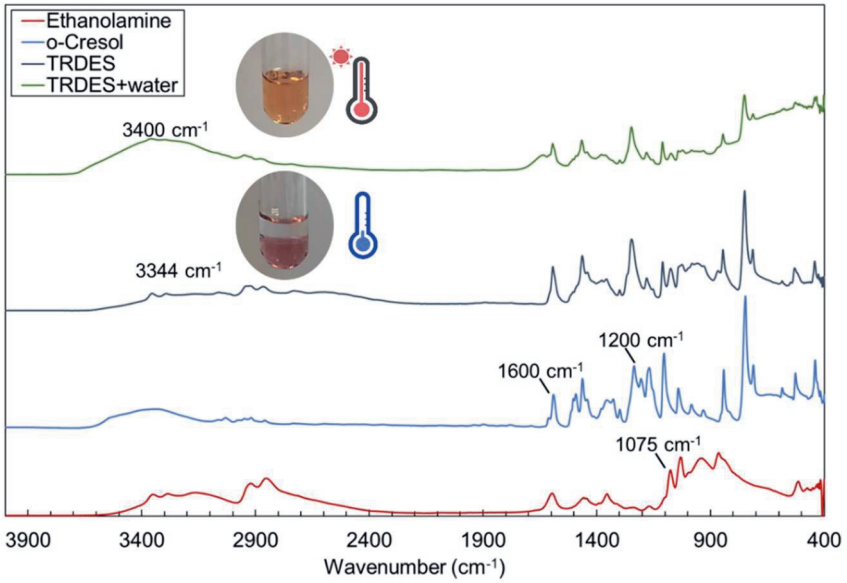


Figure 7.5 FTIR spectra of TRDES1 constituents, TRDES1 and TRDES1 containing 50 %v/v water.

7.3.5 Alginate characterisation

The alginate recovered from the TRDES was characterised for its functional groups with FTIR, for its molecular size and the M/G ratio. The FTIR spectra of alginate extracted using DES, water and alkaline treatment exhibited comparable profiles (**Figure 7.6, Table S7.4**), with characteristic absorption bands observed at 1080 cm^{-1} and 1020 cm^{-1}, corresponding to vibrations of guluronic and mannuronic acid residues, respectively [246, 300]. The bands at ~1600 cm^{-1} and ~1400 cm^{-1} are attributed to the asymmetric and symmetric stretching vibrations of the carboxylate ($–COO^-$) functional groups, respectively [244–246]. Additionally, a broad absorption band around 3500 cm^{-1} and a weak band near 2900 cm^{-1} were observed, corresponding to hydrogen-bonded O–H stretching and C–H stretching vibrations, respectively, present in alginate [245].

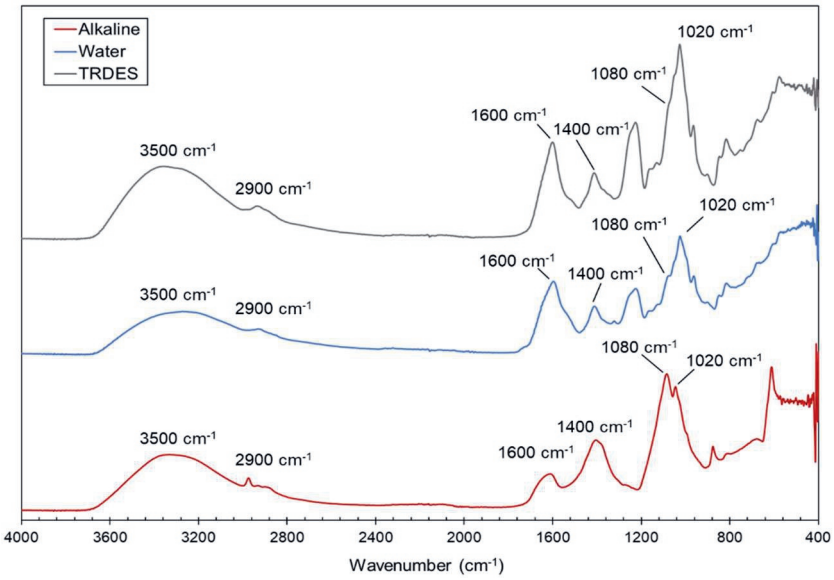


Figure 7.6 FT-IR spectra of alginate extracted with TRDES, conventional alkaline processing and with water.

The molecular weights of alginate extracted using TRDES (989 ± 227 kDa) and conventional alkaline extraction (988 ± 21 kDa) were similar, indicating comparable average molecular sizes (**Figure 7.7**). In contrast, water-extracted alginate had a significantly lower molecular weight (445 ± 71 kDa). The comparable molecular weights observed for TRDES and conventional alkaline extraction suggest that TRDES is an effective alternative for alginate extraction and recovery, achieving alginate with similar molecular weights.

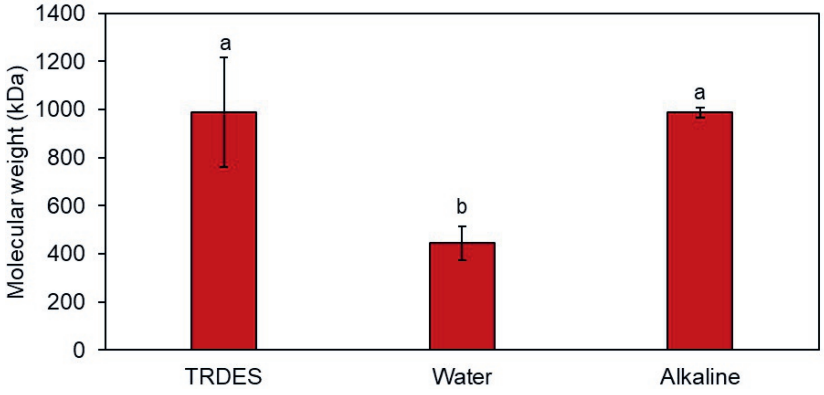


Figure 7.7 Molecular weight of alginate extracted with TRDES, water and alkaline treatment.

The mannuronic to guluronic (M/G) ratio is an important parameter in alginate characterisation, as it determines the polysaccharide's structural, physical, and functional properties [227]. Alginate gels with a high M/G ratio tend to exhibit greater permeability, while those with a low M/G ratio typically form more robust and rigid networks. The G-blocks exhibit greater rigidity due to the increased restriction of rotational freedom around their glycosidic linkages, promoting tighter cross-linking and improved mechanical strength compared to gels rich in mannuronic acid blocks [49, 247].

Alginate extracted with TRDES resulted in an M/G ratio of 2.63 ± 0.19, while for alkaline and water this was 1.15 ± 0.01 and 1.55 ± 0.02, respectively (**Table 7.3**). The M/G ratios obtained from TRDES extracts were higher than those from conventional alkaline extraction methods and also exceeded the values reported in the literature for *Saccharina latissima*, ranging from 0.8 to 1.49, depending on the extraction method [227, 248, 334]. The higher M/G ratio could be because the TRDES extraction was performed at higher pH conditions, causing an increased M/G ratio [334]. This effect may be attributed to partial degradation of alginate under alkaline conditions, coupled with differences in the solubility of the resulting shorter polymer fragments depending on their uronic acid composition. This indicates that alginate extracted using TRDES may yield more flexible, elastic, and permeable gel networks compared to alginate recovered through alkaline treatment. Such properties make this alginate particularly suitable for diffusion-dependent applications, including drug delivery systems and cell encapsulation technologies.

Table 7.3 M/G ratios of alginate extracted with TRDES, alkaline treatment and water.

	M/G ratio
TRDES	2.63 ± 0.19
Alkaline	1.15 ± 0.01
Water	1.55 ± 0.02

Based on FTIR, molecular size, and M/G ratio data, TRDES and conventional alkaline extraction yielded alginate with comparable molecular characteristics. However, TRDES could offer additional advantages due to its potential for recyclability, positioning it as a more circular alternative.

7.3.6 TRDES recycling

The recyclability of the TRDES solvent was evaluated to assess its feasibility for repeated extraction of alginate. Eight extraction cycles were performed using the same solvent to determine the impact of recycling on extraction efficiency and solvent

performance. The recycling study was conducted under the optimum extraction conditions determined previously (**Section 7.3.3**).

The extraction yield of TRDES 1 remained stable from cycle 1 to 4 (**Figure 7.8**). Starting from cycle 4, an increase in extraction yield was observed, with an extraction yield of 55.6 ± 14.4 mg/g DW at cycle 8. From cycle seven to eight, no statistically significant difference in extraction yield was observed, suggesting that the system may have approached a plateau. The larger standard deviation in the final cycle is attributed to variability between experimental replicates and analytical uncertainty, rather than incomplete phase separation or reduced solvent performance. A previous study on alginate extraction using the hydrophilic DES betaine:urea reported a recovery of 56.0 ± 0.9 mg/g, achieved through a two-step aqueous two-phase system (ATPS) [335]. In that process, alginate first partitioned into a copolymer-rich phase, after which both the copolymer and DES phases had to be separated and recycled. A second ATPS step was then required to transfer alginate into the aqueous phase while recovering the copolymer for reuse. Although the final yields are comparable to those obtained in our study, the ATPS method involves multiple sequential separation and recycling steps. By contrast, our TRDES-based process combines extraction and solvent recovery in a single step, offering a simpler and potentially more efficient alternative. In another study, Saravana *et al*. [128] used subcritical water extraction at 125 °C and 10 bar with a choline chloride:glycerol (1:2) DES containing 70% water, obtaining an alginate yield of 28%, indicating similar extraction yields compared with our study (approximately 33%). While effective, this method did not include DES recycling and relies on high-pressure equipment, which can increase capital costs.

When comparing DES recycling to other studies, Ng *et al*. [301] reported that during the extraction of ferulic acid from oil palm empty fruit bunch fibre, the addition of an antisolvent enabled ferulic acid precipitation. Using this approach, they were able to recycle the DES for up to five consecutive cycles without significant loss of performance. Chen *et al*. [336] used CO_2-triggered switchable hydrophilicity solvents for ultrasonic-assisted extraction of *Polygonatum sibiricum* polysaccharides. The solvent could be recycled five times, observing a decrease in extraction yield per cycle. Gao *et al*. [337] et al performed oil extraction from sawdust. The hydrophobic DES was regenerated through deprotonation and protonation using NaOH and acetic acid, respectively. They found a significant decrease in extraction efficiency upon recycling a hydrophobic DES five times. Compared with other DES recycling strategies, the proposed TRDES system supports a higher number of successful recycling cycles, as the recovery yield continues to increase rather than decline over successive rounds.

The trend of an increase in the extraction yield contrasts with previous TRDES recycling studies, where extraction efficiencies declined with successive cycles [165, 232]. In these studies, the accumulation of other constituents in the DES could have competed with the target compound [301], thereby reducing the solvents' effectiveness. However, other studies focused on DES recycling have found increasing extraction yields, as observed for alginate, due to compound accumulation in the DES phase [301]. The sustained and improved performance observed here may be attributed to the accumulation of alginate in the DES phase, resulting from the moderate affinity that the DES has for alginate (**Table 7.2**).

The increase in extraction yield could thus be due to incomplete phase separation of alginate into the aqueous phase in the previous cycles, due to the carryover of alginate that remains solubilised within the TRDES during cycles 1-4. During the first cycles, part of the alginate may remain dissolved in the TRDES phase as the optimal partitioning equilibrium has not yet been reached. As the TRDES system is reused, the TRDES could reach saturation. This accumulation, in turn, could influence the partition coefficient. Previous work by Cai *et al*. [165] stated a polysaccharide recovery yield of 88% from *Ganoderma lucidum*, indicating that part of the alginate could be retained as well in the TRDES.

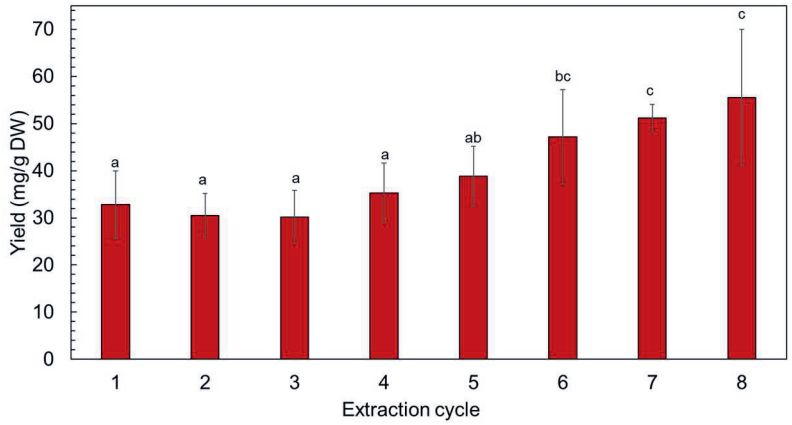


Figure 7.8 Extraction yield of alginate obtained using TRDES1 over eight consecutive recycling cycles.

To establish a theoretical framework supporting the hypothesis of potential alginate accumulation within the TRDES phase, COSMO-RS modelling was employed. The partitioning behaviour of alginate across multiple extraction cycles was assessed, incorporating an assumption that 2% of alginate remained accumulated in the DES phase after each cycle. This iterative approach allowed simulation of progressive

enrichment of alginate in the DES, enabling evaluation of its impact on the partition coefficient and the Gibbs free energy of transfer (ΔG) (**Section 7.2.3.2.2**).

The COSMO-RS modelling results showed a progressive increase in the partition coefficient and a corresponding decrease in the Gibbs free energy of transfer (ΔG) over successive extraction cycles, while having a reduction in solubility capacity (**Figure 7.9**, **Table S7.5**), indicating an increasing thermodynamic favourability for alginate partitioning into the aqueous phase. By cycle 8, ΔG becomes negative, indicating a spontaneous transfer of alginate from the DES to the water phase. This trend suggests a reduction in alginate solubility within the DES, likely due to the potential accumulation of alginate in the DES phase across cycles, leading to saturation. As a result, the driving force for alginate transfer into the aqueous phase increases and the partition coefficient increases (**Figure 7.9**). These computational findings are consistent with the experimentally observed increase in extraction yield upon solvent reuse (**Figure 7.8**). The observed changes in partitioning behaviour may diminish the DES its solvation capacity for alginate, thereby enhancing its release into the aqueous phase.

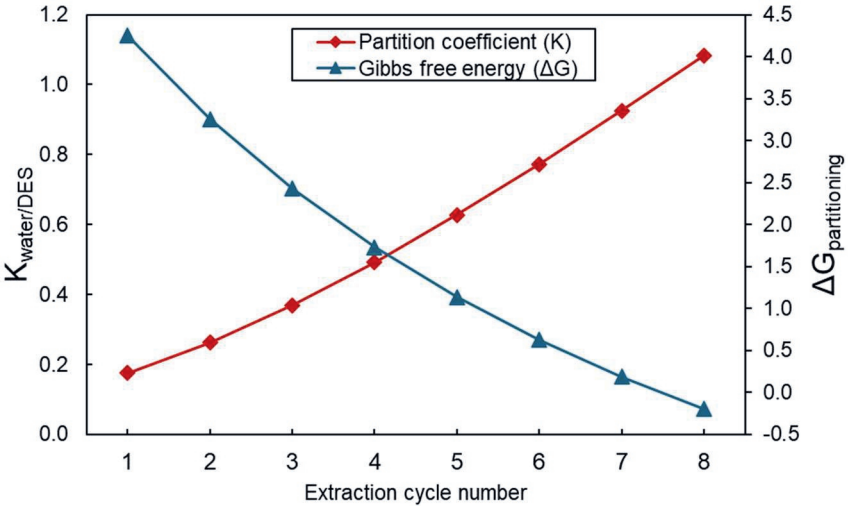


Figure 7.9 Partition coefficient and Gibbs free energy of transfer when recycling TRDES1 eight times, assuming 2% accumulation of alginate in the TRDES phase per extraction cycle.

7.3.7 Design criteria for novel TRDES

Temperature-responsive deep eutectic solvents (TRDES) effectively extracted alginate with considerable yields while enabling solvent recycling. Both COSMO-RS analysis and experimental data highlighted that the main solvent features governing extraction efficiency and recyclability are the capacity, partition coefficient and the Gibbs free

energy of transfer. The capacity (C) of the TRDES-water system should exhibit moderate capacity (10-30), thereby allowing extraction, while the capacity of the sole TRDES should be low (< 1.2), promoting alginate recovery from the TRDES. The partition coefficient (K**)** should be above 1 at room temperature, so that the compound favours the aqueous phase upon switching, indicating that the TRDES facilitates effective compound recovery. Trends in the Gibbs free energy of transfer (ΔG) across successive recycling cycles revealed that gradual accumulation of alginate enhances its partitioning into water. Together, these observations suggest that solvents with moderate affinity are optimal for balancing extraction performance with efficient recovery and recyclability.

Although the alkanolamine–phenol-based TRDES1 delivered high alginate yields with functional properties and stable recycling, these are potentially hazardous compounds. In contrast, menthol-based solvents (TRDES19-22) are non-toxic but show lower capacity. This highlights a critical design challenge: achieving effective extraction and favourable partitioning from water without relying on hazardous solvent constituents. In this study, the primary objective was therefore to gain mechanistic insights into their behaviour upon recycling. These insights guide the future development of greener, more biocompatible TRDES systems. Currently, no recyclable TRDES based on natural, non-toxic components have been reported, limiting their applicability as truly green solvents. Zhang *et al*. [338] applied a biphasic natural TRDES system composed of decanoic acid: octanoic acid (1:2) and choline chloride: levulinic acid (1:2) for extracting bioactives from *Zanthoxylum bungeanum* peels. Although lowering the temperature successfully induced phase separation of the two DES, the target bioactives still required recovery using macroporous resins. This additional step washed out the DES phase, preventing solvent recycling and thereby undermining the main advantage of the TRDES concept. Similarly, Wang *et al*. [327] designed a DES/ionic liquid/water system using natural DES. While they successfully separated rosmarinic acid and carnosic acid into distinct DES- and ionic liquid-rich phases, the compounds remained dissolved in their respective solvents, impairing the recyclability of DES and reducing the primary advantage of TRDES. This highlights the need for natural TRDES that enable product recovery and solvent recycling solely via temperature modulation. As an alternative, it would be interesting to explore LCST-type TRDES for future solvent design. LCST systems separate upon heating because hydrophobic interactions become dominant at elevated temperatures, disrupting hydrogen bonding with water [313, 328].

For future research, it is recommended to select natural HBAs and HBDs exhibiting moderate hydrophobicity, and perform computational solvent pre-screening

(capacity, partition coefficient and Gibbs free energy change) to choose suitable candidates (**Figure 7.10**). Recent advances in machine-learning-enhanced COSMO-RS workflows offer an additional opportunity to accelerate this process [339]. ML models trained on quantum-chemical descriptors can rapidly predict key solvent properties across large chemical spaces, enabling more efficient identification of promising natural TRDES candidates before experimental validation.

By modelling water–DES phase behaviour (UCST/LCST), their switchability can be assessed, followed by experimental phase behaviour assessment. Combining this data should give preferred candidates for laboratory validation on extraction, switching and solvent recycling (**Figure 7.10**). Focusing on natural compounds for designing temperature-switchable DES, supported by ML-accelerated screening, not only enhances process intensification compared to conventional DES extraction but also contributes to greater sustainability. This combined computational–experimental strategy facilitates the development and integration of DES technologies within biorefinery applications, promoting greener and more efficient biomass valorisation.

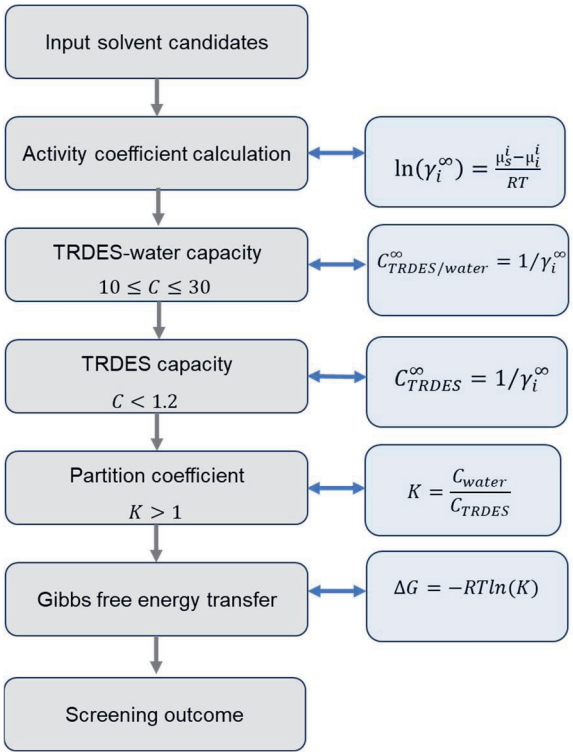


Figure 7.10 Process overview for designing natural TRDES for circular, green solvent extraction.

7.4. Conclusion

This study demonstrated the feasibility of temperature-responsive deep eutectic solvents (TRDES) as recyclable media for alginate extraction from *Saccharina latissima*. Initial solvent screening, supported by COSMO-RS modelling, identified TRDES1 as the most effective system. Under optimised conditions, TRDES1 enabled functional alginate extraction and was successfully recycled for eight consecutive cycles, with yields progressively increasing to 55.6 ± 14.4 mg/g DW. Thermodynamic modelling confirmed that this behaviour is linked to changes in alginate partitioning, with increasing partition coefficients across cycles, reflecting enhanced favourability for alginate recovery upon reuse.

Experimental data and COSMO-RS analysis showed that the capacity, partition coefficient, and Gibbs free energy of transfer were identified as the main factors influencing TRDES performance. Optimal extraction, partitioning and recyclability can be achieved with moderate TRDES-water capacity (10–30), low TRDES capacity (<1.2), and partition coefficients above 1. These findings establish preliminary design rules for future solvent development, emphasising the importance of moderate affinity to balance extraction efficiency and recovery potential.

However, the current well-performing TRDES are based on alkanolamine–phenol combinations, which limit environmental sustainability due to toxicity concerns. Bridging this performance–sustainability gap requires the development of natural TRDES composed of amino acids, sugars, and organic acids, ideally exhibiting LCST-type behaviour. To further extend the scope of this research, future work should integrate COSMO-RS with emerging machine-learning frameworks to accelerate the discovery of greener, biocompatible TRDES. ML-enhanced predictive models can rapidly screen large chemical spaces, identify promising natural HBA/HBD combinations, and guide the rational design of switchable, recyclable solvents. By uniting mechanistic understanding, thermodynamic criteria, and data-driven predictive tools, this study lays the foundation for developing non-toxic TRDES tailored for circular and sustainable biorefinery applications.

7.5. Supplementary information

Alginate is a linear copolymer composed of β-D-mannuronic acid (M) and α-L-guluronic acid (G) residues linked by β-1,4-glycosidic bonds. The relative abundance and sequence distribution of these monomers vary among seaweed species and are influenced by seasonal and environmental factors.

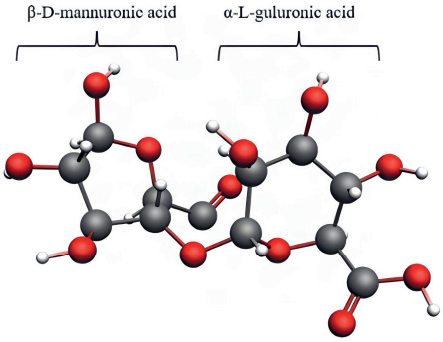


Figure S7.1 Partial chemical structure of alginic acid, illustrating the linkage between β-D-mannuronic acid (M) and α-L-guluronic acid (G) monomeric units.

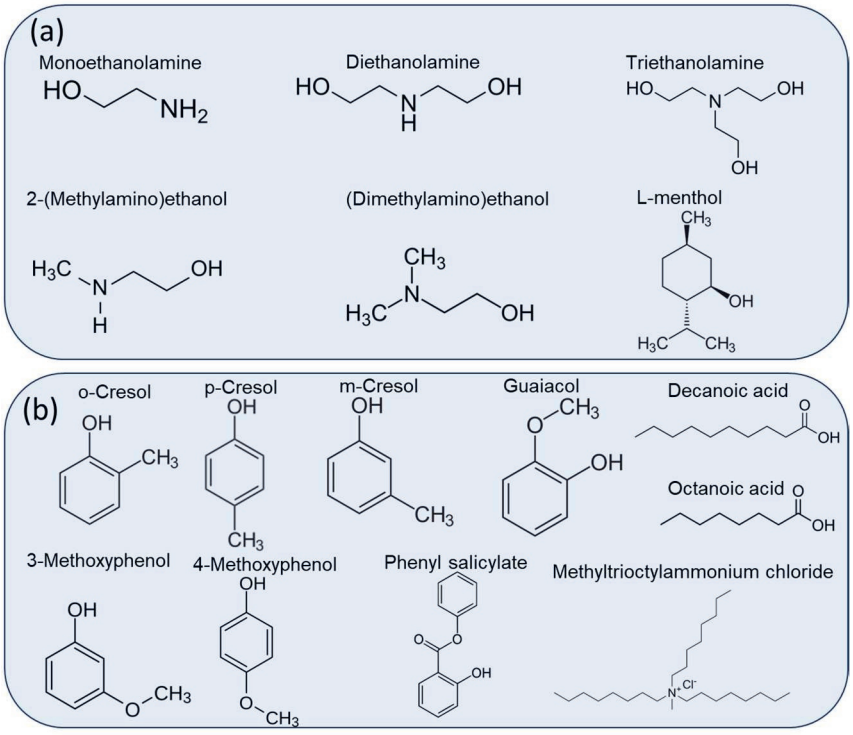


Figure S7.2 Molecular structures of the (a) HBAs and (b) HBDs used in the compositions of the DES.

Table S7.1 Phase behaviour of TRDES1 to TRDES22 with and without salt addition.

No.	HBA	HBD	Phase separation without salt	Phase separation with salt
TRDES 1	Ethanolamine	o-cresol	Yes	-
TRDES 2	Ethanolamine	p-cresol	No	Yes
TRDES 3	Ethanolamine	m-cresol	No	Yes
TRDES 4	Diethanolamine	o-cresol	No	Yes
TRDES 5	Diethanolamine	p-cresol	Yes	-
TRDES 6	Diethanolamine	m-cresol	Yes	-
TRDES 7	Triethanolamine	o-cresol	Yes	-
TRDES 8	Triethanolamine	p-cresol	Yes	-
TRDES 9	Triethanolamine	m-cresol	Yes	-
TRDES 10	Ethanolamine	Guaiacol	No	No
TRDES 11	Ethanolamine	3-Methoxyphenol	No	Incomplete
TRDES 12	Ethanolamine	4-Methoxyphenol	No	Yes
TRDES 13	2-(Methylamino)ethanol	Guaiacol	No	No
TRDES 14	2-(Methylamino)ethanol	3-Methoxyphenol	No	No
TRDES 15	2-(Methylamino)ethanol	4-Methoxyphenol	No	No
TRDES 16	(Dimethylamino)ethanol	Guaiacol	No	Yes
TRDES 17	(Dimethylamino)ethanol	3-Methoxyphenol	No	Yes
TRDES 18	(Dimethylamino)ethanol	4-Methoxyphenol	No	Yes
TRDES 19	L-menthol	Methyltrioctylammonium chloride	Yes	-
TRDES 20	L-menthol	Decanoic acid	Yes	-
TRDES 21	L-menthol	Phenyl salicylate	Yes	-
TRDES 22	L-menthol	Octanoic acid	Yes	-

The octanol–water partition coefficient (logP) was predicted using COSMO-RS to evaluate the hydrophobicity of the DES. These values were applied to assess to determine the hydrophobicity threshold associated with alginate affinity.

Table S7.2 Calculated octanol-water partition coefficients (logP) for DES and DES-water systems.

	DES	**DES-water**
TRDES 1	1.360	-0.443
TRDES 2	1.274	-0.465
TRDES 3	1.254	-0.470
TRDES 4	1.562	-0.393
TRDES 5	1.475	-0.414
TRDES 6	1.455	-0.419
TRDES 7	1.651	-0.370
TRDES 8	1.564	-0.392
TRDES 9	1.544	-0.397
TRDES 10	1.363	-0.442
TRDES 11	0.948	-0.546
TRDES 12	0.774	-0.590
TRDES 13	2.921	-0.053
TRDES 14	2.505	-0.157
TRDES 15	2.331	-0.200
TRDES 16	3.718	0.146
TRDES 17	3.302	0.042
TRDES 18	3.128	-0.001
TRDES 19	6.550	0.854
TRDES 20	7.829	1.174
TRDES 21	6.952	0.955
TRDES 22	6.550	0.854

The capacity and the partition coefficient (K) were examined across a range of temperatures for each DES that could perform reversible phase separation with water. A temperature range from 20 to 80 °C was selected to assess the influence of alginate partitioning, the capacity of water and the capacity of DES across the extraction and separation temperatures.

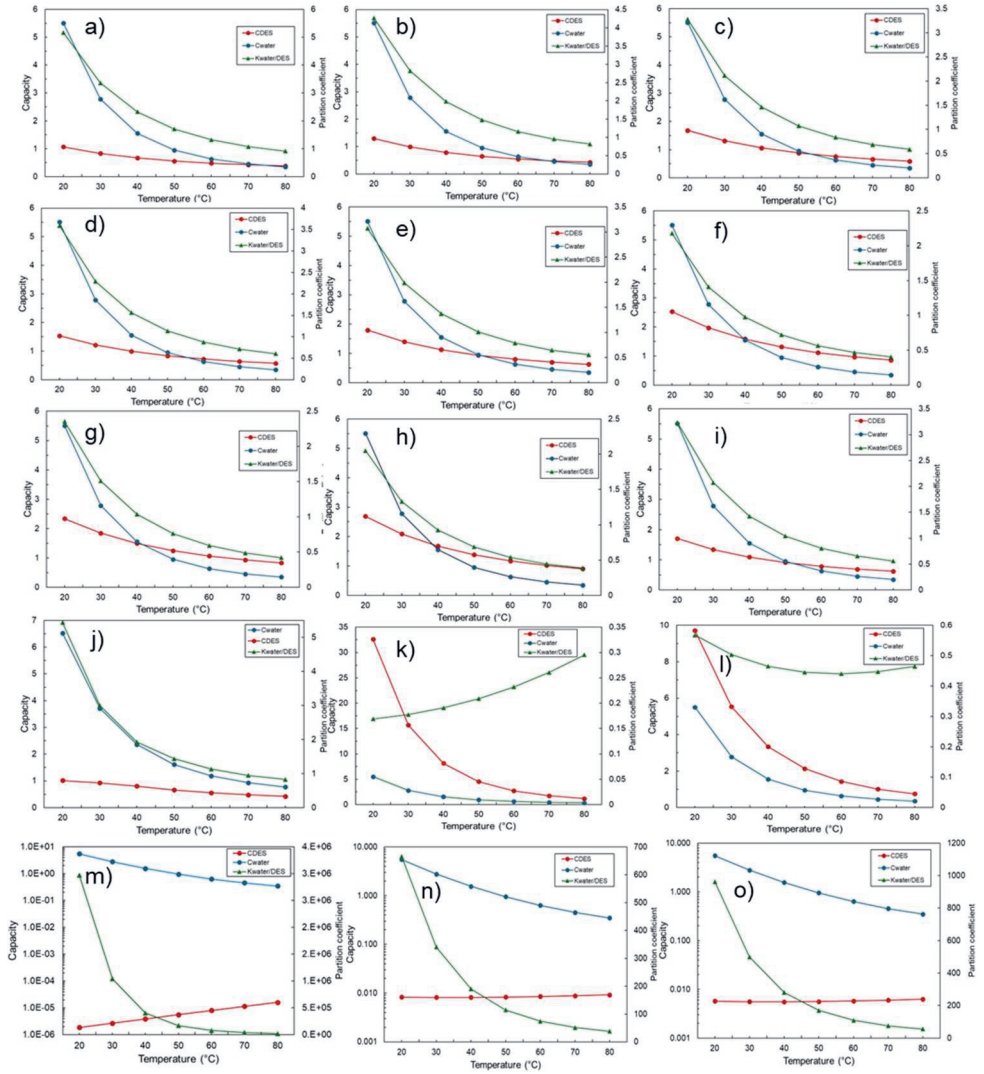


Figure S7.3 Capacity and partition coefficient (K) as a function of temperature (20–80 °C) of (a) TRDES2, (b) TRDES3, (c) TRDES4, (d) TRDES5, (e) TRDES6, (f) TRDES7, (g) TRDES8, (h) TRDES9, (i) TRDES12, (j) TRDES16, (k) TRDES17, (l) TRDES18, (m) TRDES19, (n) TRDES21, (o) TRDES22.

To confirm the temperature-responsive behaviour of the DES system, TRDES1 was characterised across the phase transition temperature with FTIR.

Table S7.3 Characteristic FTIR absorption bands of the TRDES1 constituents, TRDES1, and TRDES1 containing 50 % v/v water.

Peaks (cm^{-1})	Band assignment
1075	C–N stretching
1200	C–O stretching
1600	Aromatic C=C stretching
3344	O–H/N–H stretching
3000-3400	O–H/N–H stretching

In addition to characterising the DES in both its switched and unswitched states, the aqueous phase obtained after switching was analysed. No distinct peaks attributable to DES components were observed, suggesting the absence of detectable DES traces in the aqueous phase.

The alginate recovered from the TRDES was characterised for its functional groups with FTIR and compared with alkaline extraction.

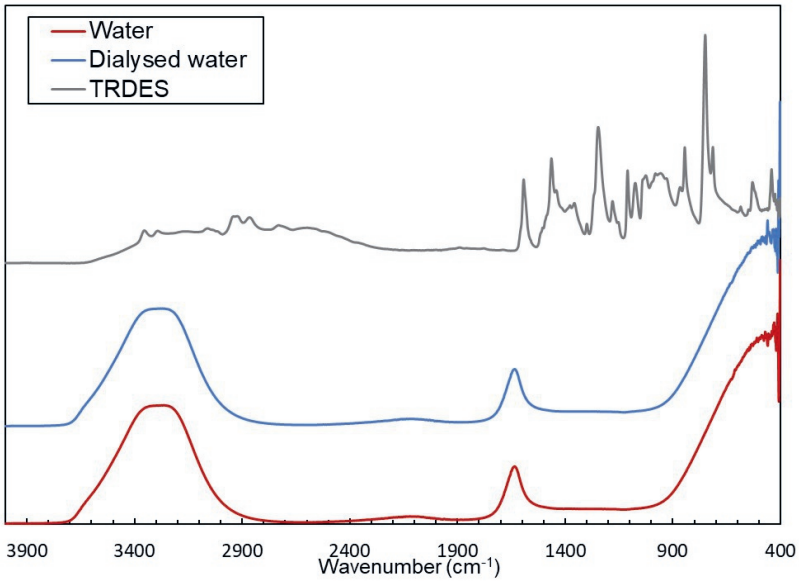


Figure S7.4 FTIR spectra of water, the aqueous phase after switching and TRDES1.

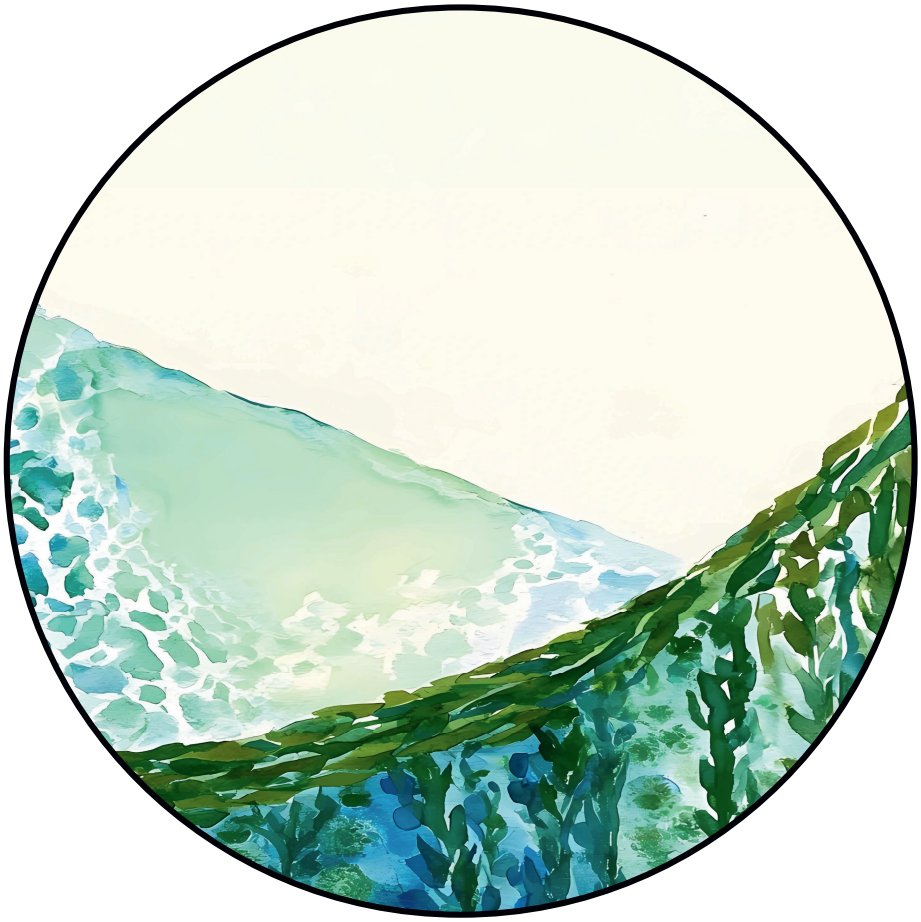
Table S7.4 Characteristic FTIR absorption bands of alginate extracted with TRDES, conventional alkaline processing and with water.

Peaks (cm^{-1})	Band assignment
1020	C-O stretching
1080	C-O-C stretching
1400	Symmetric COO^- stretching vibration
1600	Asymmetric COO^- stretching vibration
2900	C–H stretching vibration
3500	O–H stretching vibration

The recycling process was modelled using COSMO-RS to evaluate the partitioning behaviour of alginate over successive cycles. After each extraction cycle, it was assumed that 2% of alginate accumulated in the DES phase. The retained alginate was added to the solvent mixture composition for the subsequent cycle. The adapted solvent composition was used to recalculate the activity coefficient and partition coefficient of alginate in the TRDES-water system.

Table S7.5. Calculated activity coefficient, capacity, partition coefficient and Gibbs free energy when recycling the TRDES fraction eight times, assuming 2% accumulation of alginate per extraction cycle.

Cycle number	γ	C	$K_{water/DES}$	$\Delta G_{partition}$ (kJ/mol)
1	3.2×10^{-2}	3.1×10^{1}	1.7×10^{-1}	4.2
2	4.8×10^{-2}	2.1×10^{1}	2.6×10^{-1}	3.3
3	6.7×10^{-2}	1.5×10^{1}	3.7×10^{-1}	2.4
4	8.9×10^{-2}	1.1×10^{1}	4.9×10^{-1}	1.7
5	1.1×10^{-1}	8.8	6.3×10^{-1}	1.1
6	1.4×10^{-1}	7.1	7.7×10^{-1}	0.6
7	1.7×10^{-1}	6.0	9.3×10^{-1}	0.2
8	2.0×10^{-1}	5.1	1.1	-0.2
Water	1.8×10^{-1}	5.5		



Chapter 8

Direct alginate recovery and solvent recycling via interfacial precipitation in aqueous two-phase systems

Isa S.A. Hiemstra, Jinte de Jong, Michel H.M. Eppink, Rene H. Wijffels, Antoinette Kazbar

This chapter has been published as:

Hiemstra, I. S. A., De Jong, J., Eppink, M. H. M., Wijffels, R. H., & Kazbar, A. (2026). Direct alginate recovery and solvent recycling from deep eutectic solvents via interfacial precipitation in aqueous two-phase systems. *Separation And Purification Technology*, *407*, 139128. https://doi.org/10.1016/j.seppur.2026.139128

Abstract

Conventional alginate extraction from brown seaweed relies on alkaline treatments that limit sustainability and solvent reuse. In this study, a novel deep eutectic solvent (DES)–salt aqueous two-phase system (ATPS) was developed for the integrated extraction and separation of alginate as a more sustainable alternative. By incorporating the precipitation principle of three-phase partitioning at elevated salt concentrations in an ATPS, alginate was selectively recovered in an intermediate phase between the DES and aqueous salt solution, enabling direct isolation while preserving the solvent for reuse. Salt selection significantly influenced phase formation, with K_3PO_4 exhibiting stronger phase-forming ability than K_2HPO_4 due to its enhanced salting-out effect, whereas alginate recovery was primarily governed by salt concentration. The highest recovery (76.4 ± 0.1%) was achieved using betaine: urea (1:2) with 50 wt% K_3PO_4, with most alginate accumulating in the intermediate phase. The DES maintained stable recovery over six cycles (63–86%), while preserving alginate integrity. These results demonstrate the potential of DES-based ATPS as an efficient platform for simultaneous extraction, separation, and solvent recycling, providing a promising route toward more sustainable and integrated seaweed biorefinery processes.

8.1. Introduction

Efficient extraction processes are critical for the valorisation of renewable biomass. However, they commonly rely on volatile and hazardous organic solvents. The environmental burden, safety concerns, and limited recyclability associated with these solvents have driven increasing interest in alternative solvent systems compatible with sustainable biorefinery concepts [197]. One promising class of alternative extraction solvents is deep eutectic solvents (DES). DES have attracted considerable interest due to their potential advantages over conventional organic solvents, including lower toxicity, biodegradability, and the possibility of solvent recycling [87, 340]. They are typically formed by combining one or more hydrogen bond donors (HBD) with one or more hydrogen bond acceptors (HBA), resulting in a pronounced melting point depression and the formation of a liquid phase at a specific molar ratio [9, 14].

One emerging application of DES is the extraction of marine biomass constituents, particularly from seaweed [62, 88, 341]. Brown seaweed represents a renewable and abundant resource rich in structurally diverse polysaccharides, including alginate. Alginate is a linear anionic polysaccharide composed of β-D-mannuronic acid and α-L-guluronic acid residues arranged in varying block sequences (**Figure S8.1**). Owing to its gel-forming ability, biocompatibility, and rheological properties, alginate is widely used in the food, pharmaceutical, biomedical, and materials industries [50].

Despite its widespread applications, conventional alginate extraction relies on multistep alkaline treatments, typically involving multiple acidic and alkaline processing steps. This in turn results in excessive water consumption and high energy demand, generating substantial waste streams [56]. Furthermore, solvent recovery and recycling are limited, reducing overall process sustainability and efficiency. As an alternative, DES have recently been proposed as novel media for alginate extraction.

Although alginate was successfully extracted previously using DES, achieving higher yields compared to conventional processing methods [100], efficient recovery of the extracted alginate and subsequent solvent recycling remain a critical challenge. The negligible vapour pressure of DES limits separation by conventional evaporation-based techniques, thereby complicating product isolation and solvent regeneration [70]. Consequently, alternative separation strategies are required to enable efficient recovery and sustainable reuse of DES. Previous work demonstrated that three-phase partitioning (TPP) using hydrophobic DES and an aqueous salt phase can be an effective strategy for alginate recovery from seaweed [342]. This approach achieved good alginate yields while enabling DES recycling, demonstrating the potential of TPP

for integrated biorefinery processes. However, a constraint of the study was that alginate partitioned into the salt-rich phase, necessitating an additional dialysis step to isolate the polymer, thereby adding additional processing steps. In another study, the use of temperature-responsive aqueous two-phase systems (ATPS) was explored for alginate recovery and DES reuse [335]. This system employed temperature-sensitive copolymers to separate alginate from DES, enabling efficient alginate isolation while allowing the recycling of both DES and copolymer phases. Despite its effectiveness, the method required a two-step ATPS process and relied on careful temperature control, making it relatively complex and less suitable for large-scale applications. As a simpler ATPS approach, Liu *et al*. [343] employed an aqueous two-phase system composed of DES and an aqueous salt solution. In this system, polysaccharides from *Astragalus membranaceus* were extracted with DES and partitioned from the DES phase into the aqueous phase and were subsequently recovered from the aqueous phase via dialysis. By using a salt-based ATPS, the need for a second phase separation, as required in temperature-responsive systems, is eliminated. However, because the polysaccharides partition into the aqueous phase, dialysis was still necessary for product isolation.

Taken together, these studies demonstrate the potential of ATPS for polysaccharide recovery but also underscore the continuing need for simpler, more efficient strategies that enable both effective polymer isolation and straightforward solvent recycling. To avoid partitioning of the target polymer alginate into the aqueous phase, a three-phase partitioning (TPP) like strategy incorporating product precipitation could be employed. In protein separation, TPP is widely used to induce precipitation in a distinct interfacial phase between the solvent-rich and aqueous layers [344], as salt addition reduces protein solubility through charge screening and salting-out effects [218]. In turn, this leads to controlled aggregation and thereby enables simultaneous phase separation and product isolation.

Building on this, in this study, we propose a novel DES-based ATPS separation strategy that incorporates the precipitation principle of three-phase partitioning into an aqueous two-phase system, enabling direct alginate isolation while maintaining solvent recyclability. Liquid–liquid equilibria were first determined for different DES–salt combinations to evaluate their phase behaviour. Based on this, alginate was extracted using the selected DES systems. High salt concentrations were then applied to induce phase separation, mimicking three-phase partitioning conditions while promoting alginate precipitation within the ATPS. This approach enabled direct alginate recovery without the need for additional purification steps such as dialysis, which are

typically required in conventional ATPS. Finally, the optimal ATPS conditions were identified and applied for alginate characterisation and evaluation of DES recyclability.

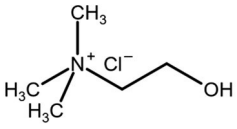
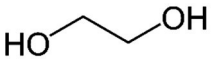
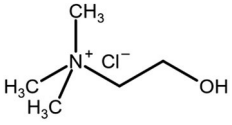
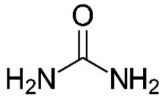
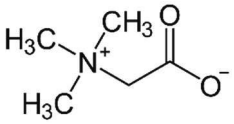
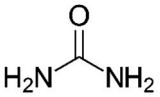
We hypothesise that this approach could be effective for alginate due to its polyelectrolytic nature, as its charged carboxylate groups may respond to salt-induced solubility shifts. In this way, alginate is recovered as a separate precipitated phase which can easily be recovered, allowing the DES phase to be directly reused without additional separation steps. This strategy aims to enable direct alginate isolation from DES while maintaining solvent recyclability. These findings provide a foundation for the development of more sustainable DES-based extraction processes that enable efficient product recovery alongside solvent reuse.

8.2. Materials and methods

8.2.1 Materials

Brown seaweed *Laminaria digitata,* was used for the alginate extractions. Sun-dried *L. digitata* was supplied by Algaia in March 2023. Prior to extraction, the material was shredded, its dry weight content was determined, and the biomass was size fractionated by sieving through 710 µm and 90 µm meshes. The intermediate fraction (90–710 µm) was retained for extractions and stored at 4 °C until use. Three different DES containing 15 wt% water were employed as candidates for ATPS separation (**Table 8.1**). The DES were prepared using either choline chloride (≥98 %) or betaine (≥99 %) as the HBA, combined with ethylene glycol (≥99.8%) or urea (≥99.5%) as the HBD. Sodium alginate standards (>88% purity) were used for characterisation. Aqueous salt solutions for the ATPS were prepared using either dipotassium phosphate (K_2HPO_4, ≥98 %) or tripotassium phosphate (K_3PO_4, ≥98 %). Chemicals were obtained from Sigma Aldrich (Merck).

Table 8.1 Composition, molecular structure and molar ratios of DES used in the study.

		Abbreviation	HBA	HBD
DES1	Choline chloride: Ethylene glycol (1:2)	ChCl:EG		
DES2	Choline chloride: Urea (1:2)	ChCl:U		
DES3	Betaine:Urea (1:2)	Bet:U		

8.2.2 DES preparation

The DESs were prepared following the heating method described by Abbott *et al*. [200]. The hydrogen bond acceptor (HBA) and hydrogen bond donor (HBD) were combined in a 1:2 molar ratio (**Table 8.1**) with 15 wt% water, which was added during preparation to

reduce viscosity and improve processability for biomass extraction applications. The mixture was heated in a water bath at 80 °C for 1 h until a clear, homogeneous solution was obtained. The resulting DES was then used for alginate extraction. The selection of DES was guided by both prior literature and their demonstrated suitability for biomass processing and aqueous two-phase system (ATPS) formation. The three DES were selected based on previous studies on *L. digitata* extraction, where these solvents showed effective alginate extraction and compatibility with downstream recovery processes, and to enable direct evaluation of recovery strategies [335].

8.2.3 Alginate extraction and quantification

Alginate was extracted from *L. digitata* using DES (**Table 8.1**), employing a solid:liquid ratio of 1:40. Extractions were conducted at 80 °C for 1 h, with intermittent vortexing to promote mass transfer and ensure homogeneity [335]. As a control, alginate was extracted using a conventional alkaline method to enable direct comparison with the DES-based extractions. For the alkaline extraction, acidified water (pH 1.9, adjusted with H_2SO_4) was added to the seaweed at a 1:1 (w/w) ratio and incubated at room temperature for 1 hour. Subsequently, Na_2CO_3 was added at a 0.0325:1 (w/w) ratio, and the mixture was further incubated for 1 h to facilitate extraction. All DES and alkaline extractions were performed in triplicate. Following extraction, the samples were centrifuged, and the supernatants were collected for alginate quantification.

Alginate quantification was performed using a colorimetric assay adapted from Cesaretti *et al*. [136]. The alginate extraction and recovery yield were defined as the mass of alginate recovered per gram of dry seaweed and were calculated according to **Equation 8.1**:

$$Yield\ \left(\frac{mg}{g\ DW}\right) = \frac{C_{extract} * V_{total}}{m_{biomass} * x_{DW}} \qquad (\mathbf{8.1})$$

where $C_{extract}$ is the concentration of the extract, $m_{biomass}$ is the weight of the initial biomass, x_{DW} is the weight fraction of the dry biomass and V_{total} is the total volume of the extract. The alginate fraction after ATPS formation was assessed in each fraction and expressed as a percentage of the alginate present after extraction.

8.2.4 Establishment and phase behaviour of DES-based ATPS

8.2.4.1 Cloud point (solubility) curves

The cloud-point solubility curves for the DES with K_2HPO_4 or K_3PO_4, combined with water as ternary systems were determined at room temperature (20 °C) using the cloud point titration method [345, 346]. Potassium phosphate salts (K_2HPO_4 and K_3PO_4) were selected due to their strong salting-out capacity and established use in DES-based ATPS systems, where they have been shown to reliably induce phase separation with choline chloride- and betaine-based DES [343, 347]. The use of two salts with different ionic strengths further enabled systematic investigation of their influence on phase formation and alginate partitioning behaviour.

Initially, a known mass of DES was titrated with a concentrated solution of aqueous salt solution under constant stirring until the first appearance of persistent turbidity, signifying the onset of phase separation. To confirm the phase boundary, the mixture was then back-titrated with deionised water until the solution returned to a clear, monophasic state. The mass of each component was recorded to calculate the mass fraction compositions at each cloud point. Cloud-point (solubility) curves were constructed from these experimental data points. The phase boundary was described using an empirical polynomial fit to guide visualization of the solubility binodal behaviour.

8.2.4.2 DES extract phase behaviour

Phase behaviour of the DES extracts was evaluated by mixing different DES extracts with aqueous salt solutions. The extracts were combined with either K_2HPO_4 or K_3PO_4 solutions at ratios selected based on the previously determined cloud point curves. The resulting mixtures were gently mixed and subsequently inspected visually to assess the occurrence of phase separation between the DES-rich phase and the salt-rich aqueous phase.

8.2.5 Alginate affinity with COSMO-RS

The Conductor-like Screening Model for Real Solvents (COSMO-RS) is an effective tool to predict the thermodynamic properties of the investigated fluid systems [67]. It can be used to describe and understand solute partitioning behaviour. COSMO-RS was applied to study the affinity of alginate in the two phases during the ATPS. Calculations were conducted using COSMO-RS version 2022.103 (Software for Chemistry and Materials BV, Amsterdam, The Netherlands) implemented within the Amsterdam Density Functional (ADF) software suite. Initial molecular structures were subjected to geometry optimisation using the universal force field (UFF), after which electronic

structure calculations were performed using density functional theory (DFT) at the GGA:BP86 level of theory with a triple-ζ polarized (TZP) basis set [93]. Direct application of COSMO-RS to polymers such as alginate is impractical, as it requires extensive quantum chemical calculations, rendering the procedure computationally demanding and time-consuming [96, 317]. Therefore, an alginate trimer was selected for modelling, as it allows feasible quantum chemical calculations while still capturing the essential structural features of the polymer [94].

Using COSMO-RS, the activity coefficients of alginate in each solvent, followed by determination of the corresponding solvent capacity. The activity coefficient (γ), defined as the ratio of a species' activity to its mole fraction, describes deviations from ideal solution behaviour and reflects the interactions between alginate and each DES and salt solution at infinite dilution. The capacity of each solvent, indicating the maximum solubility, was calculated using the inverse of the activity coefficient as described in **Equation 8.2**:

$$C^{\infty}_{alginate} = \frac{1}{\gamma^{\infty}_{alginate}} \quad (\mathbf{8.2})$$

where $\gamma^{\infty}_{alginate}$ is the activity coefficient of alginate at infinite dilution.

8.2.6 Recovery performance of DES-based ATPS

To each DES, an aqueous salt solution of either K_2HPO_4 or K_3PO_4 was added at concentrations of 40, 50, or 60 wt% (**Table 8.2**), according to the phase compositions defined by the corresponding cloud-point (solubility) curves (**Section 8.2.4.1**). Following salt addition, the mixtures were vortexed and shaken for 30 minutes to ensure thorough mixing. The samples were then allowed to stand undisturbed for at least 30 minutes to enable complete phase separation between the DES and aqueous phases. After phase separation, the two phases were carefully collected. The aqueous phase was subsequently dialysed using a membrane with a molecular weight cut-off of 3.5–5 kDa to remove residual salts. All conditions were assessed in triplicates. Alginate concentrations in both the DES-rich and aqueous phases were then quantified to evaluate the recovery efficiency of each system. Total alginate mass balances were constructed by considering all phases, including the DES-rich phase, interfacial precipitate, and aqueous phase, confirming overall mass conservation.

Table 8.2. Different ATPS variables tested per DES.

Salt type	salt/water wt%	DES: Aqueous salt solution
K_2HPO_4	40	3:2
	50	1:1
	60	2:3
K_3PO_4	40	3:2
	50	1:1
	60	2:3

8.2.7 Alginate characterisation

The recovered alginate was characterised in terms of its mannuronic to guluronic acid ratio and molecular weight. Structural features were analysed using Fourier-transform infrared (FTIR) spectroscopy.

8.2.7.1 FTIR analysis

Alginate recovered from DES and alkaline treatment was analysed with FTIR spectroscopy using a spectral range of 400–4000 cm^{-1} using a Nicolet Summit X ATR-FTIR spectrometer (Thermo Fisher Scientific). Alginate was isolated from the extracts via precipitation using a 1 % (w/v) calcium chloride dihydrate solution, followed by two consecutive washing steps with 80 % (v/v) ethanol. The resulting precipitate was dried under a nitrogen stream and subsequently characterised by FTIR spectroscopy.

8.2.7.2 Molecular weight

Size exclusion chromatography (SEC) was employed to determine the molecular weight distribution of alginate obtained via DES recovery and alkaline extraction, following a previously reported method [48]. Alginate samples (0.15% w/v) were dissolved in Milli-Q water, and 20 µL was injected into an Agilent 1290 Infinity HPLC system fitted with two PL aquagel-OH MIXED-H columns (8 µm, 300 × 7.5 mm) connected in series. Separation was performed using 0.1 M ammonium phosphate monobasic (pH 4.5, Sigma-Aldrich) as the mobile phase at a flow rate of 0.8 mL/min, with detection by refractive index (RID). Calibration was carried out using pullulan standards (PSS-PULKITR1, Agilent), and molecular weights were expressed as alginate equivalents using the Mark–Houwink relationship [48].

The average molecular weight (Mw) of alginate was calculated using **Equation 8.3**:

$$M_w = \frac{\Sigma(M_i^2 * c_i)}{\Sigma(M_i * c_i)} \quad \textbf{(8.3)}$$

where M_i denotes the molecular weight of fraction *i* at a specific retention time in the chromatogram, and c_i corresponds to the signal intensity (peak area) of fraction *i*, which is proportional to its concentration.

8.2.7.3 Mannuronic to guluronic acid ratio

The mannuronic to guluronic acid (M/G) ratio of the extracted alginate was determined by methanolysis, followed by high-performance anion-exchange chromatography with pulsed amperometric detection (HPAEC-PAD), in accordance with a previously established protocol [227]. Analyses were conducted using a Dionex ICS-6000 chromatographic system (Thermo Fisher Scientific) fitted with a 1 mm CarboPac column. Alginate samples extracted and recovered via DES-based extraction were analysed in parallel with conventional alkaline processing. In addition, a commercial sodium alginate standard was included as a reference to evaluate the efficiency of the methanolysis procedure. Prior to methanolysis, alginate samples were precipitated, subsequently redissolved in Milli-Q water, and aliquots of 50 µL were subjected to analysis.

8.2.8 DES recycling

For DES recycling, the optimal DES and salt conditions for overall alginate recovery were selected. The extraction of alginate and the subsequent separation of alginate from the DES were performed for six consecutive cycles. In each cycle, both the extraction yield and the recovery yield were quantified to assess the effect of repeated DES reuse. After every extraction step, the alginate concentration in the DES phase was determined, and following each cycle, the overall alginate recovery was evaluated.

8.2.9 Statistical analysis

Statistical analyses were conducted using IBM SPSS Statistics (version 30.0.0.0). Significant differences between groups were evaluated using least significant difference (LSD) and Duncan's multiple range post hoc tests, set at $p < 0.05$. Data are presented as mean standard deviation based on three independent experiments. Different letters denote statistically significant differences between groups ($p < 0.05$).

Figure 8.1 provides a schematic overview of the alginate extraction, the aqueous two-phase system for alginate recovery and the DES recycling.

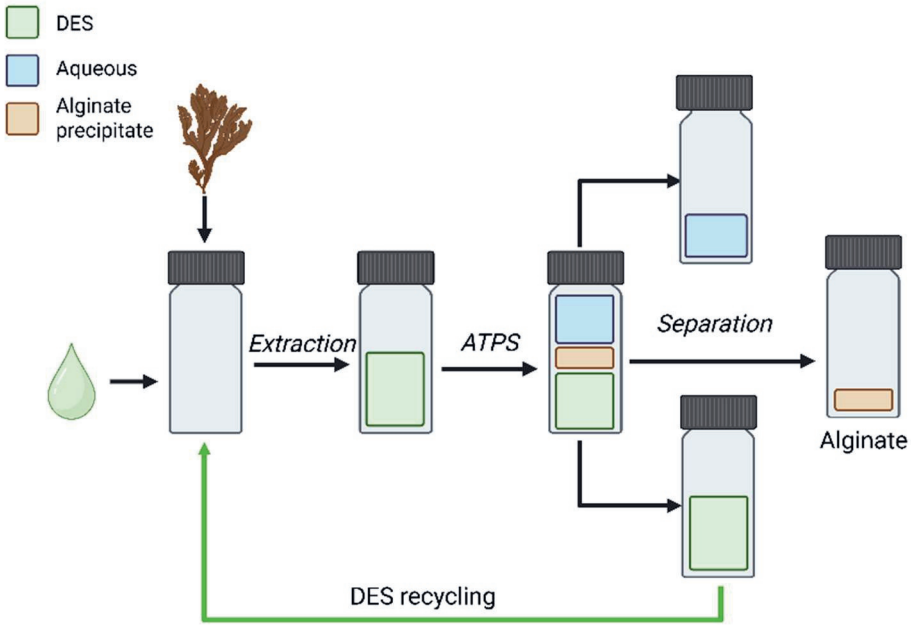


Figure 8.1 General overview of the alginate extraction and recovery procedure using deep eutectic solvent in an aqueous two-phase system.

8.3. Results and discussion

8.3.1 Aqueous two-phase behaviour

Liquid–liquid equilibria were determined to evaluate the phase behaviour of the different DES in combination with K_2HPO_4 and K_3PO_4 and to identify the concentration ranges required for aqueous biphasic system formation [348, 349]. The resulting solubility curves define the compositions at which the mixture separates into two distinct phases. Systems with compositions above the solubility curve form two phases, whereas those below the curve remain monophasic (**Figure 8.2**). Furthermore, solubility curves located closer to the origin of the phase diagram indicate stronger phase-forming ability of the DES [350, 351].

DES2 (ChCl:U) and DES3 (Bet:U) exhibited stronger phase-separation ability than DES1 (ChCl:EG), as reflected by their solubility cloud-point curves position (**Figure 8.2**). This behaviour can be attributed to differences in the HBD components of the DES. DES1 (ChCl:EG) contains ethylene glycol, whereas DES2 (ChCl:U) and DES3 (Bet:U) are based on urea. The presence of hydroxyl (–OH) groups in ethylene glycol increases the hydrophilicity of the DES and promotes hydrogen bonding with water, thereby enhancing solvent–water miscibility. As previously reported, DES with higher –OH content generally exhibit stronger water affinity and reduced tendency to form biphasic systems, which likely explains the lower phase-forming ability observed for ChCl:EG compared to ChCl:U and Bet:U containing the more hydrophobic urea [346, 348].

In addition to DES composition, the choice of salt significantly influenced phase separation. Systems containing K_3PO_4 showed stronger phase-forming ability than those with K_2HPO_4 (**Figure 8.2**). The formation of aqueous biphasic systems is primarily driven by salting-out effects, where hydrated ions compete with the DES for water molecules [346, 352]. Due to the higher charge of the phosphate anion (PO_4^{3-}), K_3PO_4 exhibits stronger hydration and therefore a more pronounced salting-out effect than K_2HPO_4 (HPO_4^{2-}). As a result, K_3PO_4 more effectively reduces DES solubility in the aqueous phase, promoting phase separation, in agreement with previous studies [353–355].

It should be noted that the phase diagrams generated in this study were based on cloud-point (solubility) curves and therefore define the onset of phase separation rather than the equilibrium compositions of the coexisting phases. While determination of tie-lines would provide additional thermodynamic insight into DES distribution and partitioning behaviour within the ATPS, the primary objective of this work was to identify stable biphasic systems capable of enabling alginate recovery

through interfacial precipitation. Consequently, cloud-point curves were considered sufficient for selection of suitable phase-forming compositions. Future studies could complement this approach with tie-line analysis to further elucidate the underlying phase behaviour.

Consequently, DES1 (ChCl:EG) was excluded from further analysis due to its weak phase-separation behaviour, resulting in poorly defined and unstable biphasic systems likely associated with its higher hydrophilicity. DES2 and DES3 were therefore selected for subsequent phase separation with the extracts and further evaluation of alginate recovery performance.

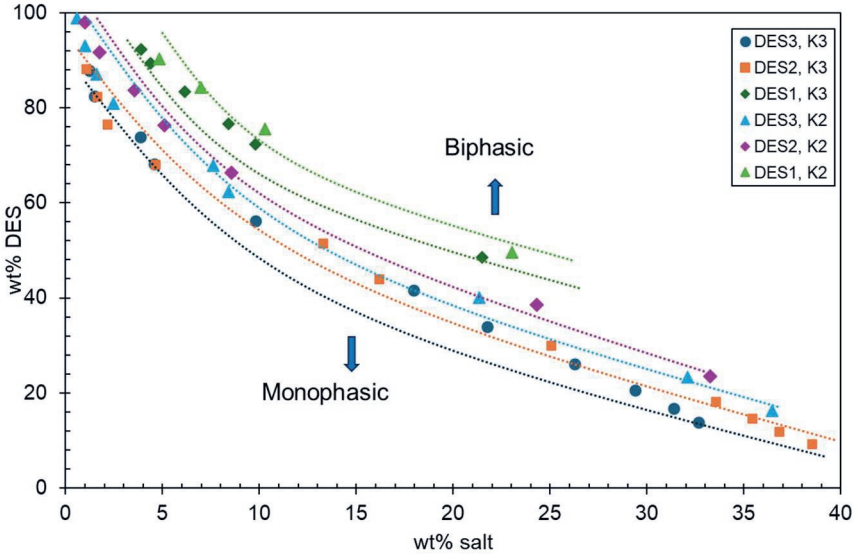


Figure 8.2 Phase diagrams of DES-based ATPS for DES1-3 combined with either K_2HPO_4 or K_3PO_4.

8.3.2 Alginate recovery performance

The extraction yields obtained ranged between 60.4 ± 4.7 and 63.2 ± 4.4 mg/g DW for DES2 (ChCl:U) and DES3 (Bet:U), respectively (**Figure S8.2**), in reasonable agreement with values reported previously [335]. Therefore, these DES were selected for aqueous biphasic system formation for subsequent alginate recovery from the DES extracts. Phase separation experiments were conducted using the DES extracts, resulting in the formation of biphasic systems for both DES in combination with the two salts (**Figure S8.3**). Phase behaviour was evaluated in terms of formulation composition (salt concentration and DES type) as a practical descriptor of ATPS conditions used for alginate recovery screening. Moreover, for each condition, a middle phase was observed, potentially containing recovered alginate (**Figure S8.4**). To evaluate alginate

recovery from DES, ATPS were established using ChCl:U and Bet:U in combination with K_2HPO_4 or K_3PO_4 at 50 and 60 wt% salt concentrations (**Section 8.2.5**). The distribution of alginate across the resulting phases was quantified to determine recovery efficiency (**Figure 8.3**, **Table 8.3**).

Alginate recovery was achieved under all investigated conditions, demonstrating that both DES systems are compatible with salt-induced phase separation (**Figure 8.3**). Recovery efficiency, however, strongly depended on DES type and salt concentration. The highest overall recovery was obtained for DES3 combined with 50 wt% K_3PO_4 (76.4 ± 0.1%) and 50 wt% K_2HPO_4 (76.0 ± 3.0%), whereas the lowest recovery was observed for DES2 with 60 wt% K_2HPO_4 (24.9 ± 1.3%) (**Figure 8.3**, **Table 8.3**). Overall, Bet:U exhibited approximately 1.5-fold higher alginate recovery compared to ChCl:U across the conditions, indicating that solvent composition plays a decisive role in phase transfer efficiency.

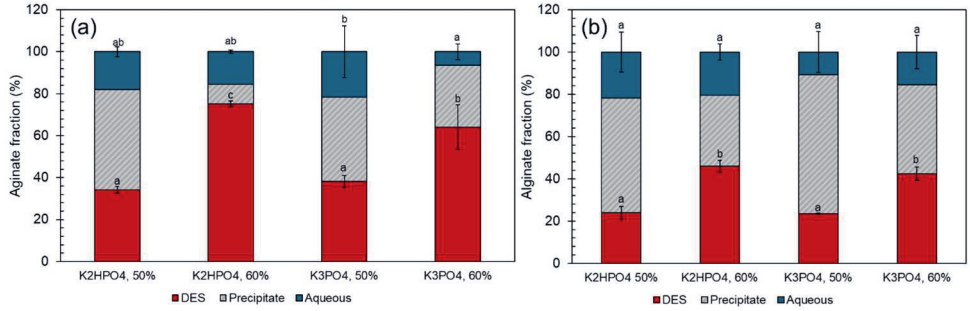


Figure 8.3 Alginate distribution (%) in the DES, aqueous and precipitate phases after ATPS formation for (**a**) DES2 (ChCl:U) and (**b**) DES3 (Bet:U).

The superior recovery performance of Bet:U compared to ChCl:U can be attributed to differences in their interaction mechanisms with alginate. In ChCl:U, the presence of free chloride ions (**Table 8.1**) increases the ionic character of the solvent and may enhance electrostatic stabilisation and solvation of the polyanionic alginate chains through hydrogen-bonding and ion-mediated interactions. In contrast, betaine is a zwitterionic hydrogen-bond acceptor without a free counterion [111], leading to interactions that are more readily disrupted upon salt addition. The increased ionic strength introduced by K_3PO_4 likely enhances electrostatic shielding and competes for water molecules, weakening alginate– Bet:U interactions more effectively and promoting its transfer into the intermediate phase. These observations are further supported by calculated capacities (**Figure S8.5**). The salt systems exhibited significantly higher capacity toward alginate compared to the DES, indicating a stronger thermodynamic affinity of alginate for the salt-rich phase. This higher interaction potential likely drives the initial transfer of alginate from the DES into the

aqueous environment. Although tie-line analysis is commonly used to describe equilibrium phase compositions in ATPS, the present study focuses on experimentally observed phase distribution and recovery behaviour across DES-rich, aqueous, and interfacial phases, as the system is additionally governed by interfacial precipitation rather than purely equilibrium partitioning.

The salt type did not show a significant effect on the alginate recovery (**Figure 8.3**). However, the salt concentration significantly influenced alginate distribution, with 50 wt% systems consistently outperforming 60 wt% systems ($p < 0.05$, **Figure 8.3**). This trend was also reflected in the formation of a distinct intermediate precipitation phase in all systems. For ChCl:U at 50 wt% salt concentration, approximately 40–48% of alginate accumulated in the middle phase, whereas Bet:U exhibited higher interfacial accumulation (54–66%). Increasing the salt concentration to 60 wt% reduced alginate presence in the middle phase to 9–29% and 33–42% for DES2 and DES3, respectively. These results indicate that moderate ionic strength promotes phase transfer and controlled interfacial aggregation, while excessive salt concentrations hinder effective alginate redistribution.

At elevated salt concentrations, the aqueous phase approaches saturation, reducing the availability of free water [219]. The resulting high ionic strength competes for water molecules and disrupts the hydration shell surrounding alginate chains. Given the high density of carboxylate groups in alginate (**Figure S8.1**), electrostatic shielding by phosphate ions further limits alginate–water interactions. While moderate charge screening promotes aggregation and phase transfer, excessive ionic strength likely reduces polymer mobility and suppresses the formation of a coherent interfacial precipitation layer. Consequently, alginate migration from the DES phase is hindered, leading to reduced accumulation in both the aqueous and intermediate phases and lower overall recovery at 60 wt% salt.

The underlying mechanism shows conceptual similarities to three-phase partitioning (TPP) systems used for protein separation, where salting-out and polarity regulation induce interfacial precipitation [356]. In classical TPP, high salt concentrations are typically employed (approximately 30–50 wt% ammonium sulphate [222, 357] to promote strong dehydration and aggregation effects. In contrast, conventional polymer–salt ATPS systems often operate at lower salt concentrations (commonly 10–25 wt% [273, 358, 359]), where phase separation is driven primarily by polymer incompatibility rather than salting-out. In both TPP and the present DES–salt ATPS system, phase formation is governed by solvent polarity modulation and dehydration effects associated with elevated ionic strength [360]. However, unlike proteins that

precipitate due to exposure of hydrophobic domains [344], alginate partitioning is primarily governed by ionic interactions and hydrogen-bond competition due to its hydrophilic and polyanionic structure. The present DES–salt ATPS can therefore be viewed as a polysaccharide-adapted analogue of TPP, combining phase separation with controlled precipitation driven by ionic strength and solvent polarity differences.

Overall, these findings demonstrate that alginate recovery in DES-based ATPS is primarily governed by solvent composition and ionic strength rather than phosphate salt identity. Moderate salt concentrations provide an optimal balance between salting-out and hydration capacity, thereby maximising phase transfer efficiency. Among the investigated systems, Bet:U (DES3) combined with 50 wt% K_3PO_4 achieved the highest total recovery (76.4 ± 0.1%), defined as the sum of alginate recovered in the aqueous and intermediate phases (**Table 8.3**), with 65.7 ± 9.7% of the total alginate accumulating in the intermediate phase, while the remainder (23.5%) remained in the DES phase (**Figure S8.3**). The separable precipitation layer formed in Bet:U at 50 wt% K_3PO_4 system facilitated efficient product isolation. Based on its superior recovery and favourable phase behaviour, this system was selected for subsequent characterisation and recycling studies.

Table 8.3 Total alginate recovery (%) from the DES phase after ATPS, defined as the combined recovery in the interfacial precipitate and aqueous phases.

Total recovery (%)	K_2HPO_4, 50%	K_2HPO_4, 60%	K_3PO_4, 50%	K_3PO_4, 60%
DES 2	65.9 ± 1.6	24.9 ± 1.3	61.8 ± 2.8	35.9 ± 10.7
DES 3	76.0 ± 3.0	54.0 ± 2.8	76.4 ± 0.1	57.6 ± 3.1

8.3.3 Alginate characterisation

Alginate recovered via DES treatment in the precipitate and aqueous phase was characterised by FTIR to assess its functional groups, alongside determination of molecular size and mannuronic to guluronic acid (M/G) ratio and compared to alginate obtained through conventional alkaline extraction. Overall, no substantial structural differences were observed between the different extraction approaches and phases.

The FTIR spectra exhibited characteristic absorption peaks around 1080 cm^{-1} and 1035 cm^{-1}, which are associated with vibrational modes of guluronic and mannuronic acid residues [246, 300], respectively (**Figure 8.4**). Additionally, bands detected near 1600 cm^{-1} and 1400 cm^{-1} correspond to the asymmetric and symmetric stretching

vibrations of the carboxylate (–COO^-) groups [155, 244, 246]. A broad absorption signal in the region of approximately 3200–3500 cm^{-1} was also observed, attributable to hydrogen-bonded O–H stretching vibrations present in alginate [245].

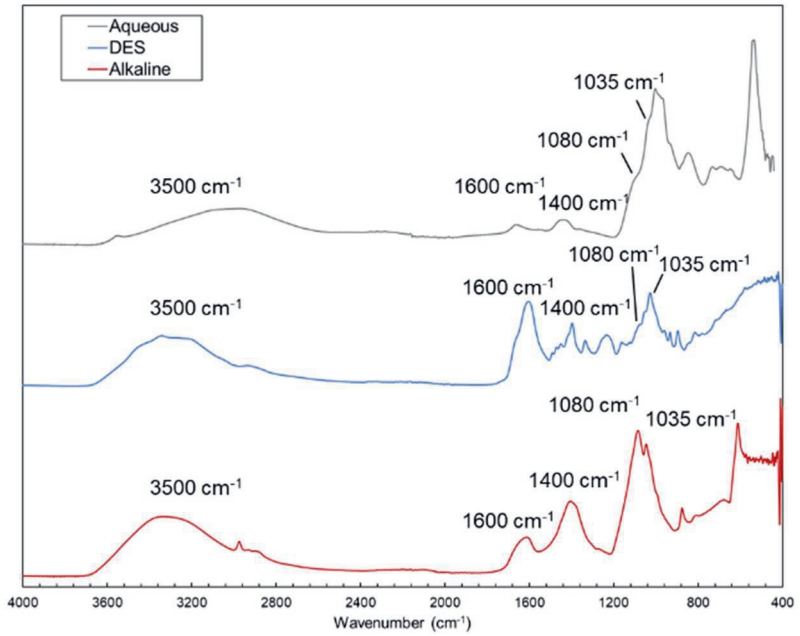


Figure 8.4 FTIR spectra of alginate extracted using DES from both the precipitation and aqueous phases, alongside alginate produced by conventional alkaline processing.

The average molecular weights of alginate recovered with DES and alkaline treatment were 438 ± 93 and 857 ± 158 kDa (**Figure 8.5**), respectively, indicating that DES extraction and recovery resulted in lower average molecular weights than the conventional process. This observation may partly result from limited depolymerisation during DES extraction, as DES have been reported to facilitate hydrolysis and depolymerisation reactions in biomass processing through their catalytic and hydrogen-bonding properties [361, 362]. In addition, the ATPS recovery step itself may introduce a degree of molecular-weight selectivity. Lower-molecular-weight alginate fractions possess greater mobility and diffusivity and may therefore partition or precipitate more readily during phase separation, whereas larger polymer chains may remain more strongly associated with the DES phase through entanglement and hydrogen-bonding interactions. Reported molecular weights for commercial alginate typically range from approximately 60 to 700 kDa [50], depending on the intended application, indicating that both fractions fall within or close to commonly utilised ranges. The molecular weight obtained for DES-extracted alginate is also comparable to values reported for greener citrate-assisted extraction

approaches (508 ± 18 kDa) [363], suggesting that reduced polymer size is not uncommon for milder or alternative extraction strategies.

The mannuronic to guluronic (M/G) ratio is an important parameter in alginate characterisation, as it influences the structural, physicochemical, and functional properties of the polysaccharide [227]. Interestingly, the M/G ratio of the recovered alginate differed between extraction methods, with values of 0.22 ± 0.02 obtained for DES-extracted alginate and 1.50 ± 0.02 for conventionally alkaline-extracted alginate (**Figure 8.5**). The relative content of mannuronic and guluronic acid residues influences the physicochemical properties of alginate. G-rich alginate typically forms stronger and more rigid gels with higher affinity for divalent cations, whereas M-rich alginate results in softer, more elastic gels with increased flexibility and lower gel strength [49, 364]. The lower M/G ratio obtained for DES-extracted alginate compared to alkaline extraction indicates selective enrichment of guluronic acid blocks, suggesting that DES extraction may preferentially recover alginate fractions with enhanced gel-forming properties.

Despite the lower molecular weight of the DES-extracted alginate, the enrichment in guluronic acid residues occurs alongside the reduced chain length, indicating that the DES-salt ATPS recovery for alginate may result in stronger and more rigid gels.

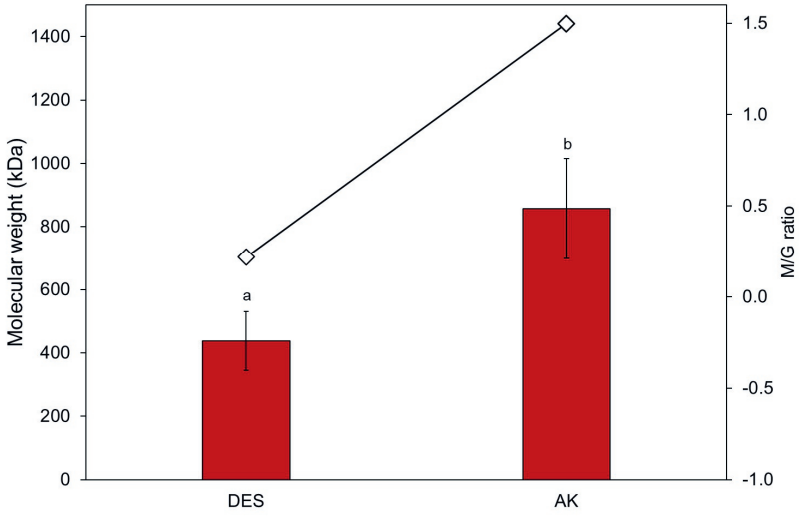


Figure 8.5 Molecular weight and M/G ratios of alginate recovered from DES and alkaline treatment.

8.3.4 Recyclability of recovered DES

The recyclability of the DES was evaluated over six consecutive extraction cycles using the selected DES3–50 wt% K_3PO_4 system (**Figure 8.6**). The overall alginate recovery remained relatively stable throughout the cycles, ranging from 63% (cycle 3) to 86% (cycle 5). Across all runs, 51–65% of the total alginate consistently accumulated in the intermediate precipitation phase.

The absence of a progressive decline in recovery indicates that the DES retained its extraction and phase-forming properties throughout repeated use. Importantly, the absence of a systematic increase or decrease in recovery suggests that the observed cycle-to-cycle fluctuations are unlikely to originate from cumulative changes in DES composition or gradual solvent degradation. Instead, the fluctuations most likely reflect the stochastic nature of the interfacial precipitation process itself. Alginate recovery in the DES–salt system relies on the formation of a transient polymer-rich layer at the interface between the DES-rich and salt-rich phases. This aligns with phase-separation models of alginate where high ionic strengths trigger rapid localised nucleation followed by aggregate growth that depletes the surrounding polymer concentration. Because these micro-separated domains are structurally pinned by local gelation, slight variations in local mixing and diffusion profiles could heavily impact the final macroscopic distribution of the polymer [365]. The exact distribution of alginate between the intermediate layer and the adjacent phases is thus governed by local nucleation, aggregate growth, interfacial transport, and phase disengagement [365], all of which depend on local concentration gradients and mixing conditions during phase separation. Consequently, relatively small differences in the formation and evolution of the interfacial layer may lead to variations in alginate partitioning between cycles without affecting the overall recovery mechanism or solvent functionality. Minor differences in residual alginate remaining in the recycled DES may additionally influence local viscosity and mass-transfer behaviour, contributing to these stochastic variations while remaining insufficient to produce a cumulative decline in performance.

The maintained formation of a distinct intermediate layer throughout all recycling cycles suggests that the DES consistently preserved the phase behaviour required for interfacial alginate precipitation and that no major alterations of the DES hydrogen-bond network occurred despite repeated exposure to high ionic strength conditions. To further assess solvent stability, the DES prior to extraction, after alginate extraction, and after ATPS separation was analysed by FTIR spectroscopy (**Figure S8.6**). While FTIR alone cannot provide definitive evidence of complete structural retention, the absence of clear spectral changes suggests that no major alterations of the dominant hydrogen-

bonding interactions occurred during recycling. This indicates that the DES framework remains largely preserved under repeated exposure to high ionic strength conditions. Together with the absence of any systematic deterioration in recovery performance, these observations support the conclusion that the DES retained its functional stability during repeated recycling. Moreover, the higher calculated capacity of the salt phase relative to the DES implies preferential alginate partitioning into the salt-rich environment, limiting solute accumulation within the DES and thereby supporting stable solvent recyclability.

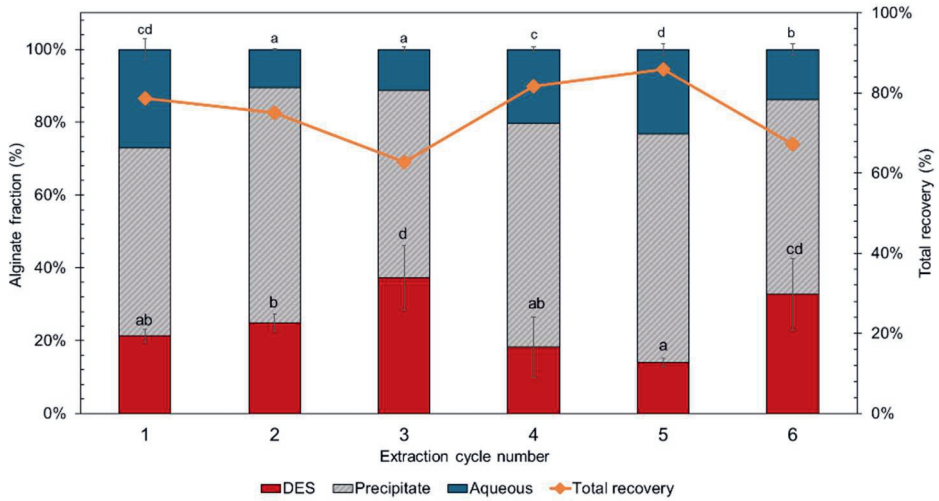


Figure 8.6 Alginate distribution (%) in the DES, aqueous and precipitate phases and overall recovery yield after ATPS formation for recycling the DES six times.

Previous studies on DES recycling within three-phase partitioning systems have reported similarly stable recovery trends over multiple cycles. For example, Chen *et al*. [222] observed only a slight decrease in tomato peroxidase recovery after five recycling cycles of the DES, while Hu *et al*. [237] reported largely stable product recovery values over five consecutive cycles during DES-based TPP. Comparable stability has also been reported for DES recycling in ATPS. For instance, in a temperature-responsive copolymer-based ATPS [335], alginate recovery remained stable between 55–65% over repeated cycles. Similarly, Wang *et al*. [366] observed relatively constant recoveries (~65%) after five recycling cycles of a ChCl:urea–K_2HPO_4 ATPS for C-phycocyanin extraction.

Taken together, the present results demonstrate that DES recyclability within high-salt ATPS is comparable to both TPP and alternative ATPS systems. Notably, the current approach enables direct product recovery via formation of a separable intermediate phase, thereby avoiding additional processing steps such as dialysis that are often

required in conventional ATPS. This feature enhances process simplicity and supports the practical applicability of the system.

From a sustainability perspective, it is important to note that the process relies on relatively high concentrations of potassium phosphate (up to 50 wt%), which may introduce constraints in terms of salt consumption, downstream handling, and potential waste generation if full recycling of the salt phase is not implemented. While K_3PO_4 is generally recognised as safe (GRAS) and widely used in food-related applications, its recovery and reuse were not experimentally demonstrated in this study and therefore remain an important consideration for future process development.

Scaling up the DES-based ATPS process may present several challenges, particularly related to the relatively high viscosity of DES, which can limit mass transfer and complicate mixing and phase disengagement at larger scale. In addition, the high salt concentrations may influence process economics and require integration of salt recovery strategies to ensure long-term sustainability. Nevertheless, process optimisation strategies, such as improved mixing configurations or continuous operation, could help to mitigate mass transfer limitations and enhance scalability. Overall, while further work is required to address salt recycling and full process integration, the demonstrated coupling of extraction, separation, and solvent reuse provides a promising foundation for sustainable DES-based biorefinery developments.

8.4. Conclusion

In this study, a novel DES–salt aqueous two-phase system (ATPS) was developed for the integrated extraction and separation of alginate, providing a more sustainable and circular alternative to conventional alkaline extraction processes. By incorporating the precipitation principle of three-phase partitioning at elevated salt concentrations into the ATPS, efficient alginate recovery was achieved via the formation of an intermediate precipitation phase between the DES and the aqueous salt phase. This approach enabled direct alginate isolation while preserving the integrity of the DES for subsequent reuse. The results demonstrated that salt selection significantly influenced phase formation, with K_3PO_4 exhibiting stronger phase-forming ability than K_2HPO_4 due to the higher charge density of the phosphate anion and its enhanced salting-out effect. In contrast, alginate recovery was primarily governed by salt concentration rather than salt type. Among the systems investigated, Betaine: urea (1:2) (DES3) combined with 50 wt% K_3PO_4 achieved the highest total alginate recovery (76.4 ± 0.1%), with the majority (65.7 ± 9.7%) accumulating in the intermediate phase. Furthermore, the DES demonstrated good recyclability, maintaining relatively stable alginate recovery yields over six cycles (63–86%). Structural characterisation confirmed the preservation of alginate functional groups indicating retention of polymer integrity. Overall, these findings emphasise the potential of DES-based ATPS as an effective platform for simultaneous extraction, separation, and solvent recycling, advancing the development of more sustainable and integrated seaweed biorefinery processes.

8.5. Supplementary information

Alginate is a linear copolymer consisting of β-D-mannuronic acid (M) and α-L-guluronic acid (G) units linked via β-(1→4) glycosidic bonds. The proportion and sequence distribution of these monomers vary depending on the seaweed species and are influenced by seasonal and environmental conditions.

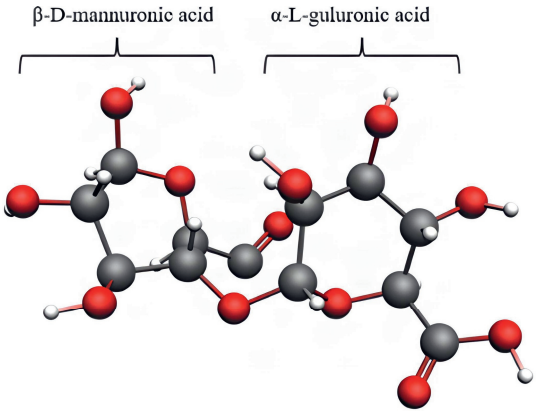


Figure S8.1 Chemical structure of part of alginate, represented by linked β-D-mannuronic acid and α-L-guluronic acid monomers.

Two DES were used (DES2, choline chloride: urea and DES3, betaine: urea) for alginate extraction. The extracts were subsequently applied for alginate recovery within an ATPS.

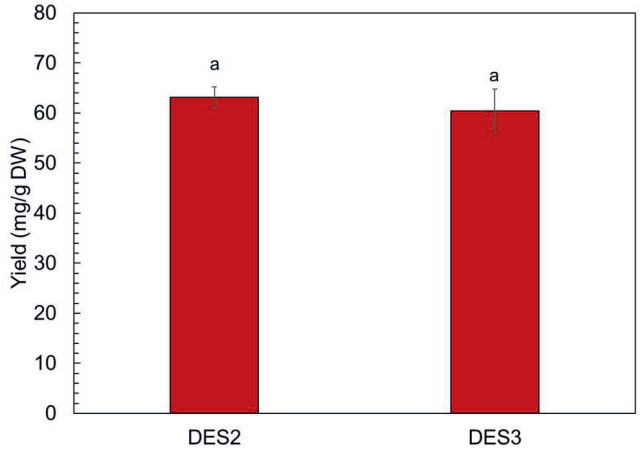


Figure S8.2 Alginate extraction from *L. digitata* with DES2 and DES3.

ATPS formation was assessed for the DES extracts of DES2 and DES3, combined with the two aqueous salt solutions consisting of different concentrations of K_2HPO_4 and K_3PO_4. From these systems, the alginate recovery yield was determined.

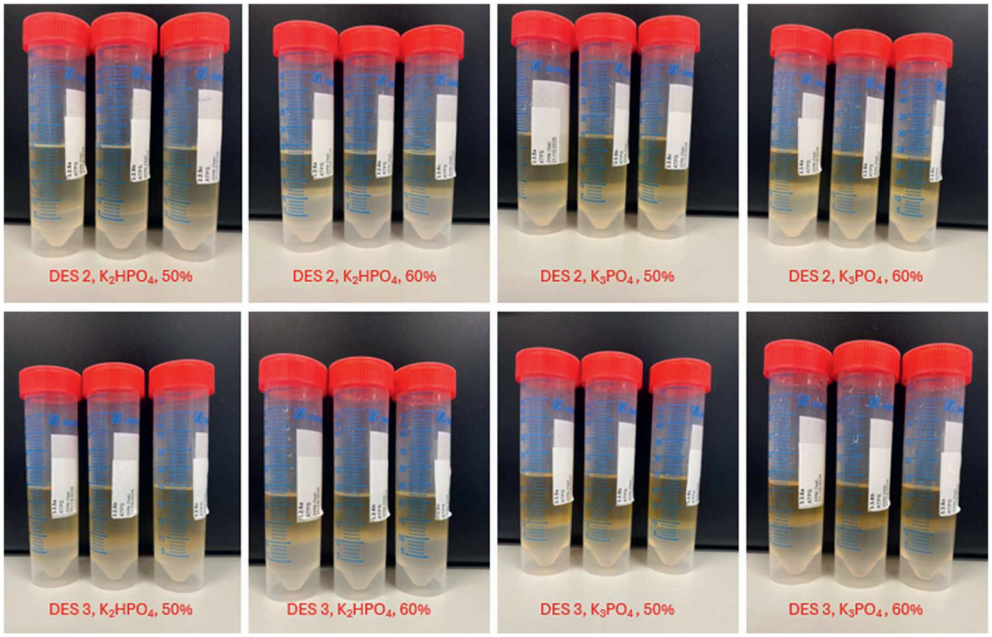


Figure S8.3 ATPS formation with DES extracts (DES2 and DES3) combined with 50 and 60 wt% of K_2HPO_4 and K_3PO_4.

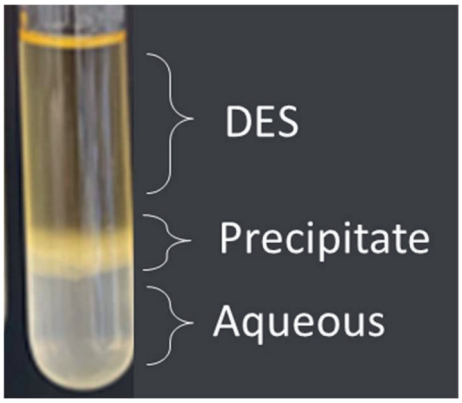


Figure S8.4 Phase separation and alginate precipitation in the DES–salt aqueous two-phase system (ATPS) formed by mixing DES3 extract with 50 wt% K_3PO_4 solution. A distinct intermediate, alginate-rich phase is observed between the upper DES phase and the lower salt-rich aqueous phase.

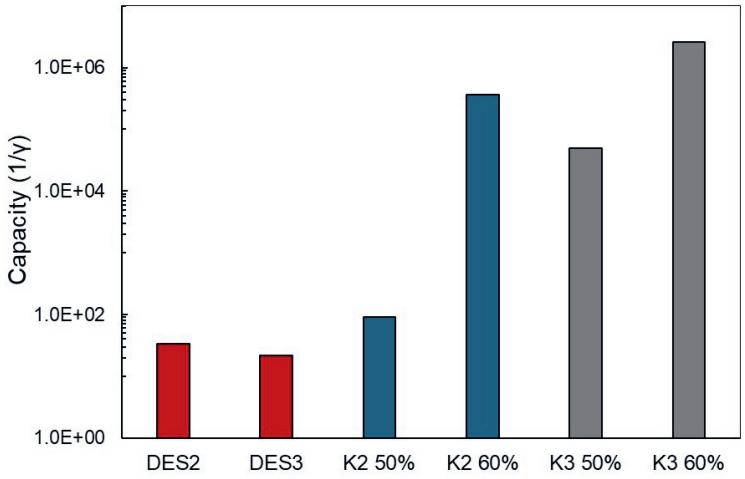


Figure S8.5 Calculated capacity values of DES2 (Choline chloride: urea), DES3 (Betaine: urea), and 50% K_2HPO_4 (K2 50%), 60% K_2HPO_4 (K2 60%), 50% K_3PO_4 (K3 50%), and 60% K_3PO_4 (K3 60%) salt solutions towards alginate.

To evaluate solvent stability, the DES was analysed by FTIR spectroscopy prior to extraction, after alginate extraction, and after ATPS separation. No significant spectral changes were observed between the samples, indicating that the DES structure was largely preserved throughout the extraction and recycling process.

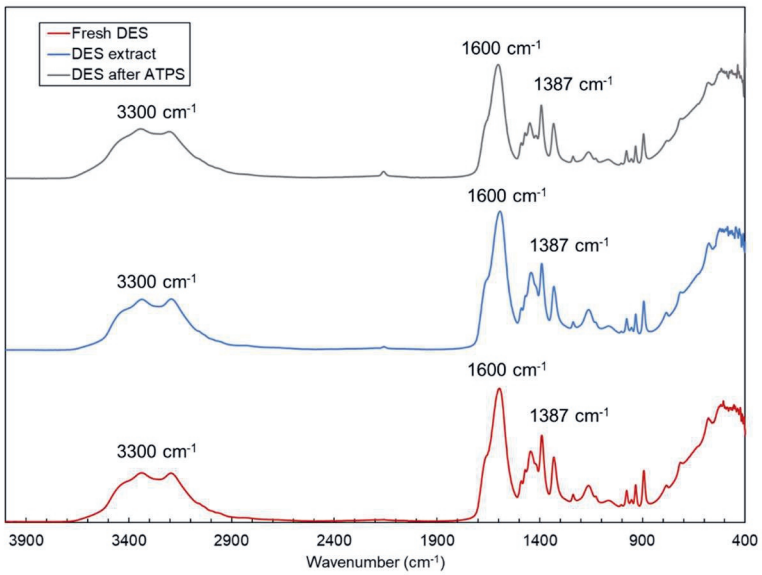
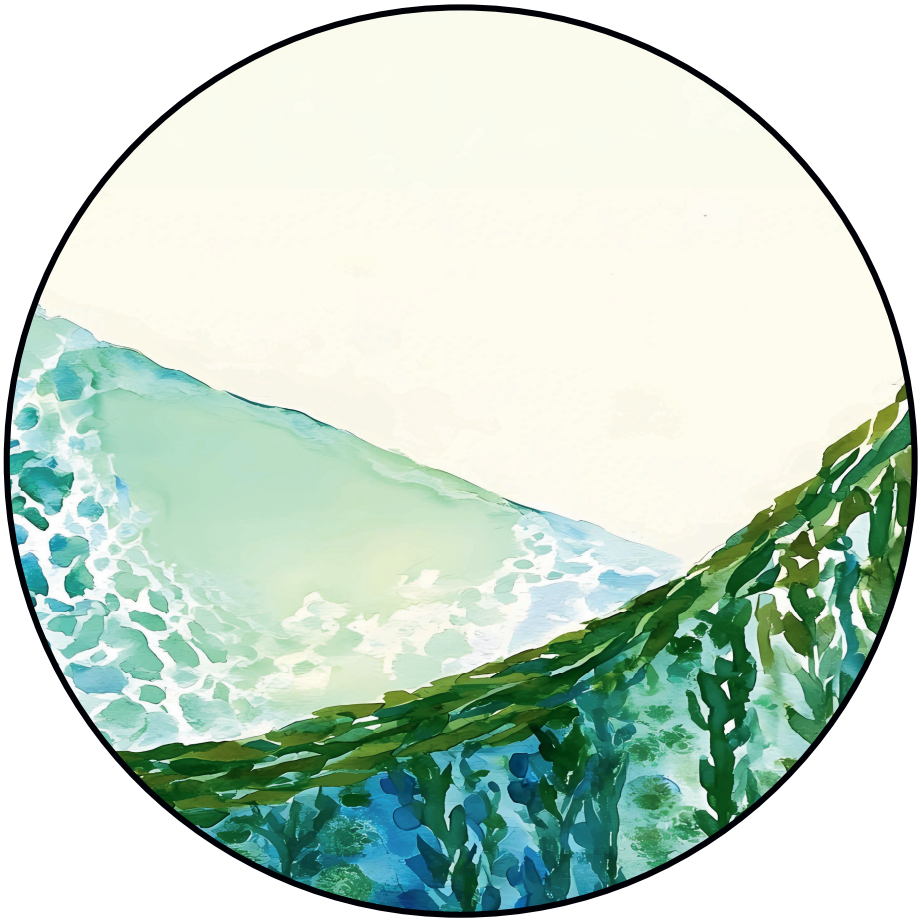


Figure S8.6 FTIR spectra of fresh DES (red), DES extract (blue) and DES after ATPS formation.



Chapter 9

Disruption or partitioning? Deep eutectic solvent biphasic systems for integrated seaweed biorefineries

Isa S.A. Hiemstra[∞], Wimar Reynaga-Navarro[∞], Rene H. Wijffels, Michel H.M. Eppink, Antoinette Kazbar

[∞] Authors contributed equally

This chapter has been published as:

Hiemstra, I. S. A., Reynaga-Navarro, W., Wijffels, R. H., Eppink, M. H., Kazbar, A. (2026) Disruption or partitioning? Deep eutectic solvent biphasic systems for integrated seaweed biorefineries. *Bioresources And Bioprocessing*, *13*(1). https://doi.org/10.1186/s40643-026-01139-9

Abstract

In this study, a DES-based biphasic system (FABU) was evaluated for the multiproduct extraction of compounds from *Saccharina latissima*. The system combined a hydrophobic fatty-acid phase (dodecanoic acid–octanoic acid, FA) for fucoxanthin extraction with a hydrophilic betaine-urea-phase (BU) for alginate recovery, together with citric acid pretreatment for fucoidan and mannitol recovery. While fucoxanthin partitioning into the FA phase was limited (41–58 µg/g), a substantially higher fucoxanthin concentration (563 ± 8 µg/g) was recovered during the subsequent alkaline extraction step. This behaviour indicates that the DES-based system likely acts as a medium that enhances biomass permeability than directly promoting partitioning. Chromatographic profiles further showed enhanced fucoxanthin preservation relative to conventional pigment extraction, suggesting a protective role of the DES matrix. These findings highlight a decoupling between biomass disruption and solubilisation in DES-based systems. Our research shows new opportunities to deploy biphasic DES systems as powerful pretreatment platforms within integrated seaweed biorefineries, thereby offering a new strategy for preserving and recovering sensitive compounds in integrated seaweed biorefineries.

9.1. Introduction

Conventional extraction processes often rely on volatile organic solvents and energy-intensive operations, limiting sustainability [176]. Deep eutectic solvents (DES) have emerged as a versatile and potentially sustainable alternative to conventional solvents [340, 367, 368]. Formed by a combination of hydrogen bond acceptors (HBA) and hydrogen bond donors (HBD), DES exhibit a depressed melting point and tuneable physicochemical properties. Owing to their adjustable polarity, hydrogen-bonding capacity, and compositional flexibility, DES are promising media for selective extraction and biomass fractionation [9, 10]. In recent years, DES have been successfully applied to various biomasses, including plant materials, microalgae, and seaweed, demonstrating enhanced recovery of various compounds [48, 100, 128, 311, 369].

Brown seaweeds represent an attractive feedstock for integrated biorefinery concepts due to their diverse chemical composition, including the polysaccharide alginate. Alginate confers unique gelling, viscosity, and chelation properties [50, 331]. In addition to alginate, brown seaweeds are also rich in other carbohydrates such as fucoidan and mannitol. Fucoidan, a sulphated polysaccharide present together with alginate in the cell wall matrix, possess reported anti-inflammatory, anticancer, antiviral, among other bioactive properties [370, 371]. On the other hand, mannitol, a sugar alcohol is widely used as a low-calorie sweetener and platform molecule in food and chemical industries [55]. In addition, a high-value pigment is present in brown seaweed; fucoxanthin (**Figure S9.1**). This carotenoid, belonging to the xanthophylls, possesses reported antioxidant and bioactive properties, making it a promising compound for nutraceutical and functional food applications [372, 373].

Despite the presence of various compounds, current industrial processing strategies remain largely focused on alginate as the primary target product, often relying on harsh alkaline and acid treatments. These conventional approaches involve high chemical consumption and energy input, limiting overall biomass valorisation and underutilising the potential of other valuable components [56, 331]. Furthermore, the complex and recalcitrant structure of seaweed biomass presents a significant barrier to efficient disruption and access to intracellular compounds [128, 374]. This limited accessibility further constrains the recovery of valuable components and often needs intensive processing conditions.

As an alternative, DES have been shown to act as effective pretreatment agents, promoting biomass disruption and enhancing the accessibility of target compounds [148, 375, 376]. In brown seaweed processing, hydrophilic DES have been shown by

our group to enable efficient alginate extraction [100] and to modify product functionality, yielding alginates with significantly higher viscosities than those obtained by conventional methods [48]. Beyond polysaccharides, hydrophobic DES showed effective extraction of non-polar bioactive compounds, while simultaneously promoting cellular disruption and facilitating polysaccharide release [342].

Building on this work, the present study represents the next step in a broader research line on DES-based seaweed biorefineries. It integrates these previously developed technologies into a single, sequential, multiproduct biorefinery process for the simultaneous recovery of multiple seaweed products, thereby potentially intensifying the process.

Our previous findings highlight that DES can go beyond their role as alternative solvents, serving instead as functional media that enable integrated, multiproduct extraction strategies. While single-phase DES systems have primarily been developed for the recovery of individual product streams, the complementary properties of hydrophobic DES for pigment recovery and potential membrane disintegration, and hydrophilic DES for cell wall disruption and the selective extraction of high-viscous alginate, suggest the feasibility of a unified, biphasic approach. By combining these two phases, alginate and fucoxanthin could be selectively partitioned within the same process, while a preceding aqueous pretreatment enables the recovery of the readily water soluble fucoidan and mannitol. Such a biphasic system exemplifies process integration and intensification by combining extraction and selective partitioning within a single workflow, thereby reducing the need for separate extraction processes and advancing toward full biomass valorisation in an integrated seaweed biorefinery.

Although promising, biphasic DES systems for multiproduct seaweed fractionation remain largely unexplored. Critical aspects such as phase interactions, extraction parameters, and component partitioning behaviour are not yet investigated. We hypothesise that the complementary properties of hydrophobic and hydrophilic DES enable selective partitioning of compounds with contrasting polarities, thereby integrating pigment recovery and polysaccharide extraction within a single process.

9.2. Materials and methods

9.2.1 Biomass

Saccharina latissima was harvested in May 2024 from the Brittany region (France) and delivered frozen (-20 °C). The biomass was subsequently oven-dried for 72 h in an industrial oven (Marius Engineering, Netherlands) without light exposure. The dried material was milled using a Retsch® SM300 mill fitted with a 1 mm sieve and stored at 4 °C until further use.

9.2.2 Biomass characterisation

Alginate, fucose, mannitol, and fucoxanthin contents were determined in the dried *S. latissima biomass* (93.6% dry weight). Alginate was quantified by methanolysis of the dried biomass [48], followed by analysis using ion-exchange chromatography (**Section 9.2.3.2**). Fucose and mannitol were determined after trifluoroacetic acid (TFA) hydrolysis of 2 mg of dried biomass and subsequent ion-exchange chromatography analysis. Fucoxanthin was quantified by extraction with methanol containing 10% water v/v at 25 °C for 2 h using a SLR ratio of 0.05 g/mL [216]. Alginate, fucose, and mannitol contents were 296 ± 10, 10 ± 1, and 73 ± 3 mg/g DW, respectively, while the conventional methanolic extraction recovered 338 ± 65 µg/g DW of fucoxanthin.

9.2.3 DES preparation

DES were prepared by mixing the compounds (HBA and HBD) in their corresponding molar ratio in a water bath at 60°C until a clear liquid was formed (**Table 9.1**). Water was added to the hydrophilic DES to reach the desired water content.

Table 9.1 DES composition and characteristics

DES nature	HBA	HBA	Ratio	Water%	Abbreviation
Hydrophobic	Dodecanoic acid	Octanoic acid	1:1	-	FA
Hydrophilic	Betaine	Urea	1:2	25, 45 and 65%	BU

9.2.4 Analytical methods and yields

9.2.4.1 Alginate quantification

Alginate extracts (1 mL) were mixed with 2 mL of ethanol-water mixture 80% v/v with 1% NaCl w/v for alginate precipitation. The samples were centrifuged at 4255 *g* for 10 min at RT (from now on these conditions will remain unless stated otherwise), the

supernatant discarded and the pellet washed with 1 mL of ethanol-water mixture 80% v/v. The samples were centrifuged, the supernatant discarded and the pellets were dried with a gentle stream of nitrogen. The dried crude alginate pellet was dissolved in milli-Q water for analysis.

The alginate concentration was determined via the colorimetric method described by Cesaretti *et al.* (2003) [136]. The extraction yield Y_{alg} (mg/g) express as dry basis is determined as follows (**Equation 9.1**):

$$Y_{alg} = \frac{C_{UA} \cdot V \cdot 0.907}{W_{sw} \cdot x_{dw}} \quad (\mathbf{9.1})$$

Where C_{UA} is the concentration of uronic acids (mg/mL), V is the volume of the sample (mL), W_{sw} is the amount of seaweed (g) and x_{DW}, and 0.907 is the correction factor to convert the concentration of uronic acids into alginate. D-galacturonic acid (≥97 % purity, Sigma-Aldrich) was used as a standard.

9.2.4.2 Ion exchange chromatography for fucose and mannitol

For fucoidan analysis, an aliquot of 1 mL of extract was mixed with 2 mL of pure ethanol and let overnight at 4 °C. Then, the mixture was centrifuged, the supernatant discarded and the pellet washed with 1 mL of ethanol 80% v/v. Finally, the pellet was dried with a stream of nitrogen. The dried pellet was then hydrolysed with 1 mL of Trifluoracetic acid (TFA) 2 M for 90 min at 120 °C, cooled down and later the TFA was evaporated with a nitrogen stream. The dried sample is then dissolved in milli-Q water, filtered and 10 µL injected into a Dionex ICS-6000 HPIC System (Thermo Fisher Scientific™) at 30 °C in a flow rate of 0.5 mL min^{-1} through a Dionex Carbopac™ PA20 (3 × 150 mm) column from ThermoFisher Scientific™ using 100 mM NaOH (A), 500 mM NaOH (B), 500 mM sodium acetate + 50 mM NaOH (C) and Milli-Q water (D) as eluents, following a protocol described previously [48]. Fucose content was used as a proxy of the fucoidan content. For mannitol determination, the extract was filtered and 10 µL were injected into ion exchange chromatographer as described previously in this section. Fucose (≥99 %, Supelco) and mannitol (≥99.9%, Supelco) were used as standards. Yields (Y_s) were expressed as follows (**Equation 9.2**):

$$Y_s = \frac{C_S \cdot V}{W_{sw} \cdot x_{dw}} \quad (\mathbf{9.2})$$

Where C_s is the monomer concentration (either fucose or mannitol), V is the volume of the sample, W_{sw} is the weight used for the extraction and x_{dw} is the fraction of dry weight.

9.2.4.3 Fucoxanthin determination

The fucoxanthin concentration was determined by ultra-high-performance liquid chromatography with diode array detection (UHPLC-DAD) using a Shimadzu Nexera X2 system (Kyoto, Japan). Samples (20 µL) were injected into a Kinetex® C18 column (5 µm, 100 Å, 150 × 4.6 mm; Phenomenex®) at a flow rate of 1 mL/min. The mobile phases consisted of (A) 0.5 M ammonium acetate in methanol:Milli-Q water (85:15, v/v), (B) 90% aqueous acetonitrile, and (C) 100% ethyl acetate. The total run time was 53 min, following the gradient programme described previously [216]. Acetonitrile, ethyl acetate, and methanol (Lichrosolv®, analytical grade) and ammonium acetate (ultra-pure) used for mobile phase preparation were purchased from Supelco™ and VWR Chemicals™, respectively. All-trans fucoxanthin (≥95% purity, Supelco™) was used as the external standard. The fucoxanthin extraction yield Y_{Fx} (µg/g dry weight) was calculated as follows (**Equation 9.3**):

$$Y_{Fx} = \frac{C_{Fx} \cdot V}{W_{sw} \cdot x_{dw}} \quad (\mathbf{9.3})$$

Where C_{Fx}, is the concentration of fucoxanthin in the sample, V is the volume of the sample W_{sw} is the weight used in the extraction and x_{dw} is the dry weight of the sample.

9.2.5 Acid-alkaline extraction as control

The seaweed biomass was mixed with a 0.2 M H_2SO_4 solution at a SLR of 1:60 (g /mL) and pretreated for 1 h at room temperature under constant mixing. The mixture was subsequently neutralised using a 3.25% (w/w) sodium carbonate solution until reaching pH 10-11 and then incubated at 55 °C for 1 h to promote alginate extraction. Later, the mixture was cooled to room temperature and centrifuged, and the supernatant was collected for alginate analysis.

9.2.6 Preliminary test of biphasic system

To evaluate the technical feasibility of the biphasic system forming, mixing tests of FA DES with BU DES (from now on FABU) in weight ratios of 1:2, with different concentrations of water (25, 45, 65%). Mixtures were centrifuged and the biphasic system formation was evaluated visually.

9.2.7 Biphasic extraction process

Later, alginate extractions were performed. Dry seaweed was mixed with FABU in a SLR of 1:60 w/w. Extraction was performed at 35°C for 1 h with constant agitation. Then, the mix was centrifuged (4255 *g* for 10 min). Subsequently, the phases were separated, and the BU phase was collected for alginate quantification.

This integrated biphasic extraction system was directly adapted from the platforms previously developed and validated. The hydrophilic phase configurations for high-viscosity alginate extraction and the hydrophobic phase configurations for pigment recovery are summarized in **Table 9.2**.

Table 9.2 Biphasic system DES phases based used.

DES phase	Components	Target compound	Reference
Hydrophilic	Betaine: urea (1:2)	High-viscosity alginate	[48]
Hydrophobic	Dodecanoic acid: octanoic acid (1:1)	Fucoxanthin	[342]

9.2.8 Pretreatment evaluation in combination with the biphasic system

Pretreatments were evaluated in combination with the biphasic extraction process (**Figure 9.1**). These pretreatments also enabled the recovery of water-soluble compounds. Two pretreatment conditions were tested: (i) extraction with water at 35 °C for 1 h and (ii) extraction with a 50 mM citric acid solution at 35 °C for 1 h [377]. After each pretreatment, the mixture was centrifuged and the supernatant collected for the analysis of fucose and mannitol. The resulting wet pellet was then mixed with the biphasic extraction system while maintaining a SLR of 1:60, and the extraction was performed at 35 °C for 1 h. Following centrifugation, the fatty acid phase and the betaine-urea phase were collected and analysed for fucoxanthin and alginate, respectively.

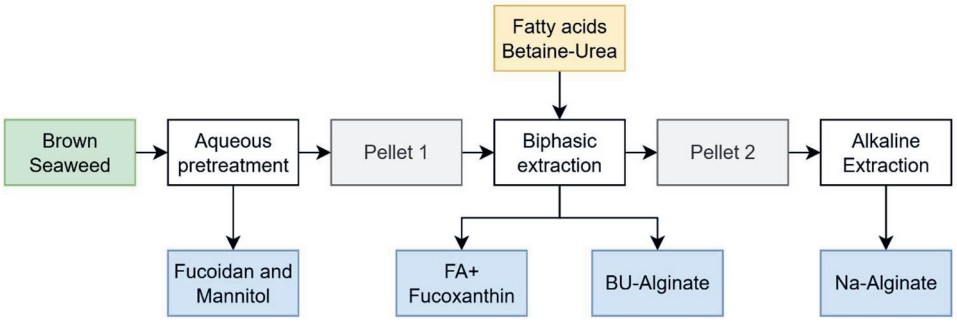


Figure 9.1 Flowchart of the experimental design combining the pretreatment and the biphasic system.

The remaining pellet was subsequently mixed with water and sodium carbonate to reach a final Na_2CO_3 concentration of 0.1 M (pH 10-11), adjusting the volume to maintain the original SLR. Alkaline extraction was then performed at 55 °C for 1 h. The

mixture was centrifuged and the supernatant collected for alginate analysis. All extractions were performed under light protected conditions.

9.2.9 Fucoxanthin recovery from the alkaline extract after the biphasic system

The alginate extract obtained after the alkaline step from the biphasic system pellet was subjected to liquid–liquid extraction with ethyl acetate at a volumetric ratio of 1:1. The mixture was vortexed and subsequently centrifuged at 21,000 *g* for 5 min at 4 °C. After phase separation, the upper organic phase was collected, diluted with methanol, and analysed by chromatography (see **Section 9.2.3.3**).

9.2.10 COSMO-RS analysis

The COSMO-RS (Conductor-like Screening Model for Real Solvents) approach was employed to predict the thermodynamic behaviour of the studied DES systems for fucoxanthin partitioning [93]. All calculations were carried out using COSMO-RS version 2022.103 (Software for Chemistry and Materials BV, Amsterdam, The Netherlands), implemented within the Amsterdam Density Functional (ADF) framework. Prior to COSMO-RS analysis, molecular structures were geometry-optimised using the universal force field (UFF), followed by density functional theory (DFT) calculations at the GGA:BP86 level with a TZP basis set [378].

Using COSMO-RS, the activity coefficient of alginate at infinite dilution was calculated according to **Equation 9.4** and **9.5**:

$$\ln(\gamma_i^{\infty}) = \frac{\mu_s^i - \mu_i^i}{RT} \quad (\mathbf{9.4})$$

$$\gamma_i^{\infty} = limit_{xi \to 0} \gamma_i \quad (\mathbf{9.5})$$

where γ_i^{∞} represents the activity coefficient of fucoxanthin (i) at infinite dilution, defined as the limiting value of the activity coefficient as the solute concentration approaches zero [378]. It is determined based on the chemical potential of the solvent μ_s and the chemical potential of the pure compound μ_i [65, 318].

With the activity coefficient, the solubility capacity (C_i^{∞}) of the DES was calculated to determine the maximum amount of solute that can be dissolved in the DES, following **Equation 9.6** [93]:

$$C_i^{\infty} = 1/\gamma_i^{\infty} \quad (\mathbf{9.6})$$

The partition coefficient was calculated to assess the distribution of the solute between the two phases [378] providing insights into the partitioning behaviour during the biphasic extraction. The partition coefficient (K) was calculated using **Equation 9.7**:

$$K_{FA/BU} = \frac{\frac{1}{\gamma_i^{\infty}(FA)}}{\frac{1}{\gamma_i^{\infty}(BU)}} \quad (\mathbf{9.7})$$

9.2.11 Statistical analysis

One-way ANOVA was performed to compare the experimental groups. When significant differences were detected ($p < 0.05$), Tukey's post hoc test was applied to determine pairwise differences between groups.

9.3. Results and discussion

9.3.1 Aqueous seaweed pretreatment

Water-soluble compounds, including fucoidan and mannitol, are readily extracted under aqueous conditions. Moreover, mild acidic conditions enhance fucoidan extraction and promote the conversion of alginate to alginic acid, facilitating its subsequent recovery [56, 377]. Therefore, two biomass pretreatments were evaluated: a water extraction and a citric acid-assisted extraction [377]. The two treatments were used to assess their potential influence on the subsequent DES extraction. To maintain mild conditions, citric acid was applied at 50 mM, at a relatively low temperature (35 °C) for 1 h under light-protected conditions. Fucose (as a proxy for fucoidan) and mannitol were quantified (**Figure 9.2**).

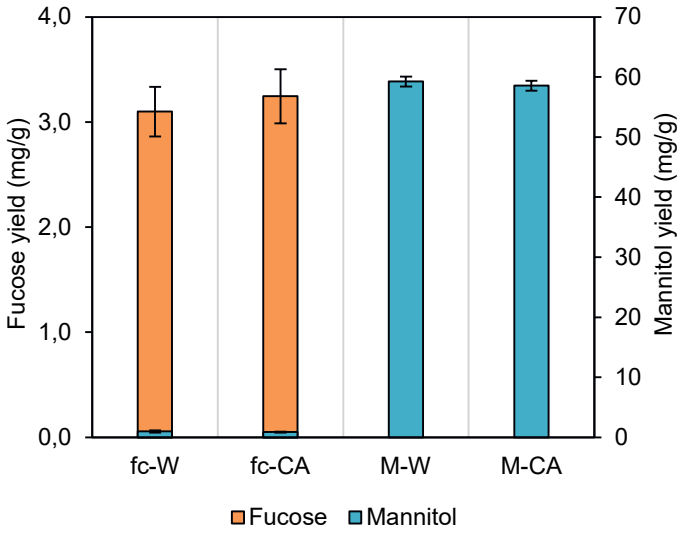


Figure 9.2 Fucose (fc) and mannitol (M) extraction yields from the aqueous (W) and citric acid pretreatments (CA).

The extraction yields of both compounds were not significantly affected by the type of pretreatment. Mannitol yields ranged from 58.5 to 59.3 mg/g for water and citric acid pretreatments, respectively, while fucose yields were 3.1 and 3.2 mg/g under the same conditions. This outcome was expected for mannitol, as a low-molecular-weight polyol predominantly located in the cytoplasm (and partly in vacuoles), which enables rapid and efficient diffusion under aqueous conditions [379]. The mannitol detected in the fucoidan extract (1.0 ± 0.2 and 0.9 ± 0.1 mg/g for water and citric acid pretreatments, respectively) likely originates from the co-extraction of water-soluble laminarin alongside fucoidan [380].

In contrast, a higher fucoidan extraction was anticipated for the citric acid pretreatment [377]. However, no significant differences were observed between treatments. This may be attributed to the relatively mild conditions employed, particularly the low temperature, which could limit acid-assisted cell wall disruption and polysaccharide solubilisation. Moreover, higher citric acid concentrations (3% or ~ 156 mM) have been reported to enhance the sequential extraction of fucoidan and alginate [377]. Notably, the impact of such conditions on subsequent fucoxanthin extraction was not addressed in the cited study.

Following evaluation of the pretreatment step, the subsequent extraction performance of the DES-based biphasic system was assessed by investigating fucoxanthin affinity toward the FA phase and its partitioning behaviour using COSMO-RS.

9.3.2 Predicting fucoxanthin partitioning in the biphasic system

To analyse fucoxanthin affinity towards the FA phase and gain mechanistic insight into fucoxanthin partitioning in the biphasic system, COSMO-RS calculations were performed to evaluate its affinity towards the individual solvent phases (**Table 9.3**). COSMO-RS analysis showed low affinity of fucoxanthin for the BU phase (capacity of $9.7 \cdot 10^{-6}$), which further decreased with increasing water content (from $2.1 \cdot 10^{-8}$ to $3.3 \cdot 10^{-11}$ for 25 to 65%, respectively), consistent with the predominantly hydrophobic structure of fucoxanthin (**Figure S9.1**).

In contrast, high affinity for the fatty-acid-based DES was observed (capacity of $2.1 \cdot 10^{3}$), suggesting partial partitioning into this solvent phase. Within the FABU biphasic system, the substantially higher capacity of the fatty-acid DES compared to the BU phase indicates preferential partitioning of fucoxanthin into the fatty-acid phase, further supported by the partition coefficient ($K = 3.8 \cdot 10^{12}$ for FA-BU45 system). Based on this predicted preferential partitioning behaviour, the subsequent step was to evaluate whether the FA and BU DES could be effectively combined to form a stable biphasic extraction system.

Table 9.3 Calculated capacities and partitioning of fucoxanthin in the different DES systems.

	Capacity ($1/\gamma_i^{\infty}$)	$K_{FA/BU}$
BU	$9.7 \cdot 10^{-6}$	$2.2 \cdot 10^{8}$
BU25	$2.1 \cdot 10^{-8}$	$1.0 \cdot 10^{11}$
BU45	$5.5 \cdot 10^{-10}$	$3.8 \cdot 10^{12}$
BU65	$3.2 \cdot 10^{-11}$	$6.5 \cdot 10^{13}$
Dodec:Oct	$2.1 \cdot 10^{3}$	-

9.3.3 FABU system behaviour

9.3.3.1 Feasibility of the biphasic system behaviour

The feasibility of forming a biphasic system was evaluated by combining betaine-urea (BU) DES at different water contents with the fatty acid (FA) DES. After centrifugation, phase separation was observed in all cases (**Figure 9.3**). Despite the clear phase division, only the systems containing BU+45 and BU+65 remained fully liquid, whereas the hydrophilic phase in BU+25 partially solidified. This indicates that a minimum water content is required in the BU phase to maintain its fluidity under the tested conditions.

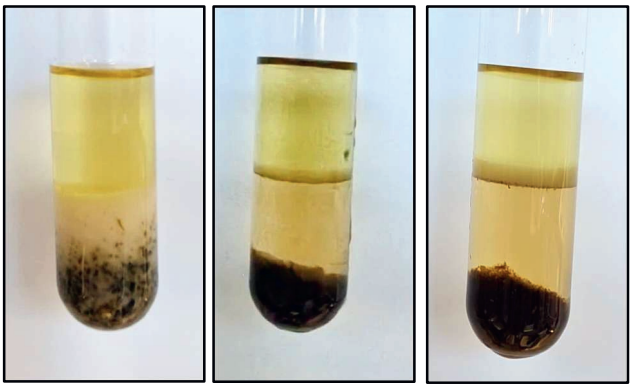


Figure 9.3 Biphasic systems at increasing water contents (from left to right): 25, 45, and 65% w/w.

The presence of a minimum water content is attributed to the role of water as a structural disruptor and plasticiser of the betaine-urea hydrogen-bond network; below a critical hydration level, the system becomes over-structured and prone to crystallisation [34, 381], an effect very likely further exacerbated by phase interaction with hydrophobic fatty acid DES. In previous research, the water content used for DES preparation was 15% (w/w), which increased to approximately 25% (w/w) after accounting for the intrinsic water content of the seaweed [48]. Under these conditions, the water level was sufficient to prevent DES crystallisation.

In contrast, the crystallisation of the BU phase observed at lower water contents upon mixing with the fatty acid DES may be attributed to competitive interactions between fatty acids and the betaine-urea hydrogen-bonding network. The carboxylic groups of the fatty acids can form hydrogen bonds with both urea and the carboxylate moiety of the zwitterionic betaine, partially disrupting the native DES network. Similar interactions have been reported in betaine-based DES systems used for free palmitic acid removal from oil, highlighting the affinity between fatty acids and the solvent

components [382]. Additionally, water may also interact with the fatty acid DES phase, reducing the amount of water available to stabilise the BU DES [383]. This redistribution of hydrogen-bonding interactions weakens the structural integrity of the betaine-urea network, lowering its capacity to remain in a liquid state and promoting crystallisation under insufficient hydration conditions.

While the formation of two distinct phases confirms the technical feasibility of the FABU system as a biphasic medium, it does not necessarily ensure effective extraction or selective partitioning. Therefore, product extraction and quantification are required to evaluate the performance of the FABU system.

9.3.3.2 FABU extraction performance

The extraction performance of the biphasic system (using BU+45) was evaluated in combination with the pretreatments described in **Section 9.3.1**. Two alginate fractions were obtained: (i) a fraction recovered from the hydrophilic phase of the biphasic system (BU DES), and (ii) a fraction extracted under alkaline conditions from the residual pellet after phase separation (**Section 9.2.7**). Furthermore, the fucoxanthin content was measured in the hydrophobic phase (**Figure 9.4**).

The observed trends of alginate yield are consistent with previous reports using BU DES [48], where the alginate recovered in the BU phase is lower than that obtained after alkaline extraction in all cases. Notably, both BU-extracted alginate and post-alkaline alginate (Na-Alg) yields were higher when citric acid pretreatment was applied. This behaviour aligns with studies employing citric acid as a pretreatment for fucoidan extraction, where improved alginate recovery has been reported [377]. This effect is likely attributed to the chelation of divalent cations by citric acid [377], promoting the conversion of alginate into its protonated (alginic acid) form. It is likely that in this form, alginate is more susceptible to interact with BU DES and can be more readily solubilised during the subsequent alkaline extraction step.

For alginate characterisation, FTIR analysis of the isolated alginate extracts (BU-alg, Na-Alg and alkaline extract) was performed. The spectra displayed similar characteristic peaks, and all exhibited characteristic absorption peaks around 1080 cm^{-1} and 1020 cm^{-1} (**Figure S9.2**), which are associated with vibrational modes of guluronic and mannuronic acid residues [246, 300], respectively, indicating the likely presence of alginate. Based on the relative intensity and size of the mannuronic acid peak compared to guluronic acid, a higher M/G ratio is anticipated for the recovered polymer. This observation is consistent with our previous characterisation study employing the same betaine:urea DES [48]. Although further characterisation was not

performed in this study, alginate extracted with BU has been characterised on quantitative M/G ratio, average molecular weight and rheological behaviour in previous works [48, 335, 384]. While the introduction of the co-existing FA DES could induce structural deviations, these prior evaluations have been proven to preserve high-viscosity alginate [48].

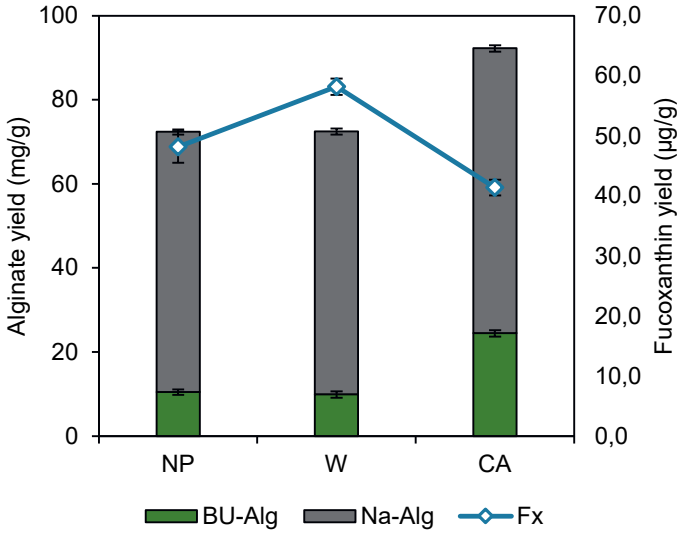


Figure 9.4 Extraction yields of BU-alginate (BU-Alg) (betaine-urea fraction), sodium alginate (Na-Alg) (alkaline extraction), and fucoxanthin (Fx) from the FABU system under different pretreatment conditions: no pretreatment (NP), aqueous (W), and citric acid (CA).

Fucoxanthin extraction yields, on the other hand, were comparable across the three treatments (no pretreatment, water pretreatment, and citric acid pretreatment), ranging from 41.4 to 58.2 µg/g DW after a single extraction cycle (**Figure 9.4**). The slightly lower fucoxanthin yield observed after citric acid pretreatment may be attributed to the acid sensitivity of fucoxanthin, which can undergo degradation or isomerisation at low pH [385, 386], potentially reducing recoverable pigment during subsequent extraction. Although statistically significant differences were observed between treatments ($p < 0.05$), the absolute differences in yield were small, indicating that pretreatment of the biomass had a limited practical impact on fucoxanthin recovery under the conditions applied. Despite the favourable thermodynamic preference of FA predicted by COSMO-RS (**Section 9.3.2**), this did not translate into effective experimental fucoxanthin solubilisation into the FA fraction remained limited, suggesting that kinetic and matrix-related limitations dominated extraction performance.

Fucoxanthin recoveries reported for *S. latissima* vary considerably depending on biomass origin, harvesting season, pretreatment, solvent system, and extraction conditions [387, 388]. For *S. latissima* harvested in May, the reported fucoxanthin content typically ranges between 300 and 600 µg/g DW [387, 388]. It should be noted, however, that these values were generally obtained using methanolic extraction. Kholany *et al.* [216] reported a higher fucoxanthin recovery from *S. latissima* using menthol-levulinic acid DES than with methanol. In contrast, the relatively low recovery obtained in the present study (~12% of the methanol extract) suggests that a substantial fraction of fucoxanthin remained associated with cellular and thylakoid membrane structures, thereby limiting its accessibility for extraction.

An important consideration is the potential increase in viscosity of the mixture as a limiting mass transfer factor. Betaine-based DES are recognised as a highly viscous eutectic systems, especially at relatively low temperatures [389]. The addition of water tends to reduce the viscosity of the DES. However, this intrinsic viscosity can be further increased due to the interfacial interactions between the two DES phases, depending on the nature of the mixture and the identity of the continuous phase [390, 391]. Additionally, water redistribution between phases may alter the local solvent environment, further affecting solvation and transport phenomena [383]. Compared to previously reported fatty-acid DES-salt systems, where an aqueous phase was employed [342], the FABU system likely exhibits higher overall viscosity. Increasing the amount of DES may raise the system's viscosity, which could in turn impede mass transfer [237] of fucoxanthin. In combination, these effects are likely to impose mass transfer limitations, hindering the diffusion of target compounds from the biomass into the respective solvent phase, even when thermodynamically favoured. This is further evidenced in the subsequent alkaline extraction step.

9.3.4 Fucoxanthin retainment in the biomass

During the subsequent alkaline step performed after the FABU system, a hazy, yellow-coloured extract was unexpectedly obtained (**Figure S9.3**) indicating potential fucoxanthin release from the seaweed. This suggests that a fraction of fucoxanthin remained associated with the biomass after the FABU extraction. Previous studies have reported values up to 1.96 mg/g DW in *S. latissima* [228], which supports that that fucoxanthin was not fully extracted during the FABU step.

To confirm the presence of fucoxanthin in this fraction, quantification was performed after liquid-liquid separation of the pigment. Interestingly, the alkaline extract obtained after biphasic DES treatment showed a more intense yellow colour (**Figure 9.5**) together with high fucoxanthin yields (563.3 ± 7.7 µg/g DW) (**Figure 9.6**). These yields

were even higher than those obtained during FA extraction in the FABU biphasic system (**Figure 9.4**). In contrast, direct sodium carbonate extraction of untreated biomass, used as a control, produced only a pale ethyl acetate phase (**Figure 9.5**) and negligible fucoxanthin recovery (**Figure 9.6**). These observations strongly suggest that fucoxanthin release during the alkaline step was mainly promoted by structural modifications of the biomass matrix induced by the DES pretreatment.

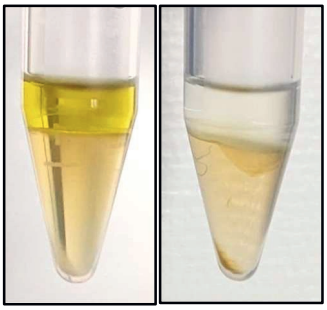


Figure 9.5 Fucoxanthin recovered in ethyl acetate (Top phases) from the alkaline extract from the FABU system (left) and from the conventional extraction process (right).

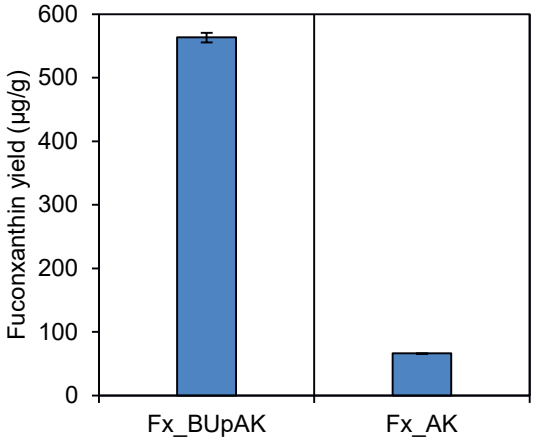


Figure 9.6 Fucoxanthin extraction yields (Fx) in the alkaline extract after the FABU biphasic system extraction (BUpAK) and in the AK extract.

During biphasic extraction, the hydrophilic phase may have promoted swelling and partial disruption of the biomass matrix, increasing pigment accessibility without directly solubilising fucoxanthin [375, 376].

Contrary to the observations of Hiemstra *et al*. [342] and the COSMO-RS predictions (**Table 9.3**), the fatty acid DES alone was unable to sufficiently disrupt the thylakoid membranes where fucoxanthin is localised [342, 371, 392]. Consequently, a

substantial fraction of fucoxanthin likely remained associated with the pretreated biomass despite the moderate extraction capacity of the FA DES. This entrapment highlights a critical limitation of thermodynamic screening models: COSMO-RS evaluates solute-solvent affinities under the assumption that the target compound is already fully solubilised and freely accessible in the fluid phase, thereby overlooking the physical mass-transfer barriers of the macroalgal cell wall.

As established in the work performed in our group, macroalgal extraction kinetics are heavily dictated by tissue density and biomass architecture, meaning that solvent accessibility represents the primary processing bottleneck, and fluid-phase thermodynamics alone cannot predict extraction yields [393]. Those findings demonstrated that potential increased cell permeabilisation on its own is insufficient to guarantee high macromolecular recovery, which instead depends strictly on the physical penetration velocity of the solvent phase into dense cellular structures [393]. During the FABU extraction, the hydrophilic betaine: urea (BU) phase could potentially enter and hydrate the complex carbohydrate network of the seaweed, inducing significant matrix swelling [48]. Because the co-existing fatty acid (FA) DES phase is highly hydrophobic, it could experience strong phase repulsion, preventing it from effectively penetrating this heavily swollen, hydrophilic, and water-rich biomass environment. Consequently, despite the high thermodynamic partition coefficients (10^{11}-10^{13}) predicted by COSMO-RS favouring the FA phase, a strict kinetic exclusion zone is established, confirming that a high theoretical partition coefficient does not equate to effective extraction performance when a physical phase barrier is present [394]. Thus, the fucoxanthin might have remained within the inner thylakoid regions, extensively isolated from direct molecular contact with the FA DES, until the subsequent sodium carbonate step transforms the mixture into an amphiphilic environment, thereby releasing the entrapped pigment.

This matrix-controlled behaviour indicates why DES treatment is mandatory to enhance pigment release, whereas highly soluble carbohydrates like mannitol and fucose undergo efficient extraction without requiring such structural modifications (**Section 9.3.1**). This contrast is governed by the spatial and compartmentalisation of these fractions within the macroalgal cell. Mannitol is a low-molecular-weight cytosolic polyol freely dissolved within the cytoplasm and vacuoles [55], while the water-soluble intercellular fucoidan (fucose) chains are loosely associated within the outer matrix boundaries [370]. Consequently, a mild aqueous solution (such as water or 50 mM citric acid) can easily permeate these outer boundaries, breaking weak ionic associations to release the sugars. In contrast, fucoxanthin is more hydrophobic and locked within the chloroplasts, chemically bound inside the lipid-protein complexes of

the thylakoid membranes and physically shielded behind the interpenetrating cellulose-alginate cell wall, thus remaining entrapped. The FABU system selectively addresses this double-shielding mechanism by leveraging a cooperative effect, where the hydrophilic BU phase could swell the seaweed cell while the hydrophobic FA is still separated from the seaweed cell wall due to hydrophobic repulsions. Upon alkaline extraction, this primes fucoxanthin release.

Given that fucoxanthin is poorly soluble in water [395, 396] and in alkaline aqueous media such as sodium carbonate, unless present at high concentrations (**Figure S9.4**), its presence in the extract is unlikely to result from true solubilisation. Instead, its co-extraction alongside alginate can be rationalised by an emulsification-driven mechanism. Residual fatty acids remaining in the pellet after the FABU treatment may facilitate the formation of protein-phospholipid-fatty acid emulsions, which can solubilise and transport fucoxanthin into the aqueous phase [342, 386]. This effect is likely enhanced under alkaline conditions, where fatty acids are converted into their corresponding sodium salts (surfactants), promoting emulsification [397, 398]. It has been reported that emulsions can exert a protective effect on pigments, although this strongly depends on the specific type and stability of the emulsion formed [396]. Elevated temperatures applied during extraction, might have contributed to the increased apparent yield as well. In addition, previous studies have found good stability of fucoxanthin in alkaline additions [385, 395]. These findings indicate that DES pretreatment enhances pigment accessibility, while the alkaline step primarily facilitates release of residual fucoxanthin rather than direct extraction from untreated biomass.

It is important to consider the potential limitations resulted from this approach. Phase separation may be hindered by the formation of stable emulsions. One feasible strategy would be the addition of a secondary solvent that can be readily recovered after extraction. Ethanol represents one of the first options, as it could simultaneously precipitate alginate and recover fucoxanthin, which could subsequently be separated by solvent evaporation [57]. Alternatively, ethyl acetate, as tested at laboratory scale, may represent a suitable option. It is considered one of the more sustainable conventional organic solvents, while its relatively high volatility facilitates solvent recovery [399].

A solvent-free strategy would involve a mild reduction in pH [400]. Re-protonation of the fatty-acid salts would reduce their surfactant activity and destabilise the emulsion droplets. This could potentially be achieved by sparging CO_2, allowing a gradual decrease in pH [401]. However, this approach should be carefully evaluated, as

acidification may also promote alginate precipitation as alginic acid [57]. In addition, acidic conditions could affect the stability of the recovered fucoxanthin [385]. Increasing the ionic strength, for example by sodium chloride addition, could represent another strategy, as high ionic strength reduces the electrostatic repulsion between emulsion droplets and promotes flocculation and phase separation [400].

In all cases, further purification, potentially using chromatographic techniques, would then be required [402]. Importantly, these approaches cannot be evaluated solely on their ability to recover fucoxanthin. Any selected separation method should also have a limited effect on alginate yield, structure and functionality to be considered suitable for process integration.

It is worth noting that the residual pellet from the conventional acid-alkaline extraction was further subjected to methanol extraction for fucoxanthin recovery. The obtained yield (328.9 ± 2.2 µg/g) indicates that a significant fraction of fucoxanthin remains in the biomass even after alginate extraction via the acid-alkaline process. However, in addition to the main peak corresponding to all-trans fucoxanthin (RT ≈ 5.2 min), several additional peaks with similar absorption spectra were observed, eluting both before and after the main peak. These peaks, hypothesised to be fucoxanthin isomers [403], accounted for approximately 39.5 ± 0.5% of the total chromatographic area (**Figure 9.7a**), suggesting substantial pigment isomerization/degradation induced by the acid-alkaline conditions. In contrast, very low levels of such potential isomerization/degradation were observed in fucoxanthin recovered from the alkaline extract following the FABU process (**Figure 9.7b**). Additionally, absorption spectra of the secondary peaks from the fucoxanthin extracted with methanol exhibited a hypsochromic shift of the main absorption band to approximately 420–430 nm, suggesting degradation of the conjugated polyene chain (**Figure S9.5**) [404]. This supports the hypothesis that FABU acts as a milder pretreatment, sufficiently disrupting the biomass to enhance pigment accessibility while preserving fucoxanthin integrity.

Improved carotenoid stability in DES has been reported previously. Xu *et al*. [93] demonstrated that fucoxanthin extracted from microalga *Tisochrysis lutea* using a thymol:dodecanoic acid DES, remained stable over 11 days without significant degradation. In another study, enhanced stability of lutein extracted from *Scenedesmus sp* in NADES compared to methanol was observed under elevated temperature and light exposure, which was attributed to hydrogen-bonding and van der Waals interactions between the solvent and pigment molecules [405]. Furthermore, Yang *et al*. [406] reported improved stability of canthaxanthin, a carotenoid present in

the green alga *Chromochloris zofingiensis,* when extracted with a fatty acid-based DES comprised of octanoic and decanoic acid. In this study, reduced pigment aggregation and a more uniform solute distribution were observed relative to conventional solvents. As a fatty acid-based DES was employed in the present study, similar stabilising interactions may contribute to the observed fucoxanthin recovery.

Taken together, these results indicate that the FABU system may fulfil a dual function within the extraction process. Although direct fucoxanthin partitioning into the fatty-acid phase was limited, the system appears to act as an effective pretreatment medium by disrupting biomass structures and increasing pigment accessibility for the subsequent alkaline step. At the same time, the chromatographic profiles suggest that the fatty-acid-based DES contributed to improved preservation of fucoxanthin, as lower levels of isomerisation/degradation were observed compared with conventional extraction. Thus, the FABU approach may decouple biomass disruption from final pigment recovery, combining enhanced accessibility with stabilising solvent interactions that help retain fucoxanthin integrity.

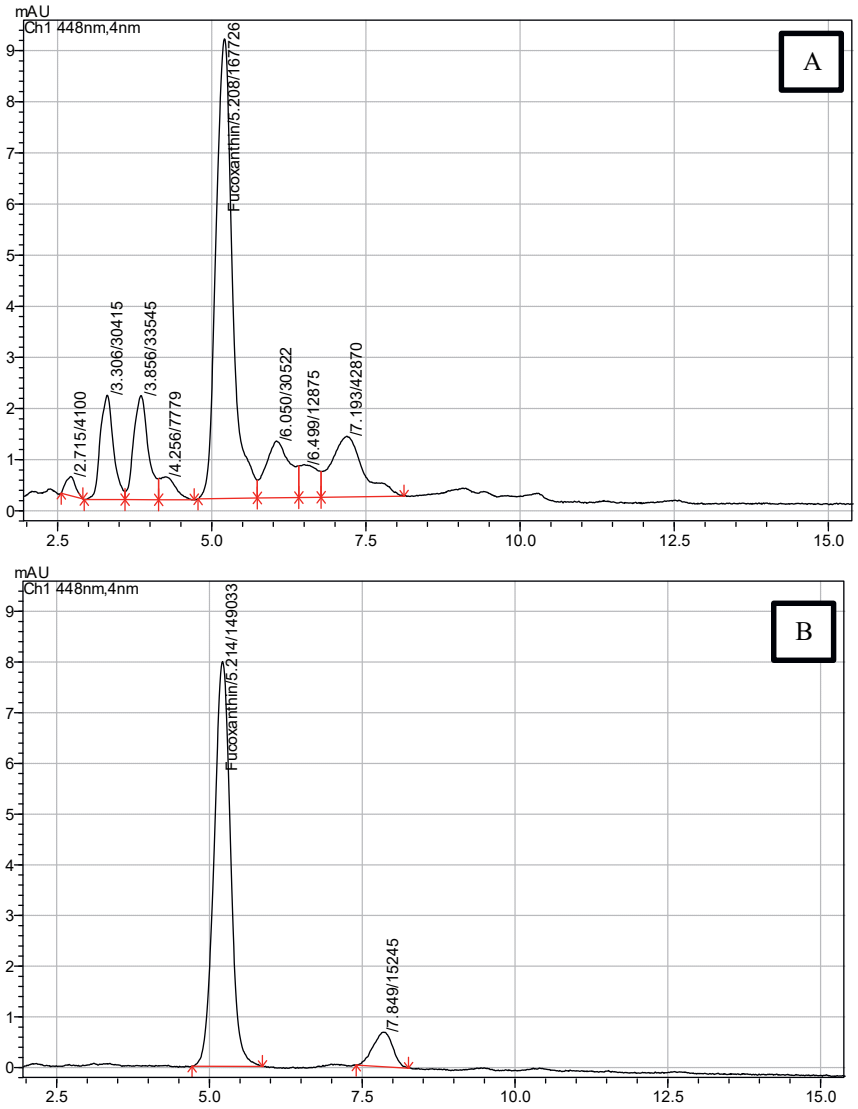


Figure 9.7 (**A**) Fucoxanthin recovered with methanol from the pellet residue after the conventional alkaline extraction. (**B**) Fucoxanthin recovered with ethyl acetate from the alkaline extraction after FABU treatment. More details regarding the UV-vis spectra of secondary peaks can be found in the Supplementary Material Section.

9.3.5 Mass balances of the proposed design

Based on the biomass composition, the recovery yield (%) of each target compound throughout the process was determined (**Table 9.4**). The alginate yields were lower than those reported by Reynaga-Navarro *et al*. [48]. One possible explanation is the

lower extraction temperature employed in the present work (35 °C versus 55 °C). Besides reducing the diffusion rate of the target compounds, the lower temperature increases the viscosity of the DES, further limiting mass transfer. Therefore, process optimisation is expected to reduce this gap or even improve alginate recovery.

Similarly, the fucose recovery (used as a proxy for fucoidan) reached only 32%, indicating that the selected operating conditions were not optimised for fucoidan extraction. In contrast, mannitol recovery was ~80%, consistent with its high water solubility [379]. Overall, the relatively mild extraction conditions, including the low citric acid concentration compared with the optimum reported for fucoidan extraction [377] and the reduced temperatures selected to preserve the integrity of fucoxanthin and alginate, favoured product quality over maximum extraction yield.

Interestingly, the conventional methanolic extraction recovered less fucoxanthin than the integrated process, resulting in an apparent recovery exceeding 100% relative to the methanolic extraction benchmark. This result suggests that the conventional methanolic extraction was not exhaustive under the conditions employed and further highlights the enhanced capability of the proposed integrated process to recover fucoxanthin from *S. latissima*.

Table 9.4 Mass balance of extracted compounds in the different fractions along the proposed FABU process.

Fraction	Alginate (mg/g)	Fucose (mg/g)	Mannitol (mg/g)	Fucoxanthin (µg/g)
Seaweed	100%	100%	100%	100%
Pretreatment	n.d.	32%	80%	0%
FABU	8%	n.d.	n.d.	12%
AK-extraction	23%	n.d.	n.d.	167%

9.3.6 FABU as powerful pretreatment

9.3.7 Proposed permeabilisation mechanism

When extracting biological compounds from structurally complex materials such as seaweed, partitioning is an important, but not sufficient, criterion for designing extraction systems. The disruptive capacity of the solvent system is equally critical, as most target compounds are embedded within or associated with complex cellular architectures that must first be “opened” before partitioning can effectively occur. The present biphasic system exemplifies this principle.

Confocal microscopy further supports the hypothesis that the FABU system promoted structural modification of the seaweed tissue rather than direct fucoxanthin extraction (**Table S9.1**). Hydrated samples exhibited a larger relative cell area compared with the intercellular cell wall space, while FABU-treated samples showed a reduced outer cell layer, suggesting partial removal of alginate and increased tissue permeability (**Figure S9.6**). These structural changes may have enhanced the accessibility of intracellular fucoxanthin release during the subsequent alkaline extraction, providing a possible explanation for its increased recovery. This interpretation is consistent with independent physiological localization studies of alginate in brown algae. In *S. latissima* embryos, Boscq *et al.* (2025) [407] showed that mannuronate-rich alginate initially occupies specific external and lateral wall domains and later accumulates in newly formed cross walls, whereas guluronate-rich alginate remains primarily associated with the external wall layers. These studies demonstrate that alginate substructures are spatially heterogeneous rather than uniformly distributed within brown-algal tissues. Although microscopic observations indicate changes in tissue architecture, further characterisation using scanning electron microscopy (SEM) would be required to confirm cell wall permeabilisation, which was beyond the scope of the present study.

The microscopy results are also supported by our previous extraction study using betaine-urea. In that study, the first fraction directly recovered with betaine-urea, BU-1, represented only part of the total alginate and had an M/G ratio of approximately 2.2, indicating preferential recovery of a mannuronate-rich fraction. Subsequent water and alkaline fractions had progressively lower M/G ratios of approximately 1.5 and 1.2, respectively. Most of the total alginate was recovered only during the final alkaline step, and the complete sequential BU process recovered 75.1 ± 2.2% of the alginate, compared with 63.5 ± 1.6% for the conventional acid-alkaline process. This fractionation behaviour indicates that betaine-urea does not directly solubilize the entire structural alginate matrix. Instead, it preferentially mobilizes a more mannuronate-rich and accessible fraction while facilitating the subsequent recovery of alginate that remains associated with the biomass.

Taken together, the quantitative microscopy, sequential extraction yields and M/G fractionation support the following mechanism: FABU induces swelling, increased porosity and partial loosening of the cell-wall matrix, permitting the recovery of a relatively accessible, mannuronate-rich alginate fraction. A substantial part of the more tightly integrated wall matrix remains in the biomass and is solubilized only during the subsequent alkaline treatment. The structural modification caused by FABU also increases access to intracellular and membrane-associated compounds, explaining

why much more fucoxanthin was recovered in the subsequent alkaline fraction than directly in the fatty-acid phase.

9.3.8 Process perspective

To transition this integrated extraction line into a circular biorefinery, efficient solvent recovery is essential. While no recycling was addressed in this specific study, our previous studies have firmly established the multi-cycle recyclability of both solvent fractions. DES betaine:urea (BU) recovery and simultaneous alginate separation have been successfully demonstrated for at least five consecutive cycles using both temperature-responsive aqueous two-phase systems (ATPS) [335] and using a DES-salt ATPS for direct interfacial alginate precipitation and solvent reuse [384]. Additionally, reuse of the fatty acid (FA) DES performed up to seven times using a circular three-phase partitioning (TPP) configuration for concurrent pigment capture [342]. These studies provide the feasibility of recycling of the DES within a circular FABU system.

Ultimately, the performance of the integrated process for seaweed must be evaluated from an economic perspective, considering solvent recovery, product purification, and overall process integration [408, 409]. The implementation of DES-based technologies introduces additional challenges, as their physicochemical properties may require dedicated equipment, increasing the initial capital investment, in addition to the different energy needed for agitation and pumping [9, 410]. Likewise, the operational costs associated with DES preparation and replenishment should be quantified, despite the recyclability of the system [411, 412]. The economic feasibility will ultimately depend on the market value of the recovered products, which is determined by their purity, functionality, and intended application [408]. Higher processing costs may therefore be compensated if the process generates products with enhanced functionality and, consequently, higher added value. In this regard, the present process demonstrates the technical feasibility of such an approach. Although the FABU biphasic system requires further optimisation, these results highlight its relevance as a starting point for the development of integrated, multiproduct seaweed biorefineries, where disruption and partitioning are strategically decoupled and sequentially exploited.

9.4. Conclusion

A DES-based biphasic system (FABU) was evaluated for the co-extraction of alginate and fucoxanthin from *Saccharina latissima*. The system combined a hydrophobic phase (dodecanoic acid-octanoic acid, FA) for fucoxanthin extraction and a hydrophilic phase (betaine-urea-water, BU) for alginate recovery.

Unexpectedly, fucoxanthin extraction into the FA phase was limited (41.4-58.2 µg/g), contradicting COSMO-RS predictions on both the affinity (capacity of $2.1 \cdot 10^3$ for FA) and partitioning ($K_{FA/BU}$ $3.8 \cdot 10^{12}$). Remarkably, a high fucoxanthin concentration (563.3 ± 7.7 µg/g) was recovered during the subsequent alkaline step, meant for full alginate recovery, indicating that the FABU system likely primarily acts as a cell permeabilization medium rather than an efficient partitioning system.

This discrepancy between predicted thermodynamic affinity and experimental extraction behaviour highlights that partitioning alone is not sufficient to describe extraction performance in complex biomass systems. Instead, factors such as biomass accessibility, mass transfer limitations, and system viscosity play a dominant role. These findings demonstrate that disruption and solubilisation can be effectively decoupled, with the FABU system enhancing accessibility while the subsequent alkaline step enables compound recovery. Chromatographic profiles further suggested improved fucoxanthin preservation compared to conventional acid-alkaline extraction, indicating the DES was likely acting as a preservative medium.

Overall, these results reveal a clear decoupling between cell permeabilization capacity and solubilisation in DES-based systems. Rather than a limitation, this uncovers the potential of DES biphasic systems as powerful pretreatment platforms for integrated seaweed biorefineries. Future work should address solvent recyclability and assess process feasibility through techno-economic and life cycle analyses and complete the characterisation of the extracted compounds.

9.5. Supplementary information

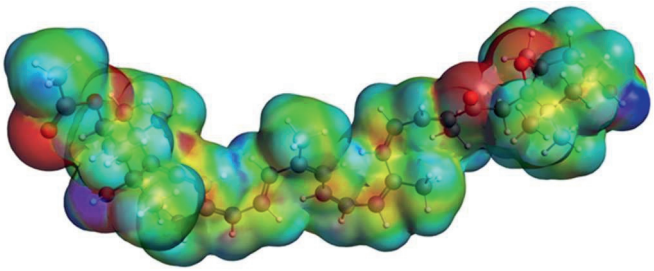


Figure S9.1 Molecular structure of fucoxanthin. Blue regions represent the hydrogen bond donating areas, red regions represent the hydrogen bond accepting areas, and green regions represent the non-polar surface areas.

FTIR analysis

To evaluate the alginate recovered from the DES extract, acid alkaline extract and the alkaline extract after DES treatment, FTIR (Fourier-transform infrared) profiles were recorded over a spectral range of 400–4000 cm^{-1} using a Nicolet Summit X ATR-FTIR spectrometer (Thermo Fisher Scientific). Prior to analysis, polymers were isolated from the extracts by precipitation with a ethanol 80% (v/v) with 1% (w/v) sodium chloride, followed by two sequential washing steps using 80% (v/v) ethanol [413]. The gathered precipitates were subsequently dried under a continuous nitrogen stream before being subjected to FTIR characterisation.

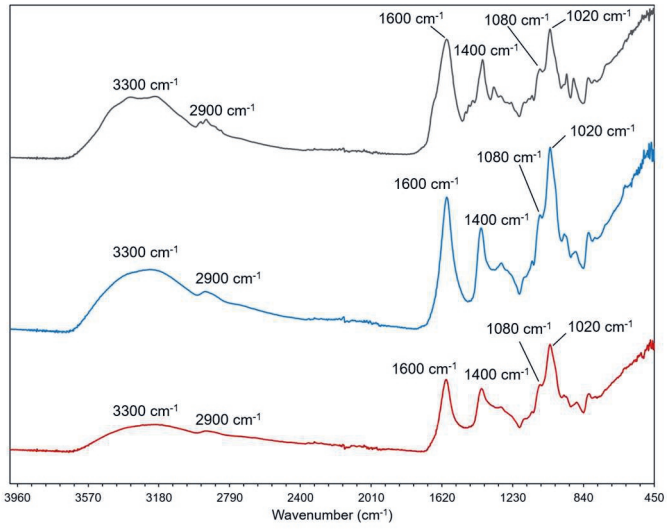


Figure S9.2 FTIR spectra of alginate extracted with acid-alkaline conventional extraction (red), alkaline extraction after BU treatment (blue) and DES BU (grey) using the FABU biphasic system.

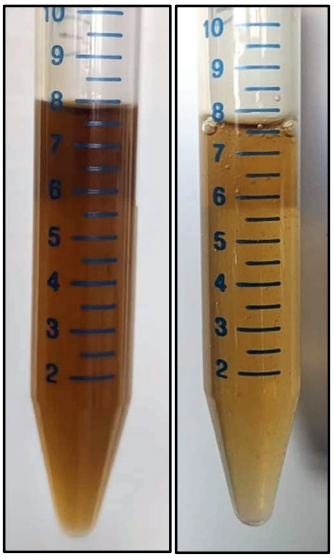


Figure S9.3 Alkaline extract from the FABU system (left) and from the conventional process (right). Extract from the FABU system was browner than the extract from the conventional method, indicating the presence of a higher concentration of fucoxanthin.

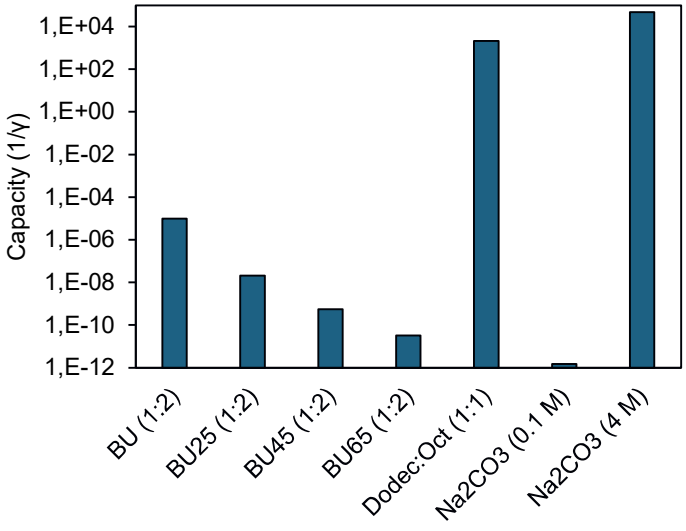


Figure S9.4 Calculated capacities of DES and sodium carbonate for fucoxanthin. From left to right: BU, betaine-urea DES. The numbers on the right indicate the water content (% w/w), while the values in parentheses represent the molar ratios. Dode:Oct, docecanoic acid-octanoic acid DES; Na_2CO_3 corresponds to sodium carbonate solutions at 0.1 and 4 M.

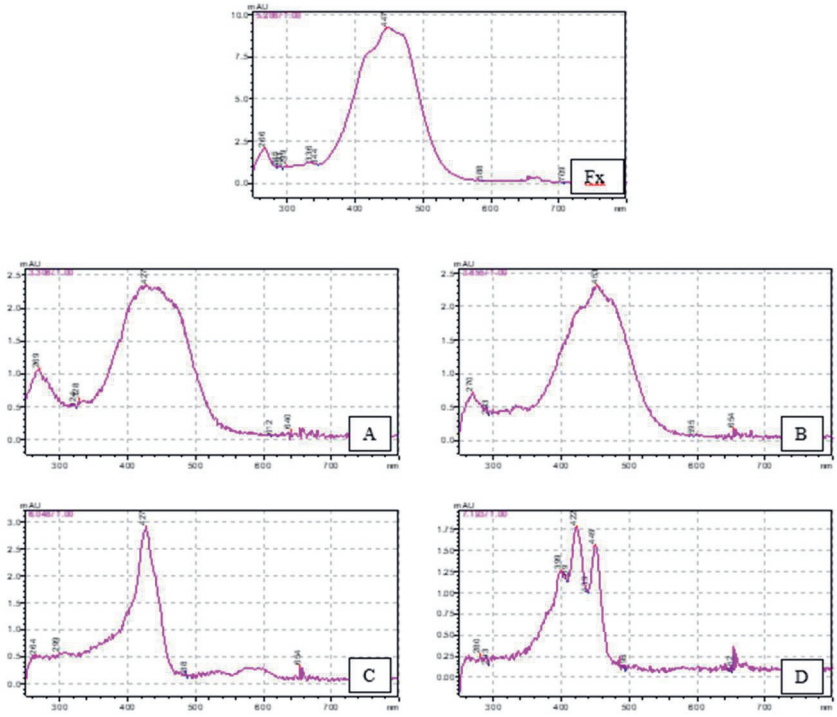


Figure S9.5 UV-Vis absorption spectra of fucoxanthin (Fx) and the four secondary peaks (A–D) observed in the chromatogram shown in **Figure 9.7a**. Peaks A, C, and D exhibited a hypsochromic shift of the main absorption band to approximately 420-430 nm, suggesting degradation of the conjugated polyene chain [414]. In contrast, peak B showed a maximum absorption at 453 nm, consistent with the presence of a potential fucoxanthin isomer [415].

Microscopy of treated biomass

Samples were imaged with a Leica Stellaris 5 confocal microscope (Leica) using a 20× objective (**Figure S9.6**). Image acquisition was performed with a white light laser (WLL) at excitation wavelengths of 485 and 680 nm, with emission bands set at 675–695 and 710–740 nm, respectively. A transmitted-light detector was used to acquire a brightfield channel simultaneously. Images were acquired at a resolution of 1024 × 1024 pixels with a scan speed of 100 Hz. Image processing and analysis were performed using LAS X software (Leica).

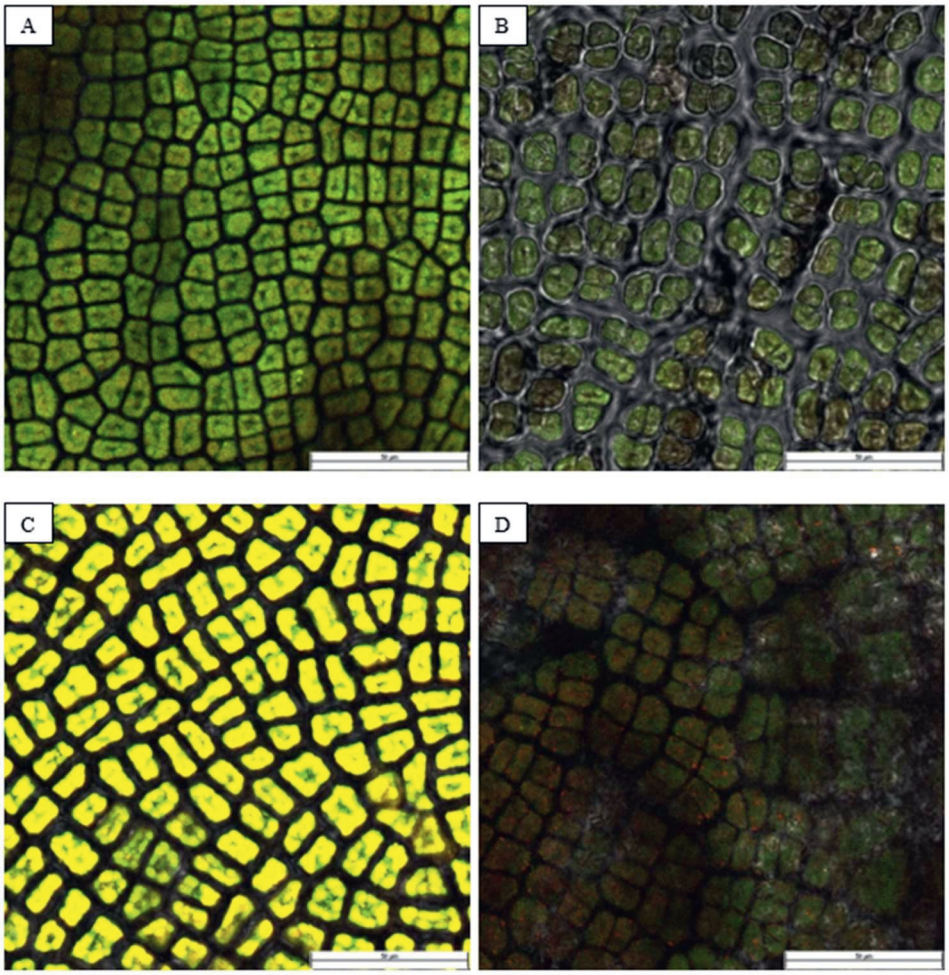
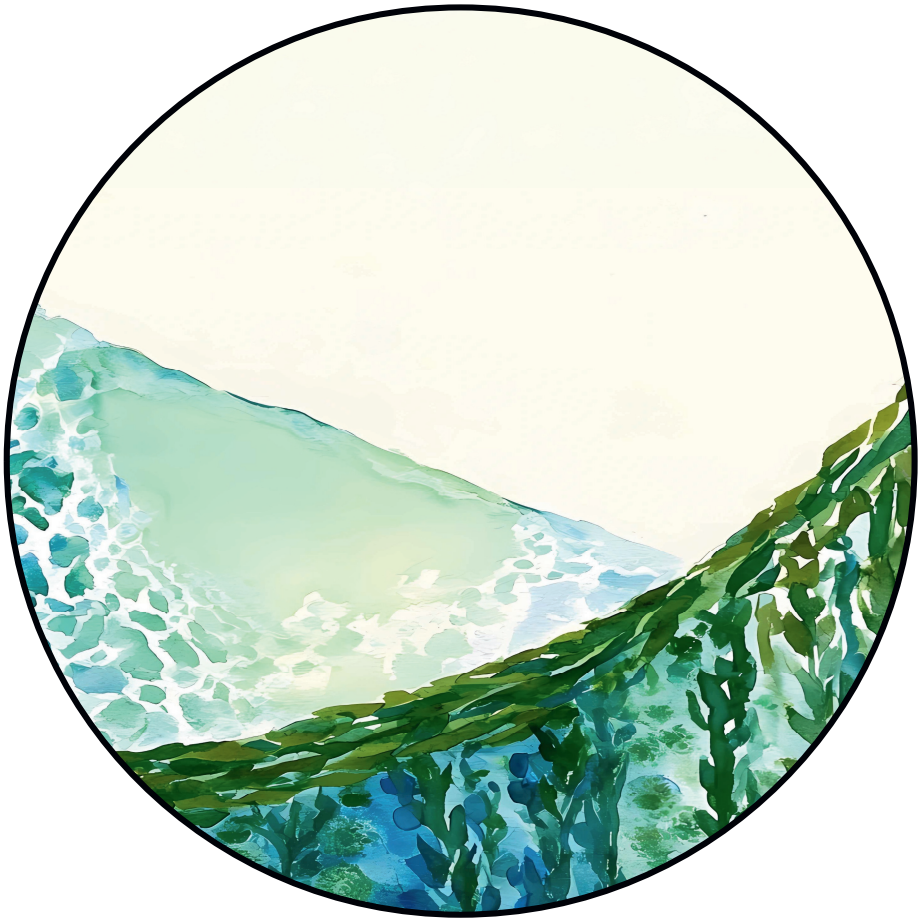


Figure S9.6 Confocal microscopy images of treated seaweed. Untreated (A); acid-alkaline treated (B); FABU treated (C); FABU-alkaline (D).

Table S9.1 Relative area of seaweed cells compared to cell walls.

Sample	Area fraction (Intra/inter) %[a]
Water	66 ± 6
FABU	54 ± 1

[a] Values represent the mean of three independent images analysed using ImageJ. The percentages for the conventional acid-alkaline and FABU-alkaline samples could not be determined due to insufficient image contrast.



Chapter 10

Techno-economic and life cycle assessment of DES-based multiproduct seaweed biorefinery

Isa S.A. Hiemstra[∞], Wimar Reynaga-Navarro[∞], Giuseppe Olivieri, Rafaela Groudou, Seppe Van der Heyden, Petronella M. Slegers, Antoinette Kazbar

[∞] Authors contributed equally

This chapter has been submitted to RSC Green Chemistry

Abstract

Deep eutectic solvents (DES) have emerged as alternatives to conventional solvents for seaweed biorefineries, yet their potential to be industrially integrated remains largely unexplored. This study presents one of the first integrated techno-economic (TEA) and life cycle (LCA) assessments of a multiproduct *Saccharina latissima* biorefinery based on a biphasic DES system. A process simulation based on literature was used to evaluate the recovery of fucoxanthin, fucoidan, and alginate and to identify the main drivers of process sustainability. Interestingly, the environmental hotspots closely mirrored the economic hotspots identified in the techno-economic assessment, where DES constituents also dominated the raw material costs (96%). The biphasic DES process reduced the environmental impacts for 16 out of the 18 evaluated midpoint impact categories compared with the conventional acid-alkaline extraction process for sodium alginate. However, it remained economically unfeasible, with a net present value of €-263.1 million, mainly due to solvent-related costs. Solvent consumption was identified as the main economic and environmental hotspots, while sensitivity analyses showed that the solvent-to-biomass ratio, fucoxanthin extraction efficiency, and product value were the key process drivers. Notably, improving product functionality and market value had a greater impact on economic feasibility than increasing extraction yield alone. These results demonstrate that the sustainability of DES-based biorefineries depends on process integration, solvent management, and multiproduct valorisation rather than on the use of DES alone.

10.1 Introduction

The transition towards a circular bioeconomy requires biorefineries capable of converting renewable biomass into multiple products while minimising environmental impacts, improving resource efficiency and being economically sustainable. In this context, multiproduct biorefineries are increasingly preferred over single-product processes because they allow several value streams to be recovered from the same biomass, thereby improving both economic performance and environmental impact [416, 417].

Marine biomass has attracted growing interest as a sustainable feedstock for such integrated biorefineries owing to its high productivity and diverse chemical composition. However, despite considerable technical progress, the industrial implementation of marine biorefineries remains constrained by the limited availability of integrated techno-economic and environmental assessments [38, 342]. Among marine feedstocks, seaweeds are particularly attractive because they can be cultivated without arable land, freshwater, or synthetic fertilizers and naturally contain a wide range of valuable compounds, including hydrocolloids, proteins, carbohydrates, and pigments [418]. Brown seaweeds, such as *Saccharina latissima*, are especially promising because they contain commercially relevant amounts of alginate, fucoidan, mannitol, and fucoxanthin, making them suitable feedstocks for integrated multiproduct biorefineries [372, 419, 420].

Conventional brown seaweed processing, however, primarily targets alginate through acid-alkaline extraction. These processes rely on harsh chemicals, generate substantial waste streams, and often compromise product functionality while leaving other valuable compounds underutilised [56, 124].

Deep eutectic solvents (DES), including natural deep eutectic solvents (NADES), have emerged as promising solvent systems for biomass fractionation due to their tuneable physicochemical properties, low volatility, simple preparation and ability to selectively dissolve different classes of biomolecules [9, 15]. In seaweed processing, hydrophilic DES have successfully been applied for alginate extraction [48, 342], whereas hydrophobic DES have demonstrated high selectivity for pigments such as fucoxanthin [216]. Recent studies have further shown that membrane-based separation can partially recover both DES and extracted products, highlighting the potential for solvent recycling within integrated seaweed biorefineries [271]. Despite these promising technological advances, the sustainability of DES-based biorefineries cannot be inferred from solvent properties alone. Recent life cycle assessments demonstrate

that the environmental performance of DES-based processes depends strongly on solvent synthesis, solvent recovery, process energy demand, downstream separation, and coproduct valorisation [152, 211, 421, 422]. In particular, unrecovered solvents can substantially increase greenhouse gas emissions and energy consumption, whereas efficient solvent recycling and process integration can significantly improve environmental performance [211, 422]. Consequently, DES-based biorefineries should be evaluated at the integrated process level rather than on solvent characteristics alone. Similarly, McReynolds *et al*. (2022) [423] concluded that although DES have become promising extraction media for marine biomass, robust environmental assessments of complete seaweed biorefineries remain scarce.

A similar conclusion emerges from the available techno-economic literature. Although relatively few TEA studies have examined DES or NADES based biorefineries directly, evidence from lignocellulosic systems consistently identifies solvent consumption, solvent recycling, and multiproduct valorisation as the primary economic drivers [38, 416, 417]. Single-product processes generally exhibit poor economic performance, whereas integrated biorefineries become increasingly attractive when multiple coproducts are recovered and solvents are efficiently recycled over multiple extraction cycles [416, 417].

Although laboratory-scale studies have demonstrated that DES enable selective extraction of multiple seaweed components and facilitate solvent recovery, the industrial feasibility of DES-based seaweed biorefineries remains largely unexplored. Most published research focuses on extraction performance or solvent recycling in isolation, while only a limited number of studies have evaluated complete process integration through combined techno-economic assessment (TEA) and life cycle assessment (LCA) [416, 417, 422]. Consequently, it remains unclear whether the technical advantages of DES translate into economically viable and environmentally sustainable industrial biorefineries.

Therefore, this study evaluates an integrated multiproduct seaweed biorefinery as a representative case study to identify the process characteristics governing the industrial implementation of DES-based biorefineries. An industrial-scale process model integrating published extraction, purification, and solvent recovery technologies was developed and assessed using combined TEA and LCA. The study investigates how process integration, multiproduct valorszation, product functionality, and solvent recyclability influence both economic and environmental performance. By identifying the critical design parameters and associated trade-offs, this work provides guidance for the development of future sustainable DES-based seaweed biorefineries.

10.2. Methodology

10.2.1 Overall methodology

To identify the key design parameters governing the sustainability of DES-based biorefineries, an industrial process model was developed using brown seaweed as a representative case study. As outlined in **Figure 10.1**, this approach was structured through a literature revision, followed by conceptual process design, SuperPro simulations and TEA, followed by parameter sensitivity analysis, and finally LCA. Experimental extraction data (**Table 10.1**) from previously published studies were integrated into a single process model describing multiproduct extraction, solvent recovery and product purification (**Figure 10.2**). The resulting mass and energy balances formed the basis for both the techno-economic assessment and life cycle assessment.

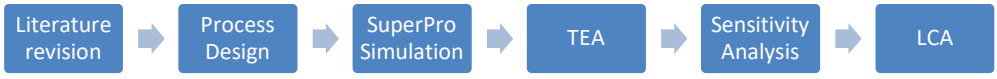


Figure 10.1 Overview of the workflow used in current research.

10.2.2 Process design

The process design was established based on the integration of previously reported DES-based extraction, recovery, and recycling strategies from literature (**Figure 10.2**). Brown seaweed *Saccharina latissima* was selected as feedstock due its relevance in the European context and in previous studies on DES-assisted seaweed processing [48, 216, 342, 378, 424].

Initially, a citric acid pretreatment step was incorporated to enable fucoidan recovery, following a previously reported study [377]. Subsequently, a biphasic DES extraction system consisting of betaine:urea (BU) and dodecanoic acid:octanoic acid (FA) was applied for the simultaneous extraction of alginate and fucoxanthin, respectively, based on earlier studies [48, 342].

The FA DES phase used for fucoxanthin extraction was recycled for six consecutive extraction cycles prior to product recovery to maximise pigment accumulation, according to previous findings [342]. Fucoxanthin separation and purification were based on the approach proposed by Kholany *et al*. [216] employing a hydrophilic choline chloride:levulinic acid DES as a secondary separation phase. In addition, an

alkaline extraction step was incorporated for further valorisation of the residual seaweed pellet following biphasic extraction, according to the method described by Bojorges *et al*. [57].

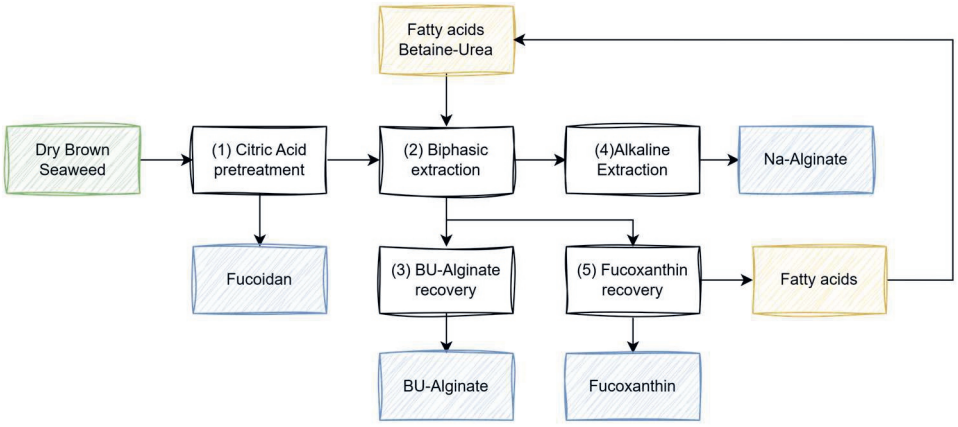


Figure 10.2 Schematic process overview of the multiproduct DES-based seaweed extraction and separation.

Table 10.1 summarises the extraction yields obtained for the different compounds across the individual process steps. Detailed extraction and processing parameters for each step are provided in **Figure S10.1**.

Table 10.1 Extraction yields (% DW) per processing step.

Section	Alginate	Fucoxanthin	Fucoidan	Reference
Citric acid pretreatment	-	-	6.55%	[377]
Biphasic extraction	4.53%	0.012%	-	[48, 342]
Alkaline extraction	11.9%	-	-	[57]
Fucoxanthin recovery	-	0.0114%	-	[216]

10.2.3 Process simulations in SuperPro Designer

10.2.3.1 Process modelling approach and assumptions

To establish the mass and energy balances required for the subsequent TEA and LCA, the proposed seaweed biorefinery was simulated using SuperPro Designer (v14, Intelligen, Inc., USA). The industrial-scale production facility was assumed to operate

in batch mode for 330 days per year, with a feedstock processing capacity of 16,000 kg of dried seaweed biomass per batch containing 10% residual moisture after drying. Scaling from the experimental data compiled in **Table 10.1** to the industrial manufacturing scale in SuperPro was executed via linear scale-up principles, as visually mapped in the process flow diagram (**Figure S10.1**).

To accommodate literature limitations and simplify the simulation framework, the following process assumptions were implemented:

1. Biomass simplification: Non-target macroalgal constituents (proteins, lipids, minerals, phenolics, and residual sugars) were not modelled explicitly but lumped into generalised "pellet" and "biomass" mass streams.
2. Phase disengagement: A theoretical 100% phase separation efficiency was assumed for the multi-phase DES systems.
3. Solvent purification: A 90% washing and removal efficiency was defined for the betaine:urea (BU) and fatty acid (FA) DES streams to ensure sufficient impurity removal.
4. Alginate precipitation: An isolation threshold of 100% precipitation efficiency was implemented for both alginate and sodium alginate fractions.
5. Solvent loss and purity: A standard 10% solvent mass loss per batch was assumed for the choline chloride:levulinic acid (ChCl:LevA) matrix, with a target fucoxanthin product purity exceeding 95% to represent an optimistic baseline scenario.

10.2.4 Economic evaluation using SuperPro Designer

The economic viability of the biorefinery was studied based on the capital investment (CAPEX) and operating cost (OPEX). Furthermore, for the economic evaluation the payback time of the investment for 10 years of operation (calculated based on total investment and the net profit), the net present value (NPV) with an interest rate of 7% and a stable net cash flow for each operating year, and the annual revenues of the process were considered. Calculations for the total capital investments, operating costs, total revenues, gross margin, return of investment (ROI) and net present value (NPV) were calculated, similar to Herrera Barragán *et al.* [409].

10.2.5 Raw material cost input and product selling prices

Data for the prices of the raw materials applied in the simulation were obtained from recent market sources and literature. These inputs in SuperPro were essential for the estimation of the raw material's annual expenses and overall operating costs. **Table S10.1** summarises the raw materials used and their corresponding costs. The alginate,

fucoidan and fucoxanthin selling prices were based on previous techno-economic literature data (**Table 10.2**) and were implemented for the TEA analysis.

Table 10.2 Unitary selling cost for alginate, fucoidan and fucoxanthin.

Product	Selling cost (€/kg)	Reference
Alginate	10	[409]
Fucoidan	300	[409, 425]
Fucoxanthin	40,000	[426]

10.2.6 Process descriptors

10.2.6.1 Citric acid pretreatment and fucoidan recovery

The process started with the citric-acid pretreatment of dry biomass, aiming to gently extract fucoidan and improve the alginate extraction in the following steps. A Solid-to-Liquid ratio (SLR) of 1:60 (w/w) and 1% (w/v) citric acid was used at 35 °C for 1 h following parameters reported by Fawzy & Gomaa [377] with modifications. The extract was later subjected to a diafiltration process to concentrate the content and remove small molecules and spray-dried to obtain a powder.

10.2.6.2 Biphasic DES extraction

Based on the set-ups reported previously [48, 342], a biphasic approach was proposed and designed. BU (betaine-urea) and FA (dodecanoic and octanoic acids) DES were prepared separately as described in the literature by applying heat, after which 45% (w/w) water was added to BU. A FA:BU ratio of 1:2 (w/w) was selected for the extraction process. The pellet stream from the citric acid pretreatment referred as “Pellet 1”, was subjected to the biphasic system extraction with a SLR of 1:60 (w/w). The extraction was conducted at 35 °C for 1 h under continuous stirring.

10.2.6.3 BU-alginate recovery and DES reuse

After the biphasic extraction the mixture was centrifuged and three fractions resulted: residual biomass (pellet 2), alginate rich BU DES and pigment rich FA DES. The FA DES was reused for 5 more consecutive cycles directly entering again the biphasic extraction system, to accumulate the fucoxanthin until saturation, while the BU DES was led to the diafiltration for alginate recovery. The diafiltration started with a pre-concentration step using a concentration factor of 9 to reduce the volume of the stream. The diafiltration step was operated such that the alginate concentration in the retentate did not exceed 2% mass composition, to minimise membrane fouling and

prevent excessive increases in viscosity. At the same time, the permeate stream was maintained at approximately 85% BU mass composition, ensuring that it was sufficiently enriched to be fed directly back into the biphasic extraction reactor without any additional processing.

To recover and purify the alginate-rich retentate, ethanol precipitation was applied. For precipitation, a ratio of 1:2 (v/v) extract to ethanol solution (80%) and 1% NaCl are selected, at 25 °C under continuous stirring [57]. The precipitated alginate recovered from the bottom of the reactor, was dried at 70 °C and grinded to a final powder product. After the reuse of the DES for 6 cycles, the extracted compounds were purified, and the wasted solvents replenished.

10.2.6.4 Alkaline extraction

The fucoxanthin accumulated in the FA DES after six consecutive extraction cycles was recovered by a liquid–liquid extraction approach, as reported [216]. Assuming a similar behaviour, the hydrophilic DES choline chloride–levulinic acid (CCLev) was used. CCLev was added to the FA fraction at a ratio of 1:4 (v/v), promoting the migration of fucoxanthin from the fatty acid phase due to the polar functional groups present in the molecule. The extraction was performed at 25°C for 10 min, after which two phases were formed. The bottom phase, containing the fucoxanthin, was then mixed with water as an antisolvent (1:1, v/v), promoting the formation of an oily phase expected to contain the recovered fucoxanthin. Finally, the FA fraction (top phase) was washed and recovered for the preparation of fresh FA DES. The water content from the CCLev acid was then removed and the DES fraction was recovered to be reused.

10.2.6.5 Fucoxanthin recovery

The fucoxanthin accumulated in the FA DES after six consecutive extraction cycles was recovered by a liquid–liquid extraction approach, as reported previously [216]. Assuming a similar behaviour, the hydrophilic DES choline chloride–levulinic acid (CCLev) was used. CCLev was added to the FA fraction at a ratio of 1:4 (v/v), promoting the migration of fucoxanthin from the fatty acid phase due to the polar functional groups present in the molecule. The extraction was performed at 25 °C for 10 min, after which two phases were formed. The bottom phase, containing the fucoxanthin, was then mixed with water as an antisolvent (1:1, v/v), promoting the formation of an oily phase expected to contain the recovered fucoxanthin. Finally, the FA fraction (top phase) was washed and recovered for the preparation of fresh FA DES. The water content from the CCLev acid was then removed and the DES fraction was recovered to be reused.

10.2.7 Sensitivity analysis

To identify the critical economic drivers of the DES biorefinery and to assess how the NPV could be improved, a sensitivity analysis was performed. Three parameters were varied against their baseline configurations to evaluate its process impact:

1. Solid-to-Liquid Ratio (SLR): To evaluate the impact of reducing the volumetric solvent load, the baseline SLR of 1:60 was varied to more concentrated ratios of 1:40 and 1:20.
2. Alginate market value: The baseline commodity selling price of €10/kg was increased stepwise to €20, €50, €100, and €200/kg. This pricing model assumes that the enhanced structural and rheological functionality of the alginate extracted via the betaine:urea (BU) platform justifies a higher functional-grade market value.
3. Fucoxanthin extraction yield: Shifting from the model baseline of 0.02% (w/w dry biomass), an optimised extraction scenario of 0.2% was evaluated, reflecting literature benchmarks where yields up to approximately 0.5% have been successfully demonstrated for the same seaweed species [228]. Additionally, 0.01, 0.1, 0.15% extraction yields were assessed.

10.2.8 Life cycle assessment

A life cycle assessment (LCA) of the biorefinery process was performed according to the guidelines of ISO 14040 and 14044.

10.2.8.1 Goal and scope

The primary objective of this attributional LCA was to evaluate whether the novel multi-product biorefinery configuration, simultaneously isolating fucoidan, alginate, and fucoxanthin, demonstrates a superior environmental sustainability profile compared to the conventional industrial acid-alkaline extraction chain that explicitly yields standard sodium alginate.

To ensure an equitable benchmark between the structurally distinct products, a performance-based functional unit (FU) was established. The FU is defined as 1 kg sodium alginate with enhanced thickening performance, expressed as consistency index (*K*) as reported [48]. Specifically, the alginate exhibited at least a 10-fold higher thickening capacity than that obtained by conventional acid-alkaline extraction from the same batch of biomass.

For the LCA, a cradle-to-gate approach was adopted, the geographical scope considers the Netherlands. The defined system boundaries encompass the upstream

operations, including seaweed cultivation under future conditions, harvesting, and transportation to the facility as well as biorefinery chain as further detailed in the previous sections, i.e. citric acid pretreatment, the biphasic and alkaline extraction stages, and the subsequent downstream purification modules, including wastewater and solid waste treatment processes for the generated effluents. Since the products have various potential end-uses, the downstream product utilization including end-of-life have been excluded.

10.2.8.2 Life cycle inventory and impact assessment

For *S. latissima* cultivation linear scaling was applied to the LCI for the future scenario cultivation and harvesting reported by Slegers *et al*. [427], while energy inputs for drying and grinding were collected from SuperPro Designer. The biorefinery process models and mass-energy balances were based on the SuperPro flowsheet simulations, including direct emissions of oxygen, nitrogen, carbon dioxide and water vapour. The background data were derived from Ecoinvent 3.8. Proxy compounds were used for betaine (based on reaction stoichiometry using trimethylamine and chloroacetic acid), octanoic acid (fatty acids from coconut oil), dodecanoic acid (fatty acids from coconut oil), levulinic acid (succinic acid) and choline chloride (trimethylamine), representing similar production processes and chemical structures. Wastewater treatment was approximated using a 50%-50% mix of wastewater treatment of vegetable oil refineries and potato starch production. The inputs for membrane production and cleaning were considered to fully account for the membranes' impact on the process. Details are provided in the Appendix.

The conventional process uses a combination of acidification and alkaline extraction, followed by microfiltration, ethanol precipitation, dewatering and subsequent purification to obtain sodium alginate. This process was modelled following Nazemi *et al.* [428]. The process description is detailed in the Appendix.

The LCA was implemented and characterised using SimaPro software (Desktop version 10.4). Environmental impacts were quantified across 18 midpoint impact categories using the ReCiPe 2016 Midpoint v1.09 methodology, applying the standard hierarchist perspective based on consensus-based characterization pathways. The evaluated impact categories comprised: Global Warming; Stratospheric Ozone Depletion; Ionising Radiation; Ozone Formation (Human Health); Fine Particulate Matter Formation; Ozone Formation (Terrestrial Ecosystems); Terrestrial Acidification; Freshwater Eutrophication; Marine Eutrophication; Terrestrial Ecotoxicity; Freshwater Ecotoxicity; Marine Ecotoxicity; Human Carcinogenic Toxicity; Human Non-Carcinogenic Toxicity; Land Use; Mineral Resource Scarcity; Fossil Resource Scarcity;

and Water Consumption. Following the comparative baseline assessment against the conventional benchmark, a detailed contribution analysis was executed to isolate which specific internal processing sub-sections within the novel biorefinery dominate the environmental footprint across each of the 18 impact parameters.

10.3. Results and discussion

10.3.1 Is the current biorefinery economically feasible?

The economic evaluation estimated a total capital investment of €135.9 million, with annual operating costs of €70.9 million. Under the simulated production capacity, the process generated 40.2 million €/year in total revenues, resulting in a negative gross margin of -76.3%, and a negative net present value (NPV) of -263.1 million € (**Figure 10.3**). Furthermore, the annual production comprised approximately 265.7 t of alginate, 94.8 t of fucoidan, and 228 kg of high-purity fucoxanthin. Assuming the same selling price for all alginate fractions (€10 kg^{-1}), alginate generated €2.66 million $year^{-1}$, representing only 6.6% of the total revenue despite accounting for the vast majority of the product mass (73.7%). In contrast, fucoidan and fucoxanthin together generated €37.56 million $year^{-1}$, corresponding to 93.4% of the total process revenue, with fucoidan contributing €28.43 million $year^{-1}$ (70.7%) and fucoxanthin €9.13 million $year^{-1}$ (22.7%). This highlights the importance of product value rather than production volume in an integrated approach.

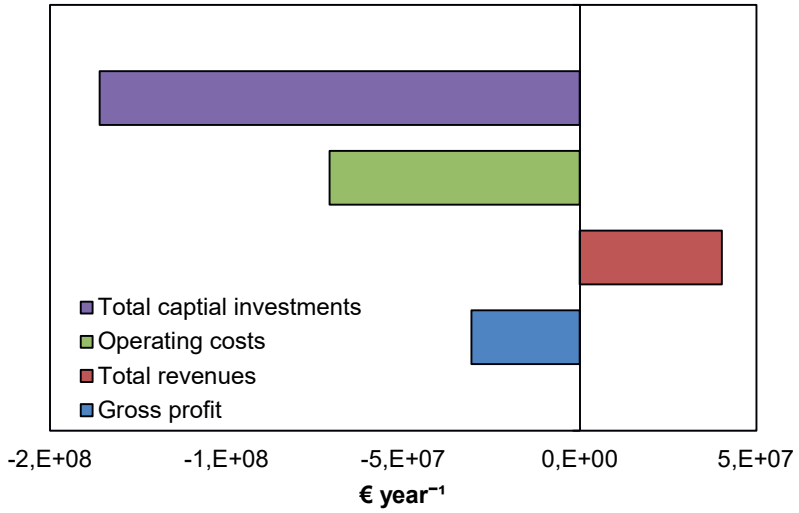


Figure 10.3 Financial summary of the multiproduct biorefinery including the annual gross profit, revenue, operating cost and total capital investment.

Under the evaluated assumptions, the proposed process was not economically feasible. This finding is consistent with the current state of DES-based biorefineries, where commercial feasibility generally depends on process optimisation rather than solvent substitution alone [408, 411]. In addition, recent reviews identify solvent

recovery, coproduct valorisation and pretreatment performance as the principal factors determining economic viability.

The revenue distribution further highlights the importance of multiproduct valorisation (**Figure 10.4**). Producing alginate alone would likely be insufficient to offset the high capital and operating costs associated with biomass processing. The incorporation of high-value co-products substantially increases the revenue potential of the process and represents the primary economic driver, as demonstrated by the contribution of fucoidan and fucoxanthin. This observation agrees with previous techno-economic studies demonstrating that DES-based biorefineries become economically attractive primarily through multiproduct valorisation. Kumar *et al*. [417], for example, identified lignin as the major contributor to process revenue in a NADES biorefinery, while Zang *et al*. [429] similarly showed that coproduct generation substantially improved the economic feasibility of a DES-pretreated lignocellulosic biorefinery. Nevertheless, it is worth noting that the alginate selling price used in the model (€10 kg^{-1}) was deliberately conservative and does not account for the enhanced viscosity observed when using the BU DES system [48]. Since viscosity is one of the main quality attributes determining the commercial value of alginate [56, 430], the production of a higher-viscosity alginate could justify a higher market price, consequently improving the economic performance of the proposed biorefinery.

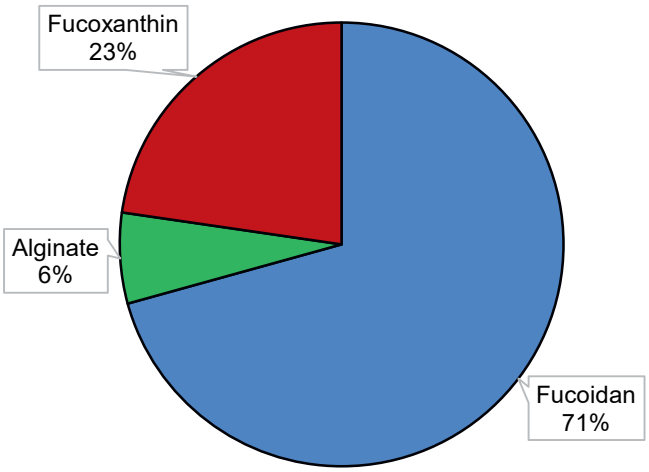


Figure 10.4 Revenue distribution of the multiproduct biorefinery using a biphasic system.

10.3.2 Main OPEX and material contributions

The annual operating expenditure (OPEX) of the proposed process was primarily dominated by raw material consumption (**Figure 10.5a**). Total raw material costs amounted to EUR 29.8 million year^{-1}, representing 46% of the total annual operating costs, followed by facility-dependent costs (18%) and depreciation (18%). This indicates that the economic performance of the process is governed predominantly by solvent and reagent consumption rather than utilities or labour.

A detailed breakdown of the raw material costs (**Figure 10.5b**) revealed that betaine and dodecanoic acid were the largest individual cost contributors, accounting for 48% (EUR 14.3 million year^{-1}) and 25% (EUR 7.5 million year^{-1}) of the annual raw material costs, respectively. Their dominant contribution can be attributed to the combination of relatively high market prices (approximately EUR 2.40 kg^{-1} for betaine and EUR 3.00 kg^{-1} for dodecanoic acid) and the large solvent quantities required during the biphasic extraction process.

The particularly high contribution of betaine is largely a consequence of the current process configuration, in which the betaine:urea (BU) DES is used only five times as extraction and the process generates losses during recovery. As a result, fresh DES must be supplied continuously, substantially increasing the annual raw material demand. BU recycling modelling is difficult due to limitations in SuperPro Designer regarding impurity accumulation. It remains unknown how the chemical composition of the DES matrix changes upon repeated recycling cycles. Buildup of co-extracted compounds such as polyphenols and residual polysaccharides could alter solvent properties and alginate extraction yields, which introduces high model uncertainty. Previous studies, however, have confirmed that recovery and reuse of betaine:urea DES is technically feasible. Hiemstra *et al*. (2025) [335] demonstrated DES recovery using a temperature-responsive aqueous two-phase system (ATPS), enabling simultaneous alginate separation and recycling of both the DES and thermo-responsive polymer. Subsequently, another study by Hiemstra *et al*. (2026) [384] reported a DES-salt ATPS that enabled direct interfacial precipitation of alginate while allowing DES reuse, whereas Elizondo Sada *et al*. [271] demonstrated the potential of pressure-driven membrane processes for simultaneous DES and alginate recovery.

Collectively, these studies indicate that integration of a DES recovery step is technically achievable and could reduce raw material consumption. Nevertheless, incorporating solvent recycling would require additional downstream separation operations, increasing equipment requirements and capital investment. Therefore, the

economic benefit of reduced solvent consumption should be evaluated against the additional capital and operating costs associated with solvent recovery technologies.

Besides solvent recycling, another important opportunity for reducing raw material costs is decreasing the solvent-to-liquid (S/L) ratio. The current process employs an experimentally optimised S/L ratio of 1:60, which was selected to maximise extraction performance at laboratory scale. However, such a high solvent loading is not optimal for industrial implementation. Consequently, reducing the S/L ratio represents a promising strategy for improving process economics and was therefore further evaluated in the sensitivity analysis.

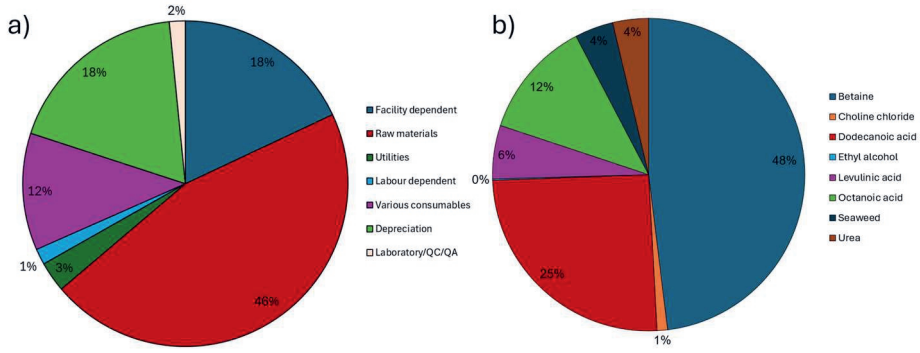


Figure 10.5 Overview of (**a**) annual operating costs breakdown and (**b**) annual raw material costs breakdown.

10.3.3 Sensitivity analysis

10.3.4 Solid to liquid ratio

As indicated previously, the major operating costs originate from the solvent components, particularly the BU fractions. Consequently, reducing the solvent-to-liquid ratio (SLR) would be expected to improve the economic performance of the process. To evaluate this effect, additional scenarios with SLRs of 1:40 and 1:20 were simulated, and the operational cost and the total revenue (**Figure 10.6**, together with the NPV (**Figure 10.7**) were used as indicators. Interestingly, only increasing the SLR to 1:20 reverted the difference between the operation costs and the total revenue, resulting in a positive NPV (€20 million). This improvement reflects the more efficient utilization of the solvent (less units per unit of product), which increases the effective processing capacity of the biorefinery and, consequently, the production of alginate, fucoidan, and fucoxanthin, leading to higher total revenues. However, this scenario represents an idealised assumption that does not account for the thermodynamic and transport limitations expected at higher biomass loadings. The affinity of the DES

towards the extracted polymers imposes a finite solubilization capacity, meaning that extraction efficiency is unlikely to increase linearly with SLR. Furthermore, increasing the biomass concentration would substantially increase the viscosity of the mixture. Given the already high viscosity of the BU system, this effect would likely hinder mass transfer and reduce extraction efficiency, ultimately limiting the practical implementation of such high SLRs.

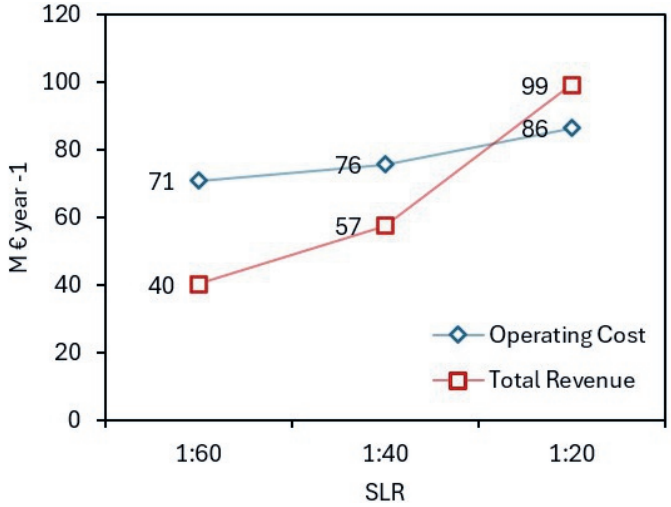


Figure 10.6 Operating costs and total revenue (M€ per year) at different simulated SLR.

It is well known that the remarkable solvent properties of DES arise from their extensive hydrogen-bonding network. However, this same characteristic also represents one of their main drawbacks, as it leads to high viscosities [9, 14]. Therefore, from an operational perspective, identifying or designing DES with a high affinity towards alginate while maintaining a low viscosity remains one of the major challenges in the development of DES-based alginate extraction processes.

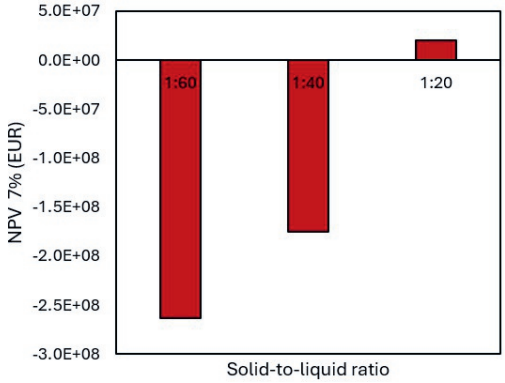


Figure 10.7 NPV (7% discount rate) for scenarios of SLR of 1:60, 1:40 and 1:20.

10.3.4.1 Alginate price

Compared to the other recovered seaweed compounds, alginate has a relatively low unit market price. However, its commercial value strongly depends on its rheological properties, particularly viscosity. To evaluate the influence of product quality on the economic performance of the process, different scenarios were simulated by increasing the alginate selling price from €10 to €200 kg^{-1} (**Figure 10.8**). Interestingly, despite alginate representing the largest fraction of the recovered biomass, its contribution to the total revenue remained limited until prices approached €200 kg^{-1}. Nevertheless, such a selling price is not unrealistic. High-purity alginates with tailored functional properties are known to command considerably higher market values due to their performance in specialized applications [431]. Considering the approximately tenfold increase in viscosity observed for the alginate extracted with the BU system [48], this product could potentially be positioned within this higher-value market segment, substantially increasing its contribution to the overall process revenue.

An additional advantage of the proposed biorefinery is that the extraction sequence inherently removes and valorises compounds that would otherwise be considered impurities in a conventional alginate production process, such as fucoidan and fucoxanthin [432, 433]. As a result, the subsequent alginate extraction is expected to produce a cleaner product while simultaneously generating value from fractions that are typically discarded, further enhancing the economic potential of the integrated process.

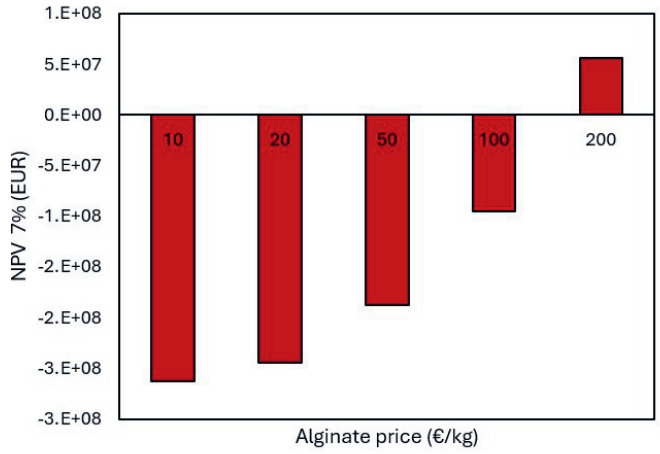


Figure 10.8 NPV (7% discount rate) obtained after simulating scenarios with different alginate prices.

10.3.4.2 Fucoxanthin yield

The economic performance of the proposed biorefinery was found to be highly sensitive to the fucoxanthin recovery yield. In the base-case scenario, a fucoxanthin yield of 0.02% (w/w dry biomass) was assumed, based on the performance reported for a TPP extraction system, although this system was focused on optimising the alginate extraction yield.

Previous studies demonstrated that considerably higher fucoxanthin yields are achievable under alternative extraction conditions. Martins *et al*. [228] reported fucoxanthin yields of approximately 0.5% (w/w dry biomass) from the same seaweed (*S. Latissima)* using an ionic liquid-based extraction system. Although direct comparison between the two processes should be made with caution, these findings indicate that substantial improvements in fucoxanthin recovery may still be possible through experimental optimisation of the biphasic system.

To evaluate the economic impact of a potential improved pigment yield, a sensitivity analysis was performed assuming enhanced fucoxanthin yields of 0.05, 0.1, 0.15 and 0.2% (w/w dry biomass) (**Figure 10.9**). These values remain below the highest yields reported in the literature while representing a technically plausible yield through process optimisation. Under these scenarios, the NPV increased from – 263 € million year^{-1} in the base case to + 225 million € year^{-1}, being the critical yield ~0.1 %DW; demonstrating that fucoxanthin recovery is an important influential parameter governing overall process profitability.

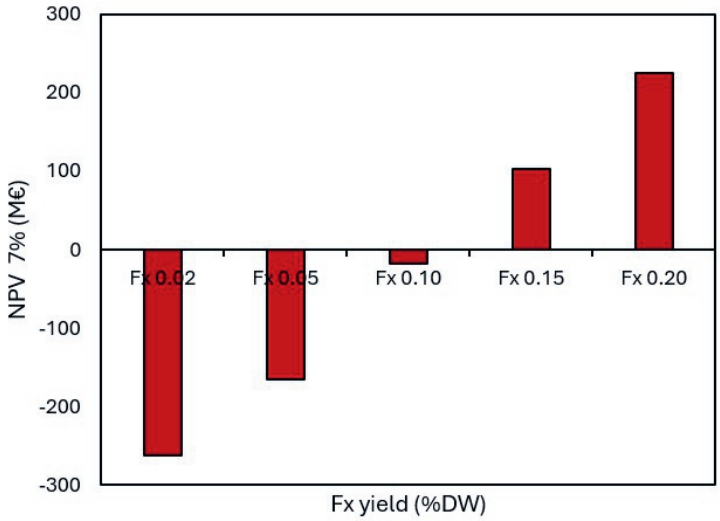


Figure 10.9 Sensitivity of the net present value (NPV, 7% discount rate) for the fucoxanthin yield.

These results highlight that economic feasibility is strongly dependent on the efficient recovery of high-value co-product fucoxanthin rather than alginate. Consequently, further optimisation of fucoxanthin extraction should be regarded as a key priority for improving the commercial viability of the process.

10.3.5 TEA overview

Overall, the sensitivity analyses demonstrate that the economic viability of the proposed biphasic system can primarily be influenced by three process parameters: solvent consumption, alginate product value, and fucoxanthin recovery. Reducing the solid-liquid ratio decreases raw material costs, while increasing the market value of alginate through the production of higher-value grades further improves the economic performance. However, the analysis identifies fucoxanthin recovery as the most influential parameter, with 10-fold improvements in fucoxanthin yield resulting in the largest increase in profitability and converting the process from an economically unfeasible to a feasible scenario. Consequently, future process optimisation should prioritise enhancing fucoxanthin extraction while simultaneously reducing solvent consumption and maximising the value of the recovered alginate through its improved functionality, as these combined improvements could impact on the overall techno-economic feasibility of the proposed biorefinery system.

Interestingly, these three parameters; solvent consumption, coproduct valorisation and solvent recovery, correspond closely to the principal economic drivers identified in recent reviews of DES biorefineries [408, 434]. The present study expands this framework by identifying product functionality as an additional design parameter that should be incorporated into future techno-economic assessments of emerging extraction technologies.

10.3.6 Environmental impact of DES-based versus conventional process

To evaluate whether the proposed DES-based multiproduct biorefinery represents an environmentally favourable alternative to conventional seaweed processing, the environmental impacts of the integrated process were compared with those of the conventional alkaline extraction process used for sodium alginate production. A worst-case perspective was taken, allocating 100% of the cultivation and biorefinery impacts to the produced alginate.

Figure 10.10 presents the midpoint impact categories, with the maximum impact fixed at 100% for each indicator. Overall, the DES-based biorefinery reduced the environmental burden in 16 out of the 18 evaluated impact categories. The largest improvements were observed for global warming potential, ionising radiation, and fossil resource scarcity, while water consumption decreased by approximately 94%. These reductions demonstrate that integrating selective extraction can substantially improve the environmental performance of seaweed processing.

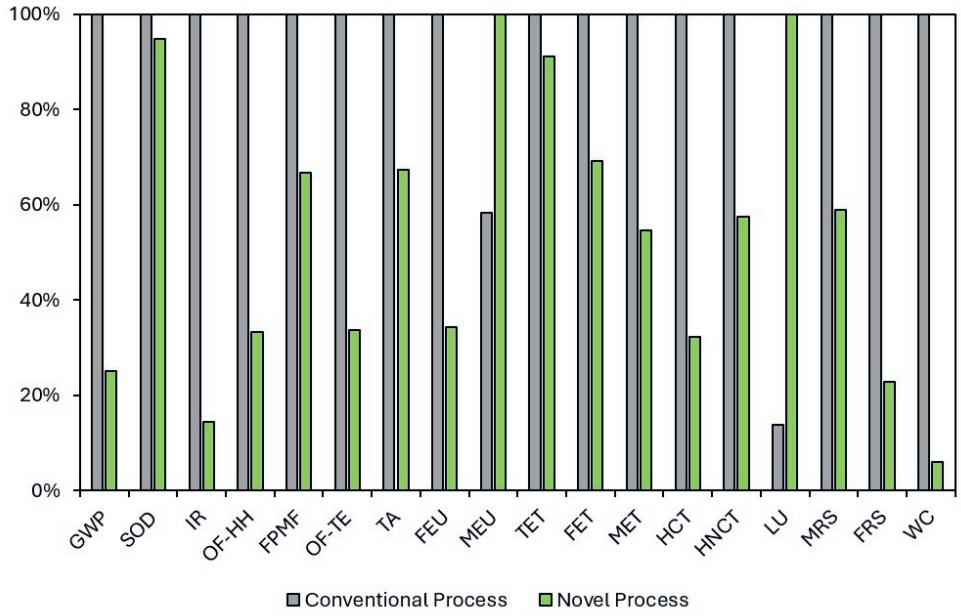


Figure 10.10 Midpoint impact assessment comparing the novel with the conventional process when the FU is the production of alginate with a thickening performance equivalent to 10 times the one obtained with the conventional process. Eighteen midpoint impact categories are shown on the x-axis, while the y-axis represents the relative contribution of each process step to the total environmental impact. Abbreviations: GWP—Global Warming Potential; SOD—Stratospheric Ozone Depletion; IR—Ionizing Radiation; OF-HH—Ozone Formation (Human Health); FPMF—Fine Particulate Matter Formation; OF-TE—Ozone Formation (Terrestrial); TA—Terrestrial Acidification; FEU—Freshwater Eutrophication; MEU—Marine Eutrophication; TET—Terrestrial Ecotoxicity; FET—Freshwater Ecotoxicity; MET—Marine Ecotoxicity; HCT—Human Carcinogenic Toxicity; HNCT—Human Non-Carcinogenic Toxicity; LU—Land Use; MRS—Mineral Resource Scarcity; FRS—Fossil Resource Scarcity; WC—Water Consumption.

The DES-based biorefinery exhibited higher impacts for marine eutrophication and land use compared to conventional alginate extraction. Process contribution analysis (**Figure 10.11**) showed that these categories were dominated by the production of the fatty acids used to prepare the hydrophobic DES, followed by the production of betaine and urea (**Figure 10.12**). In contrast, electricity, steam, cooling water and direct

process emissions contributed only marginally across most impact categories. These results indicate that the environmental performance of the proposed biorefinery is governed primarily by the production of solvent constituents rather than by the extraction process itself. This observation is consistent with recent life cycle studies demonstrating that the environmental performance of DES-assisted processes depends largely on solvent composition, recovery strategy, and overall process integration [162, 210, 416, 434]. Previous LCAs have similarly shown that the manufacture of DES constituents generally dominates the environmental footprint of DES-based extraction processes, whereas the energy required for solvent preparation contributes only a minor share [162, 210].

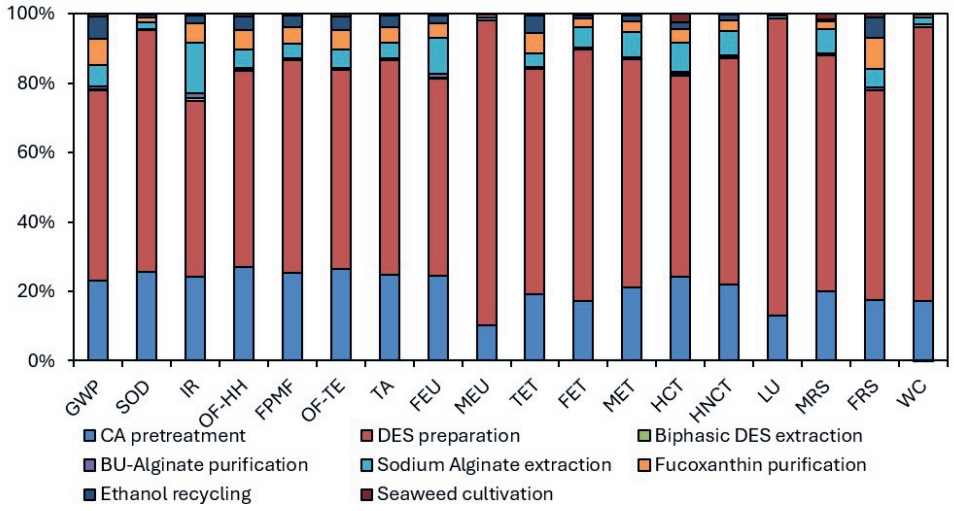


Figure 10.11 Midpoint impact assessment of the novel process based on the characterization of individual process steps across 18 midpoint impact categories. Midpoint indicators are presented on the x-axis, while the y-axis shows the relative contribution of each process step to the overall process impact. Abbreviations: GWP—Global Warming Potential; SOD—Stratospheric Ozone Depletion; IR—Ionizing Radiation; OF-HH—Ozone Formation (Human Health); FPMF—Fine Particulate Matter Formation; OF-TE—Ozone Formation (Terrestrial); TA—Terrestrial Acidification; FEU—Freshwater Eutrophication; MEU—Marine Eutrophication; TET—Terrestrial Ecotoxicity; FET—Freshwater Ecotoxicity; MET—Marine Ecotoxicity; HCT—Human Carcinogenic Toxicity; HNCT—Human Non-Carcinogenic Toxicity; LU—Land Use; MRS—Mineral Resource Scarcity; FRS—Fossil Resource Scarcity; WC—Water Consumption.

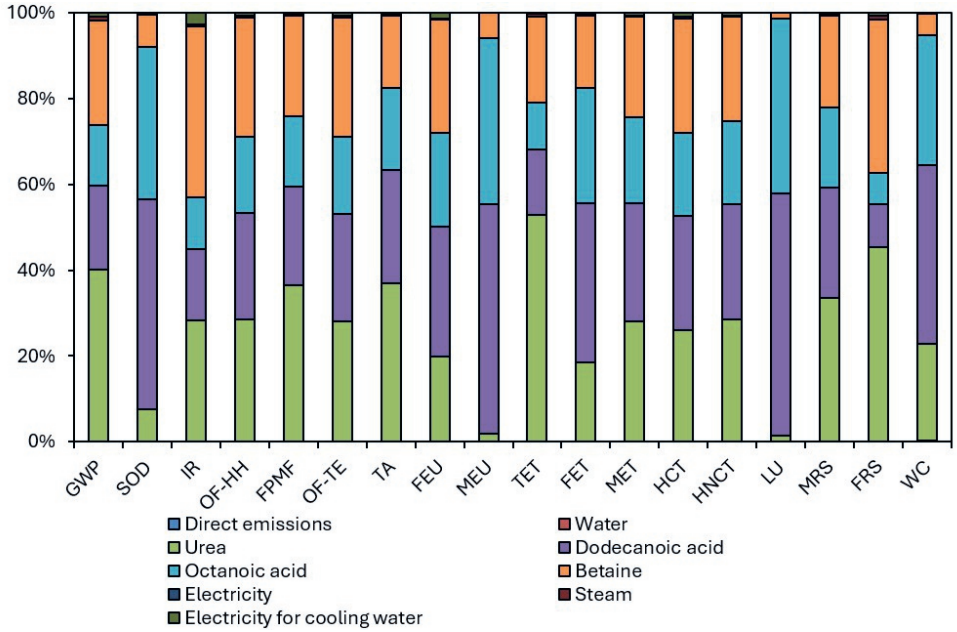


Figure 10.12 Detailed contribution in BU & FA DES preparation step across 18 midpoint impact categories. Fatty acids from coconut oil were assumed to be proxies of dodecanoic acid and octanoic acid. Midpoint indicators are presented on the x-axis, while the y-axis shows the relative contribution of each process step to the overall process impact. Abbreviations: GWP—Global Warming Potential; SOD—Stratospheric Ozone Depletion; IR—Ionizing Radiation; OF-HH—Ozone Formation (Human Health); FPMF—Fine Particulate Matter Formation; OF-TE—Ozone Formation (Terrestrial); TA—Terrestrial Acidification; FEU—Freshwater Eutrophication; MEU—Marine Eutrophication; TET—Terrestrial Ecotoxicity; FET—Freshwater Ecotoxicity; MET—Marine Ecotoxicity; HCT—Human Carcinogenic Toxicity; HNCT—Human Non-Carcinogenic Toxicity; LU—Land Use; MRS—Mineral Resource Scarcity; FRS—Fossil Resource Scarcity; WC—Water Consumption.

Because no dedicated life cycle inventories are currently available for dodecanoic acid and octanoic acid, coconut oil-derived fatty acids were used as proxy datasets. Consequently, the reported impacts largely reflect the environmental burdens associated with producing these solvent components. These findings emphasize that solvent selection should be based not only on extraction efficiency but also on the environmental impacts associated with solvent synthesis and production [37, 416]. Accordingly, selecting lower-impact solvent constituents, reducing solvent demand, and improving solvent recovery and reuse are expected to provide the greatest reductions in environmental impact.

Besides solvent production, the citric acid pretreatment represented the second largest environmental hotspot, contributing approximately 10–30% of the total impacts depending on the midpoint category (**Figure 10.13**). By comparison, alginate purification, fucoxanthin purification, ethanol recycling, and *Saccharina latissima* cultivation contributed relatively little across most impact categories. Similarly, ultrafiltration and diafiltration, membrane cleaning, electricity, steam, and wastewater treatment accounted for only minor contributions. These results indicate that pretreatment chemistry constitutes the second major opportunity for process improvement. Reducing fresh citric acid consumption through recovery and reuse or by adopting lower-impact pretreatment strategies is therefore expected to deliver substantially greater environmental benefits than further improvements in process energy efficiency. This finding is consistent with previous LCAs of biomass and seaweed biorefineries, which identify reagent production and consumption, rather than the extraction operations themselves, as the dominant contributors to environmental impacts [422, 435, 436].

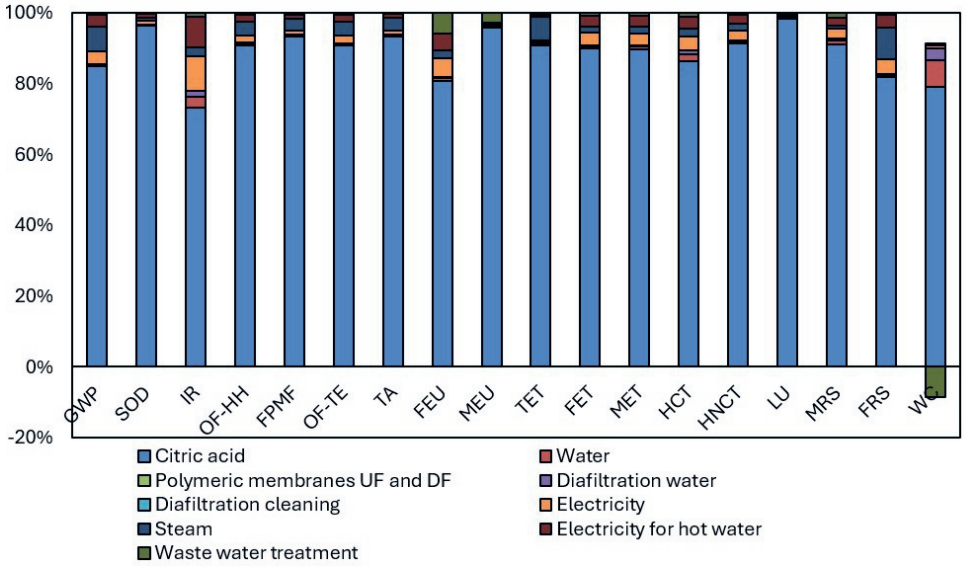


Figure 10.13 Detailed contribution in the CA pretreatment step process steps across 18 midpoint impact categories. Midpoint indicators are presented on the x-axis, while the y-axis shows the relative contribution of each process step to the overall process impact. Abbreviations: GWP—Global Warming Potential; SOD—Stratospheric Ozone Depletion; IR—Ionizing Radiation; OF-HH—Ozone Formation (Human Health); FPMF—Fine Particulate Matter Formation; OF-TE—Ozone Formation (Terrestrial); TA—Terrestrial Acidification; FEU—Freshwater Eutrophication; MEU—Marine Eutrophication; TET—Terrestrial Ecotoxicity; FET—Freshwater Ecotoxicity; MET—Marine Ecotoxicity; HCT—Human Carcinogenic Toxicity; HNCT—Human Non-Carcinogenic Toxicity; LU—Land Use; MRS—Mineral Resource Scarcity; FRS—Fossil Resource Scarcity; WC—Water Consumption.

The lower environmental impacts observed for the DES-based biorefinery differ from several recent comparative LCAs, in which DES-assisted extraction exhibited higher environmental burdens than conventional ethanol- or water-based processes due to the impacts associated with solvent synthesis [210, 211, 422, 437, 438]. Conversely, Wang *et al*. [422] demonstrated that DES-based lignocellulosic pretreatment can outperform conventional technologies when solvent recovery and process integration are incorporated into the process design.

An important aspect of the present assessment is the use of a functional unit based on equivalent thickening performance rather than product mass. Because the DES-extracted alginate exhibited higher viscosity, a smaller quantity of product was required to achieve the same functionality, resulting in lower environmental impacts per functional unit. This finding demonstrates that improvements in product quality can directly influence the environmental performance of biorefineries and highlights the importance of selecting functional rather than mass-based functional units when processing technologies modify material properties. Assessing products solely on a mass basis may therefore underestimate the environmental benefits associated with enhanced functionality.

10.3.7 Process overview and outlook

Interestingly, the environmental hotspots closely mirror the economic hotspots identified in the techno-economic assessment, where DES constituents also dominated the raw material costs (96%). Together, the TEA and LCA therefore identify solvent demand as the principal design parameter governing both the economic and environmental sustainability of DES-based biorefineries. This convergence suggests that strategies aimed at reducing solvent consumption, improving solvent regeneration and extending solvent lifetime are likely to deliver simultaneous economic and environmental benefits. A similar trend has recently been highlighted in holistic sustainability assessments of DES-based biomass processing, where solvent demand consistently emerged as the primary driver influencing both production costs and environmental impacts [434]. The present work extends these observations by demonstrating that this relationship also holds for an integrated multiproduct seaweed biorefinery and by highlighting the additional importance of product functionality as a process design parameter.

The combined techno-economic and environmental assessments demonstrate that the implementation of DES-based biorefineries requires a broader process perspective than simply replacing conventional solvents with DES. While the integrated

multiproduct concept showed clear environmental advantages over the conventional alkaline extraction route, both assessments indicate that the overall sustainability of the process is governed by a limited number of interconnected process parameters and not by the extraction technology itself.

One of the most important observations is the convergence between the TEA and LCA results. Both analyses independently identified solvent production and consumption as the dominant process bottlenecks. This suggests that future process development should prioritize reducing fresh solvent demand through lower solvent-to-liquid ratios, improved solvent affinity, or more efficient regeneration strategies. Such improvements are expected to simultaneously reduce operating costs and environmental impacts.

The results also highlight the importance of considering product characteristics (functionality) during process development. Most of current extraction technologies are typically evaluated based on extraction yield, whereas the present work indicates that product functionality may become equally important for industrial implementation. The higher viscosity obtained for DES-extracted alginate illustrates how preserving functional properties may increase product value without necessarily increasing production volumes. Future assessments should therefore integrate product functionality alongside extraction efficiency when evaluating emerging extraction technologies.

Finally, this study raises an important aspect regarding solvent recyclability. However, the present results suggest that increasing the number of recycling cycles alone is insufficient to evaluate solvent sustainability. Future studies should investigate how repeated use influences solvent composition, the accumulation of co-extracted compounds and, ultimately, product functionality. Such knowledge will be essential for designing regeneration strategies that maximise both solvent lifetime and extraction performance. Current literature generally reports the percentage of solvent recovered or the number of successful recycling cycles. However, these indicators alone may not adequately describe the long-term performance of DES systems. During repeated operation, changes in solvent composition caused by the accumulation of co-extracted compounds or degradation products may gradually alter extraction behaviour and downstream separation efficiency [384]. Consequently, future research should not only investigate how often DES can be recycled, but also how their physicochemical properties evolve during repeated use and how these changes influence extraction performance and product quality.

Overall, the framework presented in this study demonstrates how integrated TEA and LCA can be used to identify the critical process parameters that govern the industrial implementation of DES-based biorefineries. Although demonstrated here for a seaweed biorefinery, the same approach can support the development of DES-based fractionation processes for other biomass resources by guiding research towards the process variables with the greatest impact on both economic and environmental performance.

10.4. Conclusion

This study presents one of the first integrated techno-economic and environmental assessments of a DES-based multiproduct seaweed biorefinery. By combining industrial process simulation with TEA and LCA, the key factors governing the industrial implementation of DES-based biorefineries were identified and addressed. The results demonstrated that although the proposed DES-based biorefinery reduced the environmental impact compared with conventional alkaline alginate extraction, it was not economically feasible under the baseline assumptions for the production of commodity-grade alginate. Product functionality also emerged as an essential design parameter, indicating that improving the value of recovered alginate may have a greater impact on overall process feasibility than maximising extraction yield alone. Furthermore, both the TEA and LCA identified DES production and solvent consumption as the principal process bottlenecks, highlighting the importance of minimising solvent demand while maximising solvent recovery and regeneration.

Finally, future research should move beyond demonstrating solvent recyclability towards understanding solvent functionality during repeated reuse. Investigating changes in solvent composition, impurity accumulation, recovery efficiency, and regeneration strategies will be essential for developing economically viable and environmentally sustainable DES-based biorefineries. Ultimately, successful industrial implementation of DES-based biorefineries will depend not only on the development of high-performance solvents, but on integrated process engineering in which solvent design, circularity, and product functionality are optimised simultaneously.

10.5. Supplementary information

Table S10.1 Raw materials' cost in (€ kg $^{-1}$).

Raw Materials	Unit Cost (€ kg $^{-1}$)	Source
Betaine	2.40	(*Cocamidopropyl Betaine Supplier Guide: Top Chinese Manufacturers for B2B Buyers*, n.d.)
Citric acid	1.70	(*Global Citric Acid Price | Tridge*, n.d.)
Choline chloride	1.20	(*Choline Chloride 50% (Feed)	25 Kg, Bulk	Wholesale Prices at FDCM*, n.d.)
Dodecanoic acid	7.00	Henan Ruidea Industry Co., Ltd. (2026)
Ethyl alcohol	1.10	(Ethanol Price Index – Business analytiq, n.d.)
Levulinic acid	3.70	(*Levulinic Acid Market Size, Production, Average Price*, n.d.)
Sodium carbonate	0.45	(*China Battery-Grade Sodium Carbonate, Price of Sodium-Ion Battery Per Ton Today, Sodium-Ion Battery Prices Charts - Shanghai Metals Market (SMM)*, n.d.)
Sodium chloride	0.17	(*Soda Ash Price - Current & Forecasts | Intratec.Us*, n.d.)
Octanoic acid	2.00	(*Wholesale N-Capylic Acid Octanoic Acid Cas 124-07-2 Caprylic Acid*, n.d.)
Seaweed	0.80	(Paul *et al.*, 2024)
Urea	0.38	(Urea Price Index – Business analytiq, n.d.)
Water	0.004	(*Water Rates Are Rising across Europe: How Can Property Owners Prepare? | Smartvatten*, n.d.)

Table S10.2 Executive summary of the economic analysis.

Total capital investment	€135.9 million
Operating costs	€70.9 million
Total revenues	€40.2 million
Gross margin	-76.25%
ROI	-13.75%
NPV	€-263.1 million

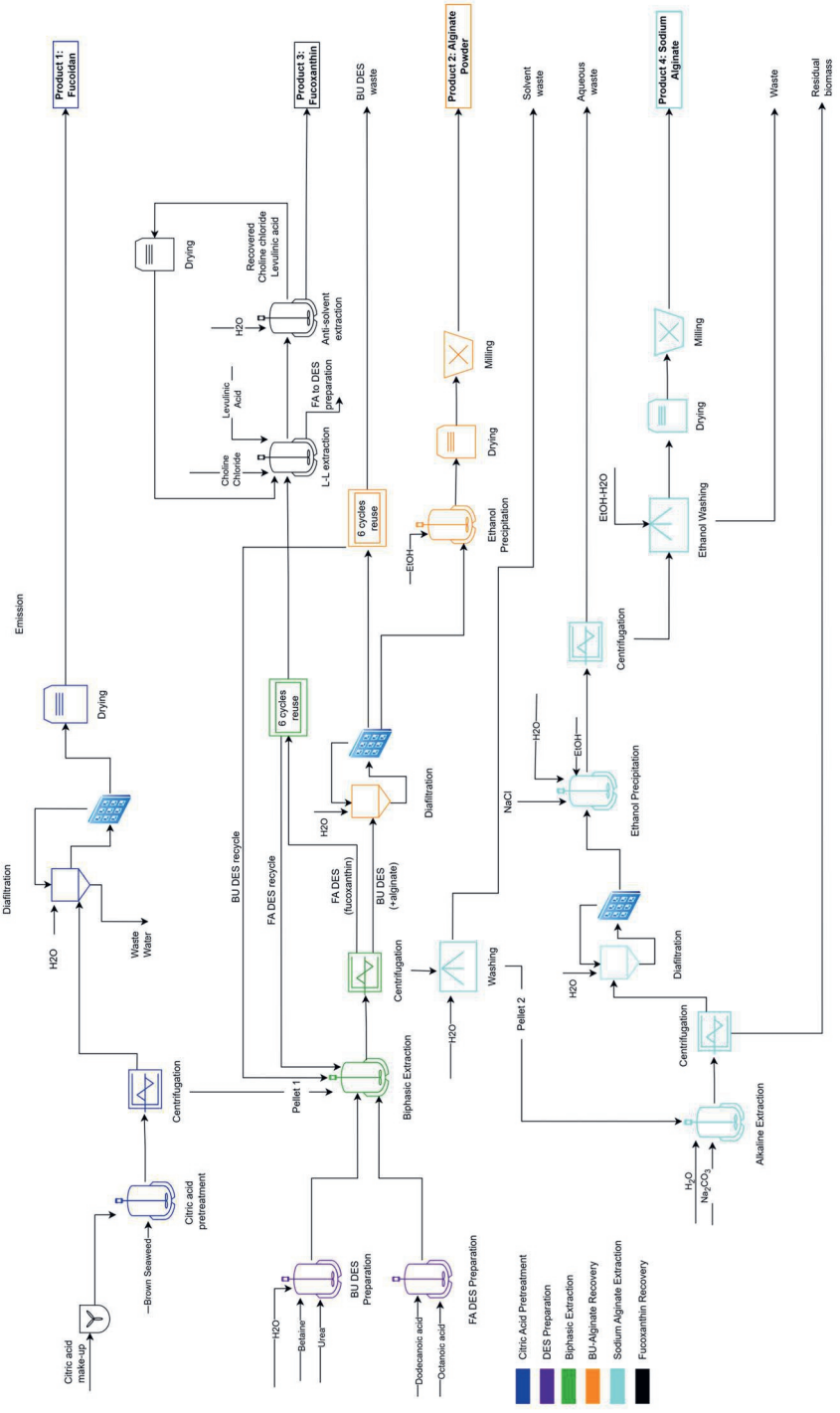


Figure S10.1 Multiproduct seaweed biorefinery flowsheet.

Life cycle inventory

Table S10.3 Background data obtained from Ecoinvent 3.8.

Input		
Seaweed	Saccharina *latissima*	[427]
Citric acid	Citric acid {GLO}| market for | APOS, S	
Water	Water, deionised, from tap water, at user {Europe without Switzerland}| market for water, deionised, from tap water, at user | APOS, S	
NaOH	Sodium hydroxide, without water, in 50% solution state {GLO}| market for | APOS, S	
HCl	Hydrochloric acid, without water, in 30% solution state {RER}| market for | APOS, S	
Urea	Urea, as N {GLO}| market for | APOS, S	
Dodecanoic acid proxy	Fatty acid {RER}| fatty acid production, from coconut oil | APOS, S	
Octanoic acid proxy	Fatty acid {RER}| fatty acid production, from coconut oil | APOS, S	
Betaine proxy		Amount based on reaction stoichiometry
	Trimethylamine {RER}| market for trimethylamine | APOS, S	
Betaine proxy		Amount based on reaction stoichiometry
	Chloroacetic acid {RER}| market for chloroacetic acid | APOS, S	
$Na(CO_3)_2$	Sodium bicarbonate {GLO}| market for sodium bicarbonate | APOS, S	
NaCl	Sodium chloride, powder {GLO}| market for | APOS, S	
Ethanol	Ethanol, without water, in 99.7% solution state, from ethylene {RER}| market for ethanol, without water, in 99.7% solution state, from ethylene | APOS, S	
Levulinic acid proxy	Succinic acid {GLO}| market for succinic acid | APOS, S	
Choline chloride proxy	Trimethylamine {RER}| market for trimethylamine | APOS, S	[127]
Electricity	Electricity, medium voltage {NL}| market for | APOS, S	
Steam	Steam, in chemical industry {GLO}| market for | APOS, S	

Water water treatment	Wastewater from vegetable oil refinery {GLO}| market for | APOS, S
Water water treatment	Wastewater from potato starch production {GLO}| market for | APOS, S
Direct emission	Oxygen (g)
Direct emission	Nitrogen, atmospheric (g)
Direct emission	Carbon dioxide (g)
Direct emission	Water (g)

In industrial membrane synthesis, polymeric membranes are typically produced by a combination of synthetic polymers, mostly polyesters due to the high stability for large scale applications and polyethylene when pore structure is important (Tan & Rodrigue, 2019). Due to the extensive use of these materials for membrane synthesis, a membrane composition of 85 % polyester and 15 % polyethylene by mass was assumed for the polymeric membrane dataset.

Table S10.4 Polymeric membrane dataset: Material and energy inputs for 1kg membrane synthesis. Emissions and waste streams are neglected.

Ecoinvent 3.5 background process	Value	Unit
Polyester-complexed starch biopolymer {RER}| production | APOS, S	0.8785	kg
Polyethylene, low density, granulate {RER}| production| APOS,S	0.1785	kg
Electricity, medium voltage {NL}| market for | APOS, S	0.33	kWh
Heat, from steam, in chemical industry {RER}| market for heat, from steam, in chemical industry | APOS, S	2	MJ

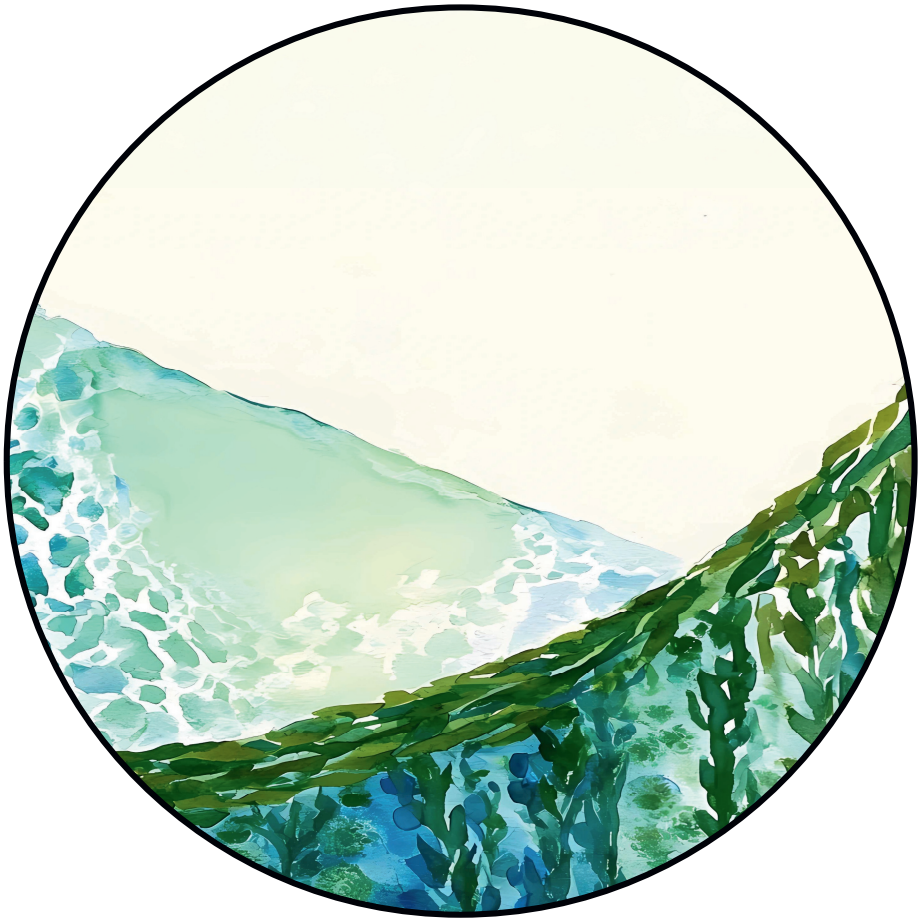
The operational inputs associated with membrane maintenance were also considered. Specifically, the consumption of water and cleaning chemicals required for membrane cleaning. For maintaining the membrane performance, cleaning-in-place (CIP) was assumed to take place after the completion of each batch. For organic fouling, an alkaline mixture of NaOH 0.1% (w/v) (corresponding to 0.025M NaOH) was selected, while for inorganic colloidal fouling, an acid cleaning step using 0.2% (w/v) (corresponding to 0.055 M) HCl solution was considered [439]. According to the literature, performing a 30-minute cleaning cycle with 3 L of solution per square meter of membrane surface is enough to bring back 90% of membrane permeability (Ahmed et al., 2006).

The operational inputs associated with membrane maintenance were also considered. Specifically, the consumption of water and cleaning chemicals required for membrane

cleaning. For maintaining the membrane performance, cleaning-in-place (CIP) was assumed to take place after the completion of each batch. For organic fouling, an alkaline mixture of NaOH 0.1% (w/v) (corresponding to 0.025M NaOH) was selected, while for inorganic colloidal fouling, an acid cleaning step using 0.2% (w/v) (corresponding to 0.055 M) HCl solution was considered [439]. According to the literature, performing a 30-minute cleaning cycle with 3 L of solution per square meter of membrane surface is enough to bring back 90% of membrane permeability (Ahmed et al., 2006).

Table S10.5 Mass balances per batch.

COMPONENT	INITIAL (kg/Batch)	INPUT (kg/Batch)	OUTPUT (kg/Batch)	FINAL (kg/Batch)	OUT-IN (kg/Batch)
alginate precipitate	0,00	0,00	576,95	0,00	576,95
betaine	0,00	57.920,00	0,00	0,00	- 57.920,00
Biomass	0,00	0,00	11.031,44	0,00	11.031,44
BU DES	0,00	0,00	213.333,34	0,00	213.333,34
Choline Chloride	0,00	2.598,25	2.598,25	0,00	0,00
Citric Acid	0,00	28.800,00	28.800,00	0,00	0,00
CO2	0,00	0,00	209,52	0,00	209,52
dodecanoic acid	0,00	24.055,80	0,00	0,00	- 24.055,80
Ethyl Alcohol	0,00	269,27	267,81	0,00	- 1,46
FA DES	0,00	0,00	41.382,77	0,00	41.382,77
fucoidan	0,00	0,00	943,20	0,00	943,20
fucoxanthin	0,00	0,00	172,25	0,00	172,25
Levulinic Acid	0,00	4.321,52	4.321,52	0,00	0,00
N2	1.325,07	47.598.253,23	47.598.489,38	1.088,92	0,00
Na2CO3	0,00	10.176,00	9.671,40	0,00	- 504,60
NaCl	0,00	2.645,54	2.645,54	0,00	0,00
O2	402,27	14.449.907,47	14.449.979,16	330,57	0,00
octanoic acid	0,00	17.419,72	92,75	0,00	- 17.326,96
S .alg. prec.	0,00	0,00	1.765,29	0,00	1.765,29
Seaweed	0,00	14.400,00	0,00	0,00	- 14.400,00
sodium alginate	0,00	0,00	121,71	0,00	121,71
Urea	0,00	59.413,33	0,00	0,00	- 59.413,33
Water	0,00	4.476.400,86	4.380.487,71	0,00	- 95.913,15
TOTAL	**1.727,34**	**66.746.580,99**	**66.746.889,99**	**1.419,49**	**1,16**



Chapter 11

General discussion:

From extraction solvents to processing platforms

11.1. General discussion

Deep eutectic solvents (DES) have emerged as a promising class of alternative solvents for biomass processing due to their beneficial solvent properties. Their tuneable physicochemical properties, potential low volatility, ease of preparation, and potential for solvent recycling enable selective dissolution of biomass components while offering opportunities to reduce chemical consumption and integrate processing steps within a single solvent platform [5–7, 177]. Conventional industrial seaweed processing relies on a fragmented sequence of at least eight distinct procedures: mechanical size reduction, acidification, alkaline extraction, solid-liquid separation to isolate soluble sodium alginate, followed by acid precipitation, neutralisation, washing, and final milling to obtain alginate. This current process is constrained by high water consumption, extensive use of harsh chemicals resulting in chemical waste, substantial energy demands and long processing times [57, 124, 432]. Moreover, only alginate is recovered in this process, leaving other valuable components unvalorised as waste.

Replacing this linear, one-product chain with a DES-centered process could offer opportunities for process intensification and less chemical waste due to circular solvent use. This intensification could be achieved by consolidating the conventional acidification and alkaline extraction sequence into a single DES-mediated extraction step, while also eliminating solvent waste through DES recycling (**Figure 11.1**).

However, such process designs depend primarily on both appropriate solvent selection and efficient recovery strategies. Due to the large possibilities of DES, computational solvent screening should be addressed for identifying promising DES candidates [440]. After effective extraction, a critical bottleneck in designing a DES-focused downstream processing design is accounting for suitable product recovery strategies [69, 70]. While polysaccharide extraction using DES has been successfully demonstrated in literature, downstream product recovery remains largely unaddressed or is reliant on high-volume organic solvent consumption [119, 207, 441, 442]. This, in turn, leaves DES recycling underperformed, which compromises the potential environmental benefits of DES-based processing compared to conventional processing.

To address this limitation, the main focus of this thesis was to investigate circular and simple configurations to recover both the alginate and the DES, while also evaluating the possibility of DES recycling over multiple extraction cycles. In an idealised DES biorefinery concept, the process workflow is streamlined into fewer core stages: seaweed size reduction, DES-mediated extraction, solid–liquid phase separation,

downstream solvent–polymer separation with integrated DES recycling, polymer purification, precipitation, and drying.

Consequently, the overall aim of this study was to assess the technical feasibility of integrated DES biorefineries by integrating solvent screening, extraction efficiency, with focus on product isolation, and solvent recycling dynamics within a unified circular process design, and to evaluate economic and environmental viability of a multiproduct DES-based extraction process.

While this thesis demonstrated that DES enables efficient extraction of alginate and other seaweed constituents through reduced processing steps, and that alginate can be recovered and DES can be recycled multiple times depending on the process (5–10 cycles), it also revealed that multiple solvent recycling rounds is a critical requirement for achieving both environmental and economic feasibility. Despite demonstrating the technical feasibility of DES recycling, this study also reveals that recovery yields are not stable upon recycling across all investigated systems. This unstable performance indicates that a mechanistic understanding of solvent–alginate interactions during recovery is required to achieve predictable process stability and a robust, economically and environmentally viable process design.

Three overarching conclusions emerge from this work:

1. Product recovery from DES-based alginate systems an essential and technically feasible step but remains the primary process engineering bottleneck.
This thesis demonstrates that both alginate recovery and DES recycling can be achieved through different downstream process configurations (**Chapters 4-8**), which is a critical requirement for obtaining an environmentally and economically viable process (**Chapter 10**). However, none of the investigated recovery strategies consistently provided a stable recovery performance, as reflected by fluctuating recovery yields and process-dependent alginate fractionation. These observations indicate that the challenge is no longer whether alginate can be recovered from DES, but how this can be achieved in a robust, reproducible and viable manner. Future research should therefore focus on improving process robustness through a better mechanistic understanding of the physicochemical phenomena governing DES–alginate systems during repeated extraction and recovery, including changes in DES composition, polymer–solvent interactions, and phase behaviour. Consequently, while future research should prioritise understanding these fluctuations and DES-alginate interactions, complete solvent–polymer separation should not necessarily be regarded as the ultimate process objective. Instead, future DES-based bioprocesses

should also evaluate whether direct utilisation of functional DES–alginate assemblies provide a more efficient and value-added alternative for polymer-based applications.

2. DES selection screening should not focus solely on solvent-solute interactions but go towards integrated dissolution–disruption screening design.
The results demonstrate that extraction performance can partially be predicted from solvent–solute interactions alone (**Chapters 2, 3, 5, 7**). While COSMO-RS provided valuable insight into molecular affinity of alginate and fucoxanthin towards DES, extraction efficiency could not always be predicted by solvent-solute interactions alone (**Chapter 3**), due to the potential structural constraints of the seaweed matrix, which led to deviations between screening results and extraction efficiencies. Future DES development should therefore integrate solvent-solute interactions screening (COSMO-RS) with molecular and transport models that explicitly account for biomass interactions and deconstruction, enabling more predictive solvent and process design focused on both dissolution and disruption performance of the DES.

3. DES processes should be engineered as multifunctional process platforms that integrate multiple process functions rather than serving solely as one unit operation for extraction in order to provide an alternative to the conventional alginate extraction.
The greatest process-engineering potential of DES lies not solely in replacing conventional solvents, but in their ability to combine several processing steps within a single solvent platform. Throughout this thesis, DES simultaneously contributed to biomass disruption, selective extraction, compound stabilisation, product fractionation, and solvent recycling (**Chapters 5, 7, 9, 10**). Designing future DES systems around these integrated process functions, focussing on processes occurring in nature, offers opportunities for process intensification by reducing unit operations, simplifying downstream processing, and improving the overall efficiency of circular seaweed biorefineries, in order to facilitate the transition from conventional extraction methods to sustainable DES alternatives.

Section 1: From product separation to DES-alginate valorisation

11.2. Rethinking product recovery and DES recycling

Product recovery and solvent recycling are essential components of any circular DES-based extraction process. While DES have demonstrated considerable potential as extraction media, their often low volatility necessitates alternative separation approaches that enable both efficient product isolation and solvent regeneration [16, 69, 443]. Life cycle assessments confirmed that efficient, multi-cycle solvent recovery, together with improved product functionality, is critical to achieving a positive environmental impact (**Chapter 10**).

To address solvent regeneration, a range of recovery and recycling strategies were investigated (**Chapters 4–8**), including membrane-based separation, three-phase partitioning, thermo-separating aqueous two-phase systems, temperature-responsive DES, and DES-based aqueous biphasic systems (**Table 11.1**). Collectively, these studies demonstrate the proof of concept that both alginate recovery and DES reuse can be achieved through multiple downstream process configurations. However, the recovery yields remained unstable upon sequential solvent recycling. This operational variance highlights that while the technical feasibility of the recovery step (yielding 75-93% alginate recovery) has been established, engineering bottlenecks remain to be overcome (**Table 11.1**). Ultimately, a deeper understanding of the recovery dynamics is required in order to stabilise these processing loops and obtain predictable process stability.

BOX 1: FROM PRODUCT SEPARATION TO DES-ALGINATE VALORISATION

Main Results & Conclusions:
By evaluating five recovery strategies, this work demonstrates that alginate isolation and repeated DES reuse are technically feasible across several process configurations. Among the evaluated options, the DES–salt ATPS emerged as the most promising configuration for direct alginate separation from DES via the formation of an intermediate precipitation phase between the DES and the aqueous salt phase, thereby enabling direct alginate isolation while preserving the DES phase for subsequent multi-cycle reuse.

However, all investigated recovery approaches were constrained by irregular recovery yields upon sequential solvent recycling. Additionally, the recovered alginate exhibited distinct variations in M/G ratios and molecular weight depending on the specific separation operation applied, indicating that the recovery methodology could dictate which macromolecular fractions are selectively isolated from the extracted polymer pool.

Opinion and Outlook:
From a process-engineering perspective, complete downstream alginate-solvent separation introduces operational complexity and auxiliary chemical or salt demands, which reduce the overall process efficiency. The LCA demonstrated that DES production represents a major contributor to the environmental and economic footprint of DES-based processing, highlighting that DES recycling is essential for commodity alginate production.

For conventional alginate applications where isolated alginate is required, future developments should focus on improving solvent recycling systems that enable efficient separation. The fluctuating yield observations indicate that DES-based alginate recovery cannot be fully investigated with recovery yields alone. Instead, detailed structural characterisation is needed to determine whether the observed differences arise from molecular modification, selective fractionation, or persistent polymer–solvent associations. A critical knowledge gap remains regarding the structural characteristics of the extracted fractions and the extent to which DES and salt counterions remain associated with the recovered alginate. Systematically quantifying these residual interactions (e.g. SEC-MALS, NMR, ICP-OES) and mapping absolute polymer and DES variations across multi-cycle runs is essential to understand and control the fluctuating yields observed upon recycling.

However, for applications where the DES contributes additional functionality, retaining the DES within the alginate matrix may represent a more suitable strategy. Rather than treating the DES-alginate extract as a downstream processing bottleneck, this combined mixture should be exploited as a process-intensification opportunity by directly formulating this mixture for end-use applications. By eliminating this separation step, the DES–alginate assembly could be directly formulated as a value-added material, potentially increasing product value beyond that of isolated alginate alone.

Consequently, the future of DES-based alginate processing may not rely on a single universal recovery strategy, but rather on matching the downstream objective to the intended application: either efficient DES recycling for commodity polymer production, or direct valorisation of DES–alginate assemblies for higher-value functional materials.

11.2.1 Membrane filtration

Membrane filtration (**Chapter 4**) demonstrated the technical feasibility of pressure-driven DES recovery using a UF–DF–NF configuration. Evaluated under controlled conditions with a simplified model mixture, the system enabled a clear baseline assessment of separation performance, yielding substantial alginate recovery efficiencies. However, this simplified matrix does not fully reflect the compositional complexity of real seaweed extracts, where co-extracted polysaccharides, salts, and phenolic compounds are expected to induce severe membrane fouling and alter overall process stability. Although membrane filtration achieved good alginate recovery, viscosity-related flux limitations, membrane fouling, and limited DES retention reduce its suitability for circular DES processing. These limitations directly motivated the exploration of the alternative phase-based recovery strategies discussed in the following sections.

11.2.2 Three phase partitioning

Three-phase partitioning enabled simultaneous extraction of alginate and pigments using a hydrophobic DES (**Chapter 5**), demonstrating strong process intensification through dual functionality of the solvent system. Alginate partitioned predominantly into the aqueous salt phase, while the DES phase facilitated pigment extraction and biomass disruption. However, the system exhibited limitations in terms of product recovery stability and downstream processing requirements. Alginate isolation required dialysis, reducing overall process integration and increasing solvent demand. In addition, partial transfer of alginate into the DES phase during recycling resulted in fluctuating yields across cycles, indicating sensitivity of phase behaviour to ionic strength and system composition. These observations highlight that while TPP enables multifunctional extraction, its circularity is limited by additional purification steps and incomplete phase control during solvent reuse.

11.2.3 DES-EOPO temperature responsive ATPS

The temperature-responsive DES–EOPO system provided an efficient and mild route for alginate recovery, enabling repeated recycling of both DES and copolymer phase over multiple cycles (**Chapter 6**). Phase separation was induced through temperature modulation, allowing controlled product partitioning without chemical additives. Despite its promising circularity, the system introduces significant operational complexity due to the need for precise temperature control, multiple recyclable components, and a two-step phase operation. In addition, polymer accumulation and changes in phase composition during recycling may influence long-term stability. While the system demonstrates strong proof-of-concept performance for circular separation, its complexity reduces its suitability for industrial implementation without further simplification.

11.2.4 Temperature-responsive DES

Temperature-responsive DES enabled direct and simple alginate recovery through thermally induced phase switching (**Chapter 7**), without the need for additional phase-forming agents or solvents. This represents one of the most operationally straightforward recovery concepts investigated in this thesis. However, the applicability of this system is constrained by the use of components with limited toxicity profiles and by incomplete phase separation behaviour in certain cycles. Although DES recycling was successfully demonstrated, long-term process robustness and product compatibility remain limiting factors for broader application. Compared with multi-component systems, TRDES offers simplicity but reduced flexibility in terms of green chemistry constraints and system design space.

11.2.5 DES-salt aqueous two-phase system

DES–salt ATPS combined salting-out-induced phase separation with interfacial precipitation, enabling direct alginate isolation without dialysis and maintaining DES recyclability (**Chapter 8**). Among the systems investigated, this approach provides one of the most integrated recovery routes, as product isolation and phase separation occur simultaneously. The system achieved consistent alginate recovery across all tested conditions; however, it requires relatively high salt concentrations (50 wt%), which may affect process economics and material efficiency. In addition, salt phase recycling was not feasible, limiting full circularity of all process streams. Nevertheless, compared with membrane-based and switchable systems, DES–salt ATPS offers a favourable balance between simplicity, direct recovery, and solvent reuse, making it one of the most promising candidates for further process development.

11.2.6 Recovery strategies comparison

A central conclusion emerging from **Chapters 4–8** is that no single recovery strategy simultaneously maximises product recovery, solvent circularity, process simplicity, and mild extraction parameters (**Table 11.1**). Instead, each approach represents a different engineering trade-off between the complexity of downstream processing, energy requirements, productivity, and the feasibility of solvent reuse. Therefore, recovery strategy selection should not be based solely on recovery efficiency, but on the overall balance between process performance and operational requirements.

Table 11.1 Comparison of recovery performance, DES recyclability, and main characteristics of the alginate recovery strategies investigated in this thesis.

Ch	System	Phase behaviour	DES type	Extraction yield (mg/g DW)	Recovery yield (mg/g DW)	Recovery efficiency (%)	Recovery steps	DES reuse	Toxicity	Salt waste	Extraction		Recovery		Thermal energy demand[e]	Vol. Productivity[f]
											T (°C)	Time (min)	T (°C)	Time (min)		
4	Membrane filtration	Single liquid phase	Hydrophilic	n.d[a]	n.d[a]	85% (from DES-alginate model extract)	5	Not studied	No	No	-[a]	-[a]	20-25	165	n.d[a]	n.d[a]
5	Three-phase partitioning	Triphasic	Hydrophobic	101.8 ± 3.1	-[b]	-[b]	3	Yes, 7 times	No	Yes	35	10	20	720	22.9 ±0.7	0.140 ± 0.0
6	Temperature-responsive ATPS	Biphasic (two stages)	Hydrophilic	83.3 ± 10.5	54.8 ± 8.1	75.4% of alginate extracted	6	Yes, 5 times (for EOPO and DES recycling)	No	No	80	60	20-60	225	115.8 ± 17.1	0.288 ± 0.043
7	TRDES	Mono- and biphasic	Hydrophilic	-[c]	55.6 ± 14.4	-[c]	3	Yes, 8 times	Yes	No	60	60	20	720	141.6 ± 36.7	0.071 ± 0.018
8	DES-salt ATPS	Biphasic	Hydrophilic	63.2 ± 4.4	48.1 ± 3.4	76.4% of alginate extracted	2	Yes, 6 times	No	Yes	80	60	20	60	138.0 ± 9.7	0.601 ± 0.042

[a] Extraction was not performed because a DES–alginate model mixture was used; therefore, no extraction or recovery yield can be reported.

[b] The recovery yield and efficiency of the TPP system could not be determined as alginate was not recovered from the DES phase but instead was present in the aqueous salt phase.

[c] The initial extraction yield within the TRDES-water phase could not be determined independently due to interference; the alginate content was measured directly from the aqueous phase after phase separation.

[d] Toxicity of the constituents reflects the established non-toxic profile of the individual precursors; however, the quantitative environmental greenness and toxicity profiles of the combined DES matrices remain unconfirmed.

[e] Thermal Energy Demand (E_{th}, MJ/kg alginate) is calculated via the thermodynamic heat equation ($Q = m * c_p * \Delta T$) relative to an ambient baseline of 20 °C and divided by the net recovered alginate mass.

[f] Volumetric productivity (P_v, $\frac{g}{L} * h$) is calculated using the formula $\frac{m_{alginate}}{V_{solvent} * t_{total}}$, where metrics are benchmarked uniformly relative to the initial primary extraction solvent volume (based on the raw biomass SLR) and total processing time, excluding auxiliary downstream fluids added post-extraction

Taken together, the comparative assessment demonstrates that DES-based recovery strategy selection cannot be based solely on recovery efficiency. Instead, industrial implementation requires balancing solvent circularity, process simplicity, operational intensity, productivity and waste generation (**Table 11.1**). Within this framework, the DES–salt ATPS with interfacial precipitation (**Chapter 8**) provides the most balanced overall configuration among the investigated systems. By enabling direct product recovery through interfacial precipitation, limiting downstream processing requirements to two processing steps, and maintaining solvent recyclability, and short processing times, this approach achieved a favourable combination of recovery performance (76.4%) and volumetric productivity (0.601 ± 0.042 g/L·h). However, the process still requires relatively high salt concentrations, resulting in salt waste generation and limiting complete solvent circularity. Therefore, while DES–salt ATPS represents the most promising recovery strategy identified in this thesis, further optimisation of phase-forming components and recycling strategies remains necessary to improve its environmental and industrial feasibility. Consequently, no single recovery strategy simultaneously optimises all process criteria. The selection of a recovery strategy should ultimately be driven by the intended application and process requirements rather than by recovery efficiency alone.

Although **Chapter 8** identified the DES–salt ATPS as the most favourable recovery strategy, the broader question is whether the overall DES-based process constitutes a process intensification compared with conventional alkaline extraction. Conventional alginate production typically requires at least eight sequential processing steps, including acid pre-treatment, alkaline extraction, precipitation, neutralisation, washing, and solvent disposal, while consuming fresh acid and alkaline chemicals in each production cycle without solvent recycling. In contrast, the integrated DES-based process developed in this thesis requires six processing steps (or seven when milling of the recovered alginate is included), while simultaneously enabling solvent recycling and reducing the consumption of fresh extraction chemicals (**Figure 11.1**). Rather than intensifying a single processing step, the process integrates extraction, product recovery, and solvent reuse within one processing platform. Consequently, the overall intensification arises from process integration and solvent reuse, rather than simply from a reduction in the number of individual process steps. Nevertheless, whether this laboratory-based process intensification ultimately translates into a reduction in overall unit operations, equipment requirements, and process complexity at industrial scale remains to be verified through integrated process simulation. Future work should therefore employ process modelling, for example using SuperPro Designer, to

quantitatively assess the extent to which DES-based biorefineries achieve a decrease in unit operations compared with conventional alkaline extraction.

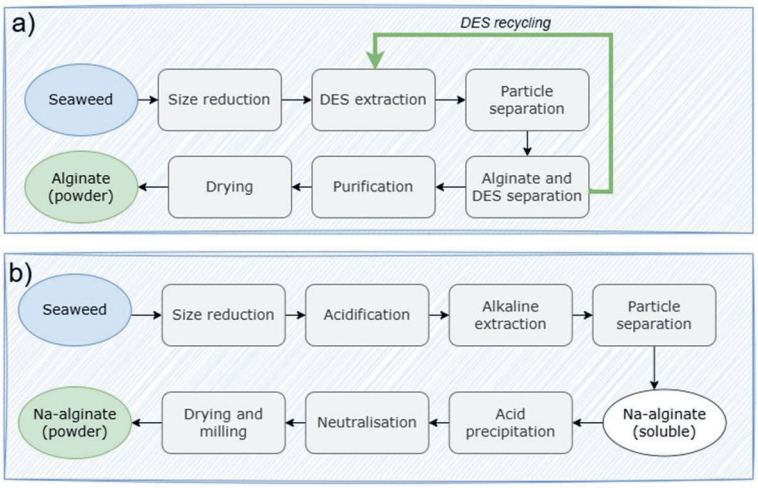


Figure 11.1 Comparisons of (a) DES-based and (b) alkaline-based alginate extraction flowsheets.

Despite the favourable performance of the DES–salt ATPS system, opportunities remain to further simplify recovery operations, improve solvent circularity, and reduce process intensity. Crucially, while **Chapter 8** optimises the recovery steps, it introduces an inorganic waste stream of potassium triphosphate. Future engineering frameworks must therefore integrate an auxiliary salt-recovery loop to achieve full circularity for both DES and salt phase. Continued development of DES-based recovery technologies is therefore warranted. The following section discusses potential adaptations of the recovery strategies investigated in this thesis, together with emerging concepts from the literature that may further enhance product recovery, solvent recyclability, and overall process integration.

11.2.7 Emerging concepts for next-generation recovery strategies

This section explores emerging directions for improving and redesigning DES-based recovery strategies beyond the systems investigated in this thesis. It is divided into (i) adaptations of the applied methodologies (**Section 11.2.7.1**) and (ii) alternative emerging recovery concepts reported in literature (**Section 11.2.7.2**), highlighting potential routes for future development.

11.2.7.1 Adaptations of applied recovery strategies

Among the recovery strategies investigated in this thesis, salt-induced phase separation was applied in three-phase partitioning (**Chapter 5**) and DES–salt aqueous two-phase systems (**Chapter 8**). In both systems, high ionic-strength salts promoted phase separation and alginate recovery but also generated salt-containing waste streams (**Table 11.1**).

While these approaches demonstrated effective product recovery and solvent recyclability, both exhibited fluctuations in alginate recovery during solvent recycling, suggesting that recovery stability is governed not only by phase formation but also by the electrostatic environment surrounding the polymer (**Section 11.2**)**.** Combined with the environmental burden associated with salt disposal (**Table 11.1**), these findings indicate that replacing ionic salting-out agents with non-ionic alternatives may improve both process robustness and circularity.

In the TPP system (**Chapter 5**), the gradual transfer of alginate into the hydrophobic DES phase during recycling could have been from electrostatic shielding of alginate carboxylate groups by ammonium ions [444], reducing the polymer's effective charge density and hydrophilicity. As a result, stronger interactions between alginate and the hydrophobic fatty-acid DES may promote partial partitioning of the polymer into the DES-rich phase during repeated cycles.

Sugar-driven TPP systems may provide an attractive alternative. Sugars such as sucrose and mannose have been successfully applied as phase-forming agents in DES-based three-phase systems for biomolecule purification [237, 445], where phase separation is induced through competitive hydrogen-bonding interactions rather than ionic charge screening. Because sugars do not neutralise alginate carboxylate groups, they may better preserve polymer hydration and favour retention of alginate within the hydrophilic phase. In addition, sugars are generally less corrosive and environmentally preferable than inorganic salts [446]. Their higher viscosity, however, may reduce mass transfer and slow phase separation [447], requiring experimental validation of their overall process performance.

A similar dependence on ionic strength was observed in DES–salt aqueous two-phase systems (**Chapter 8**), where potassium phosphate served as the phase-forming agent. Although this system enabled efficient interfacial alginate recovery, the use of up to 50 wt% salt generated substantial salt waste (**Table 11.1**), while recycling of the salt phase did not maintain stable recovery performance. Interactions between potassium ions and alginate carboxylate groups may similarly modify the polymer's local counterion

environment, thereby influencing partitioning during repeated recycling cycles [448–450].

Consequently, the sugar-based concept proposed for TPP may also be extended to DES–salt ATPS. Replacing potassium phosphate with non-ionic phase-forming compounds could minimise electrostatic screening while maintaining phase separation through hydrogen-bonding-driven "sugaring-out" mechanisms, as demonstrated for biomolecule recovery in ATPS [451–454]. Whether such systems can achieve comparable phase separation, recovery efficiencies, and long-term recyclability remains unknown and represents an important direction for future research.

11.2.7.2 Alternative classes of switchable DES

The main limitation of the temperature-responsive DES system investigated in **Chapter 7** was not the switching concept itself, but the solvent formulation and recovery time required (**Table 11.1**). Although alginate recovery and DES recycling were successfully demonstrated, the optimal o-cresol:ethanolamine formulation is not compatible with food-related or other bio-sensitive applications due to toxicity concerns. Consequently, future development should focus on identifying alternative switchable DES systems that retain the operational simplicity of stimulus-responsive recovery while improving sustainability and industrial applicability.

Several alternative switchable DES concepts have been reported in literature (**Table 11.2**). Among these, pH-responsive DES are the most mature but rely on repeated acid/base addition and associated salt generation, making them less compatible with circular processing concepts [163, 237, 455]. CO_2-responsive DES offer a more attractive alternative because switching is achieved without direct chemical addition, although current systems remain constrained by slow switching kinetics and the widespread use of toxic amine-based components [167, 262, 313, 326]. Biphasic temperature-responsive DES are particularly interesting for multiproduct fractionation [338, 456, 457], but do not fundamentally solve the challenge of product recovery because the target compounds remain dissolved in one of the DES phases upon switching [458]. The target compounds remain dissolved within one of the DES phases and therefore still require an additional recovery step, such as adsorption or resin-based separation [338, 456].

Collectively, these alternative switchable DES systems demonstrate that the concept explored in **Chapter 7** remains promising. The principal limitation lies in the development of solvents that combine reversible responsiveness with low toxicity.

Consequently, future advances in switchable DES design should focus more on developing switchable DES with low environmental impact.

Table 11.2 Types of alternative responsive DES, their advantages, limitations and relevance for seaweed biorefineries.

System	Switching mechanism	Main Advantages	Main limitations	Relevance for seaweed biorefineries
pH-responsive DES	Acid/base induced protonation	Well-established; effective phase switching and product recovery	Acid/base consumption, salt accumulation, potential biomolecule degradation	Limited compatibility with circular processing
CO_2-responsive DES	CO_2/N_2 bubbling	Reversible switching without chemical addition; reduced waste generation	Slow kinetics in viscous DES, gas-handling infrastructure, many systems remain amine-based	Promising alternative to Chapter 7
Biphasic TRDES	Temperature-induced phase separation	Selective partitioning between hydrophilic and hydrophobic DES phases; suitable for multiproduct fractionation	Additional solvent phase, increased downstream complexity, product still requires further recovery	Useful for fractionation rather than recovery

Perspective Box 1: The future of temperature-responsive DES: Multicomponent one-pot extraction using a single TRDES

TRDES could offer a conceptual basis for developing one-solvent, multiproduct biorefinery platforms. Through reversible modulation of the solvent polarity and phase behaviour, such systems could evolve into integrated one-pot processes capable of sequentially targeting compounds with different physicochemical properties.

In a seaweed biorefinery context, this would enable an initial low-temperature (<30 ◦C) hydrophobic extraction step for fucoxanthin, followed by a temperature-induced transition (> 60 ◦C) to a more hydrophilic solvent environment suitable for the subsequent extraction and recovery of alginate. In this manner, sequential fractionation could potentially be achieved within a single solvent system, while simultaneously enabling in situ phase control and solvent reuse.

A conceptual process scheme illustrating this multiproduct TRDES (**Figure 11.2**) indicates the potential of TRDES dual-solvent properties. Although this concept remains dependent on the development of less toxic and more sustainable TRDES formulations, the findings of this

thesis suggest that further improvements in solvent design and responsiveness represent a promising direction. In this context, TRDES should be viewed as switchable platforms that could enable one-pot multiproduct extractions for next-generation circular biorefinery designs.

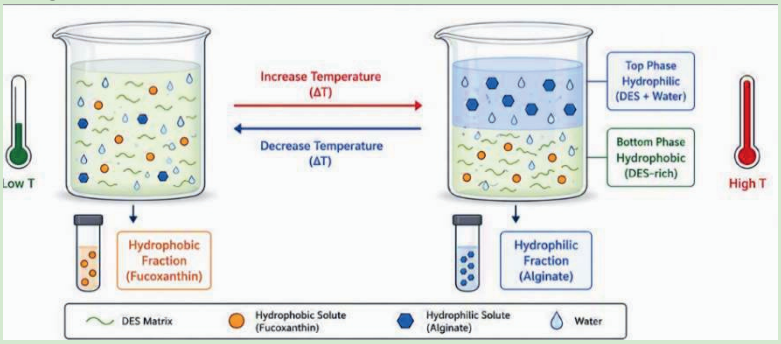


Figure 11.2 Conceptual design of a multiproduct TRDES biorefinery.

11.2.8 Alternative emerging recovery concepts

The limitations of the temperature-responsive DES system investigated in **Chapter 7** highlight the need for exploring alternative stimulus-responsive recovery strategies that avoid the use of additional chemicals while maintaining solvent recyclability. One emerging, yet largely unexplored, concept is the development of electrochemically responsive deep eutectic solvents (ERDES). Inspired by redox-switchable ionic liquids used in electrochemical and energy-storage applications [459–461] and redox flow batteries [462], ERDES could, in principle, enable reversible tuning of solvent properties through the application of an electrical potential. Such an approach may provide a reagent-free switching mechanism, potentially allowing selective product recovery while preserving the solvent for repeated reuse.

Although electrochemically switchable DES have not yet been explored for biomass fractionation, they represent a promising direction for future research. Designing DES containing redox-active yet biocompatible components could enable electrically controlled modulation of solvent polarity, hydrogen-bonding interactions, or phase behaviour, thereby facilitating controlled release of dissolved biomolecules. Such systems could overcome some of the limitations associated with thermal or chemically induced switching, while offering improved opportunities for process integration and continuous operation. Thus, a reagent-free switching mechanism can be created, which can be formulated using non-toxic components (e.g. choline chloride with urea or formic acid) [463]. Nevertheless, significant challenges remain, including the identification of suitable redox-active DES components, demonstration

of reversible switching over multiple cycles, evaluation of energy requirements, and assessment of biomolecule stability under electrochemical conditions. Consequently, electrochemically responsive DES represent a long-term research direction with the potential to further advance one-pot, multiproduct seaweed biorefineries.

Perspective Box 2: The future of responsive DES? One-pot multiproduct biorefinery using ERDES

In the context of seaweed biorefinery, electrochemically responsive DES (ERDES) could potentially enable sequential multiproduct extraction of compounds with differing polarity within a single solvent platform (**Figure 11.3**). In a reduced state, the DES could hypothetically preferentially solubilise hydrophobic compounds such as fucoxanthin. Upon oxidation, changes in local charge distribution would disrupt the hydrogen-bond network, potentially inducing a shift in solvent polarity and promoting phase separation or precipitation of the hydrophobic fraction. The regenerated hydrophilic state could subsequently be reused for extraction of compounds including alginate, enabling sequential multi-product valorisation. However, this concept has not yet been demonstrated for extraction purposes yet. Major challenges include maintaining DES formation in the presence of bulky redox-active groups, ensuring electrochemical stability, and overcoming the inherently slow mass-transfer kinetics associated with viscous DES systems. Consequently, electrochemically switchable DES should currently be regarded as a conceptual long-term research direction rather than a near-term recovery technology.

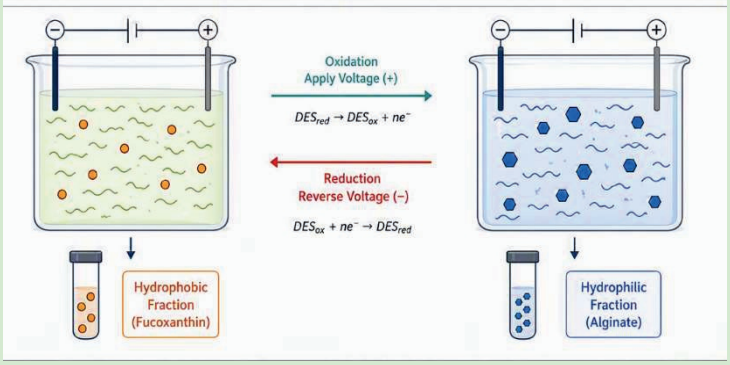


Figure 11.3 Conceptual design of a multiproduct ERDES biorefinery.

11.3. DES-alginate interactions during extraction and recovery

The recovery concepts discussed in **Section 11.2** demonstrate that several promising strategies exist to improve product recovery from DES but that recovery yields can fluctuate. Conversely, successful multi-cycle solvent reuse with stable recovery performance has been reported for a range of low-molecular-weight compounds, including metals and phenolic compounds [464, 465], indicating that DES themselves do not inherently prevent efficient product recovery. Instead, these observations

suggest that the principal challenge encountered throughout this thesis could be linked to the nature of the extracted product.

To understand why alginate recovery remains more challenging than the recovery of smaller molecules, it is therefore first necessary to examine the potential molecular interactions that develop between alginate and DES during extraction and how these may persist throughout the subsequent recovery process.

11.3.1 Alginate after extraction

During extraction, alginate is released from its native cell-wall environment, where it exists as a calcium-crosslinked network embedded within a matrix of cellulose and fucoidan [466, 467]. Disruption of these interactions requires not only dissolution of the polymer but also the cleavage of the intermolecular associations that define its native supramolecular structure. Consequently, while the primary chemical structure of the alginate remains intact, its macromolecular conformation and solvation state undergo a transition from their native biomass arrangement [48, 468]. Instead, the isolated chains associate with the solvent matrix. Since the solvent influences the alginate organisation directly [469], this may lead to the formation of new polymer–solvent interaction networks.

Consequently, the recovered alginate fraction is inherently influenced by both its location within the biomass structure (cell wall-bound versus more loosely associated fractions) and the extent to which the extraction solvent disrupts these interactions. This not only affects extraction yield, but also determines which molecular fractions become available for subsequent recovery, potentially influencing the molecular weight distribution, M/G ratio, and functional properties of the recovered alginate [48, 227].

Within DES systems, alginate is unlikely to behave as a simple isolated solute. Instead, extensive hydrogen-bonding and electrostatic interactions between the alginate polymer and DES components may partially replace its native interactions with water and counterions, resulting in solvent-mediated conformations or transient polymer–solvent assemblies [469, 470]. Depending on DES composition, additional electrostatic interactions may occur between DES components and alginate carboxylate groups [471], which could further stabilise these structures in solution.

A critical unresolved question remains regarding the extent to which DES constituents remain structurally associated with the recovered alginate after extraction and

recovery (**Chapter 3-8**). While alginate is treated as the isolated product, it remains unclear whether DES extraction and recovery yield a chemically equivalent "native" polymer or a material that retains persistent associations with DES constituents. Research has demonstrated that NADES components can partially replace native alginate–alginate hydrogen bonding with weaker, more dynamic intermolecular interactions [470]. Thus, given that conventional algal biorefining yields standard sodium alginate, extracting biomass with alternative eutectic media in **Chapters 3** and **Chapters 5-8** opens the possibility for counterion exchange along the polyelectrolyte backbone. This potential counterion shifting depends on the specific DES and recovery method used.

Previous studies have demonstrated through NMR that quaternary ammonium species, including choline and betaine, can remain associated with alginate through hydrogen-bonding and electrostatic interactions, even after washing and drying [472–474]. Similar interactions have also been reported for ammonium-containing systems [475]. These findings support the hypothesis that analogous DES–alginate or salt–alginate assemblies may have formed during the recovery processes investigated in this thesis (**Figure 11.4**).

Importantly, these potential interactions do not necessarily alter the primary chemical structure of alginate but they could influence fractionation behaviour by stabilising or selectively retaining polymer fractions during downstream processing. The spatial distribution of the negatively charged carboxylate groups differs significantly between the flexible, linear mannuronic acid (M) blocks and the rigid, buckled guluronic acid (G) blocks [448, 476]. Consequently, bulky organic cations such as choline or betaine could exhibit preferential affinities toward specific block configurations [474], potentially altering the local solubility, hydrophobicity, and hydrodynamic volume of the corresponding polymer chains.

This could indicate that the DES might not only govern alginate extraction but also dictates the affinity with which specific alginate fractions remain associated with the solvent phase during different recovery operations [48]. These differences in M/G ratios became apparent when comparing them for different recovery processes (**Chapters 5-8**).

Perspective Box 3: Are DES–alginate and salt–alginate assemblies formed during extraction and recovery?

Even though alginate was recovered using several strategies, it remains unclear whether the recovered alginate retains persistent interactions with DES or salts constituents used. During extraction and recovery, the potential extensive hydrogen-bonding network within the DES may partially replace the hydration shell and counterion environment surrounding alginate. Hydrogen-bond donor and acceptor components, such as choline chloride or betaine-based DES, may remain associated with hydroxyl and carboxylate groups along the polymer backbone through potential hydrogen bonding and electrostatic interactions (**Figure 11.4**). Likewise, ammonium or potassium ions originating from salt-based recovery systems may remain associated with alginate carboxylate groups through ion pairing or charge compensation (**Figure 11.4**). The recovered alginate may therefore comprise DES-associated or salt-associated alginate assemblies with varying degrees of residual solvent coordination.

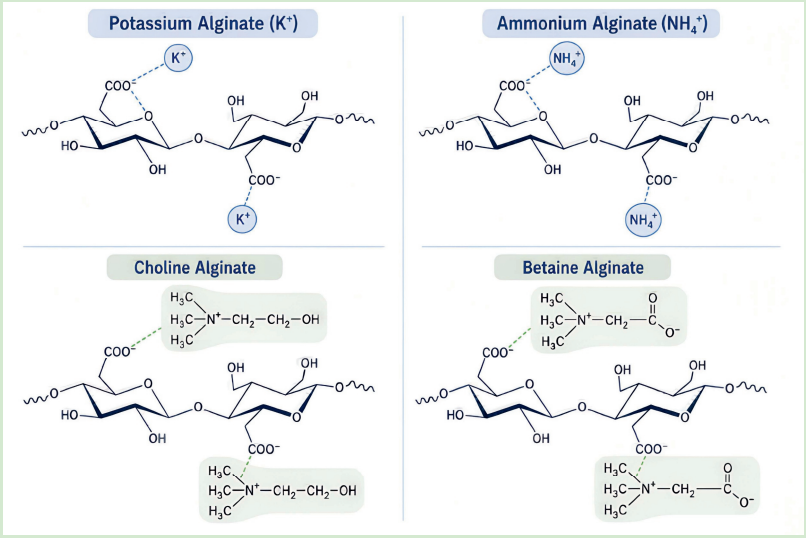


Figure 11.4 Potential alginate variants formed across the different processing approaches.

Future research should therefore establish whether these proposed assemblies exist and determine their stability and functional significance. Combining solid-state NMR, FTIR, Raman spectroscopy, X-ray photoelectron spectroscopy (XPS), ICP-OES, elemental analysis, and advanced microscopic techniques could provide direct insight into the molecular architecture of recovered alginate. Such studies would clarify whether DES-based extraction generates structurally distinct polymer–solvent assemblies with application-specific properties.

11.3.2 Recovery as selective fractionation process

The differences in molecular weight (M_W) and M/G ratio observed across **Chapters 5–8** (**Table 11.3**) suggest that recovery conditions influenced which fractions of alginate are preferentially isolated, even if extraction conditions are comparable. In the TPP system

(**Chapter 5**), alginate recovered from the salt-rich phase exhibited an M/G ratio of approximately 1.05, indicating a comparatively balanced composition of mannuronic and guluronic acid units. In contrast, DES–EOPO ATPS (**Chapter 6**) resulted in a higher M/G ratio (1.96), while temperature-responsive DES recovery (**Chapter 7**) yielded an even more pronounced enrichment in M-block content (M/G = 2.63). Conversely, the DES–salt ATPS system (**Chapter 8**) produced a markedly lower M/G ratio (0.22), indicating strong enrichment in guluronic-acid-rich fractions. These variations were accompanied by differences in average molecular weight, with relatively high M_W alginate obtained in the TRDES system (989 ± 227 kDa), whereas DES–salt ATPS yielded lower molecular weight fractions (438 ± 93 kDa), suggesting partial fractionation during interfacial precipitation and phase partitioning.

Particularly noteworthy is that **Chapters 6** and **8** employed the same DES (Bet:Urea 1:2) but yielded substantially different M/G ratios. This observation indicates that the structural characteristics of the recovered alginate are not governed by solvent composition alone but are strongly influenced by the recovery environment itself. Consequently, the recovery step may act as a fractionation process that selectively isolates different types of alginate from the extracted polymer pool.

Table 11.3 Structural characteristics of recovered alginate fractions across different downstream configurations.

Chapter	System	M/G	M_W
5	Three-phase partitioning	1.05 ± 0.00	n.d [a]
6	Temperature-responsive ATPS	1.96 ± 0.02	n.d [a]
7	TRDES	2.63 ± 0.19	989 ± 227
8	DES-salt ATPS	0.22± 0.02	438 ± 93

[a]Average molecular weight was not measured.

Mechanistically, these differences may arise because each recovery environment selectively stabilises different alginate fractions. M-block-rich regions are generally more flexible, highly hydrated, and expose accessible hydroxyl and carboxyl groups [432], potentially making them more susceptible to stabilisation within DES-rich phases through hydrogen-bonding and solvation interactions [48, 334]. In contrast, high ionic-strength recovery media, such as potassium phosphate or ammonium sulphate, could suppress electrostatic interactions and promote salting-out or partial dehydration effects around the polysaccharide, thereby reducing repulsion between chains [60, 243, 477, 478]. Previous studies have demonstrated that alginate chains in saline media become more flexible due to shielding of intra-chain repulsions [479]. Because G-block-rich sequences are more rigid and have a stronger tendency toward ordered self-association, such environments could preferentially stabilise condensed

G-rich fractions, whereas DES-dominated systems could favour retention of more flexible, hydrated M-rich regions [448, 480] favouring their selective partitioning into condensed phases rather than remaining dissolved. Consequently, downstream systems with strong dehydration or electrostatic screening effects (e.g., DES-salt ATPS, TPP) may preferentially enrich G-block-containing fractions, whereas systems dominated by hydrogen-bonding interactions or polymer compatibility (e.g., TRDES (**Chapter 7**) and EOPO-containing (**Chapter 6**) recovery methods) may favour the retention or recovery of more flexible, M-rich chains.

The observed differences in molecular weight and M/G ratio suggest that each recovery strategy selectively stabilises different alginate fractions, even when the same biomass and DES are used (as in **Chapter 6** and **8**). Hydrogen bonding within DES-rich environments and electrostatic screening in salt-rich systems likely alter polymer solvation and phase partitioning, thereby influencing which fractions are preferentially recovered. Consequently, downstream recovery should not be regarded solely as a separation step but also as a fractionation process that determines the molecular characteristics of the final alginate product.

Future work should therefore focus on understanding this fractionation depending on the downstream process. Techniques such as SEC–MALS (Size-Exclusion Chromatography with Multi-Angle Light Scattering) to determine absolute molecular-weight distributions [481], NMR spectroscopy for M/G block composition rather than only the ratios [481, 482], rheological measurements to assess network behaviour [483], and elemental analyses (ICP-OES) should be applied to quantify residual salts or DES-derived ions [484], both after extraction and after recovery. Such studies would provide important insight into the nature of the extracted and recovered alginate and clarify whether different DES recovery strategies produce chemically equivalent materials or distinct alginate fractions with application-specific properties.

Overall, alginate is a particularly challenging target for DES-based extraction and recovery systems. The proposed polymer–solvent coupling effects could offer a potential framework to explain the deviations observed across **Chapters 4–8** and highlight that successful DES-based biorefinery design must consider not only extraction efficiency but also recovery dynamics and polymer analysis. Instead, these mechanism-dependent pathways may provide a process-engineering opportunity to actively steer the characteristics of the recovered alginate based on its intended end-use application, thereby tailoring the polymer's properties for specific material demands.

Perspective Box 4: Functional DES–alginate systems: Do we even need recovery?

The recovery of alginate from DES has been considered successful when the polymer is isolated from the solvent phase. However, DES–alginate interactions are not merely a downstream separation challenge but may also provide an opportunity for designing new functional materials. Consequently, the interactions that complicate downstream separation may instead become advantageous when retained within the final application.

Several studies have demonstrated that DES–alginate systems can be utilised directly, thereby bypassing conventional solvent–product separation. For instance, DES-loaded calcium alginate hydrogel beads have been employed as green sorbents for solid-phase extraction of pesticides, exploiting the combined structural stability of alginate and the solvation properties of DES [485]. Similarly, DES–alginate hydrogel systems have been shown to enhance drug solubility and enable sustained transdermal release, with significantly improved skin permeation compared to conventional alginate hydrogels [486]. Beyond biomedical applications, DES–alginate composites have also been explored in polymer electrolyte membranes for fuel cell technologies [487] and in halochromic smart packaging for freshness monitoring [488]. In addition, recent work has demonstrated that alginate-based hydrogel matrices can be used as functional separation media themselves, for metal recovery systems where desorption of cobalt from DES-containing phases is achieved via alginate binding [489].

In this perspective, DES no longer acts solely as a temporary extraction medium, but becomes an integrated component of the final product (**Figure 11.5**). Retained DES constituents may provide additional functionalities, including enhanced molecular mobility, plasticisation, improved solubilisation capacity, or controlled release behaviour.

This concept represents a shift from separation-driven bioprocessing towards application-driven material design. Instead of aiming for separation from DES, future research should also consider whether the DES–alginate system itself provides enhanced functionality compared with isolated alginate. Such a strategy may be particularly relevant for high-value applications where material performance, rather than polymer purity alone, determines product value. This perspective expands the role of DES beyond extraction and separation, positioning DES as a potential building block of next-generation products.

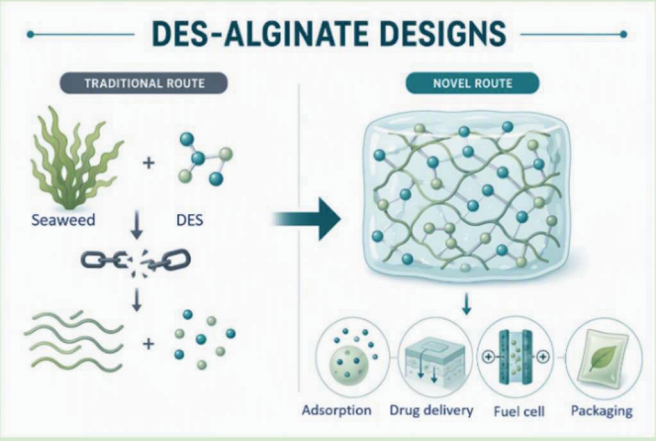


Figure 11.5 Potential combined DES-alginate applications.

Section 2: Solvent screening and extraction

11.4. DES for dissolution and disruption

The large design space of DES, arising from the wide range of possible hydrogen bond acceptor–donor combinations and compositional ratios, necessitates the use of pre-screening approaches to guide solvent selection. In this thesis, COSMO-RS-based screening (**Chapter 2, 3, 5, 7**) was used to support the identification and prioritisation of DES candidates for alginate extraction.

A central finding of this thesis is that effective DES selection for biomass processing should not be based solely on solute–solvent affinity. To the best of our knowledge, a predictive framework that simultaneously accounts for both fluid-phase solute dissolution and physical biomass matrix deconstruction does not yet exist in literature. Computational screening paradigms remain fragmented; thermodynamic tools such as COSMO-RS are routinely applied upfront to screen thousands of DES combinations for the pure dissolution of isolated target solutes, whereas Molecular Dynamics (MD) simulations are conventionally relegated to a retrospective, post-hoc role to analyse how specific ions disrupt cell wall networks on an atomic scale. Because matrix disruption modelling is utilised post-hoc rather than being integrated directly into the initial solvent screening phase, the critical coupling between physical macromolecular accessibility and thermodynamic solubility is lost.

Instead, solvent screening must account for two coupled mechanisms: (i) molecular dissolution of target compounds and (ii) disruption of the biomass matrix to enable their release. In algal systems, extraction efficiency is governed not only by thermodynamic solvation, but also by the ability of the solvent to penetrate, swell, and weaken the structural organisation of the biomass matrix. These matrix interactions are particularly critical for alginate extraction, where strong polysaccharide networks and cell wall cohesion represent a major barrier to mass transfer and solute accessibility. Additionally, future screening frameworks should integrate an environmental life-cycle assessment (LCA) upfront, prior to computational affinity simulations, to ensure that only sustainable DES candidates with low synthesis footprints are advanced through the development pipeline.

BOX 2: INTEGRATED DISSOLUTION-DISRUPTION DES SCREENING

Main Results & Conclusions:
Computational solvent screening using COSMO-RS successfully prioritised promising DES candidates based on predicted thermodynamic affinity towards target compounds, including

alginate and fucoxanthin. However, high predicted solvent affinity did not consistently translate into high experimental extraction yields from seaweed biomass, demonstrating that solute–solvent interactions alone are insufficient to predict extraction performance. COSMO-RS evaluates interactions in a homogeneous liquid phase and therefore does not account for the accessibility of target compounds within the complex biomass matrix. During biomass fractionation, extraction efficiency depends not only on solute dissolution, but also on solvent-driven interactions and disruption of cell wall structures. Therefore, future DES screening strategies should integrate dissolution capacity, biomass disruption potential, and solvent sustainability to enable more reliable prediction of extraction performance.

Opinion and Outlook:
Future DES design frameworks should transition from isolated solute-centric screening towards integrated process-oriented prediction approaches. Combining COSMO-RS with molecular dynamics (MD) simulations could provide complementary information on solvent–solute affinity and solvent-induced biomass accessibility, including solvent penetration, swelling, and matrix interactions. Furthermore, incorporating life cycle assessment (LCA) during early-stage solvent selection would enable environmentally favourable DES candidates to be prioritised before experimental validation, preventing the optimisation of solvents that perform well experimentally but have limited sustainability potential. Ultimately, integrated computational screening pipelines combining molecular interactions, biomass disruption mechanisms, and sustainability metrics could accelerate rational DES development for biomass fractionation.

11.4.1 Solvent screening

In this thesis, computational pre-screening was employed as a strategy to reduce the experimental search space and guide solvent design. COSMO-RS proved to be a versatile tool across multiple chapters in this thesis. It was applied to screen and rank DES candidates for selective alginate solvation (**Chapter 2**), to elucidate solvent–solute interactions between alginate and DES systems (**Chapter 3**), to assess the affinity of secondary target compounds fucoxanthin and chlorophyll *a* in the context of DES-based seaweed pretreatment for alginate extraction (**Chapter 5**), and to evaluate alginate partitioning behaviour between phases for product recovery in temperature-responsive DES systems (**Chapter 7**). These applications demonstrate the broader utility of molecular thermodynamic modelling for supporting rational solvent selection and process design in DES-based biorefinery systems.

Within this context, the solvent screening framework developed in **Chapter 2** demonstrated the potential of computational pre-screening to rationalise experimental DES selection and to provide molecular-level insight into observed extraction behaviour. Overall, a reasonable agreement was observed between the predicted DES capacities and the experimental extraction performance reported in **Chapter 3**. For example, Choline chloride: thiourea exhibited the highest predicted capacity (4828) towards alginate (**Chapter 2**) and, together with choline chloride:urea,

resulted in the highest experimental extraction yields (74 % after optimisation for choline chloride: urea) (**Chapter 3**). Conversely, choline chloride:acetic acid displayed a substantially lower predicted capacity (0.6) and correspondingly yielded lower alginate extraction efficiencies. These observations support the applicability of COSMO-RS as a useful tool for guiding initial DES selection.

However, the absolute magnitude of the predicted capacity values did not always directly translate to experimental performance. For instance, despite a markedly lower predicted capacity (23), choline chloride:ethylene glycol exhibited extraction yields comparable to those obtained with choline chloride:thiourea. This discrepancy highlights an important limitation of the current screening framework: COSMO-RS evaluates primarily solvent–solute thermodynamic interactions [67], focusing on the affinity between the target compound and the solvent system, thereby operating under the assumption that the solute is already freely accessible in the fluid phase. In biomass extraction, however, extraction performance is not solely governed by solubilisation of the target compound, but also by the ability of the solvent to disrupt, swell, or permeabilise the surrounding biomass matrix. DES must actively compete with the cohesive non-covalent forces stabilising the algal cell wall. It must break down inter- and intra-molecular hydrogen bonds between cellulose microfibrils and matrix polysaccharides [490–492].

Additionally, the application of COSMO-RS becomes increasingly challenging for large and structurally complex biomolecules, such as proteins and polysaccharides. The predictive accuracy of the model partially depends on the quality of the molecular structures used as input, whereas macromolecules often exhibit irregular conformations, structural heterogeneity, and extensive intra- and intermolecular interactions that are difficult to represent adequately within the COSMO-RS framework [316]. Consequently, the current screening framework using solely COSMO-RS is ideal for relatively small, well-defined molecules freely dissolved in (aqueous) solution, such as phenolic pollutants, algal toxins and pesticides [66, 493, 494], but limited predicted accuracy for larger molecules.

11.4.2 Integrated disruption-dissolution solvent screening

DES have previously been reported to induce structural modification and disintegration of algal, plant and bacterial walls through interactions with polysaccharide-rich networks, including cellulose- and hemicellulose-like components [206, 495, 496]. Given this intrinsic capability, future solvent screening strategies should explicitly

account for DES performance not only in terms of solute affinity, but also with respect to the biomass matrix interactions. Within this thesis, this is particularly relevant in the context of **Chapter 5**, where computational screening was primarily based on pigment–DES interactions, while cell wall disruption and alginate release had to be evaluated experimentally. Integrating both aspects into the screening workflow would therefore provide a more comprehensive and predictive framework for DES selection in biomass fractionation processes.

To move beyond solute-centric thermodynamic screening, a more holistic multiscale modelling framework should be integrated. Molecular dynamics (MD) simulations have already been applied post-hoc to DES–biomass systems, including seaweed, microalgal and plant cell wall models, to elucidate deconstruction mechanisms at the molecular level, such as ion-driven disruption of polysaccharide hydrogen-bond networks[148, 206, 338, 497]. As demonstrated for plant cell wall matrices, MD is capable of capturing structural swelling, wall permeabilisation, and the associated energetic penalties of biomass deconstruction [498]. These studies show that MD can resolve structure–interaction relationships governing cellulose dissolution and biomass permeabilisation and may therefore be used as a predictive screening tool rather than solely a mechanistic descriptor. Instead of utilising MD as a post-hoc mechanism, future frameworks should implement it a priori as a predictive screening tool. Therefore, a dual disruption–dissolution design framework could provide a more robust prediction of extraction performance, limiting the dependence on experimental screening (**Figure 11.6**).

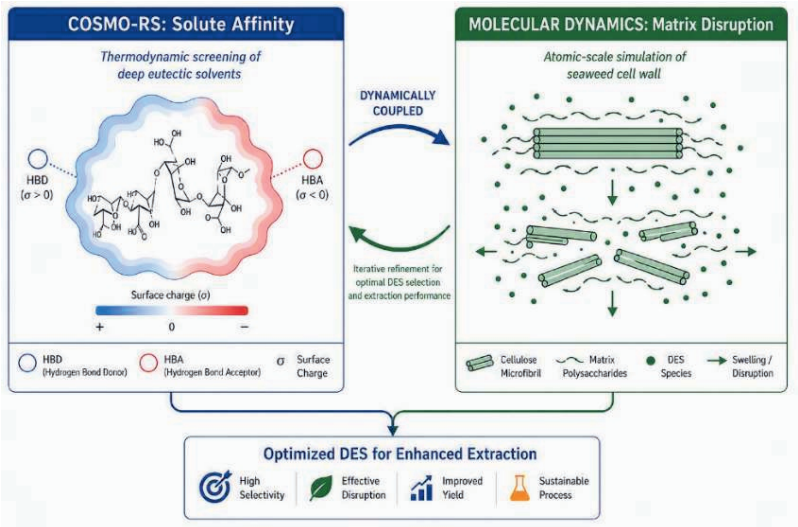


Figure 11.6 DES design approach based on combined solute affinity and biomass matrix interaction screening.

Section 3: Multifunctional DES platforms and nature-inspired processing

11.5. From extraction solvents to multifunctional process platforms

The results presented throughout this thesis indicate that DES can contribute to seaweed biorefineries beyond their role as extraction solvents alone. By combining selective extraction, biomass disruption, product stabilisation, and solvent recycling, DES-based systems offer opportunities for process intensification and integrated valorisation of multiple biomass fractions. In particular, the biphasic DES approach investigated (**Chapter 9**) demonstrates how hydrophilic and hydrophobic DES can fulfil complementary functions within a single processing platform, thereby enabling more efficient utilisation of brown seaweed biomass.

BOX 3: MULTIFUNCTIONAL DES PLATFORMS AND NATURE-INSPIRED PROCESSING

Main Results & Conclusions:
Biphasic extraction with DES (FABU) evaluated within this work demonstrated that DES could function as multifunctional process platforms that integrate several operation steps within a single medium. However, techno-economic assessments indicated that simply deploying DES as substitution for the conventional extraction solvents is economically unviable for producing low-cost alginate. Nevertheless, sensitivity analyses indicated that the process becomes economically viable if improved alginate functionality and improved preservation of fucoxanthin are rewarded with higher market prices. By demonstrating both increased yields and enhanced functionalities, this consolidated biphasic configuration could potentially be integrated in high-value advanced applications, as complemented by a promising environmental profile validated through life-cycle assessments.

Opinion & Outlook:
Although immediate commercial feasibility remains constrained by economic thresholds for commodity applications, DES represent a viable technological alternative when engineered as high-value multifunctional process platforms. In this integrated approach, the solvent is no longer solely an extracting solvent, but an active, quality-enhancing component that justifies its downstream processing costs by unlocking additional material properties. To transition beyond the limits of alginate processing and realise the full potential of DES, future bioprocess engineering should adopt biomimetic design principles. Translating how natural eutectic networks perform transportation, stabilisation and solubilisation mechanisms *in vivo* could provide a baseline, allowing to design industrial processing designs that align with biological functionalities and operational viability.

11.5.1 DES as multifunctional process media

Previous studies demonstrated that hydrophilic and hydrophobic DES can fulfil complementary functions in brown seaweed processing. Reynaga-Navarro *et al*. [48]

showed that hydrophilic DES enabled the extraction of high-viscosity alginate with improved functional properties, whereas hydrophobic DES promoted biomass disruption and facilitated fucoxanthin recovery (**Chapter 5**). Combining these functionalities within a single biphasic DES system, together with a pretreatment step enabling recovery of fucoidan and mannitol, therefore represented an attractive strategy for integrated multiproduct seaweed biorefineries, as investigated in **Chapter 9**.

The limited partitioning of fucoxanthin into the fatty acid DES phase, despite favourable COSMO-RS predictions, demonstrates that thermodynamic affinity alone is insufficient to predict extraction performance in complex biomass systems. While fucoxanthin exhibited a theoretical preference for the hydrophobic DES phase, experimental results suggest factors including biomass accessibility, mass-transfer limitations, and intracellular localisation of the pigment could have imposed stronger constraints on extraction than solvent–solute interactions alone.

Rather than representing a limitation, the enhanced fucoxanthin recovery observed during the subsequent alkaline extraction step suggests that the primary function of the FABU system may lie in increasing compound accessibility through structural biomass modification or disruption. In this context, disruption and solubilisation of fucoxanthin appear to be partially decoupled processes: the DES system facilitates release of intracellular compounds from the biomass matrix, while recovery may occur in a later processing step. The improved preservation of fucoxanthin observed relative to conventional alginate extraction alone, further indicates that DES extraction of alginate may contribute to biomass processing through protective and stabilising effects in addition to direct extraction.

These findings broaden the perspective on the role of DES in integrated biorefineries. Rather than acting solely as extraction solvents, DES may function as multifunctional process media that combine pretreatment, stabilisation, and selective recovery within a single processing platform.

11.5.2 Towards environmentally and economically viable seaweed biorefineries

The techno-economic and life cycle assessments demonstrated that the feasibility of DES-based seaweed biorefineries is primarily determined by solvent-related factors, with DES production and its constituents representing the dominant contributors to both process costs and environmental impacts. Despite these challenges, the DES-

based process showed environmental advantages compared with conventional alkaline extraction, indicating the potential of DES as a more sustainable alternative when solvent-related limitations are addressed.

The limited economic competitiveness under current assumptions is mainly attributed to the high cost of DES components and solvent consumption. However, sensitivity analyses showed that process feasibility can be improved through efficient solvent recycling and the production of higher-value alginate fractions with enhanced functional properties. These main bottlenecks were directly addressed throughout this thesis through the development of DES recycling strategies (**Chapters 4–8**) and multiproduct fractionation approaches that increased the valorisation potential of seaweed-derived compounds (**Chapter 9**).

Collectively, the TEA and LCA demonstrate that maximising solvent recycling and increasing product functionality represent the two principal strategies for improving the economic and environmental feasibility of future DES-based seaweed biorefineries.

11.6. From multifunctional DES to biomimetic process engineering

Throughout this thesis, DES were primarily investigated as extraction and separation media for circular seaweed biorefineries. However, the challenges encountered during alginate recovery highlight a broader perspective: the molecular interactions that enable DES-based extraction may also provide opportunities for applications where solvent–solute interactions are desirable rather than problematic. Therefore, DES should not only be considered as alternative extraction solvents, but as multifunctional processing environments capable of controlling molecular interactions, stabilising compounds, and influencing product functionality.

Instead, the proposed biological functions of NADES have inspired numerous technological applications, including drug delivery, cryopreservation, and biocatalysis. NADES may act as intracellular media involved in metabolite solubilisation, transport, and stabilisation [17, 499], inspiring DES-based systems that improve the solubility and stability of pharmaceutical compounds [500], protect biological materials during (cryo)preservation [3, 25, 501–503], and enhance enzymatic performance compared to in aqueous media [504–506]. Together, these developments demonstrate that DES can function as stabilising and functional process environments rather than solely extraction solvents.

Perspective Box 5: Learning from Nature - Biomimetic design of next-generation DES

NADES are increasingly recognised as intracellular liquid environments that enable living organisms to solubilise, transport, stabilise, and biosynthesise metabolites that are otherwise poorly accommodated in aqueous cellular environments. Rather than functioning as passive solubilising agents, they actively regulate molecular organisation and biological function.

Engineering perspective

The future of DES technology should not be driven solely by replacing conventional solvents, but by translating the biological functions of NADES into bioprocessing. Rather than designing DES exclusively to dissolve target compounds, future solvent systems should be engineered to actively stabilise sensitive biomolecules throughout processing, regulate molecular transport and controlled release, direct selective phase behaviour and fractionation, and, where appropriate, remain incorporated within the final product as functional material components rather than temporary processing aids. This biomimetic design philosophy fundamentally redefines the role of DES in bioprocess designs (**Figure 11.7**). Instead of acting as alternative solvents that are ultimately removed from the process, DES become functional environments deliberately designed to perform the same molecular tasks that NADES are proposed to fulfil in nature. By learning from these naturally occurring eutectic systems, future DES technologies may evolve beyond extraction towards integrated process platforms that simultaneously enhance process efficiency, product functionality, and material performance.

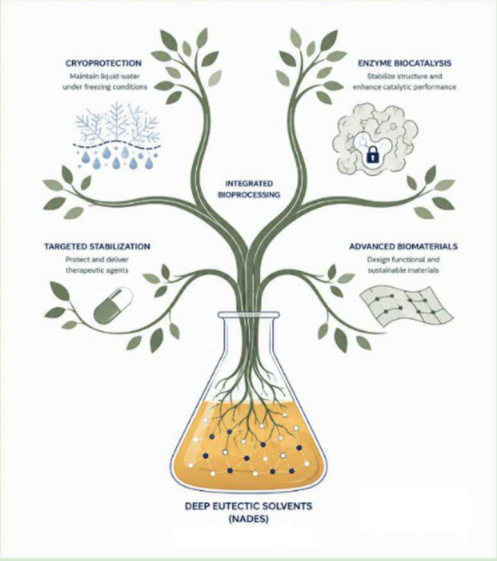
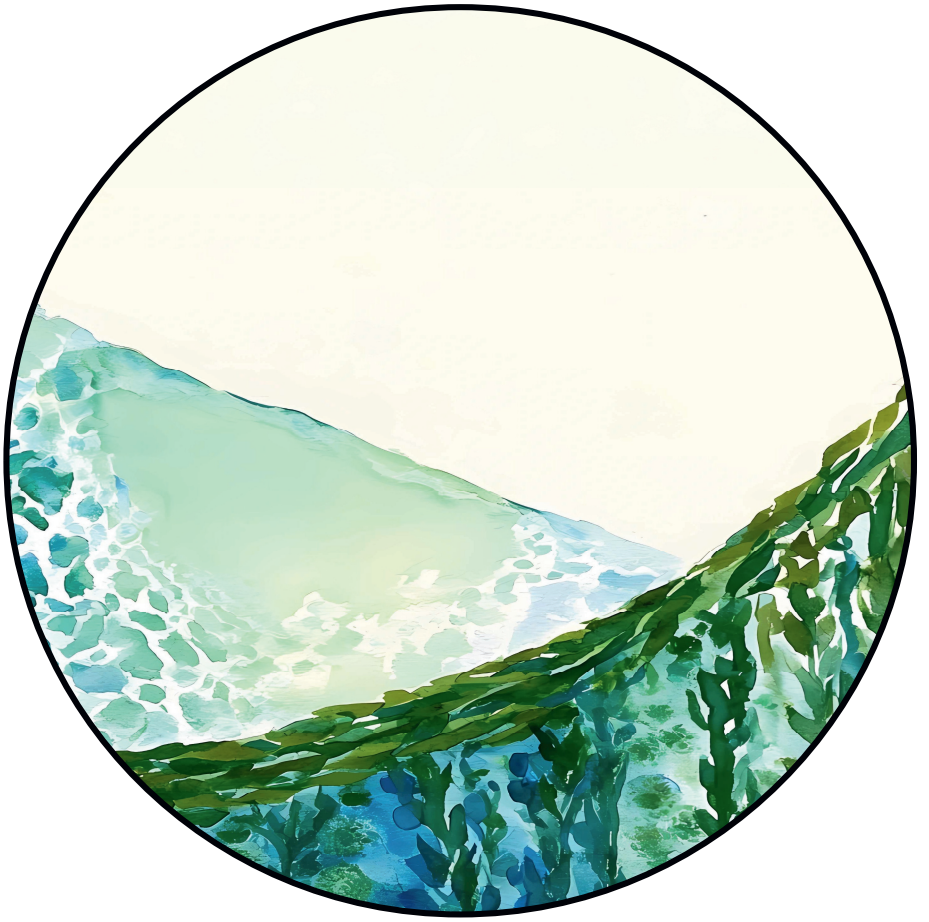


Figure 11.7 Potential nature-inspired DES applications.

From a process engineering view, this biomimetic perspective suggests a shift from designing DES exclusively for efficient extraction and subsequent removal towards designing solvents that actively contribute to the final process or product. Future DES-based systems may intentionally exploit solvent–molecule interactions for controlled

release, stabilisation of sensitive biomolecules, preservation, functional biomaterial development, and integrated extraction–formulation processes. The findings of this thesis illustrate the relevance of this concept: interactions between DES components and alginate that complicate recovery also demonstrate the ability of DES to influence polymer organisation and phase behaviour. Rather than treating these interactions only as downstream limitations, future process engineering may exploit them as a design feature. Thus, biomimetic DES design may enable a transition from solvents that simply extract molecules towards functional environments that stabilise, transport, and organise biological materials throughout processing, inspired by biological roles of DES.



References

1. Shahbaz M, Riaz M, Momal U, Rasool IFU, Naeem H, Raza N, Moreno A, Khalid W, Esatbeyoglu T (2025) Green solvent extraction and eco-friendly novel techniques of bioactive compounds from plant waste: Applications, future perspective and circular economy. Applied Food Research 5:101434. https://doi.org/10.1016/j.afres.2025.101434

2. Clarke CJ, Tu W-C, Levers O, Bröhl A, Hallett JP (2018) Green and Sustainable Solvents in Chemical Processes. Chem Rev 118:747–800. https://doi.org/10.1021/acs.chemrev.7b00571

3. Fonseca-Barahona I, Shahbaz K, Baroutian S (2026) Emerging methods to extract bioactive compounds from brown algae: a comprehensive review of performance, readiness, and sustainability. Separation and Purification Technology 395:137731. https://doi.org/10.1016/j.seppur.2026.137731

4. Mungwari CP, King'ondu CK, Sigauke P, Obadele BA (2025) Conventional and modern techniques for bioactive compounds recovery from plants: Review. Scientific African 27:e02509. https://doi.org/10.1016/j.sciaf.2024.e02509

5. Krekhova F, Shishov A, Meshcheva D, Bulatov A (2026) Deep eutectic solvents: extraction and derivatization. A review. TrAC Trends in Analytical Chemistry 200:118851. https://doi.org/10.1016/j.trac.2026.118851

6. Thamer I, Kumaravel V (2026) Natural deep eutectic solvents for bio-based industrial applications: Properties and sustainable extraction with biomedical features. Industrial Crops and Products 244:123159. https://doi.org/10.1016/j.indcrop.2026.123159

7. Yang X, Zhao L, Li L, Ai M, Wang K, Hu Z, Xu Z, Liu X (2026) Recent advances in extraction and food applications of natural bioactives using deep eutectic solvents. Food Research International 229:118407. https://doi.org/10.1016/j.foodres.2026.118407

8. Martins MAR, Pinho SP, Coutinho JAP (2019) Insights into the Nature of Eutectic and Deep Eutectic Mixtures. J Solution Chem 48:962–982. https://doi.org/10.1007/s10953-018-0793-1

9. Hansen BB, Horton A, Chen B, Poe D, Zhang Y, Spittle S, Klein J, Adhikari L, Zelovich T, Doherty BW, Gurkan B, Maginn E, Ragauskas A, Dadmun M, Zawodzinski T, Baker GA, Tuckerman M, Savinell RF, Sangoro JR (2020) Deep Eutectic Solvents: A Review of Fundamentals and Applications

10. Smith EL, Abbott AP, Ryder KS (2014) Deep eutectic solvents (DESs) and their applications

11. Fronduti M, Del Giacco T, Rossi E, Tiecco M, Germani R (2023) Insights into the structural features of deep eutectic solvents: the eutectic point as an unicum in their physical properties and the surface tension as a method for its determination. Journal of Molecular Liquids 379:121679. https://doi.org/10.1016/j.molliq.2023.121679

12. Abbott AP, Capper G, Davies DL, Rasheed RK, Tambyrajah V (2003) Novel solvent properties of choline chloride/urea mixturesElectronic supplementary information (ESI) available: spectroscopic data. See http://www.rsc.org/suppdata/cc/b2/b210714g/. Chem Commun 70–71. https://doi.org/10.1039/b210714g

13. Bhagwat P, Amobonye A, Singh S, Pillai S (2022) Deep eutectic solvents in the pretreatment of feedstock for efficient fractionation of polysaccharides: current status and

future prospects. Biomass Conv Bioref 12:171–195. https://doi.org/10.1007/s13399-021-01745-x

14. El Achkar T, Greige-Gerges H, Fourmentin S (2021) Basics and properties of deep eutectic solvents: a review. Environmental Chemistry Letters 19:3397–3408. https://doi.org/10.1007/s10311-021-01225-8

15. Omar KA, Sadeghi R (2022) Physicochemical properties of deep eutectic solvents: A review. Journal of Molecular Liquids 360:. https://doi.org/10.1016/j.molliq.2022.119524

16. Şahin S, Kurtulbaş E, Toprakçı İ, Anwar F, Khan R, Ciğeroğlu Z, İnce Yardımcı A, Torun M, Balcı Torun F, Falsafi SR (2026) Deep Eutectic Solvents for Sustainable Extraction of Bioactive Compounds from Biomass: Mechanistic Insights and Scale-Up Challenges. Molecules 31:880. https://doi.org/10.3390/molecules31050880

17. Choi YH, van Spronsen J, Dai Y, Verberne M, Hollmann F, Arends IWCE, Witkamp GJ, Verpoorte R (2011) Are natural deep eutectic solvents the missing link in understanding cellular metabolism and physiology? Plant Physiology 156:1701–1705. https://doi.org/10.1104/pp.111.178426

18. Chevé-Kools E, Choi YH, Roullier C, Ruprich-Robert G, Grougnet R, Chapeland-Leclerc F, Hollmann F (2025) Natural deep eutectic solvents (NaDES): green solvents for pharmaceutical applications and beyond. Green Chemistry 27:8360–8385. https://doi.org/10.1039/d4gc06386d

19. Alnajjar A, Onaizi SA (2025) CO2 capture and conversion using Deep eutectic Solvents: Recent progress and outlooks. Journal of Molecular Liquids 421:126832. https://doi.org/10.1016/j.molliq.2024.126832

20. Manafpour AA, Feyzi F, Rezaee M (2024) An environmentally friendly deep eutectic solvent for CO2 capture. Sci Rep 14:19744. https://doi.org/10.1038/s41598-024-70761-4

21. Dou J, Wang S, Li Y, Li H, Chen X, Yu J (2026) Toxic gas removal using deep eutectic solvents: A review of fundamentals and applications. Fuel 420:138947. https://doi.org/10.1016/j.fuel.2026.138947

22. Mao J, Ma Y, Zang L, Xue R, Xiao C, Ji D (2020) Efficient Adsorption of Hydrogen Sulfide at Room Temperature Using Fumed Silica-supported Deep Eutectic Solvents. Aerosol Air Qual Res 20:203–2015. https://doi.org/10.4209/aaqr.2019.10.0520

23. Nandgure P, Sen D, Yadav D, Methri SM, Natesan S, Yadav AK (2026) Next-Generation Green Transdermal Platforms: Integrating Deep Eutectic Solvent Chemistry with Nanotechnology. Journal of Drug Delivery Science and Technology 108396. https://doi.org/10.1016/j.jddst.2026.108396

24. Spennacchio A, Racaniello GF, Balenzano G, Iacobazzi RM, Lopedota AA, Lopalco A, Denora N (2025) Extraction of Oleanolic Acid from Olea Europaea L. leaves using a Lipophilic Deep Eutectic Solvent for direct formulation of self-emulsifying drug delivery systems. Journal of Drug Delivery Science and Technology 104:106519. https://doi.org/10.1016/j.jddst.2024.106519

25. Bryant SJ, Awad MN, Elbourne A, Christofferson AJ, Martin AV, Meftahi N, Drummond CJ, Greaves TL, Bryant G (2022) Deep eutectic solvents as cryoprotective agents for mammalian cells. Journal of Materials Chemistry B 10:4546–4560. https://doi.org/10.1039/d2tb00573e

26. Jesus AR, Duarte ARC, Paiva A (2022) Use of natural deep eutectic systems as new cryoprotectant agents in the vitrification of mammalian cells. Scientific Reports 12:. https://doi.org/10.1038/s41598-022-12365-4

27. Liu J, Liu Y, Sui L, Zhang S, Liu J (2026) Sustainable and selective recovery of valuable metals from spent catalysts by green deep eutectic solvents. Journal of Environmental Chemical Engineering 14:121890. https://doi.org/10.1016/j.jece.2026.121890

28. Mirinn E, Abbott AP, Kilpatrick AFR (2026) Deep eutectic solvents as recyclable media for metal removal from crude oil. RSC Adv 16:16211–16219. https://doi.org/10.1039/D5RA09189F

29. Soares B, Da Costa Lopes AM, Silvestre AJD, Rodrigues Pinto PC, Freire CSR, Coutinho JAP (2021) Wood delignification with aqueous solutions of deep eutectic solvents. Industrial Crops and Products 160:113128. https://doi.org/10.1016/j.indcrop.2020.113128

30. Sun X, Zhou Z, Tian D, Zhao J, Zhang J, Deng P, Zou H, Lu C (2023) Acidic deep eutectic solvent assisted mechanochemical delignification of lignocellulosic biomass at room temperature. International Journal of Biological Macromolecules 234:123593. https://doi.org/10.1016/j.ijbiomac.2023.123593

31. Aktaş H, Kurek MA (2024) Deep eutectic solvents for the extraction of polyphenols from food plants. Food Chemistry 444:138629. https://doi.org/10.1016/j.foodchem.2024.138629

32. Wojeicchowski JP, Ferreira AM, Abranches DO, Mafra MR, Coutinho JAP (2020) Using COSMO-RS in the Design of Deep Eutectic Solvents for the Extraction of Antioxidants from Rosemary. ACS Sustainable Chemistry and Engineering 8:12132–12141. https://doi.org/10.1021/acssuschemeng.0c03553

33. Tjalsma TG, Didion YP, Su Z, Malankowska M, Torres-Montero P, Martínez JL, Pinelo M (2025) Hydrophobic deep eutectic solvents as novel, sustainable aids for intracellular protein release from Saccharomyces cerevisiae. Results in Engineering 25:. https://doi.org/10.1016/j.rineng.2025.104232

34. Al Fuhaid L, Wellman GB, Kharbatia N, Farinha ASF, Vrouwenvelder JS, Verpoorte R, Choi YH, Witkamp G-J, Lauersen KJ, Fortunato L (2024) Green extraction of pigment from astaxanthin-producing algae using natural deep eutectic solvents. Algal Research 82:103668. https://doi.org/10.1016/j.algal.2024.103668

35. Xu Y, Wang Q, Hou Y (2020) Efficient Purification of R-phycoerythrin from Marine Algae (Porphyra yezoensis) Based on a Deep Eutectic Solvents Aqueous Two-Phase System. Marine Drugs 18:618. https://doi.org/10.3390/md18120618

36. Shishov A, Pochivalov A, Nugbienyo L, Andruch V, Bulatov A (2020) Deep eutectic solvents are not only effective extractants. TrAC - Trends in Analytical Chemistry 129:. https://doi.org/10.1016/j.trac.2020.115956

37. Ferreira C, Sarraguça M (2024) A Comprehensive Review on Deep Eutectic Solvents and Its Use to Extract Bioactive Compounds of Pharmaceutical Interest. Pharmaceuticals 17:. https://doi.org/10.3390/ph17010124

38. Amador S, Martins A, Matias M, Pedrosa R, Pinteus S (2025) Deep eutectic systems: a game changer for marine bioactives recovery. Marine Drugs 23:1–17. https://doi.org/10.3390/md23050211

39. Koch SJI, Rivera MA, Ciravegna E, Chatterton J, Sim S, Van Den Burg SWK (2026) Enhancing the beneficial environmental impacts of seaweed cultivation: what do we understand about best practices? J Appl Phycol 38:1381–1395. https://doi.org/10.1007/s10811-026-03822-y

40. Sen P, Kanthal S, Hore J, Hazra S, Mukhopadhyay R, Gujjar RS, Kumar R, Chatterjee A (2026) The future of food: seaweed farming, biotechnology, and global sustainability. BIOLOGIA FUTURA 77:59–83. https://doi.org/10.1007/s42977-025-00301-2

41. Afonso NC, Catarino MD, Silva AMS, Cardoso SM (2019) Brown Macroalgae as Valuable Food Ingredients. Antioxidants 8:365. https://doi.org/10.3390/antiox8090365

42. Can B, Sanlier N (2026) Secret heroes of the sea: brown macroalgae and their bioactive powers—a narrative review. Front Nutr 13:1766041. https://doi.org/10.3389/fnut.2026.1766041

43. Li Y, Zheng Y, Zhang Y, Yang Y, Wang P, Imre B, Wong ACY, Hsieh YSY, Wang D (2021) Brown Algae Carbohydrates: Structures, Pharmaceutical Properties, and Research Challenges. Marine Drugs 19:620. https://doi.org/10.3390/md19110620

44. Kenny HM, Reynolds CM, Garcia-Vaquero M, Feeney EL (2025) Keeping an eye on alginate: innovations and opportunities for sustainable production and diverse applications. Carbohydrate Polymers 366:123902. https://doi.org/10.1016/j.carbpol.2025.123902

45. Abasalizadeh F, Moghaddam SV, Alizadeh E, Akbari E, Kashani E, Fazljou SMB, Torbati M, Akbarzadeh A (2020) Alginate-based hydrogels as drug delivery vehicles in cancer treatment and their applications in wound dressing and 3D bioprinting. J Biol Eng 14:8. https://doi.org/10.1186/s13036-020-0227-7

46. Zhang S, Dong J, Pan R, Xu Z, Li M, Zang R (2023) Structures, Properties, and Bioengineering Applications of Alginates and Hyaluronic Acid. Polymers 15:2149. https://doi.org/10.3390/polym15092149

47. Charoensiddhi S, Conlon MA, Franco CMM, Zhang W (2017) The development of seaweed-derived bioactive compounds for use as prebiotics and nutraceuticals using enzyme technologies. Trends in Food Science & Technology 70:20–33. https://doi.org/10.1016/j.tifs.2017.10.002

48. Reynaga-Navarro W, Bozzo L, Wijffels RH, Eppink M, Kazbar A (2026) Characterisation of alginate extracted from Saccharina latissima with deep eutectic solvents. Food Hydrocolloids 171:. https://doi.org/10.1016/j.foodhyd.2025.111862

49. Jiao W, Chen W, Mei Y, Yun Y, Wang B, Zhong Q, Chen H, Chen W (2019) Effects of Molecular Weight and Guluronic Acid/Mannuronic Acid Ratio on the Rheological Behavior and Stabilizing Property of Sodium Alginate. Molecules (Basel, Switzerland) 24:. https://doi.org/10.3390/molecules24234374

50. Abka-khajouei R, Tounsi L, Shahabi N, Patel AK, Abdelkafi S, Michaud P (2022) Structures, Properties and Applications of Alginates. Marine Drugs 20:. https://doi.org/10.3390/md20060364

51. Rosiak P, Latanska I, Paul P, Sujka W, Kolesinska B (2021) Modification of Alginates to Modulate Their Physic-Chemical Properties and Obtain Biomaterials with Different Functional Properties. Molecules 26:7264. https://doi.org/10.3390/molecules26237264

52. Hosokawa M, Takatani N (2026) Health Benefits of the Edible Brown Seaweed Carotenoid, Fucoxanthin. In: Murakami A, Sakakibara H, Kawabata K, Miyoshi N (eds) Functional Food Factors. Springer Nature Singapore, Singapore, pp 165–174

53. Haggag Y, Abd Elrahman A, Ulber R, Zayed A (2023) Fucoidan in Pharmaceutical Formulations: A Comprehensive Review for Smart Drug Delivery Systems. Marine Drugs 21:112. https://doi.org/10.3390/md21020112

54. Karuppusamy S, Rajauria G, Fitzpatrick S, Lyons H, McMahon H, Curtin J, Tiwari BK, O'Donnell C (2022) Biological Properties and Health-Promoting Functions of Laminarin: A Comprehensive Review of Preclinical and Clinical Studies. Marine Drugs 20:772. https://doi.org/10.3390/md20120772

55. Hosseini SV, Dastgerdi HE, Tahergorabi R (2024) Marine Mannitol: Extraction, Structures, Properties, and Applications. Processes 12:1613–1613. https://doi.org/10.3390/pr12081613

56. Saji S, Hebden A, Goswami P, Du C (2022) A Brief Review on the Development of Alginate Extraction Process and Its Sustainability. Sustainability (Switzerland) 14:. https://doi.org/10.3390/su14095181

57. Bojorges H, López-Rubio A, Martínez-Abad A, Fabra MJ (2023) Overview of alginate extraction processes: Impact on alginate molecular structure and techno-functional properties. Trends in Food Science and Technology 140:. https://doi.org/10.1016/j.tifs.2023.104142

58. Rahman MM, Shahid MA, Hossain MT, Sheikh MS, Rahman MS, Uddin N, Rahim A, Khan RA, Hossain I (2024) Sources, extractions, and applications of alginate: a review. Discover Applied Sciences 6:. https://doi.org/10.1007/s42452-024-06151-2

59. Gomez CG, Pérez Lambrecht MV, Lozano JE, Rinaudo M, Villar MA (2009) Influence of the extraction–purification conditions on final properties of alginates obtained from brown algae (Macrocystis pyrifera). International Journal of Biological Macromolecules 44:365–371. https://doi.org/10.1016/j.ijbiomac.2009.02.005

60. Felicia WXL, Rovina K, Zuldin WH, Suriati L, Huda N, Nurdiani R (2026) Sustainable Valorization of Alginate, a Review of Green Extraction, Structure–Function Relationships, and Next-Generation Food Applications. Food Bioprocess Technol 19:97. https://doi.org/10.1007/s11947-025-04096-x

61. Lomartire S, Gonçalves AMM (2022) Novel Technologies for Seaweed Polysaccharides Extraction and Their Use in Food with Therapeutically Applications—A Review. Foods 11:2654. https://doi.org/10.3390/foods11172654

62. Shang X chao, Chu D, Zhang J xu, Zheng Y fen, Li Y (2021) Microwave-assisted extraction, partial purification and biological activity in vitro of polysaccharides from bladder-wrack (Fucus vesiculosus) by using deep eutectic solvents. Separation and Purification Technology 259:. https://doi.org/10.1016/j.seppur.2020.118169

63. Nie J, Chen D, Lu Y (2020) Deep eutectic solvents based ultrasonic extraction of polysaccharides from edible brown Seaweed Sargassum horneri. Journal of Marine Science and Engineering 8:. https://doi.org/10.3390/JMSE8060440

64. Praveen MA, Yu L, Selva C, Bulone V (2026) Optimization of ultrasound-assisted natural deep eutectic solvent extraction for the recovery of bioactive polysaccharides and phlorotannins from the brown alga Ecklonia radiata. International Journal of Biological Macromolecules 338:149744. https://doi.org/10.1016/j.ijbiomac.2025.149744

65. Ozturk B, Gonzalez-Miquel M (2019) Alkanediol-based deep eutectic solvents for isolation of terpenoids from citrus essential oil: Experimental evaluation and COSMO-RS studies. Separation and Purification Technology 227:. https://doi.org/10.1016/j.seppur.2019.115707

66. Fattahi N, Shiri F, Zohrabi P, Bordón Sosa FH, Hashemi B, Karimi P (2025) Using COSMO-RS in the designing and screening of different eutectic solvents for the extraction of carbaryl. Separation and Purification Technology 370:. https://doi.org/10.1016/j.seppur.2025.133278

67. Klamt A (2003) Prediction of the mutual solubilities of hydrocarbons and water with COSMO-RS. Fluid Phase Equilibria 206:223–235. https://doi.org/10.1016/S0378-3812(02)00322-9

68. Wang J, Guo Y, Liu F, Zhang X, Wang W, Peng Q (2022) COSMO-RS prediction and experimental verification of deep eutectic solvents for water insoluble pesticides with high solubility. Journal of Molecular Liquids 349:118139. https://doi.org/10.1016/j.molliq.2021.118139

69. Isci A, Kaltschmitt M (2022) Recovery and recycling of deep eutectic solvents in biomass conversions: a review. Biomass Conversion and Biorefinery 12:197–226. https://doi.org/10.1007/s13399-021-01860-9

70. Yu L, Li Z, Huang W, Ali A, Chen Y, Zhao G, Yao S (2024) Recovery and post-treatment processes for ionic liquids and deep eutectic solvents. Journal of Molecular Liquids 402:. https://doi.org/10.1016/j.molliq.2024.124767

71. Della Posta S, Gallo V, Gentili A, Fanali C (2022) Strategies for the recovery of bioactive molecules from deep eutectic solvents extracts. TrAC Trends in Analytical Chemistry 157:116798. https://doi.org/10.1016/j.trac.2022.116798

72. Zhou P, Wang X, Liu P, Huang J, Wang C, Pan M, Kuang Z (2018) Enhanced phenolic compounds extraction from Morus alba L. leaves by deep eutectic solvents combined with ultrasonic-assisted extraction. Industrial Crops and Products 120:147–154. https://doi.org/10.1016/j.indcrop.2018.04.071

73. Huang Y, Feng F, Jiang J, Qiao Y, Wu T, Voglmeir J, Chen Z-G (2017) Green and efficient extraction of rutin from tartary buckwheat hull by using natural deep eutectic solvents. Food Chemistry 221:1400–1405. https://doi.org/10.1016/j.foodchem.2016.11.013

74. Kumar AK, Parikh BS, Pravakar M (2016) Natural deep eutectic solvent mediated pretreatment of rice straw: bioanalytical characterization of lignin extract and enzymatic

hydrolysis of pretreated biomass residue. Environ Sci Pollut Res 23:9265–9275. https://doi.org/10.1007/s11356-015-4780-4

75. Bradić B, Novak U, Likozar B Crustacean shell bio-refining to chitin by natural deep eutectic solvents

76. Satlewal A, Agrawal R, Das P, Bhagia S, Pu Y, Puri SK, Ramakumar SSV, Ragauskas AJ (2019) Assessing the Facile Pretreatments of Bagasse for Efficient Enzymatic Conversion and Their Impacts on Structural and Chemical Properties. ACS Sustainable Chem Eng 7:1095–1104. https://doi.org/10.1021/acssuschemeng.8b04773

77. Lo C, Wijffels RH, Eppink MHM (2024) Lipid recovery from deep eutectic solvents by polar antisolvents. Food and Bioproducts Processing 143:21–27. https://doi.org/10.1016/j.fbp.2023.10.003

78. Wang Y, Xu F, Cheng J, Wu X, Xu J, Li C, Li W, Xie N, Wang Y, He L (2022) Natural Deep Eutectic Solvent-Assisted Extraction, Structural Characterization, and Immunomodulatory Activity of Polysaccharides from Paecilomyces hepiali. Molecules 27:. https://doi.org/10.3390/molecules27228020

79. Wu DT, Feng KL, Huang L, Gan RY, Hu YC, Zou L (2021) Deep eutectic solvent-assisted extraction, partially structural characterization, and bioactivities of acidic polysaccharides from lotus leaves. Foods 10:. https://doi.org/10.3390/foods10102330

80. Merza F, Fawzy A, AlNashef I, Al-Zuhair S, Taher H (2018) Effectiveness of using deep eutectic solvents as an alternative to conventional solvents in enzymatic biodiesel production from waste oils. Energy Reports 4:77–83. https://doi.org/10.1016/j.egyr.2018.01.005

81. Xu M, Ran L, Chen N, Fan X, Ren D, Yi L (2019) Polarity-dependent extraction of flavonoids from citrus peel waste using a tailor-made deep eutectic solvent. Food Chemistry 297:124970. https://doi.org/10.1016/j.foodchem.2019.124970

82. Tran PH, Tran PV (2019) A highly selective and efficient method for the production of 5-hydroxymethylfurfural from dehydration of fructose using SACS/DES catalytic system. Fuel 246:18–23. https://doi.org/10.1016/j.fuel.2019.02.112

83. Liang X, Fu Y, Chang J (2019) Effective separation, recovery and recycling of deep eutectic solvent after biomass fractionation with membrane-based methodology. Separation and Purification Technology 210:409–416. https://doi.org/10.1016/j.seppur.2018.08.021

84. Liang X, Zhang J, Huang Z, Guo Y (2023) Sustainable recovery and recycling of natural deep eutectic solvent for biomass fractionation via industrial membrane-based technique. Industrial Crops and Products 194:. https://doi.org/10.1016/j.indcrop.2023.116351

85. Al-Amshawee S, Yunus MYBM, Azoddein AAM, Hassell DG, Dakhil IH, Hasan HA (2020) Electrodialysis desalination for water and wastewater: A review. Chemical Engineering Journal 380:122231. https://doi.org/10.1016/j.cej.2019.122231

86. Arana Juve J-M, Christensen FMS, Wang Y, Wei Z (2022) Electrodialysis for metal removal and recovery: A review. Chemical Engineering Journal 435:134857. https://doi.org/10.1016/j.cej.2022.134857

87. Fernández M de los Á, Boiteux J, Espino M, Gomez FJV, Silva MF (2018) Natural deep eutectic solvents-mediated extractions: The way forward for sustainable analytical developments. Analytica Chimica Acta 1038:1–10. https://doi.org/10.1016/j.aca.2018.07.059

88. Zeb L, Gerhardt AS, Johannesen BA, Underhaug J, Jordheim M (2024) Ultrasonic-Assisted Water-Rich Natural Deep Eutectic Solvents for Sustainable Polyphenol Extraction from Seaweed: A Case Study on Cultivated Saccharina latissima. ACS Sustainable Chemistry and Engineering 12:14921–14929. https://doi.org/10.1021/acssuschemeng.4c06736

89. Anjana K, Arunkumar K (2024) Brown algae biomass for fucoxanthin, fucoidan and alginate; update review on structure, biosynthesis, biological activities and extraction valorisation. International Journal of Biological Macromolecules 280:. https://doi.org/10.1016/j.ijbiomac.2024.135632

90. Špadina M, Dufrêche JF, Pellet-Rostaing S, Marčelja S, Zemb T (2021) Molecular Forces in Liquid-Liquid Extraction. Langmuir 37:10637–10656. https://doi.org/10.1021/acs.langmuir.1c00673

91. Ferreira RSB, Farias FO, de Araujo EJS, Martínez J, Batista EAC (2023) Deep eutectic solvents as an alternative for extraction of flavonoids from soybean (Glycine max (L) Merrill) and okara: An experimental and computational approach based on COSMO-SAC model. Food Research International 173:. https://doi.org/10.1016/j.foodres.2023.113266

92. Peng W, Wang L, Wang X, Wang Y, Wang W, Huang J, Zhou R, Chen C, Bo R, Liu M, Li J (2025) Efficient polyphenol extraction from Moringa oleifera Lam. leaves using natural deep eutectic solvents: COSMO-RS screening, ANN-GA optimization and antioxidant activity evaluation. LWT 223:. https://doi.org/10.1016/j.lwt.2025.117687

93. Xu D, Chow J, Weber CC, Packer MA, Baroutian S, Shahbaz K (2022) Evaluation of deep eutectic solvents for the extraction of fucoxanthin from the alga Tisochrysis lutea - COSMO-RS screening and experimental validation. Journal of Environmental Chemical Engineering 10:. https://doi.org/10.1016/j.jece.2022.108370

94. Iqbal J, Muhammad N, Rahim A, Khan AS, Ullah Z, Gonfa G, Ahmad P (2019) COSMO-RS predictions, hydrogen bond basicity values and experimental evaluation of amino acid-based ionic liquids for lignocellulosic biomass dissolution. Journal of Molecular Liquids 273:215–221. https://doi.org/10.1016/j.molliq.2018.10.044

95. Baerends EJ, Aguirre NF, Austin ND, Autschbach J, Bickelhaupt FM, Bulo R, Cappelli C, van Duin ACT, Egidi F, Fonseca Guerra C, Förster A, Franchini M, Goumans TPM, Heine T, Hellström M, Jacob CR, Jensen L, Krykunov M, van Lenthe E, Michalak A, Mitoraj MM, Neugebauer J, Nicu VP, Philipsen P, Ramanantoanina H, Rüger R, Schreckenbach G, Stener M, Swart M, Thijssen JM, Trnka T, Visscher L, Yakovlev A, van Gisbergen S (2025) The Amsterdam Modeling Suite. Journal of Chemical Physics 162:. https://doi.org/10.1063/5.0258496

96. Mok SY, Sivapragasam M, Raja Shahrom MS, Bustam MA, Abidin ZZ (2023) Screening of ionic liquids for the dissolution of chitosan using COSMO-RS. Green Chemistry 26:1577–1586. https://doi.org/10.1039/d3gc03586g

97. Khan AS, Ibrahim TH, Rashid Z, Khamis MI, Nancarrow P, Jabbar NA (2021) COSMO-RS based screening of ionic liquids for extraction of phenolic compounds from aqueous media. Journal of Molecular Liquids 328:. https://doi.org/10.1016/j.molliq.2021.115387

98. Spaggiari C, Sara I, Hiemstra A, Kazbar A, Costantino G, Righetti L (2025) Towards eco-metabolomics: NADES-guided extraction enables semi-quantitative metabolomics for Melissa officinalis. 2772–5820. https://doi.org/10.5281/zenodo.12721470

99. Zurob E, Cabezas R, Villarroel E, Rosas N, Merlet G, Quijada-Maldonado E, Romero J, Plaza A (2020) Design of natural deep eutectic solvents for the ultrasound-assisted extraction of hydroxytyrosol from olive leaves supported by COSMO-RS. Separation and Purification Technology 248:117054–117054. https://doi.org/10.1016/j.seppur.2020.117054

100. Hiemstra ISA, Meinema JT, Eppink MMH, Wijffels RH, Kazbar A (2024) Choline chloride-based solvents as alternative media for alginate extraction from brown seaweed. LWT 214:. https://doi.org/10.1016/j.lwt.2024.117174

101. Alsoy Altinkaya S (2024) A perspective on cellulose dissolution with deep eutectic solvents. Frontiers in Membrane Science and Technology 3:. https://doi.org/10.3389/frmst.2024.1382054

102. Sharma M, Mukesh C, Mondal D, Prasad K (2013) Dissolution of α-chitin in deep eutectic solvents. RSC Advances 3:18149–18155. https://doi.org/10.1039/c3ra43404d

103. Chen M, Falourd X, Lahaye M (2021) Sequential natural deep eutectic solvent pretreatments of apple pomace: A novel way to promote water extraction of pectin and to tailor its main structural domains. Carbohydrate Polymers 266:. https://doi.org/10.1016/j.carbpol.2021.118113

104. Chen M, Lahaye M (2021) Natural deep eutectic solvents pretreatment as an aid for pectin extraction from apple pomace. Food Hydrocolloids 115:. https://doi.org/10.1016/j.foodhyd.2021.106601

105. Wang J, Jing W, Tian H, Liu M, Yan H, Bi W, Chen DDY (2020) Investigation of Deep Eutectic Solvent-Based Microwave-Assisted Extraction and Efficient Recovery of Natural Products. ACS Sustainable Chemistry and Engineering 8:12080–12088. https://doi.org/10.1021/acssuschemeng.0c03393

106. Tang W, Row KH (2020) Design and evaluation of polarity controlled and recyclable deep eutectic solvent based biphasic system for the polarity driven extraction and separation of compounds. Journal of Cleaner Production 268:. https://doi.org/10.1016/j.jclepro.2020.122306

107. Casillo A, Fabozzi A, Russo Krauss I, Parrilli E, Biggs CI, Gibson MI, Lanzetta R, Appavou MS, Radulescu A, Tutino ML, Paduano L, Corsaro MM (2021) Physicochemical Approach to Understanding the Structure, Conformation, and Activity of Mannan Polysaccharides. Biomacromolecules 22:1445–1457. https://doi.org/10.1021/acs.biomac.0c01659

108. Cocinero EJ, Lesarri A, Écija P, Cimas Á, Davis BG, Basterretxea FJ, Fernández JA, Castaño F (2013) Free fructose is conformationally locked. Journal of the American Chemical Society 135:2845–2852. https://doi.org/10.1021/ja312393m

109. Cunha AG, Gandini A (2010) Turning polysaccharides into hydrophobic materials: A critical review. Part 2. Hemicelluloses, chitin/chitosan, starch, pectin and alginates. Cellulose 17:1045–1065. https://doi.org/10.1007/s10570-010-9435-5

110. Li X, Wang X, Chen Q, Wu H, Huang W, Zhang W, Ren S, Ouyang R, Jiang Y, Yao C (2025) Oil-phenol separation by tetraethylammonium chloride-based deep eutectic solvents: Microscopic contribution of basic sites. Separation and Purification Technology 358:. https://doi.org/10.1016/j.seppur.2024.130296

111. Mero A, Koutsoumpos S, Giannios P, Stavrakas I, Moutzouris K, Mezzetta A, Guazzelli L (2023) Comparison of physicochemical and thermal properties of choline chloride and betaine-based deep eutectic solvents: The influence of hydrogen bond acceptor and hydrogen bond donor nature and their molar ratios. Journal of Molecular Liquids 377:. https://doi.org/10.1016/j.molliq.2023.121563

112. Di Pietro T, Cesari L, Mutelet F (2023) Influence of water on the conformations and interactions within two choline chloride-based deep eutectic solvents: a density functional theory investigation. Structural Chemistry 34:2165–2183. https://doi.org/10.1007/s11224-023-02156-6

113. Abranches DO, Silva LP, Martins MAR, Pinho SP, Coutinho JAP (2020) Understanding the Formation of Deep Eutectic Solvents: Betaine as a Universal Hydrogen Bond Acceptor. ChemSusChem 13:4916–4921. https://doi.org/10.1002/cssc.202001331

114. Suthar P, Kaushal M, Vaidya D, Thakur M, Chauhan P, Angmo D, Kashyap S, Negi N (2023) Deep eutectic solvents (DES): An update on the applications in food sectors. Journal of Agriculture and Food Research 14:. https://doi.org/10.1016/j.jafr.2023.100678

115. Duan L, Dou LL, Guo L, Li P, Liu EH (2016) Comprehensive Evaluation of Deep Eutectic Solvents in Extraction of Bioactive Natural Products. ACS Sustainable Chemistry and Engineering 4:2405–2411. https://doi.org/10.1021/acssuschemeng.6b00091

116. García-Roldán A, Piriou L, Jauregi P (2023) Natural deep eutectic solvents as a green extraction of polyphenols from spent coffee ground with enhanced bioactivities. Frontiers in Plant Science 13:. https://doi.org/10.3389/fpls.2022.1072592

117. Khandelwal S, Tailor YK, Kumar M (2016) Deep eutectic solvents (DESs) as eco-friendly and sustainable solvent/catalyst systems in organic transformations. Journal of Molecular Liquids 215:345–386. https://doi.org/10.1016/j.molliq.2015.12.015

118. Zhang Q, De Oliveira Vigier K, Royer S, Jérôme F (2012) Deep eutectic solvents: Syntheses, properties and applications. Chemical Society Reviews 41:7108–7146. https://doi.org/10.1039/c2cs35178a

119. Das AK, Sharma M, Mondal D, Prasad K (2016) Deep eutectic solvents as efficient solvent system for the extraction of κ-carrageenan from Kappaphycus alvarezii. Carbohydrate Polymers 136:930–935. https://doi.org/10.1016/j.carbpol.2015.09.114

120. Kalhor P, Ghandi K (2019) Deep eutectic solvents for pretreatment, extraction, and catalysis of biomass and food waste. Molecules 24:. https://doi.org/10.3390/molecules24224012

121. Lo C, Semerel J, van den Berg C, Wijffels RH, Eppink MHM (2021) Eutectic solvents with tuneable hydrophobicity: lipid dissolution and recovery. RSC Advances 11:8142–8149. https://doi.org/10.1039/d1ra00306b

122. Fenoradosoa TA, Ali G, Delattre C, Laroche C, Petit E, Wadouachi A, Michaud P (2010) Extraction and characterization of an alginate from the brown seaweed Sargassum turbinarioides Grunow. Journal of Applied Phycology 22:131–137. https://doi.org/10.1007/s10811-009-9432-y

123. Abdul Khalil HPS, Lai TK, Tye YY, Rizal S, Chong EWN, Yap SW, Hamzah AA, Nurul Fazita MR, Paridah MT (2018) A review of extractions of seaweed hydrocolloids: Properties and applications. Express Polymer Letters 12:296–317. https://doi.org/10.3144/expresspolymlett.2018.27

124. Dobrinčić A, Balbino S, Zorić Z, Pedisić S, Kovačević DB, Garofulić IE, Dragović-Uzelac V (2020) Advanced technologies for the extraction of marine brown algal polysaccharides. Marine Drugs 18:. https://doi.org/10.3390/md18030168

125. Bertagnolli C, Espindola APDM, Kleinübing SJ, Tasic L, Silva MGCD (2014) Sargassum filipendula alginate from Brazil: Seasonal influence and characteristics. Carbohydrate Polymers 111:619–623. https://doi.org/10.1016/j.carbpol.2014.05.024

126. Khajouei RA, Keramat J, Hamdami N, Ursu AV, Delattre C, Laroche C, Gardarin C, Lecerf D, Desbrières J, Djelveh G, Michaud P (2018) Extraction and characterization of an alginate from the Iranian brown seaweed Nizimuddinia zanardini. International Journal of Biological Macromolecules 118:1073–1081. https://doi.org/10.1016/j.ijbiomac.2018.06.154

127. Zaib Q, Eckelman MJ, Yang Y, Kyung D (2022) Are deep eutectic solvents really green?: A life-cycle perspective. Green Chemistry 24:7924–7930. https://doi.org/10.1039/d2gc01752k

128. Saravana PS, Cho YN, Woo HC, Chun BS (2018) Green and efficient extraction of polysaccharides from brown seaweed by adding deep eutectic solvent in subcritical water hydrolysis. Journal of Cleaner Production 198:1474–1484. https://doi.org/10.1016/j.jclepro.2018.07.151

129. Ci SX, Huynh TH, Louie LW, Yang A, Beals BJ, Ron N, Tsang W-G, Soon-Shiong P, Desai NP (1999) Molecular mass distribution of sodium alginate by high-performance size-exclusion chromatography

130. Li Y, Li Y, Li H, Fan X, Yan H, Cai M, Xu X, Zhu M (2023) Insights into the tribological behavior of choline chloride—urea and choline chloride—thiourea deep eutectic solvents. Friction 11:76–92. https://doi.org/10.1007/s40544-021-0575-4

131. Troter DZ, Todorović ZB, Đokić-Stojanović DR, Đordević BS, Todorović VM, Konstantinović SS, Veljković VB (2017) The physicochemical and thermodynamic properties of the choline chloride-based deep eutectic solvents. Journal of the Serbian Chemical Society 82:1039–1052. https://doi.org/10.2298/JSC170225065T

132. Hou Y, Gu Y, Zhang S, Yang F, Ding H, Shan Y (2008) Novel binary eutectic mixtures based on imidazole. Journal of Molecular Liquids 143:154–159. https://doi.org/10.1016/j.molliq.2008.07.009

133. Adeyemi I, Abu-Zahra MRM, AlNashef IM (2018) Physicochemical properties of alkanolamine-choline chloride deep eutectic solvents: Measurements, group contribution and artificial intelligence prediction techniques. Journal of Molecular Liquids 256:581–590. https://doi.org/10.1016/j.molliq.2018.02.085

134. Elik A, Durukan H, Sarac H, Demirbas A, Altunay N (2022) Application of levulinic acid-based natural deep eutectic solvents for extraction and determination of deltamethrin in food samples. Sustainable Chemistry and Pharmacy 30:. https://doi.org/10.1016/j.scp.2022.100861

135. de Almeida Pontes PV, Ayumi Shiwaku I, Maximo GJ, Caldas Batista EA (2021) Choline chloride-based deep eutectic solvents as potential solvent for extraction of phenolic compounds from olive leaves: Extraction optimization and solvent characterization. Food Chemistry 352:. https://doi.org/10.1016/j.foodchem.2021.129346

136. Cesaretti M, Luppi E, Maccari F, Volpi N (2003) A 96-well assay for uronic acid carbazole reaction. Carbohydrate Polymers 54:59–61. https://doi.org/10.1016/S0144-8617(03)00144-9

137. Youssouf L, Lallemand L, Giraud P, Soulé F, Bhaw-Luximon A, Meilhac O, D'Hellencourt CL, Jhurry D, Couprie J (2017) Ultrasound-assisted extraction and structural characterization by NMR of alginates and carrageenans from seaweeds. Carbohydrate Polymers 166:55–63. https://doi.org/10.1016/j.carbpol.2017.01.041

138. da Costa WA, de França VF, da Silva Souza LS, de Andrade ASA, de Araújo DAM, Moreira EDT, Pontes LFBL (2023) Physical–chemical and ecotoxic evaluation of different deep eutectic solvents for green analytical applications. Environmental Science and Pollution Research 30:70701–70712. https://doi.org/10.1007/s11356-023-27398-z

139. Kachangoon R, Vichapong J, Santaladchaiyakit Y, Burakham R, Srijaranai S (2020) An eco-friendly hydrophobic deep eutectic solvent-based dispersive liquid-liquid microextraction for the determination of neonicotinoid insecticide residues in water, soil and egg yolk samples. Molecules 25:. https://doi.org/10.3390/molecules25122785

140. Pires IV, Sakurai YCN, Ferreira NR, Moreira SGC, da Cruz Rodrigues AM, da Silva LHM (2022) Elaboration and Characterization of Natural Deep Eutectic Solvents (NADESs): Application in the Extraction of Phenolic Compounds from pitaya. Molecules 27:. https://doi.org/10.3390/molecules27238310

141. Loschen C, Klamt A (2014) Prediction of solubilities and partition coefficients in polymers using COSMO-RS. Industrial and Engineering Chemistry Research 53:11478–11487. https://doi.org/10.1021/ie501669z

142. Zhu R, Lei Z (2021) COSMO-based models for predicting the gas solubility in polymers. Green Energy and Environment 6:311–313. https://doi.org/10.1016/j.gee.2021.03.009

143. Xu Y, Wang Q, Hou Y (2020) Efficient Purification of R-phycoerythrin from Marine Algae (Porphyra yezoensis) Based on a Deep Eutectic Solvents Aqueous Two-Phase System. Marine Drugs 18:. https://doi.org/10.3390/md18120618

144. Yue X, Cao Y, Wang Y, Bao H, Xu Y (2022) Optimization of Deep Eutectic Solvents Extraction of Effective Components from Phellodendron chinense Schneid by Response Surface Methodology. International Journal of Chemical Engineering 2022:. https://doi.org/10.1155/2022/3881551

145. Lazović M, Cvijetić I, Jankov M, Milojković-Opsenica D, Trifković J, Ristivojević P (2023) COSMO-RS in prescreening of Natural Eutectic Solvents for phenolic extraction from Teucrium chamaedrys. Journal of Molecular Liquids 387:. https://doi.org/10.1016/j.molliq.2023.122649

146. Filly A, Fabiano-Tixier AS, Fernandez X, Chemat F (2015) Alternative solvents for extraction of food aromas. Experimental and COSMO-RS study. LWT 61:33–40. https://doi.org/10.1016/j.lwt.2014.11.021

147. Craigie JS (2011) Seaweed extract stimuli in plant science and agriculture. Journal of Applied Phycology 23:371–393. https://doi.org/10.1007/s10811-010-9560-4

148. Matchim Kamdem MC, Tamafo Fouegue AD, Lai N (2023) A Comprehensive Study on DES Pretreatment Application to Microalgae for Enhanced Lipid Recovery Suitable for Biodiesel Production: Combined Experimental and Theoretical Investigations. Energies 16:. https://doi.org/10.3390/en16093806

149. Sun B, Zheng YL, Yang SK, Zhang JR, Cheng XY, Ghiladi R, Ma Z, Wang J, Deng WW (2021) One-pot method based on deep eutectic solvent for extraction and conversion of polydatin to resveratrol from Polygonum cuspidatum. Food Chemistry 343:. https://doi.org/10.1016/j.foodchem.2020.128498

150. Yang TX, Zhao LQ, Wang J, Song GL, Liu HM, Cheng H, Yang Z (2017) Improving Whole-Cell Biocatalysis by Addition of Deep Eutectic Solvents and Natural Deep Eutectic Solvents. ACS Sustainable Chemistry and Engineering 5:5713–5722. https://doi.org/10.1021/acssuschemeng.7b00285

151. Hernandez-Carmona G, Vilchis M, Rodriguez E (1992) Recirculation of residual acid from the pre-extraction stage in the process of obtaining sodium alginate

152. Zaib Q, Eckelman MJ, Yang Y, Kyung D (2022) Are deep eutectic solvents really green?: A life-cycle perspective. Green Chemistry 24:7924–7930. https://doi.org/10.1039/d2gc01752k

153. Dardavila MM, Pappou S, Savvidou MG, Louli V, Katapodis P, Stamatis H, Magoulas K, Voutsas E (2023) Extraction of Bioactive Compounds from C. vulgaris Biomass Using Deep Eutectic Solvents. Molecules 28:. https://doi.org/10.3390/molecules28010415

154. Wan Mahmood WMA, Lorwirachsutee A, Theodoropoulos C, Gonzalez-Miquel M (2019) Polyol-Based Deep Eutectic Solvents for Extraction of Natural Polyphenolic Antioxidants from Chlorella vulgaris. ACS Sustainable Chemistry and Engineering 7:5018–5026. https://doi.org/10.1021/acssuschemeng.8b05642

155. Rostami Z, Tabarsa M, You SG, Rezaei M (2017) Relationship between molecular weights and biological properties of alginates extracted under different methods from Colpomenia peregrina. Process Biochemistry 58:289–297. https://doi.org/10.1016/j.procbio.2017.04.037

156. Imtiaz F, Saif Z, Sajid A, Nazir A, Manzoor Q, Saleem A, Mehr-un-Nisa, Farooq A, Al-Mijalli SH, Iqbal M (2024) Role of glycerol-based deep eutectic solvents for extraction of phytochemicals from Cichorium intybus seeds: Optimization by response surface methodology. Microchemical Journal 199:. https://doi.org/10.1016/j.microc.2024.110083

157. Liu Z, Sun T, Liu J, Liang N, Zhao L (2024) Natural deep eutectic solvent as a green extraction medium for the ultrasonic-assisted extraction of sinapine thiocyanate from black mustard seeds. Microchemical Journal 201:. https://doi.org/10.1016/j.microc.2024.110549

158. Chen XQ, Li ZH, Liu LL, Wang H, Yang SH, Zhang JS, Zhang Y (2021) Green extraction using deep eutectic solvents and antioxidant activities of flavonoids from two fruits of Rubia species. LWT 148:. https://doi.org/10.1016/j.lwt.2021.111708

159. Manivannan M, Rajendran S (2011) Investigation of inhibitive action of urea-Zn2+ system in the corrosion control of carbon steel in sea water

160. Cruz-Reyes IG, Mendoza-Pérez JA, Ruiz-Guerrero R, Medina-Velázquez DY, Zepeda-Vallejo LG, Morales-Ramírez Á de J (2022) Kinetics of Zn–C Battery Leaching with Choline Chloride/Urea Natural Deep Eutectic Solvents. Recycling 7:. https://doi.org/10.3390/recycling7060086

161. Song X, Hu W, Huang W, Wang H, Yan S, Yu S, Liu F (2020) Methanolysis of polycarbonate into valuable product bisphenol A using choline chloride-based deep eutectic solvents as highly active catalysts. Chemical Engineering Journal 388:. https://doi.org/10.1016/j.cej.2020.124324

162. Nejrotti S, Antenucci A, Pontremoli C, Gontrani L, Barbero N, Carbone M, Bonomo M (2022) Critical Assessment of the Sustainability of Deep Eutectic Solvents: A Case Study on Six Choline Chloride-Based Mixtures. ACS Omega 7:47449–47461. https://doi.org/10.1021/acsomega.2c06140

163. Chen X, Wang R, Tan Z (2023) Extraction and purification of grape seed polysaccharides using pH-switchable deep eutectic solvents-based three-phase partitioning. Food Chemistry 412:. https://doi.org/10.1016/j.foodchem.2023.135557

164. Wang T, Guo Q, Yang H, Gao W, Li P (2022) pH-controlled reversible deep-eutectic solvent based enzyme system for simultaneous extraction and in-situ separation of isoflavones from Pueraria lobata. Separation and Purification Technology 292:. https://doi.org/10.1016/j.seppur.2022.120992

165. Cai C, Wang Y, Yu W, Wang C, Li F, Tan Z (2020) Temperature-responsive deep eutectic solvents as green and recyclable media for the efficient extraction of polysaccharides from Ganoderma lucidum. Journal of Cleaner Production 274:. https://doi.org/10.1016/j.jclepro.2020.123047

166. Longeras O, Gautier A, Ballerat-Busserolles K, Andanson JM (2020) Deep Eutectic Solvent with Thermo-Switchable Hydrophobicity. ACS Sustainable Chemistry and Engineering 8:12516–12520. https://doi.org/10.1021/acssuschemeng.0c03478

167. Cai C, Chen X, Li F, Tan Z (2021) Three-phase partitioning based on CO2-responsive deep eutectic solvents for the green and sustainable extraction of lipid from Nannochloropsis sp. Separation and Purification Technology 279:. https://doi.org/10.1016/j.seppur.2021.119685

168. Wan W, Xiong D, Zhang Q, Wang J (2019) Miscible-Immiscible Transition of Deep Eutectic Solvents in Water Switched by CO2. ACS Sustainable Chemistry and Engineering 7:17882–17887. https://doi.org/10.1021/acssuschemeng.9b04430

169. Owhe EO, Kumar N, Lynam JG (2021) Lignin extraction from waste biomass with deep eutectic solvents: Molecular weight and heating value. Biocatalysis and Agricultural Biotechnology 32:101949–101949. https://doi.org/10.1016/j.bcab.2021.101949

170. Moncada B J, Aristizábal M V, Cardona A CA (2016) Design strategies for sustainable biorefineries. Biochemical Engineering Journal 116:122–134. https://doi.org/10.1016/j.bej.2016.06.009

171. Liew SQ, Ngoh GC, Yusoff R, Teoh WH (2018) Acid and Deep Eutectic Solvent (DES) extraction of pectin from pomelo (Citrus grandis (L.) Osbeck) peels. Biocatalysis and Agricultural Biotechnology 13:1–11. https://doi.org/10.1016/j.bcab.2017.11.001

172. Cao J, Wu R, Dong Q, Zhao L, Cao F, Su E (2020) Effective Release of Intracellular Enzymes by Permeating the Cell Membrane with Hydrophobic Deep Eutectic Solvents. ChemBioChem 21:672–680. https://doi.org/10.1002/cbic.201900502

173. Wu M, Ma H, Ma Z, Jin Y, Chen C, Guo X, Qiao Y, Pedersen CM, Hou X, Wang Y (2018) Deep Eutectic Solvents: Green Solvents and Catalysts for the Preparation of Pyrazine Derivatives by Self-Condensation of d -Glucosamine. ACS Sustainable Chemistry and Engineering 6:9434–9441. https://doi.org/10.1021/acssuschemeng.8b01788

174. Ijardar SP, Singh V, Gardas RL (2022) Revisiting the Physicochemical Properties and Applications of Deep Eutectic Solvents. Molecules 27:. https://doi.org/10.3390/molecules27041368

175. Balaraman H, Selvasembian R, Rangarajan V, Rathnasamy S (2021) Sustainable and Green Engineering Insights on Deep Eutectic Solvents toward the Extraction of Nutraceuticals. ACS Sustainable Chemistry and Engineering 9:11290–11313. https://doi.org/10.1021/acssuschemeng.1c03034

176. Paiva A, Craveiro R, Aroso I, Martins M, Reis RL, Duarte ARC (2014) Natural deep eutectic solvents - Solvents for the 21st century. ACS Sustainable Chemistry and Engineering 2:1063–1071. https://doi.org/10.1021/sc500096j

177. Elgharbawy AAM, Hayyan M, Hayyan A, Basirun WJ, Salleh HM, Mirghani MES (2020) A grand avenue to integrate deep eutectic solvents into biomass processing. Biomass and Bioenergy 137:105550–105550. https://doi.org/10.1016/j.biombioe.2020.105550

178. Liang X, Guo Y (2022) High-efficiency recovery and regeneration of choline-polyol deep eutectic solvent for biorefinery via bipolar membrane electrodialysis and ultrafiltration. Bioresource Technology 362:. https://doi.org/10.1016/j.biortech.2022.127805

179. Ruesgas-Ramón M, Figueroa-Espinoza MC, Durand E (2017) Application of Deep Eutectic Solvents (DES) for Phenolic Compounds Extraction: Overview, Challenges, and Opportunities. Journal of Agricultural and Food Chemistry 65:3591–3601. https://doi.org/10.1021/acs.jafc.7b01054

180. Suk DE, Matsuura T (2006) Membrane-based hybrid processes: A review. Separation Science and Technology 41:595–626. https://doi.org/10.1080/01496390600552347

181. Colusse GA, Carneiro J, Duarte MER, Ranga Rao A, Ravishankar GA, de Carvalho JC, Noseda MD (2022) Challenges and Recent Progress in Seaweed Polysaccharides for Industrial Purposes. In: Ranga Rao A, Ravishankar GA (eds) Sustainable Global Resources of Seaweeds

Volume 2: Food, Pharmaceutical and Health Applications. Springer International Publishing, Cham, pp 411–431

182. Al-Dawsari JN, Bessadok-Jemai A, Wazeer I, Mokraoui S, AlMansour MA, Hadj-Kali MK (2020) Fitting of experimental viscosity to temperature data for deep eutectic solvents. Journal of Molecular Liquids 310:113127. https://doi.org/10.1016/j.molliq.2020.113127

183. Abels C, Redepenning C, Moll A, Melin T, Wessling M (2012) Simple purification of ionic liquid solvents by nanofiltration in biorefining of lignocellulosic substrates. Journal of Membrane Science 405–406:1–10. https://doi.org/10.1016/j.memsci.2011.12.020

184. Haerens K, Deuren SV, Bruggen BVD (2010) Challenges for recycling ionic liquids by using pressure driven membrane processes. 2182–2188. https://doi.org/10.1039/c0gc00406e

185. W. S. Winston H, Kamalesh K. S (1992) Membrane Handbook. y Springer Science+Business Media New York

186. Aguirre Montesdeoca V, Van der Padt A, Boom RM, Janssen AEM (2016) Modelling of membrane cascades for the purification of oligosaccharides. Journal of Membrane Science 520:712–722. https://doi.org/10.1016/j.memsci.2016.08.031

187. Rizki Z, Suryawirawan E, Janssen AEM, van der Padt A, Boom RM (2020) Modelling temperature effects in a membrane cascade system for oligosaccharides. Journal of Membrane Science 610:118292–118292. https://doi.org/10.1016/j.memsci.2020.118292

188. Gabriele F, Chiarini M, Germani R, Tiecco M, Spreti N (2019) Effect of water addition on choline chloride/glycol deep eutectic solvents: Characterization of their structural and physicochemical properties. Journal of Molecular Liquids 291:. https://doi.org/10.1016/j.molliq.2019.111301

189. García G, Aparicio S, Ullah R, Atilhan M (2015) Deep eutectic solvents: Physicochemical properties and gas separation applications. Energy and Fuels 29:2616–2644. https://doi.org/10.1021/ef5028873

190. Cassano A, Donato L, Drioli E (2007) Ultrafiltration of kiwifruit juice: Operating parameters, juice quality and membrane fouling. Journal of Food Engineering 79:613–621. https://doi.org/10.1016/j.jfoodeng.2006.02.020

191. Brouwer T, Schuur B (2019) Model Performances Evaluated for Infinite Dilution Activity Coefficients Prediction at 298.15 K. Ind Eng Chem Res 58:8903–8914. https://doi.org/10.1021/acs.iecr.9b00727

192. Cui Z, Enjome Djocki AV, Yao J, Wu Q, Zhang D, Nan S, Gao J, Li C (2021) COSMO-SAC-supported evaluation of natural deep eutectic solvents for the extraction of tea polyphenols and process optimization. Journal of Molecular Liquids 328:115406. https://doi.org/10.1016/j.molliq.2021.115406

193. Verevkin SP, Sazonova AYu, Frolkova AK, Zaitsau DH, Prikhodko IV, Held C (2015) Separation Performance of BioRenewable Deep Eutectic Solvents. Ind Eng Chem Res 54:3498–3504. https://doi.org/10.1021/acs.iecr.5b00357

194. Brogioli D, Vailati A (2001) Diffusive mass transfer by nonequilibrium fluctuations: Fick's law revisited. Physical Review E - Statistical, Nonlinear, and Soft Matter Physics 63:0121051–0121054. https://doi.org/10.1103/PhysRevE.63.012105

195. Gholami M, Schuur B, Roy Y (2022) Ultrafiltration-based diafiltration for post-delignification fractionation of lignin from a deep eutectic solvent comprised of lactic acid and choline chloride. Separation and Purification Technology 302:122097–122097. https://doi.org/10.1016/j.seppur.2022.122097

196. El-Said GF, El-Sikaily A (2013) Chemical composition of some seaweed from Mediterranean Sea coast, Egypt. Environmental Monitoring and Assessment 185:6089–6099. https://doi.org/10.1007/s10661-012-3009-y

197. He S, Yin F, Wu Y, Wang M, Wang Y, Row KH, Tang W (2024) Deep eutectic solvents as extraction media for food-derived biomacromolecules. TrAC - Trends in Analytical Chemistry 171:. https://doi.org/10.1016/j.trac.2024.117521

198. Bashir I, Dar AH, Dash KK, Pandey VK, Fayaz U, Shams R, Srivastava S, Singh R (2023) Deep eutectic solvents for extraction of functional components from plant-based products: A promising approach. Sustainable Chemistry and Pharmacy 33:. https://doi.org/10.1016/j.scp.2023.101102

199. Liu J, Li X, Row KH (2022) Development of deep eutectic solvents for sustainable chemistry. Journal of Molecular Liquids 362:. https://doi.org/10.1016/j.molliq.2022.119654

200. Abbott AP, Boothby D, Capper G, Davies DL, Rasheed RK (2004) Deep Eutectic Solvents formed between choline chloride and carboxylic acids: Versatile alternatives to ionic liquids. Journal of the American Chemical Society 126:9142–9147. https://doi.org/10.1021/ja048266j

201. Santana-Mayor Á, Rodríguez-Ramos R, Herrera-Herrera AV, Socas-Rodríguez B, Rodríguez-Delgado MÁ (2021) Deep eutectic solvents. The new generation of green solvents in analytical chemistry. TrAC - Trends in Analytical Chemistry 134:. https://doi.org/10.1016/j.trac.2020.116108

202. Jahanbakhsh-Bonab P, Pazuki G, Sardroodi JJ, Dehnavi SM (2023) Assessment of the properties of natural-based chiral deep eutectic solvents for chiral drug separation: insights from molecular dynamics simulation. Physical Chemistry Chemical Physics 25:17547–17557. https://doi.org/10.1039/d3cp00875d

203. Jahanbakhsh-Bonab P, Pazuki G (2025) Enantioselective Liquid-Liquid Extraction of Omeprazole Enantiomers Using Chiral Deep Eutectic Solvents. Journal of Chemical and Engineering Data 70:2817–2830. https://doi.org/10.1021/acs.jced.5c00101

204. Jahanbakhsh-Bonab P, Khoshnazar Z, Sardroodi JJ, Heidaryan E (2024) A computational probe into the physicochemical properties of cyclodextrin-based deep eutectic solvents for extraction processes. Carbohydrate Polymer Technologies and Applications 8:. https://doi.org/10.1016/j.carpta.2024.100596

205. Jahanbakhsh-Bonab P, Sardroodi JJ, Avestan MS (2022) Electric Field Effects on the Structural and Dynamical Properties of a Glyceline Deep Eutectic Solvent. Journal of Chemical and Engineering Data 67:2077–2087. https://doi.org/10.1021/acs.jced.2c00066

206. Muhammad G, Jahanbakhsh-Bonab P, Xiong W, Lv Y, Zhang S, Zhao A, Sardroodi JJ, Xu J, Alam MA (2024) Mechanism of deep eutectic solvent-mediated microalgal biomass disintegration for enhanced lutein extraction. Industrial Crops and Products 209:. https://doi.org/10.1016/j.indcrop.2023.117940

207. Xue J, Su J, Wang X, Zhang R, Li X, Li Y, Ding Y, Chu X (2024) Eco-Friendly and Efficient Extraction of Polysaccharides from Acanthopanax senticosus by Ultrasound-Assisted Deep Eutectic Solvent. Molecules 29:. https://doi.org/10.3390/molecules29050942

208. Moreno Martínez P, Ortiz-Martínez VM, Sánchez Segado S, Salar-García MJ, los Ríos AP de, Hernández Fernández FJ, Lozano-Blanco LJ, Godínez C (2022) Deep eutectic solvents for the extraction of fatty acids from microalgae biomass: Recovery of omega-3 eicosapentaenoic acid. Separation and Purification Technology 300:. https://doi.org/10.1016/j.seppur.2022.121842

209. Moldes D, Requejo PF, Vega M, Bolado S, Wijffels RH, Kazbar A (2024) Protein extraction from seaweed Saccharina latissima with deep eutectic solvents. Microchemical Journal 205:. https://doi.org/10.1016/j.microc.2024.111275

210. Bouhzam I, Cantero R, Margallo M, Aldaco R, Bala A, Fullana-i-Palmer P, Puig R (2024) Life cycle assessment and yield to optimize extraction time and solvent: Comparing deep eutectic solvents vs conventional ones. Science of the Total Environment 955:. https://doi.org/10.1016/j.scitotenv.2024.177038

211. Song W, He Y, Huang R, Li J, Yu Y, Xia P (2023) Life cycle assessment of deep-eutectic-solvent-assisted hydrothermal disintegration of microalgae for biodiesel and biogas co-production. Applied Energy 335:. https://doi.org/10.1016/j.apenergy.2023.120758

212. Salehi B, Sharifi-Rad J, Seca AML, Pinto DCGA, Michalak I, Trincone A, Mishra AP, Nigam M, Zam W, Martins N (2019) Current trends on seaweeds: Looking at chemical composition, phytopharmacology, and cosmetic applications. Molecules 24:. https://doi.org/10.3390/molecules24224182

213. Ferruzzi MG, Blakeslee J (2007) Digestion, absorption, and cancer preventative activity of dietary chlorophyll derivatives. Nutrition Research 27:1–12. https://doi.org/10.1016/j.nutres.2006.12.003

214. Heo SJ, Ko SC, Kang SM, Kang HS, Kim JP, Kim SH, Lee KW, Cho MG, Jeon YJ (2008) Cytoprotective effect of fucoxanthin isolated from brown algae Sargassum siliquastrum against H2O2-induced cell damage. European Food Research and Technology 228:145–151. https://doi.org/10.1007/s00217-008-0918-7

215. Peng J, Yuan JP, Wu CF, Wang JH (2011) Fucoxanthin, a marine carotenoid present in brown seaweeds and diatoms: Metabolism and bioactivities relevant to human health. Marine Drugs 9:1806–1828. https://doi.org/10.3390/md9101806

216. Kholany M, Reynaga-Navarro W, Abranches DO, Wijffels R, Coutinho JAP, Ventura SPM, Kazbar A (2025) Extraction and separation of pigments from Saccharina latissima using eutectic solvents. Separation and Purification Technology 357:130053–130053. https://doi.org/10.1016/j.seppur.2024.130053

217. Liu Y, Li J, Fu R, Zhang L, Wang D, Wang S (2019) Enhanced extraction of natural pigments from Curcuma longa L. using natural deep eutectic solvents. Industrial Crops and Products 140:. https://doi.org/10.1016/j.indcrop.2019.111620

218. Chew KW, Ling TC, Show PL (2019) Recent Developments and Applications of Three-Phase Partitioning for the Recovery of Proteins. Separation and Purification Reviews 48:52–64. https://doi.org/10.1080/15422119.2018.1427596

219. Panadare DC, Gondaliya A, Rathod VK (2020) Comparative study of ultrasonic pretreatment and ultrasound assisted three phase partitioning for extraction of custard apple seed oil. Ultrasonics Sonochemistry 61:. https://doi.org/10.1016/j.ultsonch.2019.104821

220. Wang H, Geng H, Chen J, Wang X, Li D, Wang T, Yu D, Wang L (2020) Three phase partitioning for simultaneous extraction of oil, protein and polysaccharide from rice bran. Innovative Food Science and Emerging Technologies 65:. https://doi.org/10.1016/j.ifset.2020.102447

221. Yan JK, Wang YY, Qiu WY, Wang ZB, Ma H (2018) Ultrasound synergized with three-phase partitioning for extraction and separation of Corbicula fluminea polysaccharides and possible relevant mechanisms. Ultrasonics Sonochemistry 40:128–134. https://doi.org/10.1016/j.ultsonch.2017.07.007

222. Chen X, Cai C, Tan Z (2022) Deep eutectic solvents-based three-phase partitioning for tomato peroxidase purification: A promising method for substituting t-butanol. Food Chemistry 393:. https://doi.org/10.1016/j.foodchem.2022.133379

223. Jin X, Duan Q, Li X, Han Z, Wang X (2024) Dissolution of Curcumin by Deep Eutectic Solvent of Fatty Acids. Huadong Ligong Daxue Xuebao/Journal of East China University of Science and Technology 50:214–220. https://doi.org/10.14135/j.cnki.1006-3080.20230228001

224. Zhang H, Zhao W, Bai T, Fu L, Chen Z, Jing X, Wang X (2022) Sustainable extraction of polyphenols from millet using switchable deep eutectic solvents. LWT 170:. https://doi.org/10.1016/j.lwt.2022.114082

225. Gul A, Khan S, Arain H, Khan H, Ishrat U, Siddiqui M (2022) Three-phase partitioning as an efficient one-step method for the extraction and purification of bromelain from pineapple crown waste. Journal of Food Processing and Preservation 46:. https://doi.org/10.1111/jfpp.16973

226. Yan JK, Wang YY, Qiu WY, Shao N (2017) Three-phase partitioning for efficient extraction and separation of polysaccharides from Corbicula fluminea. Carbohydrate Polymers 163:10–19. https://doi.org/10.1016/j.carbpol.2017.01.021

227. Bojorges H, López-Rubio A, Fabra MJ, Martínez-Abad A (2023) Estimation of alginate purity and M/G ratio by methanolysis coupled with anion exchange chromatography. Carbohydrate Polymers 321:. https://doi.org/10.1016/j.carbpol.2023.121285

228. Martins M, Mesquita LMDS, Vaz BMC, Dias ACRV, Torres-Acosta MA, Quéguineur B, Coutinho JAP, Ventura SPM (2021) Extraction and Fractionation of Pigments from Saccharina latissima (Linnaeus, 2006) Using an Ionic Liquid + Oil + Water System. ACS Sustainable Chemistry and Engineering 9:6599–6612. https://doi.org/10.1021/acssuschemeng.0c09110

229. Baghel RS (2022) Developments in seaweed biorefinery research: A comprehensive review. Chemical Engineering Journal 140177–140177. https://doi.org/10.1016/j.cej.2022.140177

230. Shi L (2016) Bioactivities, isolation and purification methods of polysaccharides from natural products: A review. International Journal of Biological Macromolecules 92:37–48. https://doi.org/10.1016/j.ijbiomac.2016.06.100

231. Khan NM, Norman NM, Samsudin AS (2022) Studies on the effect of H+ carrier toward ionic conduction properties in alginate-ammonium sulfate complexes–based polymer electrolytes system. High Performance Polymers 34:637–644. https://doi.org/10.1177/09540083221075320

232. Cao Y, Wang H, Jian Y, Hao G, Di D, Liu J (2024) Temperature-switchable deep eutectic solvent extraction of polysaccharides from wolfberry fruits: Process optimization, structure characterization, and antioxidant activity. Journal of Molecular Liquids 398:. https://doi.org/10.1016/j.molliq.2024.124352

233. Wang G, Huang M, Li F, Li Q, Chen F, Wang S, Ling Z, Ji Z (2024) Insights into the poplar cell wall deconstruction following deep eutectic solvent pretreatment for enhanced enzymatic saccharification and lignin valorization. International Journal of Biological Macromolecules 254:. https://doi.org/10.1016/j.ijbiomac.2023.127673

234. Huang R, He Y, Yao X, Yu Y, Song W, Yang W, Cheng J (2022) Disintegration of wet microalgae biomass with deep-eutectic-solvent-assisted hydrothermal treatment for sustainable lipid extraction. Green Chemistry 24:1615–1626. https://doi.org/10.1039/d1gc03849d

235. Sed G, Cicci A, Jessop PG, Bravi M (2018) A novel switchable-hydrophilicity, natural deep eutectic solvent (NaDES)-based system for bio-safe biorefinery. RSC Advances 8:37092–37097. https://doi.org/10.1039/c8ra08536f

236. Sankaran R, Bong JH, Chow YH, Wong FWF, Ling TC, Show PL (2019) Reverse Micellar System in Protein Recovery - A Review of the Latest Developments. Current Protein & Peptide Science 20:1012–1026. https://doi.org/10.2174/1389203720666190628142203

237. Hu Y, Chen X, Tan Z (2023) Three-phase partitioning constructed by pH-responsive deep eutectic solvents and sugars for purification of radish (Raphanus sativus L.) peroxidase. Separation and Purification Technology 322:. https://doi.org/10.1016/j.seppur.2023.124353

238. Zhao W, Duan M, Zhang X, Tan T (2018) A mild extraction and separation procedure of polysaccharide, lipid, chlorophyll and protein from Chlorella spp. Renewable Energy 118:701–708. https://doi.org/10.1016/j.renene.2017.11.046

239. Tan ZJ, Wang CY, Yi YJ, Wang HY, Zhou WL, Tan SY, Li FF (2015) Three phase partitioning for simultaneous purification of aloe polysaccharide and protein using a single-step extraction. Process Biochemistry 50:482–486. https://doi.org/10.1016/j.procbio.2015.01.004

240. Liu Z, Yu D, Li L, Liu X, Zhang H, Sun W, Lin CC, Chen J, Chen Z, Wang W, Jia W (2019) Three-Phase Partitioning for the Extraction and Purification of Polysaccharides from the Immunomodulatory Medicinal Mushroom Inonotus obliquus. Molecules 24:. https://doi.org/10.3390/molecules24030403

241. El Maaiden E, El Kahia H, Nasser B, Moustaid K, Qarah N, Boukcim H, Hirich A, Kouisni L, El Kharrassi Y (2023) Deep eutectic solvent-ultrasound assisted extraction as a green approach for enhanced extraction of naringenin from Searsia tripartita and retained their bioactivities. Frontiers in Nutrition 10:. https://doi.org/10.3389/fnut.2023.1193509

242. Tabtimmai L, Jongruksavongkul C, Wisetsai A, Sonklin C, Aiamsung M, Chamsodsai P, Choowongkomon K, Sedtananun S (2024) Three-phase partitioning technique for the green separation of crude polysaccharides from Schizophyllum commune and its effect on macrophage activation. Food Bioscience 58:. https://doi.org/10.1016/j.fbio.2024.103735

243. Bojorges H, Martínez-Abad A, Martínez-Sanz M, Rodrigo MD, Vilaplana F, López-Rubio A, Fabra MJ (2023) Structural and functional properties of alginate obtained by means of high hydrostatic pressure-assisted extraction. Carbohydrate Polymers 299:. https://doi.org/10.1016/j.carbpol.2022.120175

244. Rashedy SH, Abd El Hafez MSM, Dar MA, Cotas J, Pereira L (2021) Evaluation and characterization of alginate extracted from brown seaweed collected in the red sea. Applied Sciences (Switzerland) 11:. https://doi.org/10.3390/app11146290

245. Kuzmanović M, Božanić DK, Milivojević D, Ćulafić DM, Stanković S, Ballesteros C, Gonzalez-Benito J (2017) Sodium-alginate biopolymer as a template for the synthesis of nontoxic red emitting Mn2+-doped CdS nanoparticles. RSC Advances 7:53422–53432. https://doi.org/10.1039/c7ra11011a

246. Nesic A, De Bonis MV, Dal Poggetto G, Ruocco G, Santagata G (2023) Microwave Assisted Extraction of Raw Alginate as a Sustainable and Cost-Effective Method to Treat Beach-Accumulated Sargassum Algae. Polymers 15:. https://doi.org/10.3390/polym15142979

247. Ramos PE, Silva P, Alario MM, Pastrana LM, Teixeira JA, Cerqueira MA, Vicente AA (2018) Effect of alginate molecular weight and M/G ratio in beads properties foreseeing the protection of probiotics. Food Hydrocolloids 77:8–16. https://doi.org/10.1016/j.foodhyd.2017.08.031

248. Nøkling-Eide K, Aachmann FL, Tøndervik A, Arlov Ø, Sletta H (2024) In-process epimerisation of alginates from Saccharina latissima, Alaria esculenta and Laminaria hyperborea. Carbohydrate Polymers 325:. https://doi.org/10.1016/j.carbpol.2023.121557

249. Fernandes F, Barbosa M, Oliveira AP, Azevedo IC, Sousa-Pinto I, Valentão P, Andrade PB (2016) The pigments of kelps (Ochrophyta) as part of the flexible response to highly variable marine environments. Journal of Applied Phycology 28:3689–3696. https://doi.org/10.1007/s10811-016-0883-7

250. Kurinjery A, Kulanthaiyesu A (2022) Anti-hyaluronidase and cytotoxic activities of fucoxanthin cis/trans isomers extracted and characterized from 13 brown seaweeds. Process Biochemistry 122:53–68. https://doi.org/10.1016/j.procbio.2022.09.024

251. Lim SJ, Wan WA, Maskat MY (2014) Characterisation and Stability of Pigments Extracted from Sargassum binderi Obtained from Semporna, Sabah

252. Bukman L, De Souza VR, Fernandes NRC, Caetano W, Batistela VR, Hioka N (2020) Reverse micellar extraction of dyes based on fatty acids and recoverable organic solvents. Separation and Purification Technology 242:. https://doi.org/10.1016/j.seppur.2020.116772

253. Penttila PA, Vierros S, Utriainen K, Carl N, Rautkari L, Sammalkorpi M, Osterberg M (2019) Phospholipid-Based Reverse Micelle Structures in Vegetable Oil Modified by Water Content, Free Fatty Acid, and Temperature. Langmuir 35:8373–8382. https://doi.org/10.1021/acs.langmuir.9b01135

254. Kittipongpittaya K, Panya A, McClements DJ, Decker EA (2014) Impact of free fatty acids and phospholipids on reverse micelles formation and lipid oxidation in bulk oil. JAOCS, Journal of the American Oil Chemists' Society 91:453–462. https://doi.org/10.1007/s11746-013-2388-8

255. Lafeuille B, Tamigneaux É, Berger K, Provencher V, Beaulieu L (2023) Variation of the Nutritional Composition and Bioactive Potential in Edible Macroalga Saccharina latissima Cultivated from Atlantic Canada Subjected to Different Growth and Processing Conditions. Foods 12:. https://doi.org/10.3390/foods12081736

256. Schaeffer N, Martins MAR, Neves CMSS, Pinho SP, Coutinho JAP (2018) Sustainable hydrophobic terpene-based eutectic solvents for the extraction and separation of metals. Chemical Communications 54:8104–8107. https://doi.org/10.1039/c8cc04152k

257. Chemat F, Vian MA, Ravi HK, Khadhraoui B, Hilali S, Perino S, Tixier ASF (2019) Review of alternative solvents for green extraction of food and natural products: Panorama, principles, applications and prospects. Molecules 24:. https://doi.org/10.3390/molecules24163007

258. Patrice Didion Y, Gijsbert Tjalsma T, Su Z, Malankowska M, Pinelo M (2023) What is next? the greener future of solid liquid extraction of biobased compounds: Novel techniques and solvents overpower traditional ones. Separation and Purification Technology 320:. https://doi.org/10.1016/j.seppur.2023.124147

259. Xiong Q, Yuan Z, Zhang Y, Chen Z, Wei K, Ma W (2025) A new approach for separating copper, tin, and lead from photovoltaic ribbon wastes. Solar Energy 299:. https://doi.org/10.1016/j.solener.2025.113810

260. Yang C, Li Z, Li S, Cui X, Chen Q (2025) Sustainable evaporative cooling driven by saline water sources: opportunities, challenges and solutions. Renewable and Sustainable Energy Reviews 218:. https://doi.org/10.1016/j.rser.2025.115799

261. Yi X, Qi Y, Li F, Shu J, Sun Z, Sun S, Chen M, Pu S (2019) Effect of electrolyte reuse on metal recovery from waste CPU slots by slurry electrolysis. Waste Management 95:370–376. https://doi.org/10.1016/j.wasman.2019.06.034

262. Zhang M, Zhang Z, Gul Z, Tian M, Wang J, Zheng K, Zhao C, Li C (2023) Advances of responsive deep eutectic solvents and application in extraction and separation of bioactive compounds. Journal of Separation Science 46:. https://doi.org/10.1002/jssc.202300098

263. Halder AK, Cordeiro MNDS (2019) Probing the Environmental Toxicity of Deep Eutectic Solvents and Their Components: An in Silico Modeling Approach. ACS Sustainable Chemistry and Engineering 7:10649–10660. https://doi.org/10.1021/acssuschemeng.9b01306

264. Ma H, Fu P, Zhao J, Lin X, Wu W, Yu Z, Xia C, Wang Q, Gao M, Zhou J (2022) Pretreatment of Wheat Straw Lignocelluloses by Deep Eutectic Solvent for Lignin Extraction. Molecules 27:. https://doi.org/10.3390/molecules27227955

265. Lee KY, Mooney DJ (2012) Alginate: Properties and biomedical applications. Progress in Polymer Science (Oxford) 37:106–126. https://doi.org/10.1016/j.progpolymsci.2011.06.003

266. Belattmania Z, Kaidi S, Atouani SE, Katif C, Bentiss F, Jama C, Reani A, Sabour B, Vasconcelos V (2020) Isolation and FTIR-ATR and 1H NMR characterization of alginates from the main alginophyte species of the atlantic coast of Morocco. Molecules 25:. https://doi.org/10.3390/molecules25184335

267. Mahmood Zia K, Zuber M, Ali M (2017) Algae Based Polymers, Blends, and Composites: Chemistry, Biotechnology and Materials Science

268. Qu H, Wu Y, Luo Z, Dong Q, Yang H, Dai C (2023) An efficient approach for extraction of polysaccharide from abalone (Haliotis Discus Hannai Ino) viscera by natural deep eutectic solvent. International Journal of Biological Macromolecules 244:. https://doi.org/10.1016/j.ijbiomac.2023.125336

269. Zhang L, Wang M (2017) Optimization of deep eutectic solvent-based ultrasound-assisted extraction of polysaccharides from Dioscorea opposita Thunb. International Journal of Biological Macromolecules 95:675–681. https://doi.org/10.1016/j.ijbiomac.2016.11.096

270. Zhang W, Cheng S, Zhai X, Sun J, Hu X, Pei H, Chen G (2020) Green and Efficient Extraction of Polysaccharides From Poria cocos F.A. Wolf by Deep Eutectic Solvent. Natural Product Communications 15:. https://doi.org/10.1177/1934578X19900708

271. Elizondo Sada OM, Hiemstra ISA, Chorhirankul N, Eppink M, Wijffels RH, Janssen AEM, Kazbar A (2024) Pressure-driven membrane processes for the recovery and recycling of deep eutectic solvents: A seaweed biorefinery case study. Biotechnology Reports 43:e00849–e00849. https://doi.org/10.1016/j.btre.2024.e00849

272. Moslehyani A, Ismail AF, Matsuura T, Rahman MA, Goh PS (2018) Recent progresses of ultrafiltration (UF) membranes and processes in water treatment. In: Membrane Separation Principles and Applications: From Material Selection to Mechanisms and Industrial Uses. Elsevier, pp 85–110

273. Zhang X, Han M, Han S, Zong W (2025) Aqueous two-phase system (ATPS): from basic science to applications. RSC Advances 15:9041–9054. https://doi.org/10.1039/d4ra08232j

274. Xue H, Wang W, Wu J, Xie K, Ge S, Tan J (2024) Ultrasound assisted aqueous two-phase extraction of polysaccharides from corn stigma: Process optimization, structure characterization, and immunomodulatory activity. Innovative Food Science and Emerging Technologies 91:. https://doi.org/10.1016/j.ifset.2023.103531

275. Iqbal M, Tao Y, Xie S, Zhu Y, Chen D, Wang X, Huang L, Peng D, Sattar A, Shabbir MAB, Hussain HI, Ahmed S, Yuan Z (2016) Aqueous two-phase system (ATPS): an overview and advances in its applications. Biological Procedures Online 18:1–18. https://doi.org/10.1186/s12575-016-0048-8

276. Pereira JFB, Coutinho JAP (2019) Aqueous two-phase systems. In: Liquid-Phase Extraction. Elsevier, pp 157–182

277. Leong YK, Show PL, Lan JCW, Loh HS (2015) Thermoseparating aqueous two-phase system: Recent trends and applications. Chemical Engineering Transactions 45:1249–1254. https://doi.org/10.3303/CET1545209

278. Musarurwa H, Tavengwa NT (2022) Thermo-responsive polymers and advances in their applications in separation science. Microchemical Journal 179:. https://doi.org/10.1016/j.microc.2022.107554

279. Yao T, Feng C, Hu Y, Yang S (2025) Isolation and purification of aloe anthraquinones through recoverable triple-responsive aqueous two-phase system. Separation and Purification Technology 374:. https://doi.org/10.1016/j.seppur.2025.133786

280. Lai H, Yu Q, Liu Y, Liang Z, Li Y, Pan J, Gao J (2026) Three-phase systems for simultaneous extraction and separation of bioactives from Haematococcus pluvialis: Role of thermo-switchable phase behavior. Separation and Purification Technology 382:. https://doi.org/10.1016/j.seppur.2025.135755

281. Wan J, Dong W, Hou D, Wang Z, Cao X (2018) Polymerization of a new thermo-responsive copolymer with n-vinylcaprolactam and its application in recyclable aqueous two-phase systems with another thermo-responsive polymer. Bioresources and Bioprocessing 5:. https://doi.org/10.1186/s40643-018-0231-7

282. Wang Y, Yang T, Zeng H, Wan J, Cao X (2021) Study of lincomycin partition in a recyclable thermo-pH responsive aqueous two-phase system. Process Biochemistry 109:27–36. https://doi.org/10.1016/j.procbio.2021.06.019

283. Wei Y, Chen X, Yang T, Wan J, Cao X (2021) Partition of Tea Saponin with a Novel Recyclable Thermo-pH Aqueous Two-Phase Systems. Applied Biochemistry and Biotechnology 193:3062–3078. https://doi.org/10.1007/s12010-021-03583-z

284. Marimuthu N, Chow YH, Kee PE, Lan JCW, Lai ZW, Yoon LW, Tam YJ (2025) Recovery of hyaluronic acid using thermosensitive polymer-salt aqueous biphasic system with polymer recycling. Journal of Bioscience and Bioengineering 140:79–89. https://doi.org/10.1016/j.jbiosc.2025.04.007

285. Jiang B, Zhang X, Yuan Y, Qu Y, Feng Z (2017) Separation of antioxidant peptides from pepsin hydrolysate of whey protein isolate by ATPS of EOPO Co-polymer (UCON)/Phosphate. Scientific Reports 7:. https://doi.org/10.1038/s41598-017-13507-9

286. Wang Y, Hu X, Han J, Ni L, Tang X, Hu Y, Chen T (2016) Integrated method of thermosensitive triblock copolymer-salt aqueous two phase extraction and dialysis membrane separation for purification of lycium barbarum polysaccharide. Food Chemistry 194:257–264. https://doi.org/10.1016/j.foodchem.2015.08.016

287. Ng HS, Teoh AN, Lim JCW, Tan JS, Wan PK, Yim HS, Show PL, Lan JCW (2017) Thermo-sensitive aqueous biphasic extraction of polyphenols from Camellia sinensis var. assamica leaves. Journal of the Taiwan Institute of Chemical Engineers 79:151–157. https://doi.org/10.1016/j.jtice.2017.02.018

288. Gao C, Cai C, Liu J, Wang Y, Chen Y, Wang L, Tan Z (2020) Extraction and preliminary purification of polysaccharides from Camellia oleifera Abel. seed cake using a thermoseparating aqueous two-phase system based on EOPO copolymer and deep eutectic solvents. Food Chemistry 313:. https://doi.org/10.1016/j.foodchem.2020.126164

289. Zhou RR, Huang JH, He D, Yi ZY, Zhao D, Liu Z, Zhang SH, Huang LQ (2022) Green and Efficient Extraction of Polysaccharide and Ginsenoside from American Ginseng (Panax

quinquefolius L.) by Deep Eutectic Solvent Extraction and Aqueous Two-Phase System. Molecules 27:. https://doi.org/10.3390/molecules27103132

290. Zhang R, Hong M, Wu J, Xiao Y, Tong J (2024) Effect of water on the excess properties of eutectic solvents. Journal of Molecular Liquids 414:. https://doi.org/10.1016/j.molliq.2024.126139

291. Liu Y, Gao L, Chen L, Zhou W, Wang C, Ma L (2023) Exploring carbohydrate extraction from biomass using deep eutectic solvents: Factors and mechanisms. iScience 26:. https://doi.org/10.1016/j.isci.2023.107671

292. Yeow ATH, Hayyan A, Hayyan M, Usman Mohd Junaidi M, Saleh J, Jefrey Basirun W, Roslan Mohd Nor M, Al Abdulmonem W, Zulhaziman M, Mohamed Zuki F, Diana Hamid M (2024) A comprehensive review on the physicochemical properties of deep eutectic solvents. Results in Chemistry 7:. https://doi.org/10.1016/j.rechem.2024.101378

293. Kepka C, Rhodin J, Lemmens R, Tjerneld F, Gustavsson PE (2004) Extraction of plasmid DNA from Escherichia coli cell lysate in a thermoseparating aqueous two-phase system. Journal of Chromatography A 1024:95–104. https://doi.org/10.1016/j.chroma.2003.10.028

294. Leong YK, Lan JCW, Loh HS, Ling TC, Ooi CW, Show PL (2017) Cloud-point extraction of green-polymers from Cupriavidus necator lysate using thermoseparating-based aqueous two-phase extraction. Journal of Bioscience and Bioengineering 123:370–375. https://doi.org/10.1016/j.jbiosc.2016.09.007

295. Kuznetsova IM, Zaslavsky BY, Breydo L, Turoverov KK, Uversky VN (2015) Beyond the excluded volume effects: Mechanistic complexity of the crowded milieu. Molecules 20:1377–1409. https://doi.org/10.3390/molecules20011377

296. Ng HS, Tan CP, Mokhtar MN, Ibrahim S, Ariff A, Ooi CW, Ling TC (2012) Recovery of Bacillus cereus cyclodextrin glycosyltransferase and recycling of phase components in an aqueous two-phase system using thermo-separating polymer. Separation and Purification Technology 89:9–15. https://doi.org/10.1016/j.seppur.2011.12.028

297. Leong YK, Show PL, Lan JCW, Loh HS, Yap YJ, Ling TC (2017) Extraction and purification of Polyhydroxyalkanoates (PHAs): application of Thermoseparating aqueous two-phase extraction. Journal of Polymer Research 24:. https://doi.org/10.1007/s10965-017-1307-3

298. Rabelo APB, Tambourgi EB, Pessoa A (2004) Bromelain partitioning in two-phase aqueous systems containing PEO-PPO-PEO block copolymers. pp 61–68

299. Sharma A, Kaur I, Dheer D, Nagpal M, Kumar P, Venkatesh DN, Puri V, Singh I (2023) A propitious role of marine sourced polysaccharides: Drug delivery and biomedical applications. Carbohydrate Polymers 308:. https://doi.org/10.1016/j.carbpol.2022.120448

300. Leal D, Matsuhiro B, Rossi M, Caruso F (2008) FT-IR spectra of alginic acid block fractions in three species of brown seaweeds. Carbohydrate Research 343:308–316. https://doi.org/10.1016/j.carres.2007.10.016

301. Ng MH, Nu'man AH, Hasliyanti A (2024) Recycling of deep eutectic solvent in the extraction of ferulic acid from oil palm empty fruit bunch. Journal of Separation Science 47:. https://doi.org/10.1002/jssc.202300842

302. Qiu Z, Aita GM (2013) Pretreatment of energy cane bagasse with recycled ionic liquid for enzymatic hydrolysis. Bioresource Technology 129:532–537. https://doi.org/10.1016/j.biortech.2012.11.062

303. Chen Z, Reznicek WD, Wan C (2018) Deep eutectic solvent pretreatment enabling full utilization of switchgrass. Bioresource Technology 263:40–48. https://doi.org/10.1016/j.biortech.2018.04.058

304. Ling Z, Guo Z, Huang C, Yao L, Xu F (2020) Deconstruction of oriented crystalline cellulose by novel levulinic acid based deep eutectic solvents pretreatment for improved enzymatic accessibility. Bioresource Technology 305:. https://doi.org/10.1016/j.biortech.2020.123025

305. Jeong KM, Lee MS, Nam MW, Zhao J, Jin Y, Lee DK, Kwon SW, Jeong JH, Lee J (2015) Tailoring and recycling of deep eutectic solvents as sustainable and efficient extraction media. Journal of Chromatography A 1424:10–17. https://doi.org/10.1016/j.chroma.2015.10.083

306. Xie J, Chen J, Cheng Z, Zhu S, Xu J (2021) Pretreatment of pine lignocelluloses by recyclable deep eutectic solvent for elevated enzymatic saccharification and lignin nanoparticles extraction. Carbohydrate Polymers 269:. https://doi.org/10.1016/j.carbpol.2021.118321

307. Akter A, Sobuj MKA, Islam MS, Chakroborty K, Tasnim N, Ayon MH, Hossain MF, Rafiquzzaman SM (2024) Seaweed polysaccharides: Sources, structure and biomedical applications with special emphasis on antiviral potentials. Future Foods 10:. https://doi.org/10.1016/j.fufo.2024.100440

308. de Souza Celente G, Sui Y, Acharya P (2023) Seaweed as an alternative protein source: Prospective protein extraction technologies. Innovative Food Science and Emerging Technologies 86:. https://doi.org/10.1016/j.ifset.2023.103374

309. Sadeghi A, Rajabiyan A, Nabizade N, Meygoli Nezhad N, Zarei-Ahmady A (2024) Seaweed-derived phenolic compounds as diverse bioactive molecules: A review on identification, application, extraction and purification strategies. International Journal of Biological Macromolecules 266:. https://doi.org/10.1016/j.ijbiomac.2024.131147

310. Wang H, Yang L, Yang Y (2025) A review of sodium alginate-based hydrogels: Structure, mechanisms, applications, and perspectives. International Journal of Biological Macromolecules 292:. https://doi.org/10.1016/j.ijbiomac.2024.139151

311. Ozel N, Inam A, Elibol M (2024) Exploring deep eutectic solvents for enhanced extraction of bio-active compounds from microalgae biomass. Journal of Molecular Liquids 407:. https://doi.org/10.1016/j.molliq.2024.125237

312. Sui M, Feng S, Yu J, Chen B, Li Z, Shao P (2023) Removal and recovery of deep eutectic solvent with membrane-based methodology: A promising strategy to enhance extraction and purification of Dendrobium officinale flavonoids. Industrial Crops and Products 206:. https://doi.org/10.1016/j.indcrop.2023.117638

313. Vicente FA, Tkalec N, Likozar B (2024) Responsive deep eutectic solvents: mechanisms, applications and their role in sustainable chemistry. Chemical Communications 61:1002–1013. https://doi.org/10.1039/d4cc05157b

314. Zhao C, Ma Z, Zhu XX (2019) Rational design of thermoresponsive polymers in aqueous solutions: A thermodynamics map. Progress in Polymer Science 90:269–291. https://doi.org/10.1016/j.progpolymsci.2019.01.001

315. Yan XY, Cai ZH, Zhao PQ, Wang JD, Fu LN, Gu Q, Fu YJ (2023) Application of a novel and green temperature-responsive deep eutectic solvent system to simultaneously extract and separate different polar active phytochemicals from Schisandra chinensis (Turcz.) Baill. Food Research International 165:. https://doi.org/10.1016/j.foodres.2023.112541

316. Silva GMC, Pantano DA, Loehlé S, Coutinho JAP (2023) The Challenges of Using COSMO-RS To Describe Polymer Solution Behavior. Industrial and Engineering Chemistry Research 62:20936–20944. https://doi.org/10.1021/acs.iecr.3c03310

317. Wang D, Zhang M, Law CL, Zhang L (2024) Natural deep eutectic solvents for the extraction of lentinan from shiitake mushroom: COSMO-RS screening and ANN-GA optimizing conditions. Food Chemistry 430:. https://doi.org/10.1016/j.foodchem.2023.136990

318. Al-Maari MA, Hizaddin HF, Hayyan A, Hadj-Kali MK (2024) Screening deep eutectic solvents as green extractants for oil from plant seeds based on COSMO-RS model. Journal of Molecular Liquids 393:. https://doi.org/10.1016/j.molliq.2023.123520

319. Bezold F, Weinberger ME, Minceva M (2017) Assessing solute partitioning in deep eutectic solvent-based biphasic systems using the predictive thermodynamic model COSMO-RS. Fluid Phase Equilibria 437:23–33. https://doi.org/10.1016/j.fluid.2017.01.001

320. Wang K, Peng D, Alhadid A, Minceva M (2024) Assessment of COSMO-RS for Predicting Liquid-Liquid Equilibrium in Systems Containing Deep Eutectic Solvents. Industrial and Engineering Chemistry Research 63:11110–11120. https://doi.org/10.1021/acs.iecr.4c00796

321. Shang X chao, Zhang Y qin, Zheng Y fen, Li Y (2024) Temperature-responsive deep eutectic solvents as eco-friendly and recyclable media for microwave extraction of flavonoid compounds from waste onion (Allium cepa L.) skins. Biomass Conversion and Biorefinery 14:3729–3738. https://doi.org/10.1007/s13399-022-02483-4

322. Legkov SA, Bondarenko GN, Kostina JV, Novitsky EG, Bazhenov SD, Volkov AV, Volkov VV (2023) Structural Features of Monoethanolamine Aqueous Solutions with Various Compositions: A Combined Experimental and Theoretical Study Using Vibrational Spectroscopy. Molecules 28:. https://doi.org/10.3390/molecules28010403

323. Sung JY, Ryu BK, Lee DH (2018) Structure and transmittance behavior of sol–gel silica nanoparticles synthesized using pH-stable alkanolamines. Journal of Sol-Gel Science and Technology 85:495–503. https://doi.org/10.1007/s10971-017-4561-2

324. López-García M, Martínez-Cabanas M, Vilariño T, Lodeiro P, Rodríguez-Barro P, Herrero R, Barriada JL (2017) New polymeric/inorganic hybrid sorbents based on red mud and nanosized magnetite for large scale applications in As(V) removal. Chemical Engineering Journal 311:117–125. https://doi.org/10.1016/j.cej.2016.11.081

325. Chen J, Song Y, Wei X, Duan X, Liu K, Cao W, Li L, Ren G (2025) Ultrasonic and Deep Eutectic Solvent for Efficient Extraction of Phenolics from Eucommia ulmoides Leaves. Foods 14:. https://doi.org/10.3390/foods14060972

326. Wang S, Lei T, Liu L, Tan Z (2024) CO2-responsive deep eutectic solvents for the enhanced extraction of hesperidin from Fertile orange peel. Food Chemistry 432:. https://doi.org/10.1016/j.foodchem.2023.137255

327. Wang T, Guo Q, Li P, Yang H (2022) Deep-eutectic solvents/ionic liquids/water mixture as a novel type of green thermo-switchable solvent system for selective extraction and separation of natural products from Rosmarinus officinalis leaves. Food Chemistry 390:. https://doi.org/10.1016/j.foodchem.2022.133225

328. Tang Z, Xu Y, Cai C, Tan Z (2023) Extraction of Lycium barbarum polysaccharides using temperature-switchable deep eutectic solvents: A sustainable methodology for recycling and reuse of the extractant. Journal of Molecular Liquids 383:. https://doi.org/10.1016/j.molliq.2023.122063

329. Pan X, Xu L, Meng J, Chang M, Cheng Y, Geng X, Guo D, Liu R (2022) Ultrasound-Assisted Deep Eutectic Solvents Extraction of Polysaccharides From Morchella importuna: Optimization, Physicochemical Properties, and Bioactivities. Frontiers in Nutrition 9:. https://doi.org/10.3389/fnut.2022.912014

330. Liang X, Wang S, Zhou J, Lu T, Ruan K, Xia Y, Wang T (2024) A novel deep eutectic solvent/switchable-hydrophilicity solvent/H2O system with enhanced CO2 switchability for integrated extraction of phenolics, flavonoids and essential oil from Flos Chrysanthemi Indici flower. Separation and Purification Technology 336:. https://doi.org/10.1016/j.seppur.2024.126315

331. Draget KI (2009) Alginates. In: Phillips GO, Williams PA (eds) Handbook for Hydrocolloids, Second. Woodhead Publishing Series in Food Science, Technology and Nutrition, Sawston, Cambridge, pp 807–828

332. Mahavishnu G, Malaiyarasan V, Kannaiyan SK, Ramalingam A (2024) Investigation of molecular polarity and thermal stability of monoethanolamine based deep eutectic solvents. Journal of Dispersion Science and Technology. https://doi.org/10.1080/01932691.2024.2372691

333. Lasalle BSI, Pandian MS, Ramasamy P (2023) Molecular Interactions Studies on Chloroform in the Environment of o-Cresol: FTIR Spectroscopy and Quantum Chemical Calculations. Brazilian Journal of Physics 53:. https://doi.org/10.1007/s13538-023-01309-6

334. Sterner M, Edlund U (2016) Multicomponent fractionation of Saccharina latissima brown algae using chelating salt solutions. Journal of Applied Phycology 28:2561–2574. https://doi.org/10.1007/s10811-015-0785-0

335. Hiemstra ISA, Lustig N, Eppink MHM, Wijffels RH, Kazbar A (2025) Separation of alginate and recycling of deep eutectic solvents using temperature-responsive aqueous two-phase systems. Journal of Cleaner Production 536:. https://doi.org/10.1016/j.jclepro.2025.147186

336. Chen J, Xu Y, Tan Z (2023) CO2-triggered switchable hydrophilicity solvent as a recyclable extractant for ultrasonic-assisted extraction of Polygonatum sibiricum polysaccharides. Food Chemistry 402:. https://doi.org/10.1016/j.foodchem.2022.134301

337. Gao N, Wang Y, Luo H, Xu Y, Liu J, Chen Y (2024) pH-switchable hydrophobic deep eutectic solvents for sustainable recycling extraction of high oily waste. Chemical Engineering Journal 495:. https://doi.org/10.1016/j.cej.2024.153339

338. Zhang X, Yan X, Cai Z, Fu L, Dong X, Cui J, Zheng H, Xu M, Fu Y (2024) A novel and green temperature-responsive biphasic deep eutectic solvent-based system for simultaneous extraction and pre-separation of active ingredients from Zanthoxylum bungeanum Maxim. peels. Industrial Crops and Products 221:. https://doi.org/10.1016/j.indcrop.2024.119324

339. Wu LT, Zhan YT, Li ZL, Chen PT, Hwang BJ, Jiang JC (2024) Rational electrolyte design for Li-metal batteries operated under extreme conditions: a combined DFT, COSMO-RS, and machine learning study. Journal of Materials Chemistry A 12:15792–15802. https://doi.org/10.1039/d4ta03026e

340. Ling JKU, Hadinoto K (2022) Deep Eutectic Solvent as Green Solvent in Extraction of Biological Macromolecules: A Review. International Journal of Molecular Sciences 23:. https://doi.org/10.3390/ijms23063381

341. Obluchinskaya ED, Pozharitskaya ON, Shevyrin VA, Kovaleva EG, Flisyuk EV, Shikov AN (2023) Optimization of Extraction of Phlorotannins from the Arctic Fucus vesiculosus Using Natural Deep Eutectic Solvents and Their HPLC Profiling with Tandem High-Resolution Mass Spectrometry. Marine Drugs 21:. https://doi.org/10.3390/md21050263

342. Hiemstra ISA, Eppink MHM, Bravi M, Wijffels RH, Kazbar A (2025) Process intensification of seaweed biorefinery using reusable natural deep eutectic solvents. Journal of Environmental Chemical Engineering 13:. https://doi.org/10.1016/j.jece.2025.119184

343. Liu B, Tan Z (2022) Separation and Purification of Astragalus membranaceus Polysaccharides by Deep Eutectic Solvents-Based Aqueous Two-Phase System. Molecules 27:. https://doi.org/10.3390/molecules27165288

344. Rajendran DS, Chidambaram A, Kumar PS, Venkataraman S, Muthusamy S, Vo DVN, Rangasamy G, Vaithyanathan VK, Vaidyanathan VK (2023) Three-phase partitioning for the separation of proteins, enzymes, biopolymers, oils and pigments: a review. Environmental Chemistry Letters 21:911–934. https://doi.org/10.1007/s10311-022-01540-8

345. Fernández A, Deive FJ, Rodríguez A, Álvarez MS (2020) Towards the use of eco-friendly solvents as adjuvants in remediation processes. Journal of Molecular Liquids 305:. https://doi.org/10.1016/j.molliq.2020.112824

346. Li N, Wang Y, Xu K, Huang Y, Wen Q, Ding X (2016) Development of green betaine-based deep eutectic solvent aqueous two-phase system for the extraction of protein. Talanta 152:23–32. https://doi.org/10.1016/j.talanta.2016.01.042

347. Sadeghi A, Pazuki G (2025) Separation of heavy metals using aqueous two-phase systems based on choline chloride/urea and betaine/urea deep eutectic solvents. Scientific reports 15:3948–3948

348. Marappan S, Kamaruddin AH, Gonawan FN (2023) Formation of Aqueous Two-Phase Systems Using Potassium Salt and Deep Eutectic Mixtures for Extraction of Proteins. Chemical Engineering and Technology 46:2497–2503. https://doi.org/10.1002/ceat.202200626

349. Vessally E, Rzayev R (2024) Application of deep eutectic solvent-based aqueous two phase systems for extraction of analgesic drugs. RSC Advances 14:34253–34260. https://doi.org/10.1039/d4ra05917d

350. Li P, Zhao P, Liu W, Jiang Y, Wang W, Bao L, Jin Y, Li X (2018) Determination of common ginsenosides in Kang'ai injection by aqueous two-phase extraction with deep eutectic solvents and HPLC-UV/DAD. Microchemical Journal 137:302–308. https://doi.org/10.1016/j.microc.2017.11.007

351. Xu K, Wang Y, Huang Y, Li N, Wen Q (2014) A green deep eutectic solvent-based aqueous two-phase system for protein extracting. Analytica Chimica Acta 864:9–20. https://doi.org/10.1016/j.aca.2015.01.026

352. Cai C, Wu S, Wang C, Yang Y, Sun D, Li F, Tan Z (2019) Deep eutectic solvents used as adjuvants for improving the salting-out extraction of ursolic acid from Cynomorium songaricum Rupr. in aqueous two-phase system. Separation and Purification Technology 209:112–118. https://doi.org/10.1016/j.seppur.2018.07.017

353. Cunha DR, Hsieh SA, Quinaz MB, Segundo MA, Anderson JL (2026) Aqueous biphasic systems based on deep eutectic solvents for extraction of biopharmaceuticals in downstream processing. Journal of Chromatography A 1765:. https://doi.org/10.1016/j.chroma.2025.466514

354. Moldes D, Vega M, Bolado S, Requejo PF (2026) Mild One-Step Protein Recovery from Microalgae Cultivated in Swine Wastewater Using Natural Deep Eutectic Solvent-Based Aqueous Biphasic Systems. Molecules 31:. https://doi.org/10.3390/molecules31030483

355. Zafarani-Moattar MT, Shekaari H, Ardi-Samberan P (2022) Thermodynamic Studies of l-Tryptophan and l-Threonine Partitioning in Aqueous Two-phase Systems Containing Deep Eutectic Solvents (Choline Chloride/PEG) and Potassium Salts. Journal of Chemical and Engineering Data 67:1214–1227. https://doi.org/10.1021/acs.jced.2c00062

356. Jin M, Wang E, Wang C, Wu Y, Mo L, Li L, Yu Y, Yan J (2025) Three-phase partitioning for the efficient preparation and isolation of active polysaccharides: A review. Food Biomacromolecules 2:558–570. https://doi.org/10.1002/fob2.70036

357. Jiang L, Zheng K (2024) Extraction of mucilage polysaccharides from chia seed by hydrophobic deep eutectic solvents-based three-phase partitioning system: A phase behavior-driven approach. International Journal of Biological Macromolecules 280:. https://doi.org/10.1016/j.ijbiomac.2024.135913

358. Lei T, Qin Z, Liu L, Tan Z (2025) A salt/salt aqueous two-phase system based on pH-switchable deep eutectic solvent for the extraction and separation of mulberry polysaccharides. Food Chemistry 462:. https://doi.org/10.1016/j.foodchem.2024.141024

359. Milosevic M, Staal KJJ, Schuur B, de Haan AB (2013) Extractive concentration of aqueous salt solutions in aqueous two phase systems. Desalination 324:99–110. https://doi.org/10.1016/j.desal.2013.06.008

360. Kuepethkaew S, Sangkharak K, Benjakul S, Klomklao S (2017) Use of TPP and ATPS for partitioning and recovery of lipase from Pacific white shrimp (Litopenaeus vannamei) hepatopancreas. Journal of Food Science and Technology 54:3880–3891. https://doi.org/10.1007/s13197-017-2844-9

361. Bodachivskyi I, Kuzhiumparambil U, Williams DBG (2020) Catalytic Valorization of Native Biomass in a Deep Eutectic Solvent: A Systematic Approach toward High-Yielding Reactions of Polysaccharides. ACS Sustainable Chemistry and Engineering 8:678–685. https://doi.org/10.1021/acssuschemeng.9b06528

362. Morais ES, Da Costa Lopes AM, Freire MG, Freire CSR, Silvestre AJD (2021) Unveiling Modifications of Biomass Polysaccharides during Thermal Treatment in Cholinium Chloride : Lactic Acid Deep Eutectic Solvent. ChemSusChem 14:686–698. https://doi.org/10.1002/cssc.202002301

363. Smith HA, Zhou J, Buckley HL (2026) Greener citrate-assisted extraction of sodium alginate: Process optimization and mechanical performance of alginate-based films. Green Chemistry. https://doi.org/10.1039/d5gc05514h

364. Liang X, Chen S, Liang Y, Wang M, Wang Q, Chen D, Ma X, Ding H, Zhong HJ (2026) Alginate-Based Hydrogels: Recent Progress in Preparation, Property Tuning, and Multifunctional Applications. Gels 12:. https://doi.org/10.3390/gels12020182

365. Haraguchi R, Oishi Y, Narita T (2023) Macroscopic Pattern Formation of Alginate Gels in a Two-Dimensional System. Gels 9:. https://doi.org/10.3390/gels9060444

366. Wang Q, Wei N, Wang Y, Hou Y, Ren X, Wei Q Single-step purification of C-phycocyanin from Arthrospira platensis using aqueous two-phase system based on natural deep eutectic solvents. https://doi.org/10.1007/s10811-020-02239-5/Published

367. Ivanović M, Islamčević Razboršek M, Kolar M (2020) Innovative Extraction Techniques Using Deep Eutectic Solvents and Anal ytical Methods for the Isolation and Characterization of Natural Bioac tive Compounds from Plant Material. Plants 9:1428–1428. https://doi.org/10.3390/plants9111428

368. Li X, Row KH (2016) Development of deep eutectic solvents applied in extraction and separa tion. https://doi.org/10.1002/jssc.201600633

369. Zdanowicz M, Wilpiszewska K, Spychaj T (2018) Deep eutectic solvents for polysaccharides processing. A review. Carbohydrate Polymers 200:361–380. https://doi.org/10.1016/j.carbpol.2018.07.078

370. Li B, Lu F, Wei X, Zhao R (2008) Fucoidan: Structure and bioactivity. Molecules (Basel, Switzerland) 13:1671–1695. https://doi.org/10.3390/molecules13081671

371. Wang W, Yu L-J, Xu C, Tomizaki T, Zhao S, Umena Y, Chen X, Qin X, Xin Y, Suga M, Han G, Kuang T, Shen J-R (2019) Structural basis for blue-green light harvesting and energy dissipatio n in diatoms. Science 363:eaav0365–eaav0365. https://doi.org/10.1126/science.aav0365

372. Din NAS, Mohd Alayudin 'Ain Sajda, Sofian-Seng NS, Rahman HA, Mohd Razali NS, Lim SJ, Wan Mustapha WA (2022) Brown Algae as Functional Food Source of Fucoxanthin: A Review. Foods 11:. https://doi.org/10.3390/foods11152235

373. Zhang H, Tang Y, Zhang Y, Zhang S, Qu J, Wang X, Kong R, Han C, Liu Z (2015) Fucoxanthin: A Promising Medicinal and Nutritional Ingredient. Evidence-Based Complementary and Alternative Medicine 2015:1–10. https://doi.org/10.1155/2015/723515

374. Steinbruch E, Wise J, Levkov K, Chemodanov A, Israel Á, Livney YD, Golberg A (2023) Enzymatic cell wall degradation combined with pulsed electric fields i ncreases yields of water-soluble-protein extraction from the green mar ine macroalga Ulva sp. Innovative Food Science & Emerging Technologies 84:103231–103231. https://doi.org/10.1016/j.ifset.2022.103231

375. Li P, Yang C, Jiang Z, Jin Y, Wu W (2023) Lignocellulose pretreatment by deep eutectic solvents and related tech nologies: A review. Journal of Bioresources and Bioproducts 8:33–44. https://doi.org/10.1016/j.jobab.2022.11.004

376. Loow YL, New EK, Yang GH, Ang LY, Foo LYW, Wu TY (2017) Potential use of deep eutectic solvents to facilitate lignocellulosic biomass utilization and conversion. Cellulose 24:3591–3618. https://doi.org/10.1007/s10570-017-1358-y

377. Fawzy MA, Gomaa M (2021) Optimization of citric acid treatment for the sequential extraction of fucoidan and alginate from Sargassum latifolium and their potential a ntioxidant and Fe(III) chelation properties. Journal of Applied Phycology 33:2523–2535. https://doi.org/10.1007/s10811-021-02453-9

378. Hiemstra ISA, Husna F, Eppink MHM, Wijffels RH, Kazbar A (2026) Mechanistic insights into temperature-responsive deep eutectic solvent for alginate recovery and solvent recycling. Separation and Purification Technology 388:136807–136807. https://doi.org/10.1016/j.seppur.2026.136807

379. Groisillier A, Labourel A, Michel G, Tonon T (2015) The Mannitol Utilization System of the Marine Bacterium Zobellia galac tanivorans. Applied and Environmental Microbiology 81:1799–1812. https://doi.org/10.1128/AEM.02808-14

380. Graiff A, Ruth W, Kragl U, Karsten U (2016) Chemical characterization and quantification of the brown algal storag e compound laminarin — A new methodological approach. Journal of Applied Phycology 28:533–543. https://doi.org/10.1007/s10811-015-0563-z

381. Nava-Ocampo MF, Al Fuhaid L, Santana A, Bucs SS, Verpoorte R, Hae Choi Y, Witkamp GJ, Vrouwenvelder JS, Farinha ASF (2021) Structural properties and stability of the Betaine-Urea natural deep e utectic solvent. Journal of Molecular Liquids 343:. https://doi.org/10.1016/j.molliq.2021.117655

382. Zahrina I, Nasikin M, Krisanti E, Mulia K (2018) Deacidification of palm oil using betaine monohydrate-based natural de ep eutectic solvents. Food Chemistry 240:490–495. https://doi.org/10.1016/j.foodchem.2017.07.132

383. Kivelä H, Salomäki M, Vainikka P, Mäkilä E, Poletti F, Ruggeri S, Terzi F, Lukkari J (2022) Effect of Water on a Hydrophobic Deep Eutectic Solvent. The Journal of Physical Chemistry B 126:513–527. https://doi.org/10.1021/acs.jpcb.1c08170

384. Hiemstra ISA, De Jong J, Eppink MHM, Wijffels RH, Kazbar A (2026) Direct alginate recovery and solvent recycling from deep eutectic solv ents via interfacial precipitation in aqueous two-phase systems. Separation and Purification Technology 407:139128–139128. https://doi.org/10.1016/j.seppur.2026.139128

385. Yusof Z, Khong NMH, Sim W, Chern S (2022) Opportunities for the marine carotenoid value chain from the perspecti ve of fucoxanthin degradation. Food Chemistry 383:132394–132394. https://doi.org/10.1016/j.foodchem.2022.132394

386. Zhao D, Yu D, Kim M, Gu M-Y, Kim S-M, Pan C-H, Kim G-H, Chung D (2019) Effects of temperature, light, and pH on the stability of fucoxanthin in an oil-in-water emulsion. Food Chemistry 291:87–93. https://doi.org/10.1016/j.foodchem.2019.04.002

387. Cunningham EM, O'Kane AP, Ford L, Sheldrake GN, Cuthbert RN, Dick JTA, Maggs CA, Walsh PJ (2023) Temporal patterns of fucoxanthin in four species of European marine br own macroalgae. Scientific Reports 13:22241–22241. https://doi.org/10.1038/s41598-023-47274-7

388. Marinho GS, Sørensen ADM, Safafar H, Pedersen AH, Holdt SL (2019) Antioxidant content and activity of the seaweed Saccharina latissima: a seasonal perspective. Journal of Applied Phycology 31:1343–1354. https://doi.org/10.1007/s10811-018-1650-8

389. Allahyari A, Borji M, Jahanban-Esfahlan A, Khanalipour A, Tabibiazar M, Ahmadi P (2025) Current Status and Future Perspectives of Betaine and Betaine-Based Natural Deep Eutectic Solvents: A Review. Foods 14:. https://doi.org/10.3390/foods14234122

390. DeRoussel P, Khakhar DV, Ottino JM (2001) Mixing of viscous immiscible liquids. Part 2: Overemulsification—inter pretation and use. Chemical Engineering Science 5531–5537

391. Pal R (2001) Novel viscosity equations for emulsions of two immiscible liquids. Journal of Rheology 45:509–520. https://doi.org/10.1122/1.1339249

392. Vothknecht UC, Westhoff P (2001) Biogenesis and origin of thylakoid membranes. Biochimica et Biophysica Acta (BBA) - Molecular Cell Research 1541:91–101. https://doi.org/10.1016/S0167-4889(01)00153-7

393. Agusman A, Huijgen WJJ, Eppink MHM, Wijffels RH, De Ruijter NCA, Kazbar A (2026) Extraction mechanisms of proteins from Palmaria palmata. Food Chemistry 518:149680–149680. https://doi.org/10.1016/j.foodchem.2026.149680

394. Azmir J, Zaidul ISM, Rahman MM, Sharif KM, Mohamed A, Sahena F, Jahurul MHA, Ghafoor K, Norulaini NAN, Omar AKM (2013) Techniques for extraction of bioactive compounds from plant materials: A review. Journal of Food Engineering 117:426–436. https://doi.org/10.1016/j.jfoodeng.2013.01.014

395. Fernandes V, Mamatha BS (2023) Fucoxanthin, a Functional Food Ingredient: Challenges in Bioavailabili ty. Current Nutrition Reports 12:567–580. https://doi.org/10.1007/s13668-023-00492-x

396. Ma Z, Khalid N, Shu G, Zhao Y, Kobayashi I, Neves MA, Tuwo A, Nakajima M (2019) Fucoxanthin-Loaded Oil-in-Water Emulsion-Based Delivery Systems: Effects of Natural Emulsifiers on the Formulation, Stability, and Bioaccessibility. ACS Omega 4:10502–10509. https://doi.org/10.1021/acsomega.9b00871

397. Hasenhuettl GL, Hartel RW (2019) Food Emulsifiers and Their Applications. Springer International Publishing, Cham

398. Niraula BB, Seng TN, Misran M (2004) Vesicles in fatty acid salt–fatty acid stabilized o/w emulsion—emulsio n structure and rheology. Colloids and Surfaces A: Physicochemical and Engineering Aspects 236:7–22. https://doi.org/10.1016/j.colsurfa.2004.01.002

399. Vergaelen M, Verbraeken B, Van Guyse JFR, Podevyn A, Tigrine A, De La Rosa VR, Monnery BD, Hoogenboom R (2020) Ethyl acetate as solvent for the synthesis of poly(2-ethyl-2-oxazoline). Green Chemistry 22:1747–1753. https://doi.org/10.1039/C9GC03872H

400. Xiao T, Ma X, Hu H, Xiang F, Zhang X, Zheng Y, Dong H, Adhikari B, Wang Q, Shi A (2025) Advances in emulsion stability: A review on mechanisms, role of emulsi fiers, and applications in food. Food Chemistry: X 29:102792–102792. https://doi.org/10.1016/j.fochx.2025.102792

401. Ma W, Dai S, Zhu P, Zhou R, Lu H (2021) Dual CO2 Responsiveness of an Oil-In-Water Emulsion by Usin g Sodium Oleate and Water-Soluble Tertiary Amines. Langmuir 37:750–758. https://doi.org/10.1021/acs.langmuir.0c03038

402. Pajot A, Nicolau E, Marchal L (2023) Improving the extraction and the purification of fucoxanthin from Tiso chrysis lutea using centrifugal partition chromatography. 74:. https://doi.org/10.1016/j.algal.2023.103174

403. Agung Wibowo A, Heriyanto, Shioi Y, Limantara L, Brotosudarmo THP (2022) Simultaneous purification of fucoxanthin isomers from brown seaweeds b y open-column and high-performance liquid chromatography. Journal of Chromatography B 1193:123166–123166. https://doi.org/10.1016/j.jchromb.2022.123166

404. Llansola-Portoles MJ, Pascal AA, Robert B (2017) Electronic and vibrational properties of carotenoids: From in vitro to in vivo. Journal of the Royal Society Interface 14:. https://doi.org/10.1098/rsif.2017.0504

405. Fan C, Liu Y, Shan Y, Cao X (2022) A priori design of new natural deep eutectic solvent for lutein recove ry from microalgae. Food Chemistry 376:131930–131930. https://doi.org/10.1016/j.foodchem.2021.131930

406. Yang D, Qiu W, Xu Y, Hu Z, Wang L (2023) Optimisation and modelling of ultrasonic-assisted extraction of cantha xanthin from Chromochloris zofingiensis using eutectic solvents. Industrial Crops and Products 202:117002–117002. https://doi.org/10.1016/j.indcrop.2023.117002

407. Boscq S, Theodorou I, Milstein R, Le Bail A, Chenivesse S, Billoud B, Charrier B (2025) Longitudinal growth of the Saccharina kelp embryo depends on actin fil aments that control the formation of a corset-like structure composed of alginate. Scientific Reports 15:1178–1178. https://doi.org/10.1038/s41598-024-83814-5

408. Azzouz A, Hayyan M (2024) Techno-economic feasibility analysis: The missing piece in the puzzle of deep eutectic solvents. Sustainable Materials and Technologies 39:e00795–e00795. https://doi.org/10.1016/j.susmat.2023.e00795

409. Herrera Barragán JA, Olivieri G, Boboescu I, Eppink M, Wijffels R, Kazbar A (2022) Enzyme assisted extraction for seaweed multiproduct biorefinery: A techno-economic analysis. Frontiers in Marine Science 9:. https://doi.org/10.3389/fmars.2022.948086

410. Rente D, Cvjetko Bubalo M, Panić M, Paiva A, Caprin B, Radojčić Redovniković I, Duarte ARC (2022) Review of deep eutectic systems from laboratory to industry, taking th e application

in the cosmetics industry as an example. Journal of Cleaner Production 380:135147–135147. https://doi.org/10.1016/j.jclepro.2022.135147

411. Lobato-Rodríguez Á, Gullón B, Romaní A, Ferreira-Santos P, Garrote G, Del-Río PG (2023) Recent advances in biorefineries based on lignin extraction using deep eutectic solvents: A review. Bioresource Technology 388:. https://doi.org/10.1016/j.biortech.2023.129744

412. Wang Y, Gao H, Xiao J, Yu Y, Yi Y, Wu J, Manzardo A, Zhang J, Wang Z, Luo Q (2025) Sustainable Valorization of Lignocellulose: A Prospective Life Cycle Assessment of Deep Eutectic Solvent-Based Processes and Economic Viability. Environ Sci Technol 59:24368–24379. https://doi.org/10.1021/acs.est.5c10054

413. Reynaga-Navarro W, Bozzo L, Wijffels RH, Eppink M, Kazbar A (2026) Characterisation of alginate extracted from Saccharina latissima with deep eutectic solvents. Food Hydrocolloids 171:111862. https://doi.org/10.1016/j.foodhyd.2025.111862

414. Llansola-Portoles MJ, Pascal AA, Robert B (2017) Electronic and vibrational properties of carotenoids: from *in vitro* to *in vivo*. Journal of The Royal Society Interface 14:20170504. https://doi.org/10.1098/rsif.2017.0504

415. Agung Wibowo A, Heriyanto, Shioi Y, Limantara L, Brotosudarmo THP (2022) Simultaneous purification of fucoxanthin isomers from brown seaweeds by open-column and high-performance liquid chromatography. Journal of Chromatography B 1193:123166. https://doi.org/10.1016/j.jchromb.2022.123166

416. del Mar Contreras-Gámez M, Galán-Martín Á, Seixas N, da Costa Lopes AM, Silvestre A, Castro E (2023) Deep eutectic solvents for improved biomass pretreatment: Current status and future prospective towards sustainable processes. Bioresource Technology 369:. https://doi.org/10.1016/j.biortech.2022.128396

417. Kumar AK, Sharma S, Dixit G, Shah E, Patel A, Boczkaj G (2020) Techno-economic evaluation of a natural deep eutectic solvent-based biorefinery: Exploring different design scenarios. Biofuels, Bioproducts and Biorefining 14:746–763. https://doi.org/10.1002/bbb.2110

418. Sharma A, Dubey S, Singh K, Mittal R, Quille P, Rajauria G (2025) Innovative Processing and Industrial Applications of Seaweed. Phycology 5:10–10. https://doi.org/10.3390/phycology5010010

419. Arias A, Feijoo G, Moreira MT (2023) Macroalgae biorefineries as a sustainable resource in the extraction o f value-added compounds. Algal Research 69:102954–102954. https://doi.org/10.1016/j.algal.2022.102954

420. McElroy CR, Kopanitsa L, Helmes R, Fan J, Attard TM, Simister R, Burg S, Ladds G, Bailey DS, Gomez LD (2023) Integrated biorefinery approach to valorise Saccharina latissima bioma ss: Combined sustainable processing to produce biologically active fuc oxanthin, mannitol, fucoidans and alginates. Environmental Technology and Innovation 29:103014–103014. https://doi.org/10.1016/j.eti.2023.103014

421. Verdía Barbará P, Choudhary H, Nakasu PS, Al-Ghatta A, Han Y, Hopson C, Aravena RI, Mishra DK, Ovejero-Pérez A, Simmons BA, Hallett JP (2025) Recent Advances in the Use of Ionic Liquids and Deep Eutectic Solvents for Lignocellulosic Biorefineries and Biobased Chemical and

Material Production. Chemical Reviews 125:5461–5583. https://doi.org/10.1021/acs.chemrev.4c00754

422. Wang Y, Gao H, Xiao J, Yu Y, Yi Y, Wu J, Manzardo A, Zhang J, Wang Z, Luo Q (2025) Sustainable Valorization of Lignocellulose: A Prospective Life Cycle A ssessment of Deep Eutectic Solvent-Based Processes and Economic Viabil ity. Environmental Science & Technology 59:24368–24379. https://doi.org/10.1021/acs.est.5c10054

423. Mcreynolds C, Adrien A, Castejon N, Susana CM (2022) Green Chemistry Letters and Reviews Green in the deep blue : deep eutectic solvents as versatile systems for the processing of marine biomass. https://doi.org/10.1080/17518253.2022.2065890

424. Bennett JP, Robinson LF, Gomez LD (2023) Valorisation strategies for brown seaweed biomass production in a Euro pean context. Algal Research 75:103248–103248. https://doi.org/10.1016/j.algal.2023.103248

425. Zhang X, Thomsen M (2019) Biomolecular Composition and Revenue Explained by Interactions between Extrinsic Factors and Endogenous Rhythms of Saccharina latissima. Marine Drugs 17:107–107. https://doi.org/10.3390/md17020107

426. Khaw YS, Yusoff FM, Tan HT, Noor Mazli NAI, Nazarudin MF, Shaharuddin NA, Omar AR, Takahashi K (2022) Fucoxanthin Production of Microalgae under Different Culture Factors: A Systematic Review. Marine Drugs 20:. https://doi.org/10.3390/md20100592

427. Slegers PM, Helmes RJK, Draisma M, Broekema R, Vlottes M, Van Den Burg SWK (2021) Environmental impact and nutritional value of food products using the seaweed Saccharina latissima. Journal of Cleaner Production 319:128689. https://doi.org/10.1016/j.jclepro.2021.128689

428. Nazemi F, Karimi K, Denayer JFM, Shafiei M (2021) Techno-economic aspects of different process approaches based on brown macroalgae feedstock: A step toward commercialization of seaweed-based biorefineries. Algal Research 58:102366. https://doi.org/10.1016/j.algal.2021.102366

429. Zang G, Shah A, Wan C (2020) Techno-economic analysis of co-production of 2,3-butanediol, furfural, and technical lignin via biomass processing based on deep eutectic so lvent pretreatment. Biofuels, Bioproducts and Biorefining 14:326–343. https://doi.org/10.1002/bbb.2081

430. Fernando IPS, Kim KN, Kim D, Jeon YJ (2019) Algal polysaccharides: potential bioactive substances for cosmeceutica l applications. Critical Reviews in Biotechnology 39:99–113. https://doi.org/10.1080/07388551.2018.1503995

431. (2026) Alginic Acid Medium Viscosity 9005-38-3

432. Saji S, Hebden A, Goswami P, Du C (2022) A Brief Review on the Development of Alginate Extraction Process and Its Sustainability. Sustainability 14:5181. https://doi.org/10.3390/su14095181

433. Torres MD, Kraan S, Domínguez H (2019) Seaweed biorefinery

434. Yiin CL, Lai ZY, Chin BLF, Lock SSM, Cheah KW, Taylor MJ, Al-Gailani A, Kolosz BW, Chan YH (2024) Green pathways for biomass transformation: A holistic evaluation of de ep

eutectic solvents (DESs) through life cycle and techno-economic ass essment. Journal of Cleaner Production 470:143248–143248. https://doi.org/10.1016/j.jclepro.2024.143248

435. Gaffey J, Matinez AA, Andrade TA, Ambye-Jensen M, Bishop G, Collins MN, Styles D (2024) Assessing the environmental footprint of alternative green biorefinery protein extraction techniques from grasses and legumes. Science of The Total Environment 949:175035–175035. https://doi.org/10.1016/j.scitotenv.2024.175035

436. Nilsson AE, Bergman K, Gomez Barrio LP, Cabral EM, Tiwari BK (2022) Life cycle assessment of a seaweed-based biorefinery concept for produ ction of food, materials, and energy. Algal Research 65:102725–102725. https://doi.org/10.1016/j.algal.2022.102725

437. Wang X, Wei Y, Fan Z, Chen Y, Cui Z (2024) Life cycle assessment for evaluation of novel solvents and technologies: A case study of flavonoids extraction from Ginkgo biloba leaves. Science of the Total Environment 922:. https://doi.org/10.1016/j.scitotenv.2024.171319

438. Wang Y, Kim KH, Jeong K, Kim NK, Yoo CG (2021) Sustainable biorefinery processes using renewable deep eutectic solvents. Current Opinion in Green and Sustainable Chemistry 27:. https://doi.org/10.1016/j.cogsc.2020.100396

439. Membrane chemical cleaning: why is it required and how is it performed? In: Sterlitech. https://www.sterlitech.com/blog/membrane-chemical-cleaning. Accessed 23 July 2026

440. König-Mattern L, Komarova AO, Ghosh A, Linke S, Rihko-Struckmann LK, Luterbacher J, Sundmacher K (2023) High-throughput computational solvent screening for lignocellulosic biomass processing. Chemical Engineering Journal 452:139476. https://doi.org/10.1016/j.cej.2022.139476

441. Ojulari OV, Park J-H, Lee JH, Lee W, Nam J-O, Olawuyi IF, Hahn D (2026) Optimization of Bioactive Polysaccharide Extraction from *Protaetia brevitarsis seulensis* Larvae Using Deep Eutectic Solvents. ACS Omega 11:8457–8469. https://doi.org/10.1021/acsomega.5c11323

442. Zhou D, Hu Y, Zhou T, Peng S, Li R, He J, Zhao M, Shao J, Tang Q (2025) Deep eutectic solvent extraction of polysaccharides from Gastrodiae elata with ultrasonic and enzymes assistance: Process optimization, structure, and antioxidant activity. Ultrasonics Sonochemistry 119:107383. https://doi.org/10.1016/j.ultsonch.2025.107383

443. Boateng ID (2023) Evaluating the status quo of deep eutectic solvent in food chemistry. Potentials and limitations. Food Chemistry 406:135079. https://doi.org/10.1016/j.foodchem.2022.135079

444. Zhang X, Xu P, Yao J, Hou J, Xu Y, Chen H (2026) Ultrasound-Assisted Deep Eutectic Solvent Three-Phase Partitioning System for Extraction of Polysaccharides from Longan Shell: Process Optimization, Physicochemical Properties, Structural Characterization, and Antioxidant Activities. Foods 15:2041. https://doi.org/10.3390/foods15112041

445. Chen X, Hu Y, Tan Z (2023) Innovative three-phase partitioning based on deep-eutectic solvents and sugars (sugaring-out effect) for cucumber peroxidase purification. Microchemical Journal 190:108702. https://doi.org/10.1016/j.microc.2023.108702

446. Chow YH, Sahlini A, Ng H-S, Lan JC-W (2021) Efficacy of alcohol/sugar aqueous biphasic system on partition of bovine serum albumin. Bioresour Bioprocess 8:7. https://doi.org/10.1186/s40643-021-00360-y

447. Dhamole PB, Joshi N, Bhat V (2023) A review of recent developments in sugars and polyol based soluting out separation processes. Separation and Purification Technology 312:123394. https://doi.org/10.1016/j.seppur.2023.123394

448. Donati I, Christensen BE (2023) Alginate-metal cation interactions: Macromolecular approach. Carbohydrate Polymers 321:121280. https://doi.org/10.1016/j.carbpol.2023.121280

449. Hu C, Lu W, Sun C, Zhao Y, Zhang Y, Fang Y (2022) Gelation behavior and mechanism of alginate with calcium: Dependence on monovalent counterions. Carbohydrate Polymers 294:119788. https://doi.org/10.1016/j.carbpol.2022.119788

450. Perić-Hassler L, Hünenberger PH (2010) Interaction of alginate single-chain polyguluronate segments with mono- and divalent metal cations: a comparative molecular dynamics study. Molecular Simulation 36:778–795. https://doi.org/10.1080/08927021003752853

451. Freire MG, Louros CLS, Rebelo LPN, Coutinho JAP (2011) Aqueous biphasic systems composed of a water-stable ionic liquid + carbohydrates and their applications. Green Chem 13:1536. https://doi.org/10.1039/c1gc15110j

452. Ghasemzadeh B, Shahriari S, Pazuki G (2019) Efficient separation of curcumin using tetra butyl phosphonium bromide / carbohydrates (sorbitol, fructose) aqueous two-phase system. Fluid Phase Equilibria 498:51–58. https://doi.org/10.1016/j.fluid.2019.06.015

453. Sadeghi R, Coutinho JAP (2024) Green Aqueous Two-Phase Systems Formed by Sugaring-Out Effect in Aqueous Polymer/Ionic Liquid Solutions: A Review. ACS Sustainable Chem Eng 12:15838–15874. https://doi.org/10.1021/acssuschemeng.4c05745

454. Sun Y, Zhang S, Zhang X, Zheng Y, Xiu Z (2018) Ionic liquid-based sugaring-out and salting-out extraction of succinic acid. Separation and Purification Technology 204:133–140. https://doi.org/10.1016/j.seppur.2018.04.064

455. Ataee M, Ahmadi Jouybari T, Ahmadi Jouybari H, Hosseini F, Fattahi N (2024) Fatty Acid–Based pH-Switchable Deep Eutectic Solvents for the Extraction and Preconcentration of Chlorobenzenes From Water Samples Followed by Gas Chromatography–Electron Capture Detection. Separation Science Plus 7:e202400123. https://doi.org/10.1002/sscp.202400123

456. Cai Z-H (2024) A novel temperature-responsive biphasic deep eutectic solvent-based solvent system: Integrated efficient extraction, enrichment and recovery of phytochemicals

457. Dong X, Cai Z, Wang Y, Zhou Q, Wang L, Fu Y (2025) Simultaneous Extraction and Separation of Different Polarity Phytochemicals from in Pigeon Pea Leaves with Biphasic Temperature-Switchable Deep Eutectic Solvent System. Microchemical Journal 208:112418. https://doi.org/10.1016/j.microc.2024.112418

458. Lian J, Wu Y, Xi J (2026) Temperature-responsive deep eutectic solvents: A green and recyclable extractant for efficient extraction of natural bioactive compounds. Trends in Food Science & Technology 173:105785. https://doi.org/10.1016/j.tifs.2026.105785

459. Ghahremani R, Dean W, Sinclair N, Shen X, Starvaggi N, Alfurayj I, Burda C, Pentzer E, Wainright J, Savinell R, Gurkan B (2023) Redox-Active Eutectic Electrolyte with Viologen and Ferrocene Derivatives for Flow Batteries. ACS Appl Mater Interfaces 15:1148–1156. https://doi.org/10.1021/acsami.2c18546

460. Cruz H, Jordão N, Santiago S, Mena S, Santos AFM, Viciosa MT, Zalewska K, Branco LC, Hernando J, Guirado G (2025) A Switchable Deep Eutectic System Based on Diarylethene. ACS Omega acsomega.5c04216. https://doi.org/10.1021/acsomega.5c04216

461. Wang S, Chen H, Cui Z, Liu X, Binks BP (2026) Recycling and Reuse of a Sugar-Based Nonionic Surfactant Enabled by Redox-Switchable Precipitation–Dissolution. Small 22:e73979. https://doi.org/10.1002/smll.73979

462. Minart G, Croguennec L, Olchowka J (2026) Engineering Materials for Electrochemical Energy Storage via Ionic Liquid and Deep Eutectic Solvent Synthesis Media. ACS Mater Au 6:294–312. https://doi.org/10.1021/acsmaterialsau.5c00204

463. Steffensen AK, Lundberg H, Riisager A (2026) Deep eutectic solvents as recyclable solvent–electrolyte systems for electroreductive C–O cleavage of lignin models. Green Chem 28:8176–8187. https://doi.org/10.1039/D5GC05226B

464. Feng X, Huang T, Feng J, Wang X (2026) Extraction and Recovery of Flavonoids from Tartary Buckwheat Using Deep Eutectic Solvents. Molecules 31:1261. https://doi.org/10.3390/molecules31081261

465. Lu Q, Chen L, Li X, Chao Y, Sun J, Ji H, Zhu W (2021) Sustainable and Convenient Recovery of Valuable Metals from Spent Li-Ion Batteries by a One-Pot Extraction Process. ACS Sustainable Chem Eng 9:13851–13861. https://doi.org/10.1021/acssuschemeng.1c04717

466. Alsaei A, Zarwi A, Binrajab A, Rahimi F, AlAnsari R, Kumar MP, Butler AE, Atkin SL, Deen GR (2026) Alginate-Based Biomaterials: From Fundamental “Egg-Box” Chemistry to Diverse Biomedical and Metabolic Management of Obesity and Diabetes. Gels 12:250. https://doi.org/10.3390/gels12030250

467. Terauchi M, Nagasato C, Inoue A, Ito T, Motomura T (2016) Distribution of alginate and cellulose and regulatory role of calcium in the cell wall of the brown alga Ectocarpus siliculosus (Ectocarpales, Phaeophyceae). Planta 244:361–377. https://doi.org/10.1007/s00425-016-2516-4

468. Habib M, Singh S, Jan K, Bashir K (2026) Alginate from seaweed and microbes: Sources, green extraction, functional properties, and food applications. Food Biomacromolecules fob2.70069. https://doi.org/10.1002/fob2.70069

469. Korotenko V, Smirnova I, Gurikov P (2026) Solvent-Mediated Self-Assembly and Hydrogen Bonding in Neutral Alginate: A Molecular Dynamics Study. Macro Materials & Eng 311:e00299. https://doi.org/10.1002/mame.202500299

470. Szopa D, Wróbel P, Zwolińska J, Anwar H, Kaniewski M, Witek-Krowiak A (2026) Influence of Deep Eutectic Solvents and Polyphenolic Extracts on the Structure and Functional Properties of Sodium Alginate Films. Polymers 18:186. https://doi.org/10.3390/polym18020186

471. Kowalonek J, Hamieau M, Szydłowska-Czerniak A (2024) Influence of Different Deep Eutectic Solvents and Plant Extracts on Antioxidant, Mechanical, and Color Properties of Alginate Film. Polymers 16:2084. https://doi.org/10.3390/polym16142084

472. Gulzar A, Maryam L, Khan S, Tayyeb A, Irfan M, Malik SA, Alanazi AK, Saleem M, Mansoor MA, Iqbal M (2026) Development and evaluation of choline bio-ionic liquid modified conductive

alginate hydrogels: in vitro and in vivo trials. Colloid Polym Sci 304:889–902. https://doi.org/10.1007/s00396-026-05575-z

473. Jurko L, Makuc D, Štern A, Plavec J, Žegura B, Bošković P, Kargl R (2023) Cytotoxicity and Antibacterial Efficacy of Betaine- and Choline-Substituted Polymers. ACS Appl Polym Mater 5:5270–5279. https://doi.org/10.1021/acsapm.3c00691

474. Moradiya K, Pereira MM, Prasad K (2024) Aqueous Solution of Ionic Liquid Is an Efficient Substituting Solvent System for the Extraction of Alginate from Sargassum tenerrimum. Sustainable Chemistry 5:116–129. https://doi.org/10.3390/suschem5020009

475. Tarzynska N, Bednarowicz A, Pabjanczyk-Wlazlo E, Draczyński Z (2022) The Interphase Gas-Solid Synthesis of Ammonium Alginate—The Comparison of Two Synthesis Methods and the Effect of Low Molecular Weight Electrolyte Presence. Materials 15:4321. https://doi.org/10.3390/ma15124321

476. Hernández-Fernández J, González-Cuello R, Ortega-Toro R (2026) Ion-Exchange Selectivity in Alginate Egg-Box Models: Effect of the G-Rich and M-Rich Microenvironment on the Stabilization of Divalent Metal Cations. Polysaccharides 7:54. https://doi.org/10.3390/polysaccharides7020054

477. Ahmed T, Yamanishi C, Kojima T, Takayama S (2021) Aqueous Two-Phase Systems and Microfluidics for Microscale Assays and Analytical Measurements. Annual Rev Anal Chem 14:231–255. https://doi.org/10.1146/annurev-anchem-091520-101759

478. Jablonský M, Škulcová A, Šima J (2019) Use of Deep Eutectic Solvents in Polymer Chemistry–A Review. Molecules 24:3978. https://doi.org/10.3390/molecules24213978

479. Banerjee A, De R, Das B (2022) Hydrodynamic and conformational characterization of aqueous sodium alginate solutions with varying salinity. Carbohydrate Polymers 277:118855. https://doi.org/10.1016/j.carbpol.2021.118855

480. Varadarajan A, Kearney LT, Keum JK, Naskar AK, Kundu S (2023) Effects of Salt on Phase Behavior and Rheological Properties of Alginate–Chitosan Polyelectrolyte Complexes. Biomacromolecules 24:2730–2740. https://doi.org/10.1021/acs.biomac.3c00171

481. Solberg A, Mo IV, Aachmann FL, Schatz C, Christensen BE (2021) Alginate-based diblock polymers: preparation, characterization and Ca-induced self-assembly. Polym Chem 12:5412–5425. https://doi.org/10.1039/D1PY00727K

482. Aarstad OA, Tøndervik A, Sletta H, Skjåk-Bræk G (2012) Alginate Sequencing: An Analysis of Block Distribution in Alginates Using Specific Alginate Degrading Enzymes. Biomacromolecules 13:106–116. https://doi.org/10.1021/bm2013026

483. Hilbig J, Hartlieb K, Gibis M, Herrmann K, Weiss J (2020) Rheological and mechanical properties of alginate gels and films containing different chelators. Food Hydrocolloids 101:105487. https://doi.org/10.1016/j.foodhyd.2019.105487

484. Yang N, Wang R, Rao P, Yan L, Zhang W, Wang J, Chai F (2019) The Fabrication of Calcium Alginate Beads as a Green Sorbent for Selective Recovery of Cu(Ⅱ) from Metal Mixtures. Crystals 9:255. https://doi.org/10.3390/cryst9050255

485. Karami F, Sereshti H (2023) Copolymerized Natural Deep Eutectic Solvent Encapsulated in Calcium Alginate Beads: Application as a Green Sorbent for Analysis of Multiclass Pesticides in Nonalcoholic Malt Beverages by GC–MS/SIM. ACS Sustainable Chem Eng 11:2455–2467. https://doi.org/10.1021/acssuschemeng.2c06436

486. Pedro SN, Mendes MSM, Neves BM, Almeida IF, Costa P, Correia-Sá I, Vilela C, Freire MG, Silvestre AJD, Freire CSR (2022) Deep Eutectic Solvent Formulations and Alginate-Based Hydrogels as a New Partnership for the Transdermal Administration of Anti-Inflammatory Drugs. Pharmaceutics 14:827. https://doi.org/10.3390/pharmaceutics14040827

487. Tawalbeh M, Hassan MF, Al-Othman A, Ka'ki A (2025) Facile polymer electrolyte membranes based on deep eutectic solvents and alginates for fuel cell applications. International Journal of Hydrogen Energy 136:966–977. https://doi.org/10.1016/j.ijhydene.2025.04.215

488. Su Y, Guerra NB, Herculano RD, Mussagy CU (2025) Sketching deep eutectic solvents for the development of halochromic smart packaging using blueberry residue anthocyanins and alginate-based films for monitoring food freshness. International Journal of Biological Macromolecules 321:146525. https://doi.org/10.1016/j.ijbiomac.2025.146525

489. Wang Y, Goikolea E, Ruiz De Larramendi I, Reyes E, Lanceros-Méndez S, Zhang Q (2023) Natural and recyclable alginate hydrogels as extracting media for recovering valuable metals of spent lithium-ion batteries from a deep eutectic solvent. Waste Management 171:271–280. https://doi.org/10.1016/j.wasman.2023.08.047

490. Asevedo EA, Das Chagas BME, De Oliveira Júnior SD, Dos Santos ES (2023) Recovery of lipids and carotenoids from Dunaliella salina microalgae using deep eutectic solvents. Algal Research 69:102940. https://doi.org/10.1016/j.algal.2022.102940

491. Deniaud-Bouët E, Kervarec N, Michel G, Tonon T, Kloareg B, Hervé C (2014) Chemical and enzymatic fractionation of cell walls from Fucales: insights into the structure of the extracellular matrix of brown algae. Annals of Botany 114:1203–1216. https://doi.org/10.1093/aob/mcu096

492. Nemani N, Dehnavi SM, Pazuki G (2024) Extraction and separation of astaxanthin with the help of pre-treatment of Haematococcus pluvialis microalgae biomass using aqueous two-phase systems based on deep eutectic solvents. Sci Rep 14:5420. https://doi.org/10.1038/s41598-024-55630-4

493. Guidugli LF, Cheatham R, Reza T (2025) Systematic design of hydrophobic deep eutectic solvents by VEGA, COSMO-RS, and experiments for efficient removal of Saxitoxin and brevetoxin from water. Chemosphere 385:144595. https://doi.org/10.1016/j.chemosphere.2025.144595

494. Wazeer I, Hizaddin HF, Wen NX, El Blidi L, Hashim MA, Hadj-Kali MK (2023) Extraction of Phenol as Pollutant from Aqueous Effluents Using Hydrophobic Deep Eutectic Solvents. Water 15:4289. https://doi.org/10.3390/w15244289

495. Cabo M, Mclaughlin L, LaJeunesse D (2026) NMR Spectroscopy: Molecular Insights into Cell Wall Collapse and Oxidative Stress of *Escherichia coli* Induced by Imidazole-Activated Eutectic Solvents. ACS Omega 11:35687–35699. https://doi.org/10.1021/acsomega.6c01977

496. Lu W, Alam MdA, Pan Y, Wu J, Wang Z, Yuan Z (2016) A new approach of microalgal biomass pretreatment using deep eutectic solvents for enhanced lipid recovery for biodiesel production. Bioresource Technology 218:123–128. https://doi.org/10.1016/j.biortech.2016.05.120

497. Pari RF, Uju U, Ramadhan W, Hardiningtyas SD, Toyofuku K, Wakabayashi R, Goto M, Kamiya N (2025) Deep eutectic solvent-assisted pretreatment of Ulva seaweed cellulose and in silico characterization. Journal of Molecular Liquids 435:128095. https://doi.org/10.1016/j.molliq.2025.128095

498. Khodayari A, Hirn U, Spirk S, Ogawa Y, Seveno D, Thielemans W (2024) Advancing plant cell wall modelling: Atomistic insights into cellulose, disordered cellulose, and hemicelluloses – A review. Carbohydrate Polymers 343:122415. https://doi.org/10.1016/j.carbpol.2024.122415

499. Schuh L, Reginato M, Florêncio I, Falcao L, Boron L, Gris EF, Mello V, Báo SN (2023) From Nature to Innovation: The Uncharted Potential of Natural Deep Eutectic Solvents. Molecules 28:. https://doi.org/10.3390/molecules28227653

500. Jesus AR, Paiva A, Duarte ARC (2023) Current developments and future perspectives on biotechnology applications of natural deep eutectic systems. Current Opinion in Green and Sustainable Chemistry 39:100731. https://doi.org/10.1016/j.cogsc.2022.100731

501. Gertrudes A, Craveiro R, Eltayari Z, Reis RL, Paiva A, Duarte ARC (2017) How Do Animals Survive Extreme Temperature Amplitudes? the Role of Natural Deep Eutectic Solvents. ACS Sustainable Chemistry and Engineering 5:9542–9553. https://doi.org/10.1021/acssuschemeng.7b01707

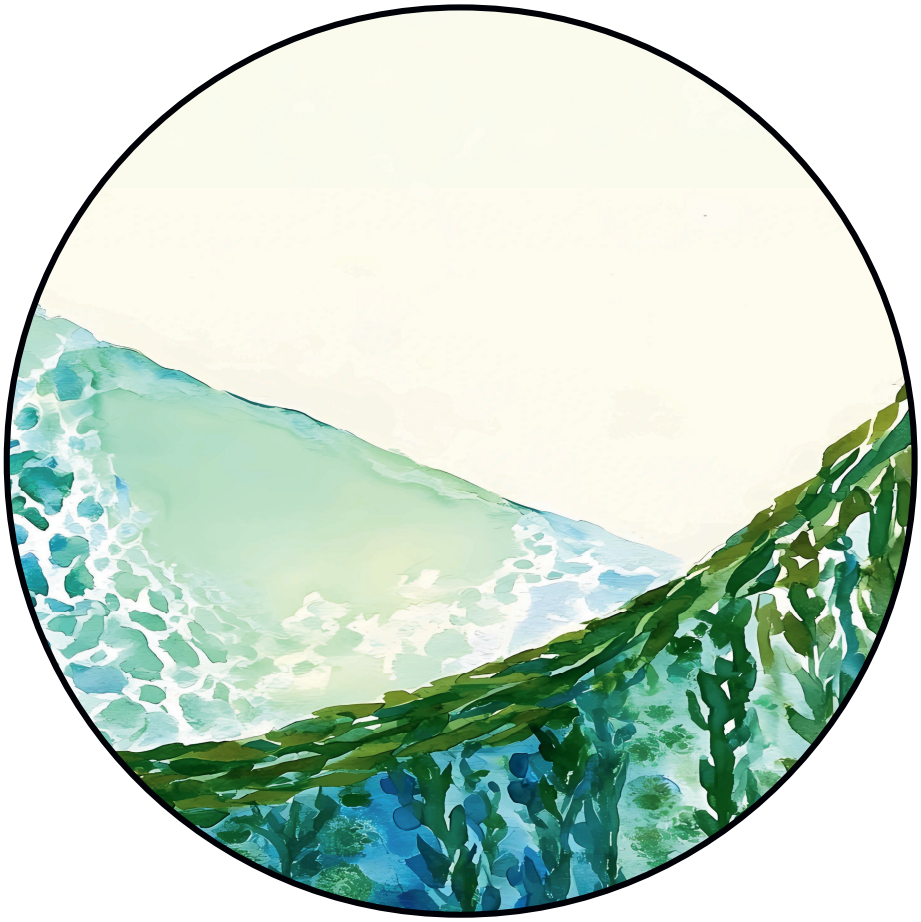
502. He W, Zhan T, Han H, Xu Y (2024) Optimization of Deep Eutectic Solvents Enables Green and Efficient Cryopreservation. Langmuir 40:624–637. https://doi.org/10.1021/acs.langmuir.3c02808

503. Tian Y, Sun DW, Xu L, Fan TH, Zhang ST, Zhu Z (2022) Bioinspired Cryoprotectants Enabled by Binary Natural Deep Eutectic Solvents for Sustainable and Green Cryopreservation. ACS Sustainable Chemistry and Engineering 10:7677–7691. https://doi.org/10.1021/acssuschemeng.2c01578

504. Nieto S, Villa R, Ruiz FJ, Velasco F, Lozano P (2026) Biocatalysis in neoteric ionic systems. Biocatalysis and Biotransformation 1–18. https://doi.org/10.1080/10242422.2026.2622470

505. Soltani-Nezhad Z, Zaboli M, Mortazavi M, Torkzadeh-Mahani M (2026) Enhancing stability and catalytic activity of urate oxidase using natural deep eutectic solvent: insights from experimental and computational approaches. Journal of Biomolecular Structure and Dynamics 44:4778–4795. https://doi.org/10.1080/07391102.2025.2486444

506. Syed Putra SS, Alias Y, Basirun WJ, Ibrahim M, A.M. Elgharbawy A, Tola H, Hayyan A, Hashim MA (2026) Biocatalytic transformation of Ganoderma lucidum by porcine pancreatic lipase in hydrophobic deep eutectic solvents. International Journal of Biological Macromolecules 340:150172. https://doi.org/10.1016/j.ijbiomac.2026.150172



Summary

Summary

The transition towards a circular bioeconomy requires sustainable technologies capable of converting renewable biomass into multiple high-value products while reducing chemical consumption, waste generation, and environmental impact. Brown seaweed represents an attractive feedstock because it contains a wide range of valuable compounds, including alginate, fucoidan, laminarin, mannitol, and pigments such as fucoxanthin. However, conventional industrial alginate production relies on harsh acid and alkaline treatments, extensive water consumption, and multiple downstream processing steps, while recovering only a single product. Deep eutectic solvents (DES) have emerged as promising alternative solvents due to their tuneable physicochemical properties, selective extraction capability, and potential for solvent recycling. Nevertheless, although DES-based extraction has been widely investigated, product recovery and solvent recycling remain major bottlenecks that currently limit industrial implementation.

The aim of this thesis was to evaluate the feasibility of a circular DES-based multiproduct seaweed biorefinery by integrating computational solvent screening, extraction process development, product recovery, solvent recycling, and techno-economic and environmental assessment. Particular emphasis was placed on developing recovery strategies that enable both efficient alginate isolation and repeated DES reuse.

Chapter 2 investigated the molecular interactions between alginate and a wide range of DES using the computational screening tool COSMO-RS. Molecular descriptors including activity coefficients, capacity, selectivity and partition coefficients were evaluated to identify DES with favourable affinity towards alginate while maintaining selectivity over other seaweed polysaccharides. The results demonstrated that COSMO-RS is a valuable first screening tool for narrowing down promising solvent candidates prior to experimental validation.

Chapter 3 experimentally evaluated the laboratory extraction performance of selected DES. Response surface methodology was subsequently used to optimise the extraction conditions. DES achieved higher alginate extraction yields compared to conventional alkaline processing while preserving polymer characteristics. However, extraction performance did not always correspond directly with the computational predictions, demonstrating that extraction efficiency depends not only on solvent–solute interactions but also on the ability to interact with the seaweed biomass matrix.

Chapter 4 investigated pressure-driven membrane filtration as a proof-of-concept recovery strategy for separating alginate from DES. A combination of ultrafiltration, diafiltration and nanofiltration successfully recovered alginate from a simplified DES

model solution, demonstrating the technical feasibility of membrane-based DES recovery. However, viscosity-related limitations, high water usage and incomplete DES retention highlighted the limitations of this approach for circular processing of complex seaweed extracts.

Chapter 5 explored three-phase partitioning (TPP) as an integrated extraction and recovery strategy for multiproduct seaweed biorefinery. A fatty acid-based hydrophobic DES simultaneously extracted pigments while pretreating the seaweed for alginate recovery in the aqueous phase. The hydrophobic DES could be reused over multiple extraction cycles, although alginate recovery yields did fluctuate upon reusing the DES and fucoxanthin remained dissolved within the DES phase. The chapter demonstrated the potential of integrating multiple process functions within a one-pot system.

Chapter 6 developed a thermo-separating aqueous two-phase system (ATPS) combining DES with a temperature-responsive EOPO copolymer. This approach enabled cyclic extraction, alginate recovery, and recycling of both DES and polymer phases. Although successful recycling was achieved, the process required multiple separation steps and relatively complex phase management, motivating the search for simpler recovery concepts.

Chapter 7 introduced temperature-responsive deep eutectic solvents (TRDES) as a one-solvent platform for alginate extraction, recovery and solvent recycling. The study demonstrated that reversible temperature-induced phase transitions can facilitate alginate recovery while allowing repeated solvent reuse. However, the optimal solvent formulation relied on amine-based components with limited suitability for food-related applications, and product recovery still required dialysis. The results indicated that the switching concept itself is promising, whereas future work should focus on developing greener temperature-responsive solvent formulations.

Chapter 8 combined the advantages of previous recovery systems (TPP and ATPS) by developing a DES–salt aqueous two-phase system with direct interfacial precipitation of alginate. This strategy enabled simultaneous product recovery and DES recycling while reducing downstream process complexity. Among all recovery strategies investigated, this process provided the most favourable balance between recovery efficiency, solvent circularity, processing time and operational simplicity.

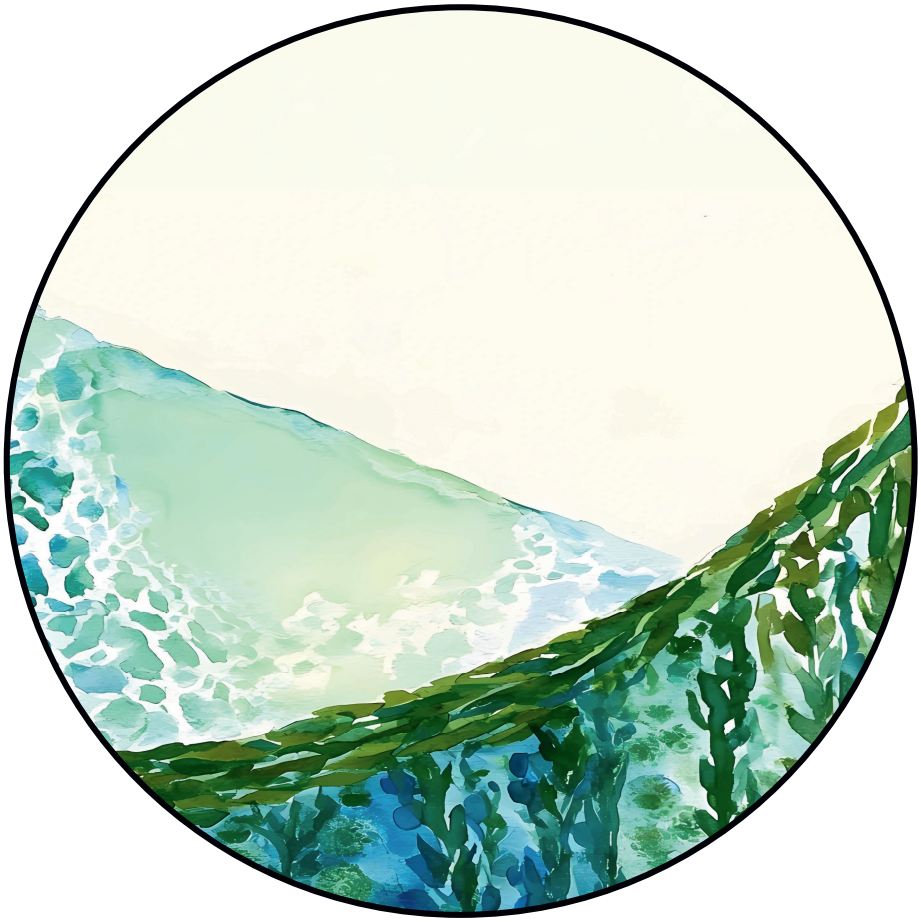
Chapter 9 expanded the role of DES beyond single-product extraction by developing a biphasic fatty acid–betaine:urea (FABU) system for one-pot multiproduct extraction. The biphasic DES simultaneously recovered alginate and fucoxanthin while improving the fucoxanthin yield and integrity after FABU pretreatment. This chapter

demonstrated that DES can function not only as extraction solvents but also as multifunctional processing platforms enabling integrated biomass fractionation.

Chapter 10 evaluated the techno-economic feasibility and environmental performance of the biphasic DES process through techno-economic assessment (TEA) and life cycle assessment (LCA). The analyses showed that DES production constitutes the largest contributor to both operating costs and environmental impacts. Nevertheless, the process becomes increasingly attractive when DES recycling is implemented, solvent consumption is reduced, fucoxanthin yields are increased, and higher-value alginate applications are considered. Compared with conventional alkaline extraction, the integrated DES process demonstrated improved environmental performance while highlighting the importance of solvent recycling for economic viability.

Chapter 11 integrates the findings of the preceding chapters and identifies three overarching conclusions. First, alginate recovery from DES is technically feasible but remains the primary process engineering bottleneck, requiring improved mechanistic understanding of DES–alginate interactions during repeated recycling. Second, DES selection should evolve from purely solvent–solute screening towards integrated dissolution–disruption design by combining molecular affinity with biomass interaction modelling. Third, DES should no longer be viewed solely as extraction solvents but as multifunctional process platforms capable of integrating biomass disruption, selective extraction, product stabilisation, fractionation and solvent recycling within a single process.

Overall, this thesis demonstrates that DES provide a promising foundation for the development of circular seaweed biorefineries. Although challenges remain in achieving robust product recovery and long-term solvent recycling, the results show that DES-based processing can intensify conventional extraction processes while creating opportunities for integrated multiproduct recovery. Future developments should therefore focus on designing DES as multifunctional processing environments that enable sustainable and economically viable biomass valorisation.



Appendices

Acknowledgements

About the author

Publications

Training activities

Acknowledgements

The past four years at Bioprocess Engineering have been an amazing journey. I found a warm and welcoming home in BPE, and I am very grateful for the people I have met here. This thesis could not have been completed without the support of many people. Looking back, what made these years meaningful was not only the research, but also the people, conversations, friendships, and experiences along the way. I would therefore like to take this opportunity to thank everyone who supported me throughout my PhD. This thesis may be the result of my work, but it is also the result of the many people who helped, encouraged, challenged, and supported me along the way.

First of all, I would like to thank my supervisor **Antoinette** and promotors **Michel** and **Rene**. **Antoinette**, first of all, thank you! You have been incredibly important to me throughout these four years, not only as my supervisor, but also as a mentor who guided me, challenged me, and pushed me to get the most out of my PhD. Thank you for having the confidence in me to take on this project, even though I started my PhD without any experience with DES. From the beginning, you gave me the trust and freedom to develop my own research ideas and explore the directions I was interested in. At the same time, you always knew when to step in or put on the brakes when I needed it. That balance helped me grow into an independent researcher. I really enjoyed the energy we shared. Our 'go-go-go' mentality often meant that there was always another idea, experiment, or project waiting around the corner. Looking back, I think that our high energy and fast pace was one of the things that made working together so enjoyable. Thank you also for treating me as a colleague rather than only as your student. I greatly appreciated being included in scientific discussions beyond my own work and having the opportunity to contribute to projects and ideas outside my thesis. And finally, thank you for all the fun along the way. I will always remember our conferences, the dinners at your place, the SeaSolv trips, and especially the slightly dangerous road trips in your car. These are the memories that will stay with me long after I have forgotten the details of many of the experiments. Thank you for believing in me, giving me the freedom to grow, and always encouraging me to get the best out of me. I could not have wished for a better supervisor to have done this journey with!

Michel, we first got to know each other during my MSc thesis, and I am grateful that our collaboration continued throughout my PhD. I have always appreciated your thoughtful feedback and the way you approached questions together with me. Your expertise in downstream processing was particularly valuable throughout my thesis and helped me look at my research from a different perspective. I am very grateful for your guidance and support over the years. You will certainly be missed at WUR!

René, thank you for giving me the opportunity to do my PhD within BPE and for the trust you placed in me from the start. I greatly appreciated your feedback during our progress meetings, as well as your sharp questions and broader perspective on my research. You gave me the freedom to shape my research and develop the different chapters in my own way, while always challenging me to think further. Thank you for your support throughout these years.

A big thank you to all the MSc and BSc students I have supervised over the past four years: **Jenne**, **Ruben M.**, **Stephanie**, **Mayank**, **Ruerd**, **Niels**, **Linn**, **Stan**, **Husna**, **Eline**, **Ruben G**. **Joost**, **Gita** and **Jinte**. It has been a great pleasure to work with all of you, and I have learned a lot from each of you along the way. **Jenne** and **Ruben M**., you were the first students to join me on the DES journey, and I really enjoyed exploring this together with you. Your questions, ideas, and enthusiasm challenged me to think beyond my own work, and our trip to Zeeland and Delft remains one of the highlights. **Stephanie** and **Mayank,** you both took on challenging thesis projects and showed great independence and perseverance in working your way through them. I am very proud of what you achieved and hope you carry that same determination into whatever comes next. **Ruerd,** you took on the challenging topic of protein extraction using NADES and brought so much positive energy and enthusiasm to the group. Thank you for your curiosity and for the energy you brought to our meetings, and I wish you all the best in your next steps. **Niels,** you laid the foundation for a new and challenging research direction that became the basis of Chapter 6, and your hard work and persistence ultimately led to part of a publication. I am very proud of what you achieved and look forward to seeing where your curiosity and determination take you next. **Linn,** you continued the challenging work on DES and proteins and made big steps towards becoming an independent researcher. It was great to see your confidence and skills grow throughout your project, and I am very proud of the work you did. **Stan,** you took on a new and challenging project on using DES as a preservative medium for seaweed storage and worked your way through it with great perseverance. You generated some really interesting results, and I hope you take the same curiosity and persistence with you into your next challenges. **Husna** and **Eline,** you were a true power couple, and I always enjoyed our group meetings with you both. Your dedication, enthusiasm and the way you encouraged each other made working with you a lot of fun, and **Husna**, part of your work ultimately became the basis for Chapter 7 and a publication. **Ruben G.**, you continued the challenging project on using DES as a preservative medium and worked hard during those six months. I am glad you persevered and completed your thesis well, and I wish you all the best in whatever comes next. **Joost,** you took on a completely new and multidisciplinary project on using DES for carbohydrate extraction from wastewater-grown algae, which took you well beyond the scope of this thesis. You

managed to develop knowledge across several different fields, which I found very impressive, and I hope you continue to explore that same broad curiosity in the future. **Gita,** you took on a novel and multidisciplinary project by bringing together virus research and DES. Through your work, you introduced me to a whole new area of research and shared a lot of new knowledge with the group. It was a pleasure working with you and I wish you all the best for the future. **Jinte,** last but definitely not least, I have never seen anyone get quite so enthusiastic about making her first DES and ATPS! You wanted a challenge and certainly took it on! Your enthusiasm, hard work, and determination laid the foundation for Chapter 9, which has now resulted in a publication. Thank you all for your dedication, enthusiasm, curiosity, and for the many discussions and ideas you brought to my PhD. It has been a privilege to supervise each of you, and I wish every one of you all the best for whatever comes next!

A big thank you to everyone in the Bioprocess Engineering group who has been part of my PhD journey. I have been incredibly lucky to work in such a great group, and I am grateful for all the friendships, conversations, coffee breaks, drinks, and everything in between.

First of all, a special thank you to my paranymphs, **Noor** and **Mels**. **Noor,** we started out as office mates for only a few weeks before we moved to having flex desks. Somehow, during those weeks, we never spoke to each other. Luckily, things changed pretty quickly afterwards, and you became a great friend. I treasure our coffee breaks, our moments of complaining about everything and nothing, and you regularly stopping by just to ask how I was doing. And of course, I will never forget all the fun nights out in Singapore and Thailand. Thank you for being such a good friend and for always being there for me throughout these years. **Mels,** the first time we met, you immediately insisted that I join the Christmas dinner organisation, which I could not say no to during my first week at BPE. From there, you became a great friend, and I will always remember our many moments of complaining in “our” office, as well as our philosophy coffee breaks, where we somehow ended up casually discussing the purpose of life. I am very glad that I got to know you, and I am happy that we are finishing this PhD somewhat together.

Thank you to my thesis twin, **Wimar**. It was really special to start this PhD journey together. I still remember our very first day, sitting together in Antoinette’s room and reading papers without having a clue what was waiting for us. Looking back now, we have both changed and grown over these four years. Thank you for all the years of figuring things out together. Thank you for always helping me with the HPLC,

troubleshooting the Dionex with me, and for all the solutions and DES I could always borrow from you! Like true siblings, we did not always agree with each other. But somehow, we always managed to move past them, and I think those moments were also part of how we grew together as colleagues and friends. I will never forget the scale-up disasters during those stormy autumn days at AlgaePARC, the late nights working on our LCA and biphasic papers, all the borrels, and of course the many trips we took together, with Korea being one of the highlights. I am really happy that I got to do this PhD journey with you. Thank you for being my thesis twin, colleague, and friend over these four years. I hope this is not the end of our collaboration. Thank you DEStie!

To my fellow biorefiners, **Iulian, Oscar, Agusman, Davey, Tim, Inge, Sylviah, Ruoxi, Jacques, Lucas, Nikhil, Lilan, Mariam** and **David,** thank you for making the biorefinery group such a fun and inspiring group to be part of. **Iulian,** you were the one who first introduced me to BPE and to the world of biorefinery during my MSc thesis. I really enjoyed working with you, and I am grateful that you sparked my enthusiasm for biorefinery and research in general. Even though we did not get to work together again directly, I have enjoyed our discussions and interactions through the biorefinery meetings over the years. **Wouter**, although we did not directly collaborate, I really appreciated our scientific discussions and your interest in my work. Thank you for sharing your expertise and perspective, and for being examiner for my students. **Oscar,** you joined the SeaSolv team at the same time as Wimar and me, so we basically had to figure out together what to do with seaweed and DES! I am very happy that we got to work together and collaborate on not one but two papers, and I always enjoyed our Dutch conversations over a beer. Thank you for all the energy you bring to the group and for always taking the initiative when it came to organising borrels and uitjes. **Agusman,** you joined Antoinette's seaweed team shortly after Wimar and I started, and it took us a little while to get to know each other. Thank you for your scientific insights, your jokes, and all the good conversations along the way. **Davey,** one of my fellow DES-ties! After having you as a student within the SeaSolv project, I was very happy to hear that you were joining the team again as a PhD and continuing your DES journey. Your enthusiasm and perseverance are a great addition to the team, and I am looking forward to seeing where your research takes you. **Tim,** I am very happy that you also joined Antoinette's team and are now stepping into the world of DES! Thank you for the enthusiasm you bring to the group, and for all the good conversations and fun moments, with Walibi as one of the highlights. **Inge,** our BPE journeys started way back together. You made doing my MSc thesis during COVID a lot more enjoyable, I was very happy when you came back for your MSc thesis and later joined us again as a PhD. Thank you for everything you do for the biorefinery team, from organising outings, drinks and dinners to taking care of all the administrative things, and of course for all your

mandatory coffee breaks with your infamous stroopwafels! **Sylviah** and **Ruoxi,** we started our BPE journeys around the same time, and I am happy that our paths crossed within the biorefinery group. Thank you for all the good conversations, your enthusiasm, and for being part of the team over these years. **Jacques, Lucas, Nikhil,** and **Lilan,** thank you for the scientific discussions during our biorefinery meetings and for all the drinks, dinners, and conferences we joined together. I really enjoyed the conversations and gezelligheid, and I wish you all the best for the future. Thank you to **Mariam** and **David**, who joined the SeaSolv group as guest PhD candidates. **Mariam,** thank you for sharing your knowledge of DES with us when you joined the team. We had only just started our DES journey, so your experience was a great help, and I learned a lot from working with you. **David,** thank you for bringing your strong chemistry background to the team, as well your statistics knowledge. I really appreciated your help and willingness to think along.

My unofficial office mates, **Guus** and **Willem**. **Guus**, you made a great start by claiming "my" desk when you first joined the group! You were a great office mate, and I really enjoyed all our discussions, coffee (and occasionally champagne) breaks, and of course the kilos of pepernoten you always brought to the office. Thank you for all the gezelligheid and for making the office such a nice place to work. **Willem,** when we first met after the Barbenheimer party, I would never have expected that you would become such a good friend. We come from different worlds and are very different people, but somehow it works, and I have really enjoyed being your vrolleeg. Thank you for all the laughs and conversations. I hope we will have many more adventures together!

The "trip after the trip" people: **Antoine, Cristina, Jenny, Kari, Matic, Nicola, Nuran, Noor** and **Wimar,** thank you for the amazing Thailand trip! The hikes, dinners, drinks, and all the adventures in between made it a memorable trip, and I am very happy that we got to share it with you. **Matic,** we started our PhD journeys around the same time, and I am glad that our paths crossed often over the years. I always enjoyed our coffee breaks and the many small conversations along the way. **Antoine,** thank you for the occasional French lessons along the way and for the positive energy you always bring. **Jenny**, thank you for connecting me to my roots by teaching me some Frisian in Singapore, and of course for organising the Veluweloop editions so well.

Pedro, thank you for all the "controversial" conversation topics you always wanted to discuss during coffee breaks and borrels. And of course, thank you for composing the WUR motto song during the PhD trip! **Sabine,** you directly made me feel welcome at BPE and brought so much positive energy to the group. I am happy to see you back at

BPE! **Kostas,** thank you for helping us with the microbial side of our students' projects and for sharing your expertise whenever we needed it. **Lyon**, thanks for all the Bongerd-gossips we shared, and of course for always calling me DES-queen! **Rutger**, thank you for regularly stopping by the "toxic office" to see how I was doing, which somehow only occurred whenever there happened to be a package of stroopwafels on my desk... **Alexandra, Antonia, Aureo, Carlos, Chantal, Claudia, Diego, Fran, Francesco, Guniz, Henrik, Igor, Ivan, Joanna, Jort, Julia, Juliette, Laura, Luca, Luka, Marcela, Martijn, Maxim, Nathan, Omnia, Ricardo, Rodrigo, Sofia, Sonia, Sophie, Stefan, Yuwei,** thank you as well for all the coffee breaks, lunches, conversations, drinks, and everyday moments we shared over the years!

I would like to thank the technicians **Wendy, Snezana, Fred, Mark v.D., Fran** and **Marsha**. Thank you for everything you do to keep the lab running. I greatly appreciate all your help with lab equipment, orders, and chemicals. Thank you for always being willing to help, and the nice chats we have had in the coffee corner. **Wendy**, a special thank you for always helping with HPLC, and especially with the Dionex. We could not have done the purchasing process, setting up and troubleshooting without you! To the AlgaePARC technicians, **Rick, Tom,** and **Brend**, thank you for your help with the upscaling experiments for our biphasic system. Working at AlgaePARC brought a new scale and set of challenges to the project. Thank you for your time, flexibility, and support!

I would also like to thank the other members of the BPE staff, **Maria, Giuseppe, Mark B., Joao, Sarah, Ruud, Dirk, Judit, Iago, Marcel, Affif, Enrique, Josue, Agi,** and **Vitor**, for their help and support throughout my PhD. **Giuseppe,** thank you for all your help with SuperPro. Your expertise made working with the process simulations much more manageable and was invaluable for the final chapter. **Maria,** thank you for chairing the algal meetings and for all the discussions and interactions within the algal group. I also really enjoyed the dinners and drinks together during the different AlgaEurope editions! **Mark B.**, thank you for your involvement in our shared 'DES to PHA' project and for always asking critical questions and thinking along with us. And of course, thank you for the occasional drinks, and for joining the PhD trip as one of our staff members! **Dirk,** thank you for your input and collaboration on the virus-DES project. I also really appreciated your expertise during the proposal writing, which helped me a lot with shaping the project. **Joao,** thank you for your last-minute help with the microscopy work, you saved our paper! **Marcel,** thank you for taking the time to examine some of my students' theses and for your involvement with the student presentations. **Miranda**, **Karen**, and **Marina**, thank you for taking care of all the administrative matters throughout my PhD. Thank you for helping me out making it all more manageable!

I would also like to thank the people I had the opportunity to collaborate with throughout my PhD. **Marco**, thank you for sharing your expertise on switchable DES. Our discussions were very valuable in shaping the direction of my research, and I am grateful that we had the opportunity to collaborate on Chapter 5. **Laura** and **Chiara,** thank you for the collaboration on your project and for introducing me to part of the research of organic chemistry. I really enjoyed working together, and I am happy that I could contribute to the COSMO-RS work in one of your papers. **Ellen**, thank you for sharing your expertise in LCA and for helping us navigate this part of the research, which was very new to us. I really appreciated your guidance and the time you took to help us understand and develop the LCA work. **Rafaela** and **Seppe**, thank you thank for your LCA insights and for helping to lay the foundation for this chapter. **Geert-Jan**, thank you for inviting me to KAUST and giving me the opportunity to experience a completely different research environment. It was a very valuable learning experience. Project partners **Sonia, Franck, Haik** and **Suzan,** and **Caroline**, thank you for your valuable contributions, input, and scientific discussions throughout the consortium meetings. **NWO**, thank you for funding this research and making the project possible.

Beyond the scientific side of my PhD, I would also like to thank people who supported me throughout these years outside BPE.

Iedereen van **RAC**, dankjewel voor alle muzikale avonden en de nodige afleiding van mijn PhD. De dinsdagavonden waren altijd een fijne onderbreking van de werkweek!

Lieve biotech-meiden, jaarclub, en schoolvrienden, dankjewel voor alle gezelligheid, vriendschap en steun, tijdens mijn PhD en alle jaren daarvoor. Hoewel jullie niet direct betrokken waren bij mijn PhD, hebben jullie de afgelopen jaren wel voor de nodige afleiding gezorgd. Dankjewel voor alle etentjes, weekendjes weg, lange wandelingen, koffies, en feestjes!

Lieve **Laurien**, **Hannah**, **Tess** en **Jan**, jullie verdienen een speciaal plekje in deze thesis. Dankjewel voor jullie liefde, steun en interesse, niet alleen tijdens mijn PhD, maar al mijn hele leven. Ik ben ontzettend blij dat ik jullie mijn zussen en broer mag noemen. Hoewel we allemaal onze eigen, verschillende wegen bewandelen, voel ik me ontzettend met jullie verbonden en weet ik dat ik altijd op jullie kan rekenen. **Laurien**, als grote zus ben je altijd iemand geweest naar wie ik kon opkijken. Dankjewel dat je altijd naar ons omkijkt, naar ons vraagt en zo vaak laat weten hoe trots je op ons bent. Dat betekent veel voor mij. **Hannah**, dankjewel voor je interesse in mijn PhD en voor de

gesprekken en steun onderweg. Ik vind het leuk dat we allebei zoveel plezier halen uit onderzoek doen, ondanks dat we in heel verschillende vakgebieden werken (lijken we dan toch niet alleen qua uiterlijk op elkaar?). Dankjewel voor je interesse en steun. Ik hoop dat jij de volgende bent die mag verdedigen! **Tess**, dankjewel voor je interesse en enthousiasme die je altijd hebt getoond. Ook al heeft mijn onderzoek niet bepaald veel met jouw vakgebied te maken, je bent altijd oprecht geïnteresseerd en enthousiast geweest over wat ik aan het doen was, zowel voor mijn PhD als daarbuiten. Dankjewel voor al die aanmoediging en warmte. Ik voel altijd jouw support. **Jan**, ook jij hebt me regelmatig gevraagd hoe het ervoor stond met mijn PhD. Dankjewel voor je interesse en aanmoediging. Nu jij zelf net bent afgestudeerd, begint voor jou ook een nieuwe fase. Ik ben ontzettend trots op je en kijk ernaar uit om te zien waar het leven je brengt! Ik houd heel veel van jullie en ben heel dankbaar dat ik jullie in mijn leven heb. Welke kanten we ook op gaan, we blijven altijd dicht bij elkaar.

Lieve **papa** en **mama**, jullie kan ik eigenlijk niet genoeg bedanken voor alles wat jullie voor mij hebben gedaan en nog steeds doen. Jullie hebben me altijd gesteund, wat ik ook deed. Of het nu om school ging, mijn studie, of accordeon, jullie stonden altijd vooraan om mij aan te moedigen en toe te juichen. Ook tijdens mijn PhD heb ik diezelfde steun altijd gevoeld. Jullie staan altijd voor me klaar, luisterden naar mij en dachten met me mee. Die onvoorwaardelijke liefde, warmte en steun hebben heel veel voor mij betekend. Ik ben ontzettend dankbaar dat ik altijd bij jullie terechtkan en dat ik weet dat jullie achter me staan, welke kant ik ook op ga en wat er ook gebeurt. Ik had geen betere ouders kunnen wensen. Ik hou heel veel van jullie en ben heel blij dat ik jullie heb gekozen!

Lieve **Marc**, als er iemand is die ik niet genoeg kan bedanken, ben jij het wel. Jij hebt als geen ander meegemaakt wat deze PhD met zich meebracht. Dankjewel voor al je liefde, steun, geduld en toewijding. Dankjewel dat je altijd zo met me meeleefde, me bij iedere stap bleef aanmoedigen en zo oprecht trots op me was. Dat je grote en kleine mijlpalen altijd met me vierde en altijd achter me stond. Dankjewel dat je me altijd de ruimte gaf om mijn eigen weg te vinden en zo veel vertrouwen in me had. Deze thesis is ook het resultaat van jouw steun, geduld en vertrouwen. Zonder jou was deze thesis niet hetzelfde geweest. Ik ben ontzettend dankbaar dat ik deze jaren met jou heb mogen delen. Jij bent mijn grootste steun. Ik hou ontzettend veel van je.

About the author



Isa Hiemstra was born on 8 April 1998 in Voorburg, the Netherlands. She attended Staring College in Lochem, where she obtained her Gymnasium diploma (pre-university education) in 2016.

Following high school, Isa studied the BSc Biotechnology at Wageningen University & Research (WUR). During her bachelor's programme, she completed a minor at the University of Limerick in Ireland. After obtaining her BSc degree, she continued with the MSc Biotechnology at Wageningen University, specialising in Environmental and Biobased Technology. During her master's, Isa developed a strong interest in sustainable bioprocess engineering and biorefineries. For her MSc thesis within the Bioprocess Engineering group, Isa investigated the acoustic properties of microalgal cell constituents to support the development of acoustic biorefinery fractionation processes. During her Research Practice within the Environmental Technology group, she focused on microbial chain elongation from ethanol-based substrates towards hexanol production and validated the process using Raman spectroscopy. She obtained her MSc degree in 2021. After graduation, Isa worked as a research assistant on the chemical and microbial recycling of polyhydroxyalkanoates (PHAs), further strengthening her expertise in sustainable bioprocesses and circular resource utilisation.

In 2022, she joined the Bioprocess Engineering group at Wageningen University & Research as a PhD candidate. Her doctoral research focused on the development of circular seaweed biorefineries using reusable deep eutectic solvents. By combining molecular solvent design, extraction process optimisation, product recovery strategies, solvent recycling, and techno-economic and environmental assessments, her work contributed to the development of more sustainable approaches for marine biomass valorisation.

Following the completion of her PhD, Isa will continue her academic career at the Environmental Technology group of Wageningen University & Research. Her work will focus on developing sustainable separation technologies for the extraction and recovery of arsenic from groundwater sludge, contributing to improved resource recovery and environmental protection. With a continuing interest in sustainable separation technologies and circular resource utilisation, she looks forward to contributing to the transition towards more sustainable chemical and environmental processes.

Publications

This thesis

Hiemstra, I. S. A., Reynaga-Navarro, W., Wijffels, R. H., Eppink, M. H., Kazbar, A. (2026) Disruption or partitioning? Deep eutectic solvent biphasic systems for integrated seaweed biorefineries. *Bioresources And Bioprocessing*, *13*(1). https://doi.org/10.1186/s40643-026-01139-9

Hiemstra, I. S. A., De Jong, J., Eppink, M. H. M., Wijffels, R. H., & Kazbar, A. (2026). Direct alginate recovery and solvent recycling from deep eutectic solvents via interfacial precipitation in aqueous two-phase systems. *Separation And Purification Technology*, *407*, 139128. https://doi.org/10.1016/j.seppur.2026.139128

Hiemstra, I. S. A., Husna, F., Eppink, M. H., Wijffels, R. H., & Kazbar, A. (2026). Mechanistic insights into temperature-responsive deep eutectic solvent for alginate recovery and solvent recycling. *Separation And Purification Technology*, *388*, 136807. https://doi.org/10.1016/j.seppur.2026.136807

Hiemstra, I. S. A., Lustig, N., Eppink, M. H. M., Wijffels, R. H., & Kazbar, A. (2025). Separation of alginate and recycling of deep eutectic solvents using temperature-responsive aqueous two-phase systems. *Journal Of Cleaner Production*, *536*, 147186. https://doi.org/10.1016/j.jclepro.2025.147186

Hiemstra, I. S.A., Eppink, M. H., Bravi, M., Wijffels, R. H., & Kazbar, A. (2025). Process intensification of seaweed biorefinery using reusable natural deep eutectic solvents. *Journal Of Environmental Chemical Engineering*, *13*(5), 119184. https://doi.org/10.1016/j.jece.2025.119184

Hiemstra, I. S.A, Meinema, J. T., Eppink, M. M., Wijffels, R. H., & Kazbar, A. (2024). Choline chloride-based solvents as alternative media for alginate extraction from brown seaweed. *LWT*, 214, 117174. https://doi.org/10.1016/j.lwt.2024.117174

Elizondo Sada, O. M. E., Hiemstra, I. S. A., Chorhirankul, N., Eppink, M.H., Wijffels, R. H., Janssen, A. E., & Kazbar, A. (2024). Pressure-driven membrane processes for the recovery and recycling of deep eutectic solvents: A seaweed biorefinery case study. *Biotechnology Reports*, *43*, e00849. https://doi.org/10.1016/j.btre.2024.e00849

Other publications

Kieffer, J. R., Kandemir, H., Stegemüller, L., Hiemstra, I.S.A., Eppink, M. H., Wijffels, R. H., & Boboescu, I. Z. (2025). Numerical analysis of a multiproduct biorefinery on a chip: Exploiting acoustic waves to process the microalgae *Tisochrysis lutea*. *Ultrasonics Sonochemistry*, *114*, 107280. https://doi.org/10.1016/j.ultsonch.2025.107280

Spaggiari, C., Hiemstra, I. S. A., Kazbar, A., Costantino, G., & Righetti, L. (2025). Towards eco-metabolomics: NADES-guided extraction enables semi-quantitative metabolomics for *Melissa officinalis*. *Advances in Sample Preparation*, *13*, 100154. https://doi.org/10.1016/j.sampre.2025.100154

Submitted work (this thesis)

Hiemstra, I. S. A., Reynaga-Navarro, W., Olivieri, G., Groudou, R., Van der Heyden, S., Slegers, P. M., Kazbar, A. (2026) Techno-economic and life cycle assessment of DES-based multiproduct seaweed biorefinery

Submitted to RSC Green Chemistry

Submitted work (other publications)

Elizondo Sada, O. M., Hiemstra, I. S. A., Reynaga-Navarro, W., De Kok, D., Wijffels, R. H., Huijgen, W. J. J., Kazbar, A. (2026) Natural deep eutectic solvents intensify enzymatic protein extraction from *Palmaria palmata* by targeting cell wall polysaccharides

Submitted to Results in Engineering

Overview of completed training activities

Category A - Discipline-specific activities

Courses	Organiser	Year
Advanced Course Downstream Processing	BioTech Delft	2023
Summer Course Glycoscience	VLAG	2023

Conferences and meetings

AlgaEurope[1]	EABA	2022
Biopartitioning and Purification Conference[2]	LIST	2024
Young Algaeneers Symposium[1]	EABA	2024
AlgaEurope[2]	EABA	2024
Seagriculture[2]	EABA	2025
International Meeting on Deep Eutectic Systems[1]	DES Solutio	2025
Green Deal Biotechnology[2]	EFB	2025
Seaweed Market Breakthrough – Korea Edition[2]	SeaweedLink	2025
Research stay at King Abdullah University of Science and Technology (KAUST)	KAUST	2025
Young Algaeneers Symposium	EABA	2026

[1]Poster presentation, [2]Oral presentation

Category B - General courses

VLAG PhD week	WGS	2022
Start to supervise BSc & MSc thesis students	WGS	2022
Scientific Publishing	WGS	2023
Efficient Writing Strategies	WSG	2024
Scientific Writing	WSG	2024
VLAG Midterm event: PhD on track	VLAG	2025

Category C - Teaching and Supervision Activities

Thesis supervision of 6 BSc and 8 MSc students	BPE	2023-2026
Laboratory assistant for Biorefinery course	BPE	2023
Lecturer and tutorial assistant for Advanced Biorefinery	BPE	2025-2026

Category D - Other activities

Preparation of research proposal	BPE	2022
PhD excursion to Singapore[3]	BPE	2023
Biorefinery theme meetings	BPE	2022-2026
Algal theme meetings	BPE	2022-2026
SeaSolv consortium meetings	BPE	2022-2026
Paper reviewing	BPE	2023-2026

[3]Including organisation

The research detailed in this thesis was conducted within the Department of Bioprocess Engineering at Wageningen University. This project was financially supported by Dutch Research Council (NWO) (The Hague, NL) under the SeaSolv project (grant number 19479).

Financial support from Wageningen University for printing this thesis is gratefully acknowledged.

Printed by ProefschriftMaken ‖ www.proefschriftmaken.nl

Classificatie: Intern

